

Contents

1	Introduction	5
1.1	Special structural design	6
1.2	Classifications	8
1.3	Structural Morphology	9
1.4	Structural design process	9
1.5	Discussion	9
2	Technology and knowledge	11
2.1	Geometry	13
2.2	Principles of Structural Morphology	22
2.3	Analogies between structural engineering, physical models and natural structures	67
2.4	Physical Modelling	67
2.5	Biomimetics	84
3	Structural concepts	121
3.1	Shells and domes	122
3.2	Cable-net and membrane structures	143
3.3	Pneumatic structures	165
3.4	Space frames	208
3.5	Kinetic and adaptable structures	277
4	Advanced computation for Structural Design	291
4.1	Theory	292
4.2	Form description and generation	294
4.3	Descriptive techniques	294
4.4	Generative Techniques	296
4.5	Form finding	324
4.6	Structural optimisation	331
A	Appendices	367
A.1	Example projects	367
A.2	Papers by Chris Williams	429

Preface

This reader belongs to the course "CT5251: Structural Design - Special Structures" of Delft University of Technology, faculty of Civil Engineering and Geosciences, of the Structural Design Lab. It covers a wide variety of knowledge, technology and examples of the field of special structures.

For comments and corrections please contact the editor.

April 2006,
J.L. Coenders, Editor (J.L.Coenders@tudelft.nl)

2nd edition

The reader has been updated with new project information, a new section on pneumatic structures and a new section on shell structures.

April 2007,
J.L. Coenders, Editor (J.L.Coenders@tudelft.nl)

3rd edition

The reader has been updated with spelling and other textual corrections.

March 2008,
J.L. Coenders, Editor (J.L.Coenders@tudelft.nl)

Acknowledgements

The editor of this reader would like to acknowledge the following persons for their useful contributions and work:

Jaap Aanhaanen, Andrew Borgart, Vincent van Dinter, Pim Dumans, Petra van Hennik, dr. Pierre Hoogenboom, Rogier Houtman, dr. Pieter Huybers, Paco Oltheten, Eline Ouwerkerk, Anke Rolvink, Michelle van Roosbroeck, Peter van de Rotten, Roel van de Straat, Matthijs Toussaint, prof. Leo Wagemans, dr. Chris Williams.

Introduction

1

Contents

1.1	Special structural design	6
1.2	Classifications	8
1.3	Structural Morphology	9
1.4	Structural design process	9
1.5	Discussion	9

1.1 Special structural design

Special structural design is a wide field of knowledge which includes many structural types, concepts, techniques, methods, etc. The field of ‘special structures’ is not very clearly defined, since:

1. Where does the boundary between ‘regular’ and ‘special’ lie?
2. This boundary shifts with increase in knowledge and experience with the structures.
3. Also terms like ‘non-standard’ do not give a clear definition of what is a ‘standard’ structure and what is a ‘non-standard’ one.
4. Terms like ‘free-form’ and the attempts made by many academics and theorists to find a clear definition for these kinds of structures unfortunately does not result in a clear boundary.

Because the geometrical definition of the structure often is not obvious, definitions tend to be aimed at the assumed lack of a mathematical definition. However, although special structures have a complex geometrical definition, they usually are very well-defined, but not recta-linear. So, in this reader no set definition for special structures will be given, except that they require knowledge, which usually is not directly part of a recta-linear building and a modified design process.

Structural concepts include among others:

- membrane structures
- pneumatic structures
- adaptive structures
- kinetic structures
- deployable structures
- retractable structures
- shell structures
- blob/free-form structures
- wide span structures
- lightweight structures
- tensegrity structures
- cable-net structures
- grid structures or grid shell structures
- lattice structures

The boundary between special structures and other structural types tends to become more vague, since high-rise structures more and more use the knowledge from this field. Recta-linear structures more often are mixed with these conventional parts and more often experiments with new materials are being performed in buildings.

Since the field of special structures and the related knowledge is such a wide field, the goal

of this reader is to introduce students of a graduate level to this field of knowledge. And to guide them to the vast array of available knowledge in the form of books, proceedings, journals, websites, etc., if they require more knowledge. For more in-depth knowledge on structural behaviour, advanced mathematics and advanced computational modelling and analysis, students are referred to the available courses around the world which each cover a small bit of in-depth knowledge.

This course collects the knowledge of structural concepts and the special design techniques, methods, etc. required for the design of these structures, such as:

- physical and computational modelling techniques
- mathematical and geometrical description
- parametric and associative design
- manual and computational analysis
- building methods and material

This introduction will continue with explanation of basic terminology, which commonly can be found in the field of knowledge for special structures (see section 2.2).

1. **Structural morphology**

Structural morphology is defined as the ‘Genesis of structures’. This definition unfortunately includes many things, but often has very much to do with the definition and design of complex regular and irregular structures. It is closely related to geometry for structures.

2. **Form finding**

Also about the definition of form finding much discussion exists in the world. The author would like to make a distinction between:

- (a) Classical form finding, which includes the definition of structural shape (form), based on the ‘form follows force’ principle. People like Antoni Gaudí, Frei Otto and Heinz Isler used this principle to find efficient shapes for their buildings. However, the resulting shape language remains quite limited to the ‘hanging chains’, inverted membrane’ analogy or minimal energy shapes of soap films.
- (b) Modern form finding, which seems to include any method and process to come to an appropriate shape in the eyes of the designer. Form finding follows no clear principle to define the shape, but includes many methods, such as NURBS definition, optimisation methods and generative methods.

3. **Form Finding versus Structural Optimisation**

Form Finding usually is related to the field of architecture and to finding the shape of a structure, and more in detail the equilibrium shape of the structure. Form Finding is usually identified with cable-nets, membranes, shells, etc. Heino Engel (Engel 1999) calls these form-active structures (systems of flexible, non-rigid matter in which the redirection of forces is effected by particular form design and characteristic form stabilization) or surface-active structures (systems of flexible, but otherwise rigid planes (=resistant to compression, tension, shear) in which the redirection of forces is effected by surface resistance and particular surface form.

4. **Form Finding by Werkman** (Werkman 2003)

Werkman describes form finding as "an iterative process where the designer determines the constraints (input) and analyses the results (output), but where he does not influence the process (black box) of the shape development itself". He divides form finding in biomorphic form finding, which researches the morphology of nature (nature is taken as a reference), and the technomorphic, which follows the principles of form of lightweight structures. He refers to Frei Otto's principle of "Form-Force-Mass" and minimal energy structures, or their components.

5. **Structural optimisation**

Optimisation can be defined as the process of searching for the minimum (or maximum) value of a set of criteria, defined by an object function, within a given set of boundaries, often defined by parameters or variables. Structural optimisation deals with the optimisation of structures.

1.2 Classifications

In the field of form finding many different classifications, subdivisions and different terminologies are used. This is probably based on the many points of view of the research fields where this technology has evolved: Architecture, Civil Engineering, Structural Engineering, Building Engineering, Mechanical Engineering, Aerospace Engineering, Mathematics, Mechanics, Informatics, etc. etc.

A classification based on four classes can be given:

- Physical modelling and optimisation
- Analytical optimisation
- Numerical and computational optimisation
- Grid generation and configuration processing

Focussed on the definition of geometry (Williams 2000)

Chris Williams, University of Bath, UK, looks at form finding and optimisation from a point of view as a definition method for geometry. A quote from one of his papers: "Form Finding is the process of establishing a structural geometry for a mechanism to carry a particular load" (Williams 2000). When looking from this point of view three categories can be seen:

- Sculptural
- Geometric
- Physical

In sculptural definition of geometry the shape is sculpted by hand and scanned in the computer or directly sculpted in the computer. In the geometric approach the form is derived from geometric objects, which requires a lot of mathematic knowledge. In the physical approach the form comes from a physical process. Williams argues that combinations of these methods should be used in projects to describe the difficult geometry.

1.3 Structural Morphology

A lot of discussion has been going over the years. Wester (Wester 1994) describes Structural Morphology as "the study of interaction between geometrical form and structural behaviour". Ramm (Ramm & Bletzinger 1993) describes it as the "study of the interaction between form and structures". He argues that structural morphology deals with the discipline of forms in general, and that structural optimisation deals with the genesis of optimal forms.

Structural Morphology is often associated with regular shapes, such as the Platonic regular shapes. Also irregular shapes built from regular elements can be included. In the past structural morphology was researched because of the use of space-trusses, which are closely related to stacking of regular geometrical shapes, such as cubes, piramids, etc. Structural Morphology can also be seen as part of form finding. By studying the morphology of structural formed by regular shapes, more complex irregular structures can be formed. It could be seen as a form of physical form finding or physical or analytical or numerical generation of shape, depending on the fact if you build models, use mathematics or use the computer to study the morphology (Coenders 2004)).

By reading "38 Years of Morphology, an Anthology" (Huybers 2000a), an impression can be acquired of structural morphology, based on papers of one of the most active people in the world, in the field of structural morphology, Piet Huybers of the Delft University of Technology. Many resources on structural morphology can also be found in the Structural Morphology Group (SMG) newsletters of the International Association of Shell and Spatial Structures (IASS).

1.4 Structural design process

The structural design process of special structures often differs from that of 'regular' structures, due to the often experimental nature of the design which requires inclusion of different steps next to the 'regular' design steps. Changes include:

- Special steps to define a unique definition for the geometry of the structure.
- Special knowledge or use of software for the analysis of these structures.
- Experimental steps to determine the behaviour of the structure, materials or conditions.
- Development of special software tools to help in the design process.

Often computation and computational modelling are required to perform even simple operations. Especially in large structures with many varying elements even the simplest of tasks often requires automation.

1.5 Discussion

Different structures Form finding and structural optimisation are techniques, technologies or driving-force for design for different structures. It is applied on many structures, especially cable-nets and membranes in the case of form finding and trusses and shells in the case of structural optimisation. Often, when looking for information on the subjects of form finding and structural optimisation, the author has experienced that people rather elaborate on the final structure of a design, the details of the structure and only make a quick remark on how the form (shape, topology, sizes, sections, etc.) of the structure was found. It seems the authors are not proud of their ingeneous methods, or do not want to share them. There are few books on the subject of form finding itself and although there are many books on structural optimisation, they all seem

to propagate one method or a few methods of solving the problems.

Maybe form finding and structural optimisation cannot be seen apart from the structures for which they work. Jörg Schlaich (Schlaich 2000), a skillfull engineer of lightweight structures for example, does not look at form finding, or optimisation, but at the lightweight structures resulting from it, as whole. Maybe this approach is a better one.

Structural optimisation usually is more related to the field of mechanics and usually is related to a more 'scientific' approach than form finding. The question here is if more mathematics means more scientific. Structural optimisation has been well-developed for specific purposes in mechanical engineering and civil engineering.

Note here that both methods are focussed on the 'form follows force' (Ramm & Bletzinger 1993) principle, where optimisation in general does not only has to focus on this. Also other criteria could be used.

Choice of method Rules can not be given for the choice of the ideal method of form finding and structural optimisation. One has to try, research, look at the general characteristics of methods and see if they fit the structural problem to solve. Isler (Isler 2000) states "The choice of form depends on the task and the importance of statical requirements: Functions and force".

Technology and knowledge

2

When designing special structures, special technology and related knowledge is required. Many techniques have been invented over the ages to create these spectacular structures. Chapter 2 will only give an overview and some insight in the technology and knowledge used by architects, engineers and contractors to build these structures.

Note that many of the techniques involve knowledge from many other fields of knowledge, such as mathematics, geometry, model building, mechanics, biology, biomechanics, etc. making it impossible to cover all these topics in depth. When the reader is interested in further knowledge, please refer to the recommended study material.

Contents

2.1	Geometry	13
2.1.1	Basics	13
2.1.2	Vector mathematics	14
2.1.3	Curve and surface geometry	15
2.2	Principles of Structural Morphology	22
2.2.1	Structural Morphology	22
2.2.2	Ordering Principles and Tessellations	27
2.2.3	The polyhedra	44
2.3	Analogies between structural engineering, physical models and natural structures	67
2.4	Physical Modelling	67
2.4.1	Catenaries	71
2.4.2	Hanging Models	72
2.4.3	Soap Film Modeling	76
2.4.4	High elasticity membranes or fabrics	82
2.4.5	Wet-cloth models	83
2.5	Biomimetics	84
2.5.1	Types of analogies	84
2.5.2	Cellular structures	85
2.5.3	Branching and tree structures	104
2.5.4	Sea shells and radiolaria	117
2.5.5	Biomechanics and muscles	117

RECOMMENDED STUDY MATERIAL

Title	Author	Year
NURBS: from projective geometry to practical use	G.E. Farin	1999
The origin of species by means of natural selection	C. Darwin	1891
Handbook of grid generation	J.F. Thompson	1999
ILEK series	Inst. für Leichtbau Entwerfen und Konstruieren	-
Applied geometry for computer graphics and CAD	D. Marsh	2005

2.1 Geometry

Geometry is derived from the greek words 'geos' and 'metria', which means 'earth' and 'measure'. Geometry therefore deals with measuring the earth primarily, which over the centuries has evolved to the mathematics of measurement of shapes and systems.

Geometry contains a wide field of mathematical techniques and applications, from simple one-dimensional points to higher-dimensional systems and complex manifolds. This section will provide an overview of characteristic terms and mathematical techniques in the field of geometry for special structures. Geometry often involves the position of objects while topology refers to the relationships between the objects.

These days geometry for special structures is often close related to the computational description and generation of structures, which will be further covered in Chapter 4.

2.1.1 Basics

The first distinction which has to be made for the description of geometry is the distinction in parametric form and the closed form. Equation 2.1 shows the parametric form of a circle with radius R and Equation 2.2 the closed form. Notice that the parametric form requires additional information, a parameter t , but allows direct calculation of the x and y coordinate, while for the closed form description first the equation has to be solved. Therefore, in computational techniques often the parametric form is preferred over the closed form of description.

$$\begin{aligned}x(t) &= R \cos(t) \\y(t) &= R \sin(t)\end{aligned}\tag{2.1}$$

$$x^2 + y^2 = R^2\tag{2.2}$$

Coordinate systems Another important fact to notice are coordinate systems. A coordinate system is a system for specifying points using coordinates measured in some specified way. Coordinates are a set of n variables which fix a geometric object (Mathworld 2008). Different kinds of coordinate systems exist, which each serve their own purpose and therefore are more or less applicable or useful in various problems.

The difference between global and local coordinate systems needs to be noted, especially for computational application. Often it is required to translate global to local coordinates and vice versa.

The two most commonly used systems are:

1. Cartesian coordinate system

If the coordinates are distances measured along perpendicular axes, they are known as Cartesian coordinates. Cartesian coordinates are rectilinear two-dimensional or three-dimensional coordinates (and therefore a special case of curvilinear coordinates) which are also called rectangular coordinates (Mathworld 2008). Often they are expressed as (x,y,z) or in parametric form as $(x(t), y(t), z(t))$ for curves and $(x(u,v), y(u,v), z(u,v))$ for surfaces.

2. Polar coordinate system

The polar coordinates r (the radial coordinate) and θ (the angular coordinate, often called

the polar angle) are defined in terms of Cartesian coordinates by Equation 2.3 and can be inverted with Equation 2.4 (Mathworld 2008).

$$\begin{aligned}x &= r \sin(\theta) \\y &= r \cos(\theta)\end{aligned}\tag{2.3}$$

$$\begin{aligned}r &= \sqrt{x^2 + y^2} \\ \theta &= \arctan\left(\frac{y}{x}\right)\end{aligned}\tag{2.4}$$

Often related to curves the parameter t is used as a measurement value along the length of the curve, scaled between 0 and 1. Zero denotes the beginning of the curve and one the end. Note that this parametric does not always have to be equally scaled over the length of the curve in cartesian space. In other words, the distance in Cartesian space (x,y,z) between a point $P(t=0.1)$ and $P(t=0.2)$, to be calculated with $\sqrt{dx^2 + dy^2 + dz^2}$, does not have to be equal to the distance between points $P(t=0.4)$ and $P(t=0.5)$. Similar parameters are used for surfaces, but since surfaces have two directions, also two parameters are used to describe the surface, often u and v .

2.1.2 Vector mathematics

Vector mathematics deal with vectors, which have been covered extensively in undergraduate math courses. Refer back to these courses to study the techniques mentioned below.

Often these basic vector techniques are used to deal with the generation of structures. Important operations are addition and subtraction of vectors, the vector norm, the vector product, the dot-product and the cross product. These techniques are very suitable for the description of systems where many linear relationships are present or where projection plays a large role. Knowledge of the basics of vector mathematics is essential for the engineer to describe simple systems.

These techniques are often applied in combination with techniques, such as curve and surface techniques, matrix techniques, etc. to simplify certain characteristics of the surfaces or systems, such as tangency and normal vectors.

Basic transformation operations Three often used operations related to vector mathematics are translation, rotation and scaling of a vector.

Translation

Translation of a vector moves the original vector V to a new vector V' with the translation described by the translation vector T without changing the direction of the vector. See Equation 2.5.

$$V'_i = V_i + T_i\tag{2.5}$$

Rotation

Rotation changes the direction of the vector. Multiplication with the matrix in Equation 2.6 will rotate the vector over an angle θ .

$$R_\theta = \begin{vmatrix} \cos \theta & \sin \theta \\ -\sin \theta & \cos \theta \end{vmatrix}\tag{2.6}$$

Scaling

Scaling changes the size or length of the vector. The vector is simply multiplied by a scalar s to perform this operation, as can be seen in Equation 2.7.

$$V'_i = sV_i \quad (2.7)$$

2.1.3 Curve and surface geometry

The geometry of curves and surfaces contains a wide field of techniques. Many techniques are available of defining and describing curves and surfaces in many forms.

Often used techniques in the field of the definition of architecture and structures are:

1. Geometrical functions
2. NURBS: Non-uniform rational B-Splines
3. Differential geometry
4. Mesh and grid geometry

Below first several general terms will be discussed.

Continuous surface techniques vs. discrete surface techniques

Surfaces (and curves) can be described in a continuous manner or in a discrete manner. The latter is often referred to as a mesh, a point grid or a point cloud. Continuous description often comes directly from a geometrical function. For this kind of description every point on the curve or surface can be determined without interpolation techniques, usually simple by filling in the parameters and computing the xyz-coordinates. With a discrete description only certain points on the surface are given. The points in between can only be derived with an interpolation technique, leading to faceted surfaces. Advantage of this technique is that often basic vector mathematics or simple transformations can be used to describe the geometry.

Ruled surfaces

Ruled surfaces are generated by sliding each end of a straight line on their own generating curve, while remaining straight parallel to a prescribed direction or plane. The generated straight line is not necessarily at right angles to the plane containing the generating director curves. Equation 2.8 shows the parametric description of the general form of the ruled surface.

$$x_i(u, v) = b_i(u) + v\delta_i(u) \quad (2.8)$$

Translational Surfaces

Surfaces of translation are generated by sliding a plane curve along another plane curve, while keeping the orientation of the sliding curve constant. The latter curve, on which the original curve slides, is called the generator of the surface.

Translating any spatial curve (generatrix) against another random spatial curve (directrix) will create a spatial surface.

Surfaces of revolution

Surfaces of revolution are generated by the rotation of a curve -the meridian- around an axis -the axis of revolution-. The results of revolution-developed surfaces are: conical shells, circular domes, paraboloids, ellipsoids of revolution, hyperboloids of revolution of one sheet, and others. Equation 2.9 shows the parametric description of the general form of the surface of revolution.

$$\begin{aligned}
x_1(u, v) &= \phi(v) \cos(u) \\
x_2(u, v) &= \phi(v) \sin(u) \\
x_3(u, v) &= \psi(v)
\end{aligned}
\tag{2.9}$$

Developable vs. non-developable surfaces

Surfaces can be developable or non-developable. Developable means that the surface can be unfolded without cuts or deformation. Mathematically developable surfaces are surfaces where the Gaussian curvature is everywhere zero. Non-developable surfaces therefore are double-curved.

For the description of structures it is important to know if a surface is developable or non-developable, since developable surfaces can be often made of simple plates without deformation or cutting. For the unfolding of non-developable surfaces computational techniques have been created, called cutting-pattern generation.

Geometrical functions Curves and surfaces can be derived directly from geometrical functions. Often a closed form or parametric form is used. Often simple functions can be used to create seemingly very complex geometrical structures.

NURBS: Non-uniform rational B-Splines A special type of a geometrical function definition which is often used for structures, are NURBS. NURBS, 'Non-Uniform Rational B-Splines', are mathematical representations of n-D geometry that can accurately describe any shape from a simple 2-D line, circle, arc, or curve to the most complex 3-D organic free-form surface or solid. Because of their flexibility and accuracy, NURBS models can be used in any process from illustration and animation to manufacturing.

Often people tend to believe that NURBS are 'random' curves, without any mathematical description. As will be shown, these curves have a unique geometrical description. However, it is not a simple one, making projection techniques, mesh techniques, etc. often a more difficult than with other techniques. On the other hand, NURBS have a very wide field of application, since they are able to model many shapes.

A NURBS curve is defined by four elements: degree, control points, knots and an evaluation rule.

1. Degree

The degree is a positive whole number. This number is usually 3, but can actually be any positive whole number. NURBS lines and polylines are usually of degree 1, NURBS circles are degree 2 (quadratic), and most free-form curves are degree 3 (cubic) or 5 (quintic).

It is possible to increase the degree of a NURBS curve and not change its shape, called degree elevation.

Generally, it is not possible to reduce a NURBS curve's degree without changing its shape.

2. Control Points

The control points are a list of at least (degree+1) points. One of the easiest ways to change the shape of a NURBS curve is to move its control points.

The control points have an associated number called a weight. With a few exceptions, weights are positive numbers. When a curve's control points all have the same weight (usually 1), the curve is called non-rational, and otherwise the curve is called rational. The

R in NURBS stands for rational and indicates that a NURBS curve has the possibility of being rational. In practice, most NURBS curves are non-rational. A few NURBS curves, circles and ellipses being notable examples, are always rational.

3. Knots

The knots are a list of (degree+N-1) numbers, where N is the number of control points. The number of times a knot value is duplicated is called the knot's multiplicity. For example, for a degree 3 NURBS curve with 11 control points, the list of numbers 0,0,0,1,2,2,2,3,7,7,9,9 is a satisfactory list of knots. The knot value 0 has multiplicity 3, 1 has multiplicity 1, 2 has multiplicity 3, 3 has multiplicity 1, 7 has multiplicity 2, and 9 has multiplicity 3. A knot value is said to be a full-multiplicity knot if it is duplicated degree many times. In the example, the knot values 0, 2, and 9 have full multiplicity. A knot value that appears only once is called a simple knot, such as knots 1 and 3 of the example.

Duplicate knot values in the middle of the knot list make a NURBS curve less smooth. At the extreme, a full multiplicity knot in the middle of the knot list means there is a place on the NURBS curve that can be bent into a sharp kink. For this reason, some designers like to add and remove knots and then adjust control points to make curves have smoother or kinkier shapes. Since the number of knots is equal to (N+degree 1), where N is the number of control points, adding knots also adds control points and removing knots removes control points. Knots can be added without changing the shape of a NURBS curve. In general, removing knots will change the shape of a curve. Knots that are not uniform are called non uniform. The N and U in NURBS stand for non uniform and indicate that the knots in a NURBS curve are permitted to be non-uniform.

If a list of knots starts with a full multiplicity knot, is followed by simple knots, terminates with a full multiplicity knot, and the values are equally spaced, then the knots are called uniform.

4. Evaluation Rule

A curve evaluation rule is a mathematical formula that takes a number and assigns a point.

The NURBS evaluation rule is a formula that involves the degree, control points, and knots. In the formula there are some things called B-spline basis functions. The B and S in NURBS stand for 'basis spline'.

The number the evaluation rule starts with is called a parameter. You can think of the evaluation rule as a black box that eats a parameter and produces a point location. The degree, knots, and control points determine how the black box works.

The equation for a B-spline is

$$s(t) = \sum d_i N_i^P(t); d_i \in \mathfrak{R}^3 \quad (2.10)$$

Differential geometry Differential geometry is officially the study of Riemannian manifolds, but usually this term is used for any type of geometry derived from a base of differential equations. These techniques are often used for curves and surfaces, and for grid generation techniques in a structured manner. The field of differential geometry is part of complex mathematics and will not be further covered in this course.

Interested readers can refer to Dirk J. Struik's, Lectures of Classical Differential Geometry

(Struik 1950).

It is also possible to generate geometry (and topology) from analytic functions and equations. Various examples of this will be discussed below. Many examples of geometry are available, less are known of topology.

Geometry from differential equations and functions Geometry can be generated from differential equations and functions. The Great Courtyard roof of the British museum in London is an example of this. What is not well-known is that the shape of the roof has been determined as a function (Williams 2000) instead of form finding by physical or computational models. Afterwards some adjustments have been made.

Many mathematical books exist on this subject, "Differential Geometry" (Struik 1950) and "Analytical and projective Geometry" (Struik 1953) by Struik are recommended for reading.

Gaudí Many people know Gaudí for his architecture, his learning from nature and of course his hanging models, but little people know that Gaudí used mathematical generation techniques to shape his buildings. In 'The Essential Gaudí' (i Armengol 2001) Jordi Bonet describes the tree columns of the Sagrada Familia in Barcelona. The columns are generated by a simple mathematical equation (2.11) but create complex shaped columns, which also make sense in a structural manner.

$$H = n + n/2 + n/4 + n/8 + n/16 + n/32 + \dots = 2n \quad (2.11)$$

where n is the number of sides and H the height of a column. The column height and the series to elevation are determined by the number of sides of each column, or depending from which point one looks, the elevation is determined by the height and the number of sides. The twists in the column are produced in the same manner. Figure 2.1 shows the column and its sections.

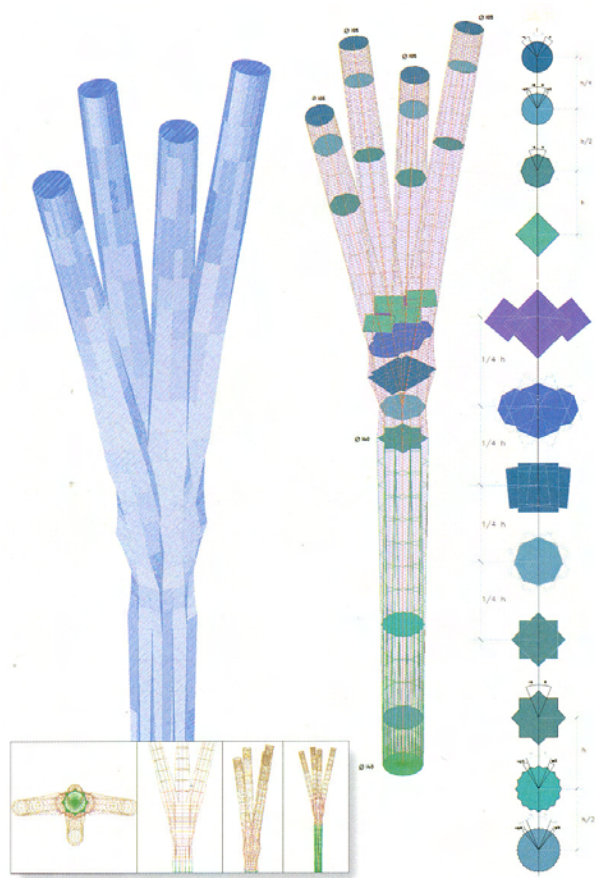


Figure 2.1: Tree column and the sections. Image from (i Armengol 2001).

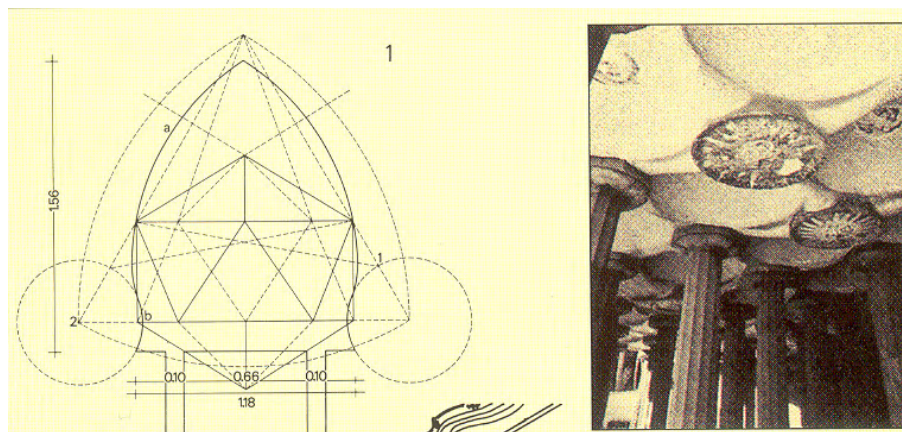


Figure 2.2: One of the geometry definitions which was found in Gaudí's buildings. Image from (Zerbst 2002).

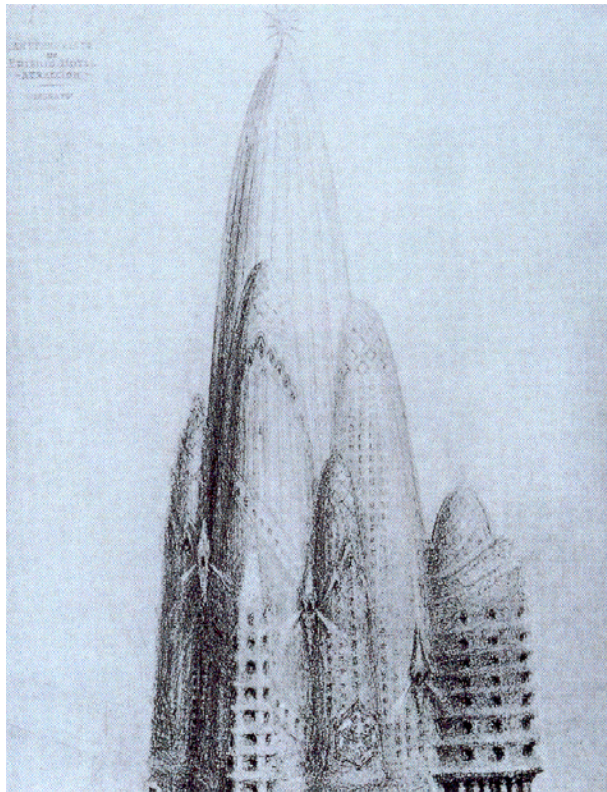


Figure 2.3: Proposal by Gaudí for a hotel. Image from (Zerbst 2002).

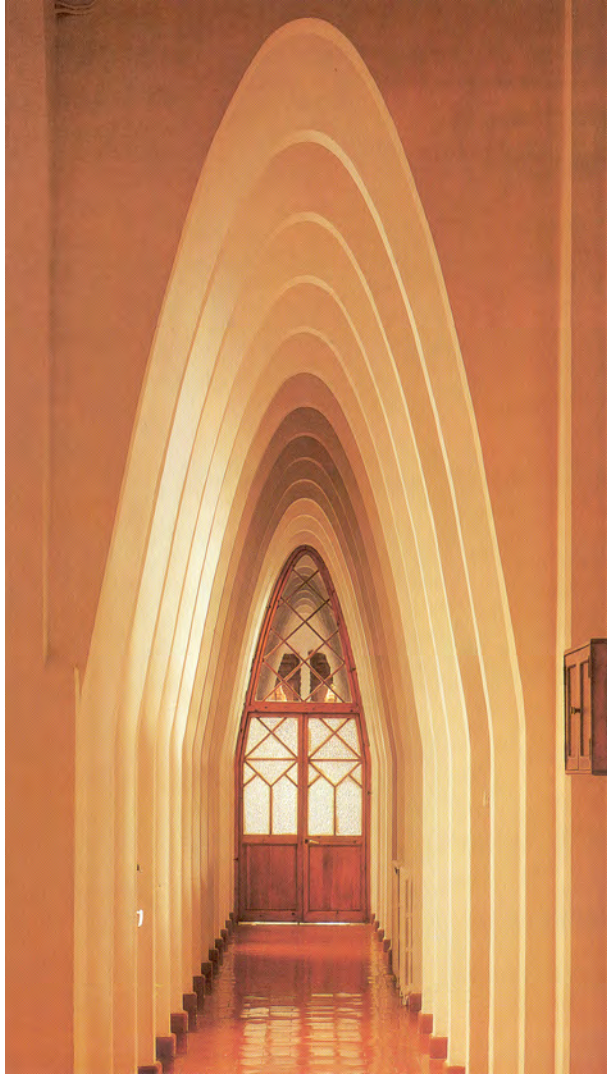


Figure 2.4: Parabolic shape in one of Gaudí's buildings. Image from (Zerbst 2002).

Grid and mesh geometry Grid and mesh geometry often involve computation and generation. The computational techniques for grid and mesh geometry generation will be further discussed in Section 4.4.

Formex mathematics Formex mathematics are a special kind of mathematics, developed by Nooshin and Disney of the University of Surrey. It is used for the processing of configurations, such as curves, surfaces and all kinds of vector-based configurations. Computational implementations of Formex mathematics are Formian and pyFormex. Formex mathematics will also be further discussed in Section 4.4.

2.2 Principles of Structural Morphology

2.2.1 Structural Morphology

Morphology; Goethe's (Goethe, Johann Wolfgang von, 1749-1832) term for the study of form and structure, in its broadest sense, dealing with every aspect of form you can think of. These aspects might be physical or abstract, perceptual or symbolic, functional or social, spatial or temporal. Structural morphology implies: the study of describing and calculation of shapes; the shapes of structures, buildings, or towns, the shapes of cells, crystals, mountains, or living organisms, or the arrangements of atoms and stars. The same shape may occur in a variety of unrelated situations, in various sizes, materials and colors; it may be stationary or moving, rigid or constantly changing. In addition to the physical form, one can look at abstract or non-physical form, the form of ideas or human relationships. Geometry occupies a central place in such a study which Buckminster Fuller describes as "explorations in geometry of thinking". The need to explore the different aspects of forms comes from several different motivations; the need to search for alternative ways to define architectural space, to span space, to discover design principles in nature, and the need to develop a formal language. In computational sciences, this aspect is being referred to as shape grammar.

To be able to create an optimum structure you have to completely understand the form. Different groups did research in this field. These basic forms can also be found in nature.

Structures in Nature As a response to the action of forces nature creates a great diversity of forms from an inventory of basic principles. The form of an object is a diagram of forces (Thompson 1963). There are innumerable examples in nature of forms and structures which are generated from the combinations of physically as well as chemically different components; snowflakes, soap bubbles, honey combs, etc. Section 2.5 covers more information about this subject.

Closest packing Closest packing is a structural arrangement of inherent geometric stability that finds expression in the three-dimensional arrangement of polyhedral cells. It can be found in biological systems as well as in dense arrangement of spherical atoms in the structure of certain metals. The closest packing develops because nature creates forms and structures according to the requirements of minimum energy (Thompson 1963).

If circles are tightly packed, as dense as possible, and their centers are joined, triangles are formed. When centers of packed hexagons are jointed, an array of triangles also results (see Figure 2.7. The principle of closest packing is equivalent to that of triangulation. When packing many circles together, more circles can be placed in a given area with triangular packing. In the limit of very many circles, all of a common size, approximately 7 percent more circles may be placed (Loeb 1966). Figure 2.6 shows some minimal energy packings with figures drawn by connecting centers. In a three-dimensional array of closest packed equal spheres, each sphere is

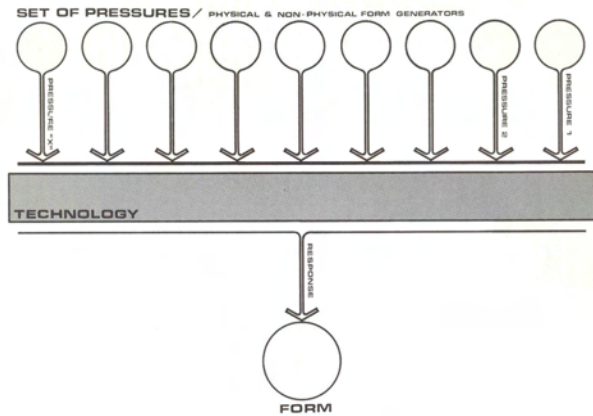


Figure 2.5: Basic pressure-response diagram showing relationship between the set of pressures and the form. A change in any of the pressures within the set or in the technology which stands at the interface between pressure and form will alter the diagram and ultimately the form. Image from (Clark 1970).

exactly surrounded by twelve others. The centers of the outer spheres are the 12 vertices of a polyhedron known as the cuboctahedron. Some other examples are shown in Figure 2.8.

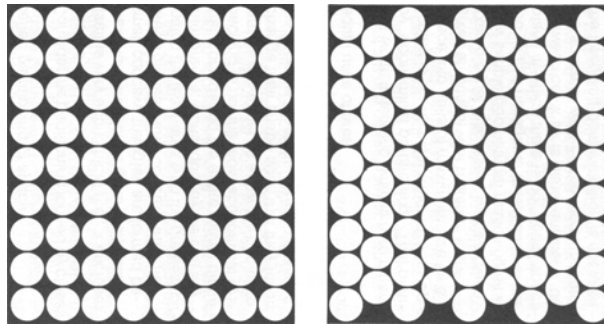


Figure 2.6: Comparison of square and triangular packings of equal circles in a given area, with triangular packing approximately 7 percent more circles may be placed. Image from (Pearce 1978).

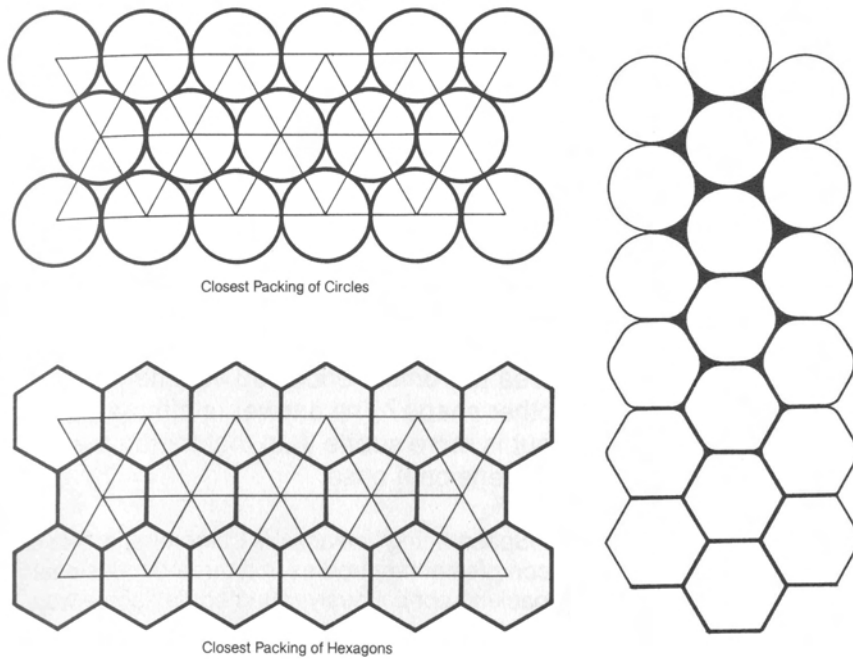


Figure 2.7: Triangulation of two-dimensional closest packed arrays. Changing closest packed circles into closest packed hexagons. Image from (Pearce 1978).

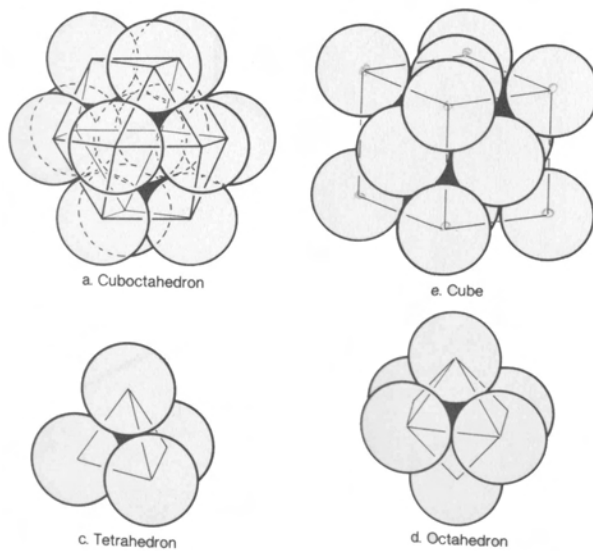


Figure 2.8: Figures formed by closest packed equal spheres. Image from (Pearce 1978).

The Soap Bubble Array as Model Some research with closest packings has been performed by Macior and Matzke (Macior & Matzke 1951) by using soap figures. This soap film behavior gives an elegant demonstration of minimal principles. Because tension is not the same in every bubble nor pure rhombic dodecahedra neither pure truncated octahedral appear. After observing 600 bubbles Matzke found an average of 13.53 faces, for each polyhedron. The majority of the faces were pentagons.

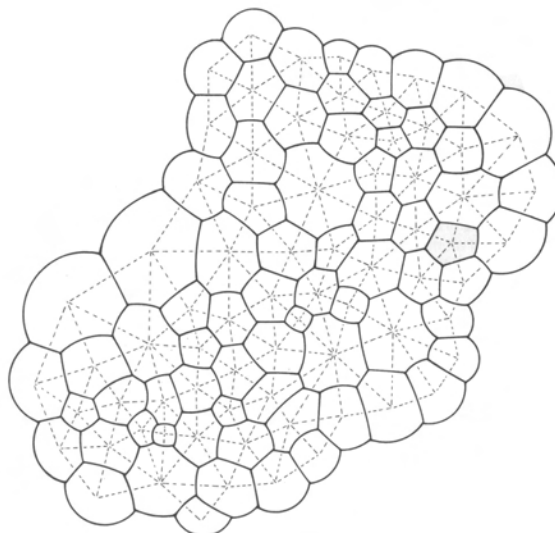


Figure 2.9: Soap Bubbles. Image from (Pearce 1978).

With soap bubbles the law of closest packing and triangulation can be proposed; "when compact arrays of volumetric (morphological) units (cells, bubbles, atoms, etc) are formed by any external, internal or attractive forces, they tend to have the greatest possible numbers of neighboring units, while equalizing as nearly as possible distances between their centers" (see Figure 2.9 (Pearce 1978).

Beside the soap bubbles a remarkable series of papers have discussed the cells of various plants and human fat cells (Lewis 1923), (Marvin 1938), (Matzke 1939). A in general consistent behavior is remarked in these diverse groups (realms). The forms of the systems are manifestations of the least-energy principle. All of the systems tend to conform to the law of closest packing and triangulation, although there are many other forces at work. Smith states (Smith 1952): "It seems that astonishing at first that the cells of things as different as a metal and soap foam can be almost indistinguishable in shape (see Figure 2.10 and 2.11). Only a crystal growing freely without contact with others can have the highly symmetrical polyhedral shape that is usually thought to typify a crystal."

The soap bubble packing can be taken as the model or type of all systems in which there is an economical association of cellular modules.

Closest Packed Unequal Spheres Frank and Kasper (Frank & Kasper 1959) have described the structures of complex metal alloys in terms of packing of spheres, in which the allowance of small variations of sphere diameters permits denser packings than the characteristic twelve-around-one packing of equal spheres.

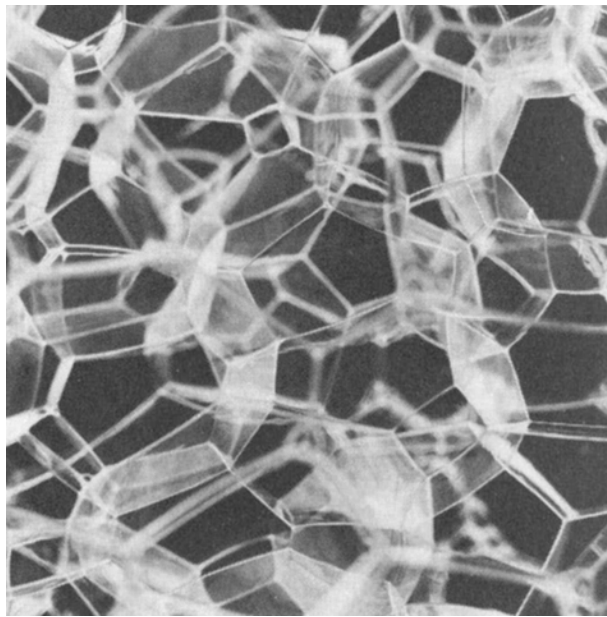


Figure 2.10: Triangulation of planar array of random bubbles viewed form above. Image from (Pearce 1978).

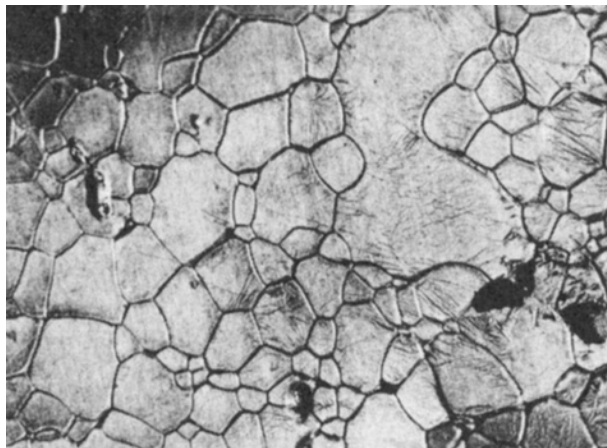


Figure 2.11: Surface of heated aluminum sheet. Image from (Smith 1952).

2.2.2 Ordering Principles and Tesselations

Spatial structures can be described in 3-dimensional elements. However, it is convenient to think of built structures as 0-, 1-, 2- and 3-dimensional structures composed of 0-, 1-, 2- and 3-dimensional elements. These four classes of built structures are composed of four elements; vertices, edges, faces and volumes. Example; in space frames the vertices are the nodes, the edges are the struts, the faces are the panels, and the cells are the 3-dimensional modules.

N-Dimensional Tables N-dimensional tables are complex versions of 2-dimensional tables. These higher tables are n-dimensional cubes (n-cubes) which chart all combinations of n independent variables. These variables could be n different structures, transformations, properties or attributes of structures.

N-cubes are determined by an n-star, a star of n distinct non-collinear unit vectors. The total number of combinations to create a polygon equals 2^n . N-cubes for cases n= 0,1,2,3,4 can be found in Figure 2.12.

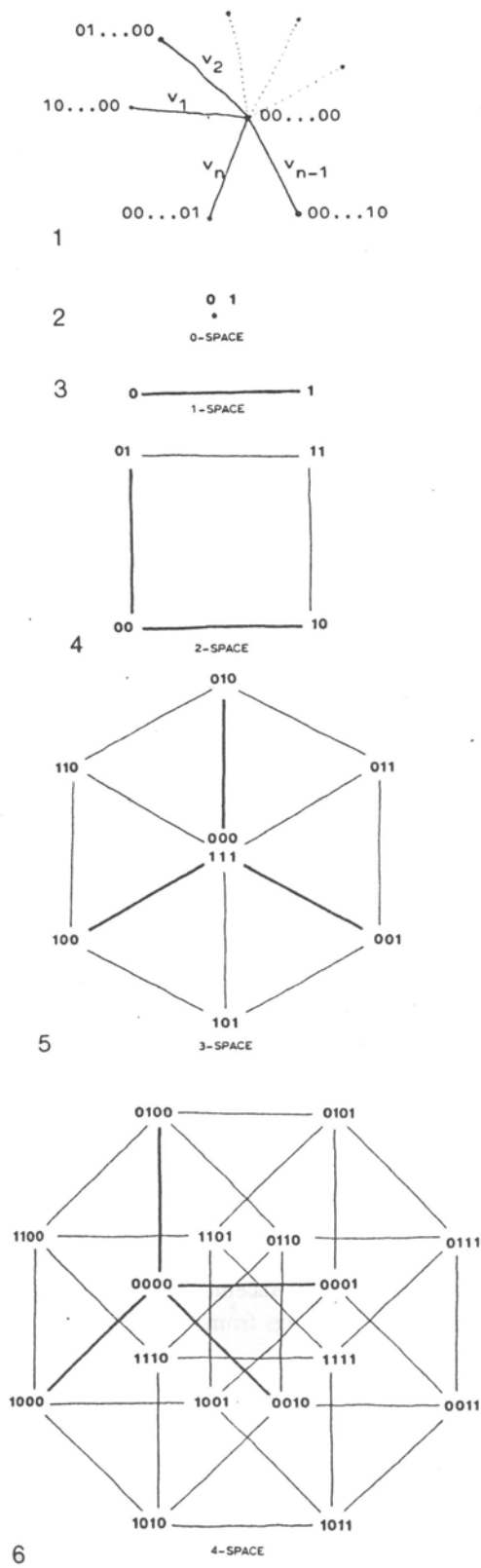


Figure 2.12: n-dimension table.

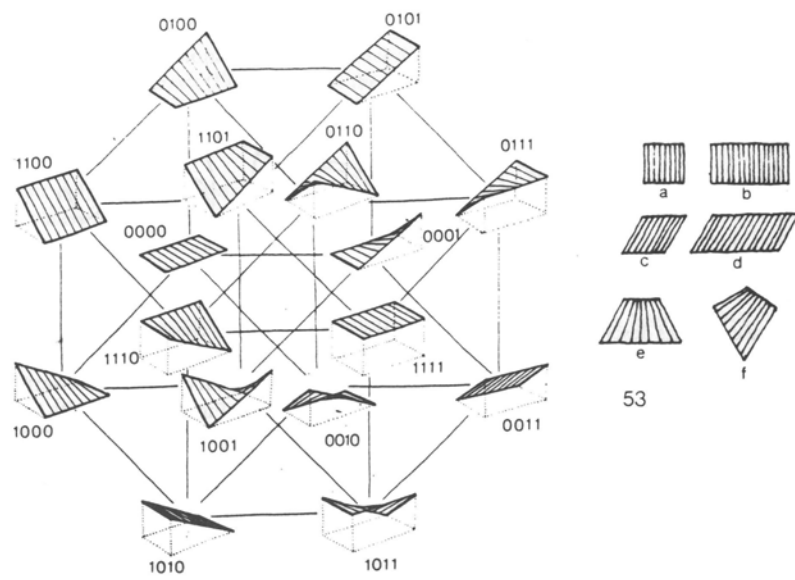


Figure 2.13: 4-sided polygon. Image from (Lalvani 1991).

Polygons Polygons are the simplest structures with a bound region, a face. The number of vertices and edges are equal here. Polygons are faces of more complex structures like polyhedra plane and space grids, and can be symmetric or irregular, convex or non-convex, have straight or curved edges, and plane or curved faces. They can transform from one to another by changing their angles, lengths, number of sides or curvature.

An infinite class of convex polygons corresponding to the sequence of natural numbers exists. Of these a special class consists of regular polygons having a plane face, straight and equal edges and equal contained angles. Curved polygons are produced by curving the edges or the face of the polygon. This produces four classes of curved polygons;

1. a plain face with straight edges (00)
2. a plane face with curved edges (10)
3. a curved face with straight edges (01)
4. a curved face with curved edges (11)

The 00 are regular polygons; the other three are classes of non-Euclidean polygons. Here we are interested in the straight edges for the space frames. There are two cases depending on whether the straight edges are co-planar or non-planar. When the edges are non-planar interesting double-curved surfaces can be produced. These include the familiar "warped" surfaces and the minimal surfaces obtained from soap films. A general method for generating warped polygons is by raising/lowering the vertices, mid-faces, or mid-edges in combinations out of the polygonal lane. Structures 1000, 0100, 0010, 0001 have one point lowered; 1100, 1010, 1001 and their complements 0011, 0101, 0110 have two points lowered; their complements 0111, 1011, 1101, 1110 have three points lowered; and 0000 and 1111 respectively have none and all points lowered. Warped parallelograms, squares, rectangles and rhombii (See Figure 2.13(a, b, c, d)) can be generated by a parallel translation of an edge over its two adjacent edges, and quadrilaterals (e, f) require a non-parallel translation.

Zonogons An infinite class of convex polygons with parallel edges, termed zonogons, expands the repertoire of polygonal structures. The even sided regular polygons, described before, are part of the infinite family of zonogons with equal edges. The edge directions of zonogons are determined by distinct combinations of i vectors ($i=0, 1, 2, 3, 4, \dots, n$) from a planar n -star. Zonogons with equal edges are 2-dimensional projections of n -dimensional regular polygons. Though any arbitrary direction for vectors can be chosen, a useful class of modular structures can be derived from the stars of regular polygons. An example is given in figure 2.14 with a 4-star, where the four directions 1, 2, 3 and 4 are determined by an octagon. The combinations of the four directions produce 16 structures.

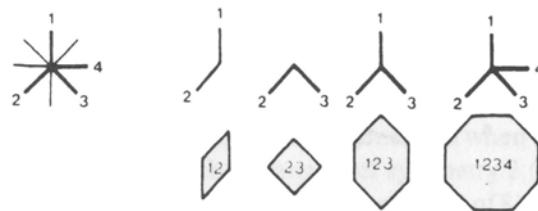


Figure 2.14: 4-star. Image from (Lalvani 1991).

All zonogons from regular polygonal stars can be tabulated. On the horizontal the star numbers are given on the vertical the number of different edges (See Figure 2.15).

$i \backslash n$	2	3	4	5	6	7	...
2	2_1 						...
	2_2						
	2_3						
	⋮						

Figure 2.15: Table with zonogons derived out of regular polygonal stars. Image from (Lalvani 1991).

Subdivided polygons All polygons can be subdivided in various ways leading to families of inter related polygonal compounds. The compound polygons provide basic geometries for subdividing polygonal space and could be faces of polyhedral structures. Centralized Churches of the Renaissance and numerous Islamic building used many of these square subdivisions as space diagrams for their (floor) plans.

Plane Tessellations A plane tessellation is an infinite set of polygons fitting together to cover the whole plane just once, so that every side of each polygon belongs also to one other polygon (H.S.M.Coxeter 1963).

Plane tessellations are a natural extension of polyhedra, infinite polyhedron, and provide their limiting cases. When the sum of angles at every vertex is equal to 360, the surfaces are flat and are known as plane tessellations. The methods of generating polyhedra from the fundamental regions extend to the derivation of plane tessellations. There are three broad classes of plane tessellations: periodic, central and non-periodic. These can be converted into tessellations with curved polygons, 2-dimensional space frames, or the entire plane could be curved into a curved surface. Plane tessellations can be seen as sections or layers of 3-dimensional space structures, or projections of higher-dimensional structures.

Regular Tessellations In modular structural systems such as single or double-layer grids, it normally is considered advantageous if the number of different member lengths can be limited and connection angles at the joints standardised. Resulting in regular patterns. This approach can be rather restrictive as there are only three regular polygons that can be used exclusively to completely fill a plane. These are the equilateral triangle with angles of 60° , the square with angles of 90° and the hexagon with angles of 120° which all have a minimum of three axes of symmetry. Square configurations are described as two-way grids as they have members in only two directions. The grid lines can be parallel to the edges of the grid or set on the diagonal, usually at 45° to the edges. See Figure 2.17 and 2.18.

Plane grids of triangles and hexagons produce three-way grids with members orientated in three directions. See Figure 2.19 and 2.20. There are only 17 plane symmetries; eight have triangular-form bases, and nine have four-sided-form bases (Shubnikov & Kopstik 1974), (Buerger 1968).

Semi Regular Tessellations A second class of planar partitioning is known as semi regular tessellations. This class requires that all polygons are regular and that all vertices be congruent, but permits the use of more than one type of polygon. There are only eight possible cases of semi regular plane tessellations, which consist of triangles, squares, hexagons, octagons and dodecagons (12 sides). One of these, consisting of triangles and hexagons, can be assembled in right - or left-handed form. Such figures, called enantiomorphs, are mirror images of one another. See Figure 2.21 (8 and 9).

- | | | |
|----|-----------------------------|---|
| 1 | hexagons | - triangles 60° - 60° - 60° |
| 2 | squares | - squares |
| 3 | octagon/squares | - triangles 45° - 90° - 45° |
| 4 | squares/triangles | - pentagons (semi-regular) |
| 5 | squares/triangles | - pentagons (semi-regular) |
| 6 | hexagons/triangles | - rhombii |
| 7 | dodecagons/hexagons/squares | - triangles 30° - 60° - 90° |
| 8 | hexagons/triangles | - pentagons (semi-regular) left-handed |
| 9 | hexagons/triangles | - pentagons (semi-regular) right-handed |
| 10 | hexagons/squares/triangles | - four-sided-polygons |
| 11 | dodecagons/triangles | - triangles 30° - 120° - 30° |

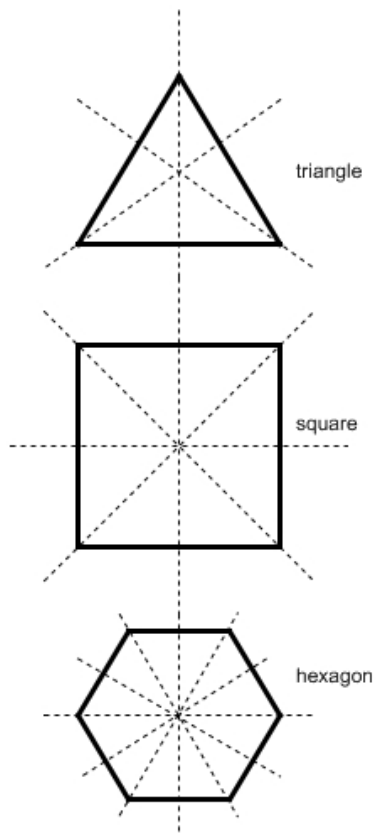


Figure 2.16: Axes of symmetry.

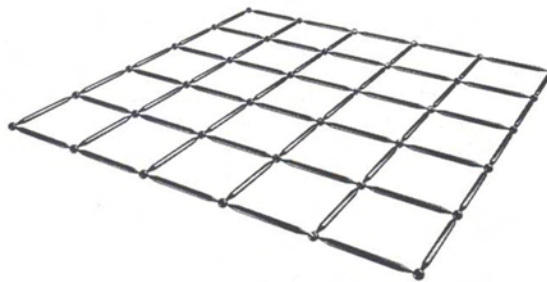


Figure 2.17: Tessellation of flat plane with squares. Image from (Chilton 2000).

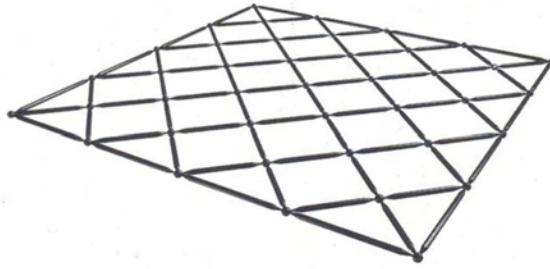


Figure 2.18: Tessellation of flat plane with rotated squares. Image from (Chilton 2000).

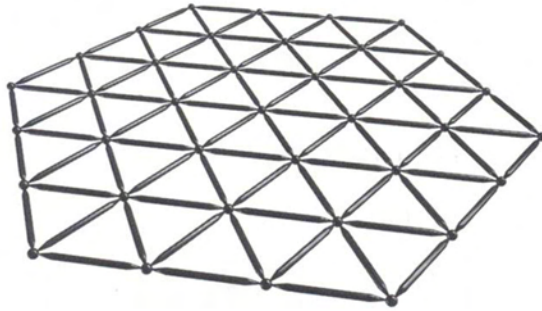


Figure 2.19: Tessellation of flat plane with triangles. Image from (Chilton 2000).



Figure 2.20: Tessellation of flat plane with hexagons. Image from (Chilton 2000).

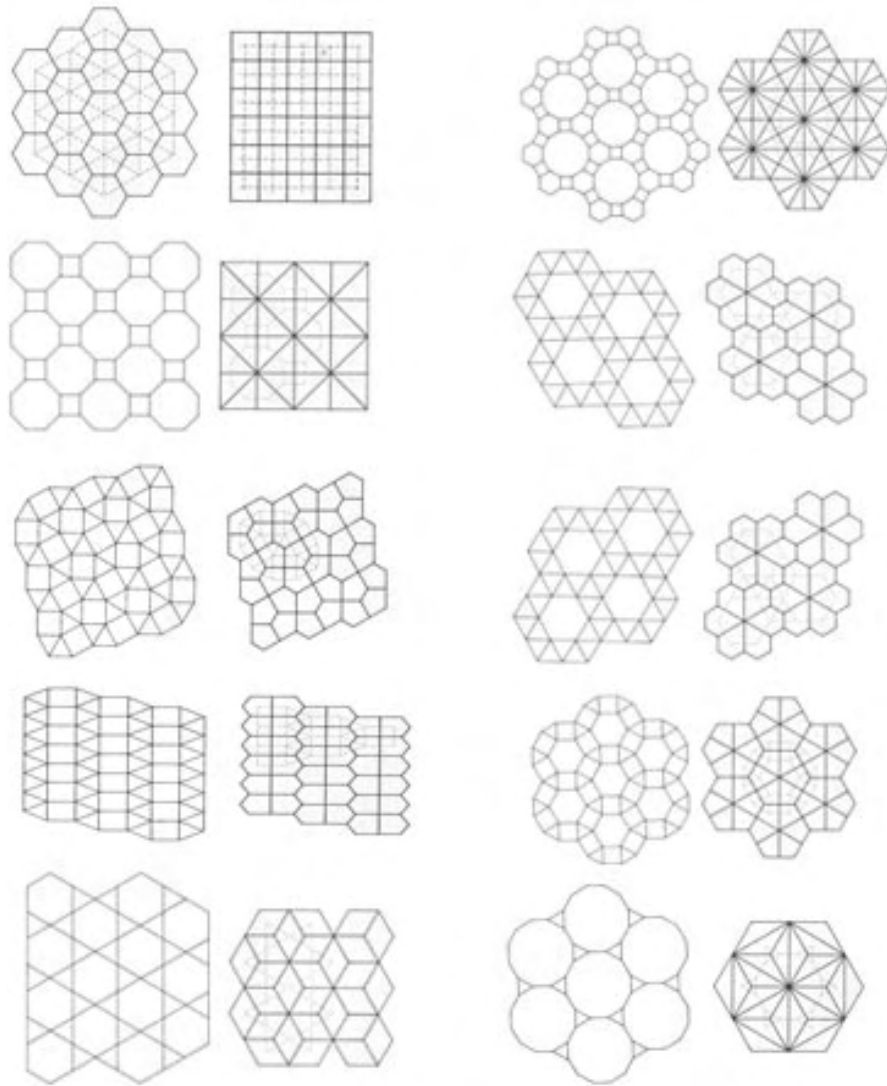


Figure 2.21: Regular and semi-regular plane tessellations (left) and their duals (right). Image from (Pearce 1978).

Dual Tessellations The concept of the reciprocal or dual network is important in the closest packed systems. It is also fundamental to the understanding of the properties of all spatial systems. A dual network is formed by joining the centers of each polygon to all neighboring polygons through the shared edges. Only one of the regular and semi regular plane tessellations is dual to itself; the square grid. Polygonal domains will have always the same number of edges as there are edges meeting at the vertex it encloses.

Other Tessellations When some of the conditions are relaxed an entirely new range of possibilities emerges. Numerous morphology researches have been performed in the past. When variation in lengths of elements is allowed a lot of other configurations are possible. Most grid configurations, however, look far too difficult to use in building practice because of the high numbers of nodes and different lengths of bars. However, with the modern computer-programs it is quite easy to produce members with many different lengths and nodes without an excessive cost penalty. This is called 'mass customization'; producing huge amounts of unique products. Greg Lynn can be seen as the pioneer in the field of mass customization. His project Embryologic Houses is an good example of this. The owner can act as a designer of his own house.

In the basic periodic plane tessellations a lot of other tessellation can be produced by placing a vertex in one region which is reflected throughout the plane. Connecting the vertices in the adjacent generates different tessellations.

A lot of different tessellations are shown; Islamic patterns, parallelogram and rectangular, zonogonal, non periodic, non periodic pattern-generation and non-convex polygons (see Figures 2.22 and 2.23).

Tessellations with Regular Polygons The entire plane is filled with regular polygons but do not require that all vertices are surrounded by equal angles. An infinite number of patterns are possible.

Tessellations and Symmetry The rotational symmetry of any figure is determined by counting the number of times it repeats or reproduces itself in one revolution about an axis. Only four kinds of rotational symmetry are possible in the uniform subdivision of space: 2-fold, 3-fold, 4-fold, 6-fold. A polygon has mirror symmetry when one side is the reflection of the other side about a common line which divides the polygons.

Open patterns with regular polygons If not all of the plane have to be filled and not all vertices should be congruent, open patterns emerge. With no need to fill all spaces with polygons, it is no longer necessary that polygons are used with face angles that can be combined summed up to 360 degrees. There still are 360 degree at each vertex but this vertex is not entirely surrounded by regular polygons.

Compound Tessellations and Islamic patterns Compound tessellations can be derived from the basic tessellations and duals by subdividing the polygons, or through recursive subdivisions as in polyhedra.

Parallelogram and Rectangular Tessellations Parallelogram and rectangular tessellations are characterized by four types of centers (axes) of symmetry. Their fundamental regions are parallelograms, rhombii, rectangles or squares.

Triangular Tessellations The three basic forms of the triangles which fill space are the equilateral triangle $60^\circ-60^\circ-60^\circ$, and the two rightangled triangles $45^\circ-90^\circ-45^\circ$ and $30^\circ-60^\circ-90^\circ$ (see Figure 2.24).

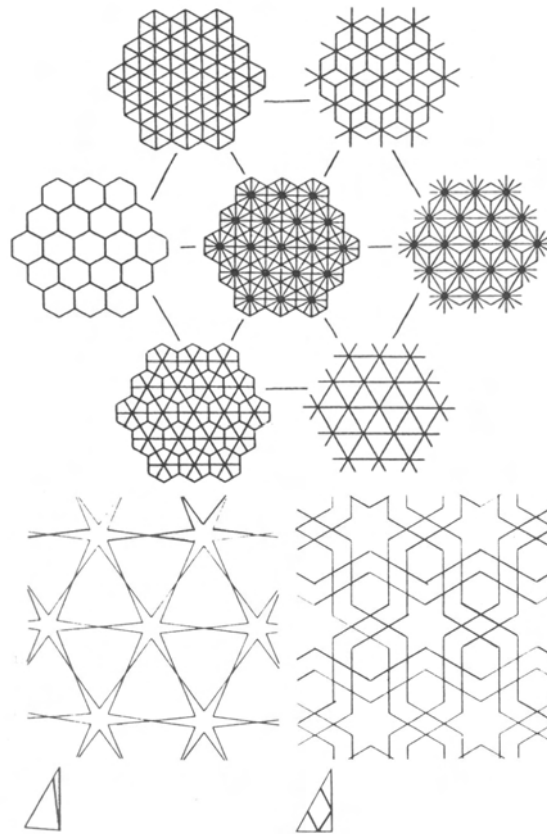


Figure 2.22: Compound Tessellations and Islamic patterns. Image from (Lalvani 1991).

Zonogonal Tessellations All rhombii and zonogons with $i \leq n$ can be used as modules to generate rhombic and zonogonal tessellations. One can use a single rhombii, but combinations of different rhombii give more variation. See also non-periodic tessellations.

Central Tessellations Central tessellations have a single center of symmetry. The class of such tessellations is infinite.

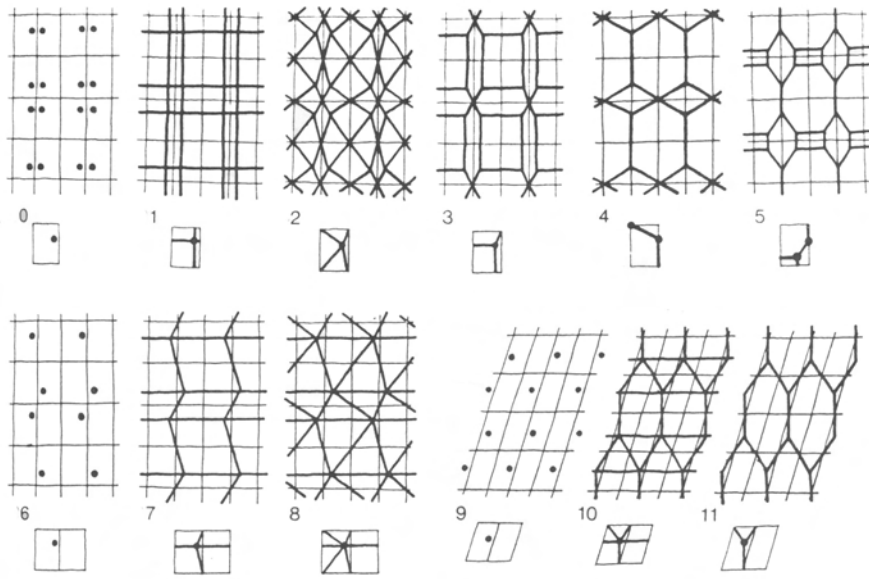


Figure 2.23: Parallelogram and rectangular tessellations and vertex placements. Image from (Lalvani 1991).

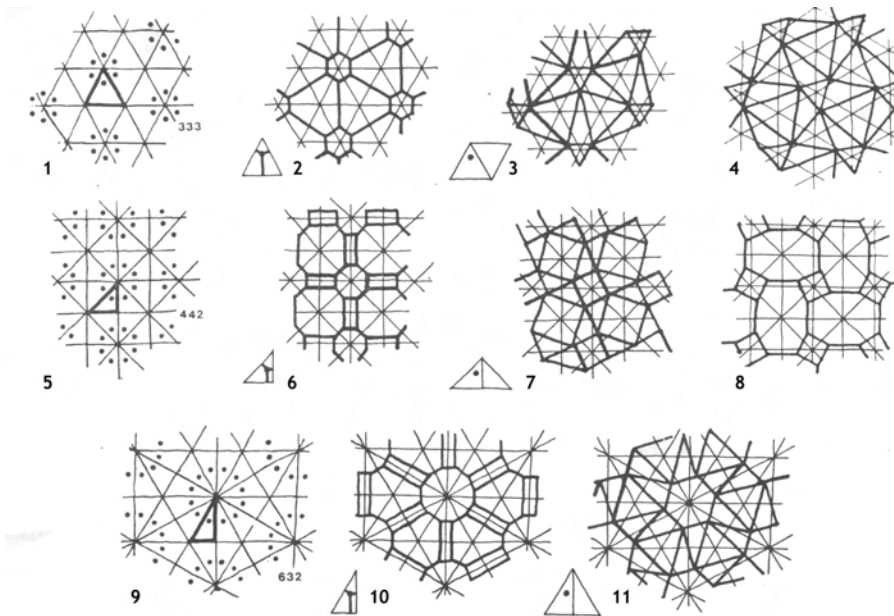


Figure 2.24: Triangular tessellations and vertex placements. Image from (Lalvani 1991).

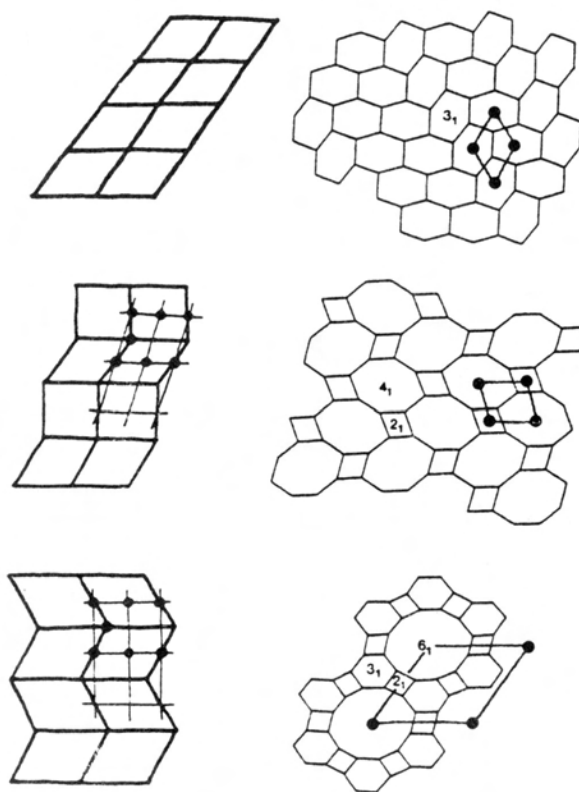


Figure 2.25: Zonogonal tessellation. Image from (Lalvani 1991).

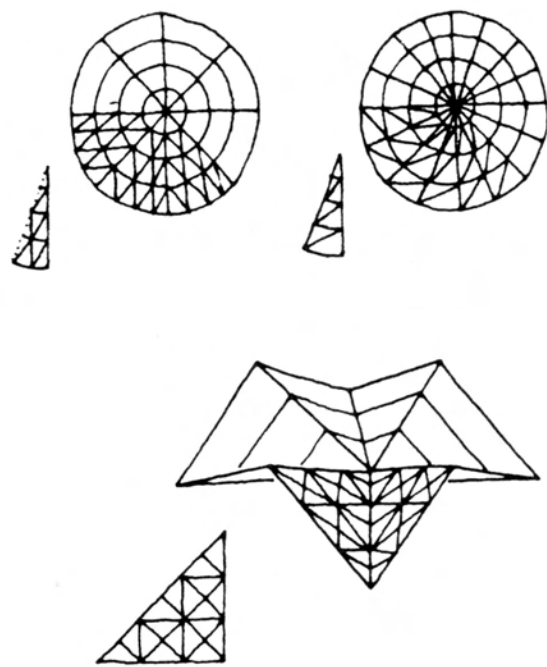


Figure 2.26: Central tessellations. Image from (Lalvani 1991).

Concentric Patterns with regular Pentagons Although the pentagon does not tessellate the plane, it has the curious property that it generates infinite concentrically repeating open patterns. Such concentric open patterns have only one axis of rotational symmetry, about the center of the central polygon which is the only one which shares all of its edges with other pentagons. Because the decagon has twice as many sides as a pentagon, their symmetry properties are similar. In fact any regular polygon which is not divisible by 2, 3, 4 or 6 will be capable of generating concentric patterns with a center of symmetry. One exception: a regular polygon which is divisible by 5 can generate concentric polygons.

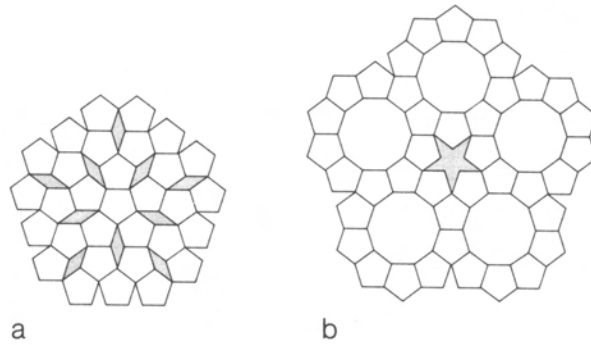


Figure 2.27: Concentric repeating patterns with regular pentagons with regular decagons. Image from (Pearce 1978).

Non-periodic Tessellations The rhombii and zonogons have a remarkable property of filling the plane non-periodically. Non-periodic tessellations are of recent origin and are characterized by lack of any translational symmetry.

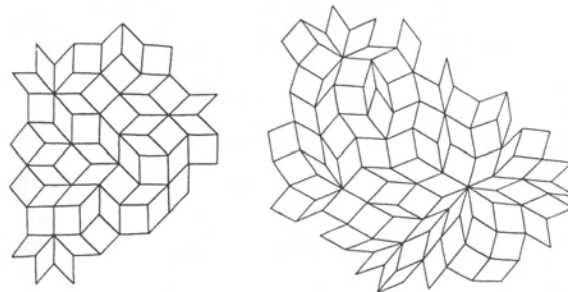


Figure 2.28: Non-periodic rhombic tessellations and non periodic hexagonal tessellations. Image from (Lalvani 1991).

Non-periodic Pattern-generation The method of deriving plane tessellations by vertex placement within the fundamental region, or by subdivisions, can be applied to the rhombic tessellations.

Tessellation with Non-convex polygons A special class of such polygons having equal edges can be derived from the difference between two overlapping polygons. This produces crescent-

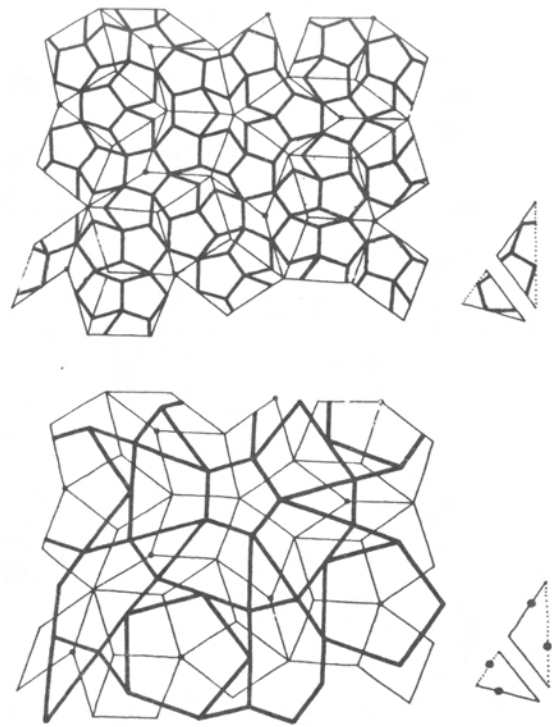


Figure 2.29: Non-periodic Pattern-generation. Image from (Lalvani 1991).

and bow-shaped polygons. It can be separated and their complementary polygons are rhombii and zonogons. Many other, infinite, tessellations are possible.

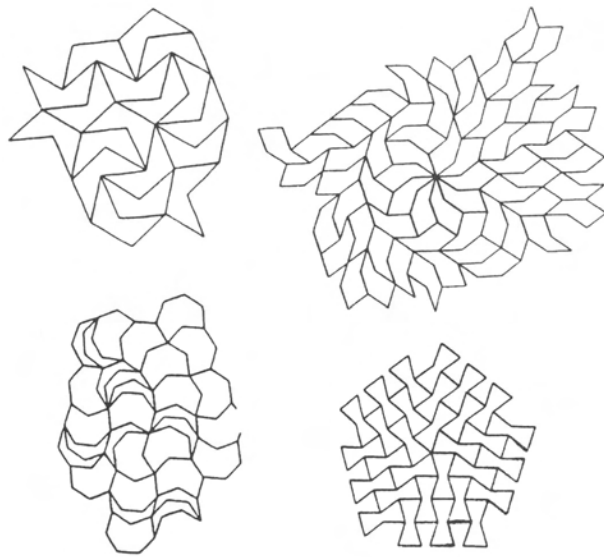


Figure 2.30: Tessellation with Non-convex polygons. Image from (Lalvani 1991).

2.2.3 The polyhedra

Polyhedral forms are bodies in three-dimensional space. They can be used as modules that fit edge-to-edge to produce a large variety of surface structures. When the sum of angles at every vertex is equal to 360° , the surfaces are flat and are known as plane tessellations. When this sum is less than 360° , the surfaces have a positive curvature at every vertex and enclose a space or volume. Such surfaces are polyhedra (having many faces), though strictly speaking these are convex polyhedra. Non-convex polyhedra have a sum greater than 360° leading to negative curvature. Convex polyhedra are composed of V vertices, E edges and F faces related by Euler's equation $V + F = E + 2$.

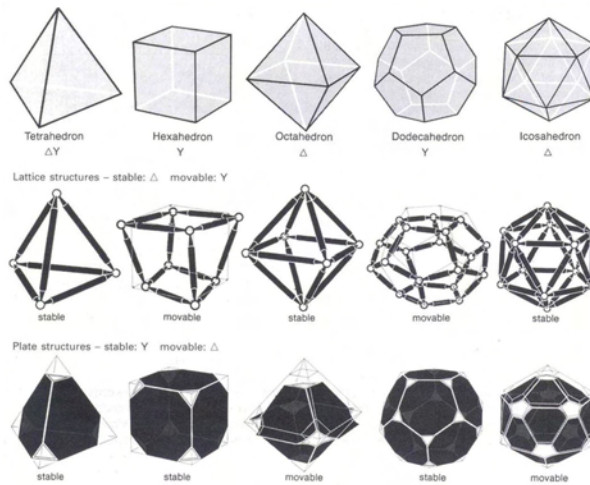


Figure 2.31: Platonic polyhedra as bar and node or pure plate structures. Image from (Chilton 2000).

Mathematicians in ancient times, before the Greek civilization, have studied and ascribed special properties to them. Crithclow (Crithclow 1980) has pointed out that Platonic solids were known to the Neolithic culture of northern Britain over a thousand years before Plato (427-347 BC). Plato was apparently the first person to attempt a geometrical description of structure in nature. He also explored the possibility of developing an inventory of basic shapes which could be recombined to form the five regular polyhedra.

The most basic of these forms are termed the Regular or Platonic polyhedra and consist of the tetrahedron, hexahedron (cube), octahedron, dodecahedron and icosahedron. Each of these is composed of similar or regular polygons. In other words; the sides of each face are the same length and each polyhedron has faces of only one polygonal shape. By space grids the lattice structures with bars and nodes are important. However, to understand stability of three dimensional structures in general, it is advantageous to study the behaviour of simple, regular, polyhedral shapes.

Most double layer space truss geometries are based on stable polyhedral forms. When the same polyhedra will be formed with flat plane surfaces the tetrahedron, cube and dodecahedron found to be stable. Research has been carried out by Ture Wester at the Royal Academy of Fine Arts, in Copenhagen, into stability and structural duality of polyhedra where bars and nodes were connected with plates (see Figure 2.31).

Semi-regular Polyhedra There are 13 semi-regular polyhedra, termed "Archimedean" solids, which use more than one type of regular polygon and which also meet alike at every vertex (see Figure 2.33). 11 Out of the 13 Archimedean solids are formed by a process called truncation. Truncation is the process of removing all the corners of a polyhedron in a symmetrical fashion. The remaining two Archimedean solids are formed by snubbing the cube and dodecahedron. Snubbing is an interesting process which, roughly speaking, amounts to loosening all faces of a polyhedron and rotating them all slightly in the same direction (clockwise or counterclockwise), creating 2 triangles for each edge and one m-sided polygon for each vertex of degree m. A polyhedron and its dual have the same snub(s)! If a polyhedron has k edges, its snub has 5k edges, 2k vertices and 3k+2 faces. Note that that neither the pentagon nor decagon appears in the plane tessellations and that the dodecagon, which appears in the plane tessellations, does not appear in any of these polyhedra.

Both Platonic and Archimedean polyhedra have only one vertex-type. Less regular polyhedra have several vertex-types and can be derived from these by subdividing their faces, by projections from higher dimensions, or by other methods.

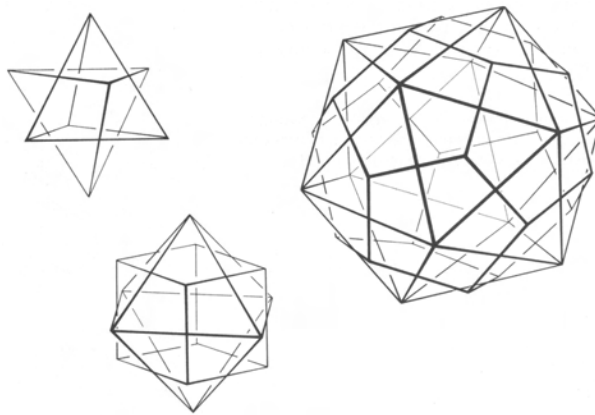


Figure 2.32: Dual regular polyhedra. Image from (Pearce 1978).

Stability To form a stable pin-jointed truss structure composed of nodes interconnected by axially loaded bars only, a fully triangulated structure must be formed. In a three-dimensional pin-jointed space frame, it is a necessary condition for stability. Maxwell's Equation or Föppl's Principle:

$$n = 3j - 6$$

n = number of bars in the structure.

j = number of joints in the structure

6 = the minimum number of support reactions.

In almost all cases space frames are based on Platonic polyhedra or Archimedean polyhedra or plate structures. See Figure 2.31. Not fully triangulated structures can be made stable if suitable and sufficient additional external supports are provided.

Polyhedra and their duals The dual polyhedron is formed in a manner analogous to that described for the plane tessellation. However, for polyhedra the reciprocation process is somewhat more complicated: the point perpendicularly above the center of each face of a given polyhedra

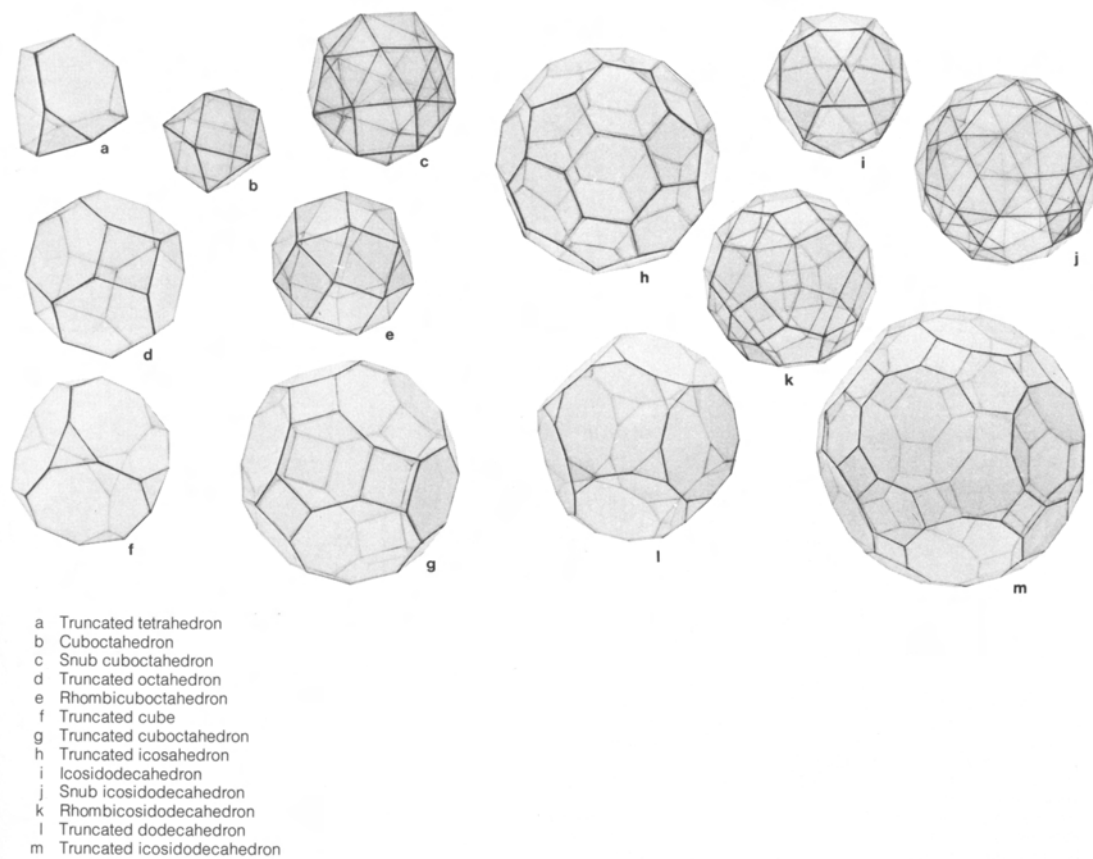


Figure 2.33: The 13 Archimedean polyhedra. Image from (Pearce 1978).

is joined with new edges similar points above all neighboring faces such that the new edges that connect these points intersect the edges of the original polyhedron, forming the edges of a new dual polyhedron. It is usually true that the respective edges of dual polyhedra perpendicularly bisect each other. Both will have the same number of edges and the inventories of faces and vertices will be exactly reversed. There is only one polyhedron self-dual: the tetrahedron.

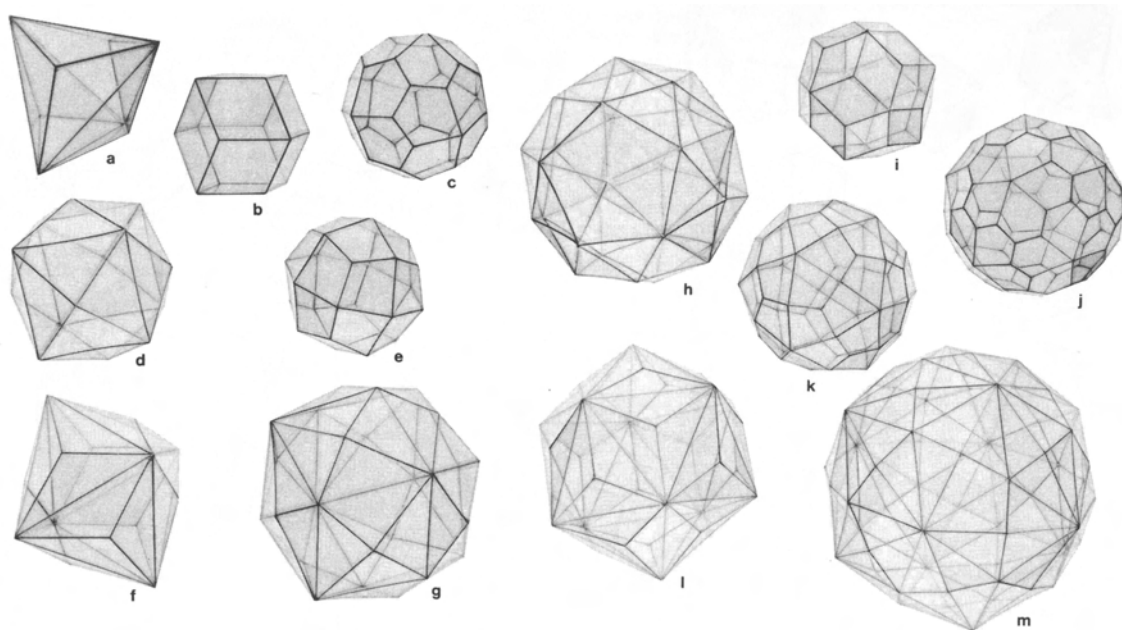


Figure	Dual of
a	Truncated tetrahedron
b	Cuboctahedron
c	Snub cuboctahedron
d	Truncated octahedron
e	Rhombicuboctahedron
f	Truncated cube
g	Truncated cuboctahedron
h	Truncated icosahedron
i	Icosidodecahedron
j	Snub icosidodecahedron
k	Rhombicosidodecahedron
l	Truncated dodecahedron
m	Truncated icosidodecahedron

Figure 2.34: The duals of the 13 Archimedean polyhedra. Image from (Pearce 1978).

Prisms and pyramids In addition to the Archimedean figures there are two infinite groups consisting of prisms and anti-prisms which correspond to the infinite number of possible polygons. A semi-regular prism is made up of two parallel regular polygons of any number of sides, connected in equatorial fashion by square faces. The anti-prisms are like prisms except that the equatorial polygons are equilateral triangles. The cube and the octahedron fall into both categories. The duals of prisms are called di-pyramids (double pyramids), whose faces are congruent isosceles triangles. The duals of the anti-prisms are called trapezohedra.

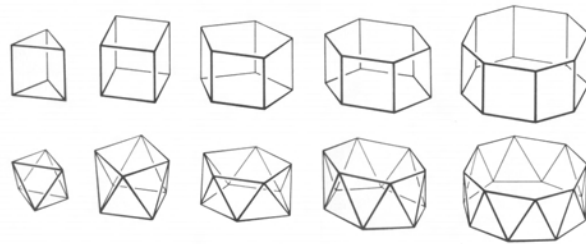


Figure 2.35: Semi-regular prisms (top) and semi-regular anti-prisms. Image from (Pearce 1978).

Convex polyhedra composed of regular polygons Triangulated polyhedra noted special interest because of their effectiveness as physical structures. In addition to the five Platonic polyhedra, there are five others all bounded by equilateral triangles, although it is only in the Platonic figures that all vertices are equidistant from a center.

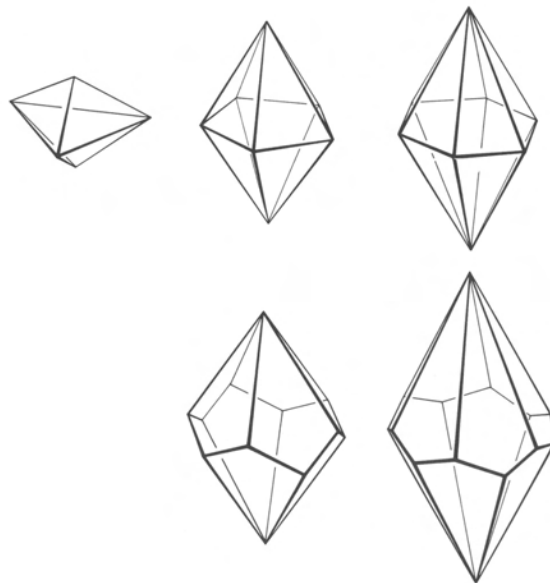


Figure 2.36: Dipyramids (top), the duals of prisms (top) Trapezohedra (down), the duals of antiprisms. Image from (Pearce 1978).

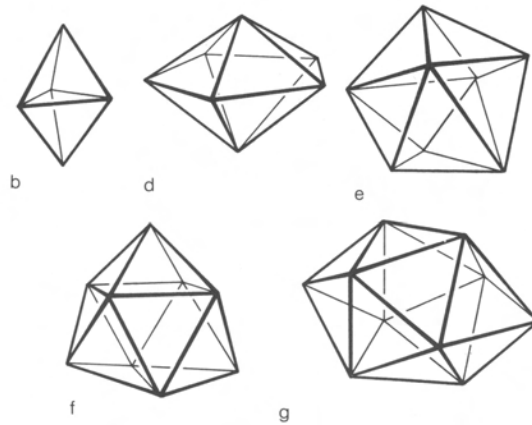


Figure 2.37: The convex deltahedra. b: Triangular dipyramid. d: Pentagonal dipyramid. e: 12-hedron. f: 14-hedron. g: 16-hedron. Image from (Pearce 1978).

Families in Polyhedra There are four families of polyhedra; the first is an infinite of prisms with general symmetry. The remaining three families correspond to the three regular polyhedra and are the tetrahedral, octahedral and icosahedral families. Each family has polyhedra with mirror-symmetry and rotational symmetry, and regular and semi-regular polyhedra belong to these four families.

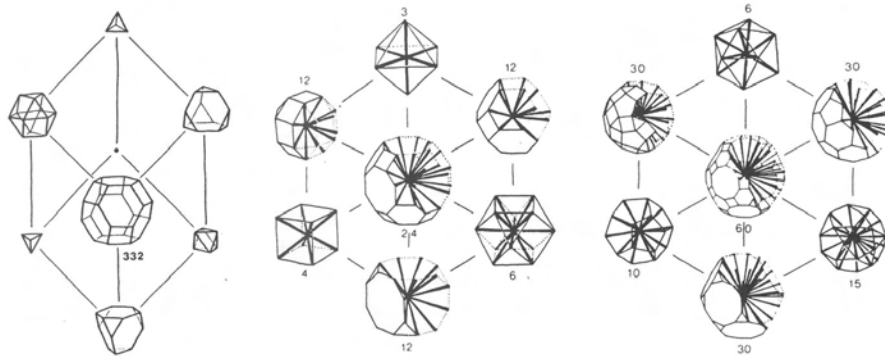


Figure 2.38: Three families of polyhedra: tetrahedral, octahedral and icosahedral, the last two families are here turned into n-stars. Image from (Lalvani 1991).

In the field of polyhedra a lot of research has been done which goes far beyond the goal of this reader; for instance curved polyhedra, saddle polyhedra, Kepler-Poinset solids etc.

Simple polyhedra could be combined together in a system to produce a higher-dimensional table: a space frame.

Zonohedra and Rhombohedra Zonohedra are polyhedra with parallelogram faces and are a natural extension of the zonogons described before. A three-dimensional zonotope is called a zonohedron. The method of derivation is the same, the one difference being that the n -star is spatial and can be derived from vertex directions to the center of any symmetric or arbitrary polyhedron. The number of vectors, n , is determined by the number of non-collinear vertices. Zonohedra provide alternative geometries for space structures that define architectural space. The octahedral and icosahedral families (see polyhedra section) each produce seven distinct stars with the following values of n : 3, 4, 6, 12, 12, 12, 24 and 6, 10, 15, 16, 30, 30, 30, 60.

Consider any star of n line segments through one point in space such that no three lines are coplanar. Then there exists a polyhedron, known as a zonohedron, whose faces consist of $n*(n-1)$ rhombii and whose edges are parallel to the n given lines in sets of $2 * (n - 1) * [i]$ Furthermore, for every pair of the n lines, there is a pair of opposite faces whose sides lie in those directions (Coxeter & R.W.W.Ball 1947). A zonohedron is therefore a polyhedron in which every face is centrally symmetric (Eppstein 1996).

From the n -stars, zonohedra can be derived from all distinct i -stars ($i \leq n$) which determine their edge directions. They are the shells of i -cubes (or i -cells), and all its faces are rhombii ($i=2$). All zonohedra can be decomposed into 3-dimensional building blocks or 3-cells, termed rhombohedra ($i=3$), which are regular cubes in higher dimensions. Rhombohedra and zonohedra are cells or space fillings. Polyhedra from different symmetry classes generate their own set of rhombohedra.

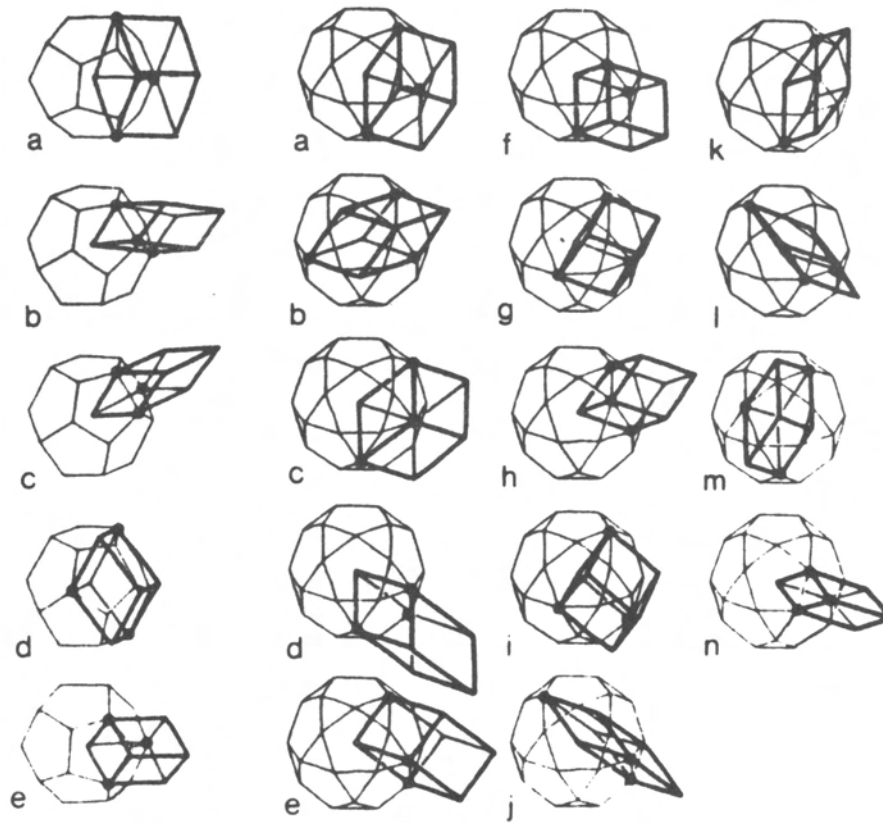


Figure 2.39: The dodecahedron has 5 rhombohedra from two types of rhombii, $70^{\circ}32'$ and $41^{\circ}49'$, and the icosidodecahedron has fourteen types of rhombohedral cells from four types of rhombii 90° , 72° , 60° , 36° . Image from (Lalvani 1991).

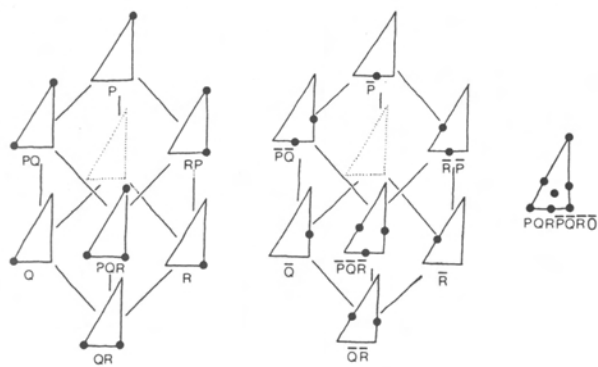


Figure 2.40: Vertex placements. Image from (Lalvani 1991).

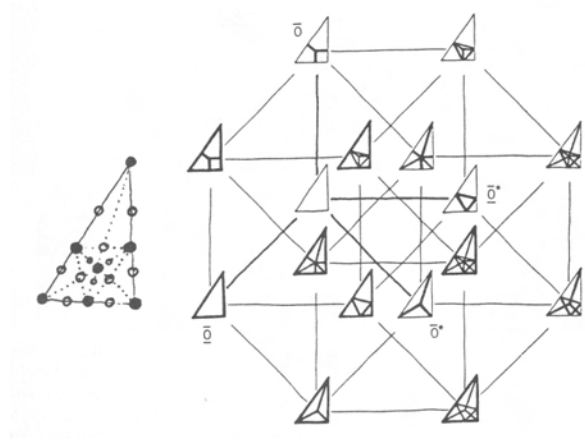


Figure 2.41: Edge combinations. Image from (Lalvani 1991).

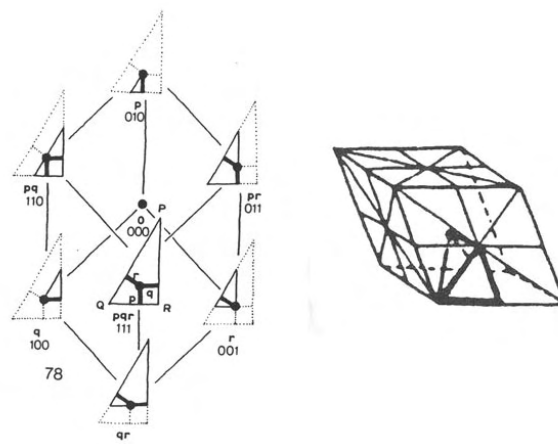


Figure 2.42: The fundamental regions of a single rhombohedron, a cube in higher space, are shared. Image from (Lalvani 1991).

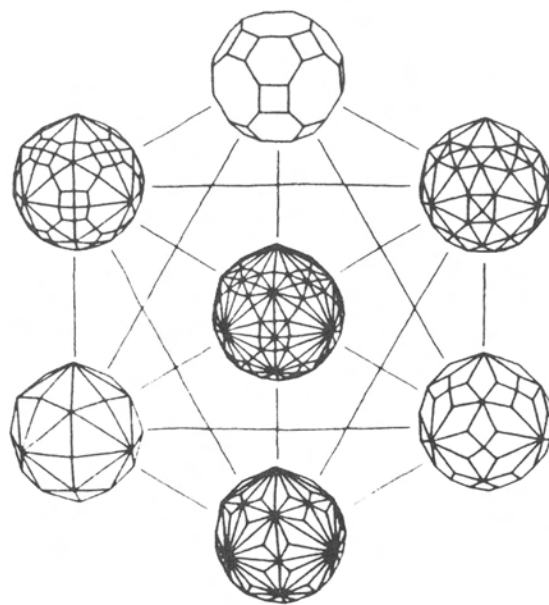


Figure 2.43: Seven polyhedra of octahedral symmetry corresponding to one cube. Image from (Lalvani 1991).

2.2.3.1 Generation of Polyhedra

The method of subdividing polygons can be applied to the faces of polyhedra to generate new polyhedra. Just like polygons were added to other polygons, polyhedra can be added to other polyhedra to generate new polyhedra. There are two possible methods; vertex combinations and edge combinations.

2.2.3.2 Divisions of spherical surfaces

Besides the Recursive Surface Subdivisions there are other divisions possible. When the demand is made that the space frames must consist of (stable) triangles only three polyhedra will do: tetrahedron(4), octahedron(8), icosahedron(20). Other polyhedra must be subdivided in triangles, where every summit of the triangles must lay on the defined sphere, before they can be used.

Class I The Platonic polyhedra are subdivided in smaller triangles.

1. Tetrahedron
2. Octahedron (useful horizontal and vertical connections)
3. Icosahedron (easy to split in two parts with even division frequencies)

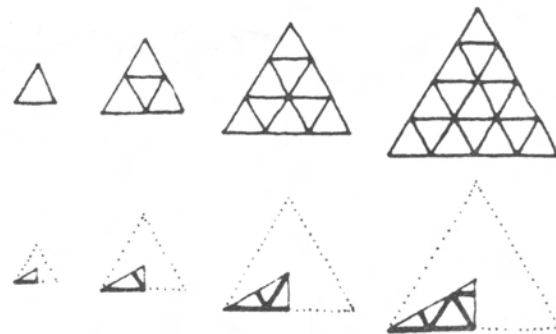


Figure 2.44: Triangles of frequencies 1 to 4 (top) and minimal triangles. Image from (Lalvani 1991).

Regularity of division As can be seen in Figure 2.46 a subdivision there is needed for the curved polyhedron-edges. Mostly one of the two following methods is used: (also see Figure 2.47)

- Method I. Equal pieces on a straight line. Projected on the sphere. The subdivision in triangles can be found by connecting the points on the edges of the polyhedra triangle.
- Method II. Equal sizes on a curved line, the centers of the small triangles are used to create further subdivision

Both methods use geodesic lines, which is the shortest distance between two points on a curved surface.

Recursive Surface Subdivisions

Polygons and polyhedral faces can be subdivided again and again to produce infinite classes of finer subdivisions of a surface. For structures of a fixed size, this produces finer meshes and on

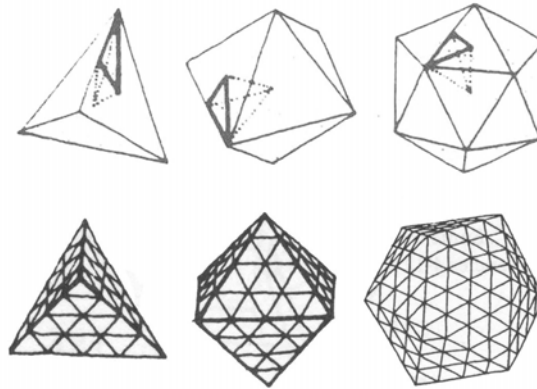


Figure 2.45: Division of spherical surfaces Class I Method I. Image from (Lalvani 1991).

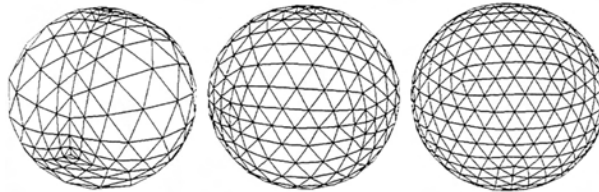


Figure 2.46: The tetrahedron, octahedron and icosahedron can be converted into a sphere by using the minimal triangle. Image from (Knebel & et al. 2002) (Huybers & Ende 1994).

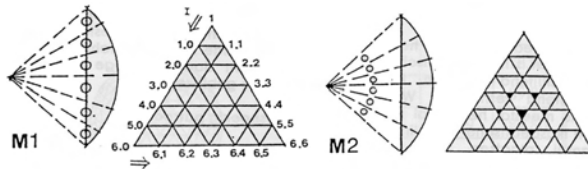


Figure 2.47: Two methods for the subdivision of polyhedron-edges and surfaces. Image from (Huybers & Ende 1994).

the other hand, for elements of a fixed size, larger and larger structures can be produced. The geodesic dome of Fuller is an example, and is based on special subdivisions of the triangular faces of a tetrahedron, octahedron or the icosahedron. These subdivisions are described in terms of frequency, the number of times the edge of the polygon, and hence a polyhedron, is subdivided. When the vertices are found by subdivision, a pattern can be made with connection-lines. Also here there are two possibilities.

- Triangular pattern; many different triangles needed
- Hexagons and pentagons, 12 in a whole closed sphere, combination of the triangles

The Fuller Dome

The basis of the Fuller dome is either the Icosahedron or the Dodecahedron. The two polyhedra

have to be placed as "duals" with respect to the centre of the sphere. The corners of the vertices of the icosahedron in the resulting network can be recognized by their pentagonal symmetry and they correspond with the midpoints of the dodecahedron's faces. The so-called "characteristic" triangle is defined by the icosahedron point I2, the dodecahedron point D1 and the icosahedron's edge midpoint DI-1' projected on the surface of the sphere (see Figure 2.48). This triangular surface is the smallest symmetry part of the whole spherical network. It is also called after Fuller as the "lowest-common-denominator-" or LCD-triangle.

It is possible to subdivide the spherical surface in 120 minimal symmetry parts. The actual specifications of geometric and connectivity properties of the whole network can be reduced to this minimal triangle.

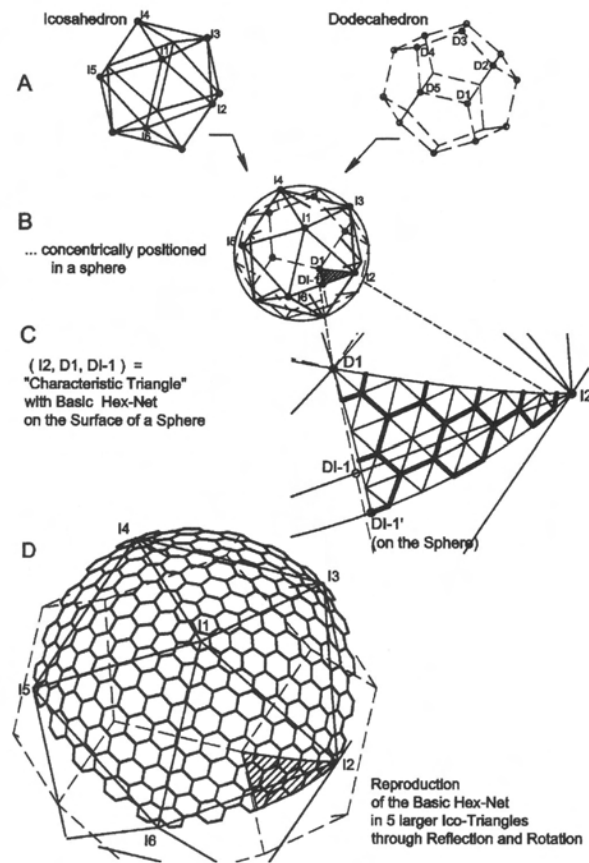


Figure 2.48: Generation of the Fullerdome. Image from (Knebel & et al. 2002).

In nature many domes can be found. The most expressive is the Bucky ball also called after Buckminster Fuller: "Fullerenes". These Fullerenes are large carbon-cage molecules. By far the most common one is C_{60} in morphology called the truncated icosahedron.

Fullerenes cages are about 7-15 angstroms in diameter, which is around a billionth of a meter, or 6-10 times the diameter of a typical atom. On molecule level they are used to create nanotubes.

Another remarkable comparison can be made with the Volvox: a freshwater colonial protozoan. Volvox are spherically organized colony of several hundreds to several thousands smaller elements.

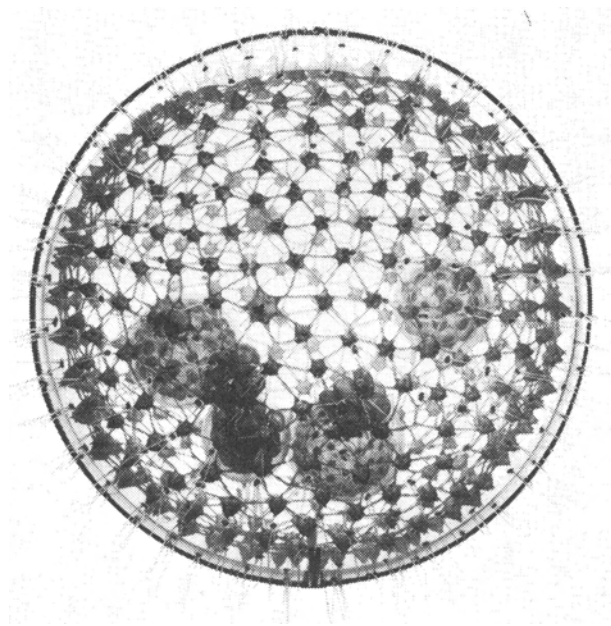


Figure 2.49: Volvox. Image from (Pearce 1978).

Class II An equilateral triangle can be subdivided in 6 by perpendicular lines. The icosahedron can be divided in 120 equal parts. Rhomboids are formed by connecting these right-angled triangles. Subdividing these many different divisions can be made.

1. Cubic (regular rhombic)
2. Rhombic dodecahedron
3. Rhombic triacontahedron

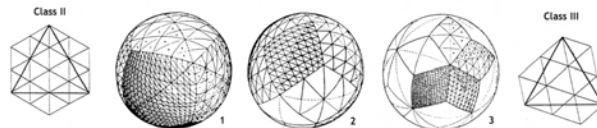


Figure 2.50: Class II and III and their subdivisions. Image from (Huybers & Ende 1994).

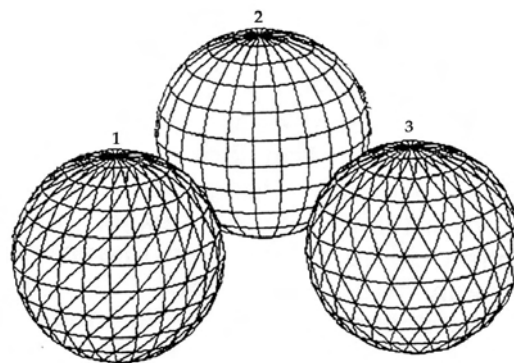


Figure 2.51: Other basis divisions of spheres. Image from (Huybers & Ende 1994).

Class III A division called 'skew networks', based on twisted snub solids (see Figure 2.50).

Class IV (see Figure 2.51)

1. Meridians and parallelcircles ('orange peel')
2. Schwedler
3. Lattice dome

2.2.3.3 Space Fillings

Space filling means the combining of similar or complementary bodies in a three-dimensional packing continuously repeated, in such a way that there is no unoccupied space. Space fillings are space structures composed of 3-dimensional modules that fit face-to-face to fill space. They are similar to plane tessellations where polygons fit to fill a plane. Rhombohedra, prisms and various other polyhedra are units of corresponding space-fillings. Same as in the 2-dimensional case there are three different types of fillings; periodic, central and non-periodic. Applications in architecture include the use of multi-layered or multi-directional geometries for space frames, or 3-dimensional habitats to live in.

Close packings of polyhedra form space-fillings, their edges define space grids. These space grids form the basis of architectural space frames. In fact they are the skeleton of the space structures.

Dihedral Angle The dihedral angle is the angle formed between the planes of two adjacent polygons, the angles taken in a plane perpendicular to the common edge. All of the dihedral angles for each of the regular polyhedra are equal. However, of the semi-regular polyhedra, only the cuboctahedron and the icosidodecahedron have equal dihedral angles. There are nine Archimedean figures with two dihedral angles and two which have three. The dihedral angle will become quite important as the problem of space fillings is considered (Cundy & A.P.Rollett 1961).

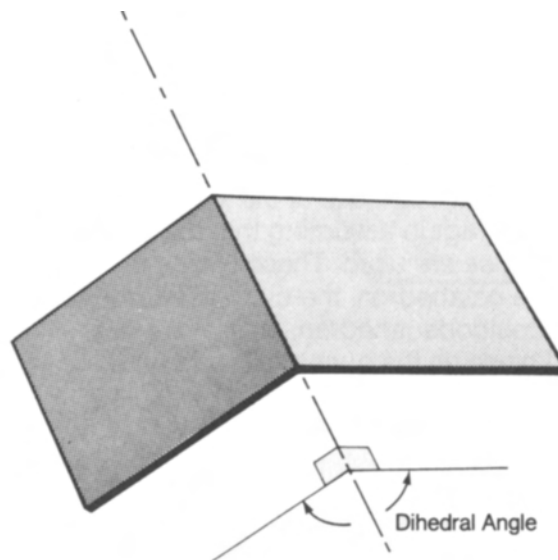


Figure 2.52: Dihedral Angle. Image from (Pearce 1978).

Periodic Space Fillings The cube is the only Platonic polyhedron that will repeat to fill all space. It is the most symmetrical variation on the infinite class of three-dimensional figures known as parallelepipeds. The parallelepipeds are prisms whose bases and sides are parallelograms; they are, therefore, six faced polyhedra. The subdivision of space by means of congruent parallelepipeds may be characterized in terms of six symmetry classes or systems. These classes form six of the seven crystal systems of crystallography. The seven crystal classes rely upon various combinations of 2-fold, 3-fold, 4-fold and 6-fold or no rotational symmetry.

Together they provide a descriptive scheme of space partitioning.

As already said the cube is the most symmetrical, it has the greatest number of symmetry axis. A cube has three axes of 4-fold symmetry, four axes of 3-fold symmetry and six axes of 2-fold symmetry. Ranking by the total number of symmetry axes of each class: (see Figure 2.53

1. Cubic - 13 axes (a)
2. Hexagonal - 7 axes (g)
3. Tetragonal - 5 axes (b)
4. Orthorombic - 3 axes (c)
5. Trigonal - 1 axis (d)
6. Monoclinic - 1 axis (e)
7. Triclinic - no symmetry axis (f)

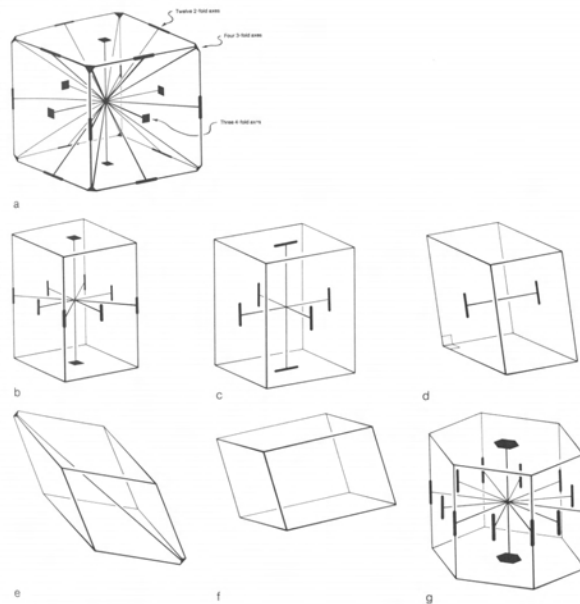


Figure 2.53: The seven symmetry classes. Image from (Pearce 1978).

Bravais lattices In 1848 Bravais (Auguste Bravais, 1811-1863) showed that there was a maximum of fourteen space lattices or points of groups differing by symmetry and geometry whose translational repetition in space maintained the symmetrical arrangements of points of a unit cell. Bravais perceived that these fourteen space lattices corresponded to the seven crystal symmetry classes. In crystallography, a unit cell is well defined as the basic repeating unit or module that by simple translation will define the infinite structure.

For four of the seven primitive lattices, we can add additional points to face centers and cell body centers so that more lattices can be formed in which all the points are symmetrically equivalent (see Figure 2.54) (2006).

- Cubic (3 lattices)
- Tetragonal (2 lattices)
- Orthorhombic (4 lattices)
- Hexagonal (1 lattice)
- Trigonal (1 lattice)
- Monoclinic (2 lattices)
- Triclinic (1 lattice)

Federov (1880) and Schoenflies (1891) determined independently that the 14 Bravais lattices maximally generate 230 space groups. For complete descriptions see Chalmers (Chalmers, Holland, Jackson & Williams 1965).

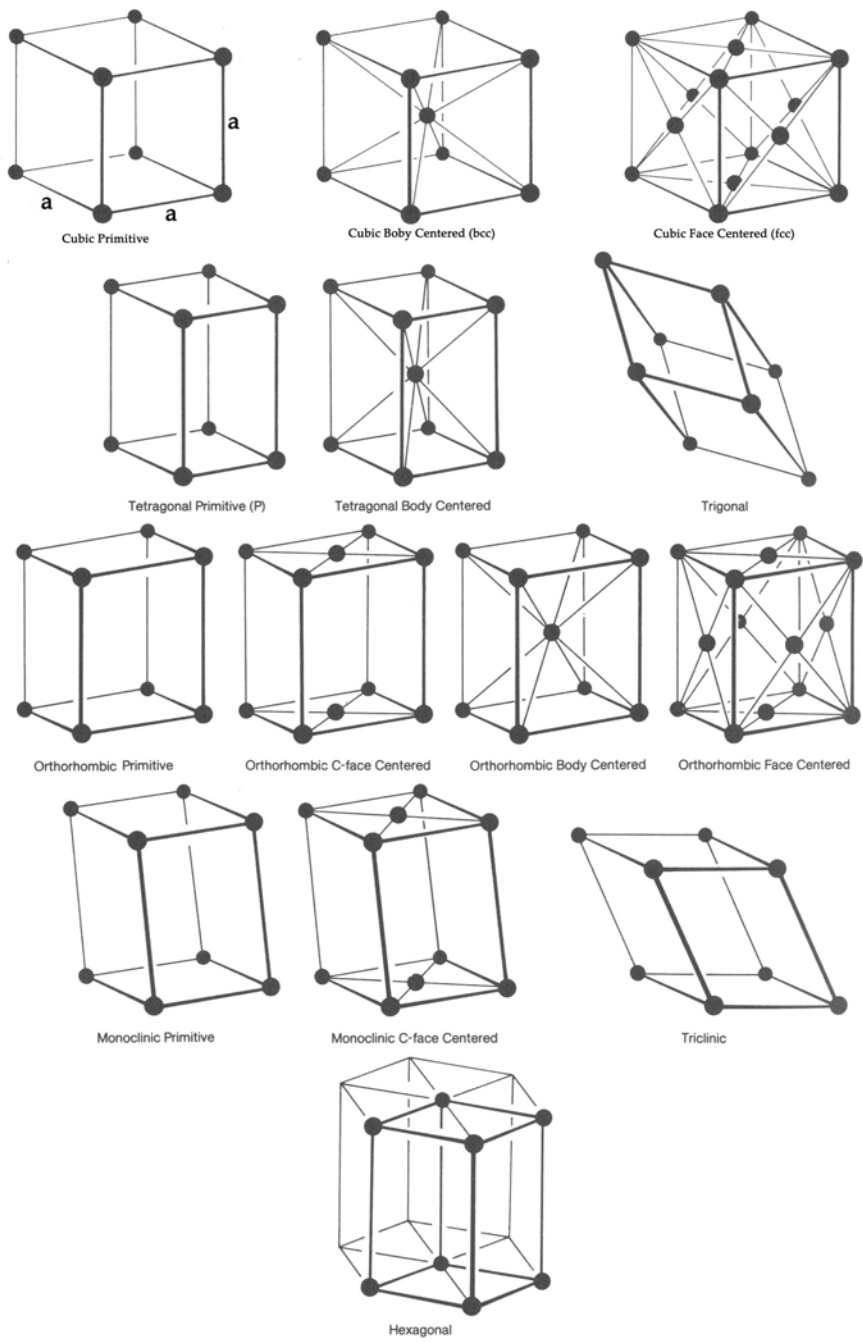


Figure 2.54: Bravais lattices. Image from (Pearce 1978).

Space Filling Polyhedra Among the Archimedean polyhedra and in the infinite family of prisms and anti-prisms there are exactly three space fillers: the truncated octahedron, the hexagonal prism and the triangular prism. Of the thirteen Archimedean duals, only the rhombic dodecahedron will fill all space. Both the rhombic dodecahedron and truncated octahedron have full cubic symmetry. Symmetry is not the only factor that allows us to discover candidates for space filling. Another factor is the complementary of adjacent dihedral angles. In a space filling array of polyhedra the dihedral angles formed by faces meeting around a common edge must sum to 360° . This is equivalent to the requirement of 360° around each vertex of plane tessellation.

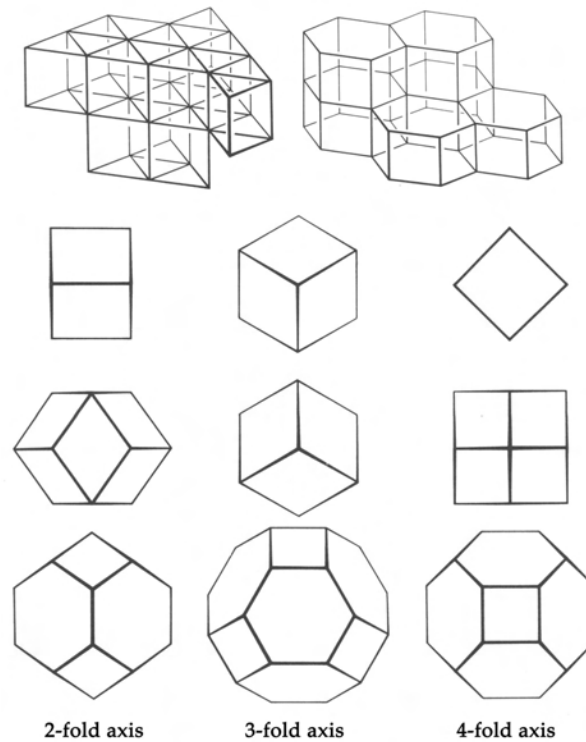


Figure 2.55: Space fillings: Triangular prisms, hexagonal prisms, cube, rhombic dodecahedron and the truncated octahedron. Image from (Pearce 1978).

The tetrahedron and octahedron space filling Because the octahedron is the dual of the cube, it has the same symmetry. However, it will not space. Although the symmetry is there, its dihedral angle of $109^\circ 28'$ makes it impossible for the octahedron to pack with itself to occupy all of space. In combination with the tetrahedron it forms a fully triangulated network, which in turn describes a space filling array of these polyhedra. In fact it is a face centered cubic (Bravais). Octahedra and tetrahedra will space when packed 1:2. See figure. The result is a space filling parallelepiped with six rhombic faces with angles of 120° and 60° . The dihedral angle of the tetrahedron is $70^\circ 32'$, which is compatible with the $109^\circ 28'$ dihedral angle of the octahedron. The tetrahedron is less symmetrical than the octahedron (or cube). It has four axes of 3-fold symmetry and three axes of 2-fold symmetry.

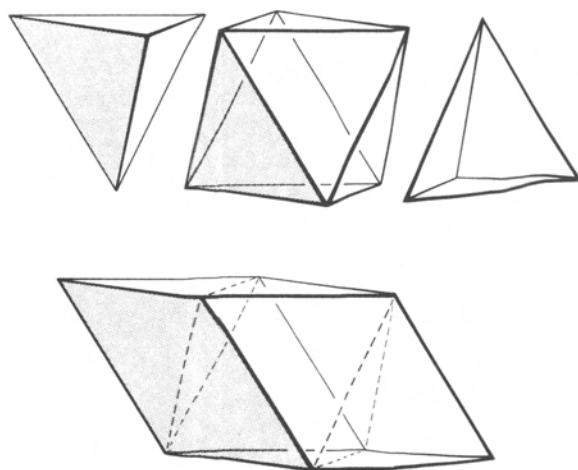


Figure 2.56: Tetrahedron-Octahedron space filling. Image from (Pearce 1978).

The icosahedron and dodecahedron space filling The icosahedron and the dodecahedron are dual to each other so they have the same symmetry. The icosahedron is the most symmetrical of all possible polyhedra. It has six 5-fold axes, ten 3-fold axes and fifteen 2-fold axes. The icosahedron has twenty equilateral triangular faces. There is no convex polyhedron with more than 20 identical regular faces. But both will not fill space. The dihedral angles of the dodecahedron are $116^{\circ}34'$ which can not fill a space.

Regular and semi-regular Polyhedra as multiple space fillers Of the Archimedean and Platonic figures there are altogether nine polyhedra that qualify as candidates for multiple space filling systems. In a larger class of semi-regular polyhedra, which includes prisms as well as the Archimedean figures, a look at the semi-regular plane tessellations reveals which of the prisms will qualify for multiple space filling. Triangles, squares, hexagons, octagons and dodecagons are the polygons that can be combined in various arrangements to form a plane tessellation. This forms the basis for the prisms with square sides. There are eight multiple-prism (from the semi-regular tessellations) space filling systems.

The multiple space fillings can be classified according to how many different types of polyhedra the system requires. A space filling consisting of one type of polyhedron is called a unary, two - binary, three - ternary, four - quaternary. Systems with more than four types of polyhedra can not be composed.

The first requirement of multiple space filling is that different polyhedra must have matching parallel faces in common. Of the Platonic and Archimedean figures there are nine polyhedra that qualify as candidates for multiple space filling systems. There are eleven space filling possibilities utilizing these Archimedean and Platonic polyhedra.

Dual Space Filling Following from the definition; if all vertices in a space filling array are congruent, the dual network will form a unary space filling system composed of a single kind of polyhedron. If there is more than one kind of vertex in a space filling structure, its dual space filling will be composed of as much different kinds of polyhedra as there are kinds of vertices. The 23 space filling systems consisting of regular and semi-regular polyhedra give 20 unary space fillings, while three systems have dual space filling systems which are also comprised of regular and semi-regular polyhedra. In total 20 new polyhedra are formed with the dual space filling

systems.

Central Space-Fillings Central Space-Fillings have one clear center. However central space-fillings which use single rhombohedra give nice forms it is doubtful if they are interesting for (kinetic) space frames.

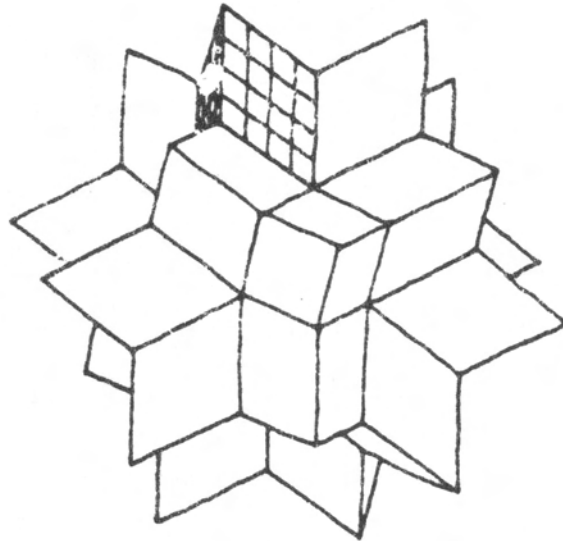


Figure 2.57: Central space filling with a single rhombohedron, hexacontrahedral star ($n=6$) with icosahedral symmetry. Image from (Lalvani 1991).

Non Periodic Space-Fillings These fillings work with the non-periodic tessellations and consist of rhombohedra, zonohedra (and affine polyhedra). It results, just like the tessellations, in rather difficult fillings. A simple example is given in Figure 2.58.

Stellated polyhedra There is a very large class of nonconvex uniform polyhedra. They are loosely referred to as Stellated polyhedra (H.S.M.Coxeter, Longuet-Higgins & Miller 1954).

Loose-Packings Loose packings are a class of orderly structures which cover all space but leave empty spaces in-between. An easy way is to remove cells from the closest packings leaving holes in various places. The space becomes a sponge. Another way to create a loose-packing is with the polyhedra placement method.

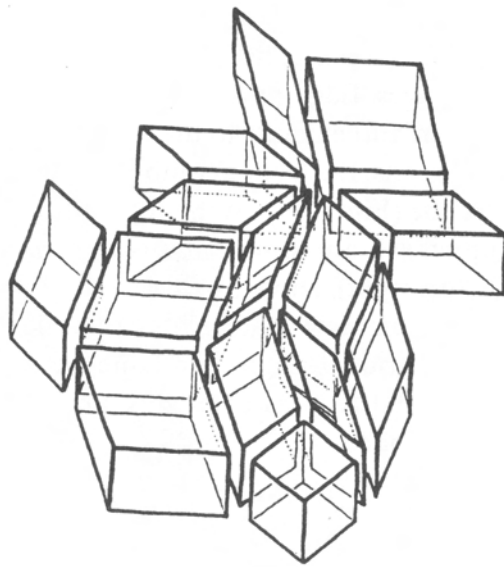


Figure 2.58: Non periodic space fillings. Image from (Lalvani 1991).

2.3 Analogies between structural engineering, physical models and natural structures

It is useful to discuss analogies in general before covering techniques, such as physical modelling and learning from nature. Analogies are traditionally used in arguments; explaining a specific case by drawing attention to the similarities with another, mostly better understandable example.

Every analogy between two dissimilar cases have something similar. The more similarities two cases have, the stronger the analogy is. Some people will focus on the dissimilar parts, while others focus more on the similar parts. Both ways of dealing with analogies are needed to make use of an analogy in a proper way. Find inspiration and stimulation in the parts in which the two cases overlap, but keep in mind that it is an analogy, and in that way it is not possible to treat the cases like they are similar. One has to distinguish the similarities and the dissimilarities.

For example; a tree is a beautiful natural structure and in some aspects it can be an useful inspiration source for man-made structures. The fact that a tree divides the available 'building material' as optimal as possible over its structure, is an useful principle. On the other hand; saying that a tree-structure as a whole can function as a good example for a building structure, would be making a doubtful statement. The main function of a tree is collecting as much energy as possible. A tree with its branching branches is well adopted to fulfill this task, however which man-made structure has the same purpose? Instead of copying nature we have to focus on the principles which form the basis of natural structures.

The example of the tree demonstrates the fact that an analogy between two cases is never valid for 100%. Nevertheless it is interesting to look for analogies between physical models, structures in biology and structural engineering. The potential usefulness of such analogies lies in the way in which our awareness of remarkable and, to us, novel examples of structures in biology can stimulate our own design imaginations. In short, 'we are engaged in an exercise of "inter-disciplinary cross-fertilization of ideas", which seems one of the key characteristic for the design of special structures' (Calladine 1998).

2.4 Physical Modelling

Physical modelling techniques are manual techniques to model certain characteristics of structures. "Physical" refers to the distinction with "Virtual" or "Computational", which are techniques to model characteristics of structures in computer models and applications.

Model building is often viewed upon as "child's play" until the architect, engineer or students attempts to build his or her first models. Physical modelling is a technique is are easy accessible, but on the other hand different to execute and control properly. Deriving the correct conclusions from physical modelling is an art.

This section introduces several of the basic techniques for model building. The best way to learn how to make and control these techniques is to attempt building these models at home, based on earlier written down hints and tips, such as in the IL series (published by the Institut für Leichtbau Entwerfen und Konstruieren).

Model building One special technique is model building. With model building the builder studies the shapes, grids, etc. by making a physical model. An example of this are the folded paper models of Huybers (see Figures 2.59 and 2.60) and various other builders (see Figure 2.61).

These models can be used for study and formulas can be derived from these models (Huybers & Ende 1994) (Huybers 2000b). Finally entire structures can be studied with these techniques.

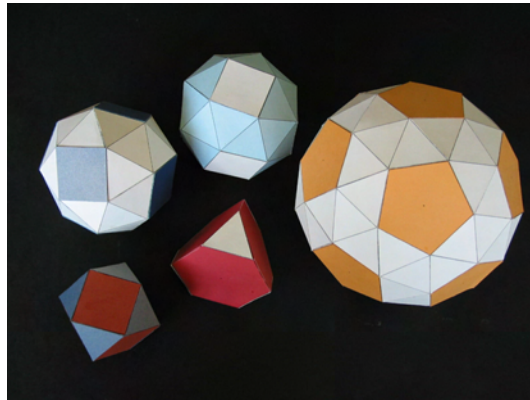


Figure 2.59: Models built by Pieter Huybers.

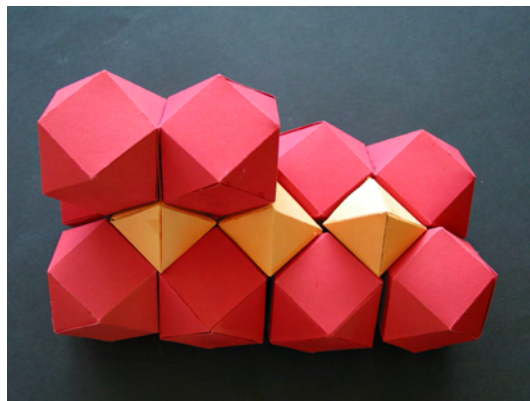


Figure 2.60: A study of stacking regular shapes. Models by Pieter Huybers.



Figure 2.61: Some shapes from the field of Structural Morphology.

There are many techniques, too many to discuss all and for each structural type or topology at least one or more techniques often exist. Before a structural engineer starts building a model, it is a good idea to first research existing techniques, since often model building can be quite complicated when inexperienced. Cattan(Cattan & Reissig 2000) provides an interesting classification model for built models for structural morphology.

Tekkit is an example of such a model building material, which can be seen in Figure 2.62, for building space trusses.

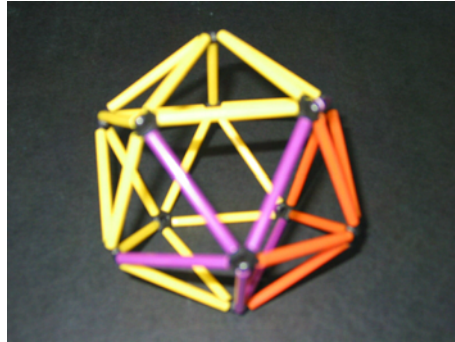


Figure 2.62: A model in Tekkit.

Another system, which can be seen in Figure 2.63, is the model building material of the Mero space trusses system.

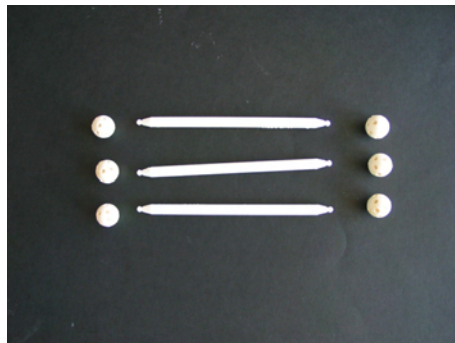


Figure 2.63: Mero model material.

2.4.1 Catenaries

The catenary form has been used by famous architects, such as Gaudí, to find the shape of their buildings. Because the catenary form follows the tension line for gravity, it is very suitable to design masonry structures when inverted. However, for these masonry structures the dead weight of the brick has to be dominant over other loads, such as the overturning moments and shear-forces of the wind, or unequal loading due to snow for instance. Usually this is the case for the buildings of architects like Gaudí. The catenary form can be easily derived from mechanics. Figure 2.64 shows the geometry of the catenary.

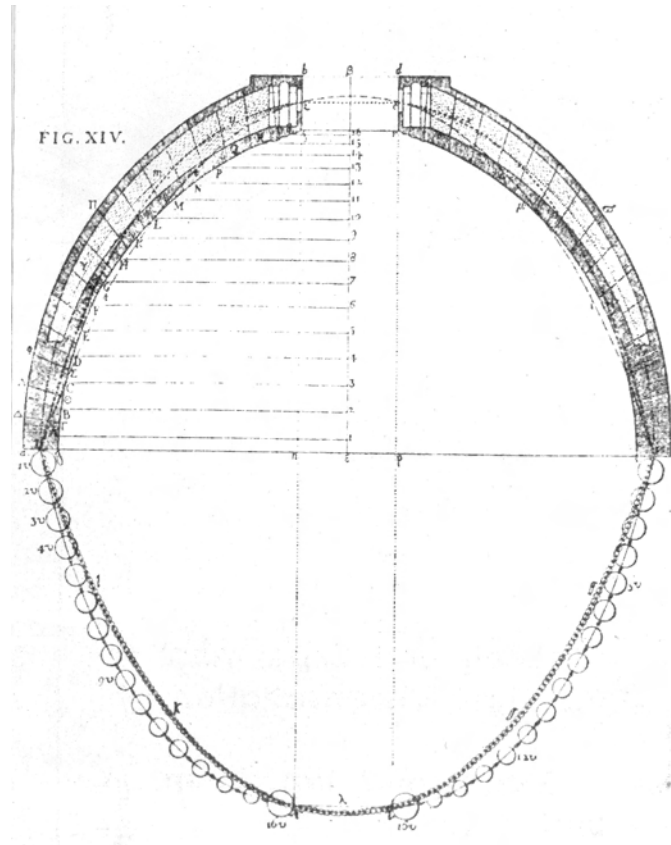


Figure 2.64: The earliest presentation of a tensile-stressed suspended model describing the load-bearing behaviour of a compressive stressed vaulting structure by Giovanni Poleni (1748), used to check the stability of the dome of St. Peter's in Rome. Image from (K. Bach 1988).

As a first step the hanging chain under a equally distributed load can be considered. The theoretical shape for a hanging chain under a distributed model is the parabola ().

$$q = -H \frac{d^2w}{dx^2} \quad (2.12)$$

Equation 2.12 shows the differential equation for a cable under an equally distributed load. When integrated twice, in Equations 2.13 and 2.14, the parabola follows as the shape for an equally distributed shape.

$$\frac{dw}{dx} = \frac{-q}{H}x + C_1 \quad (2.13)$$

$$w(x) = \frac{-2q}{H}x^2 + C_1x + C_2 \quad (2.14)$$

From $w(0) = 0$ and $w(L) = 0$ follows that:

$$\text{for } \begin{cases} w(0)=0 & : & C_2 = 0 \\ w(L)=0 & : & C_1 = \frac{2qL}{H} \end{cases} \quad (2.15)$$

$$w(x) = \frac{2q}{H}(Lx - x^2) \quad (2.16)$$

However, this model is too simple for the hanging chain hanging under its own weight. Since it cannot be assumed that the load is equally distributed, an alteration has to be made to the model. Equation 2.17 and 2.18 describe the new model.

$$q_x = q_0 \sqrt{1 + \left(\frac{dy}{dx}\right)^2} \quad (2.17)$$

$$\frac{dy}{dx} = \frac{V_x}{H} = \frac{\int p_x dx}{H} \quad (2.18)$$

These can be resolved to Equation 2.19 for the catenary in parametric form.

$$x(t) = ty(t) = a \cosh\left(\frac{t}{a}\right) \quad (2.19)$$

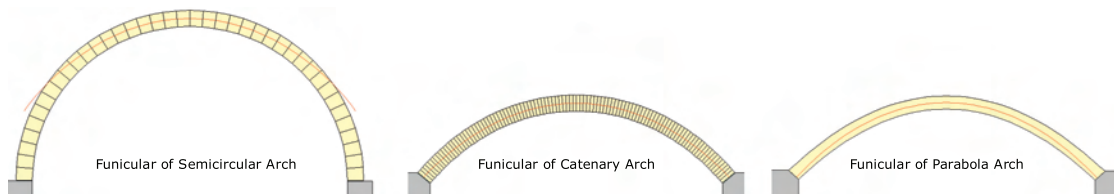


Figure 2.65: Funiculars of a semi-circular, a parabola and a catenary arch.

2.4.2 Hanging Models

As stated before Antonio Gaudí used the principle of hanging models intensively. When a hanging model is turned upside down a pure compression model arises. Figure 2.65 shows the funicular of a semi-circular, a parabola and a catenary arch. The catenary arch is the optimised structure for the self weight of the structure.

The parabola is the optimised shape for an equally distributed load. Figure 2.130 *a* shows a hanging model. As a result of its structural principle, the form of a suspended model is self-forming and is capable of transferring its own weight and area load distributed according to this, solely by means of tension. The grid shell (Figure 2.130*b*) is the inverse structure of the hanging model and is thus loaded by pure compression. Nevertheless, when unequally distributed loads occur in addition, as is the case with snow or wind loads, the initial coincidence between the structural task and the form is no longer given. The bending stresses and deformations which occur result in a form which is less favourable for the transmission of forces - in particular

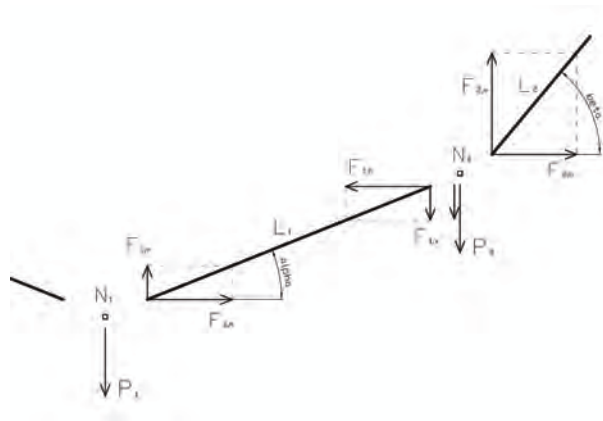


Figure 2.66: Model geometry used to model hanging lines.

with regard to snow loads in the softly curved apex area (Figure 2.130c). The form can be raised in its apex by adding small weights to the suspended model (Figure 2.130d). The deformation which occurs gives the shell a more suitable form for load transmission. The hanging model can also be adjusted for wind loads (K. Bach 1988).

Gaudí used hanging models to determine the configuration of his buildings. Brick experiments to determine a slender structure are time-consuming and difficult, where hanging models (catenaries) show many similarities to brick compression structures, except that where in catenaries tension is the most important force, compression is the most important for brick structures. Both structures also are less good for bending forces, however the dead weight of the masonry compensates the bending forces for most buildings because of their limited height and/or span. By adjustment and observation Gaudí could make various configurations.

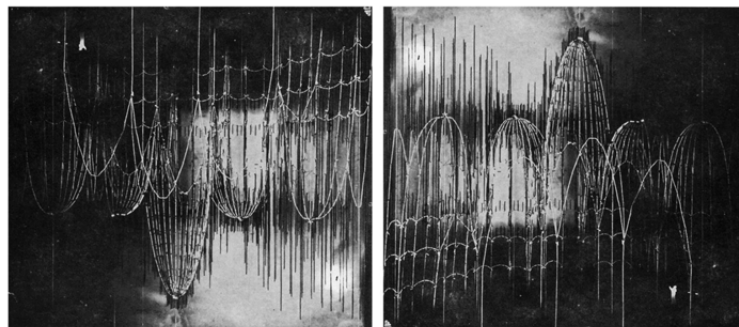


Figure 2.67: Two hanging models by Gaudí. Image from Williams.

Some models which have survived the ages can be seen in Figure 2.67, 2.68 and 2.69. Gaudí created the Sagrada Familia, the Guell crypt and several other buildings using these techniques.



Figure 2.68: Hanging model by Gaudí. Image from (i Armengol 2001).



Figure 2.69: Hanging models by Gaudí.

Hanging chain models Probably the most famous form finding techniques are the hanging chain and hanging net models, made famous by Antoni Gaudí. The hanging chain is a linear element which finds its equilibrium shape, the catenary line, caused by its own dead weight and gravity. There are many techniques for building these models. Many materials can be used for modeling: rope, small chains, large shackled chains, paperclips, etc. It is possible to hang weights, in the form of simple weights, small sand bags, etc. to simulate the loads on a structure. With pulleys it is possible to simulate loads in the other direction too. Photographing these models and inverting them shows the pressure line for the load, as shown in Figure 2.70 and 2.71. In Section 2.4.1 the mathematical formulation of catenaries is covered.



Figure 2.70: Hanging chain model.



Figure 2.71: Hanging chain model upside down to find the pressure shape.

Hanging net models Hanging net models are very similar to hanging chain models, except that they are three-dimensional nets built from individual linear chains instead of two-dimensional chains. Figure 2.72 shows a hanging net model built from paperclips.



Figure 2.72: A hanging paperclip model.

In IL10 (Bach 1974) basic characteristics for hanging nets are given:

- The nets are self-forming: they form themselves without external manipulation.
- The nets are unique: they form only one configuration.
- The nets form an equilibrium configuration.

IL10 (Bach 1974) also covers the building of hanging net models and their various purposes: architectonic, form finding models, test models for determining geometry and for determining forces. The book also covers good model photography and measuring the forces.

2.4.3 Soap Film Modeling

Soap films find the equilibrium shape of a minimal surface between preset (closed) boundaries. The soap film is often made from a special mixture which is stronger than normal dishwashing soap so that it lasts longer and forms easier. Pustafix is a good soap to use.

Many phenomena can be modeled with soap films. Two main directions can be derived: the use for membrane structures and shells, where usually only the minimal surface between set boundaries needs to be found and the use for pneumatic structure, where by applying an overpressure in the soapbubble an internal (pneumatic) load is created to drive the forming process. In this manner not only minimal surfaces can be found.

Note that soap film models are very good for studying shapes and finding minimal surfaces, but it is not possible (or hardly possible) to measure forces, stresses, shapes, etc. directly from the model. Of course, photographing and analysing solves some of those problems.

For more indepth theory on the subject of soap film modeling, refer to "Seifenblasen" (Bach, Burkhardt & Otto 1987) or "Tensile structures" (Otto 1973). These explain why soap bubbles always come together with three 'surfaces' in one 'node' in a two-dimensional plane and why the angle between it is always 120 degrees. Also more background theory is given about minimal surfaces and minimum energy shapes, which soap films are.

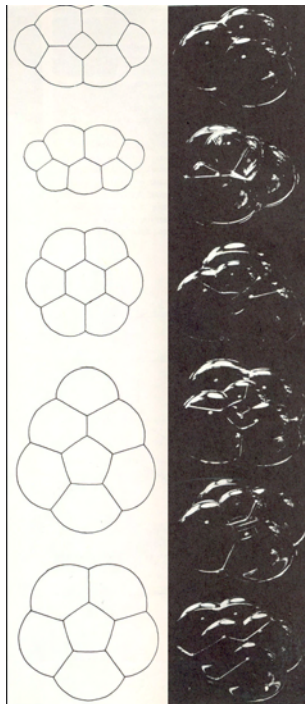


Figure 2.73: Soap bubbles. Image from (Otto 1973).

In Figure 2.74 and 2.75 two complex boundaries can be seen with their soap film minimal surface. The soap film forms the minimal surface between the wireframe.



Figure 2.74: Soap film model.

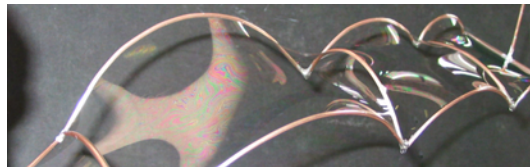


Figure 2.75: Soap film model.

In Figure 2.76 the analogy between a soap film hyper (hyperbolic paraboloid) and its structural counterpart is shown. The relationship of the shape is clear. The soap film finds the optimal (equilibrium) shape according to which the structure can be build.

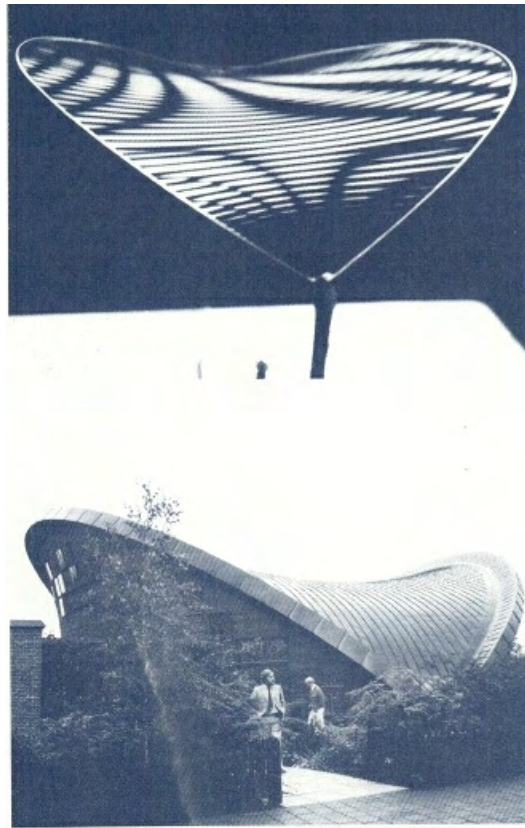


Figure 2.76: Soap film model. Image from (Bach et al. 1987).

For pneumatic structures the soap film is blown in a certain shape possibly with a closed preset boundary. The overpressure in the soap bubble again forms an equilibrium, but not necessarily a minimal surface. The possible shapes for pneumatic structures can be studied in this manner. In Figure 2.77 an example of this can be seen.

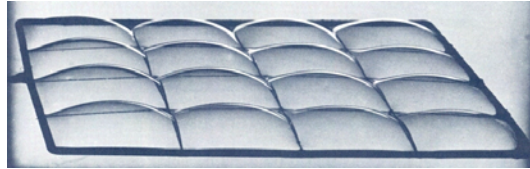


Figure 2.77: Soap film model. Image from (Bach et al. 1987).

In Figure 2.78 a soap bubble with increasing overpressure on the inside can be seen in its different stages.

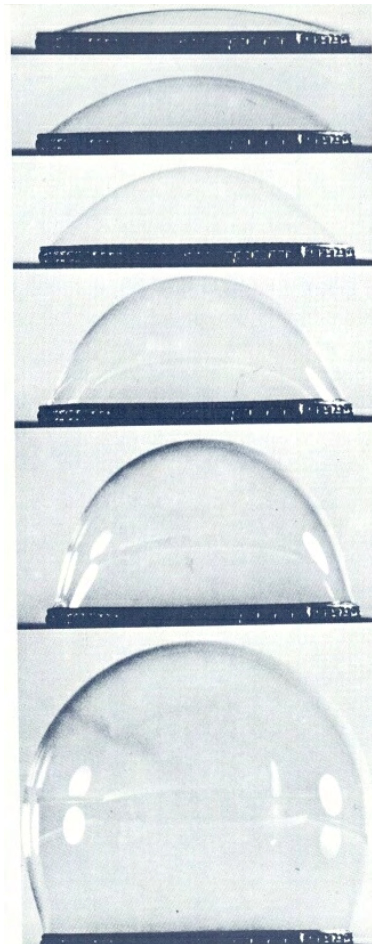


Figure 2.78: Soap film pneumatic model. Image from (Bach et al. 1987).

In Figures 2.79 and 2.80 two examples are given of pneumatic soap films which are created on an edge. Note that the soap films are not one piece, but consist of various compartments, with the angles explained in the references (see also Section 2.5.2).

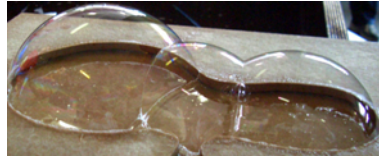


Figure 2.79: Soap film pneumatic model.



Figure 2.80: Soap film pneumatic model.

2.4.4 High elasticity membranes or fabrics

In Figure 2.81 a panty model is shown, which is an example of a high elasticity membrane (fabric) model. Prestressed panties have an analogy with prestressed membranes. Although the material and the scale is different, aspects can be studied of the panty model, such as the curvature related to the stiffness of the membrane (more curvature usually means more stiffness) by pressing and feeling the fabric and the forces.



Figure 2.81: Two prestressed pantymodels.

A pneumatic structure can be modeled in more or less the same way as a membrane structure with the main difference that an overpressure inside the model must 'blow' the model in a certain direction. Instead of using panty fabric or other fabrics, it is possible to use a high elasticity membrane which is air tight, or lets very little air through. In this manner it is possible to simulate the behaviour of the pneumatic structure in a model. Note however that is very hard to scale down the model and the parameters appropriate, and that it might be better to use such models only in shape studies. Figure 2.82 shows an example of a pneumatic model.



Figure 2.82: Picture of the physical pneu model. Image courtesy of P.C. van Hennik.

2.4.5 Wet-cloth models

Another technique of making models for membranes and when inverted for shell structures, is the use of wet cloth. The heavy of moist cloth will approximate the equilibrium shape.

Various techniques exist to make inversion of these models possible to structure shells: freezing, plastering, glueing, etc. Heinz Isler made very thin shells in this manner.

Figure 2.83 shows an example of a hanging cloth model which was strengthened with plaster.



Figure 2.83: Inverted hanging cloth model, strengthened with plaster. Models by P.C. van Hennik.

2.5 Biomimetics

One of the oldest methods of finding form is to learn from nature and imitate its structural behavior. Many examples can be given of optimal structures in nature, since nature has its own optimising law, the Darwinian law of survival of the fittest (Darwin 1859) and evolution resulting from it. For many 'structures' in nature gravity is an important load and the structures are optimised accordingly. Not always is gravity or optimisation the main reason we can learn from nature, sometimes the shapes themselves are inspiring for architects and engineers.

A seasoned structural engineer can distinguish many structural principles in nature. With his knowledge about structural engineering he is able to understand structural principle in nature. It is generally accepted that nature is adopting itself by evolution to its ever changing surrounding (Darwin 1859). Not the principles of *Evolution* and *Growth* themselves are useful for structural designers, but the results of these, the optimised natural structures, are. They can function as an inspiration for structural design.

Although the learning-curve of man-kind is much steeper than that of nature (it may sound a bit strange to place man-kind opposite to nature, man-kind is of course a product of evolution itself), we can still not compete with the solutions nature found in the struggle to survive. Nachtigall used his own words to express a similar thought (Nachtigall 2001):

Die Natur hat über Jahrmillionen Erfindung auf Erfindung getürmt. Deshalb erinnert der Erfindewettstreit zwischen Mensch und Natur ein wenig an den Wettlauf zwischen dem Hasen und dem Igel.

Sir D'Arcy Thompson discussed in his work 'On Growth and Form' (Thompson 1942) many natural structures. For example the analogy between the back of a horse, which has to carry the self-weight and the principles of bending of a beam. There are direct similarities between the muscles and bones of animals and the tension and pressure elements of a bridge. On cellular level similar analogies exist. The buckling of a microtubule in a cell that is about to divide is essentially the same as the buckling of an elastic bar at a much larger scale (Calladine 1998). For most of the structural engineers the analogy of the back of a horse and a structural beam is much clearer than the latter analogy, nevertheless it is possible to find analogies between nature and structural design on different scales.

Famous examples of learning from nature as a form finding technique. Antoni Gaudí is well-known as an architect and structural engineer who learned from nature. Many of his buildings show a strong relationship with nature.

The Institute for Lightweight Structures of the University of Stuttgart has made many studies of nature in relationship to structures and building in the period 1970-1990 which are reported in various books (Bach 1971), (Bach 1973), (Bach 1975). Below some fields of which can be learned will be discussed with references to more detailed information.

Whalley (Whalley 2000), director of Nicholas Grimshaw & Partners describes the importance of nature for the Eden project and how they have learned from nature to create the shape of the structure.

2.5.1 Types of analogies

To place the natural structures in their context it seems useful to start with an investigation of statical natural structures (deployable structures will not be covered in lecture notes). It should be noted that this section can not and does not offer an exhaustive listing and description of all existing natural structures.

- Statical natural structures

- cellular structures
 - * honey combs
 - * bone structure
 - branching and tree structures
 - * tree structures
 - * leaf structures
 - skeleton structures
 - web structures
 - sea shell and radiobria
 - biomechanical structures
- Deployable and retractable structures

2.5.2 Cellular structures

In their books Gibson and Ashby and D’Arcy Thompson have covered the subject of cellular structures, and structures built from cellular or cell-like material, either natural or artificial (Gibson & Ashby 1997) (Thompson 1942).

In 1917 D’Arcy Thompson explains, partly in a mathematical manner, the forms of cells, which are minimal surfaces. He explains minimal surfaces for various forms, cell types and droplets of water. In another part he extensively explains the clustering of bubbles, minimal energy surfaces and their hexagonal formed minimal shape.

Surface-tension is the leading parameter for the relative orientation of cells. The effect of this surface-tension will manifest itself in surfaces *minimae areae*. The underlying principle of surface-tension is described as follows; The part of the total energy available in a certain system, which is ‘located’ at the surface, is called the *surface energy* and is proportional to the surface of contact between the system and its surrounding substances. Each boundary between two substances has its one particular property. The *surface energy* is also proportional to this particular property. Equilibrium, which is the condition of minimum potential energy in the system, will accordingly be obtained by the utmost possible reduction of the surfaces in contact (Thompson 1942).

With this principle Thompson explains the forming of thin films of oil on water and small drops of water on tree leaves. Based on an old seventeenth-century theorem, called Lamy’s Theorem:

”if three forces acting at a point be in equilibrium, each force is proportional to the sine of the angle contained between the directions of the other two.”

$$\frac{P}{\sin \phi} = \frac{R}{\sin \rho} = \frac{S}{\sin \varsigma} \quad (2.20)$$

where P , R and S represent the forces in the partition walls acting on the intersection point of the working lines of the three forces; ϕ is the angle between R and S ; ρ is the angle between P and S and ς is the angle between P and R .

Lamy’s Theorem describes a closed (force) triangle. The Cosines Rule is used;

$$P^2 = R^2 + S^2 - 2RS \cos \varphi$$

$$R^2 = P^2 + S^2 - 2PS \cos \alpha$$

$$S^2 = P^2 + R^2 - 2PR \cos \beta \quad (2.21)$$

In Figure 2.84 the used forces and angles are shown.

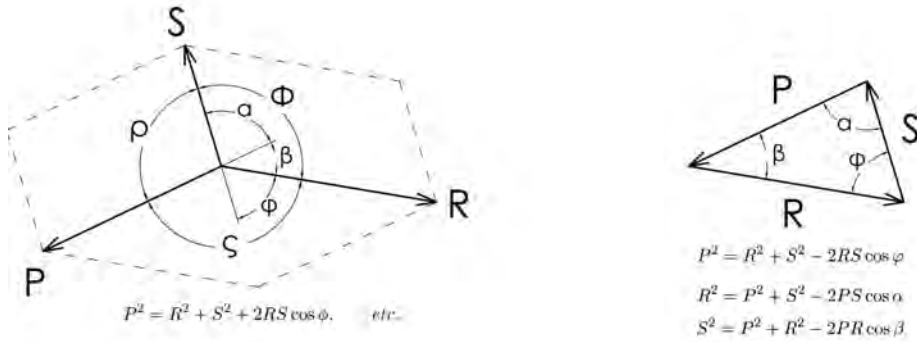


Figure 2.84: Relation between Lamé's Theorem and the Cosines Rule.

Because;

$$-\cos(\varphi) = +\cos(-\varphi) = +\cos(2\pi - \varphi) \quad (2.22)$$

and

$$2\pi - \varphi = \phi \quad (2.23)$$

Equation 2.21 becomes;

$$P^2 = R^2 + S^2 + 2RS \cos \phi, \quad \text{etc.} \quad (2.24)$$

Equation 2.24 shows clearly that the angle between three equal substances must be 120° . As long as there is no difference in external pressure applied. And of course the sum of the three angles must be 360° .

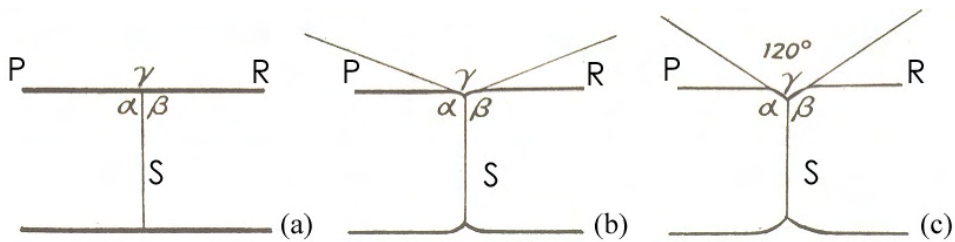


Figure 2.85: Three situations (a) $P = R \gg S$; (b) $P = R$ and S is a little smaller; (c) $P = R = S$.

According to Gibson and Asby, a cellular solid is made up of an interconnected network of solid struts or plates which the edges and faces of cells. There are several typical structures,

such as the two-dimensional honeycomb, the three-dimensional foam with open cells and three-dimensional foam with closed cells (see Figure 2.86).

They derived that there are several cell shapes (see Figure 2.87, 2.88 and 2.89).

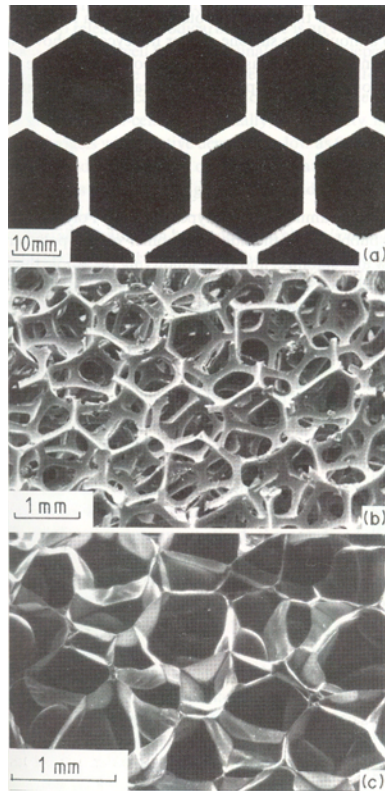


Figure 2.86: Different types of cellular structures. Image from (Gibson & Ashby 1997).

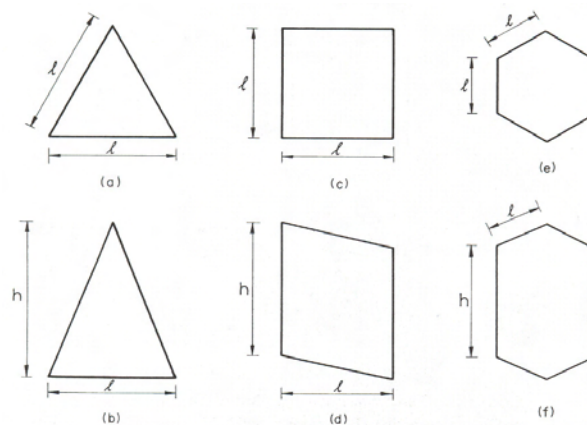


Figure 2.87: Different types of two-dimensional shapes. Image from (Gibson & Ashby 1997).

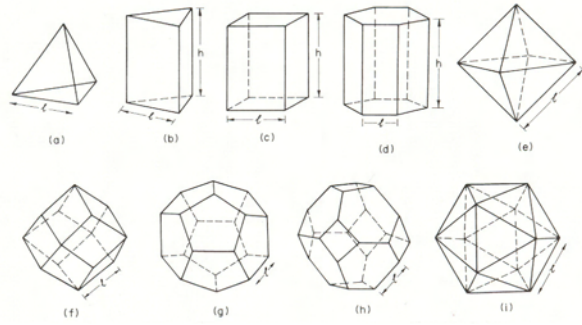


Figure 2.88: Different types of three-dimensional shapes. Image from (Gibson & Ashby 1997).

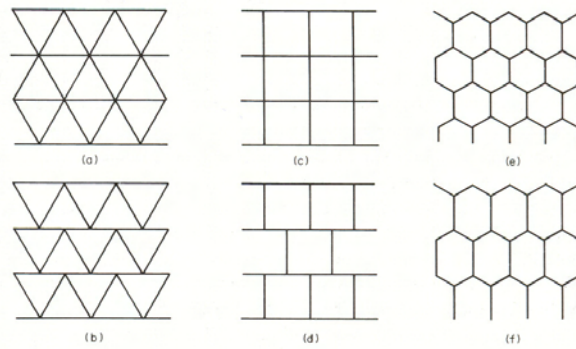


Figure 2.89: Different types of grid topologies. Image from (Gibson & Ashby 1997).

These cell shapes have to comply with Euler's Formulas:

$$F - E + V = 1 \quad (2.25)$$

for two dimensions

$$-C + F - E + V = 1 \quad (2.26)$$

for three dimensions

where

- V number of vertices
- E number of edges
- F number of faces
- C number of cells

Gibson and Asby also derived several formulas for the angles of the edges of the cells. These formulas could be seen as the natural equivalent of optimisation. As nature optimises its cells to a certain equilibrium.

Another interesting property of cell partition, described by Sachs, known as Sachs's Rule, is that one cell-wall always tends to set itself at right angles to another cell-wall (Figure 2.93a). This fact can be explained with Equation 2.24; assume for example that $R = S \gg P$ and $R^2 + S^2 = 2RS = a$ Equation 2.24 transform in the following equation;

$$1 = a + a \cos \phi \quad (2.27)$$

$$for a \Rightarrow \infty \quad \frac{\frac{1}{a} - \frac{a}{a}}{\frac{a}{a}} \approx \frac{0 - 1}{1} = -1 \quad (2.28)$$

$$\cos \phi = -1 \quad \Rightarrow \phi = 180 \quad (2.29)$$

Sachs' Rule looks contradictorily with the fact that three substances with the same properties have to form angle of 120° with each other. Nevertheless, among plant-tissues it commonly happens that one cell-wall has become solid and rigid before another partition-wall impinges upon it (Thompson 1942).

Figure 2.90 shows a part of the wing of a dragonfly, the characteristic angles of 90° and 120° are easy to recognize. Figure 2.91 gives an indication of the distribution of the angles measured in a part of the wing.

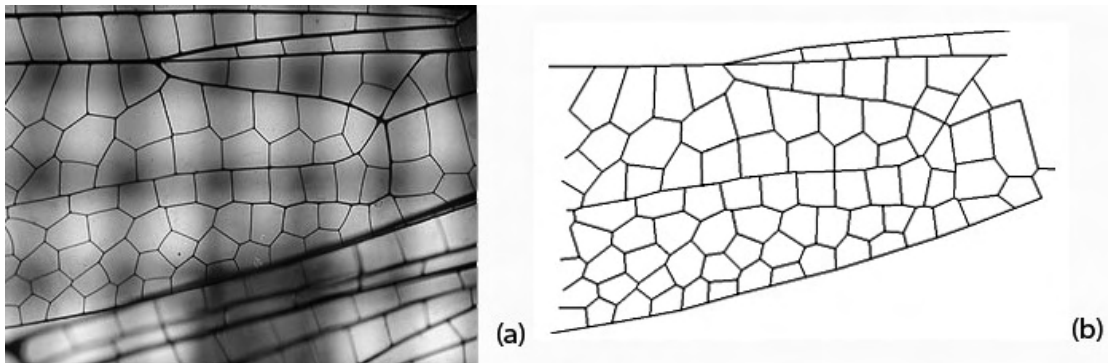


Figure 2.90: (a) Picture of a part of a dragonfly wing; (b) vector drawing of the venation. Based on this vector drawing the distribution of the 235 angles of Figure 2.91 is made.

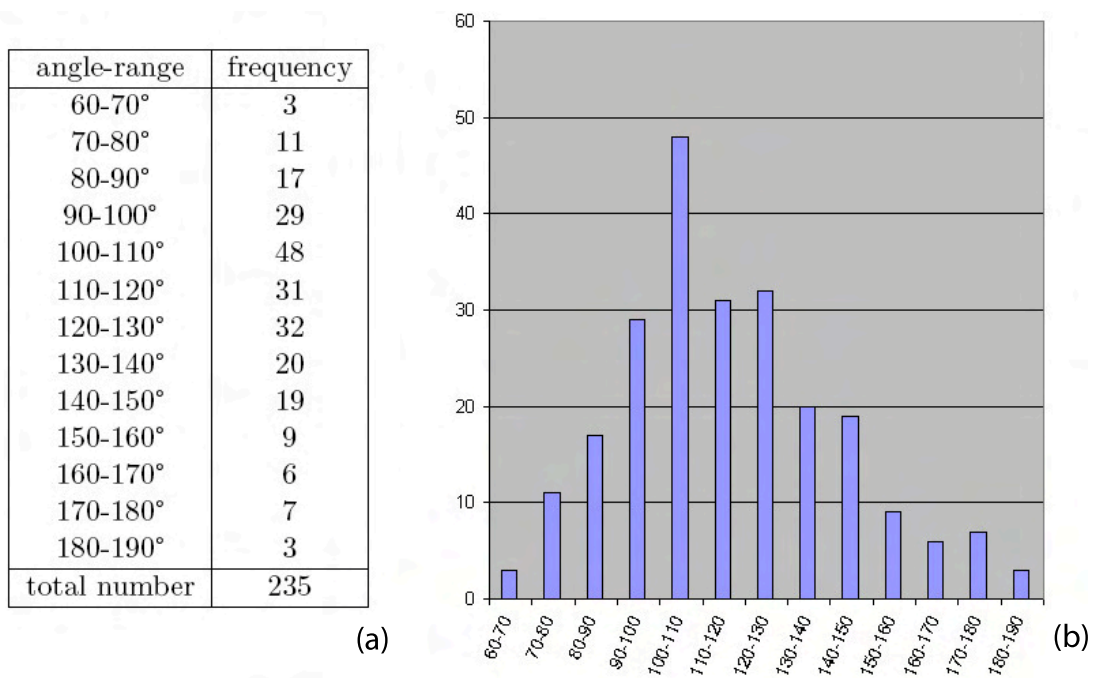


Figure 2.91: (a) Distribution of 235 angles between cell partition walls; (b) Graphical illustration of the distribution of 235 measured angles between the partition walls of a dragonfly wing. Image from Dumans 2005.

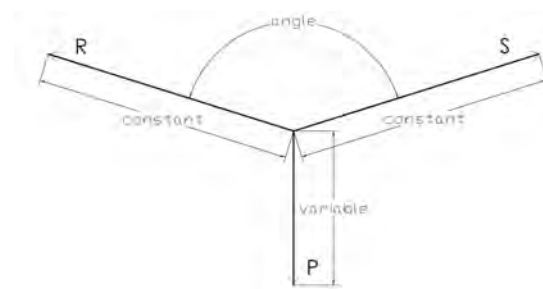


Figure 2.92: Introduction of the parameters used for the calculations.

The distribution of the angles shows not exactly the expected result. Although a significant part of the angles fits in the sub-groups of $80\text{--}100^\circ$ (19.6%) and $110\text{--}130^\circ$ (26.8%), the dispersion of the angles is quite big.

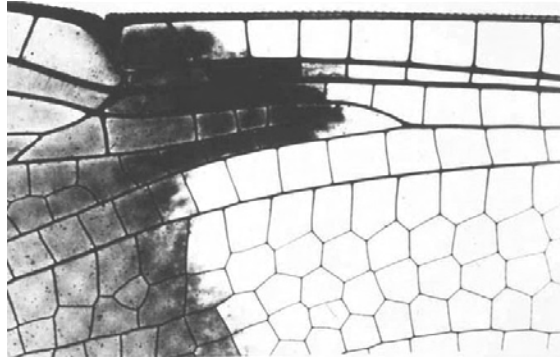


Figure 2.93: Detail of the wing of a dragonfly. The characteristic angles 90° and 120° are clearly visible.

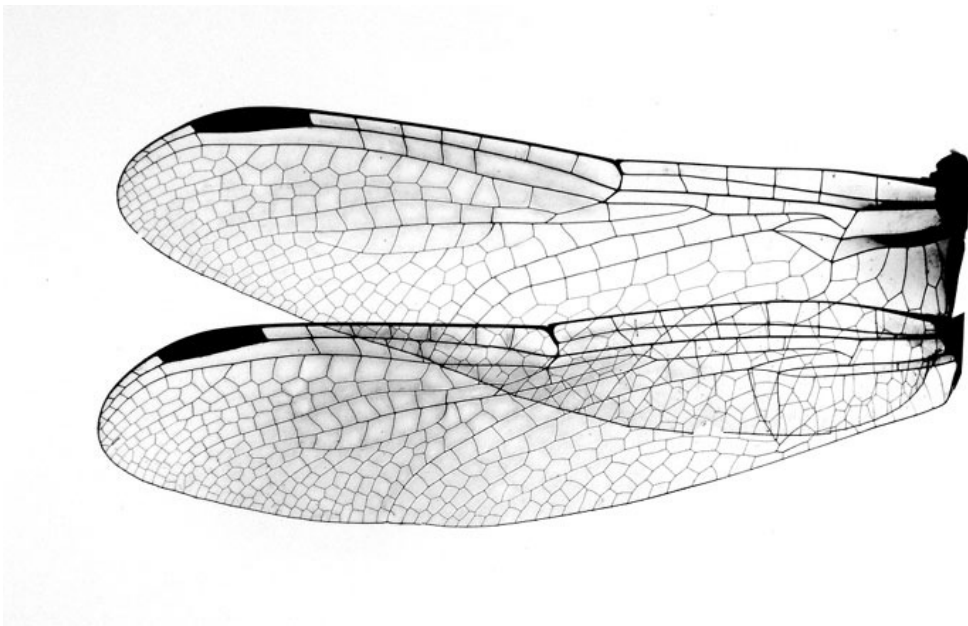


Figure 2.94: Two wings of a dragonfly, a fore and a hind wing. Both wings look quite similar, although they differ at some points, nevertheless, nature seems to have reasons to form the venation in this way and it may be assumed that is not a random configuration.



Figure 2.95: Fresh and dried leaf of *Dieffenbachia*. Nature does not always follow the ‘simple’ laws and rules made by human beings. In this leaf the regular pattern with 180° and 120° which may be expected based on Equation 2.24 is missing. Nature has its own, more complex reasons to form the partition walls the way they are formed.

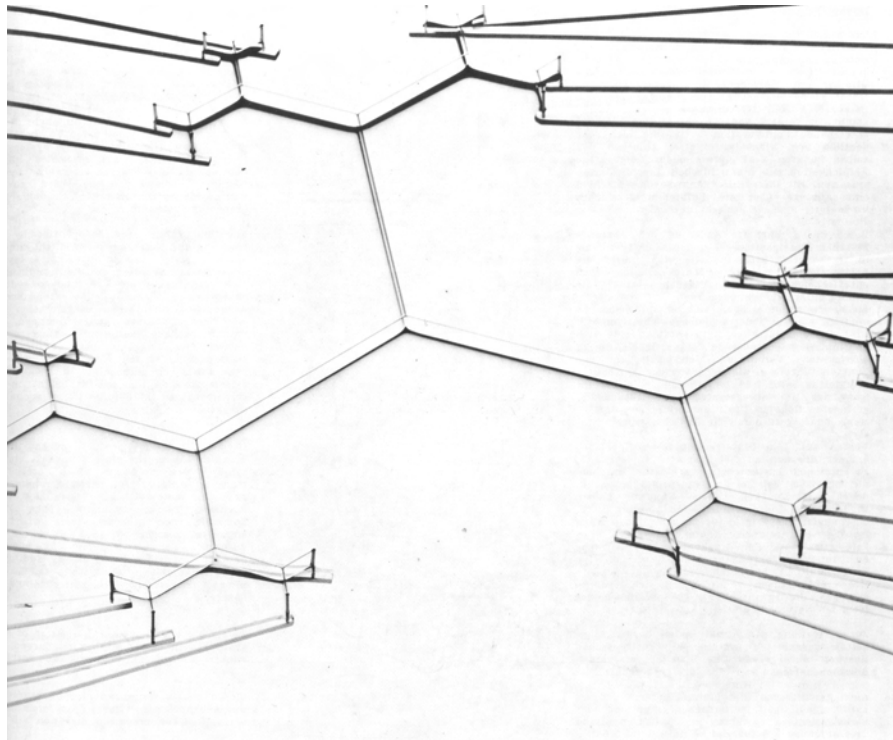


Figure 2.96: Pattern of soap-partition walls. The characteristic angle of 120° is easy to recognize. Image from (K. Bach 1988).

2.5.2.1 Honeycombs

Honeycombs are a special kind of cellular structures, and an inspirational source for many structures. They are usually hexagonal cells made by bees, but there are also man-made examples of honeycomb structures.

Figure 2.99 shows a honeycomb structure made by bees. Agreement exists on the fact that these structures are optimal structure, but exactly why they are optimal and why bees make them in an optimal way is not agreed on. D'Arcy Thompson (Thompson 1942) elaborates extensively on this and on their relationship of various spatial shapes. He also studies the wingshape of various flies, which have cell (or grid) like structures. Also the ILEK refers to dragonfly wings in the book IL18 (Bach et al. 1987).

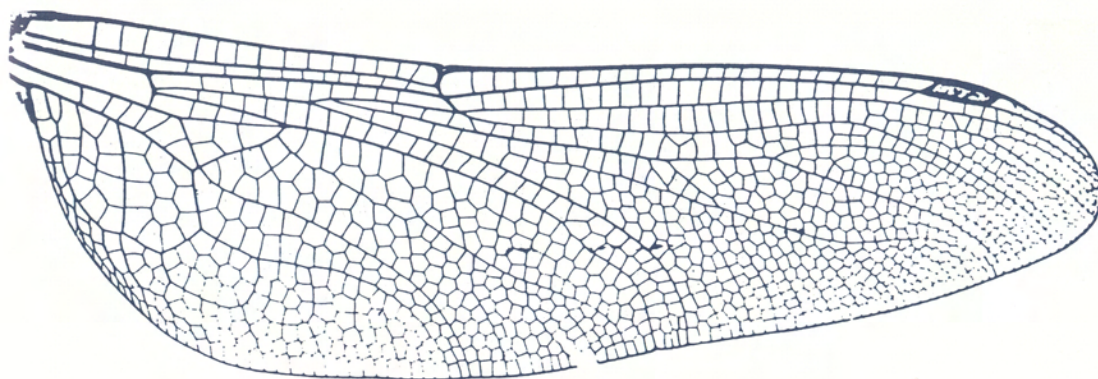


Figure 2.97: Dragonfly wing. Image from (Bach et al. 1987).

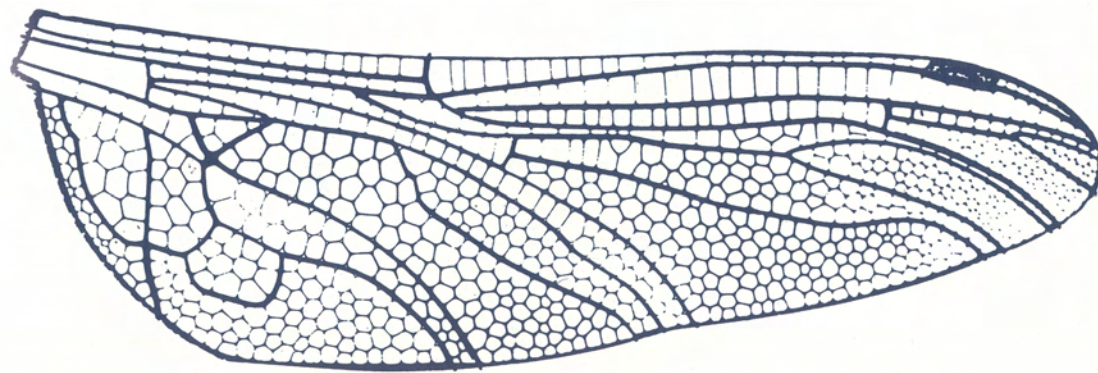


Figure 2.98: Dragonfly wing. Image from (Bach et al. 1987).

Gibson and Asby (Gibson & Ashby 1997) see honeycombs more in a general sense, as two-dimensional cellular solids with certain mechanical and biological properties. They cover both the natural as the arteficial side of honeycomb structures.

When circular sections (e.g. sections of bubbles) are pressed together a regular hexagonal pattern arise. Three partition walls of the same material and loaded, by symmetry, by the same load touch each other at angles of 120° .

From observations of connected bubbles it is known that the 'ends of the cylinder' become (or better; stay) spherical. When, in the case of bee's cells, to obtain the closest packing, the ends of one layer of cells fits in the ends of a second layer of cells, the spherical ends disappear and trihedral pyramids appear. One cell-end of the first layer fits in the gap between three cell-ends of the second layer.

Many diverse proofs have been given of the minimal character of the bee's cell (Thompson 1942). A mathematical model of the bee's cell, used by Maclaurin to prove the optimal form of the bee's cell is given in Figure 2.100.



Figure 2.99: The most famous hexagonal structure; the bee's cell.

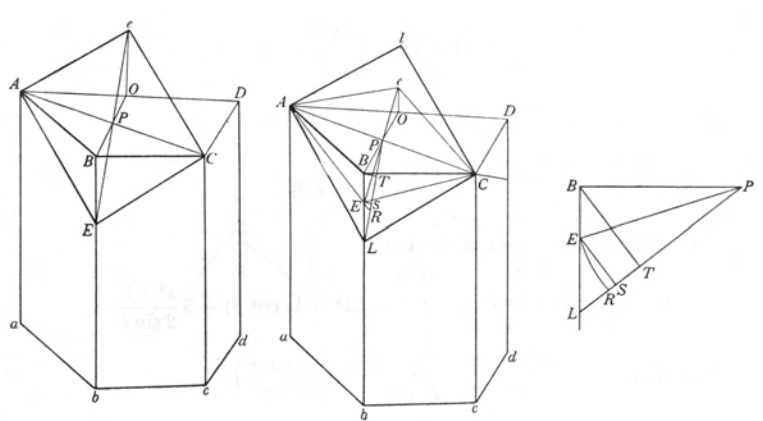


Figure 2.100: Mathematical model of the bee's cell. Image from (Thompson 1942).

The honey comb structure is often called 'an optimised natural structure', but it is important to mention for which parameter the structure is optimised. There is little doubt that the bee's cell provide the biggest volume-material ratio for a configuration of two layers of compartments with an opening to the one or the other side. But is the honey comb so optimal with respect to

the transfer of loads?

A triangle is the only two-dimensional form which is rigid by itself. All poly angles with more than three hinges are instable without external support. Thus a honeycomb, which is a hexagonal structure with six 'potential' hinges, needs stiffening of the hinges or external support. The deformation of the hexagon is presented schematically in Figure 2.101.

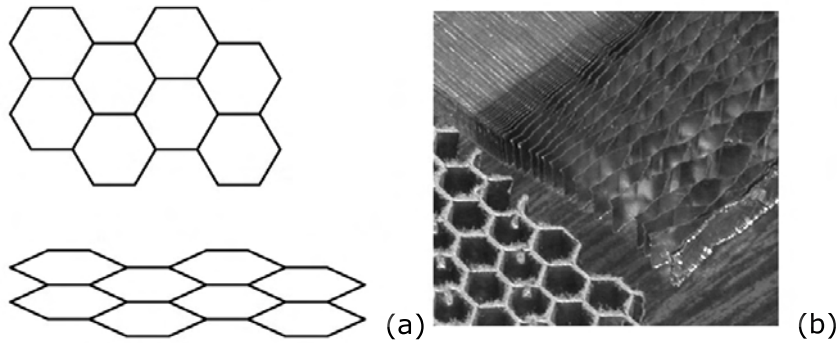


Figure 2.101: (a) Schematically representation of the folding of eight hexagons. (b) Foldable bee's cell structure. Image from (n.d.).

Part of the stability of the bee's cells is provided by the semi-fixed joints and partly by external stiffening elements. The chambers at the border of the honeycomb are not hexagonal. According to Thompson the chambers or cells which constitute the outer layer, retain their original spherical surfaces and these still tend to meet the partition-walls connected with them at constant angles of 120° (Thompson 1942). The form of the cells in the outer layer can be explained by pointing at the principle of occurring angles between partition-walls; the partition-walls will fit the (stiff) boundary at almost right angles (see Figure 2.90). This boundary distortion has a structural function, the distortion prevents the deformation of the hexagonal structure as in Figure 2.101. The partition walls at the boundary of the comb function as a bracing. This model is valid when we assume that all connections are pin-joint connections.

A more realistic approach, assuming that the joints are semi-fixed is carried out [Mechanics of Honeycombs (Honeycombs n.d.)]. Figure 2.102 shows the model used for this analysis. It is possible to calculate the bending moment M , on the angled beam, from which the deflection, d , can be determined.

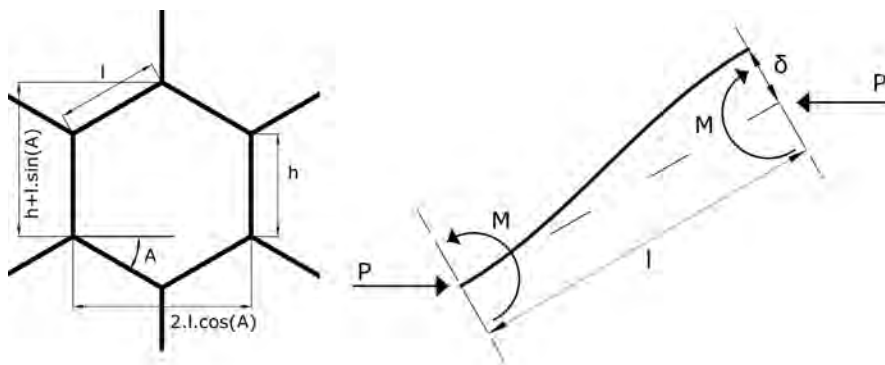


Figure 2.102: Model for elastic analysis of hexagonal structure.

$$M = \frac{Pl \sin A}{2} \quad (2.30)$$

and;

$$P = \sigma_1(h + l \sin A)b \quad (2.31)$$

where σ_1 represents the stress in the X_1 direction and b stands for the depth, out of plane, of the honeycomb. P is a point load. It is the resultant of the stress σ_1 working over the area $(h + l \sin A)b$. Substitution of Equation 2.31 into Equation 2.30 gives;

$$M = \frac{\sigma_1(h + l \sin A)bl \sin A}{2} \quad (2.32)$$

The deflection can be expressed by;

$$d = \frac{Ml^2}{6EI} = \frac{\sigma_1(h + l \sin A)bl \sin Al^2}{12E_s \left(\frac{bt^3}{12} \right)} \quad (2.33)$$

The component of deflection in the X_1 direction is just $d \sin A$ acting over a length $l \cos A$ hence the strain in the X_1 direction is;

$$\begin{aligned} \varepsilon_1 &= \frac{d \sin A}{l \cos A} = \frac{\sigma_1(h + l \sin A)b.l \sin A.l^2 \sin A}{12E_s \left(\frac{bt^3}{12} \right) l \cos A} \\ &= \frac{\sigma_1 \left(\frac{h}{l} + \sin A \right) l^3 \sin^2 A}{E_s t^3 \cos A} \end{aligned} \quad (2.34)$$

Since the modulus of elasticity is the ratio of stress to strain, we can re-arrange the above equation to;

$$\frac{E_1}{E_s} = \left(\frac{t}{l} \right)^3 \cdot \frac{\cos A}{\left(\frac{h}{l} + \sin A \right) \cdot \sin^2 A} \quad (2.35)$$

where E_s is the modulus of elasticity of the solid of which the beam is made and E_1 is the modulus of elasticity of the cell in X_1 direction. When the honeycomb consists of regular hexagons in which $h = l$ and $A = 30$ then the above equation reduces to;

$$\frac{E_1}{E_s} = \frac{4}{\sqrt{3}} \left(\frac{t}{l} \right)^3 \quad (2.36)$$

A similar procedure can be followed in the X_2 direction and it seems that $E_1 = E_2$ and this means that a regular hexagonal honeycomb is isotropic. Thus, from structural point of view the orientation of the cells does not matter. The floor of a cell has a V -shape. Figure 2.103 shows a section of two layers of cells. The cells are not placed horizontal but they are placed under a small slope. The combination of the small slope and the V -shape of the cells results in the collection of the honey in the lowest part.



Figure 2.103: Section over two layers of bee's cells. The small slope results in the collection of the honey in the lowest part of the cell.

2.5.2.2 Bone and skeleton structures

What can be learned from cancellous or trabecular bones is shown by Gibson (Gibson & Ashby 1997). The structure of the bone is closely related to optimal shapes of Michell structures (which is also explained by Thompson in "On Growth and Form" (Thompson 1942)). Gibson also shows that bone has a cellular structure, which grows in such a way that it adapts to the loads it has to support (note the resemblance to form finding). The cells will try to strengthen in the direction where the load is larger.

Also the book IL6 (Bach 1973) covers the adaption of bone-structures to their forces.

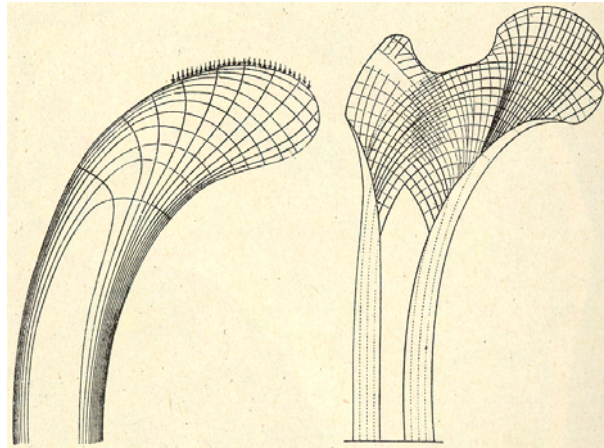


Figure 2.104: Bone analogy with Michell structures (see Section 4.6.8). Image from (Thompson 1942).

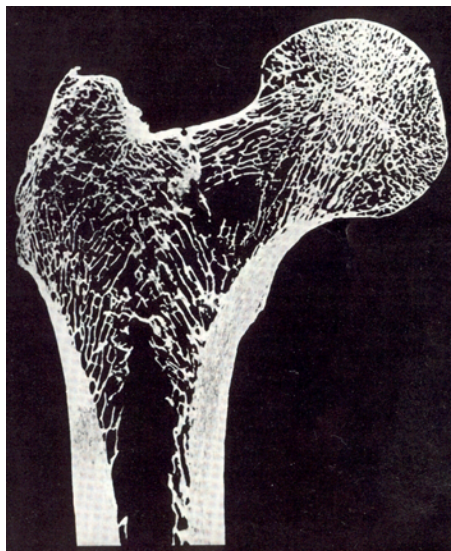


Figure 2.105: Bone structure. Image from (Bach 1973) .

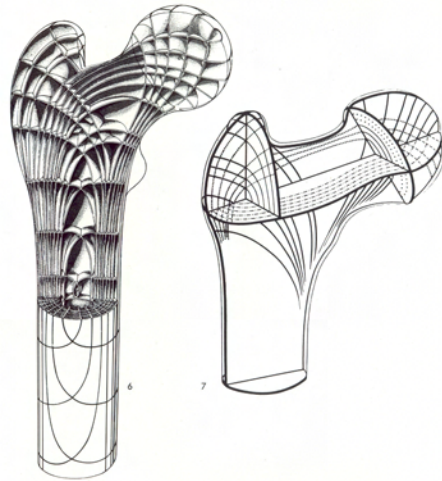


Figure 2.106: Bone structure. Image from (Bach 1973) .

Bones form a beautiful example of natural optimisation of material. D'Arcy Thompson discussed the cancellous (Thompson 1942) or spongy human bone. He focussed on the *tibia* and the *femur*, the human under and upper leg. The outside bone-cells of the *tibia* form a solid cylinder. From structural point of view a cylindrical cross-section is quite efficient; torsion stiff and most of the material at the outside to take the bending forces.

The 'head' of the *tibia* is some what widened out compared to the middle part of the bone. The head is capped with a relative flat plate. Figure 2.107(a) illustrates a very simplified model of the human *tibia*, a cylindrical wall and a flat cover plate. Based on differences in stiffness the displacements may be assumed as presented in (b). From a structural point of view it seems logical to reinforce the part located directly under the flat plat (c).

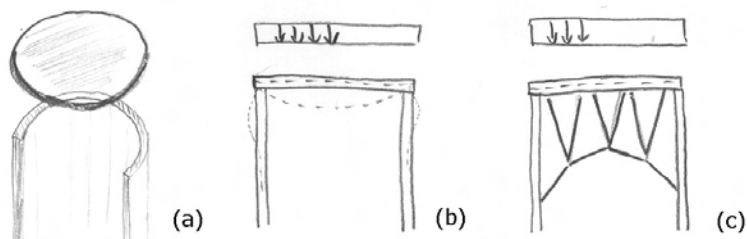


Figure 2.107: Very simple model of the human *tibia* (a) The bone can be simplified as a cylinder with a flat top plate. (b) Without stiffening-elements, the flat plate shows significant deflections. (c) With stiffening-elements, the deflection is much less. The stiffening-elements in bone structures have strong similarities with Michell structures.

This is exactly what occurs in the bones under pressure like the *tibia*. The Figure 2.108 shows an x-ray photo of the same head and Figure 2.109 shows an drawing of the head of the *femur* after Culmann and Wolff.

A fine lattice-work of bone material supports the head of the *femur*. Similar patterns can be seen

in x-ray photos of the *tibia*. Hermann Meyer (and afterwards in greater detail by Julius Wolff and others) described the pattern of the cancelli in human bones under compression. The cancelli, as seen in a longitudinal section of the *femur*, spread in beautiful curving lines from the head to the hollow shaft of the bone. And that these linear bundles are crossed by others, with such a nice regularity of arrangement that each intercrossing is as nearly as possible an orthogonal one (Thompson 1942).

Figure 2.109 shows these cancelli meeting at (nearly) right angles. The 'compression-lines' run down the concave or compression side of the bone and the 'tension-lines' run upwards at the convex or tension side of the bone. The 'compression-lines' bend to a perpendicular angle with the 'tension-lines' and the other way around.

As mentioned before this pattern of perpendicular tension and compression lines shows strong similarities with the Michell structures presented in the Figure 2.110 and 2.111. Michell structures are structures designed to transmit load from specified points of application to supports using a minimum weight of linear elements Holgate.

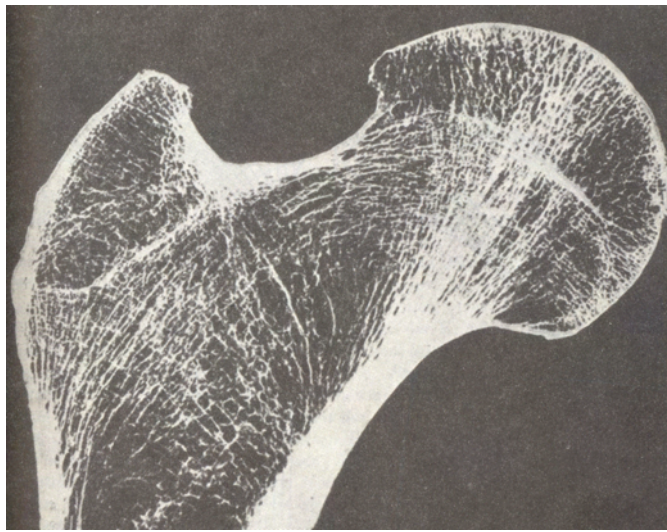


Figure 2.108: X-ray photo of the head of the human *femur*. Image from (Thompson 1942).

The *humerus*, *radius* and *elna* bones of the bird wing which are mainly loaded by tension are hollow (Nachtigall 1985).

A team of international researchers, working under the name SHASTRA using MRI scans and photos to make 3D computer models (Figure 2.112) for finite element analyses (2005a). The flat plate on top of the *tibia* is divided in two parts, that is why it is not very easy to recognize the stress trajectories in the *femur*.

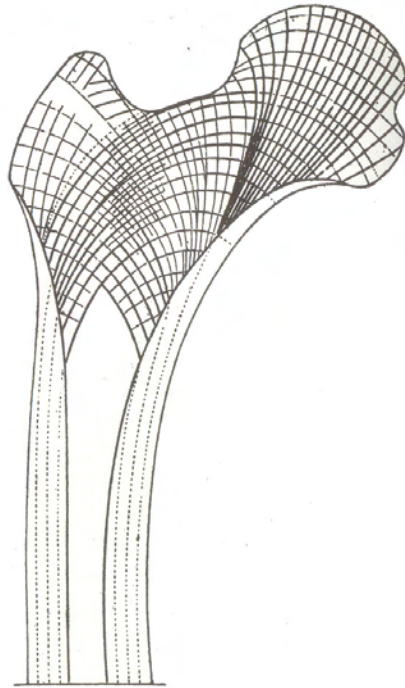


Figure 2.109: Head of the *femur* (upper leg). Image from (Thompson 1942).

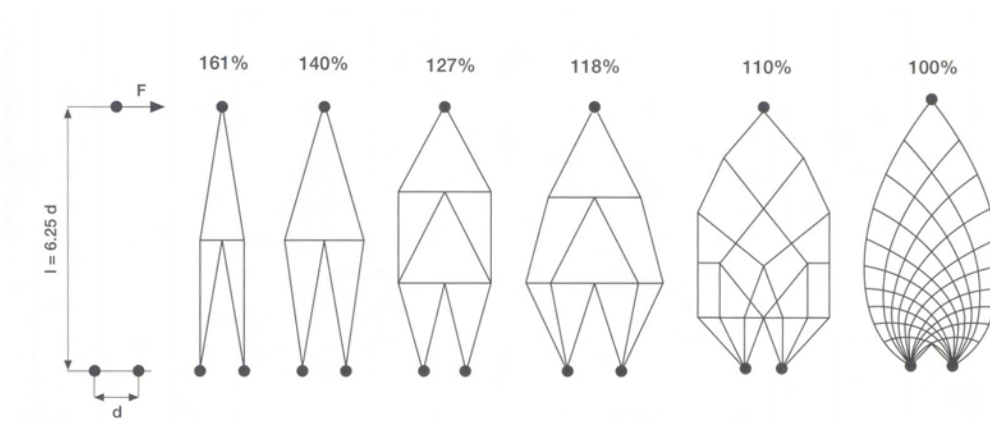


Figure 2.110: Optimisation of a structure. In every step the required bars are thinner. The most complicated one is called 'Michell structure'. Image from (Beukers & Hinte 2001).

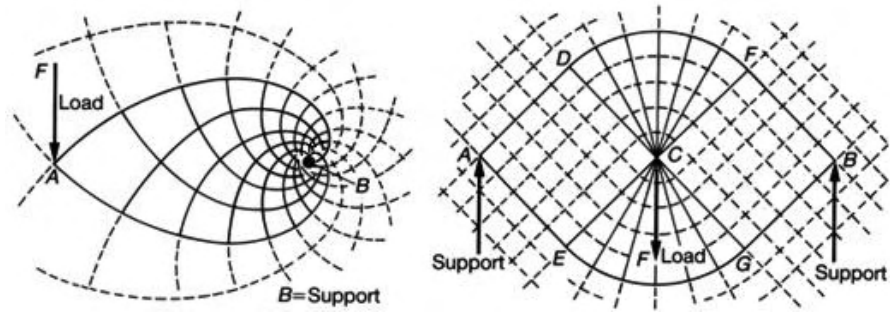


Figure 2.111: Michell structures for two different configurations; a cantilever structure and a structure one two supports loaded by a force in the center. Image by (Holgate 1986).

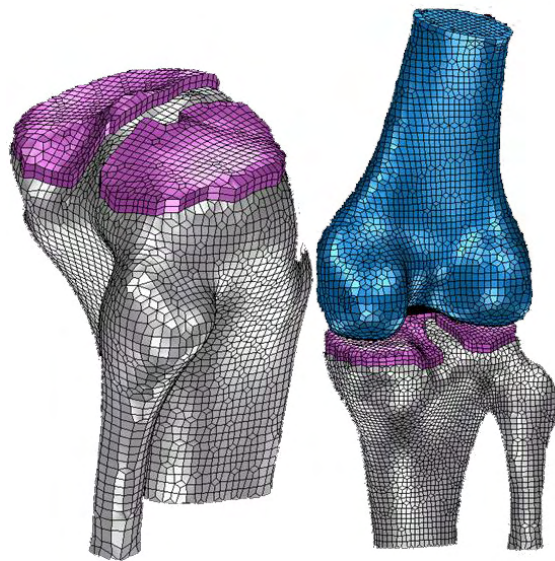


Figure 2.112: 3D model of joint *tibia* and *femur*, the flat plate on top of the *tibia* is clearly visible. Image from (2005a).

2.5.3 Branching and tree structures

As can be seen in Figures 2.113 and 2.114, also the structure of leaves can be used as an analogy for structures. Although, the leaf looks to be structural optimal, we'll have to consider a point which Jorg Schlaich makes: the tree (and the leaves) optimize (grow) themselves to the maximum quantity of sunlight and not necessarily to a good use of force. Copying nature without thinking is therefore senseless.

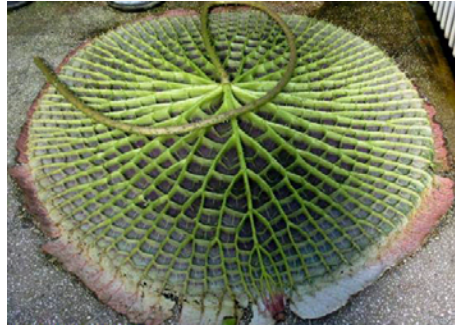


Figure 2.113: Leaf structure of the Victoria Amazonica.



Figure 2.114: Hangar structure by Nervi.

Ribs are frequently used in nature to stiffen 'plates'. For example the wings of butterflies and moths are a ribbed structures. Their wings are not membranous, rather they are covered with small scales¹. The ribs which stiffen the scales are clearly visible in Figure 2.115.

By adding ribs to a structure the moment of inertia is enlarged, which makes the structure respond stiffer than without ribs. Furthermore the nerves of leaves may be seen as ribs, giving a leaf its stiffness. A well known example of a natural ribbed leaf is the *Victoria amazonica* (Nachtigall 2001).

The principle of ribs is widely adopted by architects and structural designers. The beautiful hangars and halls designed by Pier Luigi Nervi (1891–1979) in the end of the thirties are good examples of a human 'translation' of the natural principle of ribbed structures (Figure 2.117).

It is broadly assumed that Sir Joseph Paxton, the builder of the Crystal Palace in London (1850–1851) was inspired by the underside of the leaf of the *Victoria amazonica*.

¹<http://www.arthropod.net> Access-date: 5-2005.

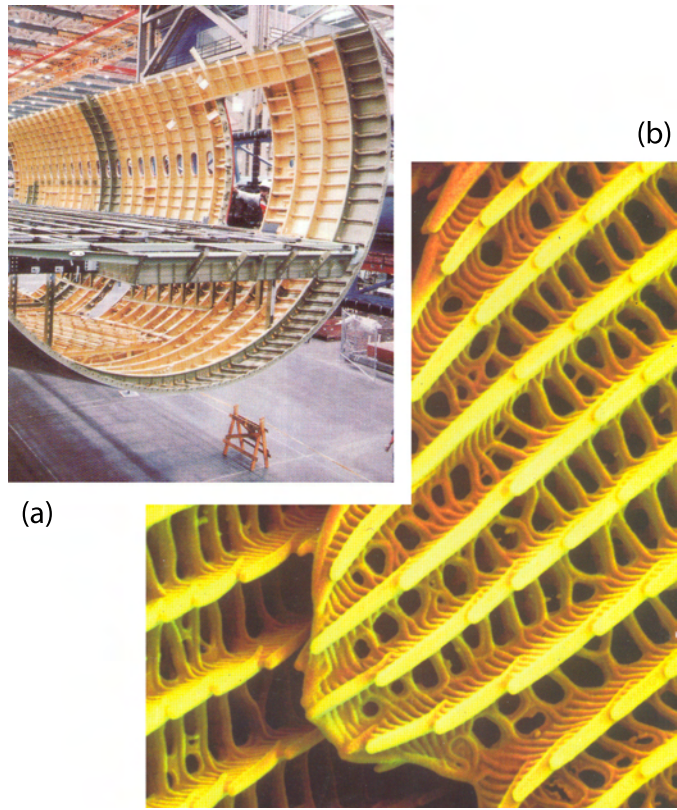


Figure 2.115: (a) The ribs of a Boeing airplane show strong similarities with (b) the rib structure of the wings of butterflies at micro-level. Image from (Nachtigall 2001).



Figure 2.116: Underside of the *Victoria amazonica*, a typical example of a natural rib structure.

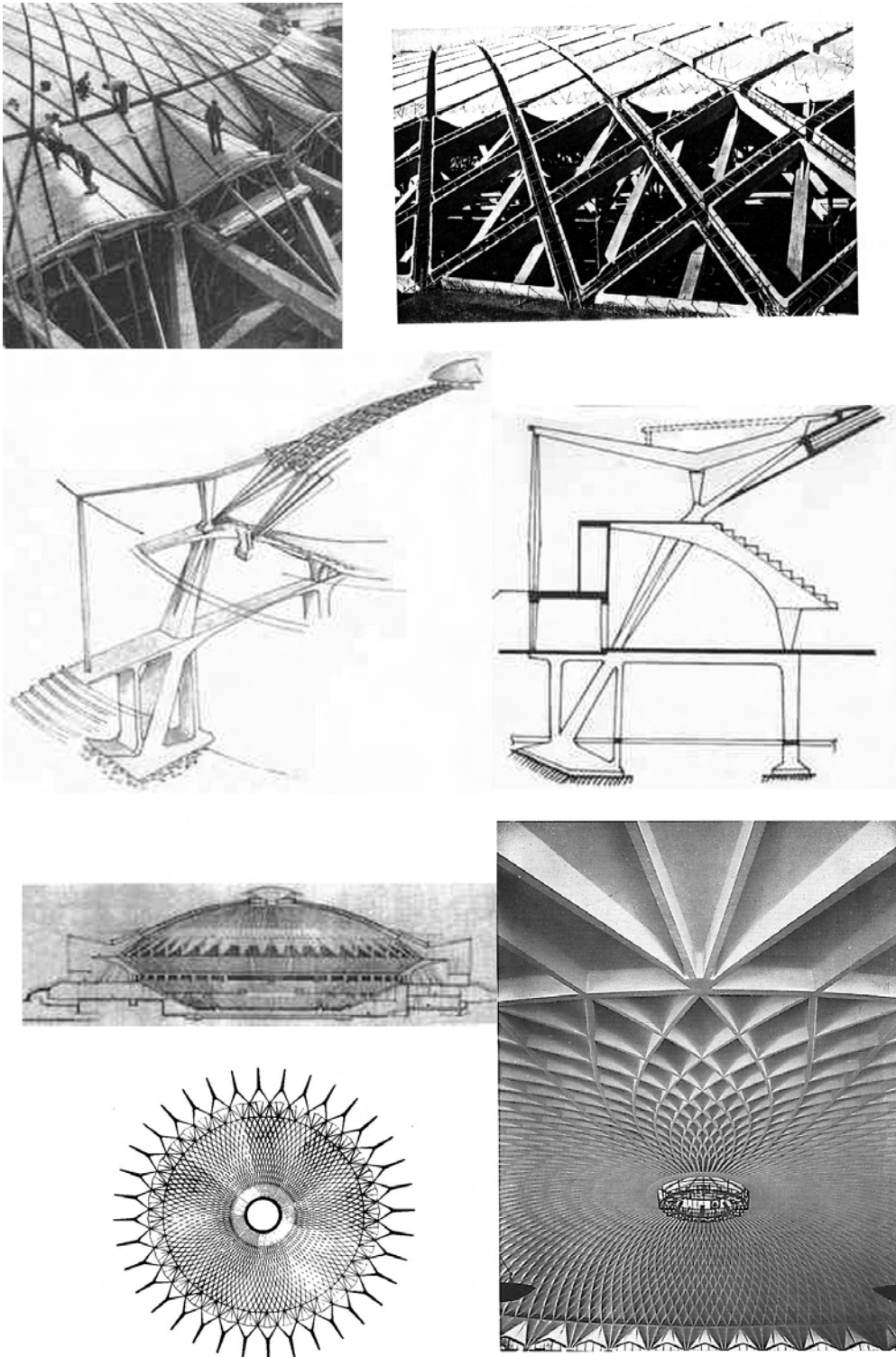


Figure 2.117: Compilation of pictures of the Palazzetto dello Sport in Roma. Especially the picture at the right-bottom side shows in a nice way the ribs. They have strong similarities with the Michell structures which can be found in bones.

D’Arcy Thompson (Thompson 1942) explains the growth of trees from a biological and growth point of view. A famous example of a structure which imitates trees to bear loads is the Sagrada Familia in Barcelona by Gaudí (i Armengol 2001). Gaudí uses an analogy to trees to create his columns.

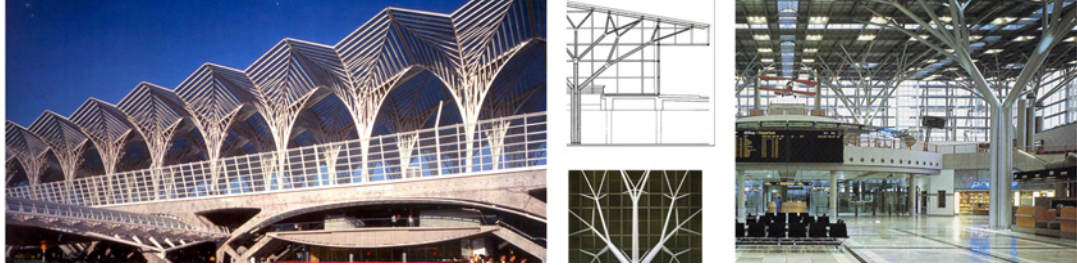


Figure 2.118: Oriente railway station, Lisbon, Portugal and departure hall Stuttgarter airport.

Branching structures can be determined by repeated division of mostly linear elements. The principle can be seen at different levels in nature. A tree is an obvious example, but there are more; electrical discharges in flashes of lightning, division of a river in a delta, cracks in dry mud, dunes in the Sahara Dessert and many others.

The branches of a tree inspired some architects and structural designers to develop tree-like structures. The enclosure of the Oriente railway station in Lisbon, Portugal, by Calatrava and the departure hall of the Stuttgarter airport by Jörg Schlaich are famous examples of tree-like structures. In their book *The Algorithmic Beauty of Plants*, Prusinkiewicz and Lindenmeyer discuss in a mathematical way the forms of plants. Figure 2.119 shows output from a model based on their algorithms (Prusinkiewicz & Lindenmayer 1990).

Mathematically there are only five things which have to be described to draw such figures.

1. the starting point
2. the length of member 0
3. the direction of member 0
4. the angle β
5. the factor R defined as

$$R = \frac{L_n}{L_{n+1}}$$

Figure 2.120 shows the basic idea of the model.

With this five parameters it is possible to describe all different regular two-dimensional branching structures.

It is possible to rewrite the algorithms of Prusinkiewicz (Prusinkiewicz & Lindenmayer 1990) in such a way that they ‘produce’ three-dimensional branching structures. The 3D-representation of the load-bearing structures in Figure 2.121 of the Stuttgarter airport departure hall is not ‘produced’ by an algorithm, but by reconstruction of pictures from the structure.

In IL25 (K. Bach 1988) the difference of a branching structure being tensile-stressed and a structure under compression is mentioned. Tensile-stressed structures are optimised systems for transmission of tensile forces which have straight connections between the force and the support (Figure 2.124b). On the other hand, structures subjected to compressive and bending stress have branching systems with increasing slenderness (Figure 2.122c and d). According to (K. Bach 1988) the ratio of the length and the thickness is constant;

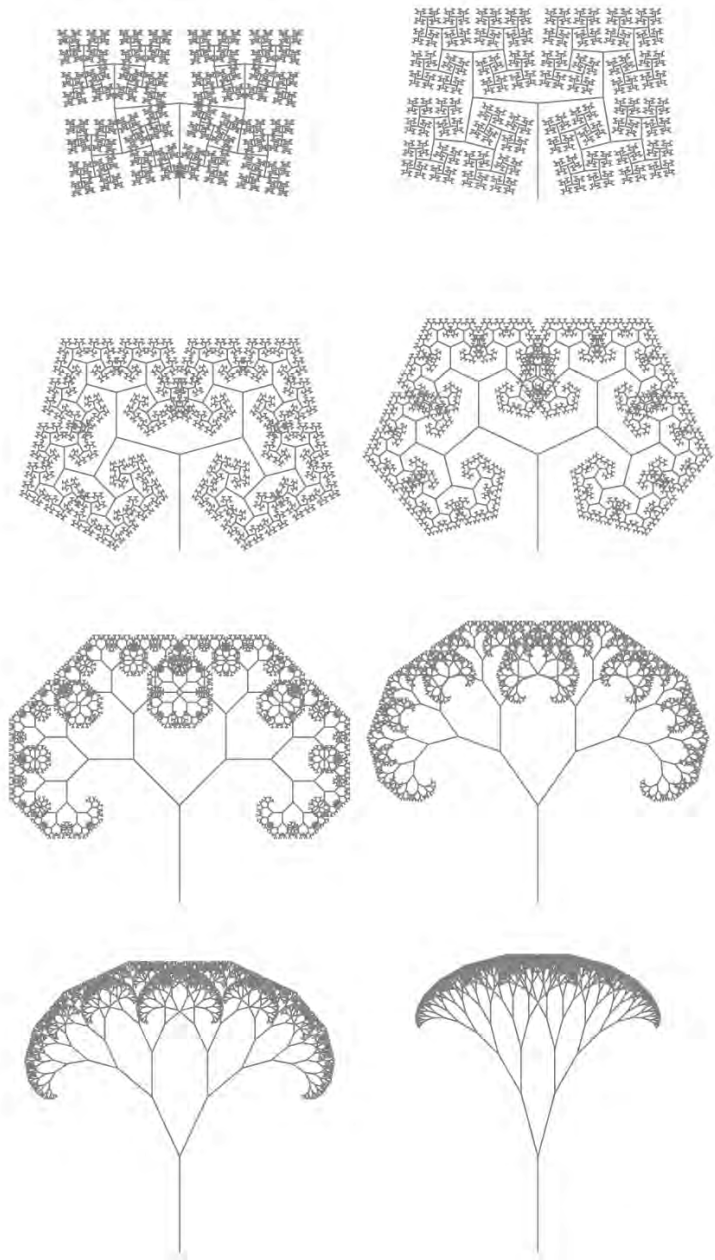


Figure 2.119: Generated branching structures for $L_0 = 1$, $n = 10$, $R = 0.6868$ and a changing angle α (95° , 85° , 75° , 65° , 45° , 35° , 25° and 15°).

$$\frac{L_1}{D_1} = \frac{L_2}{D_2} = \frac{L_3}{D_3} = \dots = \text{constant} \quad (2.37)$$

To demonstrate the structural behaviour of a branching structure like a tree a simple two-

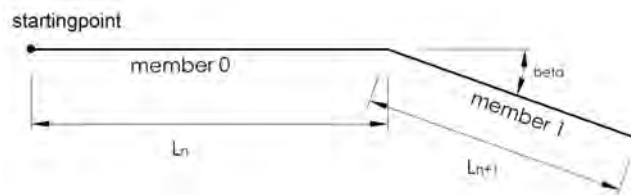


Figure 2.120: Explanation of parameters used in model.

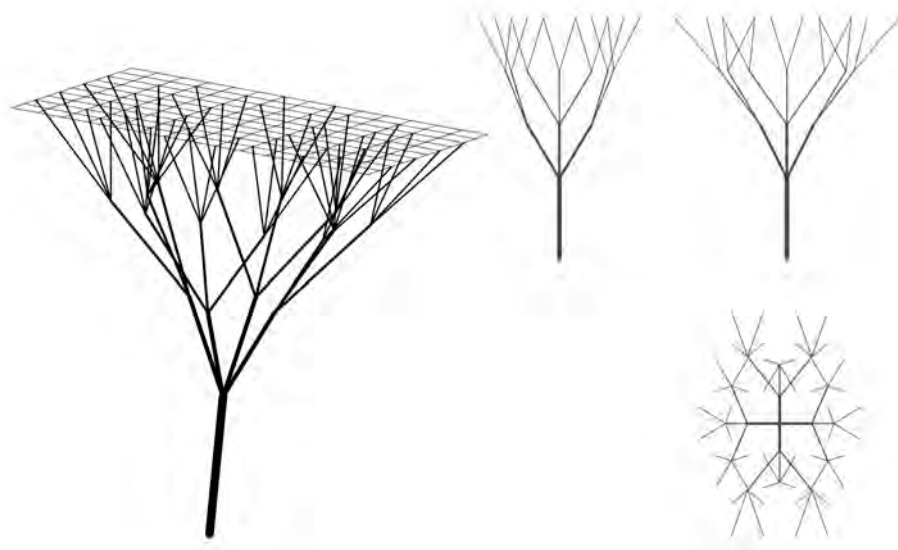


Figure 2.121: Three-dimensional representation of branching structure of the Stuttgarter airport.

dimensional model is made. Figure 2.122 shows a symmetrical and regular branching structure ($\alpha = 30^\circ$ and n is 2). The structure is loaded by two different load cases; the first one is a load in the direction of the structure, as may be expected to be a good representation of the natural load, for it is reasonable to assume that a tree grows in a way which is the most favorable to carry the load. The second load case is a pure vertical loading, which represents the load which a tree-like structure has to carry, when it supports a flat roof, as in the departure hall of Stuttgart. Figure 2.122c and e shows the axial-stresses and the bending stresses resulting from the loads. GSA8.0 is used to calculate these stresses. Based on this model it must be concluded that Equation 2.37 does not result in the most optimal structure with respect to the axial stresses in this particular case ($R=0.6868$). It is assumed that Equation 2.37 does not 'produce' optimal structures with respect to the axial forces for any value of R , nevertheless it is possible that Equation 2.37 is valid when R is variable, this is not investigated.

The figures 2.122d and e demonstrate that a tree structure is not optimal for supporting a flat roof.

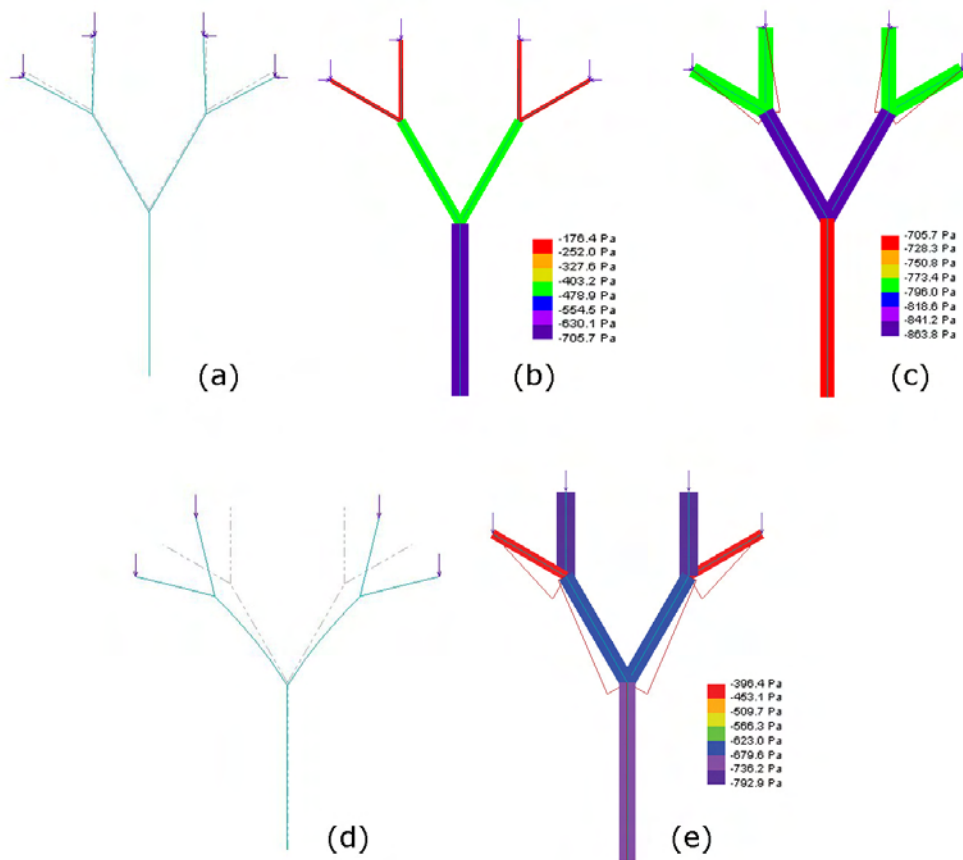


Figure 2.122: Output from GSA8.0 (a) Displacements by point loads in the direction of the structure; (b) Axial-stresses belonging to the loads of (a); (c) Axial-stresses after the sections are changed according to formula 2.37; (d) Displacements by point loads in vertical direction; (e) Axial-stresses after the sections are changed according to Equation 2.37.



Figure 2.123: (a) Feasibility study Tree Structures for an exhibition hall, Yale University, USA 1960 (Students of Frei Otto during a seminar) (b) Support pillars of a six-angle gridshell in the Kings Office, Council of Ministers, Majlis al Shura, Riyadh, Saudi Arabia, 1979 (Rolf Gutbrod, Frei Otto, Buro Happold, Ove Arup and Partners.)

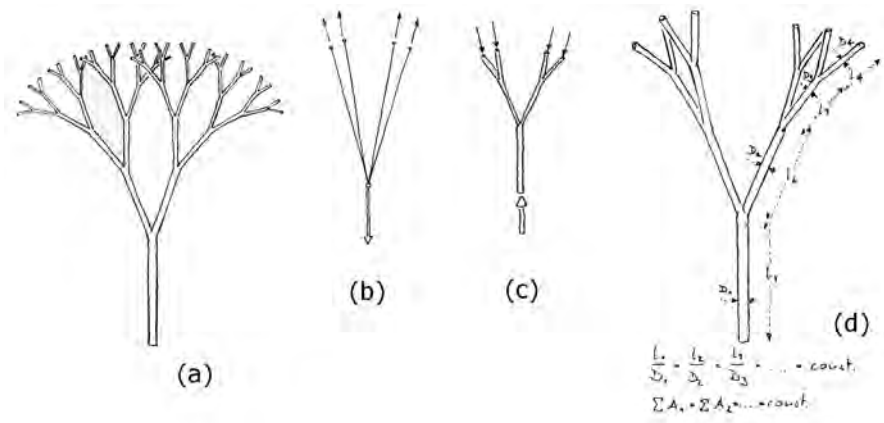


Figure 2.124: (a) Tree-like branching structure; (b) tensile-stressed branching structure; (c) under compression; (d) slenderness increase from top to bottom. Image from (K. Bach 1988).

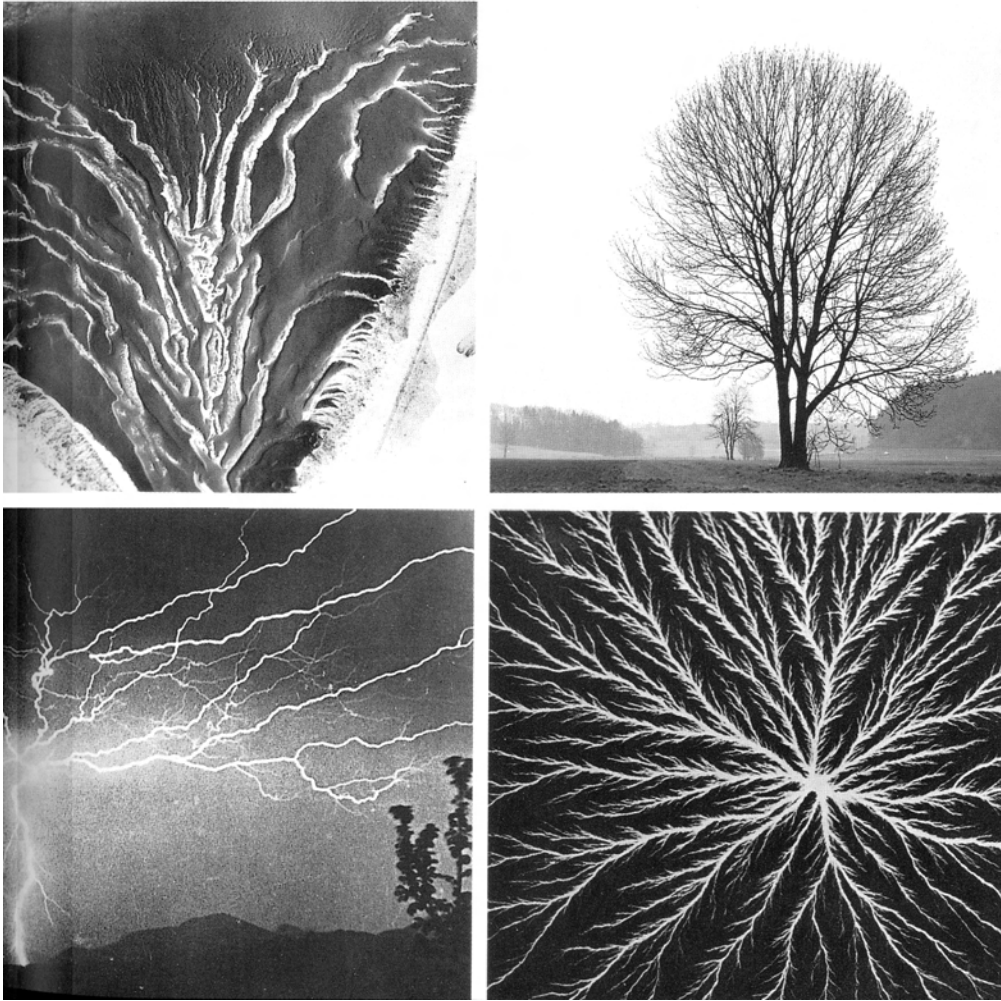


Figure 2.125: Different examples of branching structures found in nature. Image from (K. Bach 1988).

2.5.3.1 Spider webs



Figure 2.126: A spiderweb.

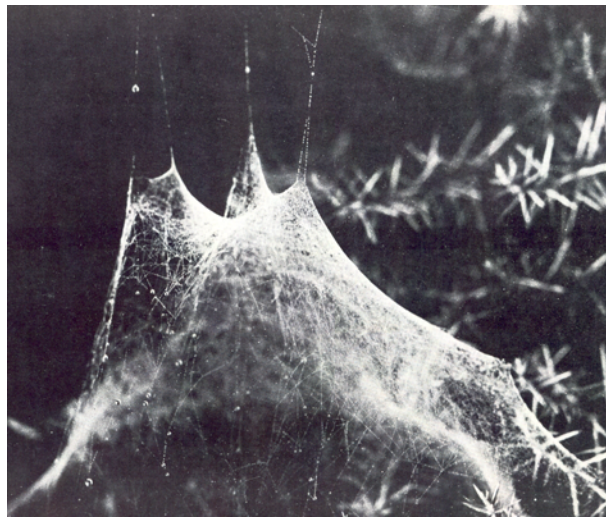


Figure 2.127: Spider web analogy of a membrane structure. Image from (Bach 1975).

Spider webs are investigated in the past by many researchers. D'Arcy Thompson (Thompson 1942) covers spider web's and their principles of surface tension in his book. The books IL6 (Bach 1973) and IL8 (Bach 1975) from the *Institut für Leichttragwerke*, Stuttgart, deal with the similarities between spider webs and cable structures. In the book IL6 (Bach 1973) a start is being made with the comparison of the spider webs from nature and cable-net and membrane structures.

This is continued in the book IL8 (Bach 1975) which extensively covers the analogy of spider webs with structures. The authors describe the thread material, the elements of a web, the web edges, etc. each time with the relationship to structures. The book also reflects on the biological aspects of webbing. Mutoh (Mutoh 2002) describes the use of an analogy of a spiderweb for structural use.

The threads produced by the spider are pure tension elements. The web is fixed at its boundaries, where the tension forces from the web form an equilibrium with the support forces. The web is loaded by its own weight, dew drops, wind loads and the impact of a prey (see Figure 2.128).

Not all spiders make webs. They are all capable of producing silk, but the prey-catching technique of web building is not universal. There are many different kind of webs; the 'ordinary' web



Figure 2.128: Dewdrops on the threads of a spider web.

or orb web, the sheet-like webs, tangle webs, triangle webs, and webs that just look like a jumble of sticky threads (2005b).

All webs exist of tension members incapable of taking moment forces, so the principle of pure tension in the threads is valid for all different types of web.

The angles between the threads explain to the engineer what the ratio between the forces is. The magnitude of the forces is still unknown but the ratio is fixed.

The orb web exist primary of two types of threads; the radial and the spiral threads. A radial thread supports spiral threads. The spiral threads carry blob-like drops. They are made of a viscous liquid (Figure 2.129). The spider uses the sticky blobs to catch its prey.

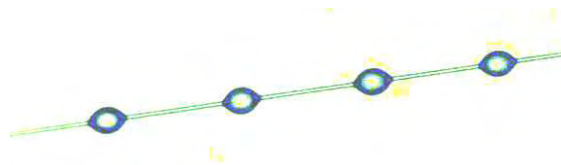


Figure 2.129: Microscopic photo of a thread of a spider web. The small blobs are made of a sticky viscous liquid.

On a damp morning, drops of water may form on the blobs. Sometimes there is one drop per blob; at other times the drops may hang on two blobs each. The weight of the water makes the threads droop into beautiful shapes (see Figure 2.128). If the blobs are equally spaced and the drops are of equal weight, the curves of the threads are close to being catenaries (2005c)(see Figure 2.132).

Finally we have to conclude that the shapes of spider webs arise automatically because of simple physical principles, without any specific action by the spider. In this respect the webs differ from the honeycombs of bees, in which the cells are arranged to use smallest possible amount of wax while retaining enough strength. The bees make hexagonal cells. There is no physics to make this happen automatically - the bees are “programmed” to do it.

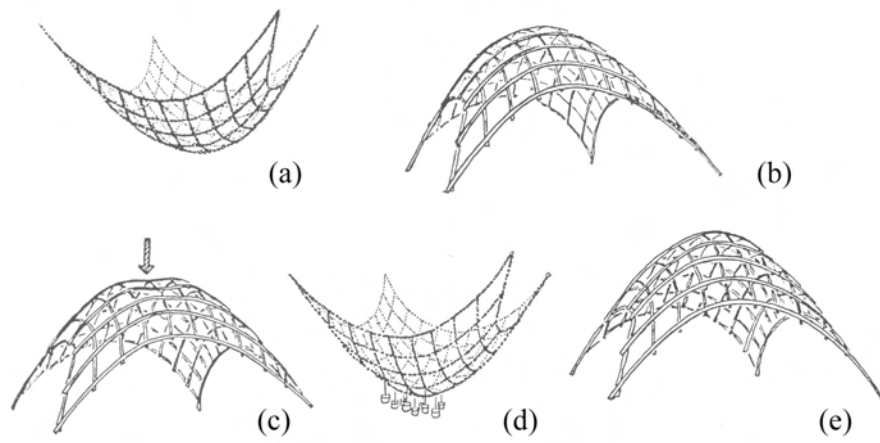


Figure 2.130: Grid shells based on hanging models. Image from (K. Bach 1988).



Figure 2.131: Reconstruction of hanging model from Gaudí. Image from (K. Bach 1988).

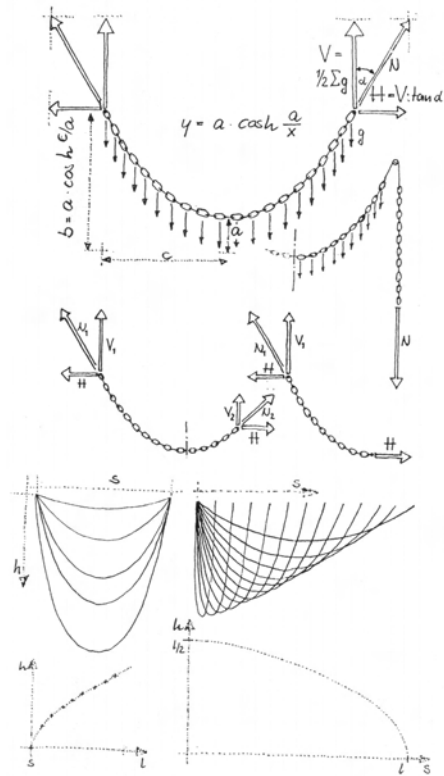


Figure 2.132: Basic geometry of catenary curves. Image from (K. Bach 1988).

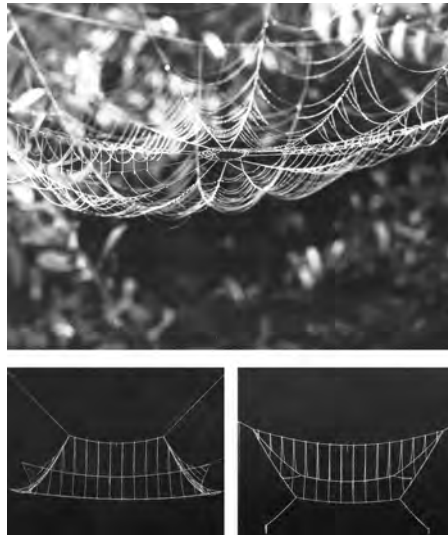


Figure 2.133: Spider web and structures based on webs. Image from (K. Bach 1988).

2.5.4 Sea shells and radiolaria

Beukers (Beukers & Hinte 2001) and the ILEK (Bach 1990) cover the subject of radiolaria, which are creatures in the depth of the ocean which grow lightweight skeletons. The skeletons are optimal for their use and shaped in a hexagonal manner, which often points to the fact that high stresses have to be transferred (see Figure 2.134).

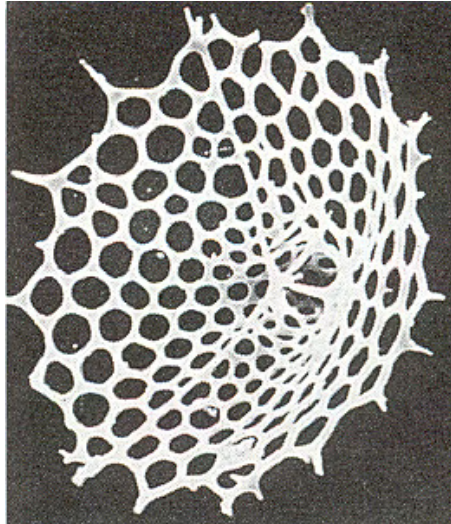


Figure 2.134: Radiolaria. Image from (Beukers & Hinte 2001).

D'Arcy Thompson (Thompson 1942) describes various shell shapes and skeletons of various creatures, such as radiolaria. He shows many examples of structures, which are optimised by growth or form the influence of their surroundings and relates them to mathematical theorems and cellular structures.

A special case he covers is the equiangular spiral (an example of this can be seen in Figure 2.135 and the mathematical counterpart in Figure 2.136), which is thoroughly researched with mathematical formulas from various theorems and base shapes, measurements, etc. Here he clearly shows that nature and mathematics can be very closely related and that although something is mathematically determined, it does not have to be square or triangular. Nature deals with very simple principles which form very complex shapes.

2.5.5 Biomechanics and muscles

From biomechanics and muscles various aspects for the future might be learned. However, currently in structural engineering only very specific aspects could be learned based on the principles that current structures mainly are static and biomechanics mainly is dynamic. However, in mechanical and aerospace engineering many aspects could be learned from nature.

An example of an aspect which could be learned for the near future would be for instance the combination of muscles and tendons. The muscles provide the raw pulling power and the tendons make the system efficient by storing and delivering energy by acting as a spring system (Alexander 1992). This might be used in adaptive structures in the future.

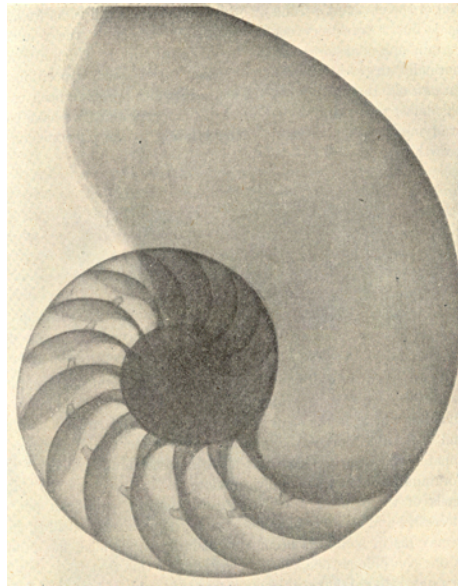


Figure 2.135: Spiral shell. Image from (Thompson 1942).

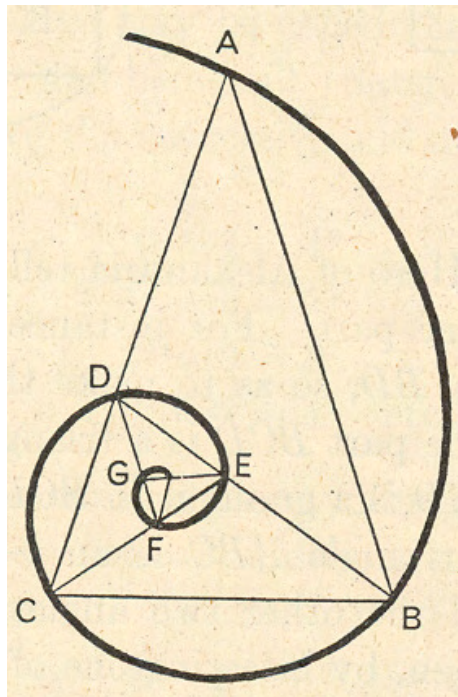


Figure 2.136: Spiral analogy of the spiral shell. Image from (Thompson 1942).

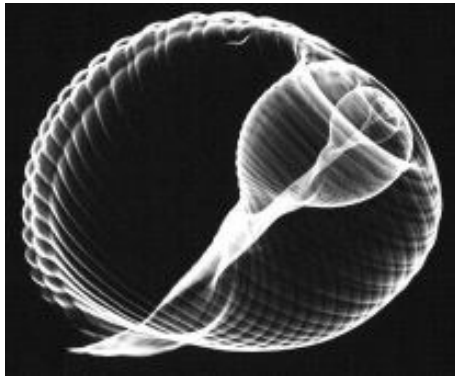


Figure 2.137: X-ray image of a sea shell.

3

Structural concepts

Contents

3.1	Shells and domes	122
3.1.1	Introduction in shell structures	122
3.1.2	Simplified methods to calculate shell structures	122
3.1.3	Instability of shell structures	133
3.2	Cable-net and membrane structures	143
3.2.1	Introduction	143
3.2.2	Evaluation of the computer model	143
3.2.3	Cutting Pattern Generation	147
3.2.4	Post Processing the Cutting Patterns	150
3.2.5	Examples	155
3.3	Pneumatic structures	165
3.3.1	Introduction	165
3.3.2	Principles of form	170
3.3.3	Materials	173
3.3.4	Air pressure	179
3.3.5	Making-up of the fabric	183
3.3.6	Anchorage	185
3.3.7	Building physics	187
3.3.8	Regulations	191
3.3.9	Stabilizing the shape	194
3.4	Space frames	208
3.4.1	Space Frames	209
3.4.2	Formal definition	217
3.4.3	Single layer systems	219
3.4.4	Systems with multiple layers.	222
3.4.5	Polygons as base element for spatial structures	223
3.4.6	Parallel rasters	230
3.4.7	Sphere-shaped truss frames	241
3.4.8	Aspects of construction	249
3.4.9	Stability	271
3.4.10	Calculation	275
3.5	Kinetic and adaptable structures	277
3.5.1	Adaptive structures	277

3.1 Shells and domes

3.1.1 Introduction in shell structures

RECOMMENDED STUDY MATERIAL

Title	Author	Year
Vormgeving in hout	J.H. Pestman	

3.1.2 Simplified methods to calculate shell structures

3.1.2.1 The relationship between form and force of curved surfaces: The Rain Flow analysis

Introduction There is great knowledge of the mechanical behavior of geometrically regular curved surfaces like most shells structures are formed by (Flügge 1960). This is mainly caused by the fact that these surfaces are relatively easily described by analytical mathematical functions. For describing irregular curved surfaces, like those in Free Form Architecture, very little analytical mathematical functions exist and therefore it is very hard to derive formulas to describe their mechanical behavior. One way of dealing with this problem is to calculate the stresses and strains of these irregular curved structures with computer programs based on the finite element method. However the problem is that you only obtain quantitative information about the results (like the magnitude of the forces) but no qualitative information. This does not always give clear insight into the structural behavior. For example, what is the relation between the shape of the curved surface and the flow of forces. In analytical formulas for regular curved surfaces there is a quantitative relation between the magnitude of the forces and the shape of the shell, like the radius. Because of the lack of insight it can be difficult to design irregular curved surfaces which have shell-like behavior that is mainly extension forces and little bending moments.

In 2D structures the load and the supports determine the line of thrust of the load. If the system line of a structure deviates from the line of thrust of the load it will cause "corrective" bending moments in the structure. In 3D structures like shells, for example a dome, the line of thrust of the load can be corrected by the hoop forces so to coincide with the system line of the shell so there are no bending moments in the dome. For a dome where the line of thrust of the load falls outside the system line the hoop forces are compression, and where the line of thrust of the load falls inside of the dome the hoop forces are tension (see Figure 3.1). If we know the "3D line" (surface) of thrust of the load in regards to it's supports and we combine this with any (irregular) curved surface it is possible to determine the forces in the shell. A way of determining the flow of forces of (irregular) curved surfaces is the "rain flow" analysis of the geometry of the curved surface.

Presently there is a tendency to integrate design, calculation and production driven by the possibility to exchange data between CAD-program (Computer Aided Design) and FEM-program (Finite Element Method). This has lead to a wide range of designs for buildings with complex shapes (Free Form Architecture), which sometimes seem to have shell-like behaviour. Shell-like behaviour consists of mainly extension forces and little bending moments, due to the curvature of the surface. These buildings are often calculated by first importing the data of the geometry of the shape made by the CAD-program to the FEM-program, where the structural model is build and calculated. For describing irregular curved surfaces, there are very little simple analytical mathematical functions available and therefore it is very hard to derive formulas to describe their mechanical behaviour. Because of this only quantitative information about the results (like the magnitude of the forces) but not any qualitative information is obtained. This quantitative information doesn't always give clear insight into the structural behaviour. Therefore it is convenient to get insight in the mechanical behaviour of (irregular) curved surfaces, without

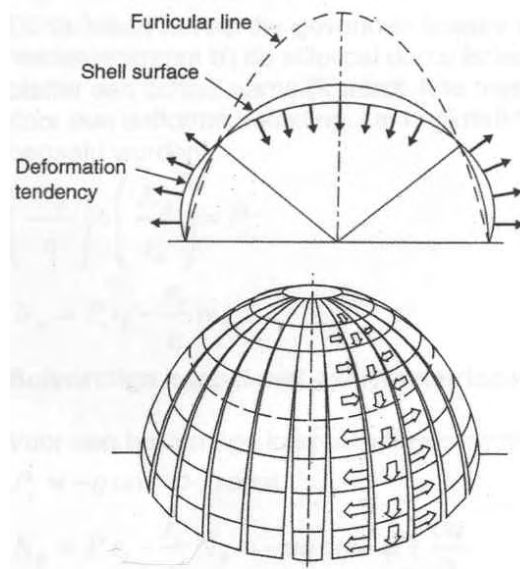


Figure 3.1: Line of thrust of the load (Funicular line) in relation to the Shell surface and the corrective hoop forces. Image from (Schodek 1998).

use of FEM-program or very complicated analytical formulas.

Analytical and graphical solutions for shell structures Many shell theories have been developed to analyse the mechanical behaviour of shell structures. A well-known theory is the membrane theory for thin shallow shells. In the membrane theory it is assumed that the thickness of a shell is far smaller than the overall dimensions. Due to this the flexural rigidity is far smaller than the extensional rigidity. A thin shell subjected to external applied loads therefore mainly produces membrane forces, which are actually resultants of the in-plane normal and shear stresses that are uniformly distributed across the thickness. In the regions where the membrane theory will not hold, because for example edge disturbances, some (or all) of the bending field components are needed to compensate the shortcomings of the membrane field in the disturbed zone. These disturbances have to be described by a more complete analysis, which leads to a bending theory of thin elastic shells. Because of its simplicity the membrane theory gives a direct insight into the structural behaviour and the order of magnitude of the expected response without elaborate computations.

There are several ways to make a classification of surfaces: by using the definition of Gaussian curvature and by using the way the surface is generated. The Gaussian curvature is defined as the product of the two principal curvatures of a surface in a point. When the Gaussian curvature is positive both curvatures are pointing in the same direction and the surface is called synclastic. If the Gaussian curvature is negative both curvatures are pointing in another direction and the surface is called anticlastic. When both the curvatures are zero the surface is flat and is called zeroclastic. When one curvature is zero the surface is called monoclastic. There are several ways to develop surfaces. The main ways are revolution, translation and ruling. Surfaces of revolution are generated by the revolution of a plane curve, called the meridional curve, about an axis, called the axis of revolution. Surfaces of translation are generated by sliding a plane curve along another plane curve, while keeping the orientation of the sliding curve constant. Ruled surfaces are generated by sliding each end of a straight line on their own generating curve, while remaining

the straight line parallel to a prescribed direction or plane. It is also possible to combine several surfaces.

For several well known shells the mechanical behaviour has been formulated by using the membrane theory. The bending moments caused by the edge disturbances can be calculated separately and superimposed with the result of the membrane solution. The predominantly load case is most often its own weight. For the surfaces of revolution shells subjected to its own weight it is always possible to determine the mechanical behaviour with a graphical solution, to give more insight in the flow of forces. By this graphical method it is easily to construct a polygon of forces. This polygon represents the "corrected" line of thrust, whereby the hoop forces correct the line of thrust of the load to coincide with the system line of the shell. A nice example of this graphical method is used to calculate the forces in a masonry dome (see Figure 3.2).

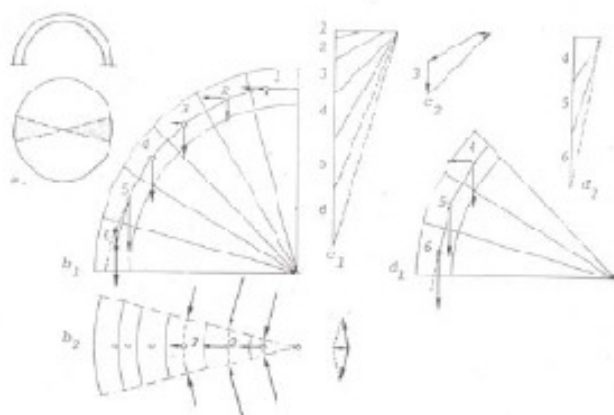


Figure 3.2: Graphical determination of the forces in masonry dome due to its own weight. Image from (Beranek 1988a)

Rain Flow analysis The next hypothesis for the flow of forces in shell structures has been the basis of this method:

Like a rain flow loads will flow along curves with the steepest ascent on the shell surface to its supports.

These curves can be derived from a gradientplot of a surface, which plots the normal vectors of the surface in a view from above. These curves are always orthogonal to the vertical contours of the surface, which are easily to plot. The gradient forces in the vertical sections between curves can then be obtained in the same way as with the masonry dome through the vertical equilibrium of forces. The hoop forces have to be in equilibrium with the horizontal forces, which have to ensure that the pressure surface (line of thrust of the load) converges with the system (line) surface of the shell. The hypothesis has been formulated from studying the way which plates transmit their loads. The maximum shear force in a plate is a vector with the magnitude of the carried load and points in the direction of the flow of the shear force to the supports. The vector of the maximum shear force can be derived from the gradientplot of the surface which represents the sum of the curvatures because the shear force is the derivative of the sum of the bending moments (M):

$$M = \Delta w = \frac{d^2w}{dx^2} + \frac{d^2w}{dy^2} \quad (3.1)$$

As an analogy (the rainflow analogy ((Beranek 1976)) this surface also represents an air inflated membrane, on which the rain flows along curves with the steepest ascent to the supports. In the case for the flow of forces of shells (the hypothesis) the surface of the sum of the curvatures for plates or the surface of the air inflated membrane is replaced by the surface of the shell itself. It is possible to combine straight edge hypars to get a shell as shown in Figure 3.3. It is assumed that the separate hypars act as like a single hypar with diagonal compression and tension parabola. But according to (Lauletta 1961) however the compression forces are dominant and the tension forces merely distribute the loads towards the compression trajectories. This gives in a stress distribution (a results of tests) as shown in Figure 3.4, which resembles the contourplot and gradientplot of the flow of forces according to the hypothesis, shown in Figure 3.5.

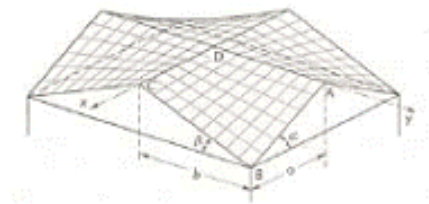


Figure 3.3: Shell combined of several straight edge hypars.

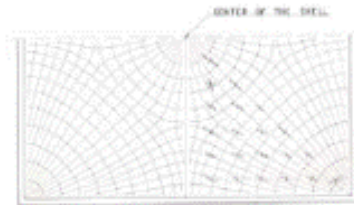


Figure 3.4: Principal stresses in a shell model combined of several straight edge hypars. Image from (Lauletta 1961)

This hypothesis has been tested on a Free Form design at the Faculty of Architecture (Hanselaar 2003) and comprehends of a shell-like structure for a indoor ski-slope (Figure 3.6). The structure spans in the short direction, so that the long sides are pin fixed. A gradientplot of the surface (Figure 3.7) represents the flow of the forces (loads) according to the hypothesis. There are two different kinds of free edges on the short sides. On the left side a raised edge is visible. Because of this raised edge the loads run away from the edge towards the support direction, which leads to a desirable membrane stress distribution. On the other side however the loads run towards the free edge, which then has to transfer the loads towards the supports. This leads to an undesirable situation. In the gradient plot also a couple of drain curves are visible. Loads from curves leading to these drain curves can be transferred by these drain curves like membrane forces under certain conditions. However when the curves leading to these drain

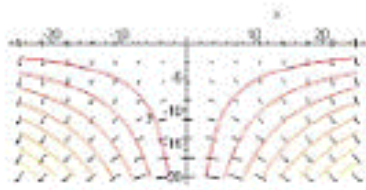


Figure 3.5: Contourplot and gradientplot of the flow of forces of a shell combined of several straight edge hypars.

curves are orthogonal to them large bending moments can be expected. This is visible by the dark bleu color representing large vertical deformations as shown in Figure 4. Looking along a curve large hoop forces can be expected at places where the slope changes rapidly. This is due to the sudden change of the horizontal force that has to ensure that the pressure surface converges with the system surface. These large hoop forces can also result in bending moments.

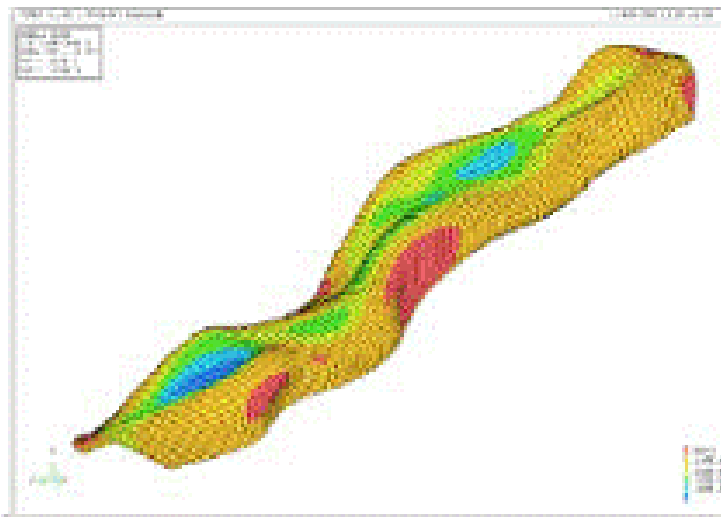


Figure 3.6: Shell-like structure with contourplot of the vertical displacements determined with an elastic calculation (FEM).

3.1.2.2 The relationship between form and force of curved surfaces: A graphical solution

Introduction Because of the geometric complexity of Free Form Architecture it is important to develop systems which are relatively easy to construct. It is also important to develop accessible methods for designers to understand the principle mechanical and structural behavior of these complex structures. These methods are complimentary to computer models, like Finite Element Methods (FEM), which does not always give an insight to the principle mechanical behavior of complex structures. Researchers like Frei Otto made physical models for the



Figure 3.7: Sketch of gradientplot in top view.

understanding of the mechanical behavior of complex structures. We try to develop analytic and semi-analytic / semi-numerical methods.

The aim of this section (Baecke 2005) is on one hand to extend a graphical method (Beranek 1988b) to derive the section forces in an axisymmetric shell and to be able to study the mechanical behavior of these types of shells. The graphical method compared with a FEM calculation gives a very good result. The great advantage of the graphical method is it also gives a good understanding of the mechanical behavior, besides the numeric result.

Graphical solution for shells (Domes) In 2D structures, like arches, the load and the supports determine the line of thrust of the load. If the centerline (axis) of an arch deviates from the line of thrust of the load it will cause "corrective" bending moments in the arch (see Figure 3.8). In 3D structures like shells, for example a dome, the line of thrust of the load can be corrected by the hoop forces so to coincide with the axis of the dome surface so there are no bending moments in the dome (see Figure 3.9).

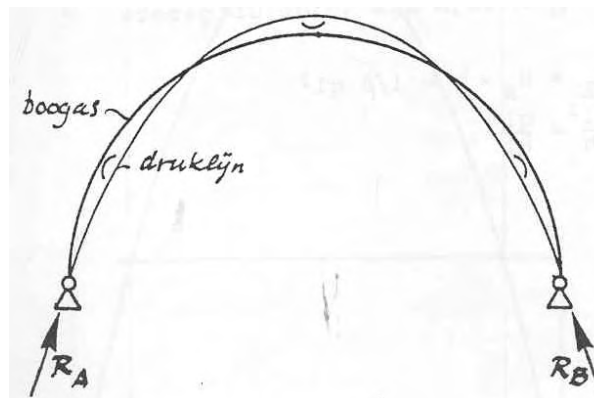


Figure 3.8: Line of thrust of the load (funicular line) in relation the axis of a circular arch.

The stress distribution in domes (in this case a hemispherical dome) is easily verified by means of a funicular polygon. Two "orange peels" are regarded as a linear arch (see Figure 3.10). The loads of the various parts of this arch are easily determined. The shape of the funicular polygon will not coincide with the centerline (axis) of the arch, unless extra horizontal forces are added. If these horizontal forces need to be directed outwards, they can be produced by tangential compressive forces (hoop forces). And if the horizontal forces need to be directed inwards, they can be produced by tangential tensile forces. Thus a true membrane stress distribution may be expected in the dome. The above described example (see Figure 3.10) we take into account that the deformations of the dome under loading are not constrained. For the stresses and deformation

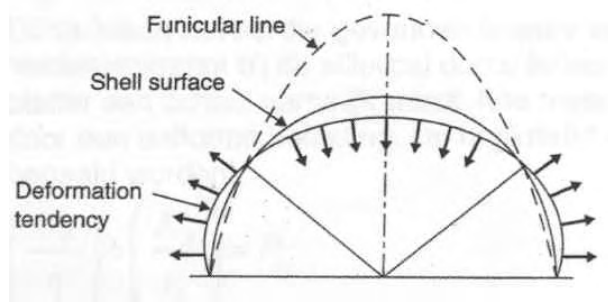


Figure 3.9: Line of thrust of the load (funicular line) in relation to the dome (shell) surface.

is this case see the top two pictures in Figure 3.11 and 3.12. But for most structural uses the base of a dome will pinned round its hemisphere, thus preventing deformations at its spring due to loading (bottom two pictures in Figure 3.11 and 3.12). This has as a consequence for the tensile hoop forces at the spring; these will be zero in stead of maximum in the unconstrained case.

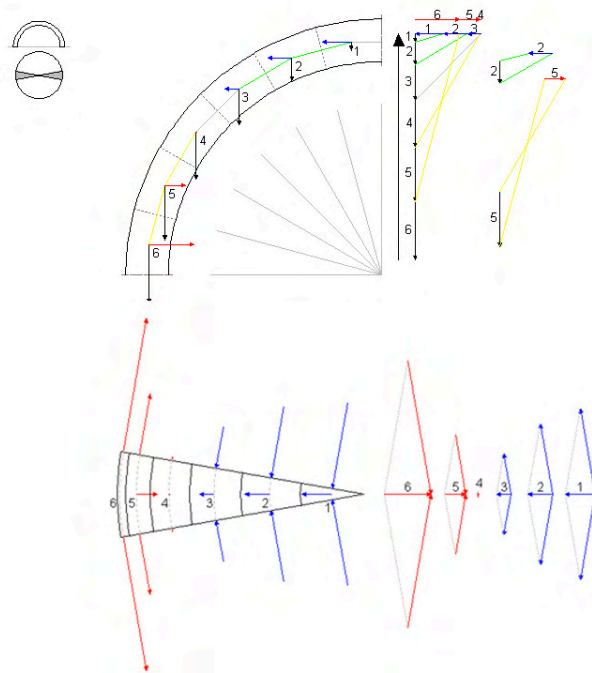


Figure 3.10: Polygon of forces in dome section.

Graphical solution for a dome with an oculus If we take a section of a (in this case a top part of a) dome with an oculus and determine the forces needed to make global equilibrium with the loads we need an outward horizontal force in the top and an inward horizontal force in the spring (see Figure 3.13). A tangential compressive "ring force" (hoop forces) in the top can produce the outward horizontal force and a tangential tensile "ring force" (hoop forces) in

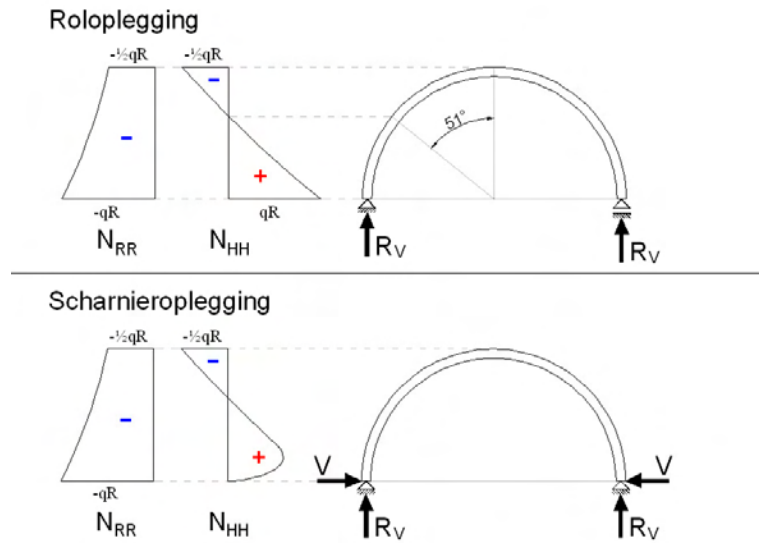


Figure 3.11: Hoop forces (N_{HH}) and meridional forces (N_{RR}) in a dome pinned in one point and on rollers round the hemisphere at its spring (picture above) and a dome pinned round the hemisphere at its spring (picture below).

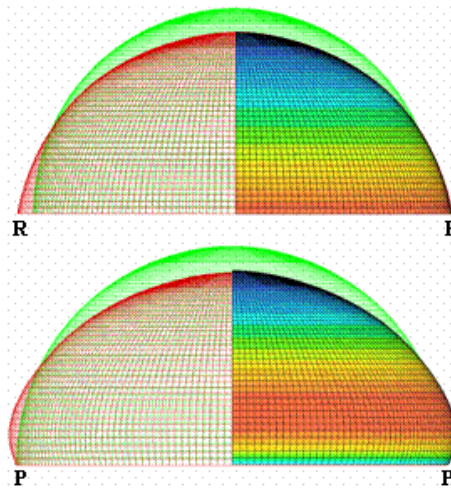


Figure 3.12: Deformation of a dome pinned in one point and on rollers round the hemisphere at its spring (picture above) and deformation of a dome pinned round the hemisphere at its spring (picture below).

the spring can produce the inward horizontal force in the spring (Figure 3.14). If we compare this with the hoop forces in a dome without an oculus we can see as a similarity compression hoop forces in the top and tensile hoop forces at the spring, the difference is that because of the oculus the hoop forces will be more concentrated towards the oculus at the edge to form a "ring force" (Figure 3.15), the numerical result verifies this (top picture in Figure 3.17). If

we again take two "orange peels" and regard those as a linear arch we can determine the stress distribution by means of a funicular polygon (Figure 3.16). This graphical result is verified by a numerical calculation (Figure 3.17), the graphical solution gives the correct analysis and the correct magnitudes compared to the numerical solution. Because in this case not a hemispherical dome was taken but only the top part of a dome the support reaction will not only have a vertical resultant (carrying the weight) but also a horizontal resultant (Figure 3.18), which would not be needed for a hemispherical dome, which deformation are unconstrained (Figure 3.10 and top picture of Figure 3.11).

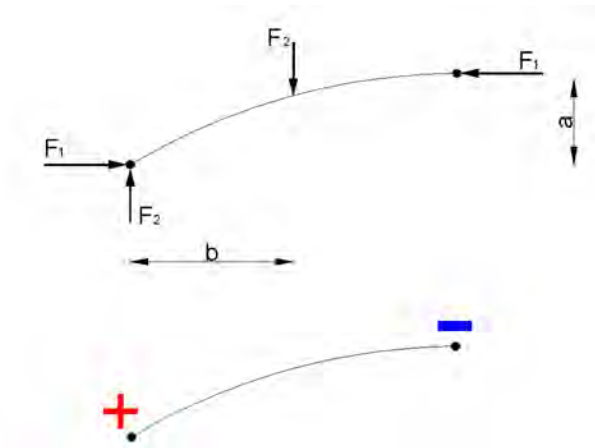


Figure 3.13: Equilibrium of forces in a section of a dome with an oculus.

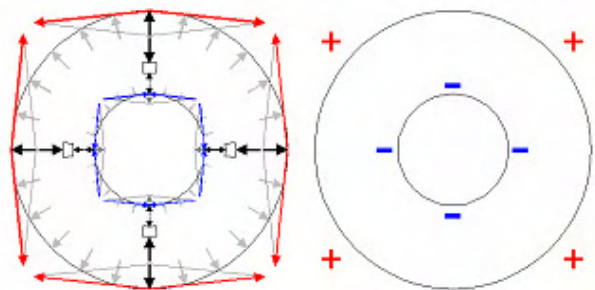


Figure 3.14: Hoop (ring) forces in a dome with an oculus.

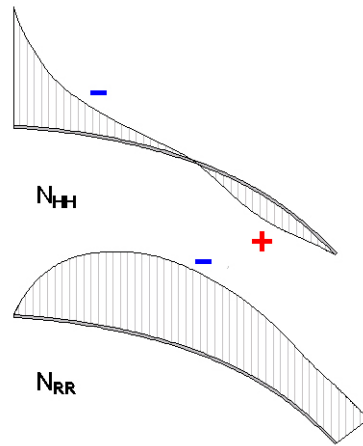


Figure 3.15: Hoop forces (N_{HH}) and meridional Forces (N_{RR}) in a section.

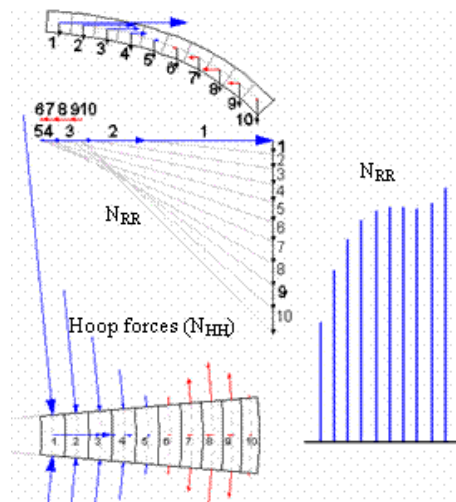


Figure 3.16: Polygon of forces in a section.

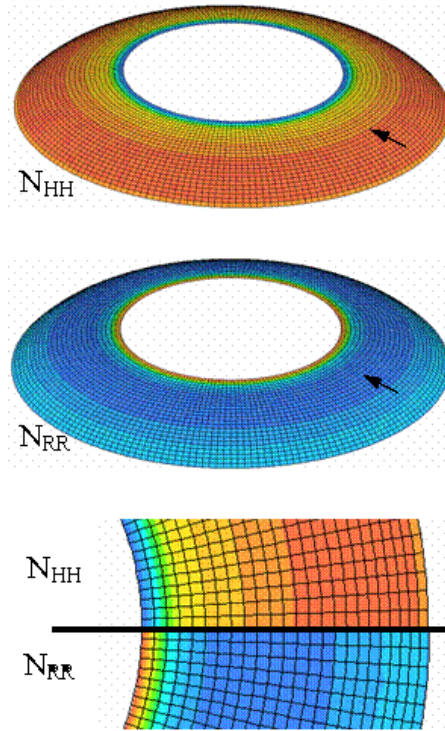


Figure 3.17: Hoop forces (N_{HH}), above, and meridional forces (N_{RR}), below, numerically calculated.

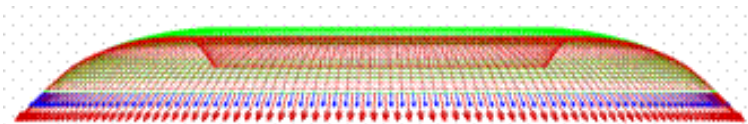


Figure 3.18: Support reactions.

Graphical solution for an axisymmetric "Donut like" shell In the following case we examine a axisymmetric shell with a hole, like the dome with an oculus, but in this case the highest point in the section is not at the inner ring next to the oculus but somewhere between the spring and the inner ring (see Figure 3.19).

For the global equilibrium with the loads this means the outward horizontal force will be in the highest point, which in this case, does not coincide with the inner ring next the hole as it did with the dome with an oculus, thus creating the greatest arm for equilibrium (see Figure 3.20). As a consequence the tangential compressive "ring force" (hoop forces) needed to produce the outward horizontal force is also in the highest point (see Figure 3.21), the graphical solution (see Figure 3.22) and the numerical calculation verifies this (see Figure 3.23). Another interesting aspect with this example is the type of meridional forces. In the case with the dome and the dome with an oculus the meridional forces are compression, they carry the loads straight down to the supports. In this case the loads first have to be carried up from the inner ring next to the hole to the highest point, by tensile meridional forces, and from there down to the supports by compressive meridional forces (bottom picture, Figure 3.21 and Figure 3.24). The graphical solution gives the correct analysis, as it does with the dome and the dome with an oculus.

Both graphical as numerical solution give a remarkable result in respect to the hoop forces in the highest point. As pointed out the compressive "ring forces" are in the highest point, but the hoop forces on both sides of these compressive "ring forces" are tensile hoop forces, this is a result of the equilibrium. This sudden change in hoop force from tension to compression to tension again has a large impact on the deformations. Hoop forces will cause extensions in the tangential direction, the compression hoop forces will shorten the rings and the tensile hoop forces will elongate the rings (see Figure 3.27), thus resulting in a sharp dip in the deformations (see Figure 3.25 and 3.26).

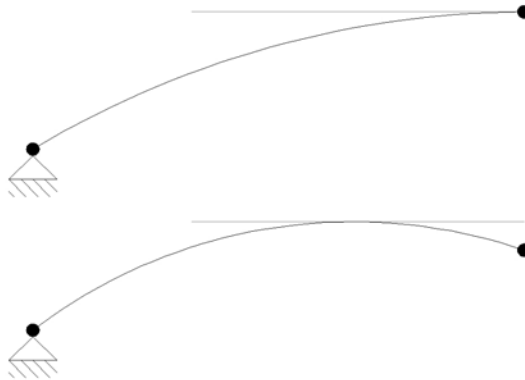


Figure 3.19: picture above: dome with an oculus, picture below: axisymmetric "donut like" shell.

3.1.3 Instability of shell structures

Shells are very efficient in carrying load. However, this efficiency comes at a price. If a shell fails it fails with a bang. There will be no warning and it will collapse faster than we can run.

Ferrybridge. Three reinforced concrete cooling towers collapsed in Ferrybridge UK on November 1st 1965 (Fig. 1). Strong winds triggered the successive collapses. All chunks of concrete fell inside the towers. There were no fatalities or injuries because there were no workers either

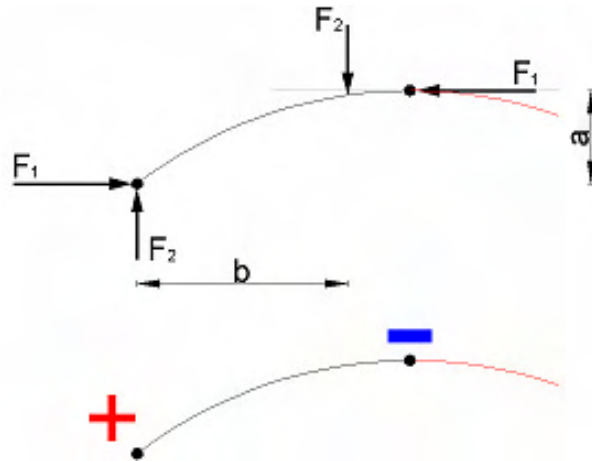


Figure 3.20: Equilibrium of forces in a section of an axisymmetric "donut like" shell.

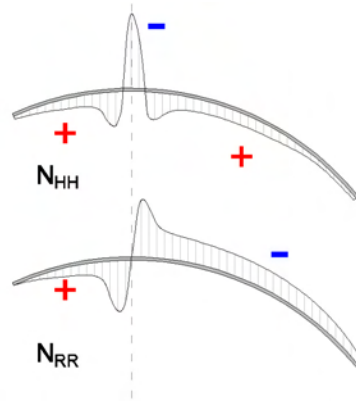


Figure 3.21: Hoop forces (N_{HH}) and meridional Forces (N_{RR}) in a section.

on or inside the tower at the time. The cooling towers were part of a group of eight at a power station. The remaining towers sustained severe structural damage. The towers were 115 m high.

Two factors caused the collapse. The average wind speed over a one minute period, was used in design whereas, in reality, the structures are susceptible to much shorter gusts. The wind loading had been based on experiments using a single isolated tower. The grouping of the towers created turbulence on the leeward towers that collapsed.

In-extensional deformation. An in-extensional deformation is a deformation in which only bending occurs while membrane extension and contraction do not occur. Shells that have zero Gaussian curvature over large areas are susceptible to in-extensional deformation. Since shells are thin they have very little bending stiffness. Therefore, a shell needs to be designed such that in-extensional deformations cannot occur. A scaled down physical model of a shell can be used to study in-extensional deformations that might be possible. Also a finite element program can be used. The smallest natural frequencies and especially the associated normal modes will show any in-extensional deformations that might be possible.

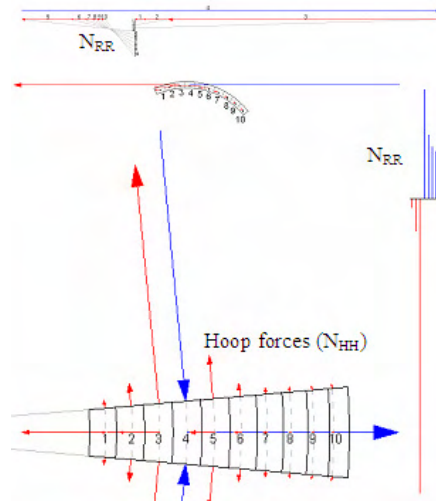


Figure 3.22: Polygon of forces in a section.

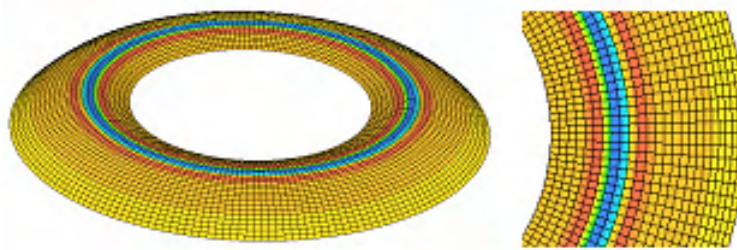


Figure 3.23: Hoop forces (N_{HH}) numerically calculated.

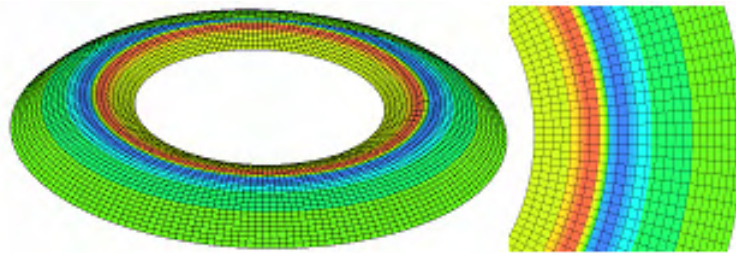


Figure 3.24: Meridional forces (N_{RR}) numerically calculated.

Differential equation for shell buckling The structural behaviour of shells including large displacements is described by an eight order differential equation (Hoefakker & Blaauwendraad 2003)

$$\frac{Et^3}{12(1-\nu^2)} \nabla^2 \nabla^2 \nabla^2 \nabla^2 u_z + E t \Gamma^2 u_z = \nabla^2 \nabla^2 p_z - n_x x u_{z,xx} - 2 n_{xy} u_{z,xy} - n_{yy} u_{z,yy} \quad (3.2)$$

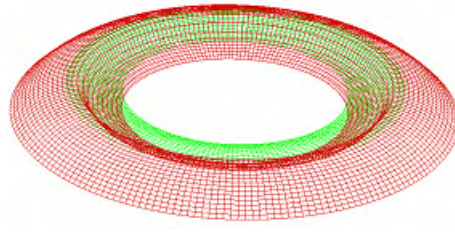


Figure 3.25: Deformations with sharp dip at the hole.

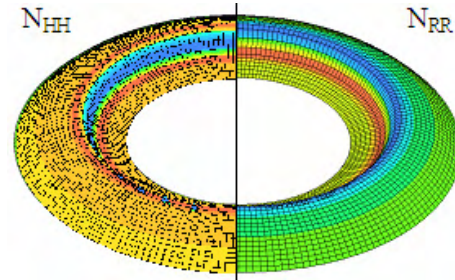


Figure 3.26: Hoop forces (N_{HH}) and meridional forces (N_{RR}) plotted on the deformed surface.

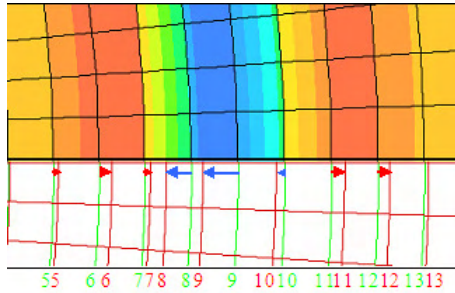


Figure 3.27: The hoop forces will cause extensions in the tangential direction, compression hoop forces will shorten the rings, and tensile hoop forces will elongate the rings, thus resulting in a sharp dip of the deformations.

where u_z is the displacement perpendicular to the shell surface, p_z is the loading perpendicular to the surface. Γ^2 and ∇^2 are operators.

$$\begin{aligned} \nabla^2 &= \frac{\partial^2(\cdot)}{\partial x^2} + \frac{\partial^2(\cdot)}{\partial y^2} \\ \Gamma^2 &= k_x * \frac{\partial^2(\cdot)}{\partial y^2} - 2 * k_{xy} \frac{\partial^2(\cdot)}{\partial x * \partial y} + k_y * \frac{\partial^2(\cdot)}{\partial x^2} \end{aligned} \quad (3.3)$$

The x and y direction often are not linear but are plotted on the surface of the shell. The differential equation can be solved analytically for elementary shell shapes and elementary loading (Table 3.1.3). E is Young's modulus, ν is Poisson's ratio, t is the shell thickness and a is the radius of the middle surface of the shell.



Figure 3.28: Three collapsed cooling towers at Ferrybridge.

Yoshimura pattern. The buckling shape of an axially loaded cylinder can be a "ring pattern" or a "square pattern" (Figure 3.29). Which one occurs depends on the shell thickness and its radius. When buckling progresses the "ring pattern" can transform into the "square pattern". When the material starts to deform plastically the shape adopts a "rhombic pattern". The latter is called a Yoshimura pattern (Yoshimura 1955) (Figure 3.30). Remarkable about the Yoshimura pattern is that it is in-extensional. Fortunately, large extensions are needed before the Yoshimura pattern is obtained.

Imperfection sensitivity. Experiments on axially compressed cylinders show that the maximum load is much smaller than the critical load (Figure 3.32). This is caused by extreme softening of a cylinder after buckling. Figure 3.33a shows the behaviour of a perfect cylinder under perfect loading. This result can only be obtained analytically because in reality perfect cylinders do not exist. Figure 3.33b shows that small imperfections cause a large reduction of the maximum load. Imperfections include dents, residual stresses, temperature stresses, inhomogeneities, creep, shrinkage, eccentricity of loading and first order deformations. Not only compressed cylinders but also bent cylinders and radially compressed domes are very sensitive to imperfections. Hyppars are not sensitive to imperfections.

Experiment. What is the carrying capacity of an axially loaded empty beer can? We model the can as an open cylinder. The wall thickness is $0,08\text{mm}$ the radius is $32,8\text{mm}$, Young's modulus is $2,1 \cdot 10^5 \text{ N/mm}^2$ and Poisson's ratio is 0.35. According to Table 3.1.3 the critical loading is:

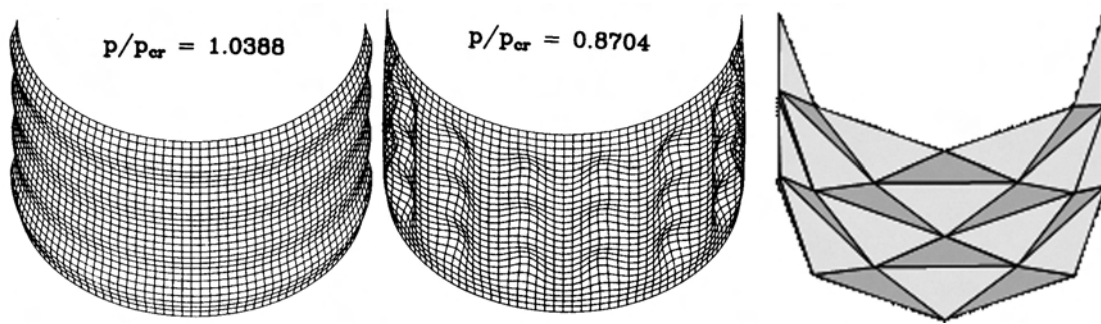


Figure 3.29: Buckling modes of an axially compressed cylinder (Baant & Cedolin 1991) (only half the cylinder is shown).



Figure 3.30: Experiment on an aluminium cylinder (Note the Yoshimura pattern).

$$n_{cr} = \frac{-1}{\sqrt{3(1-\nu^2)}} \frac{Et^2}{a} = \frac{-1}{\sqrt{3(1-0,35^2)}} \frac{2,1 \cdot 10^5 \cdot 0,08^2}{32,8} = -25,3 N/mm \quad \alpha \quad (3.4)$$

$$F_{cr} = 2\pi a n_{cr} = 2 * 3,14 * 32,8 * (-25,3) = -5200 N$$

Therefore, it should be able to carry a mass of 520 kg, Carefully stand on the can and it will - probably - carry your weight. Subsequently, use your thumbs to push many little dents in the can and push them out again. Doing so makes typical clicking sounds. Notice that the imperfections you made are hardly visible. Now, try standing on the can again. It will collapse abruptly. The explanation is imperfection sensitivity. When folded back you can recognise the typical Yoshimura buckles.

Prof. Koiter. Warner Tjardus Koiter (1914-1997) was professor at Delft University of Technology at the faculties of Mechanical Engineering and Aerospace Engineering (1949-1979). He wrote his dissertation during the Second World War and published it just after the war (Koiter 1945). The English translation appeared in 1967 (Koiter 1967). In this he developed a theory for initial postbuckling behaviour of structures. It became famous because it explains the considerable difference that was found between critical loads and experimental maximum loads.

	Critical loading $p_{cr}[N/m]$	Critical membrane force $n_{cr}[N/m]$	Imperfection sensitive
Open cylinder, radially loaded (in-extensional deformation)	$\frac{1}{4(1-\nu^2)} * \frac{Et^3}{a^3}$	$\frac{-1}{4(1-\nu^2)} * \frac{Et^3}{a^2}$	no
Open cylinder, axially loaded		$\frac{-1}{\sqrt{3(1-\nu^2)}} * \frac{Et^2}{a}$	yes
Open cylinder, torsion loaded		$\frac{1}{3\sqrt{2}(1-\nu^2)^{\frac{3}{4}}} * E\sqrt{\frac{t^5}{a^3}}$; shear force	no
Hyperboloid, axially loaded (cooling tower)		$\frac{-1}{\sqrt{3(1-\nu^2)}} * \frac{Et^2}{a}$	yes
Closed cylinder, loaded in all directions	$\frac{2}{\sqrt{3(1-\nu^2)}} * \frac{Et^2}{a}$	$\frac{-1}{\sqrt{3(1-\nu^2)}} * \frac{Et^2}{a}$; hoop direction	yes
Sphere	$\frac{2}{\sqrt{3(1-\nu^2)}} * \frac{Et^2}{a}$	$\frac{-1}{\sqrt{3(1-\nu^2)}} * \frac{Et^2}{a}$	yes
Dome; base radius $> 3, 8\sqrt{at}$	$\frac{2}{\sqrt{3(1-\nu^2)}} * \frac{Et^2}{a}$	$\frac{-1}{\sqrt{3(1-\nu^2)}} * \frac{Et^2}{a}$	yes
Hyppar	$\frac{2}{\sqrt{3(1-\nu^2)}} * \frac{Et^2}{a}$	$\frac{-1}{\sqrt{3(1-\nu^2)}} * \frac{Et^2}{a}$	no

Table 3.1: Critical loading and critical membrane forces for elementary shells.



Figure 3.31: A simple beer can.

Koiter's laws. The equilibrium of a perfect system can be described by

$$\lambda = \lambda_{cr}(1 - c_1 w - c_2 w^2) \quad (3.5)$$

Where λ is the load factor, λ_{cr} is the critical load factor, w is the amplitude of the deflection, c_1 and c_2 are constants characterising the given structure. There are three types of post critical behaviour (Figure 3.34). Type I behaviour occurs when $c_1 = 0$ and $c_2 < 0$. The structure is not sensitive to imperfections. Type II behaviour occurs when $c_1 = 0$ and $c_2 > 0$. The structure is sensitive to imperfections. The maximum load factor is equal to

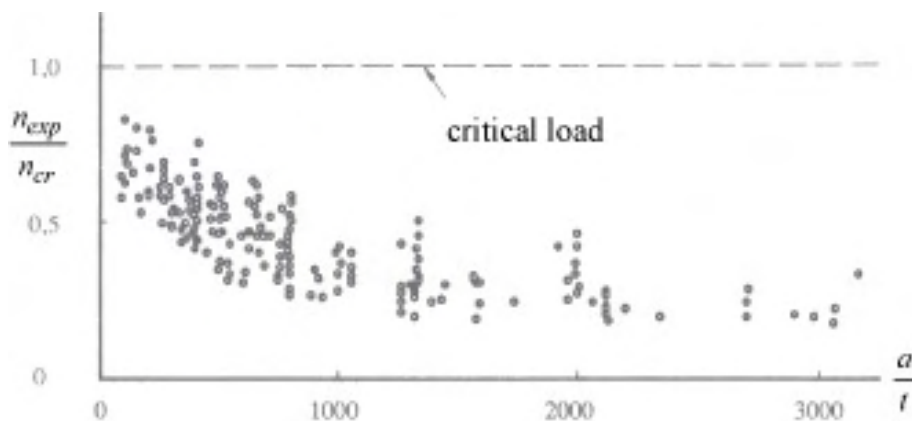


Figure 3.32: Experimental maximum loads of 172 axially loaded cylinders. (Weingarten et al. 1965)

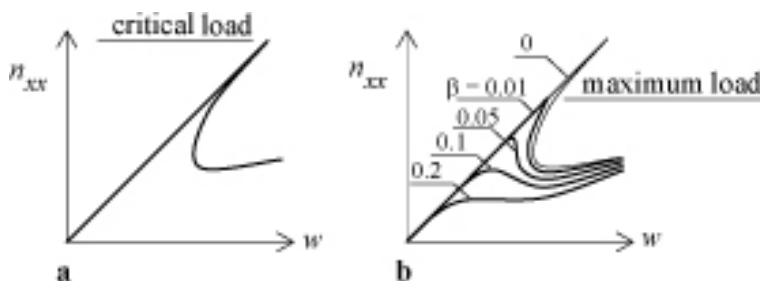


Figure 3.33: Buckling of cylinders for different unevenness size β . (Weingarten et al. 1965)

$$\lambda_{max} = \lambda_{cr} \left(1 - 3 \left(w_0 \frac{1}{2} \rho \sqrt{c_2}\right)^{\frac{2}{3}}\right) \quad (3.6)$$

Where ρ is a coefficient depending on the imperfection shape and w_0 is the imperfection amplitude. This is called the $\frac{2}{3}$ -power law. Type III behaviour occurs when $c_1 > 0$. The structure is very sensitive to imperfections. The maximum load factor is equal to

$$\lambda_{max} = \lambda_{cr} \left(1 - 2(w_0 \rho c_1)^{\frac{1}{2}}\right) \quad (3.7)$$

This is called the $\frac{1}{2}$ -power law (Figure 3.35).

Knock down factor. In shell design often the following procedure is used. First the critical loading is computed by using formulas or a finite element program. Then this loading is reduced by a factor that accounts for imperfection sensitivity. The result needs to be smaller than the design loading. This factor is often called "knock down factor". It is experimentally determined. For example for reinforced concrete cylindrical shells loaded in bending the following knock down factor C is used.

$$C = 1 - 0,73 \left(1 - e^{-\frac{1}{16} \sqrt{\frac{a}{t}}}\right) \quad (3.8)$$

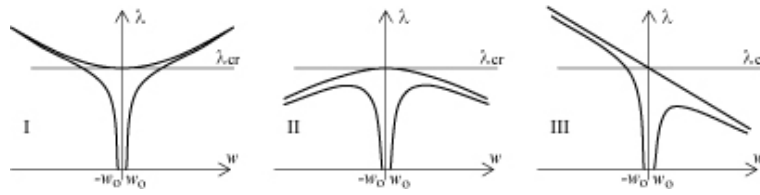


Figure 3.34: Basic types of post buckling behaviour.

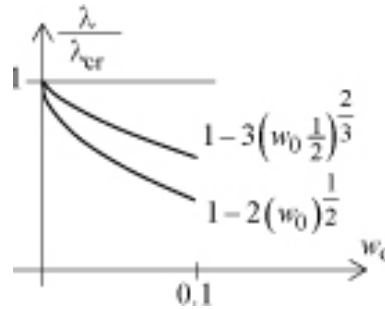


Figure 3.35: Maximum load as a function of the imperfection amplitude.

The range in which it is valid is $0,5 < \frac{l}{a} < 5$ and $100 < \frac{a}{t} < 3000$ where l is the cylinder length (Farshad 1992).

Finite element analysis of buckling. Finite element programs can compute critical load factors and the associated normal modes. The real critical load is represented by the smallest load factor because a shell will buckle at the first opportunity it gets. If the second smallest buckling load is very close (say within 2%) to the smallest buckling load we can expect the structure to be highly sensitive to imperfections. This is because the interaction of buckling modes gives a strong softening response after the critical state. For shells that are sensitive to imperfections the maximum load factor might be as small as 1/6 of the critical load factor.

Nonlinear finite element analysis. If a shell is sensitive to imperfections a different kind of finite element analysis is necessary. In this geometrical nonlinear analysis the loading is applied in small increments for which the displacements are computed. Such analyses should be only performed by experts. It involves equilibrium iterations, path following methods and termination criteria. (See the course CT5142 Computational methods in nonlinear solid mechanics). Figure 3.36 shows the results of different finite element computations of a simply supported shallow dome.

Design formula. Using the formulas in Table 3.1.3 and the knock down factor in Figure 3.32 we can derive a formula for the required thickness of a shell

$$t = \sqrt{10 \frac{-n_2 a}{E}} \quad (3.9)$$

Where E is Young's modulus, a is the shell radius in the direction of n_1 and n_2 is the smallest principal membrane force. Note that n_2 needs to have a negative value because shells buckle only due to compression. For hyppars the factor 10 in the formula needs to be replaced by 1.7.

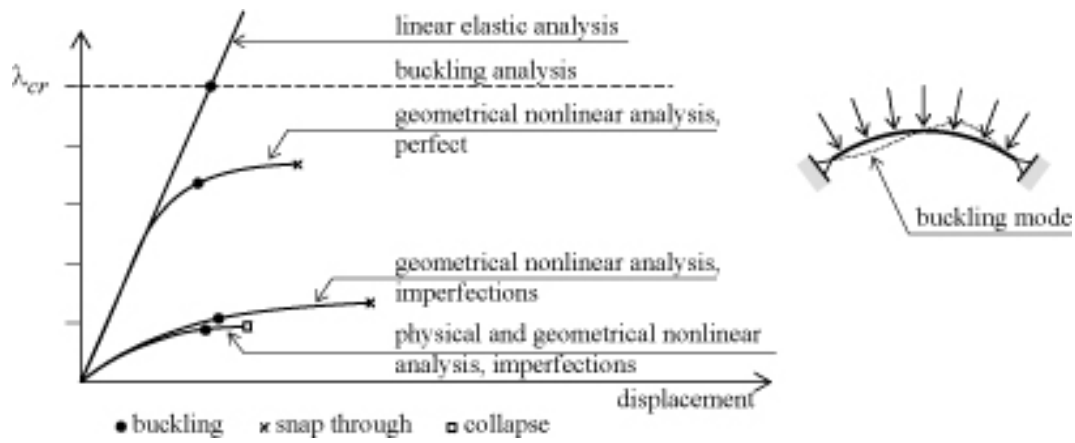


Figure 3.36: Shell finite element analysis of a shallow dome (Farshad 1992).

Small shells of reinforced concrete often will be thicker than this formula predicts because there needs to be sufficient cover on the reinforcing bars.

3.2 Cable-net and membrane structures

RECOMMENDED STUDY MATERIAL

Title	Author	Year
European Design Guide for Tensile Surface Structures.	B. Forster, M. Mollaert	2004

3.2.1 Introduction

Nowadays membrane structures are produced by using computer software. A model of the required shape is generated and load analyses are performed. A large benefit of using computer software for the analysis of tensile structures is the possibility to determine reaction forces on the supporting structure in extreme situations. When no computer software is used, these forces have to be obtained by means of physical modelling. In this case, the scale factor of the physical model causes large deviations in the forces, so a large safety factor needs to be used.

Another benefit of using computer software for the realisation of tensile structures is the ability to generate cutting patterns. These are needed to enable the creation of larger membranes out of small parts. The parts need to have a specific form. When they are assembled, they must form the required shape. The generation of these patterns can be done precise and convenient by means of computer software.

There is one serious drawback of using computer software. It is difficult to get feeling with the structure. It is represented as a computer model, an estimation of reality. Very often large structures are visualised at the size of the computer screen, which makes it difficult to understand the size of the structure. It requires experience and common sense to translate computer data into useful data for manufacturing.

3.2.2 Evaluation of the computer model

The starting point for the evaluation is the computer model. The model is generated to represent the required shape. During the form finding stage the shape is adapted to the limitations and requirements of the customer. And the eye of the designer has checked the shape for its aesthetics. Load analyses are performed to get reaction forces and to dimension the supporting structure. The final stage is the translation of the computer model into usable data. However, the model needs to be checked on several points:

- What kind of model exist to represent the shape?
- Is this model capable of representing the required shape?
- Is the way of representing the fabric in accordance with the way of the cutting pattern generation?

What kind of computer models exists? A computer program needs a way to order the information about the surface to be described. When a finite element method is used, the surface is cut into small pieces and for each piece the forces are calculated. The way of cutting the surface into pieces is called the discretisation of the surface. The purpose of the discretisation is to make the best approximation of reality possible. A very common way of discretisation of membrane surfaces is to generate a mesh. The mesh is triangulated to be able to make planar elements. The mesh is stretched into the right shape. Another way to discretise the surface is to project a mesh upon the plan view of the surface and cut it with the boundaries. In this way the mesh is not deformed to fit to the boundaries. This approach is used within EASY.

The discretisation of the surface divides the surface into small pieces, the elements. An

element can have different properties. It can be, for example, a cable element of a membrane element. A cable element is a 1-dimensional element. It represents the stiffness of a cable only in the length direction of the cable. A membrane element is a 2-dimensional element. It represents the membrane, so it has to take into account the stiffness of an area. When the surface is triangulated, one triangle represents a membrane element and therefore the area of the triangle represents the membrane. When the surface is not triangulated, one bar element represents half the width towards both sides of the bar to be the membrane.

When a radial type of roof is used, a radial mesh is generated. This mesh can again be stretched into the right shape or projected upon the plan view of the structure and being cut by the boundaries. It is much better to have a radial mesh when a radial structure is used.

Depending on the type of program that is used, a form can be calculated according to the chosen mesh. There are different approaches. It is possible to generate a minimal surface; this is a surface with the same stresses in all directions. Such a shape is only valid for one load case. When the loads change, the form should change as well, in order to stay a minimal surface. But it is regarded as a good starting point for an initial form. Programs based upon this principle are called dynamic relaxation programs.

Another approach is the Force Density approach. This method is based upon linearization of the non-linear equation system by introducing a new parameter; the force divided by the length of the bar. The non-linear equation system, meant to solve the equilibrium of internal and external forces, now suddenly is a linear system which is easy to solve. Therefore very quick form finding is possible. EASY is based upon this system. It is possible to generate a minimal surface with this approach, it then requires more iterations.

Not every shape is suitable to be a minimal surface; especially radial roofs cannot be a minimal surface. The top of the structure has always higher stresses than the perimeter of the structure.

Does the model represent the required shape? After choosing the model and doing the form finding, the model needs to be evaluated:

1. Does the model look like the required shape?

If not, the shape must be adapted by changing the internal stresses in the fabric or changing the fixed points. This is a matter of aesthetics. With the assistance of a software package, in principle all tools are present to adapt the shape completely to the wishes of the designer. If more elevation or curvature is wanted, it can be adapted, within the restrictions of the starting points.

2. Are all the necessary parts modelled?

For example, if there is a hole in the fabric, is there a hole in the model too. This seems to be a very obvious remark, but it is very easy to simplify the structure too much. When there is a hole in the fabric, it has great influence upon the stress behaviour of the material. Another aspect is use of ridge and valley cables. Are they attached to the membrane or just adjacent to the fabric. When the cables are attached to the fabric they will carry a part of the stresses. If not, all the stresses are transported to the tensioning points, which results in high stresses.

Something that easily can be forgotten, are the links between the fixed points and the fabric. The fabric does not reach to the fixing points exactly, there is always a connection needed. This link can cause changes in shape, so it should be modelled. The same holds true for the elastically supported fixed points. These points can slightly move and therefore can influence the shape, which means that they should be modelled as well.

Also of large influence upon the stress behaviour of the shape is the width of the mesh in proportion to the size of the structure. When the structure is much curved and only a few elements are used to represent the surface, the elements need to be deformed very

much to answer the equilibrium equations. Firstly the shape usually does not answer to the expected aesthetic qualities and secondly a very high stress surface originates. Therefore always choose elements in such a manner that they are not deformed too much during form finding. It may take more form finding runs to find the right mesh.

Can the model be used for cutting pattern generation? One of the most important purposes of using computer modelling is the generation of cutting patterns. But the model must be useful for the generation of cutting patterns; else it is of no use having such a model. The model represents the membrane and the membrane is materialised with a fabric. A fabric is a woven material. The warp threads are between the loom and the weft threads are woven in between. The warp threads are tensioned during the weaving process, and the weft threads therefore pace up and down. When the weft direction is tensioned, it will strain much more than the warp direction. So fabric is a non-homogenous material which cannot resist shear forces. Warp and weft threads are orthogonal to each other, so the model must represent this feature of the material. The direction of the mesh indicates the direction of the warp and weft direction of the fabric. When the form finding is executed, it must be checked whether the cutting pattern orientation is according to the mesh orientation.

For the statical analysis, a stiffness is entered, for both warp and weft direction a different value. Does this stiffness still represent the directions of the threads in the cutting patterns? Usually the mesh is oriented in the direction of the primarily curvature. Then there will occur less shear in the surface. So the cutting pattern orientation will also need to be in the direction of the principle curvature to get the best results when the patterns are assembled. When the model is not a good base for creating cutting patterns, it must be decided whether the model will have to be adapted or not. Adapting the mesh will change the shape, so a new form finding procedure is started. But when good results are requested, it is better to have a good model to start from.

Example Following example is a preliminary design for a mobile stage covering. The design is made by Mick Eekhout (Eekhout 1989). The first attempt to model the preliminary design, is showed in Figure 3.37.

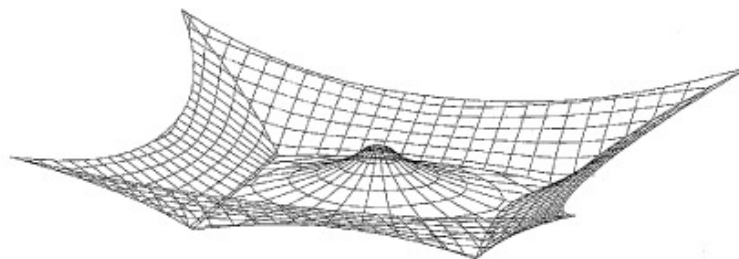


Figure 3.37: Preliminary design for a mobile stage covering.

There are four lower points, which will be supported by masts and which form the corner points of the stage. The rest of the points are supported by a space frame which is situated above the membrane. In principle this form answered the preliminary design requests. Next phase is to examine this shape to make sure it can be used for generating cutting patterns.

First mandate is to think of the type of modelling that is used. For this particular case is made use of EASY, which is based upon Force Density form finding, so the found shape is

not a minimal surface. Because a cone is used, there is no need to make a minimal surface; it would give a non-realisable structure. So a model based upon the Force Density approach is appropriate. The mesh used is not too large; it gives a good approximation of the expected curvature.

Second mandate is to investigate if the model represents the required shape. The purpose of the membrane is to cover a stage. All the necessary parts of the stage can be covered with this shape, so that's OK. The space frame which is situated above the membrane has enough space to be dimensioned functionally. At the other hand the curvature of the fabric is not very strong so it will result in higher stresses than when there would have been more curvature. The appearance of the structure is also better. So the modeller is not quite content with the shape.

Another important question to ask is if all the needed parts are modelled. It seems to be quite OK, but when thinking about to connect the supporting structure to the lower four points, it occurs that there is something missing. When poles need to be put under the lower points and they must be connected to the space frame that is situated above the membrane, it is clear that there should be some holes in the membrane to put the poles through. So there are some holes missing in the model. Here again the danger of simplification turns up. Because only the membrane is regarded, it is very easy to forget how to connect the membrane to the supporting structure. Conclusion of investigation the second problem is to change the model. Before starting to change the model, first the third mandate must be checked.

The third mandate is to check if the model can be used for cutting pattern generation. This turned out to be a very important question for this structure. When is looked at the orientation of the mesh, is clear that the cutting patterns for the saddle shaped parts will be aligned horizontally. The cutting patterns of the radial midpart of the roof, will meet the cutting patterns of the midpart at right angles. This will create difficulties in manufacturing. Besides, the combination of radial cutting patterns with normal cutting patterns is aesthetically poor and does not seem to fit for this structure. So it seems to be better to change the model to be a structure with all radial parts. It is then also possible to create the holes for the supporting structure at the lower points.

The model has been changed to have five radial parts. Four of the parts are having a low point as midpoint. One part, the midpart, has a high point as midpoint. The result of the new model is shown in Figure 3.38. All mandates are checked and it can be concluded that the

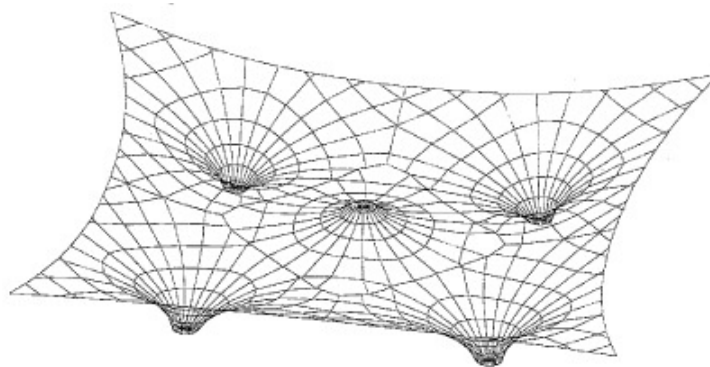


Figure 3.38: New model for the mobile stage covering.

new model is a much better approximation of the required shape. There is much more curvature, the different area's flow naturally into each other. The shape is much more satisfactory for the eyes. Also the holes in the membrane are obvious, so no mistakes can be made on their behalf. All the needed parts are modelled. This new model is a good starting point for the generation of cutting patterns.

3.2.3 Cutting Pattern Generation

After the form finding and statical analysis stage, it is needed to translate the found form into realisable pieces. These pieces are the so-called cutting patterns. It is up to the designer to determine these pieces. Because the designed form is double curved, it is not possible to flatten the form into the plane, like can be done for a cube for instance. A cube can be build up from 6 equal flat planes. When they are sewn together, the cube originates. The anticlastical shaped membrane cannot be build up from flat planes. So how to define pieces to be able to assemble the membrane? Now the features of the material need to be taken into account. Normally a rather stretchable type of material is used, compared to the supporting structure. The value of the Young's modulus varies between 400 and 1000 kN/m² for PVC coated polyester. Compared to steel, which has a Young's modulus of $210 \cdot 10^6$ kN/m² this is rather small. So it is not too difficult to deform the membrane a little bit to obtain the requested shape. The way to develop cutting patterns for a doubly curved membrane is to introduce deformation. The introduction of deformation is done by a computer program. The extend of the deformation is an indication of the quality of the program (Houtman 1996).

In this Section first the pattern orientation will be discussed. Next the generation of the cutting patterns will be discussed.

Cutting pattern orientation The starting point of the cutting pattern orientation is the computer model after form finding. The mesh of the computer model models the threads in the fabric. The fabric cannot resist shear forces, so the orientation of the mesh is supposed to be in the direction of the principal curvature. Then there will be very little shear forces. Because the mesh is representing the fabric, the patterns must be orientated in such a way that the threads in the patterns correspond with the mesh orientation. Patterns are cut out of a roll of fabric. Normally the warp threads are orientated along the roll of fabric. The weft threads are orientated at right angles with the warp direction, so in the width of the roll of the fabric. When the patterns are cut out of the fabric, the warp direction is in the length of the cloth and the weft direction is in the width of the cloth. So when the cutting patterns are orientated in the same direction of the mesh, the threads of the fabric will be in the right position to take up the forces, assuming that the mesh is orientated according to the principal curvature of the structure.

When a radial roof is made use of, normally the mesh should be radial too. The fabric used does not have radial threads. But this is approximated by the use of triangular cutting patterns. In conclusion, it can be said that the direction of the mesh is an important directive for the orientation of the cutting patterns.

Another important directive is the number of different areas in the structure. It is not always possible to model the structure with only one area. One area consists out of a closed polygon, which represents the edge cables. When two edge cables are adjacent to each other, they are the border between two areas. These cables can have a important contribution in creating the required shape, because they have a higher stiffness than the surrounding fabric so they can take more forces and thus influence the shape. It is also possible to have them just as dummies to indicate the border between two areas. Actually very often a structure is composed out of more areas. For each area separately the cutting patterns must be generated. So each area

can have a different orientation of the cutting patterns. This is of course theoretically spoken. The cutting patterns of the different areas must form a consistent unity after orientation. Just think of what it looks like. Does it create a nice view for the spectators or does it give a rather confusing image of the structure. (see Figure 3.39) The seams of the pattern have a large visual

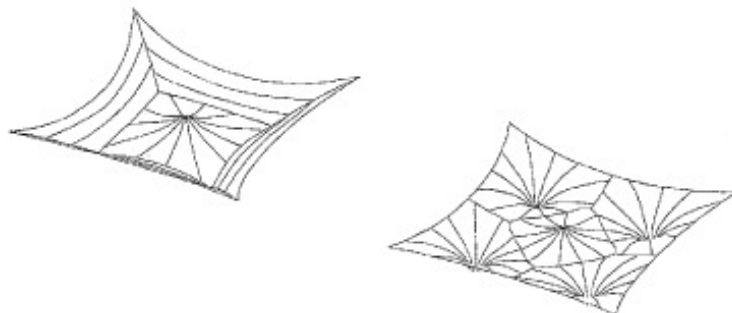


Figure 3.39: The left figure has cutting patterns which meet at right angles. The other figure has cutting patterns which flow into each other.

effect on the appearance of the structure. They can be used to guide the spectators or to surprise them. It is up to the designer to create a satisfying outlook of the structure. It is also very important to regard the meeting of the cutting patterns of the different areas. When the pattern of one area meets the patterns of another area at right angles, there is no problem in theory. The forces can flow from the warp threads of one cloth into the weft threads of the other cloth. But as soon as there originates another angle, this is not possible anymore. So there needs to be taken some shear forces by the fabric. The threads will rotate and the shape changes unverifiable. In the worst case, wrinkles are the result. So orientating cutting patterns is always a matter of trying to get patterns which lie in the length direction of each other.

Cutting Pattern Generation The starting point for cutting pattern generation is the computer model and the ideas of orientation. The model describes the three dimensional surface and the cutting patterns are used to approximate this shape by means of flat strips. Because the material used can deform easily, this usually gives a very good approximation of the shape. The width of the strip determines the amount of approximation. A very wide strip gives a rough estimation of the shape and creates large stress concentrations at the boundaries. This is because the deformation is added at the boundaries when the strips are flattened. When a very small strip is used, the shape is approximated very precisely. It is a matter of economics which is the optimal width of a strip. Many small strips mean a lot of work and a lot of waste material. Few wide strips mean less work and less waste material. So before generating the patterns, first must be decided what the minimum required width of the cloths is. This is of course also depending on the structure. When it is a curved structure, it will be necessary to use very small strips. So for each structure it will be necessary to determine the minimum width for each separate structure. The maximum width is determined by the width of the roll in the fabric. Depending on the type of fabric, this varies from 1.8 till 2.5 metres. Also the seam width must be taken into account. This must be added to the flattened cloth and decrease the available width.

Next step is to add the lines to the surface of the model to indicate where the patterns will have to originate. These lined are the so called geodesic lines. Geodesic lines are defined as being the shortest distance line over a given surface between two points in space. It is very

useful to have a straight line on a curves surface because when the strip is flattened, it will create a boundary which is as straight as possible. So the generated patterns are as optimal as possible.

It is also possible to use the mesh to generate cutting patterns. But what then happens is that highly curved patterns are created, the so called bananas. So it is better to use geodesic lines. Now the problem occurs how to determine the width of the strips upon a curved surface. This is a problem which is still not solved. It is just a matter of estimating the number of patterns on the basis of the lengths of the borders. The program EASY has a graphical interface to give an indication of the width. But it is just an indication. The whole process of generating cutting patterns has to be repeated until all cloths have an acceptable width.

It is also necessary to think of the places of the geodesic lines. They form the borders of the cloths, so when the cloths are sewn together, there will originate seams. A seam is a double layer of fabric, twice as stiff as the other fabric. Therefore seams "attract" stresses. So seams can be used on places where there is little curvature and danger of water sags. They will stiffen the fabric there, for example in flat corners. So place the geodesic lines deliberately.

When all the needed geodesic lines are placed, they need to be calculated. This depends on the program how to do it. EASY calculates them interactive. When they are calculated the strips are cut out of the surface on the spot of the geodesic lines. Now there are individual three dimensional strips. Next stage is to flatten them and to remove the inner mesh so only borderlines remain. Now the cutting patterns are ready for post processing.

3.2.4 Post Processing the Cutting Patterns

After generation of the cutting patterns, some more things need to be finished. The cutting patterns must be checked if they are right or not, stress compensation must be done, the seam lines and the cable pockets must be added. These actions require practical experience and 'feeling' with membrane structures. It can be considered as the most difficult part of the design and realisation of membrane structures. In this section is tried to explain the reasons of these actions.

Checking the cutting patterns The flattening of the strips is a numerical process and therefore small deviations in the patterns occur. For example the borders of adjacent strips can have different lengths while they ought to have the same length. Because this occurs often, most cutting pattern software packages have a module to adjust the border lengths. So the length of the borders is changed. It is up to the modeller to check if the adjustment of the border lengths is done properly. So compare the lengths of the borders before adjustment with the border lengths after adjustment. The differences must not be too large. If this is the case, check the differenced graphically; it is possible that some corners are cut off. It is always possible to adjust that, it is just that the modeller must be aware of it.

Next thing to check is the starting angle that the outer edges of the strips make with the seam line. Calculate or measure the angle of the flattened strip and compare it to the three dimensional angle of the edge cable with the geodesic line in the model. It is to check if the curvature will originate when the patterns are assembled.

Adding stress compensation When the patterns are satisfying, stress compensation can be added. Stress compensation is done because the found shape in computer modelling is a shape under prestress. So actually pieces are cut out of a stressed skin. When the pattern is cut, it should have to shrink according to the stress that was in the different parts of the pattern. This is not the case when the patterns are cut; the lengths of the mesh stay the same. The needed shrinkage must be added by the modeller. The needed shrinkage is called compensation. The amount of compensation can be derived from the stresses in the computer model. At places with high stress there will be needed much compensation. It would be possible to add the compensation automatically by the computer software. But this is not preferred. Not at all places compensation is needed or even desired. Several things need to be taken into account:

- Large forces indicate relatively large stress compensation, small forces indicate relatively small compensation.
- When there are small stresses, maybe it is not needed to add stress compensation, because with a little bit of displacement the right prestress is reached. This is particularly the case when it is an indoor structure. There will be no applied loads, so very little prestress is needed. Therefore hardly any compensation is needed, when the shape does not demand high prestress.
- The fabric used for tensile structures is a synthetic material. It suffers from stress relaxation which brings about certain strain of the material. In the course of the years this will result in unstressed areas. When compensation is added, it must be enough to remain tensioned for the expected lifetime of the structure. At the other hand areas of the fabric near tensioning points are easy to restress after stress relaxation has occurred. So these are not very dangerous areas, which do not need special attention. When an area relaxes which is not easy to restress, this area requests extra attention. Here needs to be done very accurate stress compensation, to prevent the area from going slack.

- Preferably both sides of the cutting patterns are curved, and compensation is added to both sides of the cloths, although it is more easy to have one straight border of a cloth.
- When adding compensation to one part of a cloth, it has to be done for the whole cloth.
- The welding machine has certain welding length. The adjustments made should not be in such a way that because of a too large welding length the adaptations are lost.

The amount of compensation is depending on the forces in the model. The unstressed length of the links can be calculated, but are depending on the Young's modulus used for the fabric in the computer model. The fabric is a non-linear material. So the stress-strain curve is not a straight line. This is the case for most of the materials, but the problem here is that this curve differs for every roll of fabric that is produced. Of course there is a tolerance, but this is too large for precise working. Stress/strain curves are produced by the manufacturer of the fabric. These curves are always having a ratio for the stress in warp and weft direction, because both of the directions have to be measured at the same time. For example 1 to 1, or 1 to 2 , 2 to 1. But in reality the ratio of stress in warp and weft direction differs largely and can be 1 to 4 or 5 or even more. So often more information is needed about the material behaviour than is present. Because the material is non-linear, the Young's modulus is dependent on the stress in the computer model. When there is a high stress, the stiffness is lower. The right Young's modulus needs to be found in an iterative way. One computer run is made with an initial Young's modulus, the stresses are checked and another run is made with a Young's modulus adapted to the found stresses. When the stresses do not change a lot, the right Young's modulus is found. Sometimes it is needed to have different Young's moduli for different areas, when there is a large difference in stresses. There is always a different Young's modulus in weft and warp direction. With the right Young's modulus the unstressed lengths can be calculated, so a value for the compensation is present.

Compensation is not good at all places. At the border of the membrane for example, where a pocket is made to place a cable. A cable does stretch very little when it is pretensioned. The fabric stretches much more than a cable at the same stress. The cable cannot move in the pocket because of the friction between pocket and cable, so the fabric is bound to have the same strain as the cable. Therefore the pockets should have the same length as the cables so no compensation is allowed.

Example In Figure 3.40 a flattened cloth is showed. The cloth has 2 separate boundaries. At these places compensation is not desired. The material between the boundaries should have compensation. But the boundaries are having an angle so the compensation is disabled for these parts. How to do the compensation? What will happen when the borders are stressed? They move outwards. So it is possible to add compensation in such a way that the boundaries are rotated a little bit with the rotation point at the top of the cloth and meanwhile the borders keep the same length.

Adding seam lines and cable pockets When stress compensation is added, the computer generated cutting patterns are ready. The patterns can be plot out or the coordinates of the border points can be listed. It is however not very convenient data for the manufacturers. Therefore first the manufacturing process is regarded. Two different cloths must be welded together. This happens by means of a welding machine, which is very large and immobile (see Figure 3.41). The seams of the adjacent cloths are put under the welding strip, and are welded. The length of the welding strip depends on the curvature of the surface. When there is much curvature, the cloths are highly curved too and then only a small length at a time can be welded. When the manufacturers start welding, they put the ends of the cloths together and

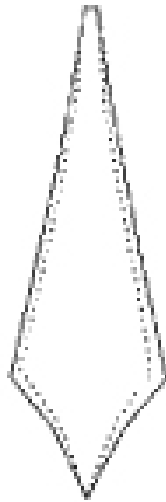


Figure 3.40: By means of a dotted line the stress compensation is indicated. It is on a scaled base. The boundaries should stay at the same length and just rotate a little bit. After stressing they will rotate into their meant position. Because the opening angle at the bottom point will become larger, this needs to be regarded when designing the detailing.

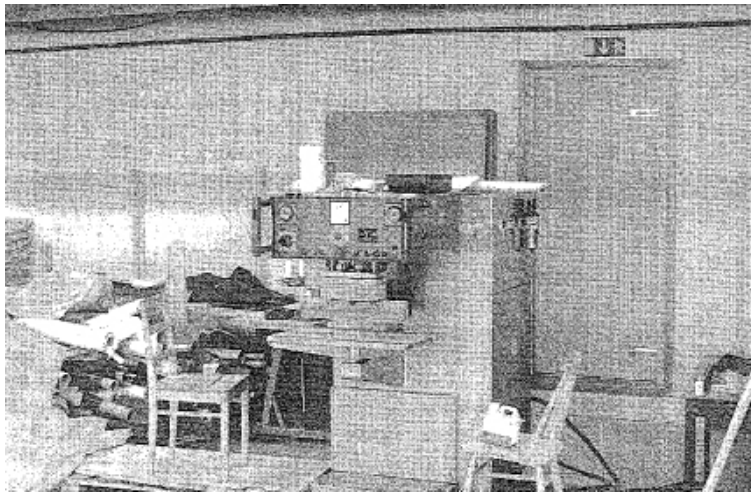


Figure 3.41: A welding machine.

start welding. They put the seams piece by piece together, till the end of the cloths is reached. When there originates an overlap, the welding has not been very good. But because there was no possibility to check along the way, it was not possible to discover it before the end of cloth is reached. So along the seam line points are needed at a certain distance which corresponds with points at the same distance upon the adjacent cloth. Then it is possible to check if along the way. When a difference is discovered, it can be adjusted within some marked points. Therefore the assignment is to define points at a fixed distance along the boundaries of the cloths.

When the right data is gained to draw the patterns upon the fabric, the question arises how to orientate the patterns upon the fabric. When the width of the pattern is somewhat too wide, it is possible to rotate the patterns a little bit to make it fit. Normally only one part of the pattern is somewhat too wide, so there is some room to rotate the pattern. Fact is that because of the rotation of the pattern, the orientation of the treads is changing to. This will be no problem when is taken into account that the threads of adjacent cloths meet at the same angles at the seam line. So it is best to rotate the patterns in pairs.

Before the cutting patterns are drawn upon the fabric, there must be thought of a seam line and of the pocket manufacturing. First the seam lines:

The width of the seam is determined by the required strength of the seam. When a string fabric is used, also a strong seam is needed. Because the seam originates by the welding as the coating of the fabric, the seam is as strong as the coating is attached to the fabric. Therefore a stronger seam is made by using a wider seam. For fabric type 3 normally a seam of 4 centimetres is used. The seam is not added to the data of the pattern. One possibility is to tell the manufacturer which side of the pattern needs to get a seam and how wide it should be. It is then added manually to the data of the cutting patterns, only at one side.

Another method is to add a seam at both sides of the pattern, just by adding a strip to the data of the cutting patterns. Now at both sides the seam is located. To place the welding marks, another measuring cycle must be done

Also a pocket for the cables must be added. A cable is used to tension the membrane. Therefore it needs to be added to the membrane. Usually is made use of a pocket with the cable inside. This pocket can be added to the cloth in a few ways:

- Lengthen the border of the cloth twice the width of the pocket and fold it back to the border of the cloth. This is possible when the border is not very curved. When the boundary is highly curved, the length of the border of the overlap is much smaller than the length of the border of the cloth. This can be solved by perpendicular cuts of the pocket, but this is not elegant (see Figure 3.42).
- Add a rectangular strip to the boundary of the cloth which has a warp and weft direction which makes 45 degrees with the border of the cloth. This makes it possible to let the pocket follow the curvature of the border by stretching it a little, which can be done very easily because the fabric cannot take any shear forces.

Now all the necessary actions are done to cut out the patterns from the fabric and to weld them together. The cutting patterns are ready.

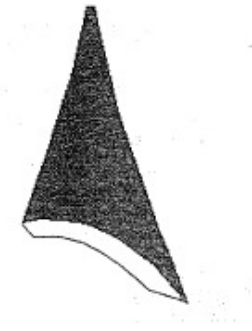


Figure 3.42: In the overlap of this pocket is folded back, the border will be much too short. By means of perpendicular cuts it will be possible to solve this problem. It is not a very nice solution. It is better to use a strip of fabric which has threads which make an angle of 45 degrees with the boundaries and add it to the cloth. Because of the disability to resist shear forces, it is easy to deform the strip to make it follow the boundary of the cloth.

3.2.5 Examples

A round wood dome structure The first project handles about a round wood dome structure (Huybers 1983). It is meant as an exhibition stand and therefore a covering of the domed space is needed. The round wood dome consists out of an antiprisma and half a boll. In the boll part of the dome the membrane is situated (see Figure 3.43). The membrane is generated by means of the software package EASY.

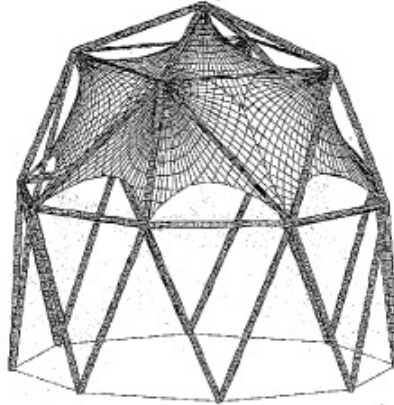


Figure 3.43: A round wood dome structure generated with EASY.

Modelling the membrane into the computer program The first stage of modelling the membrane is to decide which way of modelling needs to be chosen. At the perimeter there are 8 fixed points, and furthermore there are 5 points which can be used to attach the membrane to. It is most easy to model simple saddle shapes between the available points. To get some curvature in the membrane, there need to be cables between the different areas. A sharply shaped membrane originates (see Figure 3.44).

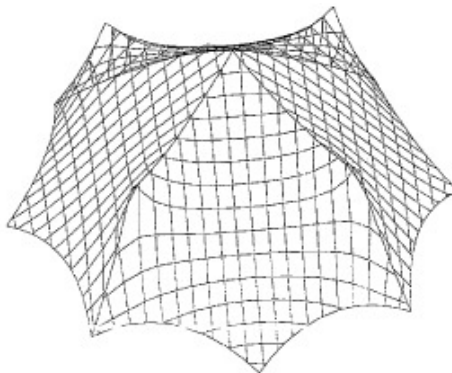


Figure 3.44: Modelling the membrane.

Checking the generated computer model At first the type of modelling seemed OK. There was very little curvature in the plane, but because of the usage of cables between the different

areas, the stresses were not very high. However, the outlook of the structure was not satisfactory. The cables were creating too sharp edges and the little curvature did not give the structure a nice appearance. When thinking of the second checkpoint of Section 3.2.2, another important point is the missing of the holes in the membrane to connect the cables to the supporting structure. The model needs some adaptation. To do this in the right way, the choice is made to use radial mesh orientation. It then is possible to easily create holes in the membrane and there will occur much more curvature.

The third checkpoint of Section 3.2.2 handled about the usability of the model to create cutting patterns. The first model is consistent for generating cutting patterns, except for the holes in the membrane

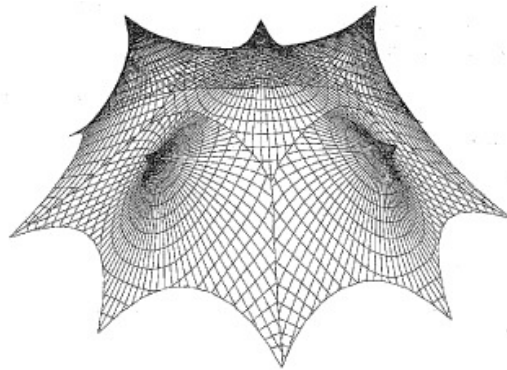


Figure 3.45: Radial pattern orientation.

Figure 3.45 shows a radial patterns orientation. The result is a more curved membrane. The cables between the different areas are dummies, they do not have a function in determining the shape. The Figure still does not show any holes in the fabric, but when is looked properly, it can be seen that the centre points of the radial mesh are modelled as being small cones which have a slightly different shape. The model is suitable for generating cutting patterns. The mesh flows fluidly into each other, and meeting cutting patterns have the same warp and weft orientation.

Orientation of the cutting patterns For orientating the patterns, the plan view of the shape is considered (see Figure 3.46). It can be seen that the shape consists out of 5 areas. 4 of the areas are identical, only the midpart is different. So only for two parts the cutting patterns need to be generated. The midpart has three axes of symmetry, so only 1/8 of the part needs to be generated.

Because for the modelling is made use of radial meshes, the cutting pattern orientation will be radial too. At the edges of the areas they will meet each other. Normally it is very useful to have seam lines in the corners. But in this particular case many parts meet at the corners. It is not good to have too many parts meet at one place, because it is not possible to weld more than three layers of fabric. This must be taken into account when the seam lines are placed.

Generating the cutting patterns The cutting patterns generation program used, is quite a special program. It grows a new mesh over the existing surface which is much easier to flatten. The starting and ending line of the growing process is a geodesic. So when the starting line is flattened, it becomes a completely straight line. This is not very desirable, therefore the pattern to be generated, is divided into two parts. The dividing line is the starting line for the program.

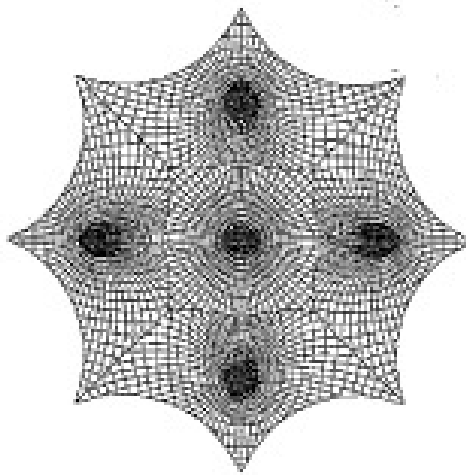


Figure 3.46: Planview of a radial pattern orientation.

So the surface is grown towards two sides. After the pattern parts are flattened, they are sewn together by the program. A very precisely cutting pattern is obtained.

When this program is used, twice as much geodesic lines need to be added to the surface as is needed for normal cutting programs. The program is called STGEN and is a module of EASY. The following geodesic lines are added to the surface (see Figure 3.47). The lines marked with a

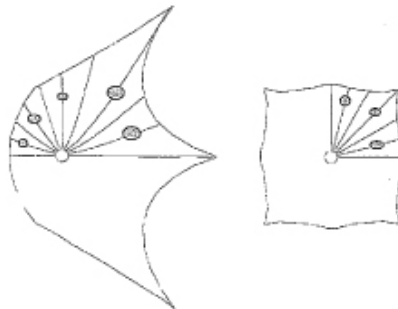


Figure 3.47: Geodesic lines.

grey oval are starting lines for the program. The other lines are cutting lines. The total number of cloths to be generated is 16, after the generation there will only remain 8 of them. From the midpart is generated, because only three patterns will remain. Now there is a possibility to check if the patterns are the same or not.

The geodesic lines are added and calculated. Next stage is the growing of the new surface over the existing one. After growing the patterns are far too large. Therefore they are cut with the cutting geodesics. After cutting they are flattened. Now the rough cutting patterns are ready. The patterns are checked whether they are good or not and the different parts are sewn together. The patterns are shown in Figure 3.48. The starting geodesic lines have disappeared. The result is 8 cutting patterns which are ready for post processing.

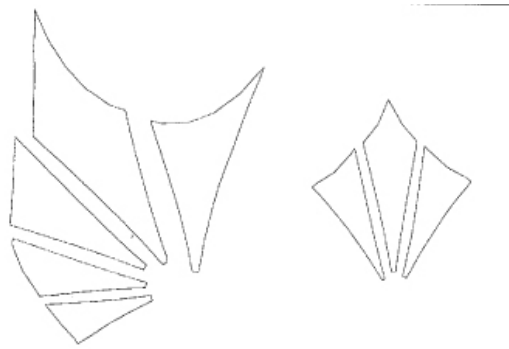


Figure 3.48: Eight cutting patterns.

Postprocessing The purpose of the round wood dome is to function as an exhibition structure, so always for short periods and very often inside. Therefore it is not necessary to do stress compensation for this membrane. Additional must be mentioned that radial roofs are very easy to stress. By lifting the cone a little bit, there comes an equal pretension in the membrane. And because this membrane is very small, it will be just a little bit of elongation of the material before the right stress is reached. When stress compensation is added, always must be thought of the effect of it. What will happen after stress compensation? It must be taken into account that the material type used for this roof is Ferrari's 502. This is a very thin fabric with equal strain in warp and weft direction. This is because of the special patented weaving techniques used by the company. When a traditional type of material is used, it will be necessary to do some compensation, else the weft direction will give too much strain. So the post processing is quickly done for these patterns. A module of EASY is used to find points along the border with a minimal distance of 25 centimetres. These points can be used for welding the parts together.

Entrance Canopy in Helsinki For a new restaurant in Helsinki an entrance canopy is requested. It is quite a long building so it is helpful for the visitors when the entrance is indicated properly. The building has a very fragile design so the canopy must be very fragile too. The canopy is added afterwards to the design so the possible fixing points needed to be indicated after the design was ready. The possible membrane resulted in a quite flat design. This was because of the restrictions made by the architect. But at the building side was made a mistake in placing the fixing points. This resulted in a much flatter design as was proposed. As a result of this the fabric had to resist high forces when snow load is present. Therefore the type of fabric used is Ferrari's 1002, which is a very heavy type (see Figure 3.49).

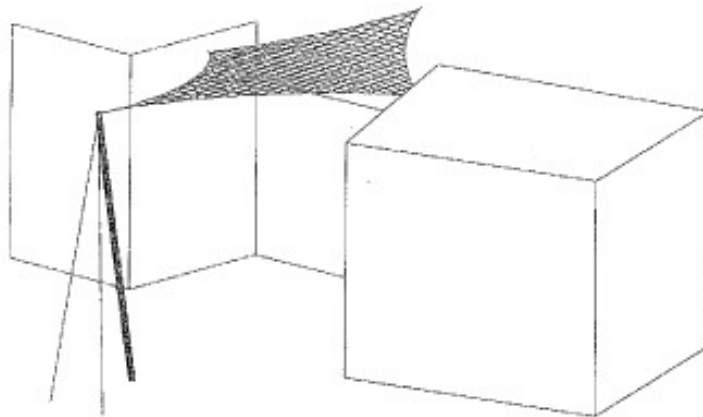


Figure 3.49: Entrance canopy in Helsinki.

Modelling the membrane into the computer program The required shape is a simple saddle shape, so it is very convenient to use a square mesh to model the shape. The principle curvature of the shape goes from the fore point to the front point and from one side point to the other side point. So this is the direction that the mesh must have. It can be seen in Figure 3.49 that the modelled mesh is according to the principal curvature. What stands out is the very fine mesh of the model. This is because of the small size of the membrane and the little curvature. When a larger mesh is used, precious curvature will be lost because the mesh draws a straight line between two points. Less points means less curvature. Therefore such a small mesh is

used. It would be nice to introduce some more curvature, but this is not possible because of the restrictions of the architect.

Checking the computer model The first question is if all the necessary parts are modelled. There are no holes in the membrane or cables at the surface missing. The architect wanted a certain distance between the membrane and the mast. In Figure 3.49 can be seen that there is a link between the membrane and the mast. The mast and the ties are also modelled because the ties can deform elastically too. The strain of them influences the shape. It therefore is necessary to model them. So all the necessary parts are modelled. The mesh orientation is according to the principal curvature so it can be used for cutting pattern generation. It can be concluded that the model is OK.

Orientation of the cutting patterns There are two possibilities to orientate the cutting patterns. From the fore point to the back point or from one side point to the other side point. Both options follow the principal curvature of the surface so which one to choose. To make this decision, the extra stiffness of the seam must be taken into account. When the seams are orientated from one side point to the other, the extra stiffness of the seams is not used. When there is snow load, this curvature direction will be relaxed while the other curvature direction will take the load. Especially in this case it would be very wise to use the extra stiffness because of the very flat membrane. So when the seams are orientated from the fore point to the back point, the extra stiffness of the seams is used. When there is applied load, the seam will take more of it. This will prevent the appearance of sags. (see Figure 3.50) Because of the very small membrane,

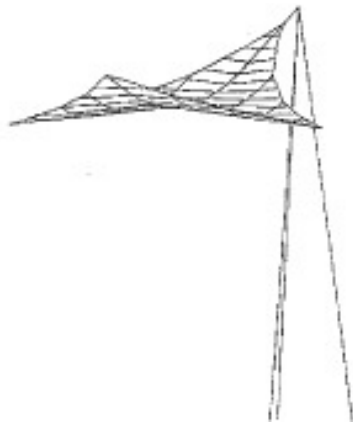


Figure 3.50: To examine the influence of the seam in the middle, the created cutting patterns are sewn together and re-analyzed under snow load. It can be seen that the middle line takes much force under load. The use of the seam line in the middle prevents the occurrence of sags.

only two cloths need to be made and two small corner parts. A seam line is orientated in the middle in the fabric to make the most of it. The orientation can be seen in Figure 3.51.

Generation of the cutting patterns The cutting patterns are generated with the module STGEN from EASY. So a new surface is grown over the existing surface. For the large cloths there is made use of starting lines at the middle of the cloths. They are not displayed in Figure 3.49. For the small cloths it was not necessary to use starting lines at the middle, because cloths are nearly flat so the cutting edge would have been flat to. After generation of the patterns the two

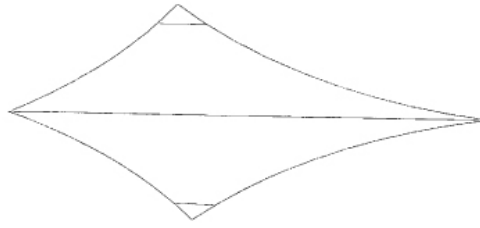


Figure 3.51: The seam line in the middle of the fabric.

parts of the large cloths are sewn together. They are ready for post processing (see Figure 3.52).

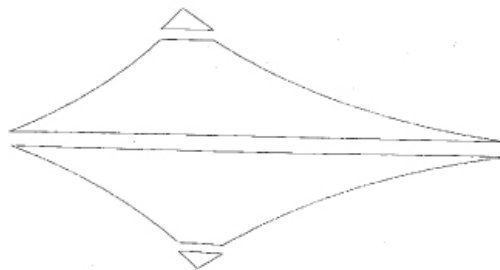


Figure 3.52: Two parts of the large cloths are sewn together.

Post processing The chosen type of fabric makes it unnecessary to use stress compensation. There is an equal stress distribution in the fabric and there are actually only two cloths. The needed compensation will be very small which indicates that it will have small effect. The chosen type of fabric does not strain more in weft direction than in warp direction. Also a safety factor 10 is used for the fabric so the deformation of it is always in the elastic zone. This is much better for the life span of the fabric and it does not give problems with stress relaxation. At the borders of the cutting patterns new points are defined at an equal distance of 0.5 metres.

After the patterns are cut and welded, the angles of the tension points are measured and the connections to the supporting structure are designed. The installation can be done.

Installation The fabric, mast, anchor plates, cables and connections are transported to the spot. The foundation and fixing points are applied by the primarily contractor, so only the installation of the membrane needs to be done. Figure 3.52 shows the building to which the membrane must be attached. The first action is the positioning of the anchor plates upon the foundation (see Figure 3.53). Then the membrane is transported to the roof of the building, where the installation starts. The membrane is just a very small package which is easily to carry by one person. The fabric is laid down upon a piece of plastic to prevent it from getting dirty. (see Figure 3.54). The fabric is rolled out and the side points are attached to the fixing points (see Figure 3.55). After that the back point is connected to its fixing point. The mast foot is placed into the anchorage plate. The ties and the membrane are connected to the top of the mast. Now the mast is lifted up by means of a winch and man power. The ties are connected to the anchorage plates while the winch cable is ensuring the stability of the mast during erection

(see Figure 3.56). After tensioning the structure, the covering of the mast is removed and the installation is ready (see Figure 3.57).

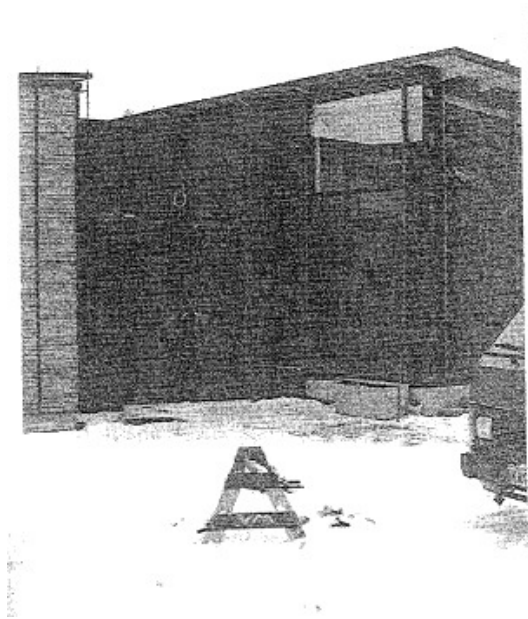


Figure 3.53: The building without the membrane.



Figure 3.54: The anchoring points.

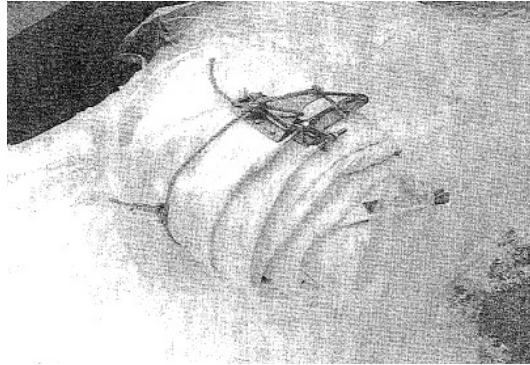


Figure 3.55: The membrane.

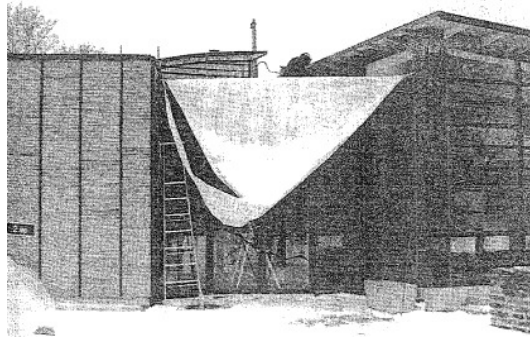


Figure 3.56: Installing the side points.



Figure 3.57: Erecting the mast.

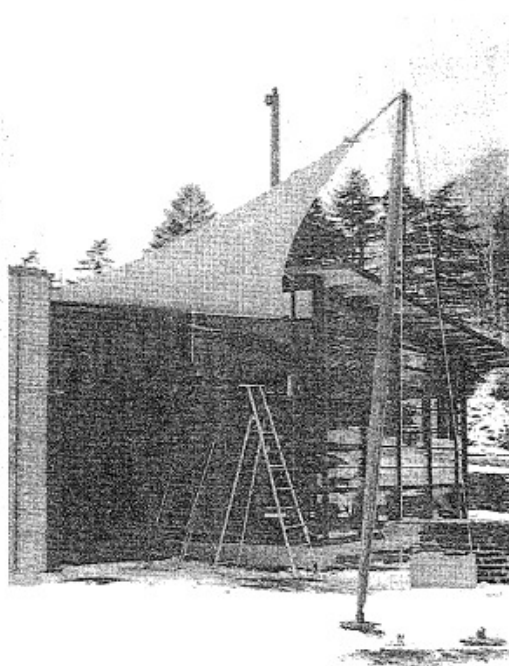


Figure 3.58: The membrane after pretensioning.

3.3 Pneumatic structures

3.3.1 Introduction

Membranes with a positive curvature can only be achieved by having over pressure in the enclosed space. The medium allowing for this pressure can take many forms, amongst others gaseous, liquid, expanding foam, sand. In most cases, however, air is used. In these cases it is spoken of as pneumatic or air-supported structures (Dutch: pneumatische constructies/draaglucht-hallen; German: 'Tragluft-hallen'; French: 'structure gonflable';).

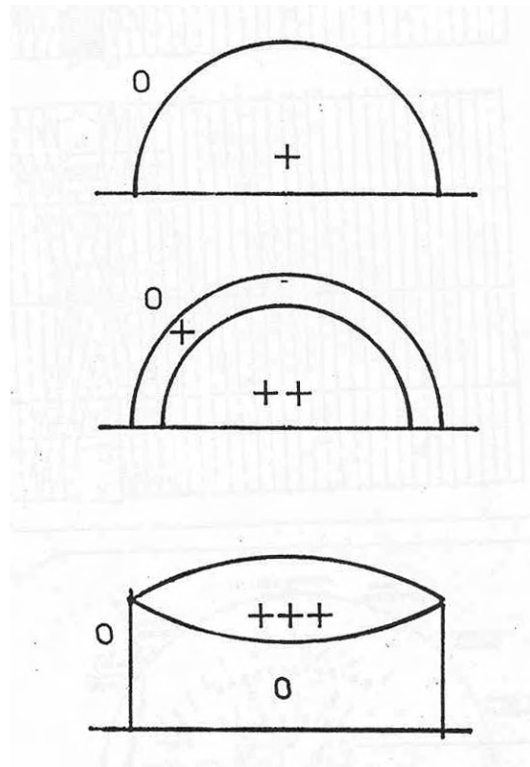


Figure 3.59: The principles of the air-supported structure.

The idea of using air-over-pressure to hold up thin membranes to use as a roof structure dates back to 1917. This year Lancaster filed an appeal for a patent on a field hospital with a dome shaped canvas roof (Figure 3.60). Lancaster also made calculations on domes with diameters up to 650m and worked on solving many technical problems, like passing into the pressurized room by an air lock, heating, lighting ventilation and fire safety.

In December 1942 H.H. Stevens published an even further elaborated proposal in *Architectural Record*, on a aircraft factory with a circular plan and a lightly curved roof made from thin steel (Figure 3.62). The sphere shape should have been created through a 1% plastic deformation of the material by an overpressure of $420g/m^2$. This proposal, which had a total span of 400m, got a quite reserved welcome. The publisher thought it necessary, for instance, to place the following remark accompanying the article: *'His theories and calculations have been checked by several prominent consulting engineers without discovering fallacies in the reasoning.'*

The world had to wait till 1949 before W. Bird realised the first real inflatable structure. This concerned a inflatable 2/3 sphere, with a diameter of 18m and a height of 12m, made from

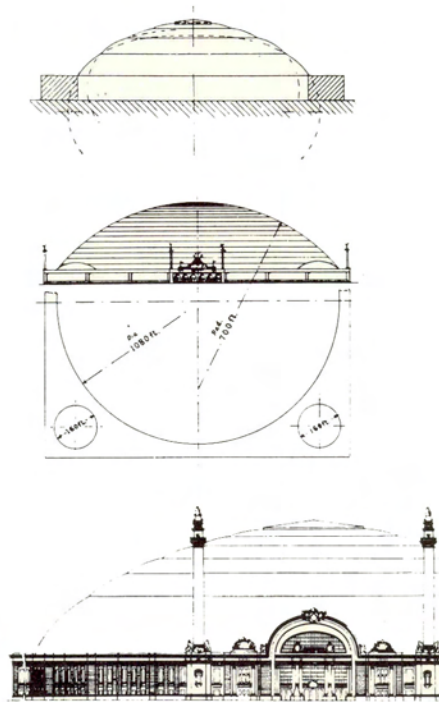


Figure 3.60: The first designs for an air-supported structure by Lancaster.

a nylon weave, impregnated with rubber (Figure 3.63).

Bird's work meant the needed impulse to an explosive development. Since the construction of this first pneumatic structure, many daring design have been constructed by companies like Scheldjahl, U.S. Rubber, Goodyear, Irving, Stromeyer, Texair, Krupp, Ogawa, Taiyo Kogyo and many more. Most of these structures serve as storage depots, exhibition space, swimming pools or temporary assembly halls creating the possibility of winter production.

One of the largest radomes ever built has a diameter of 70m. It was fabricated by Scheldahl and is in use for the so-called Telstar project in Maine. (Figure 3.64)

Cylindershaped halls with a quarter sphere on each end, have been built with lengths up to 100m and width to 40m. A well known example from the early years of the developments, is the exhibition pavilion for the Hannover Messe, built by Krupp. The size was 106 x 35 x 17m and the total weight was 5,2 tons, while the skin weigh only a mere 1 kg/m^2 .

Also Japanes companies, like Ogawa Tent Co. Ltd., have come up with interesting and daring applications of the air support principle. They are involved in most larger projects realized all over the world.

Air-supported structures have a number of clear advantages compared to traditional structures, namely:

- modest investing and transport costs
- light foundations
- demountable

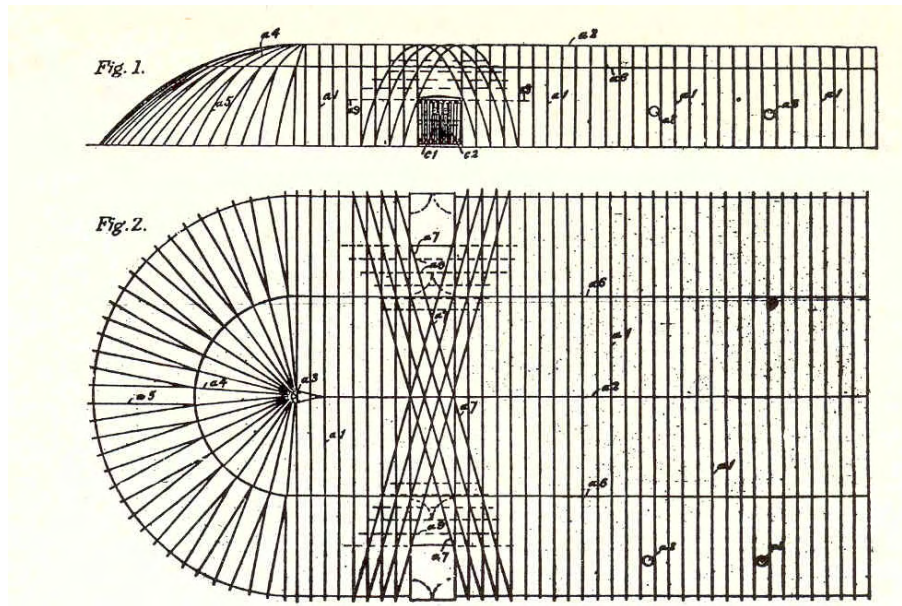


Figure 3.61: Patent request by F.W. Lancaster.

- fast warm up

This means it is possible to create a large and cheap covered space within a short timespan and for relatively low cost.

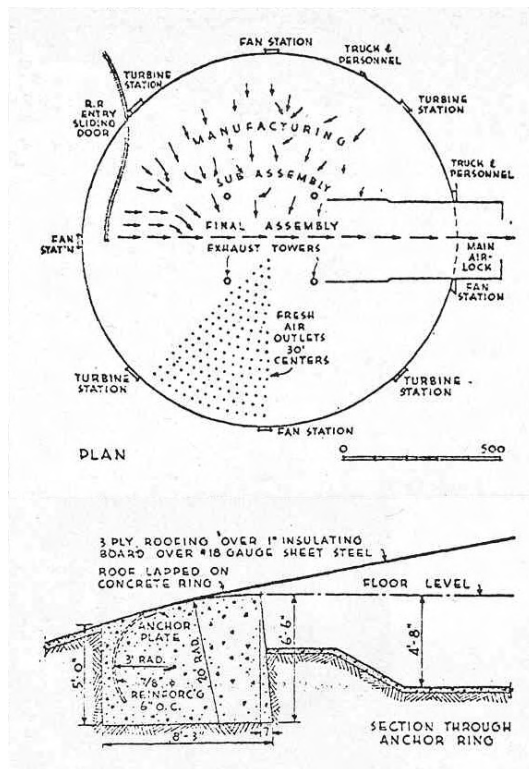


Figure 3.62: A design for an aircraft hangar by H.H. Stevens.

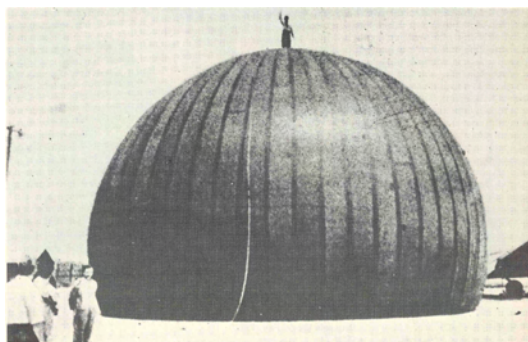


Figure 3.63: The first pneumatic dome structure ever built; design by W. Bird (1949).

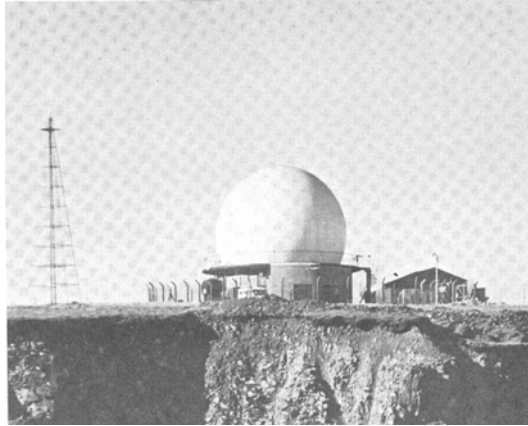


Figure 3.64: The Telstar radome in Maine.



Figure 3.65: An exhibition hall by Krupp in Hannover, shape like a toroid (=part of a cylindrical ring).

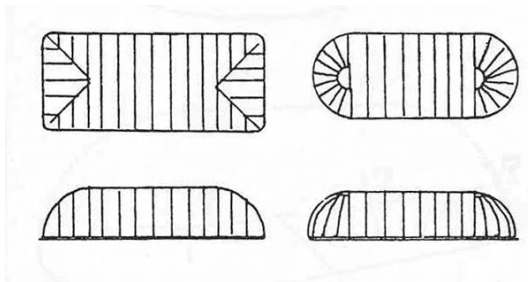


Figure 3.66: Air-supported halls on a longitudinal base; often applied shapes.

3.3.2 Principles of form

Normal force in the meridional direction:

$$n\theta = \frac{p_i R_2}{2} \quad (3.10)$$

Other direction:

$$n\phi = p_i R_2 \left[1 - \frac{r_2}{2R_1} \right] \quad (3.11)$$

Equilibrium equation:

$$\frac{n\theta}{r_1} + \frac{n\phi}{R_2} = p_i \quad (3.12)$$

Where p_i is the over-pressure, R_1 and R_2 are the main radii of curvature. This leads to the conclusion that the normal force in the circumferential direction becomes negative when $2R_1 < R_2$.

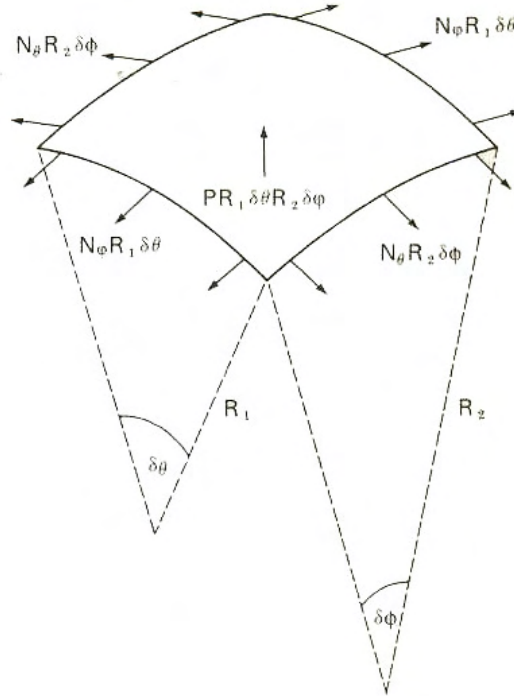


Figure 3.67: The common stress distribution in a double curved surface under internal pressure.

For a cylinder is true:

$$R_1 = \infty; n\theta = \frac{p_i}{R_2}; n\phi = p_i R_2 \quad (3.13)$$

For a sphere:

$$R_1 = R_2 = R; n\theta = n\phi = \frac{p_i R_2}{2} \quad (3.14)$$

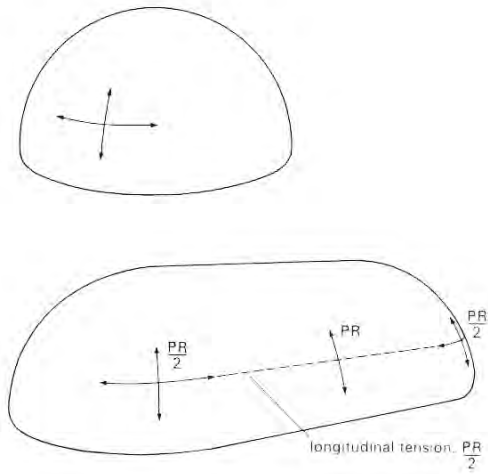


Figure 3.68: The stress distribution in spherical and cylindrical shaped roof surfaces.

A much used main shape is the cylinder combined with two quarter spheres on both ends. At the connection between the two different parts a discontinuity arises, because the stress in the longitudinal direction -and with it the elongation- doubles. Nevertheless, this main shape is very popular, because the cylinder part can be easily made from parallel bands of fabric. Much material is lost in cutting and sizing when using double curved shapes.

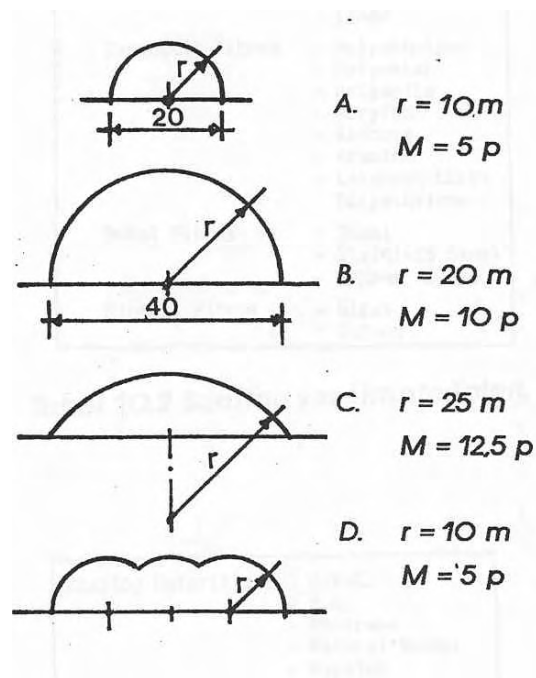


Figure 3.69: The effect of the shape on the membrane stresses; $M = p * \frac{r}{2}$.

When it is considered to realize an as equally divided stress as possible, the structural shape is a direct derivative of the circumference of the plan. An equal divided stress occurs when $N_x = N_y$ and $N_{xy} = 0$. On the average it is very difficult to analytically define the shape of the an air supported membrane with a random plan. This is why the shape of these structures are usually approached numerically and often also by measuring small scale physical models.

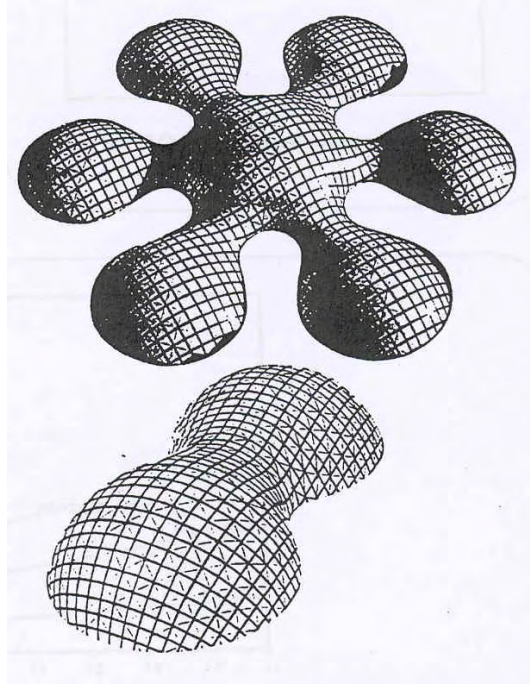


Figure 3.70: Shapes of air-supported surfaces over random plans.

3.3.3 Materials

It is thinkable to use isotropic foils, like PVC, saturated polyester, polyaramide, polypropylene, PVF or synthetic rubber, for this type of structures. However, it is usually very hard to create a stable shape due to excessive deformation (low E-modulus) or creep of the material.

This why the most commonly used materials are membranes with a more complicated build up. To create the desired stiffness and strength weaves are often chosen. For smaller structures this can be made from natural fibres like cotton, the majority is, however, made from linear polyester fibres (Terlenka Trevira).

In many other cases also nylon or glassfibre weaves are used. The last mentioned mainly in large structures. To protect the weave and to create water- and airtightness, the weave is covered with a covering layer on both sides. For this layer a number of plastics are suitable. In over 90% of the cases in Europe, however, these layer are made from plasticized PVC. This has as advantage that it is weldable thermally or high frequency. Also synthetic rubbers, like chlorosulfonrubber (Hypalon), polychloridebutadene (Neoprene), ethene-propene rubber and Teflon (PTFE), are used as a covering material.

On average a covering needs to be at least 0,2mm. This leads to a thickness of PVC-polyester membranes varying between 0,7mm and 1,2mm. The weight of this membrane is 800-1100 kg/mm^2 . The tensile strength lies between 0,6 and 1,2 kN/cm width.

Average strength ($kN/5cm$)	Internal pressure (mm water column)	max. radius	
		cylinder	sphere
3,5	30	23	46
	50	14	28
	70	10	20
	100	7	14
	150	4,5	9

Table 3.2: Max. radii depending on the material strength and internal pressure.

Natural fibres	- Cotton - Linnen
Synthetic fibres	- Polyethylene - Polyester - Polyamide - Acrylic - Viscose - Aramide - Extended Chain Polyethylene
Metal fibres	- Steel - Stainless Steel - Copper Alloys
Mineral fibres	- Glass - Carbon

Table 3.3: Different types of fibre materials

Sometimes a totally different material is used, like thin steelplate. In Halifax in 1979 a design by Carruthers and Wallace was realized, which was a roof structure on a superelliptical plan of

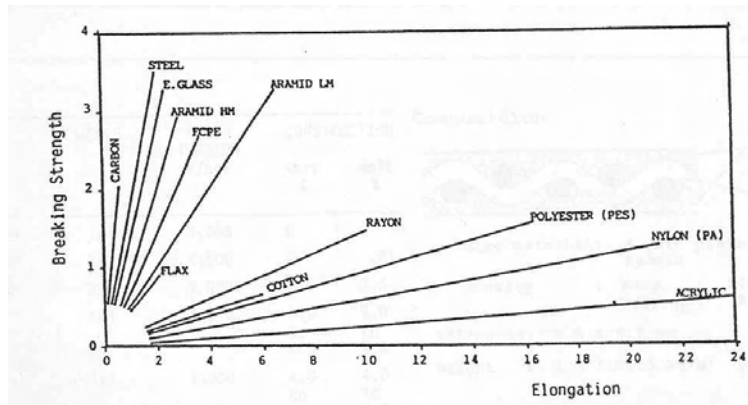


Figure 3.71: Stress-strain curves for different types of fibres.

Coating materials	<ul style="list-style-type: none"> - P.V.C. - P.U. - Neoprene - Natural Rubber - Hypalon - P.T.F.E. and F.E.P. - P.V.F. - Silicone Rubber - P.V.D.F.
-------------------	---

Table 3.4: Applied coating materials.

82x64m. The membrane was made from 1,5mm thick stainless steel.

A super ellipse can be pictured by the following expression:

$$\frac{x_v}{a_n} + \frac{y_n}{b_n} = 1 \quad (3.15)$$

n can have every positive value. For $n = 2$ the regular ellipse is found with axis a and b . When $n > 2$ the circumscribed rectangle is approached. For $n = 1$ a rhomb is found with straight edges and for values $n < 1$ a more or less asymptotic shape is found.

When $a = 1$ and $b = E$ (or Expansion), then equation 3.15 becomes:

$$x^n + \frac{y^n}{E^n} = 1 \quad (3.16)$$

Yarn	Weave	Strip Tension (N/mm^2)	Construction	
			Warp (%)	Weft (%)
Polyester	1x1	3,000	0	2
Polyester	2x2	4,5000	0	0,81
Polyester	3x3	9,000	-0,5	3,5
Glass	1x1	4,000	+0,5 to -0,5	2,0 to 4,0
Glass	1x1	7,000	+0,8 to -0,3	4,0 to 6,0

Table 3.5: Fibre properties

MATERIAL	COST/m²	UTS (for 1000 g foil)	EL	DURABILITY	TRANSLUCENCY	FIRE RESISTANCE	COLOUR RANGES	APPLICATION
Foils								
PVC Foil	£1.50			E	90%	Not if Clear	All Inc. Clear	
Polyester ("MYLAR")	£5			D	95%	Not	All	Greenhouse glazing, air cushions for Tokyo Roof.
FEP	£10	2.5	200%	A	95%	A	Clear	Durable clear foils for high light transmission roofs. Span limited to 1.0 m for FEP and 2.0 m for ETFE. Can be reinforced with wires overlaid.
ETFE 'Tefzel'	£10	YS 5 kN/m US15 kN/m	300%	A	90%	A	Clear	
Coated Fabric								
PVC Coated Polyester Cloth with Acrylic Lacquer	£2-£7	20-200	16%	D	85-30%	B	All	Widely used for air-houses and fabric structures. Can be coloured opaque etc. High translucent materials are less durable. PYDF laquer is now available to give a more durable surface.
PVC Coated Nylon	£2-£7	20-200	20%	D	85-30%	B	All	As above, but less popular because of poor dimensional stability and creep.
PVC Coated Kevlar	?	100-400	5%	C	Opaque	B	All	Would only be used where high strength stiffness is required. Jointing problems. Must be opaque to protect Kevlar.
Hypalon Coated Polyester	£8-£20	20-300	16%	C+	Opaque	Not	All	Used for radar domes. Hypalon degrades and powders on the surface - can be repainted to extend life.
PVC Coated Polyester with Tedlar (PVF ₂ Laminate)	£3-£8	50-200	16%	C	75-20%	B	All	Used occasionally in USA. Laminate provides a stay-clean surface. Welded joints have low strength.
PYDF Coated Polyester or Glass	£15-£20	50-150	16%	B	35%	B	White or Milky	New product - RF weldable. In the course of development - not commercially available.
PTFE Coated Glass Cloth	£25-£45	30-150	6%	A	5%-15%	I	Ivory, some colours	Has been widely used for "permanent" fabric structures. 1st example now 15 years old.
PTFE Coated Kevlar	?	50-250		B	0	A	Ditto	Used for radomes.
Silicon Coated Glass	£20	30-150	6%	B-A	20%-50%	B	Clear	New material. Several structures have been completed in America in the last 2 years by ODC.
Reinforced Films								
Polyester Reinforced PVC Laminate	£1.50	10-30		E	80%	B	Some colours	Widely used for windows in structures and clear sheeting on scaffolding.
FEP or ETFE Film Reinforced with Glass, Kevlar or Steel Wire Mesh	?			A	50%-80%			Considerable research has gone into this material but at present it is not in commercial production.

NOTES: Durability Grading : A >25 years
 B 20-25 years
 C 15-20 years
 D 10-15 years
 E <10 years
 F <5 years

Fire Resistance Grading : I Virtually incombustible
 A Inherently flame resistant
 B Flame resistant with the addition of flame retardant salts

A and B Grades meet the requirements of BS3120 or DIN4102.

Figure 3.72: Often applied types of membrane (costs are not realistic anymore).

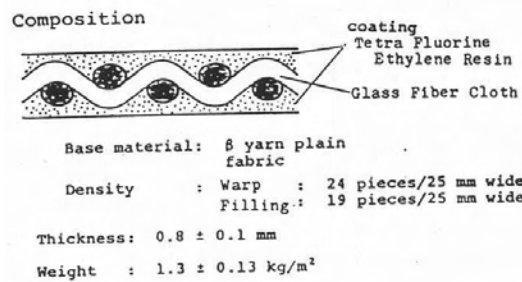


Figure 3.73: An example of a high strength membrane build up.

When it is furthermore stated that $x = R \sin \phi$ and $y = R \cos \phi$ then the equation can also be written as: (also see Figure 3.75)

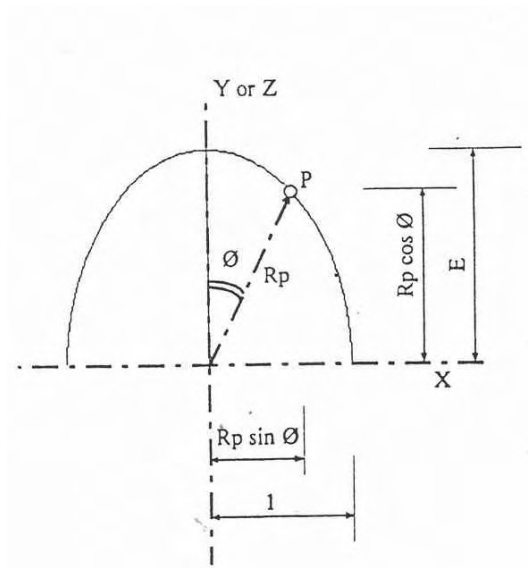


Figure 3.74: The basic shape of an ellipse.

$$R = \frac{E}{E^n \sin^n \phi + \cos^n \phi}^{\frac{1}{n}} \quad (3.17)$$

The most interesting aspect to this structure is the so-called ‘contraction joint’ (see Figure 3.78), designed by D.A. Sinoski. In first instance the seam has the shape of an Ω and it is stretched when the roof is inflated. This creates the possibility to construct the roof on a flat surface, while it gets its final shape during the inflation procedure (up to 38mm watercolumn¹). A layer of acoustic and thermal glass wool insulation hangs 30cm underneath the outer plane.

¹1N/m² = 1Pa = 0,102mm water column

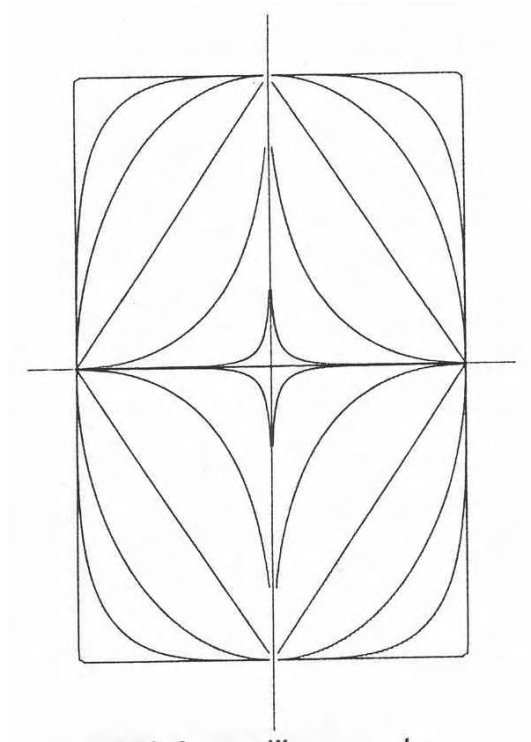


Figure 3.75: Superellipses with different values for the exponent; in this case a proportion of 1,5 between the axis is chosen.

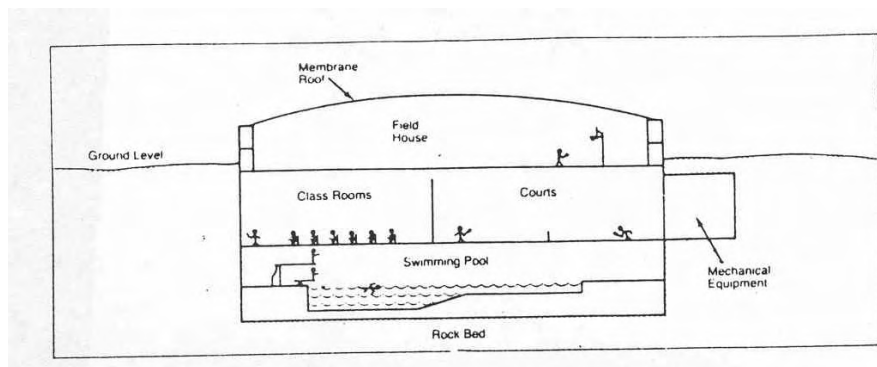


Figure 3.76: Section through the stainless steel roofstructure in Halifax.

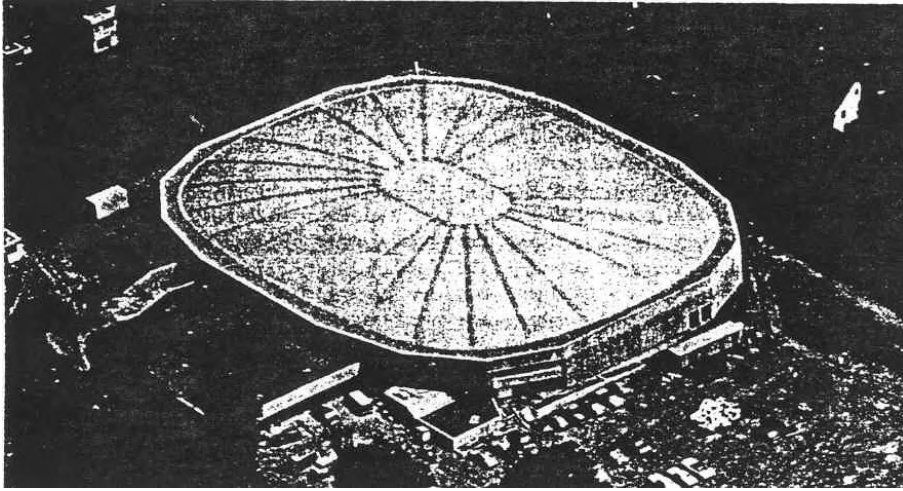


Figure 3.77: Overview Halifax.

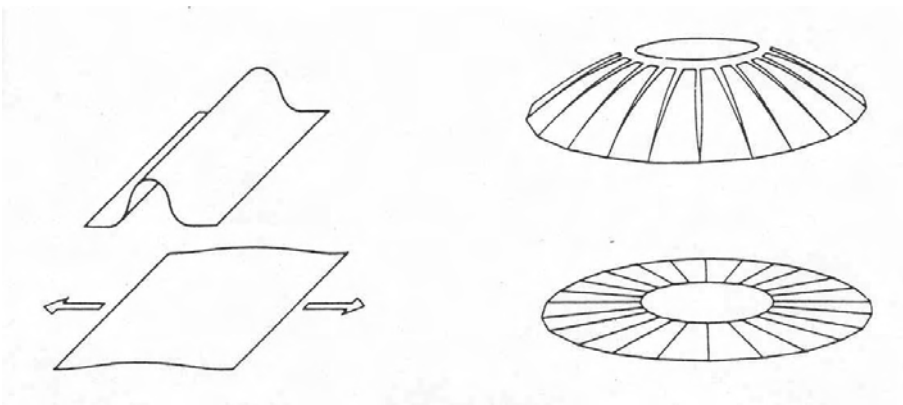


Figure 3.78: Structural lay-out of the air-supported stainless steel roof (82mx64m) with contraction joint.

3.3.4 Air pressure

The overpressure needs to be fairly low, because of the very low self weight of the structure. An overpressure of 10-30mm watercolumn (0,001-0,003 atm) is sufficient in almost all cases. This is a very small pressure and is comparable to the change of airpressure over an altitude of 8-35m. This means that the same airpressure that needs to be overcome when climbing to the 8th floor of a building is enough to hold up a pneumatic structure. This clearly shows that the difference in airpressure is hardly noticeable for persons entering an air-supported structure.

The only precaution that has to be taken is that the inner space has to be protected from loss of pressure by an airlock, when entering. In many cases a revolving door is sufficient.

The amount of over-pressure also has some relation with the shape of the structure. Relatively high structures need to be able to take up large horizontal forces due to windload. In radardomes usually 2/3 or 3/4 spheres are used. To obtain enough shape stability in these cases, the over-pressure has to be increased up to 5- or 10-fold the regularly used pressures.

The sphere-shaped observatory in Bochum, built by Krupp in 1964, has a height of 24,5m and a maximum diameter of 39 m. In this structure an over-pressure of 40-150 mm watercolumn is used.

Force Beaufort	$v_{max}[m/s]$	$q_0[N/m^2]$	Official description
1	1,5	2	Light air
2	3	6	Light breeze
3	5,5	19	Gentle breeze
4	5,5	19	Moderate breeze
5	11	76	Fresh breeze
6	14	122	Strong breeze
7	17	181	Near gale
8	20	250	Gale
9	24	360	Strong gale
10	28	490	Storm
11	32	640	Violent storm
12	>32	>640	Hurricane

Table 3.6: Comparison of windspeeds and wind pressures;

In order to maintain the over-pressure, relatively small cold air ventilators are needed, though every air-supported structure has many -however small- airleaks, mainly on seams, at the airlock and at the connection to the ground.

In calculating the use of power, the following rule of thumb is often used: covered area [m^2]/200=KW. When a hall with a plan of $800m^2$ is considered, a power of $\frac{800}{200} = 4KW$ is found.

In such case 2 ventilators of 3KW each would be enough. The second ventilator is then mainly as a back up if the first one fails. Depending on the needed over-pressure and the use of the enclosed space, extra safety precautions can be taken, like emergency generators. The air-pressure is by the way always tuned to the current windspeeds, so the skin is never higher stressed than needed.

According to H. Ruhle one should use the following working pressure in calculations: (working pressure: $p = p_i = p_e$, so internal over-pressure minus external pressure by loading)

Practical values for p_i/q_w

3/4 sphere	> 1 > 0,8 (when large deformations are allowed)
1/2 sphere	> 0,7
1/2 cylinder with 1/4 sphere as ending	> 0,6

For spheres:

$$\begin{aligned}
 &1,5R < h < 1,05R \\
 &p = 0,85 * q_0 = 47\text{mm water column}
 \end{aligned}
 \tag{3.18}$$

$$\begin{aligned}
 &1,05R < h < 0,75R \\
 &p = 0,65 * q_0 = 35\text{mm water column}
 \end{aligned}$$

For cylinders and torusses:

$$p = 0,55 * q_0 = 30\text{mm water column}
 \tag{3.19}$$

Where q_0 is the thrust of the wind; here $q_0 = 0,55kN/m^2$ was used. The actual value of the loading can be calculated from the airspeed. So:

$$\begin{aligned}
 q_0 &= 5 * \rho(\text{air}) * v^2, \text{ where } v \text{ in m/s} \\
 \rho(\text{air}) &= 0,125 \\
 q_0 &= \frac{v^2}{1,6} N/m^2
 \end{aligned}
 \tag{3.20}$$

The most important loadcase is: working pressure + wind pressure.

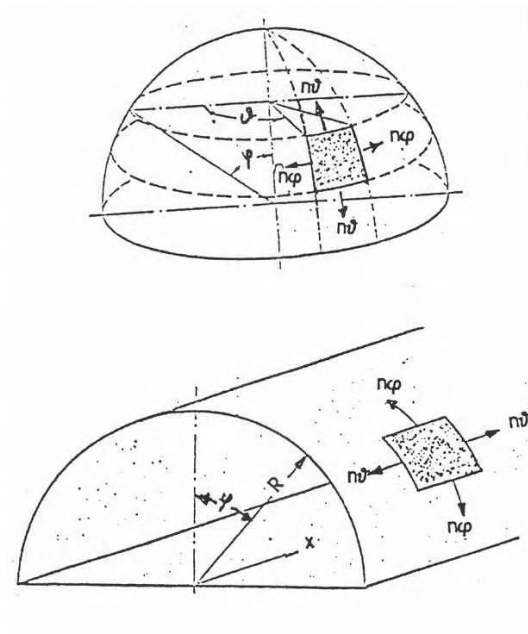


Figure 3.79: Cylinder and sphere.

For spheres:

$$\begin{aligned}
 &1,5R < h > 1,05R \\
 &n\phi = n\theta = \frac{\Delta p * R}{2} + q_0 * R \\
 &1,05R < h > 0,75R \\
 &n\phi = n\theta = \frac{\Delta p * R}{2} + 0,75 * (max\ c) * q_0 * R
 \end{aligned}
 \tag{3.21}$$

The last equation (3.21) is taken from F. Rudolf. The factor (*max c*), or shape constant, was determined by G. Beger and E. Macker for a number of values of p/q_0 .

$\frac{\Delta p}{q_0}$	1,3	0,65	0,55	0,34	0,27
(<i>max c</i>)	1,05	1,1	1,3	1,6	1,8

Cylinders:

$$n\theta = 0,58(1,8q_0 + \Delta p)R \tag{3.22}$$

Quarter spheres:

$$n\phi = n\theta = \frac{\Delta p R}{2} + 1,3q_0 R \tag{3.23}$$

Basket handle arches (Dutch: *korfbogen*): In the cylinder part:

$$n\phi = n\theta = 0,58(1,8q_0 + \Delta p)R \tag{3.24}$$

In the sphere part:

$$n\phi = n\theta = 0,8\Delta p R + 1,6 - q_0 R \tag{3.25}$$

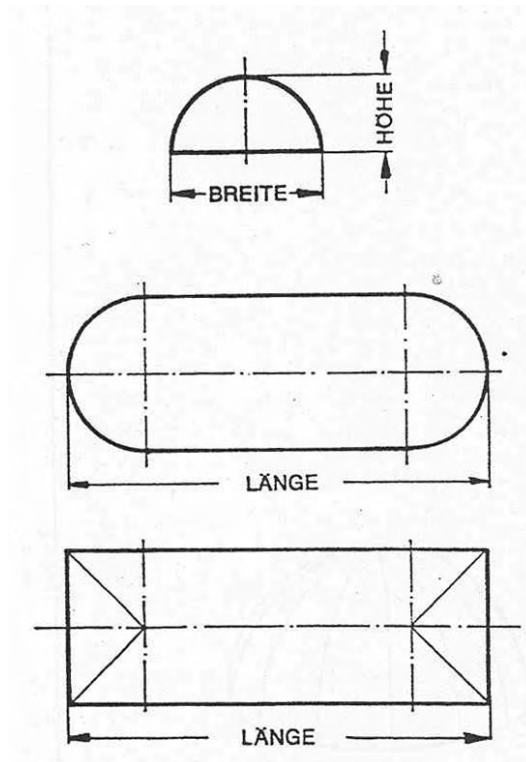


Figure 3.80: The two hall types, compared in Tables 3.7 & 3.8.

Hall no.	Plan area m^2	Length m	Width m	Height m	Volume m^3	Circumference m	Average needed energy kW/h
1	222	22.52	11.00	5.50	900	57.6	1.65
2	314	27.24	12.84	6.42	1490	69.1	1.65
3	423	31.96	14.68	7.34	2290	80.7	2.25
4	570	38.10	16.50	7.95	3300	95.0	2.25
5	713	42.82	18.34	9.17	4850	106.6	2.25
6	872	47.54	20.18	10.09	6520	118.1	3.00
7	1045	52.24	22.00	11.00	8530	129.6	3.00
8	1270	58.40	23.84	11.92	11260	144.0	4.10
9	1553	66.00	25.68	12.84	14870	161.3	4.10
10	1823	72.16	27.52	13.76	18720	175.7	5.60
11	2114	78.32	29.36	14.68	23190	190.1	5.60
12	2425	84.46	31.18	15.59	28260	204.5	8.25
13	2758	90.62	33.02	16.51	34070	218.9	11.25
14	3112	96.78	34.86	17.43	40620	233.3	11.25
15	3539	104.36	36.68	18.34	48650	250.5	11.25

Table 3.7: Needed energy for keeping hall type one from Figure 3.80 pressurized.

Hall no.	Plan area m^2	Length m	Width m	Height m	Volume m^3	Circumference m	Average needed energy kW/h
1	222	22.52	11.00	5.50	690	67.0	1.65
2	314	27.24	12.84	6.42	1590	80.2	1.65
3	423	31.96	14.68	7.34	2440	93.3	2.25
4	570	38.10	16.50	7.95	3520	109.2	2.25
5	713	42.82	18.34	9.17	5140	122.3	2.25
6	872	47.54	20.18	10.09	6910	135.4	3.00
7	1045	52.24	22.00	11.00	9025	148.5	4.10
8	1270	58.40	23.84	11.92	11890	164.5	4.10
9	1553	66.00	25.68	12.84	15650	183.4	5.60
10	1823	72.16	27.52	13.76	19690	199.4	8.25
11	2114	78.32	29.36	14.68	24360	215.4	8.25
12	2425	84.46	31.18	15.59	29670	231.3	11.25
13	2758	90.62	33.02	16.51	35740	247.3	11.25
14	3112	96.78	34.86	17.43	42580	263.3	11.25
15	3539	104.36	36.68	18.34	50940	282.1	11.25

Table 3.8: Needed energy for keeping hall type two from Figure 3.80 pressurized.

3.3.5 Making-up of the fabric

Air-supported structures are assembled from strips of weave with a working width of appr. 130cm. Cylinders can be made from parallel strips and thus material loss is minimal. In sphere-shaped structures a radial division is normally used. The strips then have to be cut up into long stretched triangles. To diminish material loss as much as possible, and to reduce the number of strips coming together in the top, a new division is adopted when two strips together have become as wide as one strip.

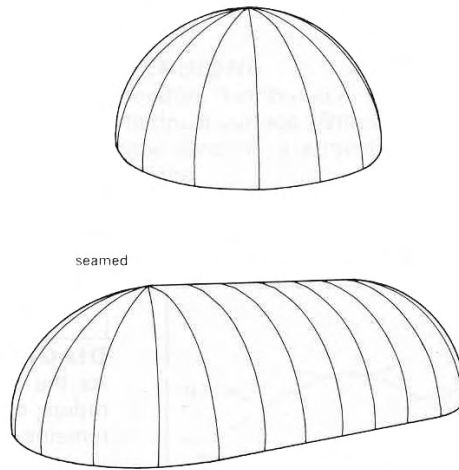


Figure 3.81: Often used patterns in two common shapes.

The connection between the strips is usually made by seams formed in a double overlap. Glueing is also possible, however, the available methods are often do not offer enough weather resistance. When the surface layers are made from a thermoplastic material, for instance PVC, the connection can also be made by welding. This method is only used for smaller structures, because the connection is only superficial, which means that the weave that provides the strength is not through-connected.

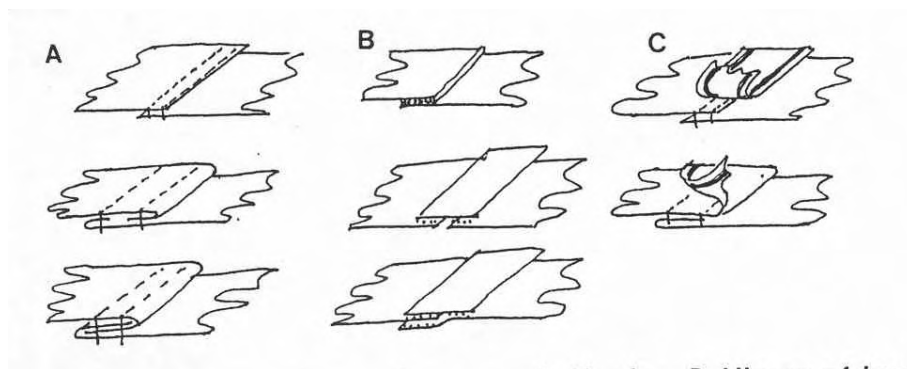


Figure 3.82: Different possibilities for seams: A. Sewing; B. Gluing or welding; C. Combinations.

Welds are sometimes used to improve the water- and airtightness as well as the weatherproof-

ness of the seams, by welding a strip of thermoplastic foil over the sown seam.

Material losses:

Cylinder:	5-10%
Sphere:	20-30%
Torus:	10-15%

3.3.6 Anchorage

The anchorage has two main functions:

1. Transfer of all membrane forces caused by the over-pressure and wind forces to the underground
2. Airtight connection of the skin to the underground

In Figure 3.83 a number of often used anchorage technics is shown. The simplest one is with a circumferential tube filled with sand or water. The size of the anchorage forces in cylinder shaped halls is mainly defined by the radius R of the structure (when the same maximal over-pressure is considered for all different sizes of the halls).

In most cases an over-pressure of 30mm water column is sufficient with a wind thrust of $0,95kN/m^2$ (appr. 140km/h). According to H.J. Schulz (Schulz 1962):

$$\text{Anchorage force:} \quad Z = 0,7R \text{ kN/m (R in m)}$$

$$\text{Vertical component:} \quad Z_v = 0,67R \text{ kN/m}$$

$$\text{Vertical force with } R = 5,5m \quad Z_v = 0,67 * 5,5 = 3,7kN/m$$

When using a sand-filled tube ($\rho = 1,7kg/dm^3$) and a safety factor 2, a diameter of 75cm is needed. This means that already with relatively small radii other systems are needed, to prevent building absurd tube dimensions.

The most used system is the one where thread anchors with pull eyes are put into the ground with a c.t.c distance of approximately 1m. Then a steel tube is pulled through a seam in the structural skin and through the eyes in the anchors. The seam is of course interrupted at the anchors. A slab of weave is pressed to the ground on the inside of the structure to maintain the needed over-pressure. When the soil conditions are too poor, it may be necessary to provide an extra load, for instance in the form of concrete blocks or a poured foundation. When the anchorage forces increase even further (especially in radomes), the interruptions in the seam are no longer desirable and clamping connections are most often used.

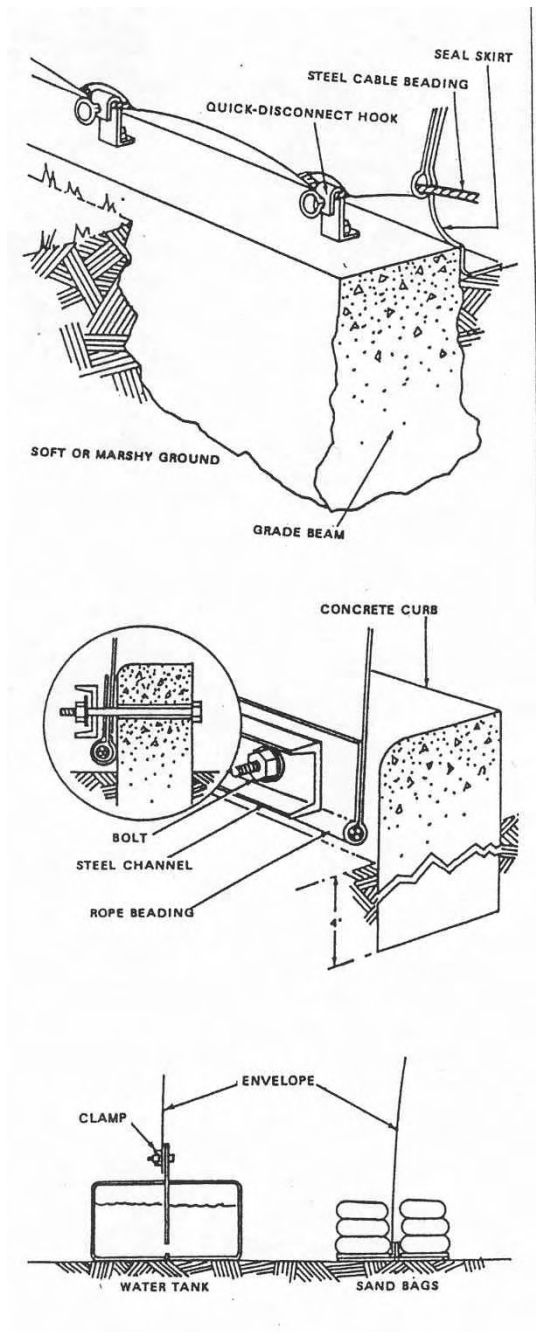


Figure 3.83: Some characteristic principles of anchorage.

3.3.7 Building physics

3.3.7.1 Indoor climate

The thermal insulation of the very thin skin is of course very small, even though the fairly high thermal conductivity ($\lambda = 0,10$) of the material. The K-value of the material is:

$$K = \frac{1}{\frac{1}{\alpha_i} + \frac{\delta}{\lambda} + \frac{1}{\alpha_e}}$$

$$K = \frac{1}{\frac{1}{5} + \frac{0,0008}{0,10} + \frac{1}{20}}$$

$$= 4Kcal/(m^2hK) \quad (3.26)$$

For a double layered skin:

$$K = \frac{1}{0,20 + 2 * 0,0008 + 0,15 + 0,05}$$

$$K = 2,5Kcal/(m^2hK) \quad (3.27)$$

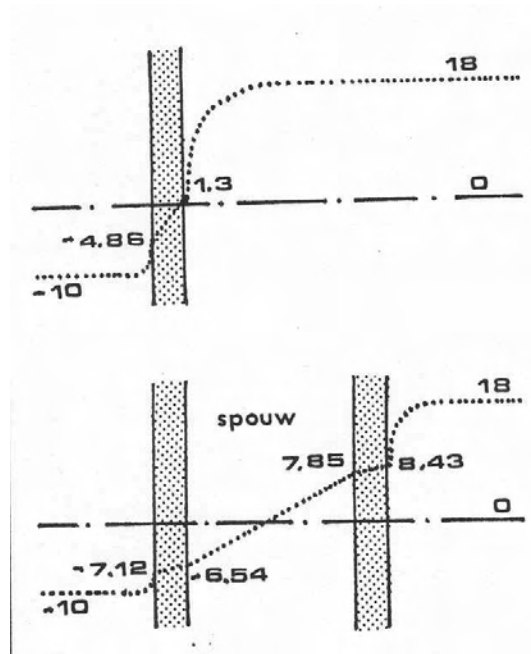


Figure 3.84: The temperature profile for single and double layered skins.

An example:

A pneu with a plan of $500m^2$, a volume of $1800m^3$, a skin area of $800m^2$ and $t_i = +20^\circ C$, $t_o = -5^\circ C$ ((Wellesley-Miller 1972).

To prevent unnecessary loss of heat, ventilation is only performed once each hour, so $n=1$. This frequency is of course dependant on the use of the internal space. When a large amount of people needs to be present at the same time, n_{min} should be taken as $40m^3$ per person. When the loss of air through the airlocks is large, a separate contribution should be accounted for.

When a 10cm thick concrete floor is considered as a floor structure, then a constant temperature of $10^\circ C$ is maintained at 2cm below ground level. The K-value of the in total 2,1m thick floor layer is 0,47.

For a single skin now holds:

$$\begin{aligned}
W_{single} &= (20 + 5) * 1 * 18 - - * 0,31 + (20 + 5) * 4 * 800 + (20 - 20) * 0,47 * 500 \\
W_{single} &= 13.950 + 80.000 + 2.350 \\
W_{singel} &= 96.300Kcal/h
\end{aligned}
\tag{3.28}$$

For the double-layered skin:

$$\begin{aligned}
W_{single} &= (20 + 5) * 1 * 18 - - * 0,31 + (20 + 5) * 2,5 * 800 + (20 - 20) * 0,47 * 500 \\
W_{single} &= 13.950 + 50.000 + 2.350 \\
W_{singel} &= 66.300Kcal/h
\end{aligned}
\tag{3.29}$$

This shows that a multiple-layered skin results in a significant reduce of needed energy when a normal -and for air-supported halls: fairly high- inside temperature needs to be maintained. According to U. Bauer (Bauer 1968) the total heat flow adds up to:

$$Q = K * F * (t + 5^{\circ}C) \tag{3.30}$$

Wher F is the total area of the skin and T the desired temperature difference. The extra 5°C is a practical value, considering losses due to airleaks. For an average cylinder hall of 40x18x8m and a demanded temperature difference of 20°C a energy consumption of 112.000kcal/h. R. Brylka (Brylka 1970) uses the following rule of thumb:

area of plan[m²]*240 at temperature difference of 20°C, so: 100 * 240 = 168.000kcal/h. This is clearly on the very safe side.

The forming of condense is a problem especially encountered at swimming pools, because of the high internal temperatures and the large evaporation surface. According to Bauer a ventilation coefficient of 1,25 per hour is enough to prevent the forming of condense. In extreme situations, like the forementioned swimming halls, this can be achieved by forming gutters, using the seam covering strips. By puncturing these in strategic place the possibly formed condense can be diverted.

Direct solarization can be prevented by using light coloured materials. In the summer, however, the temperature of the outside skin can still accumulate to 55°C. Usually, this does not impose great objections, because the air is refreshed several times each hours. If it still poses problems, the outside can be cooled by spraying water. In smaller halls -where this problem is most urgent- also the use of mechanical coolers can be considered.

3.3.7.2 Air locks

To maintain the internal over pressure, the entrances to a air-supported structure need to be provided with air locks. A number of considerations need to be made in the design of such locks:

- A hole needs to be made in the tensioned outer skin. This can not be done without taking precautions: the force from the skin needs to be diverted and brought down to the foudnation. This is usually done by giving the hole a smoothly run, mostly circular, shape and leading a cable through the edge seam.
- The entrance itself can be constructed in several manners:
 - A simple door opening against the air pressure, so inward.
 - A rectangular lock with single or double doors on both sides.
 - A revolving door.

- Special solutions, like flaps falling over each other or cushion shaped elements.
- The transfer from the outer skin to the lock needs to be made in such a way that the airpressure can be taken in the transfer area, as well as movements are allowed to prevent undesired stresses in the skin.

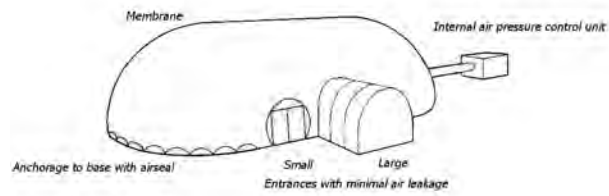


Figure 3.85: Necessary provisions for entering while maintaining the over-pressure.

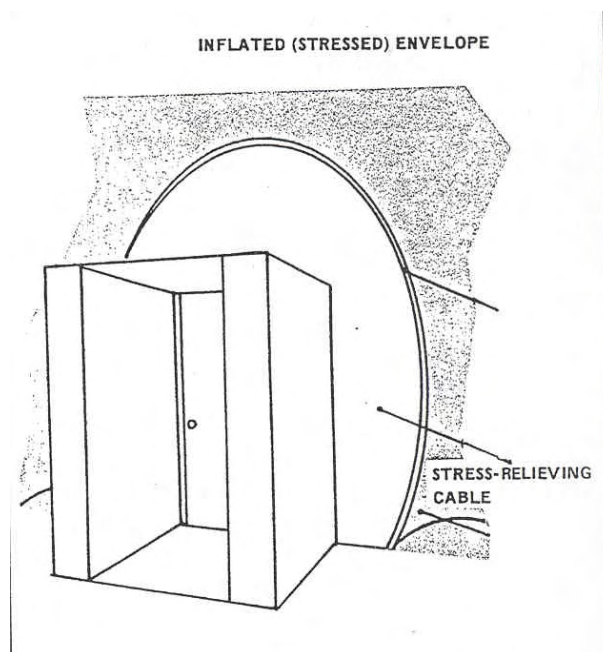


Figure 3.86: Tensioning around a door.

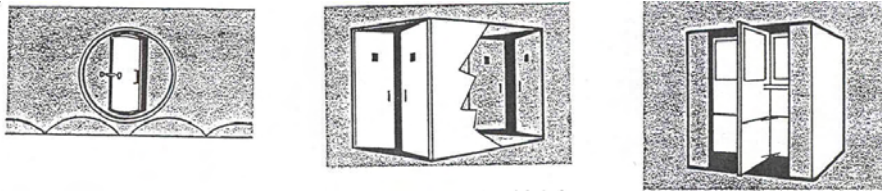


Figure 3.87: Different solutions for an airlock.

3.3.8 Regulations

There are no regulations in the Netherlands. A German proposal, dating back to July 1971, on the design of the 'Arbeitskreis Tragluftblauten' of the 'Fachkommission Bauaufsicht der Argebau' (Argebau 1971), can be summarized as follows:

1. Building permits are provided for a timespan of maximum of 5 years. After 5 years requests can be made for every time a duration of 3 years.
2. For the calculation the windloading on half cylinders can be schematized by a uniformly distributed radial suction force of $-0,9$ *the local value of the wind thrust (Figure 3.88). For the anchorage a horizontal load of $0,6$ *wind thrust*height should be considered. A more accurate calculation, based on the division of the windload of Figure 3.88.4 *may* be used for half cylinders, but *has* to be used for sphere shaped structures.
3. Snow loading does not have to be considered when it made sure that the inside temperature never falls below $12^{\circ}C$. If one wants to get permission not to consider snow load anyhow, one should take care that the snow is removed in an early stage. For instance with a cable hangin from the top of the structure. Concentrated loads should always be avoided.
4. The safety on the occurrence of folds due to compressive stresses in the skin needs to be:
 - For cylinders: $V = \frac{p_i * r}{max n_D} = 2,0$
 - For spheres: $V = \frac{p_i * r}{max n_D} = 1,2$

Where n_D is the largest membrane compression force that occurs when the inner pressure p_i is left out of consideration.

5. For cylinders holds for the inner pressure, when $h/r \geq 1$:
 - $min p_i = 0,3kN/m^2$, for $h > 8,00m$
 - $min p_i = 0,2kN/m^2$, for $h < 8,00m$
 - $min p_i = 0,12kN/m^2$, for $h < 3,50m$ and covered area $< 200m^2$
6. The skin material needs to be secured for tearing for at least 5x the maximal tensile stress. The seams need to have a safety factor of 3,5.
7. Air-supported halls, where 11-30 people need to be staying, have to have 2 cold air ventilators, each capable of maintaining the overpressure. In halls where over 30 people can reside, the second ventilator needs to be equipped with a self starting engine, non dependend of outside power. In this case also at least two exits need to be available for fire safety. An air-supported hall is, however, not considered as unsafe regarding fire. They are considered as very safe structures. In the first place the skin is very light, so collapse is not always disastrous. Also, the collapse is very slow due to the very low over-pressure, even when the ventilators fail or large holes appear. During a fire large holes usually appear locally at the fire, because the materials are often flame stopping. Collapse is furthermore counteracted by the warming up of the internal air, which will expand and initiate a rising motion. (Figure 3.89)

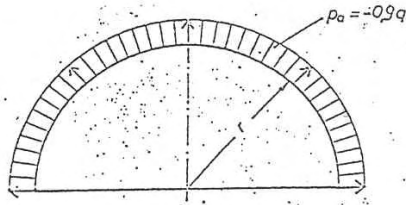


Bild 1

Vereinfacht angenommene Belastung eines Halbzylinders durch Windsog

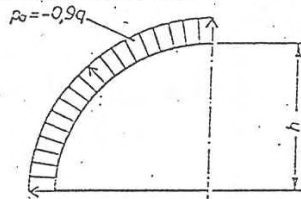


Bild 2

Vereinfacht angenommene Belastung einer Viertelkugel durch Windsog

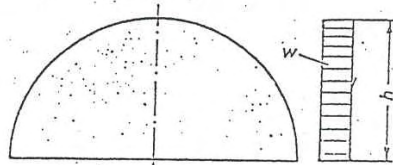


Bild 3

Vereinfacht angenommene Belastung für Verankerungen

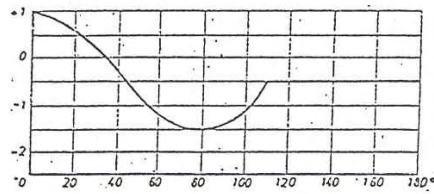


Bild 4

Beiwerte c zur Ermittlung der Windbelastung

Figure 3.88: Loading on circular shaped air-supported halls.

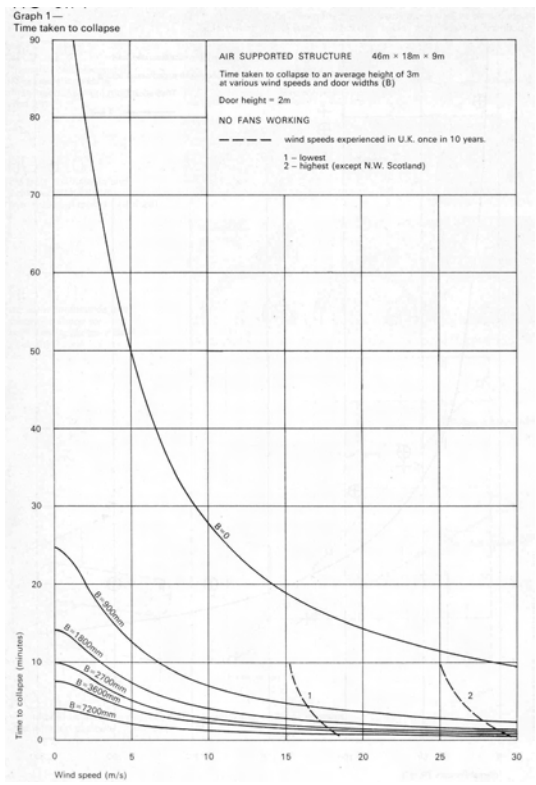


Figure 3.89: Time taken to collapse at different door widths.

3.3.9 Stabilizing the shape

3.3.9.1 tying down

The shape of the structure can be influenced by tying it down line or point shaped. Frei Otto (Otto, Trostel & Schleyer 1962) gives many possibilities for this. One of the oldest known applications is the Brassrail snackbar by V. Lundy, built for the New York World Fair of 1965 by Birdair.

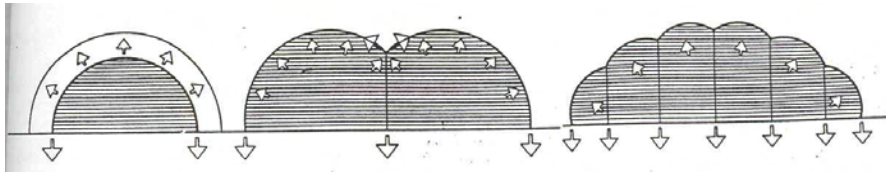


Figure 3.90: The principle of stabilisation by tying down.

Lineshaped indentations can be created by spanning cables over the skin (Figure 3.91) or by walls underneath the skin, like was done in a twin tennishall by Stromeyer.

These cables and walls exert, in most cases, an extra stabilizing effect on the structure, because it becomes less sensitive for asymmetrical or local loading. This creates the possibility of very large spans, especially when the height is chosen small. In this case the radius for a skin that has not been tight down will be very large and it will be very sensitive for local disturbances. The tension in the skin will also be very high. This skin stress will be lowered by decreasing the radii. (See Figure 3.69 and (Schippers 1975))

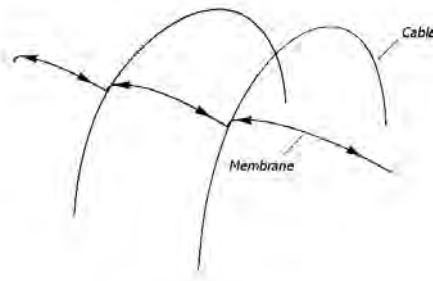


Figure 3.91: The principle of tying down with line shaped ties.

The pattern of these cables on the surface of the roof is most often radial (in circle shaped plans), parallel (in rectangular plans), rectangular or even geodetic (built up from triangles). The most famous example of a rectangular cable pattern is the U.S.A. pavilion on the World Fair in Osaka 1970 (Architectural design: Davis Brody; Structural design: David Geiger), shown in Figure 3.92. The membrane consists of a glassfibre weave with a PVC coating. It has a plan of 83x142m, shaped like a super-ellips. In this case exponent $n=2,5$ was used (Chapter 3.3.3).

Another example is the 135x50m measuring Canadese pavilion for the 1986 Expo in Vancouver by E. Zeidler; the so-called B.C. Place Amphitheatre. Furthermore the Lindsay Park Aquatic Centre in Calgary, Canada. This last one has a roof in the shape of a supercircle with a diameter of over 200m. In a supercircle $a=b$ is chosen (also Chapter 3.3.3).

In this structure much attention was payed to the thermal insulation. The roof is built up



Figure 3.92: The American pavilion at the Osaka World Fair.

from multiple layers. The outer layer is a glasfibre weave with a PTFE coating. Underneath a layer of 10cm so-called Fibair isolation material is hung and all the way on the inside a dampproof layer of Tedlar foil is installed. This total layer is still not entirely airtight.

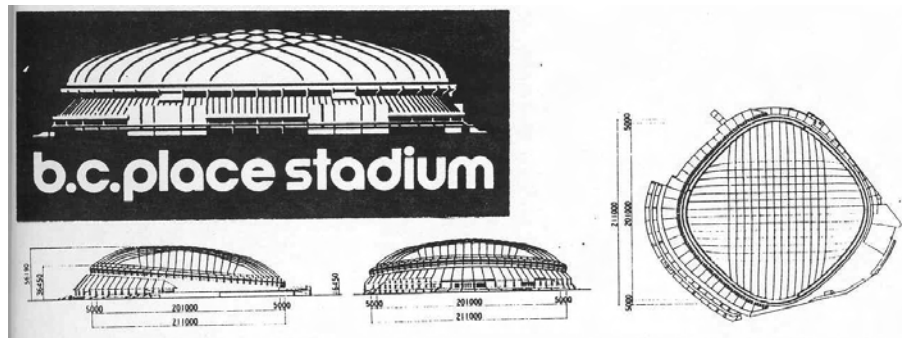


Figure 3.93: The B.C. Place Amphitheatre in Vancouver (top) and the Aquatic centre in Calgary, Canada (bottom).

Research into soap bubbles (mainly based on visual judgement) can provide information about the most appropriate way and shape of the tying down by interior walls. Moreover, studying the laws to which conglomerations of two or more soap bubbles apply, gives insight in the origin and appearance of inflated foams and some single cell organisms, of which the interior walls are stiffened and are part of the skeleton (Figure 3.94).

The shape of the dividing wall of two soap bubbles follows from:

$$\frac{1}{R_A} + \frac{1}{R_{AB}} = \frac{1}{R_B} \quad (3.31)$$

so: $R_{AB} = \frac{R_A * R_B}{R_A - R_B}$

When considering two bubbles of the same size the following holds:

$$R_{AB} = \infty \quad (3.32)$$

And when $R_A = 2R_B$:

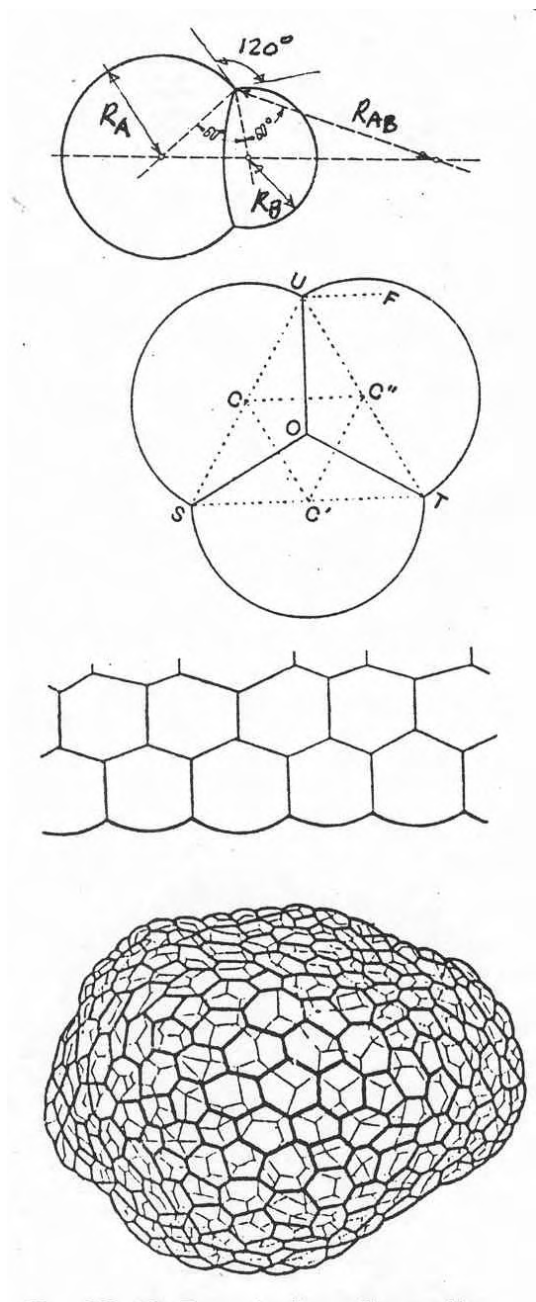


Figure 3.94: Soap bubble configurations.

$$R_{AB} = R_A \tag{3.33}$$

3.3.9.2 Double layered structures

The necessity to enter an air-supported structure through an air lock, to prevent the loss of pressure, is felt like a hindrance in many areas of application. When the skin is made double, the loss of pressure between inside and outside can be made obsolete. When this is done one should speak of an 'air inflated structure' rather than an 'air supported structure'.

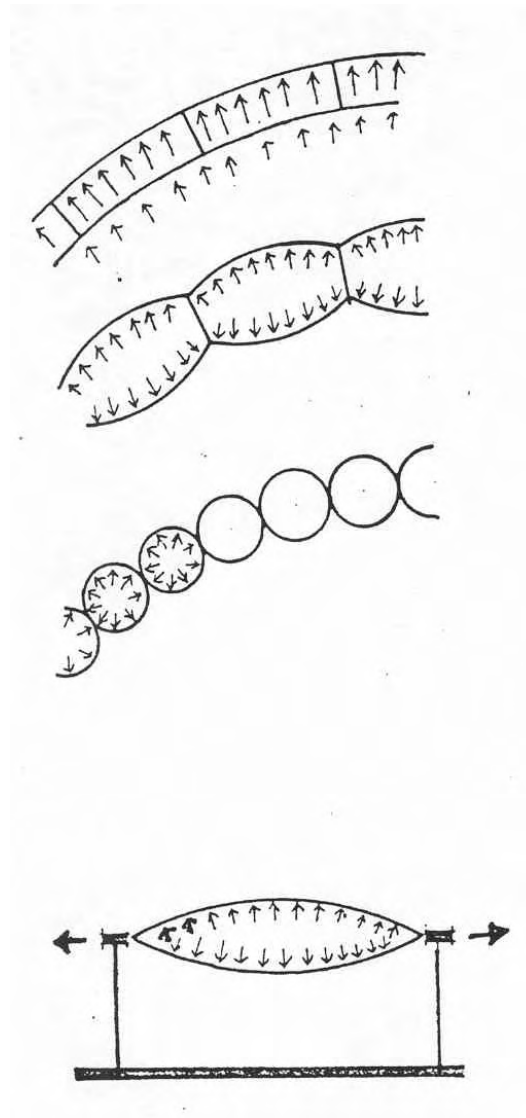


Figure 3.95: Principles of double layered pneumatic structures.

An early example of such a solution is the Boston Arts Centre Theater by Koch, Ross and Weidlinger. Two nylon skins, spanned between a steel circular compression ring with a diameter of 35m, are inflated into a cushion with a thickness in the centre of 6m (Figure 3.96).

When covering a shopping street in Marl Germany, cushions of approximately 30m wide and 60m long were used. These were modelled to a more or less flattened shape by a number of tying cables on both the top and bottomsides, on a c.t.c. distance of 7,5m. The material that was used

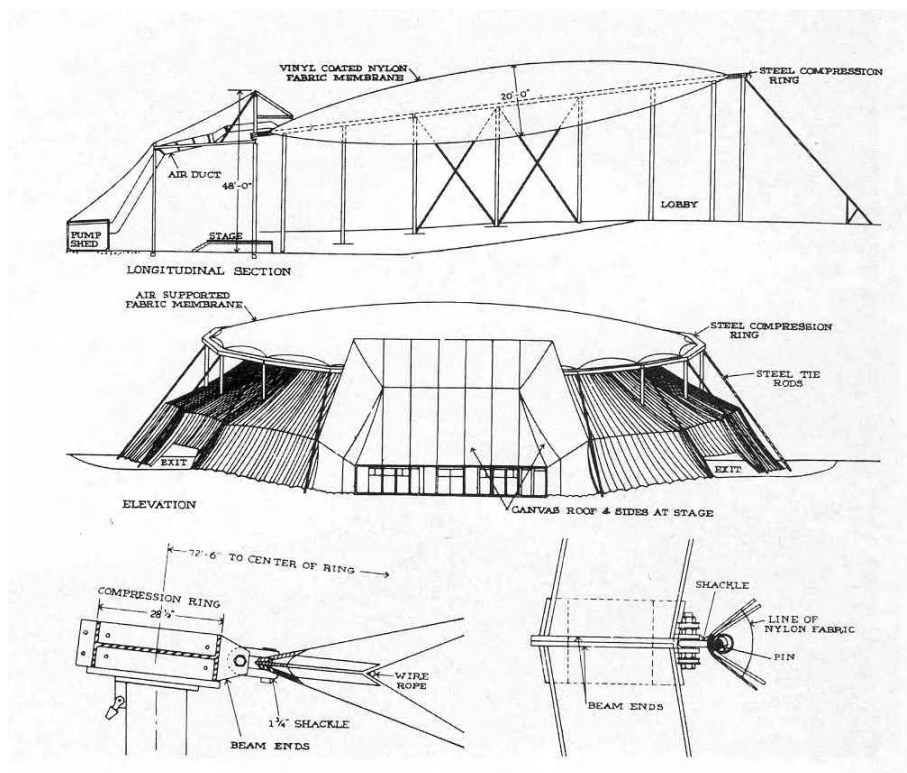


Figure 3.96: The Boston Arts Centre Theatre by Koch, Ross and Weidlinger.

here was linear polyester for the weave (Terlenka or Diolen) and PVC for the coating on both sides. This led to a total weight of the membrane of $850g/m^2$ and a tearstrength of $4,15kN/5cm$ the thickness of the cushions was approximately 8cm.

In a similar way the engineering company ABT realized a roof in Burger's Bush in Arnhem. It measured 90x150m and was covered with cushions consisting of three layers of PTFE foil, measuring 3x6m each. This tying down with cables was used to reduce the disadvantage of very thick cushions needed for large spans.

This can also be reached by using internal walls. This was for instance done in the exhibition hall for the nuclear energy committee of the U.S.A., designed by V. Lundy (Figure 3.99) The spanning distance for the skin was thus fixed at 1,2m. To be able to give the internal and external skin a fluent look, it was decided to use over-pressure in the room and choosing a slightly higher over-pressure for the cushions themselves (respectively 38 and 49mm water column). This leads to the impression of inflated tubes at the free ends of the entrance parts, which are used as portalframes.

Constructing with inflated tubes has been used in many different shapes. For instance the Fuji Group pavilion (Osaka, 1970, Figure 3.100) where the architect Yukata Murata used portal frames shaped like giant tubes with a span of around 50m to create an interconnected arched roof.

At the so-called Showboat of the Electric Energy pavilion by the same architect, three portal shaped like tubes, spanning 23m were used as a support for a double membrane spanned in between. In these double membranes an *under*-pressure was created (Figure 3.101). The video pavilion by the ERG Group in Sonsbeek in 1970 was based on a similar principle (Figure 3.102).

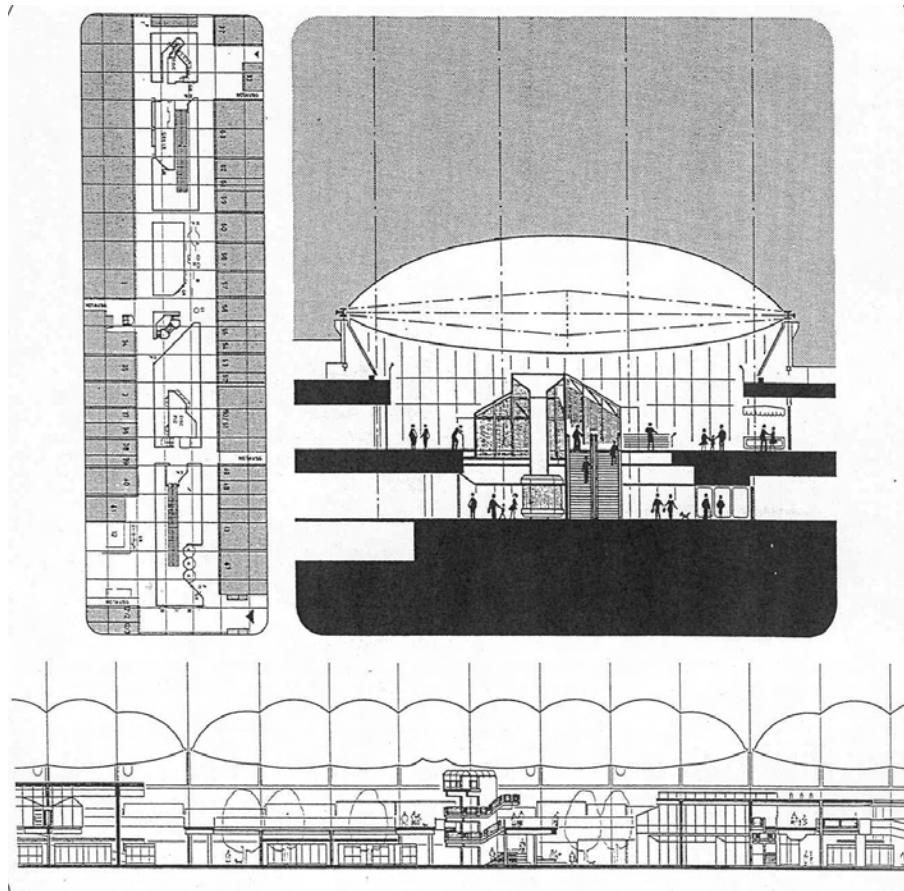


Figure 3.97: Structural lay out of the covering of a shoppingcentre in Marl.

The principle of the tube was not only used for roofstructures. An interesting example is the inflatable bridge, developed by P.S. Bulson for the army engineers. The bridge has a free span of 6m and can carry the weight of a car. The in this case high tensile forces are taken up by inbedded steel cables, while the compression stress is taken up by timber elements layed in the width direction of the bridge (Figure 3.103).

Another important area of application is that of the inflatable barrier (Figure 3.104). The internal pressure is provided by water let into the structure. It is possible to get such a dam up to height in a very short matter of time. The oldest example is the so-called 'Fabridam', built by Imberson in Los Angeles in 1957. In Vezzer in France this solution is used to be able to adjust the height of the dam to the ever changing run-off of the river. This way the effects for the people living in the direct neighbourhood are kept small.

Closer to home an entirely foldable storm surge barrier, proposed by ir. J.C. Buyze, was built by Vredestein. During normal weather it is stored underneath steel covers and it only is used when the dikes collapse.

Besides by using interior walls, the skins of double-layered inflated structures can be held together by threads. By creating a fine mesh of threads between both layers of skin, a total flatness of both outer skins can be achieved. This way pneumatic sandwich panels can be created.

R. Buckminster Fuller, in cooperation with Berger Brothers, developed rubber inflatable domes, assembled from rhomb- or triangular-shaped panels. The English firm M.L. Aviation

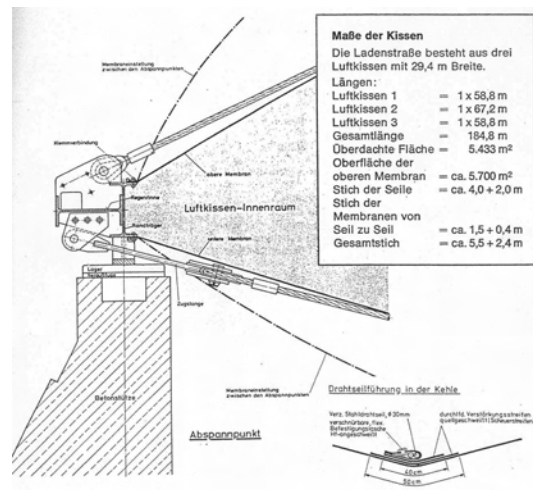


Figure 3.98: Structural detail of the covering in Marl.

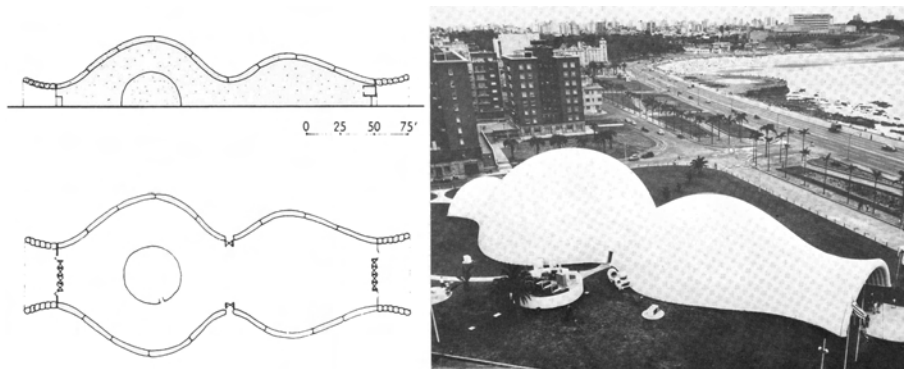


Figure 3.99: Double layered exhibition hall by V. Lundy.

Co. used to have a standard system in its program, called 'airmat-shelters', with which different combinations between quarter spheres and half cylinders are possible. It is interesting to note that hall of 18x9x5m can be pack in a box of 1,5x1,0,5m.

Using airmats fairly large spans can be reached. A pavilion by P. Jutras, for the Expo 1985 in Tsukuba, Japan, has a span of 27m with a largest thickness of 4,5m.

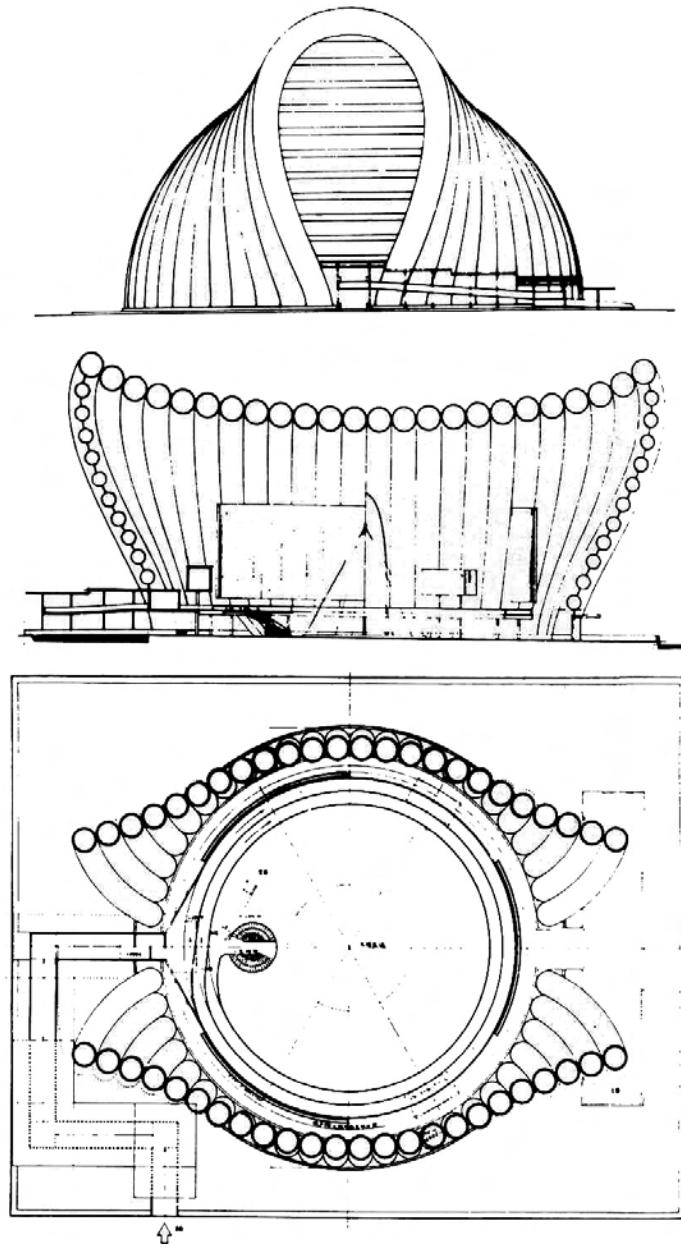


Figure 3.100: Fuji Group pavilion in Osaka.

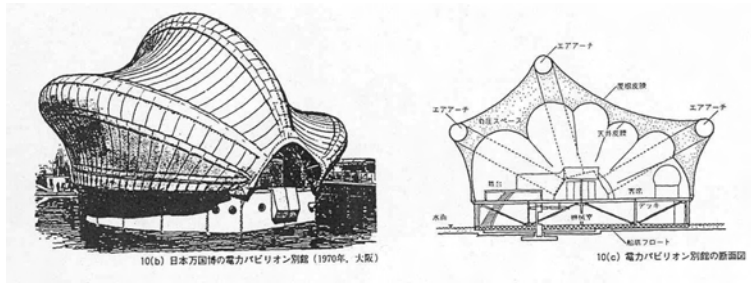


Figure 3.101: Showboat of the Electric Energy pavilion by Y. Murata.

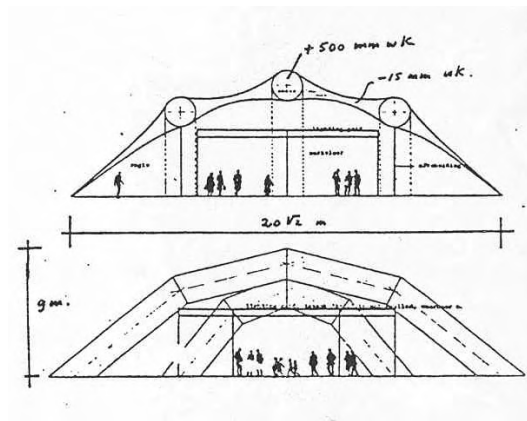


Figure 3.102: The video-pavilion in Sonsbeek by the ERG-group.

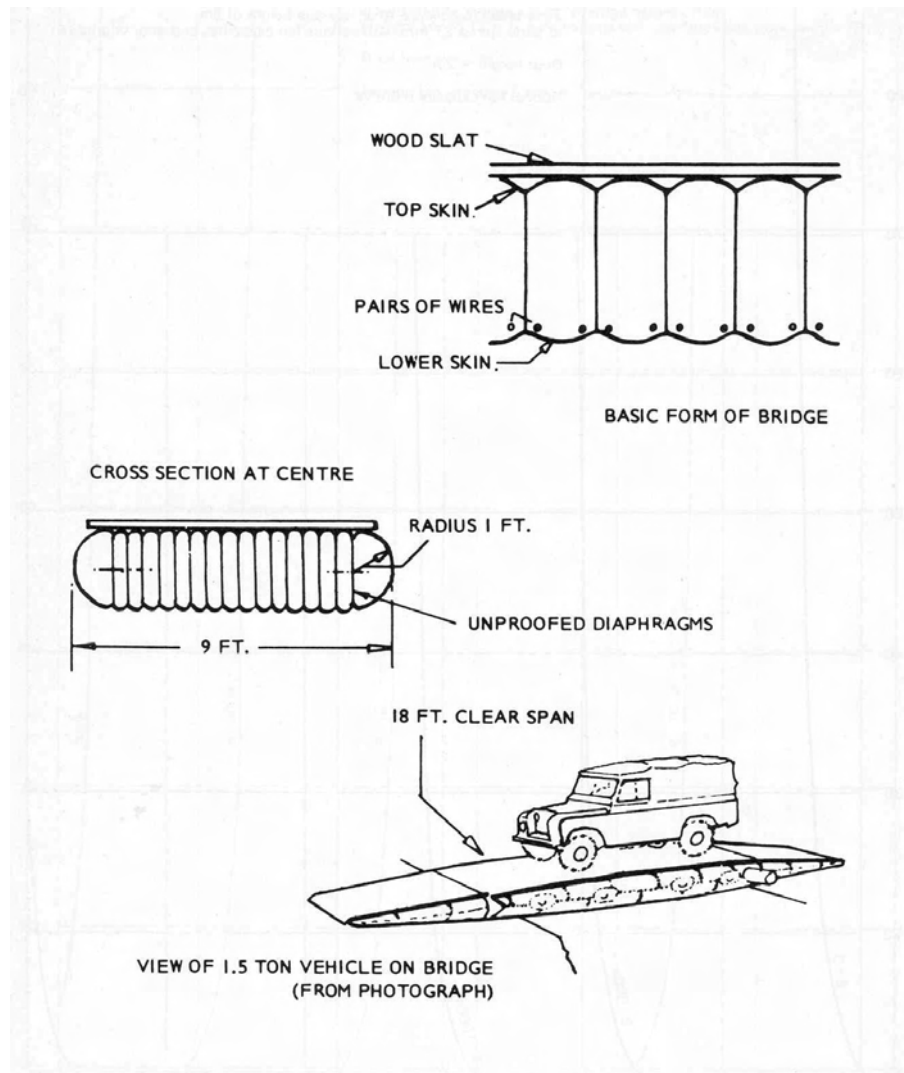


Figure 3.103: Inflated bridge structure by P.S. Bulson.

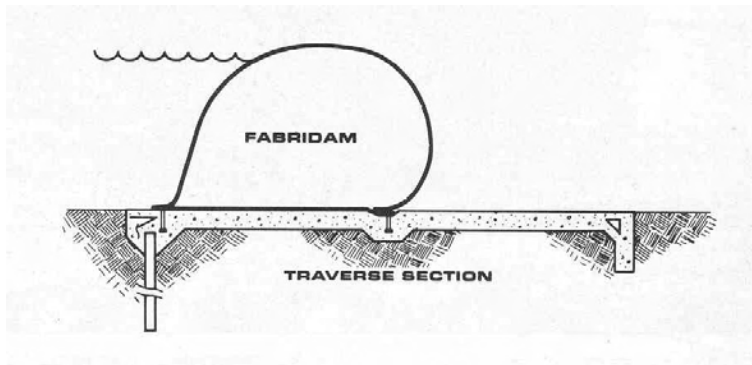


Figure 3.104: An inflated dam structure, with water as medium.

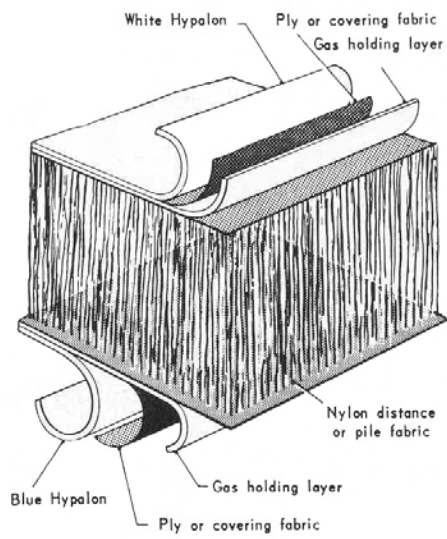
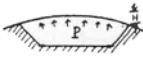
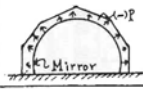
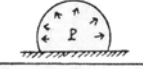
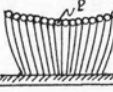
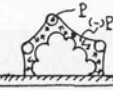
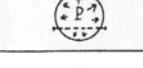
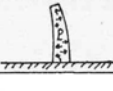


Figure 3.105: Principle of the air sandwich.

NOTEWORTHY PNEUMATIC STRUCTURES AT EXPO'70, OSAKA

Sectional Shape	Structure	Size	Main Material	Ref. Pic.	Sectional Shape	Structure	Size	Material	Ref. Pic.
	Roof of U.S. Pavilion	L: 142m W: 83m H: 6.1m A: 9,500m ² (* Above concrete ring)	PVC coated Glass-fiber Fabric	8		Grand Roof of Festival Plaza	L: 292m W: 108m H: 30m A: 28,900m ² (A Unit: 10.8m x 108m)	Polyester film	13
	Interior Mirror of Pepsi Pavilion	D: 30m H: 18m A: 700m ²	surface aluminized Polyester Film	9		Mush Balloon (5 Balloons)	D: 30m (1) H: 29m (1) D: 20m (1) H: 20m (1) D: 15m (3) H: 15m (3)	PVC Coated Polyester fabric and PVA fabric	14
	Exhibition Dome of American Park Pavilion	D: 23m H: 18m A: 420m ²	Neoprene coated Nylon fabric (2 ply)	10		Fuji Group Pavilion	L: 64m W: 50m H: 31m A: 2,000m ² (Beam Dia 4m)	Hypalon coated PVA fabric (2 ply)	15
	Balloon of Ricoh Pavilion	D: 25m H: Max 75m	Rubber coated Nylon fabric	11		Floating Theater of Electric Power Pavilion	D: 26m H: 26m A: 450m ²	Hypalon coated Polyester fabric	16
	Dome of Information Booth	D: 9m H: 12m	transparent PVC film Laminated Polyester fabric	12		TOWER OF Mitsui Pavilion	D: 15m H: 50m A: 175m ²	PVC coated Polyester fabric	17

Remarks: L=Length W=Width H=Height A=Projected Roof Area

Figure 3.106: Noteworthy pneumatic structures at the Osaka World Fair 1970.

3.3.9.3 Rigidising air-supported structures.

As can be concluded from the German proposed regulations, air-supported structures are mainly regarded as temporary structures. The vulnerability and easily deformable skin are the most important considerations in this regard. It has been tried -not always succesful- to change these aspects by making the skin rigid, by spraying polyurethane foam or glasfibre polyester onto the skin.

When using polurethane foam it can be chosen to spray it on the inside as well as on the outside of the structure, because the material has a strong sticking immidiately when expanding. People who have used this technic are G. Günschel and F. Otto in cooperation with W. Mühlau.

In 1967 the first two test structures with polyurethane foam, constructed by sparying it onto a PVC air-supported hall, were build in the Netherlands by P.B. Hangelbroek of the Instituut Landbouwbedrijfsgebouwen Wageningen. The PVC foil was held in its right shape by using a net of sisal rope.

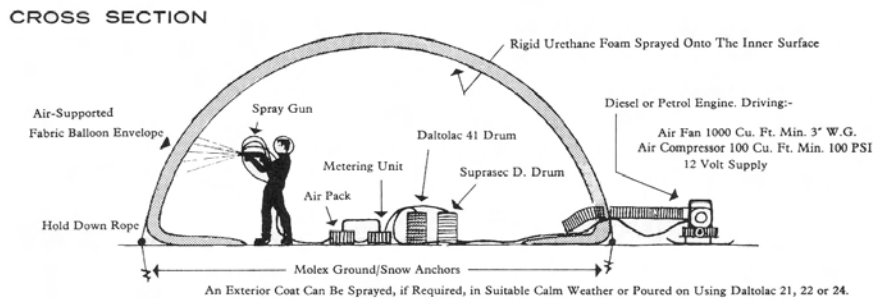


Figure 3.107: The principle of rigidising air-supported structures.

Bayer made half-sphere residential units, by spraying polyurethane foam spirally over an inflated model. The spray head was moved up along a meridian arch, while at the same time the model was turned round a vertical axis. After hardening, the mold was removed. Many hundreds of these structures have been built in Turkey and Guatemala, where they were use as emergency housing. In Tilburg a temporary project, the so called 'Iglonium, arose around 1972, where a series of the fore-mentioned units were coupled by connecting pieces from the same PU-foam.

Burger Eisenwerke in the same way created a building out of glassfibre polyester, with a footprint of 4x8m and a height of 2,5m, while the material thicknes was a mere 5,5mm. The hardest thing in glassfibre polyester is the fact that a fairly tough underground is needed to be able to drive out the enclosed air in the laminate.

The character of the inflatable structure changes radically when the stiffening material is hardened out and the over-pressure is released. It can only be concluded that the original structure was used merely as a mold to build a totally different structure with a totally different structural principle. Now other considerations regarding the structural shape will begin to play an important role.

The use of inflatable structures for mold purposes is also look into in the concrete industry, amongs others by Bini in the Bini-shell principle, by Wallace Neff, by Hangelbroek, Poort and Grabovski for the Airform-procedure for covering silo's and by the Australian company Dome Constructions. The latter has constructed spheres to up to 80m span, by first spraying a layer of PU-foam onto the inside of a pneu. After this concrete an reinforcement were added. In the end the pneu was removed and a watertight coating is applied to the outside in the desired colour.

The problem that is encountered usually, is that as a result of the local pouring or spraying of the concrete many small cracks occur in the end result. This is why the concrete is applied in many thin layers.

The procedure of making air-supported structures rigid by using foam or glassfibre polyester has to take place at the building site. Depending on the climate conditions, this can pose difficult problems.

3.4 Space frames

RECOMMENDED STUDY MATERIAL

Title	Author	Year
<i>Title first entry</i>	<i>Author first entry</i>	<i>YoP first entry</i>

3.4.1 Space Frames

A space frame is normally a light weight structure, it is stiff, built out of tension and compression elements and the nodes are, at least in calculations, working like hinges. The term space structures will be used as a generic term for spatial arrangements, geometric configurations, forms, patterns and structures. The architectural or built space structures have various characteristics which include physical perceptual, functional economic, symbolic, or spatial aspects. The physical aspects deal with weight, size, force, and strength, method of construction or fabrication, and spatial aspects deal with dimension, topology, geometry and symmetry. The flat shape, of space frames, is used quite often. In space frames a lot of repetition is used which makes it less expensive and easy to build. Different structures and their families transform from one to another.

3.4.1.1 Introduction

Designing in three dimensions 1-dimensional space structure ($n=1$) are organized around a 'line' as in a modular tower or a linear truss. 2-dimensional space structures ($n=2$) are organized around a 'plane' as in a single- or double-layered space frame. 3-dimensional space structures ($n=3$) are organized in '3-dimensional space' as in a multi-layered or multi-directional space frame. N-dimensional space structures must be projected down to 3-and lower dimensions for us to realize them physically. These four classes of built structures are composed of four elements, vertices (nodes), faces (panels), edges (struts), cells (3-dimensional modules).

Most of the time engineers and architects think in terms of planar (2D) structures such as beams, trusses and portal frames when considering methods of spanning space. However, in many cases there are advantages to be gained from thinking in three dimensions and apply spatial structures for medium to long spans. Especially when heavy loads points or moving loads are to be supported.

Among architects, engineers and others in the building and construction industry the general term 'space frame' is commonly used to describe three-dimensional structures that may be either frames or trusses in the engineering definition of the terms. In fact, practically all 'space frames' are space trusses in the engineering sense. 'Space grid structures' is an accepted alternative name that encompasses both structural systems. They are systems of inter-connected elements.

A short overview on the development of the space frame In the 19th century several domes were designed and built with cast iron elements. August Föppl (1854-1924) is generally recognized as one of the first scientists having introduced consequent research work concerning 3-D steel trusses. However the first real attempts to design and realize metal space frames are known to have been made by Alexander Graham Bell (1847-1924). In spite of the fact that in structural engineering the space trusses by Eiffel can be regarded as an assembly of 2-D trusses, the aero plane designs showed explicitly that 2,5-D and 3-D entities had to develop further, because the spatial stability had to be absolute.

- Eiffel tower, Gustave Eiffel (1832-1923)
- First industrial Space Frame, Graham Bell (1847-1922)
- MERO system, Max Meringhausen (1903-1988)

- Fuller Sphere, and study on closest packing of spheres, developed the Octet Truss System, Richard Buckminster Fuller (1895-1981)

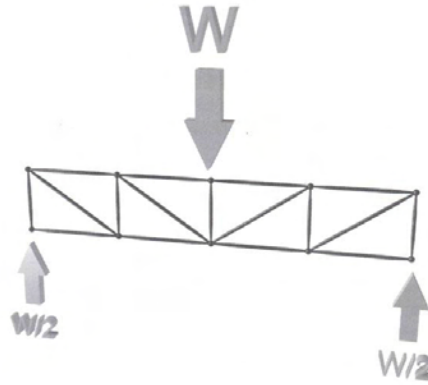


Figure 3.108: A point load supported by one individual simple truss. Image from (Chilton 2000)

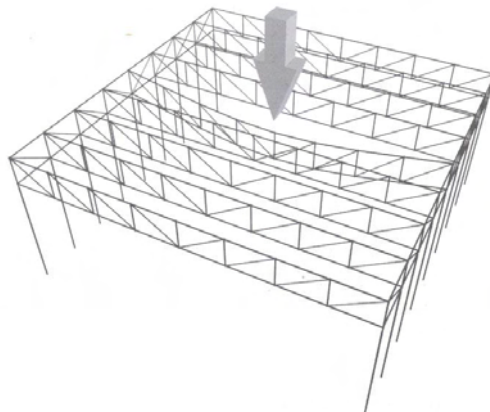


Figure 3.109: Deflection of a system of individual trusses. Image from (Chilton 2000)

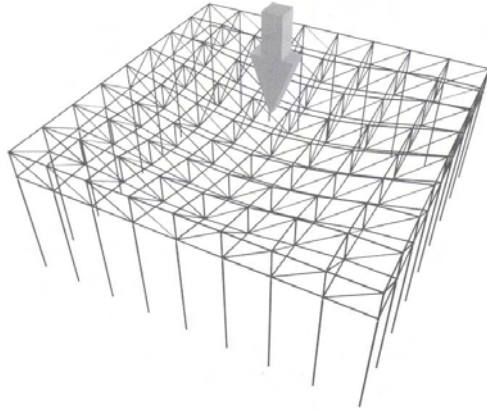


Figure 3.110: A point load supported space grid of intersecting trusses. Image from (Chilton 2000)

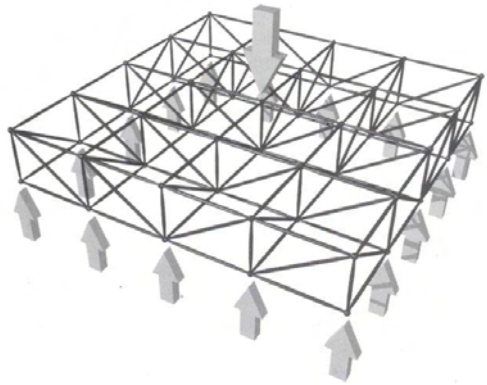


Figure 3.111: The deflection of a two-way spanning double-layer grid of intersecting trusses demonstrating the load distribution advantage. Image from (Chilton 2000)

During the 1950s and 1960s, space grid systems were built all over the world as architects explored the aesthetic of the modular grid and engineers experimented with jointing systems, materials and configurations. Some people believe that the use of space grids reached its climax in the 1970s. However, space structures are still being used widely for medium and long span structures of innovative form. In the more developed world their use diminishes but in the developing countries there is a huge potential for their widespread use. The materials are expensive, labour is cheap and simple efficient structures are in demand.

3.4.1.2 The advantages of two way spanning

The principle and benefit of using a two-way spanning structure can be demonstrated as the woven canvas webbing often used for seats or to support chair hassocks are considered. If webbing strips are used only in one direction, a load applied to one strip will cause it to sag and transfer loads to only two sides of the supporting frame. However, if the webbing strips are interwoven in two orthogonal directions the loaded strip is partly supported by all others. This reduces the sag of the loaded strip and distributes the applied load even more evenly to all sides of the frame. In the second case, each strip does not have to be capable of carrying the full applied load on its own and a lighter structure can be used for the supporting frame. Another advantage is that, if one of the webbing strips breaks, the seat as a whole will still support loads. Similar benefits may accrue from the use of two-way spanning structures in architecture and engineering. See Figures 3.108-3.111 (Chilton 2000).

When the span of the structure exceeds about 10 m, the use of beam elements in a single layer grid becomes less economical. And open web trusses or Vierendeel girders may be substituted for the solid beams. Connected with a pattern of vertical and/or inclined 'web elements' between the two plane girders results in a double layer grid. Double layer grids are the most efficient and lightweight structural systems because of their ability to share the task of load carrying through the whole structure.

3.4.1.3 Aspect Ratio

The benefit of two-way spanning is the greatest if the ratio of the lengths of strips is around 1. The roof will be square in this situation (square bays). It is also possible to modify the load distribution characteristics; by increasing the size of the chord members in the long span direction.

The decision whether to use a three-dimensional space grid or a one-way spanning structure is often influenced by the plan form of the building and the location of the supporting structure. If support is only possible along two opposing sides of a rectangular building one-way spanning will almost certainly be more economical. If supports can be provided along all sides it is more difficult to decide. It depends on several factors, in particular the ratio of the spans in each direction; the span aspect ratio. The influence of the span aspect ratio on load distribution within a two-way spanning structure is illustrated by a simple point load W applied at the intersection of two orthogonal beams of span L and L . The beams are connected at their midpoints (perpendicular) and form in that way a simple single-layer beam grid. The Young's Modulus (E) and second moment of area (I) are the same for both. The relationship between the span aspect ratio (L_1/L_2) and the loads carried out by each beam W_1 and W_2 can be found by the following equations:

Mid-span deflection with hinge and roller support:

Span ratio ($\frac{L_2}{L_1}$)	1.0	1.2	1.5	2.0	3.0
Beam 1(W_1)	0,500W	0,633W	0,771W	0,889W	0,964W
Beam 2(W_2)	0,500W	0,367W	0,229W	0,111W	0,036W

Table 3.9: Span Ratio. (Chilton 2000) Note: E and I constant, L_2 longer span and L_1 shorter span.

$$\delta = \frac{1}{48} \frac{WL^3}{EI} \quad (3.34)$$

If connected the deflections must be equal. The term $48EI$ is constant and the equation follows;

$$W_1(L_1)^3 = W_2(L_2)^3 \text{ or } W_1 = W_2 \frac{(L_2)^3}{(L_1)^3}; \quad (3.35)$$

with $W_1 + W_2 = W$

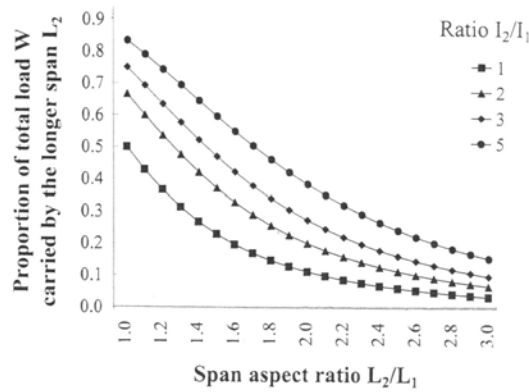


Figure 3.112: Relationship between span aspect ratio and proportion of the total load carried out by the longer span beam, L_2 of the simple two-beam intersection grid ratio L_2/L_1 , equal to 1, 2, 3, 5. Image from (Chilton 2000)

Seen these results it can be concluded that in large space grid structures, a double layer grid is more usual and there are many more intersecting members but the basic principle of using aspect ratios close to 1.0 still applies. When an economical solution is to be achieved and the aspect ratio is much greater than the 1.0 the possibility of dividing the longer span by introducing intermediate columns should be considered. If a clear span is essential, additional lines of support in the form of stiff edges or intermediate beams on grid lines may be used to break the structure in approximately square bays. It is also possible to increase the depth of the longer beam and thus the magnitude of its second moment of area I (stiffness). See Figure 3.112.

3.4.1.4 Advantages and disadvantages of space frames

Disadvantages of space frames Space frames have some disadvantages which must be offset against the considerable number of advantages described further on in this section.

- **Cost** The costs can sometimes be high when compared with alternative structural systems. Particularly when space frames are used for relative short spans; spans less than 20 to 30 meter can probably be considered as short for most space frames. Choice of grid configuration and the depth between the chord layers will affect the economy of the space frame. Prefabricated elements are produced in limited number of standard sizes and depths. The nodes are the most expensive part of the frame. Reducing the amount of nodes makes the frame more economical and the erection time is shorter.
- **Regular Geometry** To some eyes the space frames can appear very busy. The regular nature of the geometry is lost and at some viewing angles, the 'lightweight' structure appears to be very dense indeed. The upper and lower grid sizes as well as the grid depth have a considerable influence on the perceived density of the double layer structure and charisma of the building. On the other hand the space frame can give a nice view on the curves of the structure. See Figure 3.113.

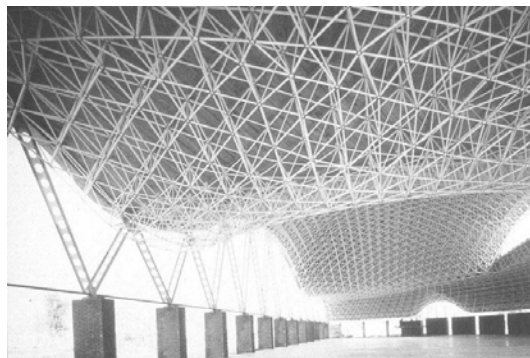


Figure 3.113: Regular geometry can gives nice views. Pallafoflls sports hall. Image from (Chilton 2000)

- **Erection time** The number and complexity of joints can lead to longer erection times on site. Designing the grid to contain the most practical minimum number of nodes is good practice; they are usually the most expensive components. This leads to economy of material costs and faster erection time.
- **Fire protection** Most of the times space frames are used at places where normally nominal or no fire resistance is required. However, when necessary it is difficult to achieve economically due the high number and relative large surface area of the space grid elements.
- **Load sharing at supports** Space frames are called high redundant structures. But also with the freedom of placing support are limits; some examples are known of roofs which collapsed under snow-loads of $78 - 88 \text{ kg/m}^2$. In space trusses supported at the bottom nodes there are usually four diagonal web members converging on each support and these are in compression. Failure of only one of this due accidental damage or buckling under excessive compression owing to an unforeseen load can lead to the partial or total collapse of the whole structure, as the load originally carried by the failed member transfers to the remaining three in turn causes their failure.

Advantages of space frames Space frames have a considerable number of advantages which make them useful as structures.

- **No bending moments by external forces** If loads are directly applied to the nodes the bars within the space frame carry either axial tension or compression forces because space frames have hinge connections which can not pass on moments. Bending is only present due the self-weight of the bars.
- **Installation of services** The open nature of the structure allows easy installation of mechanical and electrical services and air-handling ducts within the structural depth.
- **Load sharing** The prime advantage of space grid structures is that generally all elements contribute to the load carrying capacity. This in contrast with planar beams or trusses which must be individually capable of carrying any possible concentrated or heavy moving loads. However in space grids such concentrated loads are distributed more evenly throughout the structures and all supports. The maximum deflections are reduced, lighter or shallower three dimensional structures may be used, which can result in reducing costs of the supporting structures.
- **Robustness** Failure of one or a limited number of elements, for instance buckling of a compression member under excessive loading, does not necessarily lead to overall or progressive collapse of the structure. Space frames are also called highly redundant structures. The redundancy of space grid structures also assists with their resistance to damage of space grid , which allows heat and smoke (in fire) or the force of the blast (in explosion) to escape.
- **Modular components and prefabrication** Space frames are almost all prefabricated in the factory. Therefore the product is usually produced with high dimensional accuracy, high quality of surface finishing and generally easily to transport. Without difficulty it can taken down and reassembled elsewhere. In the past many different systems have been brought on the market. The most famous are the MERO system and Space Deck. See Figure 3.114 and 3.115.
- **Regular geometry and simplicity of erection** The use of space grids is the efficiency of erection for large-span roof structures and especially on sites with limited access. The whole roof can be assembled safely at or near ground level and then jacked into its final position. Large structures can be assembled out of small elements, on site, with limited disruption to other activities.

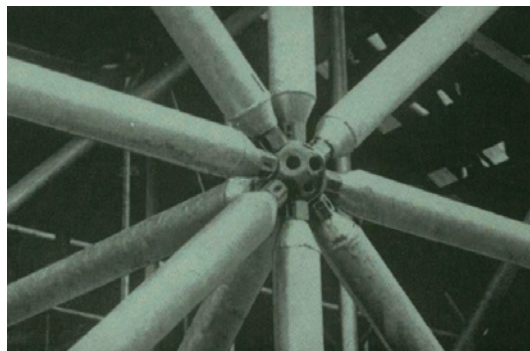


Figure 3.114: MERO System. Image from <http://www.columbia.edu>

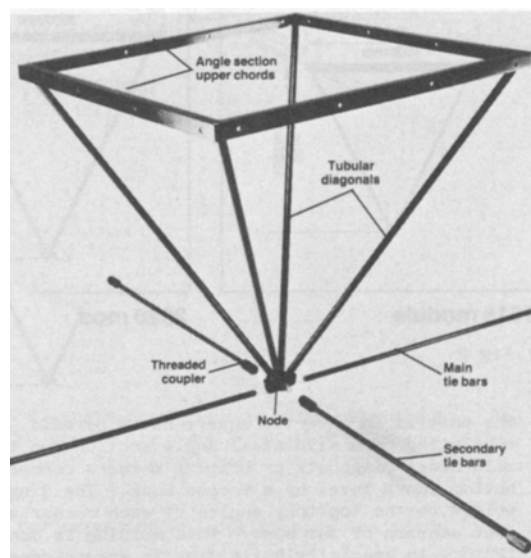


Figure 3.115: Space Deck System. Image from (Nooshin, Space Structures Research Centre, Department of Civil Engineering, University of Surrey, Guildford, UK 1984)

- **Supporting structures, freedom of placing** Within reason, space frames can be supported at any node of the grid and at practically any location in plan. This gives the architect considerable freedom in space planning beneath the grid. As mentioned before square bays are preferable. To avoid high forces in one point tree structures are used to lead the forces to the supports.

3.4.2 Formal definition

A space frame (Dutch: 'ruimtevakwerk') is a structure, which consists of bars, all connected by hinges. The bars will be purely loaded in axial direction and will not have to take any bending moment. Together they need to have such a spatial configuration, in order for a stable system to be formed. This means that the bars in the structure need to form triangles in two or more directions.

The term 'space frame' is normally used for systems, which have a clear upper and lower layer of bars - usually parallel to each other - with in between a network of bars, which keeps the outer layer in place. Another term used for spaceframes is 'spacedecks'. These systems have at least two layers, but sometimes also three or more.

To be complete single-layer systems will be dealt with in short. However, in principle they can be interpreted as translations of shells. They also have a lot in common with the earlier mentioned space frames.

A framework (Dutch:'staafwerk') is - according to common opinion - considered a structure, built up from bars which are connected with a certain amount of bending stiffness.

This stiffness is never infinitely large and can also be different in two perpendicular directions. However, this does mean that the bars have to be able to resist the bending moment in the given direction. The bars will be loaded in bending and/or normal force.

The main shape of a framework or a truss system can be:

- flat (slab)
- kinked
- singular curved (barrel vault, cylinder)
- multiply curved (sphere, hyperpar)
- combinations (especially cylinder with sphere)

A flat system is in essence always in two or more layers, all others can also be single-layered.

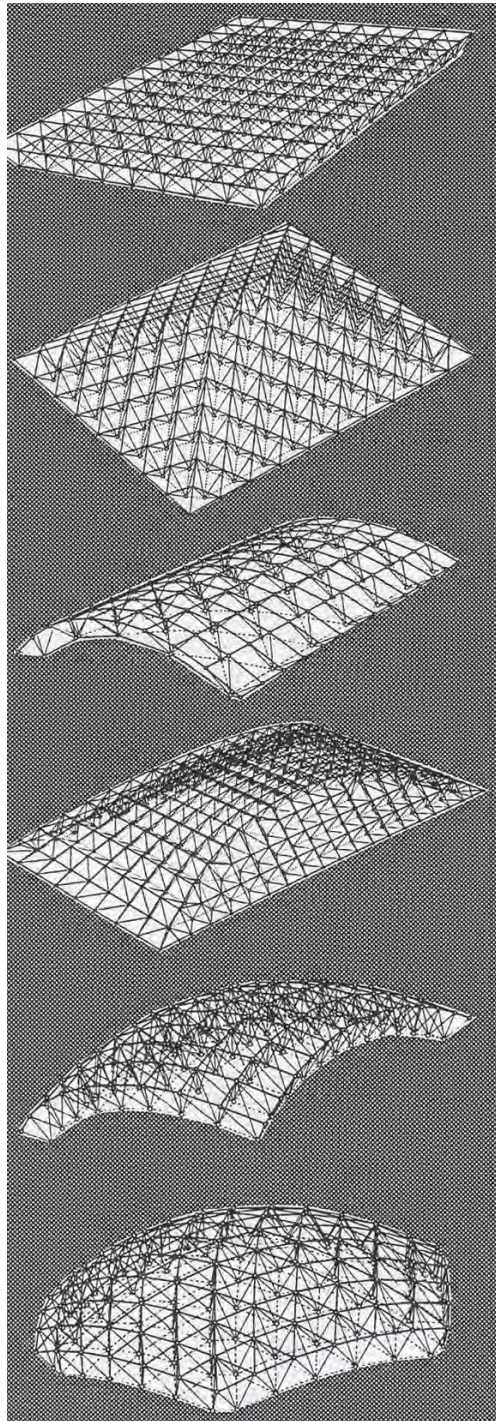


Figure 3.116: Different principle shapes of spaceframes

3.4.3 Single layer systems

3.4.3.1 Flat;

A single-layer structure will normally not be designed flat. In case of flat structures it should be considered as a combination of beams and columns. In that case the loads are transferred by bending moments; this requires a large construction depth, in order to get a large inner moment-arm.

3.4.3.2 Single folded or curved;

This type of structures is easily made single folded or curved with one type of bar. The joints must have at least four or six directions of connection to allow for respectively square or triangular subdivisions. Dependent of the applied type of division - or pattern - these can be of one and the same type.

3.4.3.3 Double curved;

To create such structures multiple bartypes are needed. The amount of different types depends on the shape and the chosen method of division. There are also multiple types of joints required. The number of directions of connection usually does not exceed six. The connections of the members at the joints can be executed as hinges when the bars together form a stable system. This criterium is met if:

$$s = 3k - 6 \quad (3.36)$$

where s = number of bars and k = number of joints.

3.4.3.4 Combinations;

Parts of single and double curved surfaces can be joined into one surface. Parts of cylinders are fairly easily combined with parts of spheres. It is for instance also possible to create a cross vault, by combining perpendicular cuts from two equal cylinders, or the opposite shape. Spheres can also be built up from sectors in the shape of cylinderparts.

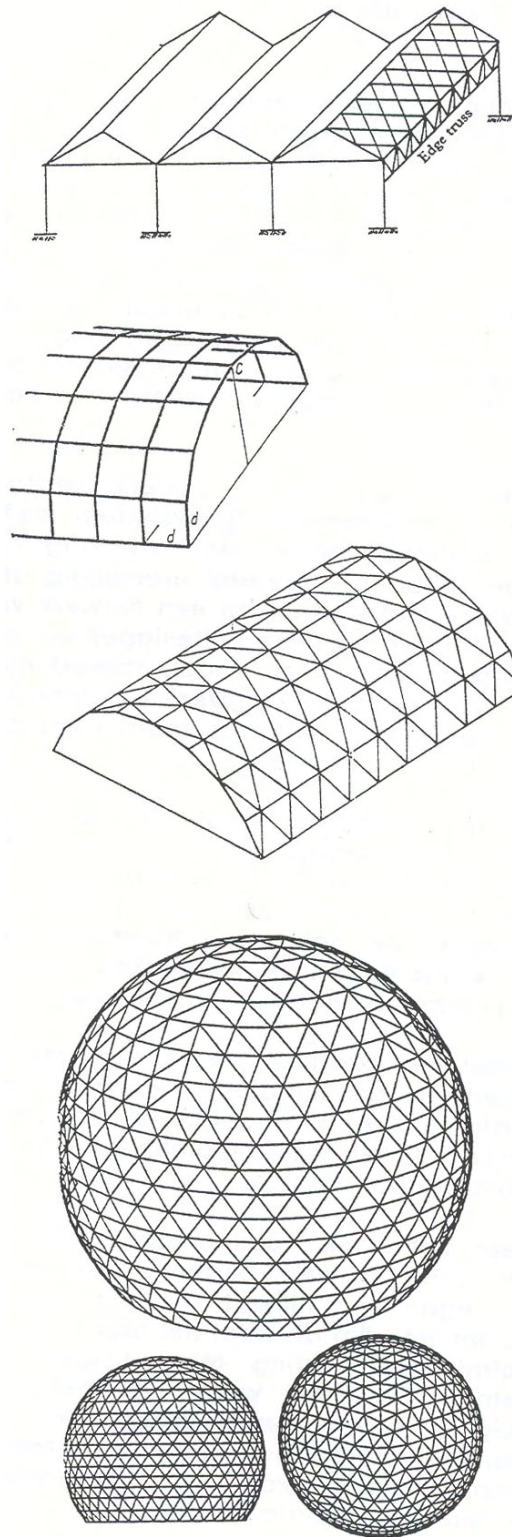


Figure 3.117: Different single layer shapes

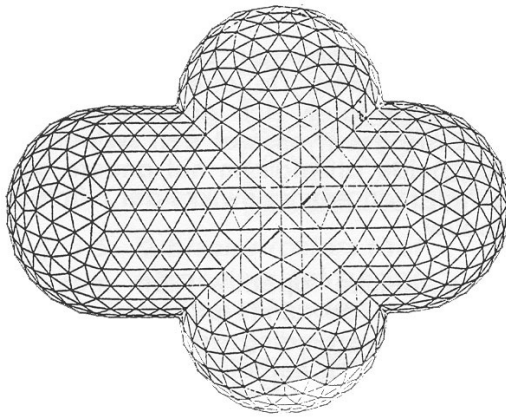


Figure 3.118: Combinations of single and double curved systems

3.4.4 Systems with multiple layers.

3.4.4.1 Double layered

Borrego (Borrego 1967) discerns the following principally different methods:

Direct Grid Two parallel, identical rasters, directly above each other. Upper and lower plane are connected by flat vertical trusses.

Offset Grid Two parallel, identical rasters, in at least one but mostly in two directions shifted regarding each other in plane, but not rotated. The upper and lower plane are connected by sloping bars.

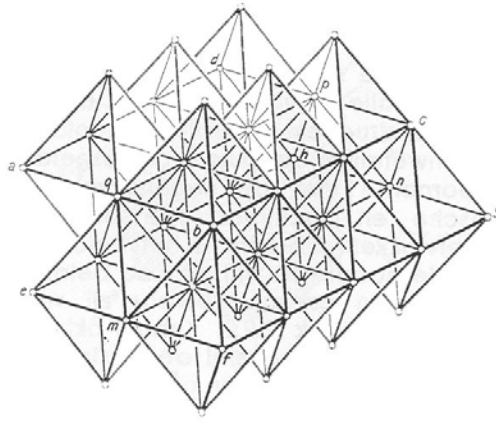


Figure 3.119: Stacking of octahedrons and tetrahedrons, in which the most often used offset grid appears as horizontal layer

Differential Grid Two parallel, but not-congruous rasters, chosen regarding each other in such a way that they can work together properly, in combination with the connecting bars between upper and lower plane. Furthermore Borrego names the 'lattice girders', built up from prefabricated beam, but these are not essentially different from the first group.

3.4.4.2 Three or more layers

These can be a stacking of multiple flat systems. The *direct grids* and the *offset grids* are very suitable for stacking. In the first case a system of coupled prisma is created, in the other case a more complicated spatial build up is found.

A built up like this can be stretched out into infinity, where the connecting bars meet each other according to a regular, repeating pattern under carefully defined angles. From this view parts can be selected which suit the regarded design problem. Vertical parts can for instance be taken out to create a tower structure, cavities can be made in the outside perimeter, or pieces can be taken of and put on. On a rough base practically every building shape can be approached.

Three-layered trusses are taken into account much more often these days, when dealing with large spans.

3.4.5 Polygons as base element for spatial structures

Spatial frameworks or trusses can in practically all cases be considered as structures in which the principal form is based on the so-called Platonic and Archimedic polygons. That is why it is important to know their most important characteristics.

The cube, octahedron and tetrahedron are usually the base elements for the well known types of spaceframes.

As shown in (Huybers 1994), every polygon also has an inversed or 'reciprocal' shape. The rhombic dodecahedron and rhombic triacontahedron (Dutch: ruitentwaalf- en dertigvlak) are in this context the most important representatives for this group. The direction of the ribs of the rhombic dodecahedron are in a cube and therefore this shape is in certain perspectives suitable as concept for the geometry and as an alternative for the node-element. The rhombic triacontahedron is - just like the triangular Platonic figures (octahedron and ikosahedron) - often used as concept for sphere divisions. Aside from that, certain structures often called quasi-crystalline, are based on this shape.

3.4.5.1 Spacefilling stackings of polyhedrons.

Some of these polyhedrons can be put together in larger numbers, into closed spatial packings. This is used in spaceframes. The directions of the ribs, their mutual angles and the position angle between the planes are therefore interesting data, because these are directly linked to the trusses based upon them.

Prismatic Systems. In a plane some prisms can be joined into one. In this way *direct grids* are formed. With the square, prism or cube a system is made of perpendicularly intersecting truss beams. The square -or rectangular- faces of prisms must be stiffened to get a stable system.

Cubic Sections In every face of a cube a diagonal can be installed in such a way that all these diagonals together form a tetrahedron. Such braced cubes can be coupled alternately -horizontally and vertically- and this way the most often used spatial configuration is derived. The original MERO-system, for instance, is based on this. In this system two lengths of bars exist: length a (cube rib) and length $a\sqrt{2}$ (brace). When the ribs of the cubes are taken out, a system of coupled tetrahedrons is left, with the open spaces in between shaped like octahedrons.

A horizontal cut gives the best known raster, the earlier mentioned *offset grid* with a rectangular pattern in upper and lower plane. A diagonal cut, so alongside a series of triangles, gives the by R. Buckminster Fuller introduced *octet-truss*, with triangular rasters in upper and lower plane. Grigorievich(IASS 1985) and Mengerinhausen/Eberlein(Mengerinhausen 1975)(Popko 1968) point out the possibilities to realise different sorts of truss systems with a different build up, based on cubic packings.

An orthogonal *offset grid* according to the cubic system is in fact a layer of upward aimed pyramids with the shape of half an octahedron, of which the tops are connected by the rectangular bar pattern in the upper plane.

Rhombic Dodecahedron Build-up When in the cube, apart from the plane diagonals, also the body diagonals are accepted, then the possibility arises to create rhombic dodecahedrons. This means that in this system also edge-endings under 45 degrees become possible. So it will be easier to work around the corner, for example from roof to wall. The main layout of the truss

system can be very similar to the normal cubic system and can therefore also be shaped like an *offset grid* of pyramids, but they will now have sideplanes under 45 degrees. In the joints a new direction is introduced, namely $\arctan(\frac{1}{\sqrt{2}}) = 35.26^\circ$. Though there are two bar lengths needed: a for the horizontals and $\frac{a}{\sqrt{2}}$ for the diagonal ribs.

Other Systems. Apart from the cubic and the rhombic dodecahedron system also some other configurations are known, which can be suitable as principle. There is mainly much interest in the so-called quasi-crystalline build-up. With two types of spatial cells, a thick and a thin one, with rhomb-shaped (Dutch: 'ruitvormig') side planes, interesting structures can be built. Depending on the point of view they have a very different appearance.

There is little concrete information available yet. This is also true for the *zone-eder-build-up*, for which amongst others S. Baër (Baer 1970) and, in the Netherlands, O. Hanegraaff (Hanegraaf & et al. 1975) are conducting a lot of pioneering work. They are trying to further explore the field of the 5-axle symmetry, which is found in the isohedron and the rhombic triacontahedron. Besides some incidental and small scale applications there have not been many practical developments.

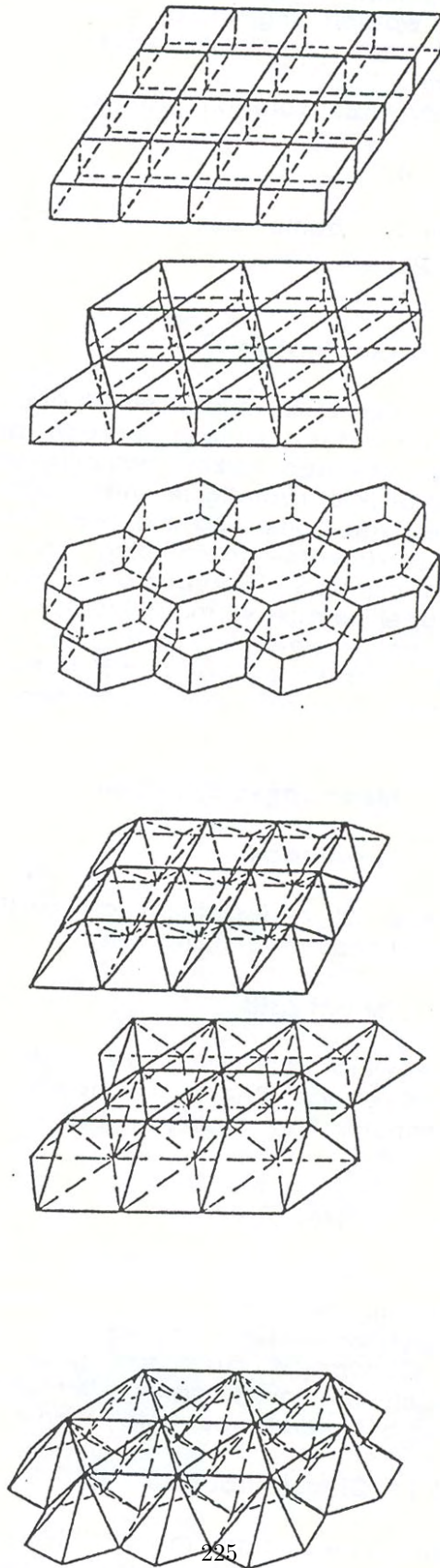


Figure 3.120: Two-layered systems

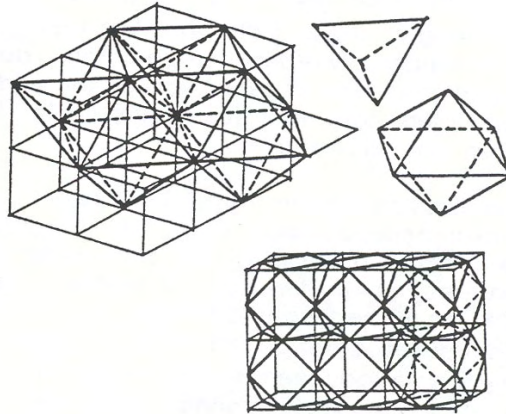


Figure 3.121: Cubic rasters with octahedrons, tetrahedrons and cuboctahedrons

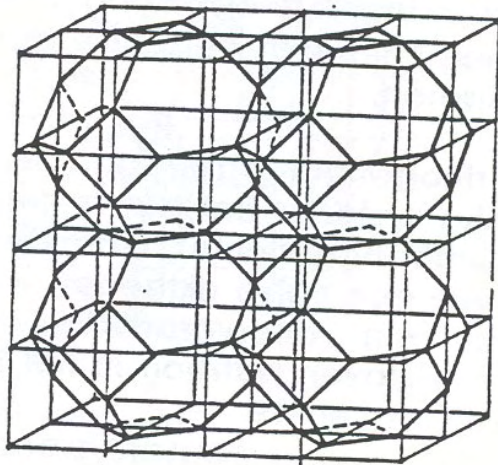


Figure 3.122: Spacefilling stacking of a 14-plane

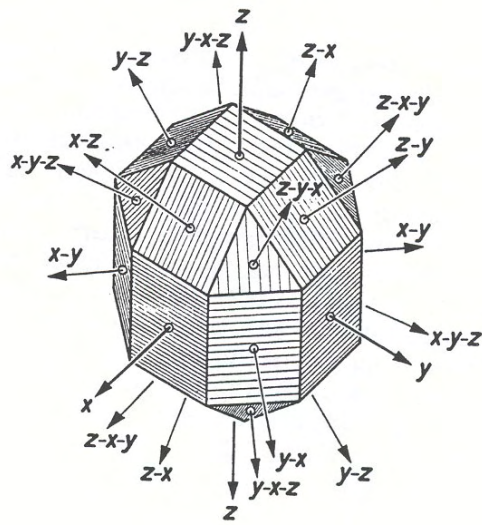


Figure 3.123: Typical node element in a cubic system

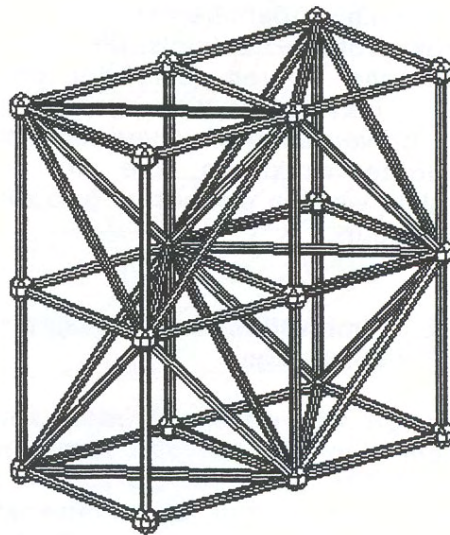


Figure 3.124: Spatial system of cubes with plane diagonals

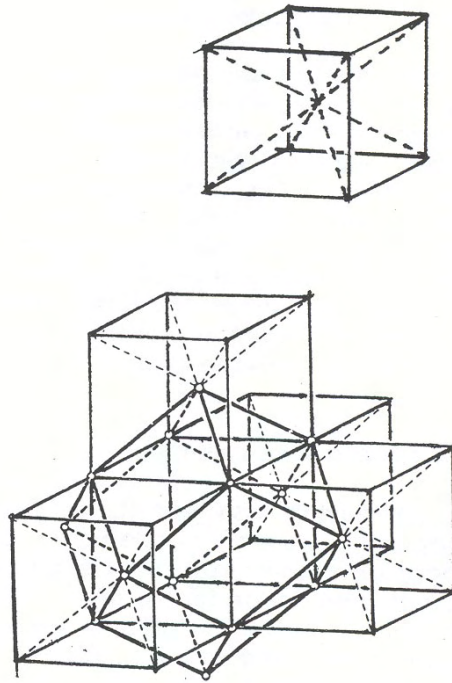


Figure 3.125: rhombic dodecahedron

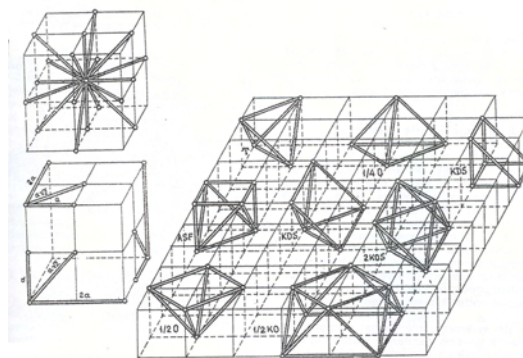


Figure 3.126: Spatial view of cubic systems

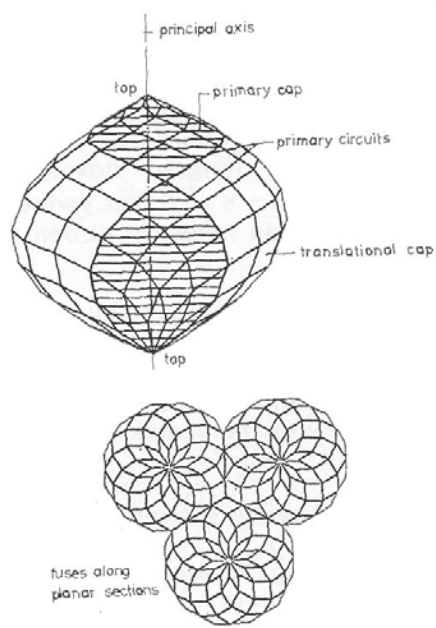


Figure 3.127: Zone-eders

3.4.6 Parallel rasters

When space frames are considered, most of the time mainly planar configurations with parallel upper and bottom planes are meant.

3.4.6.1 Often applied shapes

Most popular are the grids which have as many the same bars, so as little different types of bars. These grids are almost always dual, which means that the bottom plane is divided in connecting polygons (3-,4-,6-, or higher level polygons) and that every joint of the upper plane is centered above one of these polygon-planes. This creates a layer of upward aimed pyramids, of which the tops are interconnected.

With the systems, previously indicated as 'cubic', in fact only the diagonals from the square faces are used. One of the two possible diagonals is chosen in a way that a certain spatial pattern is created. All diagonals have the same length and they become the ribs of two of the most often used systems.

With the rhombic dodecahedron-systems all ribs of the cubes are used, along with the inner diagonals. This creates two diagonal lengths: $l = 1$ and $l = 1/2\sqrt{2}$. In this system the shorter diagonals form the ribs of the pyramids.

3.4.6.2 A cut from a spatial configuration

The chosen cut from the total spatial grid of bars has direct consequences for the characteristics of the space frame.

Two-way grid A two-way grid can be created by taking orthogonal cuts from both the cubic grid as the rhombic dodecahedron or rhombic grid. In both cases a system is found consisting of upward aimed pramids with a height of respectively $1/2a\sqrt{2}$ and $1/2a$, in which a is de modular size of the pyramid base.

Positioning on a plan A two-way grid can be placed on an orthogonal system -or rectangular plan- in two ways. These two variants have a clearly different structural behaviour.

Parallel

The edges of the base of the pyramids are parallel to the edges of the rectangular plan. This means that these are in the longitudinal direction of the span.

Diagonal

The edges of the bases of the pyramids are diagonal. This causes strips to be formed that cross diagonally. This is especially very advantageous for plans tending towards a square-shape. The sagging moment will be relatively small, because the span is just $1/2\sqrt{2}$. In the corners it is even possible to get a change in the direction of the bending moment. When the size of the plan is large in the direction of the span, a space frame like this can have weak behaviour, because there is little stiffness in the diagonal direction.

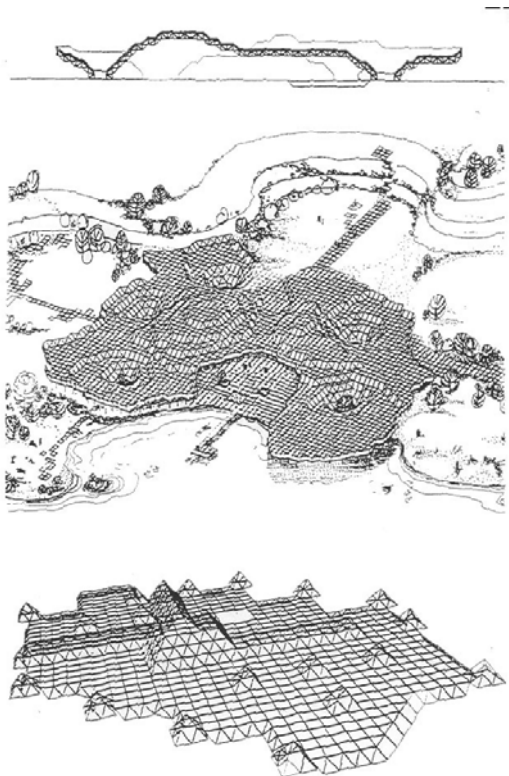


Figure 3.128: Examples of cubic rasters in possible applications

3.4.6.3 Three-Way grid

With a three-way grid the bars go in three directions in both parallel planes and not in two, as with the two-way grids, which were treated in the previous paragraphs. It is just another cut from the cubic grid. It can also be built up from just one type of bar with a length of $a\sqrt{2}$. The height of this grid is $1/3a\sqrt{6}$ and it consists of regular octahedrons and tetrahedrons.

An alternative is a grid, which follows the diagonal plane in the cube (See Figure 3.134). This consists of bars with a length of $a\sqrt{2}$ and a . It has a height of $1/6a\sqrt{6}$

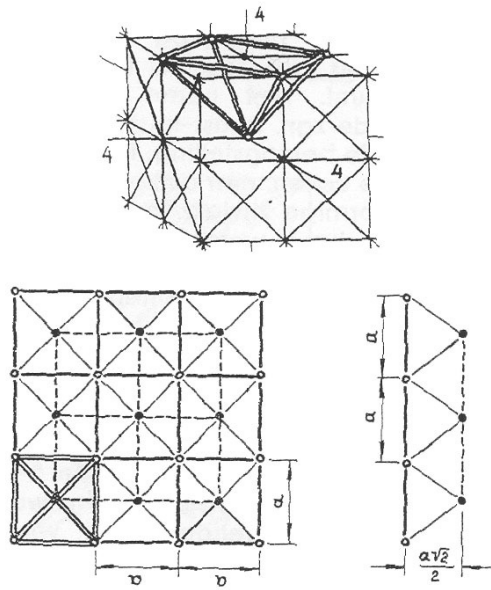


Figure 3.129: Principle of a two-way grid

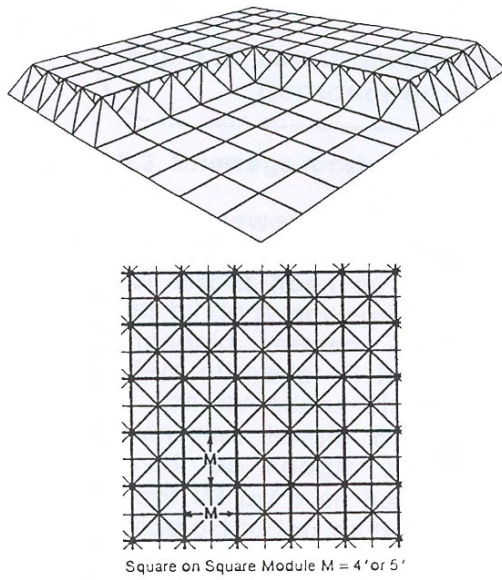


Figure 3.130: parallel raster

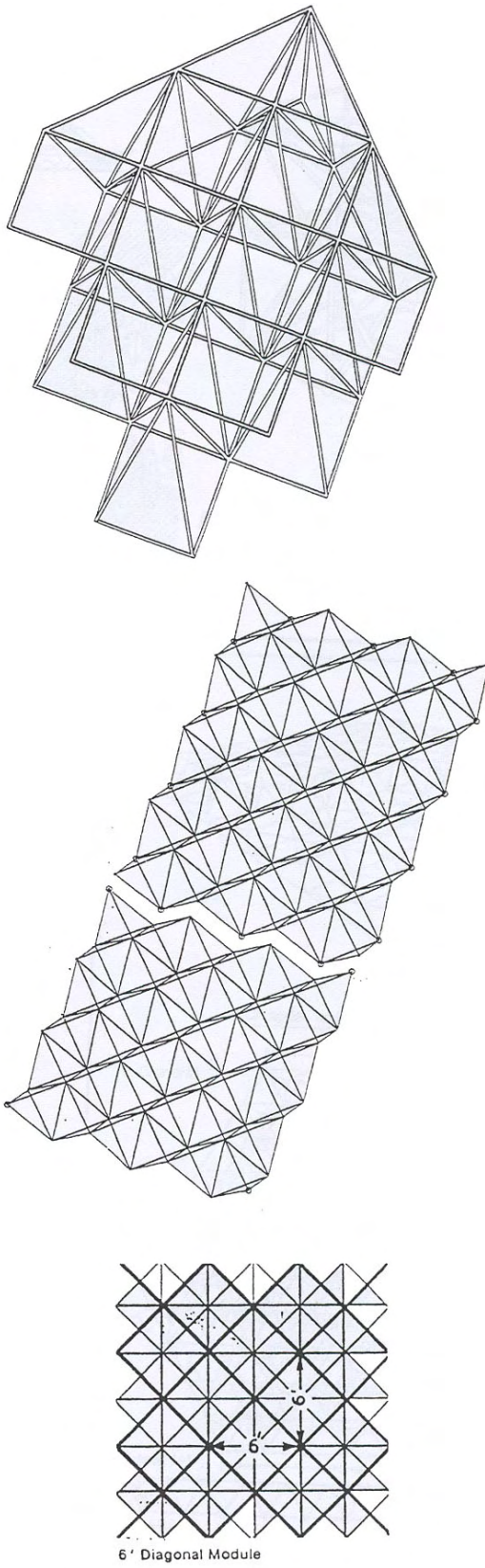


Figure 3.131: Two-layered, 236-directional diagonal raster

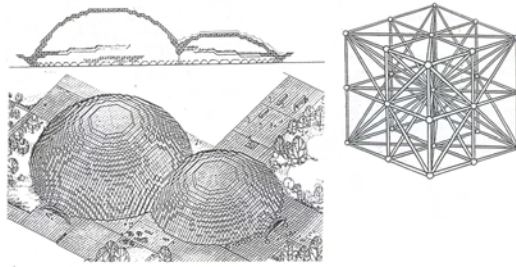


Figure 3.132: A sphere shaped spaceframe based on a cubic raster

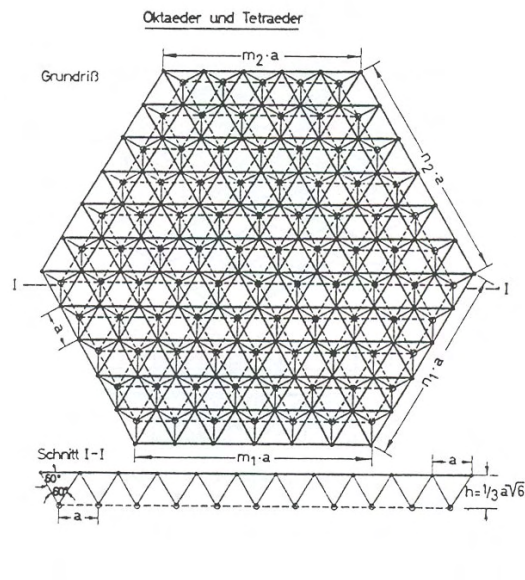
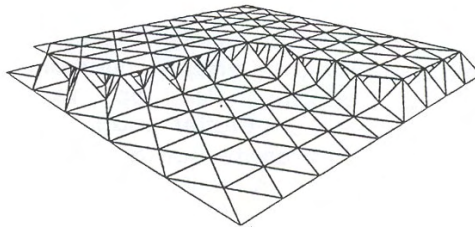


Figure 3.133: A three-way grid with a reduced height

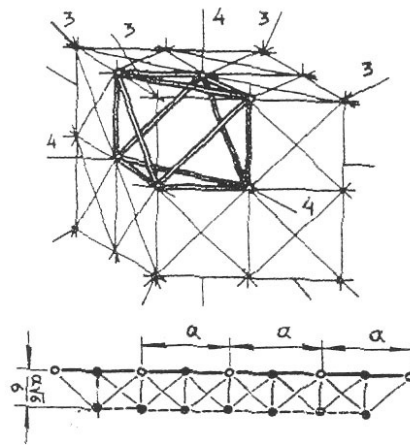


Figure 3.134: A three-way grid built from identical bars

3.4.6.4 Edge-endings

The sides of a normal offset grid are in an angle with the horizontal plane, which is equal to half the dihedral angle (Dutch: ‘standhoek’) of an octahedron: 54.74° . With grids based on the rhombic dodecahedron this angle is 45° . With the three-way type two types of edge angles are found, one that is equal to the dihedral angle of the tetrahedron, 70.53° , and one that is equal to the dihedral angle of the octahedron, 54.74° .

This edge-ending can have a cantilever or be drawn back. The terms used for this are:

- *Mansard Edge*
The lower plane has the largest size, the roofplane is drawn back. The structure is usually supported from the outside.
- *Cornice Edge*
The upperplane is larger than the lower plane. When the structure is supported at the outermost points of the lower plan, the upperplane still protrudes half a triangle.
- *Vertical Edge*
The sides can also be finished vertical, for instance to create an easier connection to the facade. When using a square mesh offset grid, placed parallel regarding the plan, it is needed to use extra bars with deviating lengths. When such a grid is placed diagonally onto the plan, vertical edge-endings will automatically occur. With triangular grids this can only be realized by adding different dypes of bars. Grids with identicle lower and upper layers, which can be interpreted as collections of vertical prisms, by definition have vertical edge-endings.

3.4.6.5 Modifications

Reduction of the number of bars for economical reasons Not in every case all bars appearing in parallel grids are absolutely necessary. In order to economize, some bars can be left out, creating a reduced frame. Of course this has to be done with the utmost care and without creating a partially or entirely instable frame.

Aside from the usual grids, of which the upper and lower plane are identical but shifted half a triangle in two directions, also alternative combinations can be created in this way. With the rectangular square grids we already distinguished the following:

- *Fully filled:*
 - square on square
 - diagonal on diagonal

Aside from these for instance the following are known:

- *Reduced:*
 - Square on larger square
 - Diagonal on square
 - square on diagonal

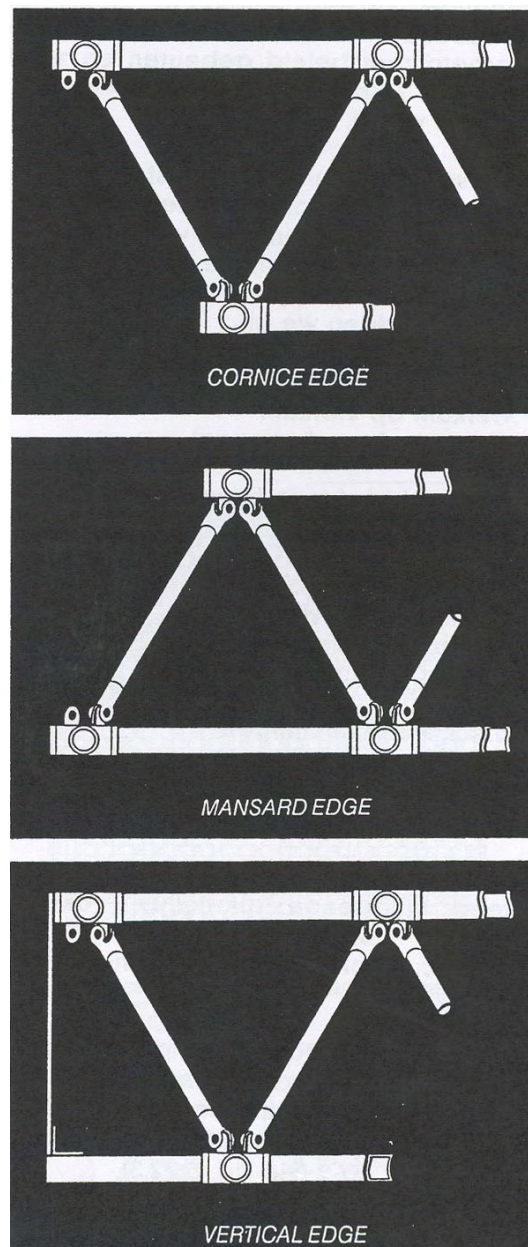


Figure 3.135: Edge-endings of two-layered spaceframes

Supports

- Point support: Underneath a layer or a high point
- *spread*: By spatial frames widening from bottom to top and support different points at the same time, thus spreading the loads.
- *Linear*: The support is made with the edges formed by trusses. The bay size used in vertical sense is most of the times the double height of the truss, so: $2 * 1/2\sqrt{2} = \sqrt{2}$.

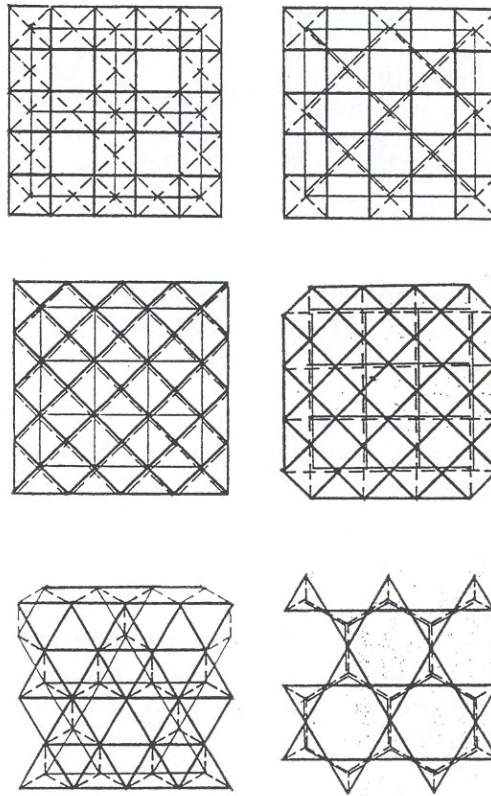


Figure 3.136: Reductions

Discontinuities Creating holes in the frame structure has to be done with care and of course without essential discontinuities in the transfer of forces. In general this will not lead to problems, due to the large surplus in stiffness of the most used configurations.

Adjusting the dimensions of bars Around discontinuities, above large openings in the wall, with large spans or near the supports, it is often useful to adjust the dimensions of the bars. This has little influence on the visual aspect of the structure, because the geometry does not change. Moreover it is possible to look for variation in wall thickness of the elements and thus keeping the outer dimensions of the tube or bar the same.

Multiple-layered trusses Most trusses -and especially the flat ones- are double-layered. There is, however, a large advantage in stiffness to be achieved by using more than two layers. There are still not many examples of three-layered, let alone multiple-layered, trusses. The number of bars will increase drastically. With three-layered trusses a neutral centre layer is found and it is often hard to initiate this layer into the division of forces in an economical way. An advantage is that the lengths of the bars are relatively short, which is very positive in relation to the buckling-behaviour of the bars when under compression.

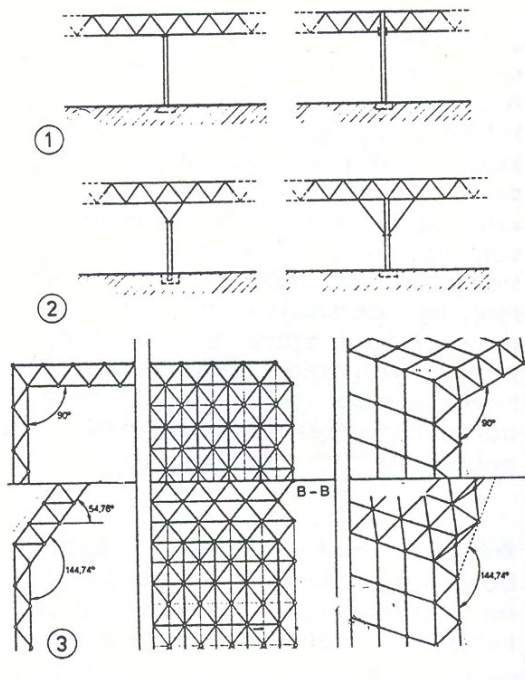


Figure 3.137: Support types

A start is just to increase the height of the frame in places of high loads. In a shopping centre in Rijswijk for example, just the middle part of the structure is built as a three-layered truss, to reduce the vertical sag.

Aluminium can also be a reason for applying a three-layered truss, because the E-modulus of aluminum is three times lower than the E-modulus of steel. The maximum deflections and buckling-stresses will otherwise be reached much sooner.

With very large spans it is also necessary to increase the construction height, without using longer bars. Especially hangars for large planes like the Boeing 747 with spans of 80-100m and doors with almost the same span, need such considerations. Figure 3.139 shows a graduation thesis of J. Poland, with a design for a hangar in India. The basic geometrie can be characterized as follows: Diagonal to square to diagonal. The inner square is $\sqrt{2}$ times as big as the other two planes, which creates a favourable division of forces.

Research has been performed, especially by Makowsky c.s., which shows that spans up to 300m are possible with three-layered grids.

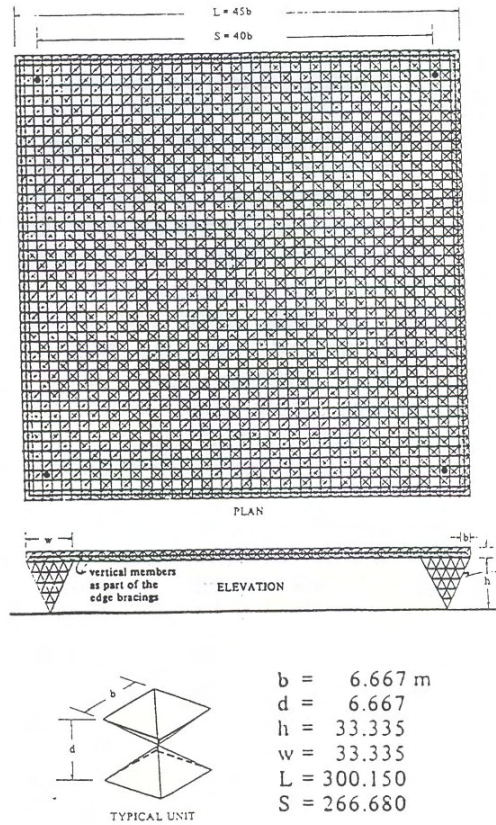


Figure 3.138: Design for a three-layered spaceframe with a span of 300m

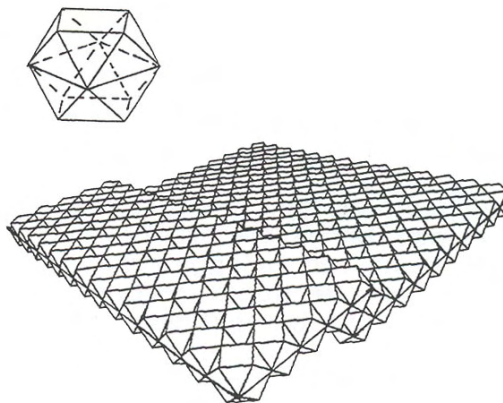


Figure 3.139: Design of a three-layered structure for a hangar in India, with the cubeoctahedron as base element

3.4.7 Sphere-shaped truss frames

The sphere is the geometrical place of all points at a given distance to a fixed point. This distance is called the radius of the sphere.

The properties of a sphere are:

- Every cut with a flat plane results in a circle as cutting edge, with a radius which is always smaller than that of the sphere, except when the cut is through the centre of the sphere. These circles are called ‘small circles’.
- If the cut is over the centre of the sphere, the cutting edge is called ‘large circle’.
- A unique large circle is defined by the centrepoint and two points on the outer perimeter of the sphere. Except when these two points are the outer endings of a diameter.
- The shortest distance between two points on a sphere are formed by a piece of the large circle in between. This shortest path is called a ‘geodesic line’.

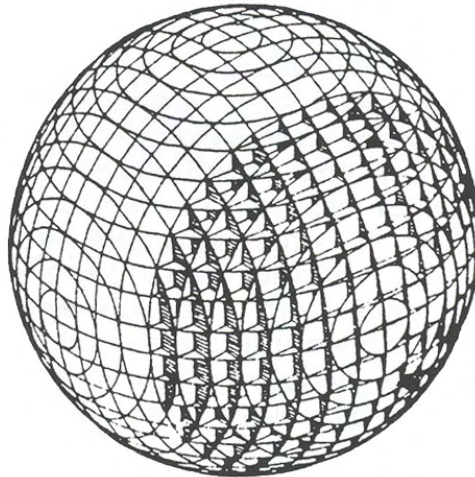


Figure 3.140: Large and small circle on a sphere

3.4.7.1 Polyhedron faces

When it is required that a truss is built up from triangles, then just three of the known polyhedrons fulfill this requirement: the tetrahedron (4), the octahedron (8) and the icosahedron (20).

To make the other polyhedrons suitable for use as a dome structure, it is needed to subdivide the polygons of which they consist, into triangles of which all tops are on the circumscribed sphere. The advantage is then not yet very large. The radius of the sphere can be expressed in the rib of the equilateral polygons of which the polyhedron consists.

The largest value for this radius that occurs in one of the known polyhedrons is 3.8024. This means that in this case the diameter of a dome shaped like half a sphere is $2 * 3.8 = 7.6$ times

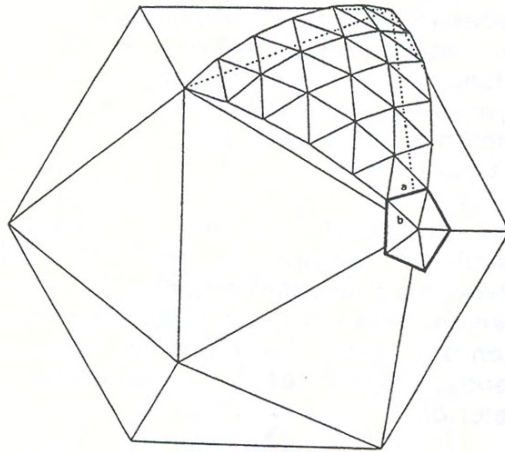


Figure 3.141: Projection of a triangular division of the circumscribed sphere

the largest riblength. This maximum riblength has a practical upper boundary, depending on factors like fabrication techniques, transportability or manageability at the construction site. With a build up of bars also the buckling-length can play a role.

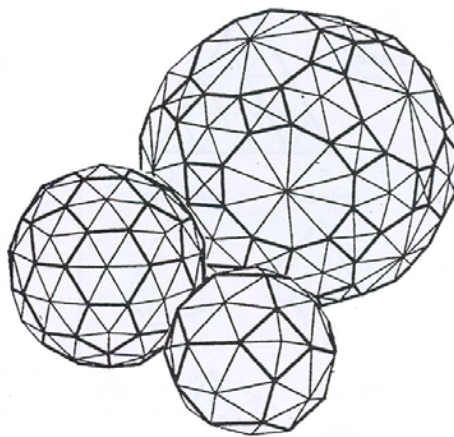


Figure 3.142: First degree subdivisions of polyhedrons

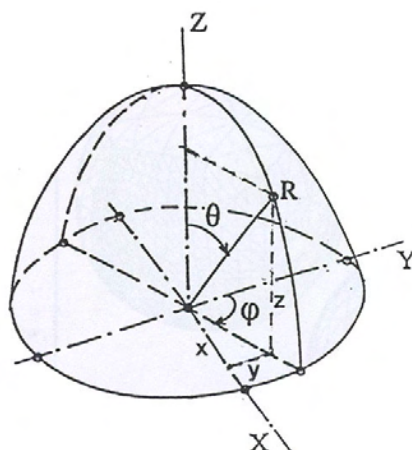


Figure 3.143: Orientation on a sphere

$$\begin{aligned}
 z &= R \cos\theta \\
 x &= R \sin\phi \sin\theta \\
 y &= R \cos\phi \sin\theta \\
 x^2 + y^2 + z^2 &= R^2
 \end{aligned}$$

$$\text{When } R = 1 : \tag{3.37}$$

$$\sin^2\phi \sin^2\theta + \cos^2\phi \sin^2\theta + \cos^2\theta = 1$$

Distance between the points (x_1, y_1, z_1) and (x_2, y_2, z_2) :

$$d = \sqrt{(x_1 - x_2)^2 + (y_1 - y_2)^2 + (z_1 - z_2)^2}$$

On themselves these polyhedrons have little use for practical application on a larger scale. Unless one should create the polygons of which they consist as flat trusses and then put them together into a larger whole.

If it is required to reach larger spans, then the polygons will most of the times be further subdivided and the thus found pattern will be projected from the centrepoint onto the sphere. With the by R. Buckminster Fuller introduced principle this is initiated from the three earlier mentioned polygons: the tetrahedron, octahedron and icosahedron -with a slight preference for the last mentioned- which already consist of triangles. The original triangle will be subdivided into smaller triangles and the points that are thus found will be projected onto the sphere.

3.4.7.2 Geodesic subdivisions

The subdivision of the surface of the sphere is in principle performed by large circles intersecting at discrete points. There are many possible starting points for this.

Methods of division or classes In the further subdivisions the original polyhedron triangle is used as a starting point for this division. Joseph D. Clinton calls this triangle the ‘Principal Polyhedral Triangle’ (PPT).

There are three main principles, called ‘classes’, named:

Class I The face is divided into smaller, identical, equilateral triangles. For this the Platonic polygons, which are built up from triangles, are used as a starting point:

1. Tetrahedron
2. Octahedron (with suitable horizontal and vertical connection faces)
3. icosahedron (easily divided into two pieces with even division frequencies)

Class II

A equilateral triangle can be divided by the isolines of the altitude into six equal, two by two mirrored rectangular triangles. With the icosahedron this gives in total 120 equal parts. These can be combined into lozenge-shapes en further subdivided following many different conventions (Kitrick 1990).

When starting with the three Platonic polygons of Class I this gives a series of new possibilities:

1. A cube, with the square interpreted as a regular lozenge shape.
2. rhombic dodecahedron
3. rhombic triacontahedron

Class III

A division called ‘Skew networks’ based on twisted snub solids (Dutch: Een volgens de zgn. afgesnoten figuren gedraaide verdeling.)(Tarnai 1987)

other basic divisions

1. meridians and parallel circles (‘orange peel’)
2. Schwedler
3. Lamellas or lattice domes

regularity of the division The further subdivision of the original polyhedronrib is mostly done according to one of the two following methods:

- *Equal parts on a cord* (Dutch: ‘koorde’) This method is also called the ‘alternative’. The rib of the original polyhedron is divided into equal parts and after that the found points are projected from the system’s centre (the origin of the coordinate system) onto the sphere’s surface.

With the subdivisions of the Platonic triangles the points lying in between are found by connecting according points on the ribs of the polyhedron-triangle. This creates a pattern of identical, equilateral, smaller triangles. The intersecting points that are found in this way can also be projected onto the sphere.

- *Equal parts on the arch*

In this method the angle under which the rib is seen from the centre-point, is subdivided into equal, smaller parts. The result is that the arch on the sphere is subdivided into equal parts, so equal ribs are created. When connecting lines are drawn on the original polyhedron-triangle in the same manner as in the previous case, these no longer intersect exactly in one point. At every intersecting point small triangles or ‘windows’ appear. The further subdivision is made by projecting the centre points of these ‘windows’ onto the sphere.

Though this second method is slightly more complicated, it often is still used because it usually gives a more regular subdivision, which means that the dimensions are closer to each other. This is shown in Figures 3.146 in which the three Platonic classes and the two methods are compared.

The choice between a division according to the rib or the arch can also be applied for the other classes for the division of heights. In these cases there looked into the connecting line between the foot and top of the sphere. For further subdivision it is usually chosen to have an equal division by the sectors.

Connecting pattern When the distribution of the junctions on the sphere’s surface has been defined by above mentioned methods, the choice concerning the pattern of connectinglines is, within certain boundries, free.

1. **Triangular pattern**

A often used pattern is of course a triangular pattern. Though such a pattern can look very regular most of the times, still there are often a lot of different triangles involved. The reason for that is made clear in the previous paragraphs.

2. **Hexagonal pattern**

Triangles can be combined into hexagonals. A hexagonal can be designed as a stiff panel or as a spatial element.

With domes that do not just consist of a small ‘sphere-cap’ but of a larger part of the sphere-surface, it is theoretically possible to get a closing pattern out of hexagonals. When -which is done in most cases- an isokahedronic division is assumed, there will still be places where pentagonals are needed to close the shape. (twelve with a closed sphere).

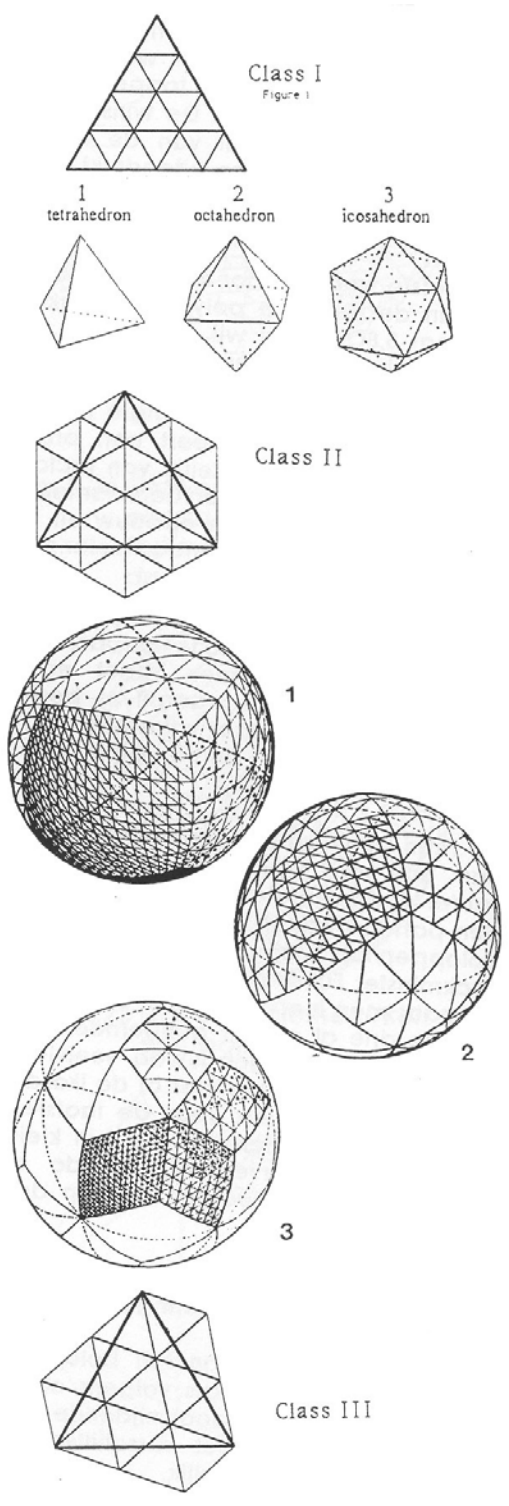


Figure 3.144: The different classes of subdivision

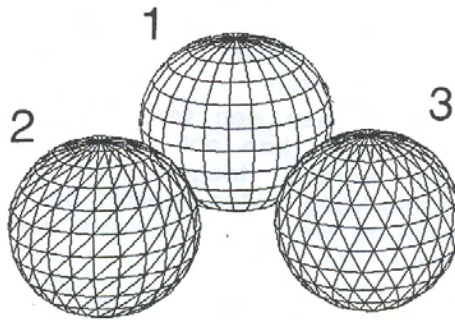


Figure 3.145: Some other types of often used sphere subdivisions

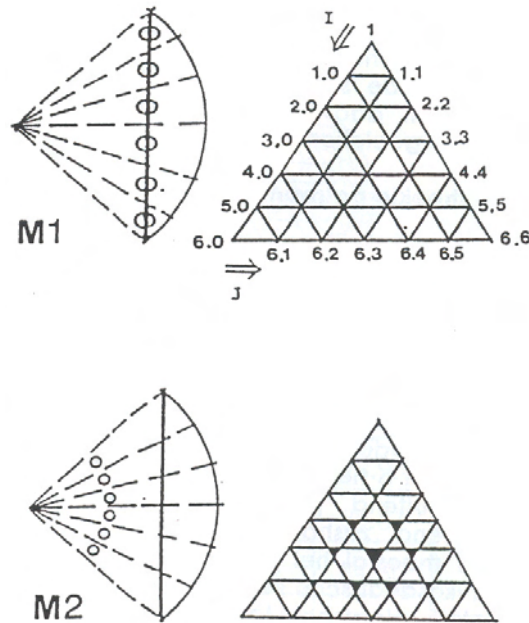


Figure 3.146: The two most important methods of subdividing triangular planes

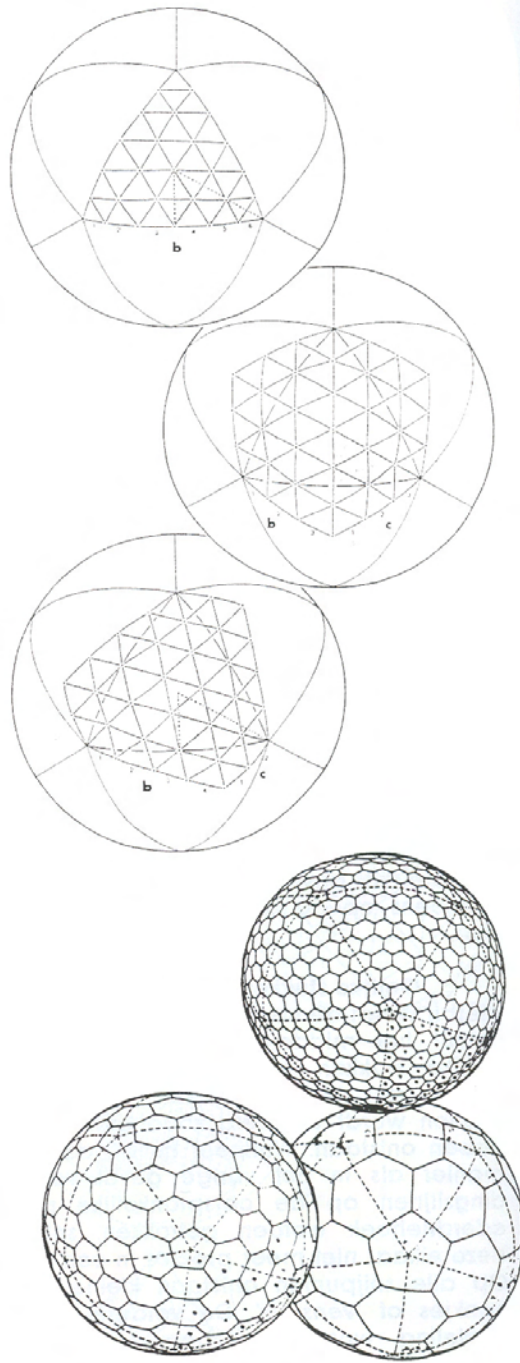


Figure 3.147: Different possible connection patterns, after the definition of the topological division of the points

3.4.8 Aspects of construction

3.4.8.1 Prefabrication of larger units

With a number of systems the bar is not the basic element, but are elements preassembled into a larger, prefabricated element.

Pyramids This element is usually shaped like a pyramid. It does not need to consist of bars, but can also be made partly or entirely from plates. There are multiple examples in steel bar-based pyramids, like Pyramitec, Czaplinski and Space-deck. There have even -some already quite some time ago- been some experimental projects constructed with concrete bar-based pyramids. H. Caminos, R.P. Burns, P.A. Kurpitz, (Popko 1968). One realized design is a system for the construction of halls up to 39 by 39 meters by Mihailesc, Ionescu and Catarich.

Pyramids entirely constructed by plates have been built in aluminium (Makowski) and plastic (Robak, Piano, Huybers). The last type can be found in a porter's lodge in Delft.

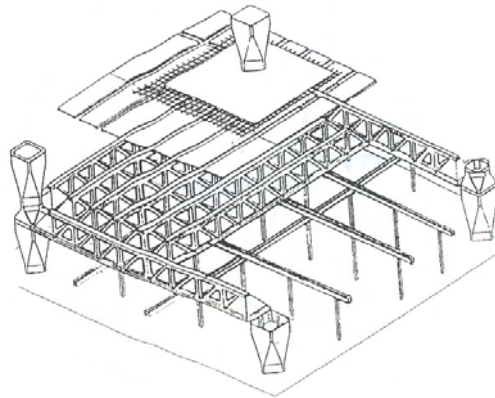


Figure 3.148: Project: Structural Bay System by H. Caminos

Tetrahedrons *Aluminium*

A number of the well-known dome-systems consists of tetrahedrons of which half is made from fold plate and the two thus created high tops are connected by a crossbar. Interesting examples of this are domes by the American product TEMCOR (In the Netherlands: Zoetermeer, The Hague, Tilburg, Schiphol).

Plastics

Examples exist of plastic tetrahedrons, mainly in glassfibre reinforced plastic (Wachsmann 1962). These have in general not passed the experimental phase for several reasons, mainly fire safety and economy-related. A structure like this could be found in Delft on the terrains of the faculty of Civil Engineering and Geo-Sciences, near the Stevin laboratories. This one has actually been built up from separate tetrahedrons, interconnected by bolts. In Wollaston, England, there is a building of which the roofstructure consists of a number of 15m long V-shaped beams with triangular partitions. These were constructed in one part, but have a internal build up of tetrahedrons.

Timber

In the system ‘Tetragrid’ by L.C. Booth and B.T. Key the spaceframes are composed of triangular plywood panels and wooden planks.

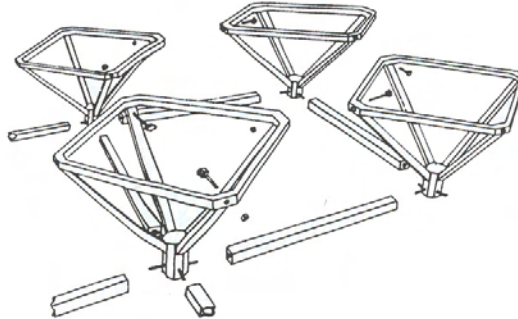


Figure 3.149: System of prefabricated pyramids

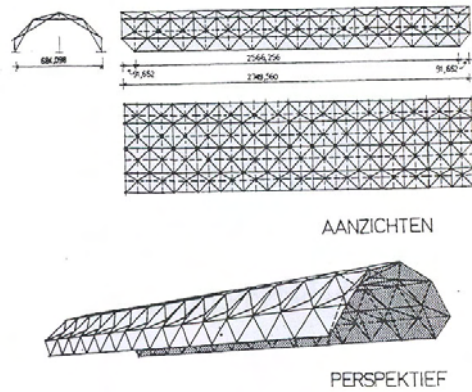


Figure 3.150: Cylindershell of plastic tetrahedrons

Folded lozenge-shapes When two isoscelic triangles are placed with the bases to each other and are folded a little bit under an angle regarding each other, then half a tetrahedron is found. With elements of which the base is large in comparison to the width, it is possible to create cylindrical spatial structures, which remind of a accordeon. The system also behaves like one. When these folds are made in a piece of paper, then it is also possible to entirely flatten them out. This is a transistion shape, which belongs to folding structures.

3.4.8.2 Fabrication and Measurements of Parts

Bars The fabrication of the bars is of course material bound. Roughly three groups can be distinguished:

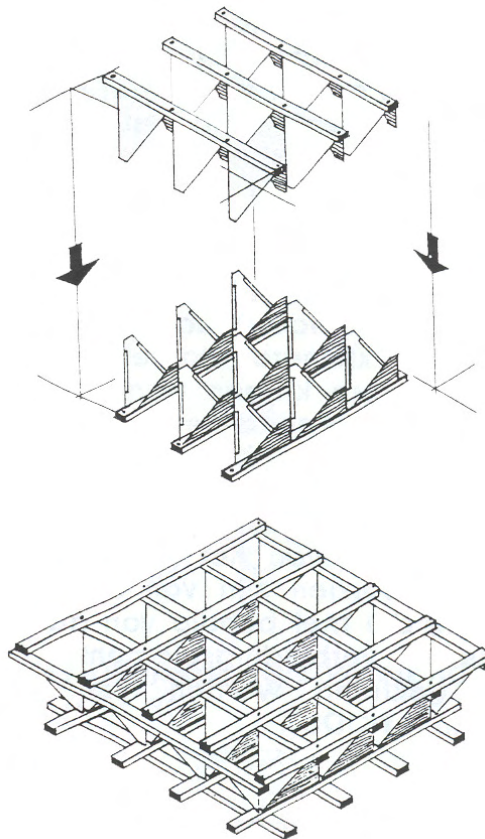


Figure 3.151: Tetragrid System consisting of multiplex and planks

1. Steel

- *Welded connections;*
Some systems, like the SDC-system, make use of cast or pressed connections to which the bars are welded on site.
- *Open standard profiles;*
The transfer of forces is done by shear through the web and/or the flanges, or axial through endplates. In the last case it is hard to handle the deformations caused by bending in these plates.
- *Rectangular, square or circular tubes;*
A tube is pinchable in the width direction, which is why it has to be mechanically flattened or strengthened by welding enplates on at the tube endings in order to take flanking force transfer. With axial loads the tube endings are usually provided with welded or screwed on lump with a hole in the direction of the tube. Du Chateau uses circular tubes in the Spherobat-system, of which the diameter is made smaller towards the tube-endings. These will therefore also get a larger wall thickness and there will be enough material to tap bolt holes (Dutch: 'draadtappen').
- *Clamp- or clasconnections;*

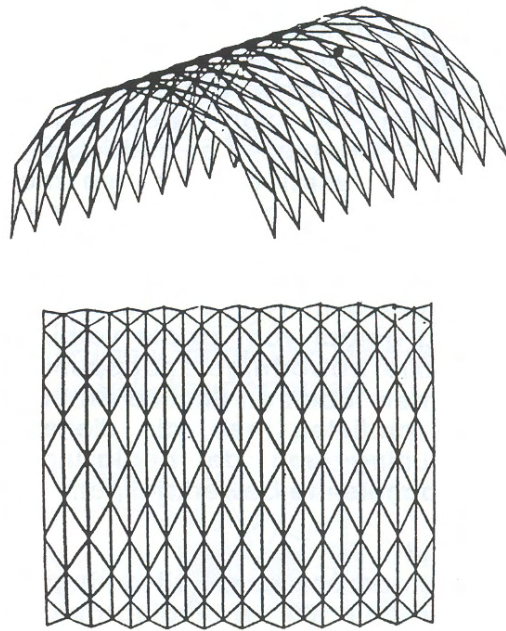


Figure 3.152: Antiprismatisch vouwsysteem

The ends of the profile or tube can be provided with special endpieces, which can be clamped together with especially fitting clamp-elements. An example is NODUS.

2. Aluminium

For aluminium in general the same counts as for the steel bars. Because of the three times lower E-modulus the bars will mostly have much larger diameters. This can have consequences for the production. This material has, however, as special characteristic that it can be extruded. The cross section can therefore have a very varying profile. This aspect is often used. Du Chateau uses profiles of two concentric tubes, of which the middle one is connected to the outer tube with longitudinal plates. This is extruded in one cycle, after extrusion the profile is made to the appropriate length and finished. In the endings of the inner tube threads are made to provide for axial connections to the hollow sphere-shaped connections. In the systems Tuball and Schuco extra profiles extruded in the same way onto the elements, which are meant for the connections of glazing or panels.

3. Timber

There are also some examples in timber. The methods of connection are approximately the same as in steel, because mostly steel transition elements are used between the timber member and the joint. The joint solution can even be identical to the steel version. There is for instance a version of pieces of MERO-bar, which are pressed into a rectangular timber beam and fastened with steel dowels. A comparable solution is offered by the ASB-system. In this system a U-shaped steelplate is put into two slots in the head end of square laminated

timber beams and fixated with steel pins. The U-shape is made smaller in the direction of the pins and has a hole in the narrow crossplate, onto which a sphere shaped connection can be fixed. In Delft a system for roundwood poles was developed. In this system a steelplate is inserted in a slot in the pole tip and fixed by hollow steel dowels. Through these dowels steelthreads are pulled and fixed. The plates in the poles are connected by bolts to circular connector plates with welded on flanges.

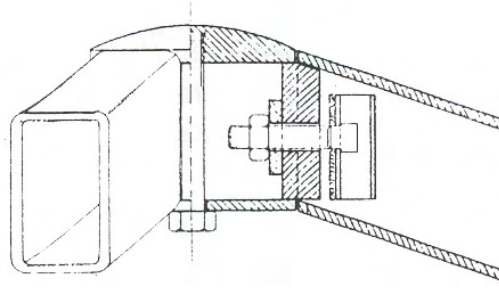


Figure 3.153: Spaceframe in rectangular tubes

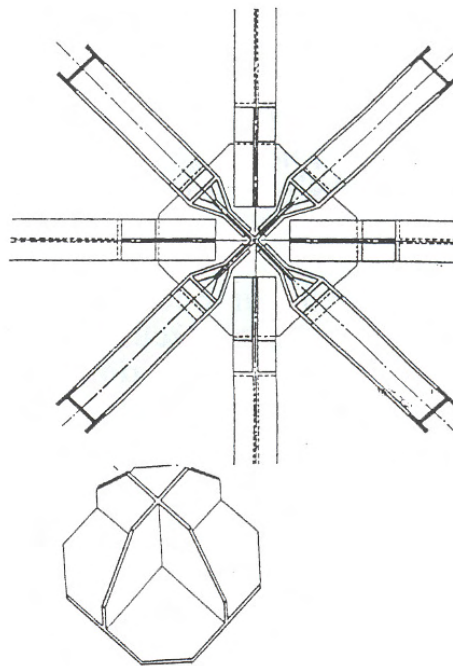


Figure 3.154: Detail with pinched profiles and eight cornered nodeplates, by W. Beckett

Joints

1. Joints in Steel

These can be shaped as follows:

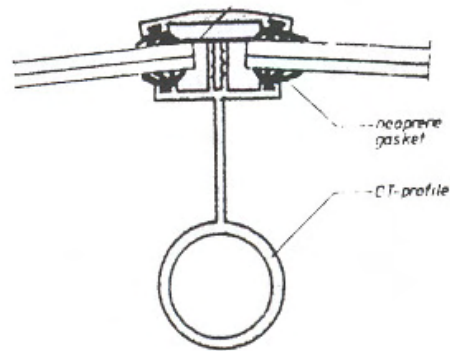


Figure 3.155: Cut over a bar according to the Tuball-plus system

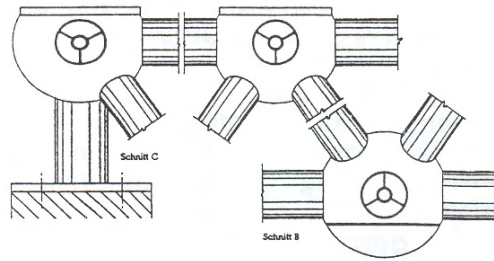


Figure 3.156: Composed cut over a bar, by Schuco

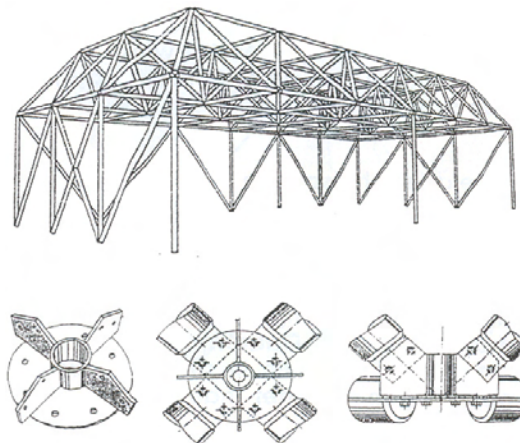


Figure 3.157: Spaceframe in roundwood poles

- *Cast spheres or faceted shapes (polyhedrons)*, usually provided with screw holes with internal threads. Sizes can be very large, diameters up to 35cm have been used

(MERO-stadium in Split). The contactplanes must be carefully made and treated to provide for a correct system size and can not be fit with a compressable protective layer, as for instance a powdercoat-layer. In these joints it must be possible to variate the direction of the hole under two angles: horizontally and vertically. This demands programmable boring equipment. Especially in Japan these techniques are pretty far developed.

- *Cast or pressed hollow spheres.* In principle the same counts as for massive spheres. They are easier to deform, so the wall thicknesses should be enough. Usually they are made in two parts, of which one is a pressed plate. With SDC two shell parts are pressed, which roughly follow the wrapping shape of the connecting bars. Measurements are no problem in fabrication, but are in construction. With Unistrut U-shaped profile-bars are bolted to a cold pressed form, in which also dents are pressed, which exactly fit into the holes of the bars. This guarantees exact measurements.
- *welded tie plates (Dutch: 'schetsplaten').* When joints are constructed from pieces of plate, then holes can be predrilled into them. The orientation of the holes is very important, because this defines the c.t.c. distance. That is why this drilling has to be done with programmable machines or precise boring molds.

2. Joints in aluminium.

This material is very suitable for precisioncasting, which enables the production of very precise and detailed elements like the jointelements. The material is also easily deformed cold. This characteristic is used in the Triodetic system. The joints in this system are slab shaped and have toothed incisions. The elements are made by extrusion and sawn to discs. The bars fit into the the joints because they are tubes with flattened ends, which have been equiped with rims corresponding to the toothed incisions. Sometimes these rims have to be pressed under an angle with the axisdirection, like for instance in diagonal joints.

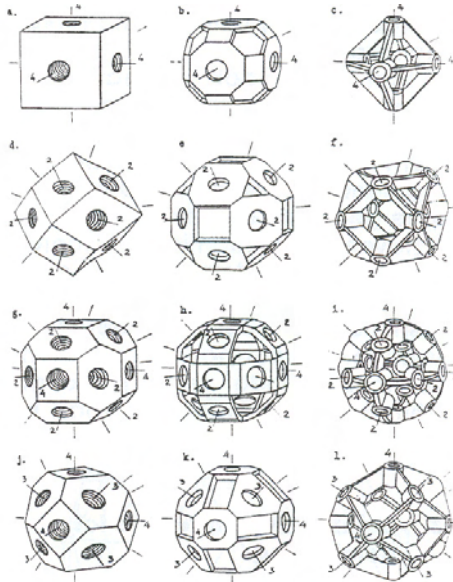


Figure 3.158: Some examples of faceted nodes

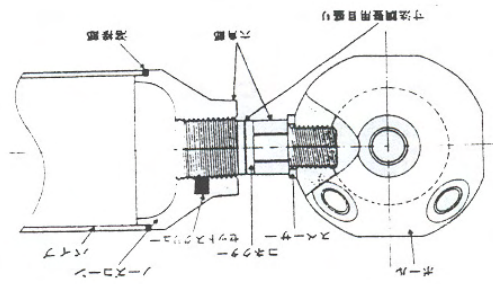


Figure 3.159: A Japanese sphere-shaped node

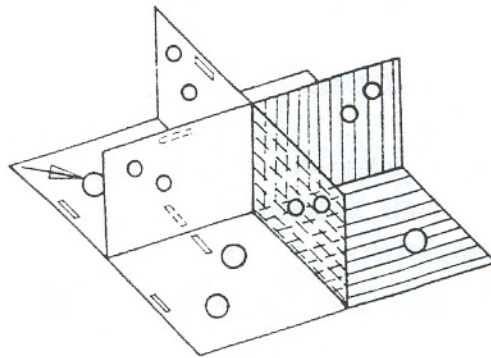


Figure 3.160: A solution with tie plates, with which most common spaceframes can be built

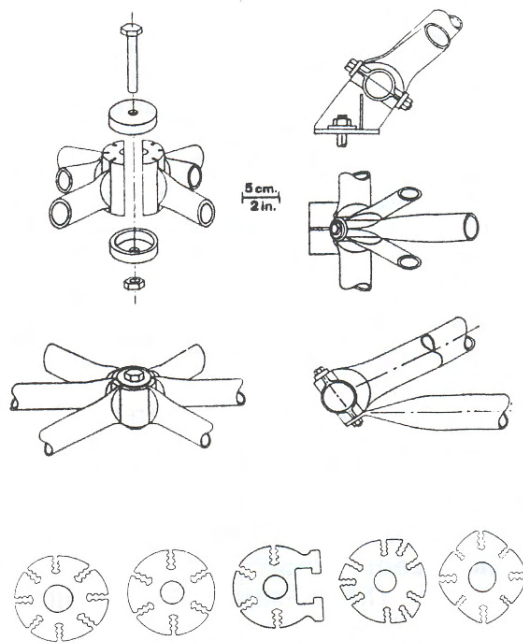


Figure 3.161: The triodetic system with aluminium nodes and bars

3.4.8.3 Measurements in relation to the detailing.

In structures, built up from a large number of relatively small elements, measurements are very important. Small deviations can accumulate to an intolerable total deviation compared to the design. That is why measurements in fabrication have to be controlled very tightly. The influence of these deviations can be system-bound.

- *Welded connections*

In systems like the SDC-system, tubes are welded between two shell shaped connecting elements. It is clear that there are no high demands for the measurements of the bars. In fact the problem is shifted to the construction site. In construction supports are needed to create the total shape. This can be partly neutralized by constructing the structure with temporary bolts. The welding on site, often under difficult angles and under harsh climate conditions, is a restrictive factor.

- *Shear-bolt connection.*

In joint solutions in which flanking transfer of forces occur, like flanges and tie plates, hole tolerances are important. The holes should be made slightly larger than the bolt diameter, because assembly can be a problem. Normally a minimal tolerance in the order of 0,5mm is demanded. This tolerance also depends on the finishing of the bar and the joint. If one of the two is steel, then it will be galvanized and the thickness of this layer needs to be added to the initial tolerance. Usually finishing of the holes and contact surfaces is needed, because drops and roughness can be formed by the galvanizing, which need to be removed (of course without damaging the conservative properties). With powdercoating and painting the same problems arise, though the layer on the contact surface is much softer. Usually the contact surfaces are kept blank or another type of finishing is used. The center to center distance is of course dictating the end measurements in the assembly phase. This dimension can be found within very slim tolerances by using precise boring equipment. The total tolerance of the hole is, however, influencing the total dimension in loaded condition and can require special care for for instance the displacements.

This can usually be solved by giving the structure a pre-camber, This does imply that the bars on the the bottom side need to be made longer in at least one direction.

- *Connection with axially loaded bolts.*

One should think of the type of joint in which the bar is bolted to a massive or hollow sphere. The spheres are usually cast and therefore relatively rough. The distance of this plane to the center of the sphere as well as the length of the bar need to be precisely measured. When these planes are properly finished, a very precise measurements can be achieved. This finishing is, however, not always possible due to the needed surface protection; that is why the measurements are sensitive to imperfections in the contact surfaces. This method has as an important advantage, that the bar can be slightly lengthened fairly easily, by using rings put in between. This can be used to create a pre-camber in the structure.

3.4.8.4 A Connection without separate joints

In some cases the bars are interconnected without using separate joints.

1. Connections by dihedral angles (Dutch: 'standhoeken') Two different solutions are used:
 - In the first case the ends of a tube are provided with welded on attachments with wings, that are placed under the desired angles. These angles are the same as the dihedral angles of the tetrahedron (70.53°) and the octahedron (109.47°). Examples of

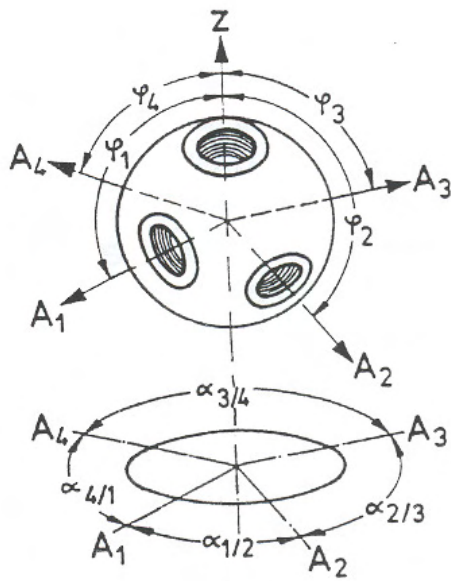


Figure 3.162: The positioning of the holes in a node

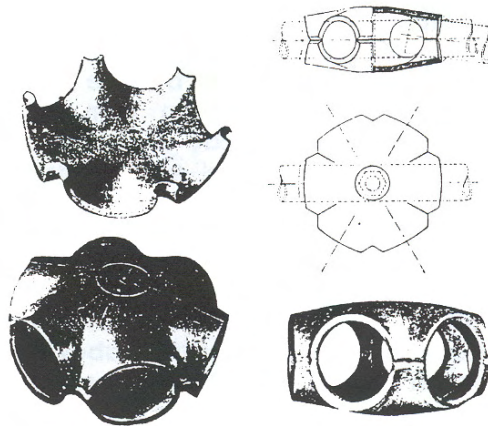


Figure 3.163: The SDC-system

this are a system by R.B. Fuller and the Pearce-system. The structure of the famous biosphere is made with a system like this, presumably the last mentioned.

- In another solution an extruded aluminum profile is used with webs and flanges, which are under these angles over the entire length.

Both methods have an objection; in the heart of the system -where the jointelements normally are- no material is found. This can lead to rather large displacements in the connection, especially when not all directions of connection are taken up. This is definitely the case in double layer systems and most definitely along the edges.

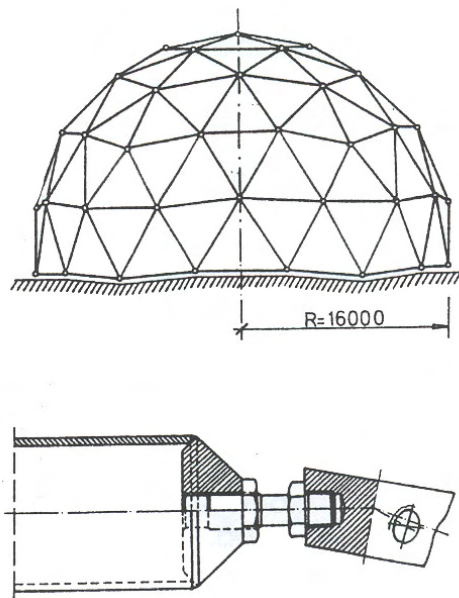


Figure 3.164: A disc joint in a single layer sphereshaped frame

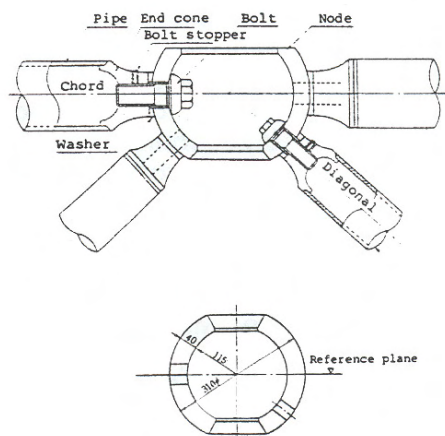


Figure 3.165: The Japanese NS space truss system

2. The ends of the bars are machined;

- Corner elements.

The bars are provided with small welded corner elements, which fit around each other like a wing of a mill and butt (Dutch: 'stuiken') along the horizontals. This has been applied in a roundwood spaceframe in Rotterdam. The corner elements have in this case been welded to tie plates, which are put into a slot in the end of the pole and connected with tubeshaped pins and steel wire.

- Flattened bar endings

Something like that is the case in the RADIAL system. In this system the trusstubes of the sloping diagonal bars are flattened at the endings and put under the required angle. These flat pieces are bolted tight in the joining of the horizontals which pass each other with some sort of a half-‘timber’ overlap.

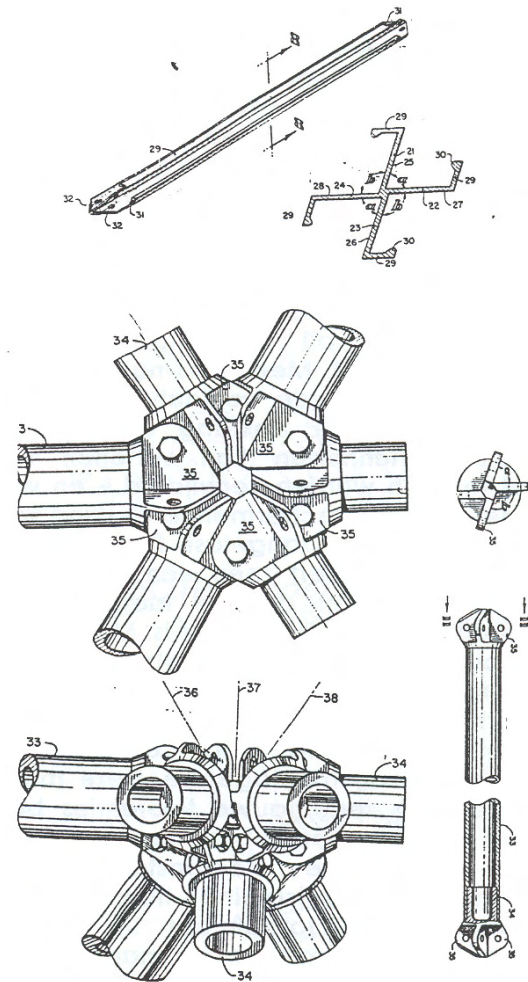


Figure 3.166: Solutions by R.B. Fuller without separate joints

3.4.8.5 Connection with separate node elements.

Types of nodes

- **Welded:**
 - Connected directly (For example Kolowski)
 - onto a sphere shaped element (Oktaplatte)
 - Between arched, pressed plates (SDC)

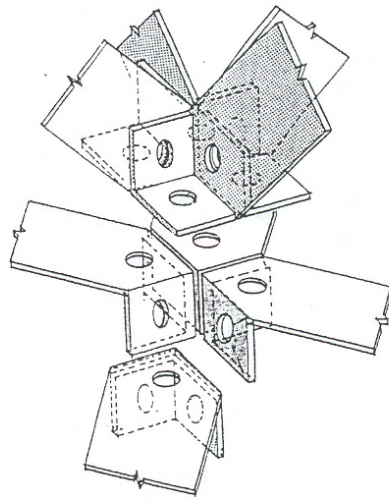


Figure 3.167: A system, developed by TU Delft, with a U-shaped bar-ending

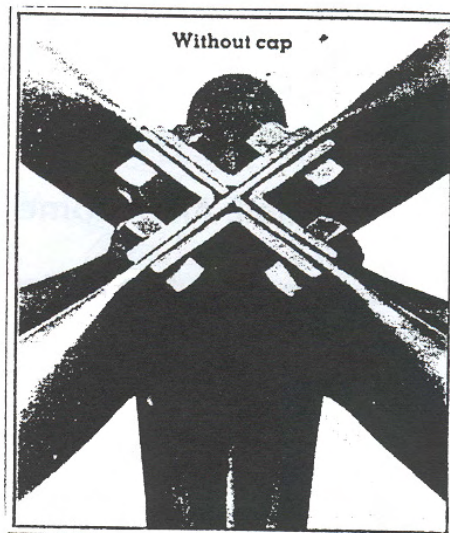


Figure 3.168: The Radial System

– Clamping systems (NODUS)

- **Disc-joints** (Mero, Triodetic)

- **Massive sphere**

M. Mengerhausen visualized the cuboctahedron (P10) as a node element. In this idea all needed connection directions of the ribs and planar diagonals of a cube appear, in total 18 directions. This joint is in principle shaped like a cube, chamfered in multiple directions under an angle of 45 degrees. With a diagonal on every plane of the cube a tetrahedron can be formed which entirely consists of equilateral triangles. The MERO-node gives the

possibility to not only connect the ribs of the cube, but also the diagonals in the planes. The strange effect then arises with these nodes, that not only angles of 45 degrees or multiples of 45 degrees can be made, but also angles of 60 degrees. Most other systems are based on the same connection directions. Many examples exist:

- Netherlands: van Thiel Space System
- Japan: Pantadome, Tomoe Unitruss, TM Truss(Taiyo Kogyo), KT Truss.
- USA: Steve Baer (dodekahedron)
- Germany: Mero, Zublin, Krupp, W. Kuhn (mainly rhombic dodecahedron)
- **Hollow sphere** (Spherobat, Tuball, Alco-dome, Schuco)
- **placed** (bended or forced plate and/or bar (Unistrut, Power strut)
- **Assembled**
 - From cast elements (Wachsmann)
 - Standard half-fabricates
 - Tie plates (Octatube, TU-roundwood system, RAI-joint)

This list is probably far from complete. Often a new solution is sought, to avoid paying licenses needed to use existing systems. The differences with existing systems are therefore often very small and many systems look very similar.

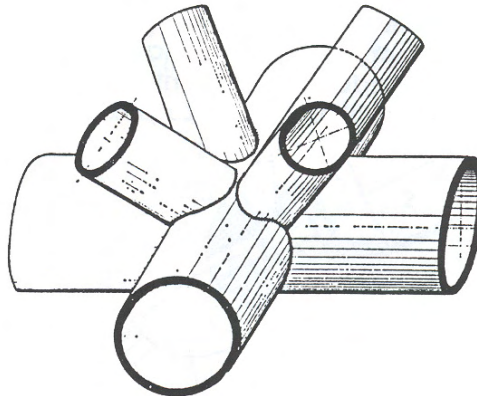


Figure 3.169: A welded joint

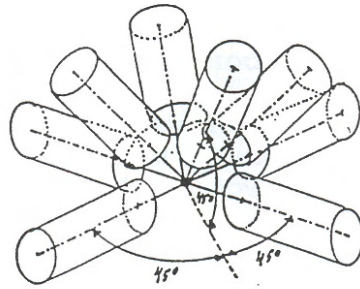


Figure 3.170: The meeting of different bars in a common spaceframe

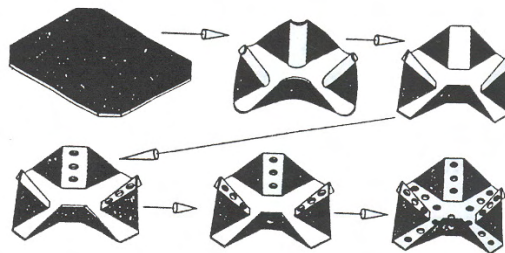


Figure 3.171: The Unistrut system

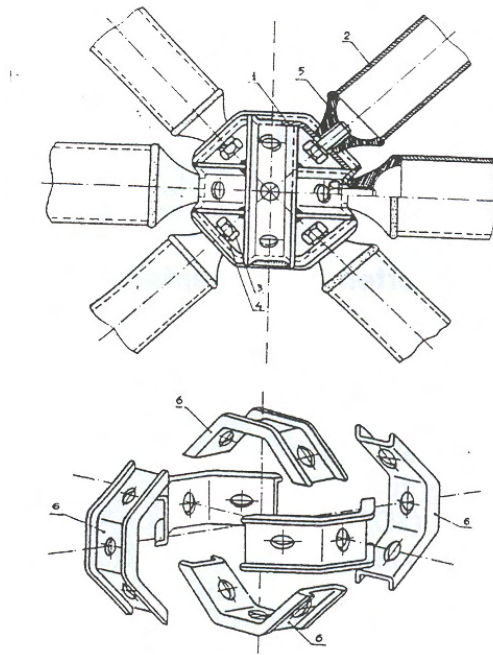


Figure 3.172: A composed joint according to a Russian patent

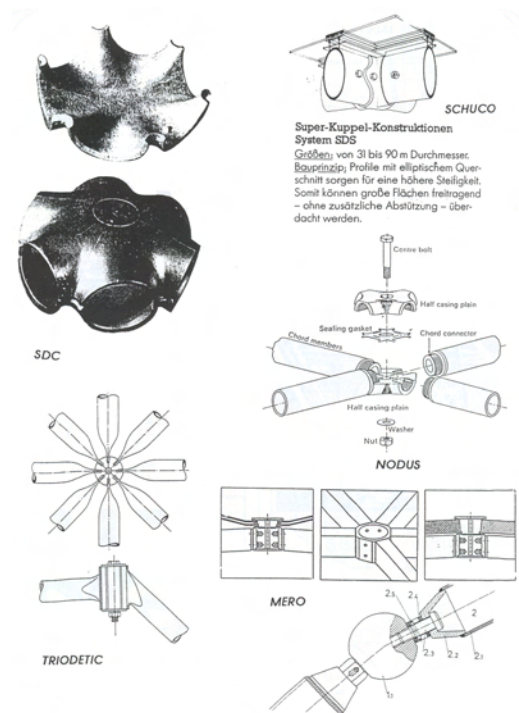


Figure 3.173: Some examples of solutions for single layered spaceframes

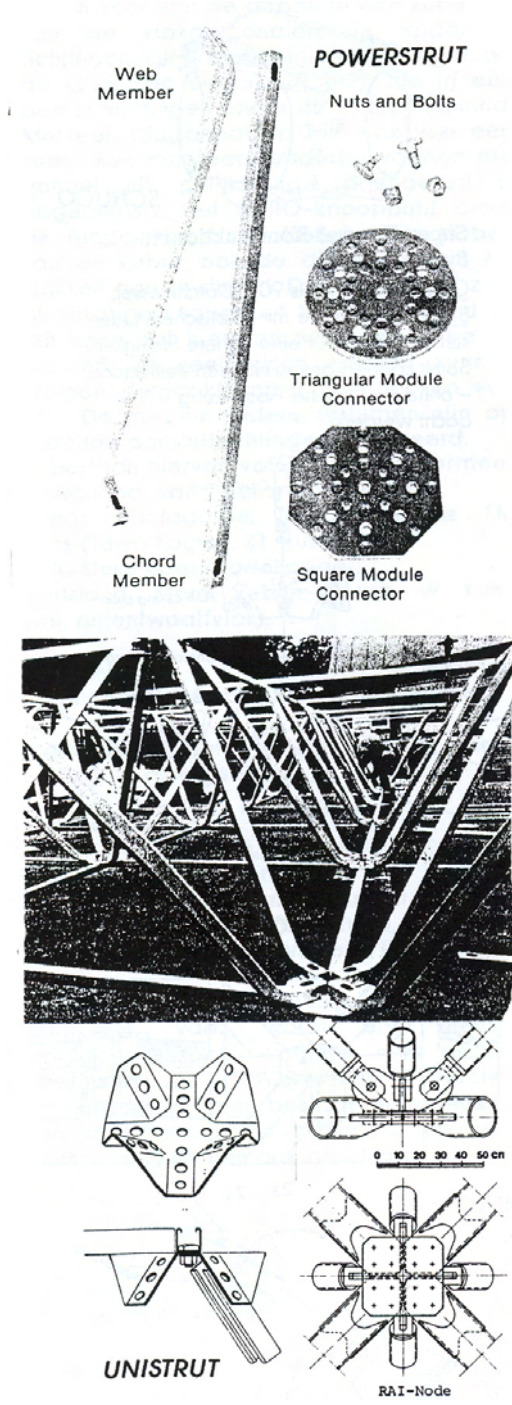
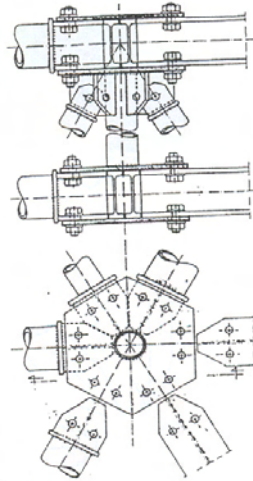
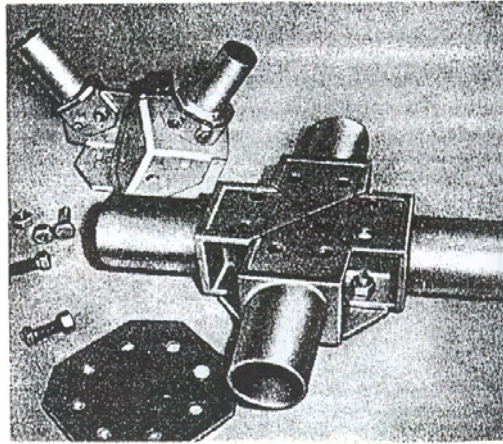


Figure 3.174: Some special solutions with clamping or slide connections

TRIDIMATIC



TRIDIMATIC

OCTATUBE

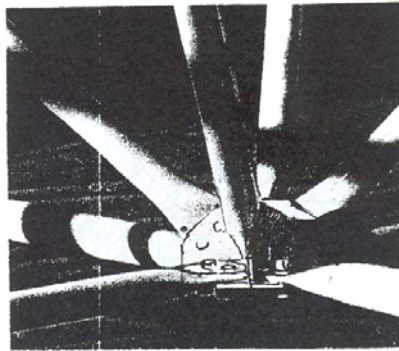


Figure 3.175: Joints with tie plates

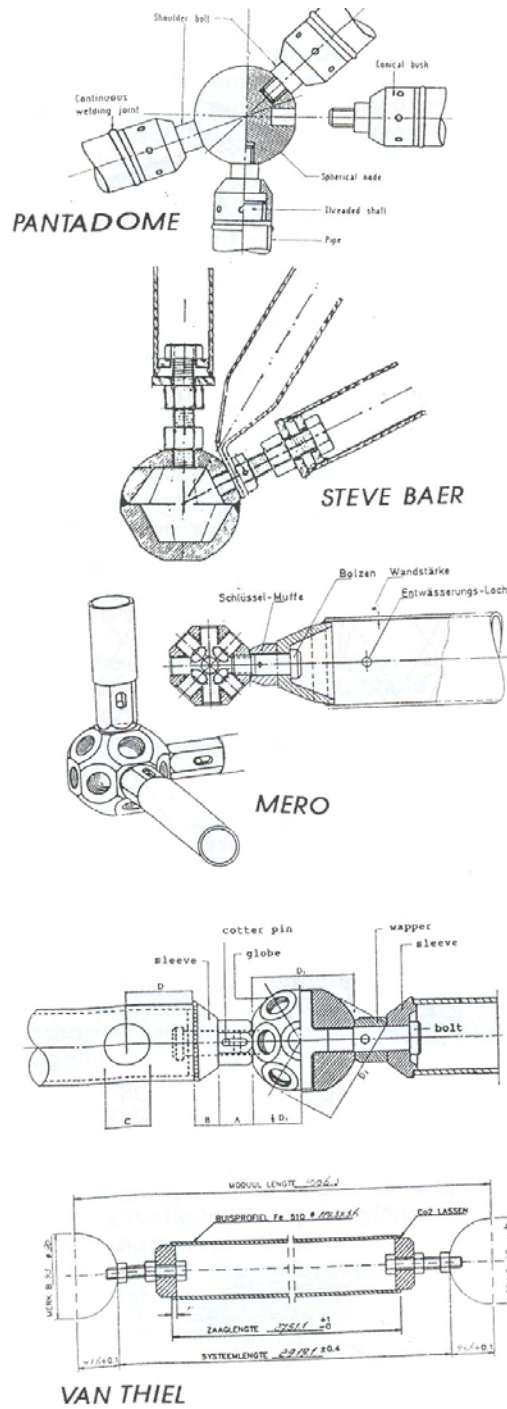


Figure 3.176: Different massive sphere shaped joints

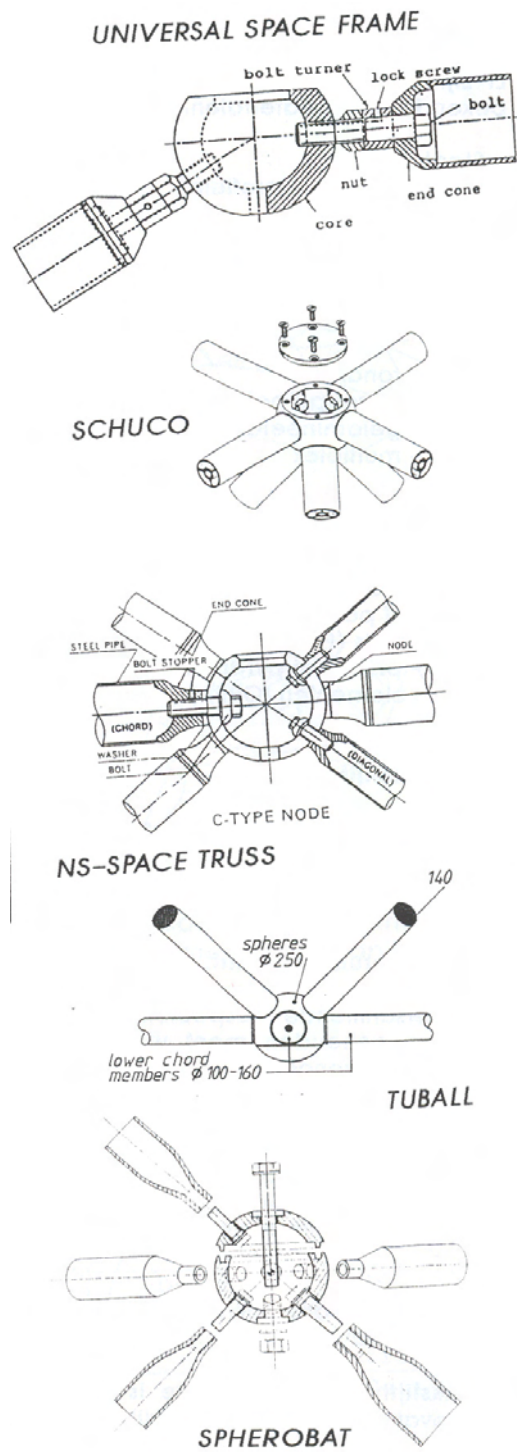


Figure 3.177: A number of hollow sphere shaped joints

Used materials There are variants known in almost all known building materials:

- Steel
 - Tubes or profiles
- Aluminium
 - Tubes or profiles
 - Pyramids
- Timber
 - Roundwood
 - Sawn timber
 - Glue-laminated timber
 - Multiplex
- Concrete
- Plastics
 - Rods (Glassfiber Reinforced epoxy or polyester (GRP))
 - Tube (PVC)
 - Plates or pyramideshaped elements (GRP)

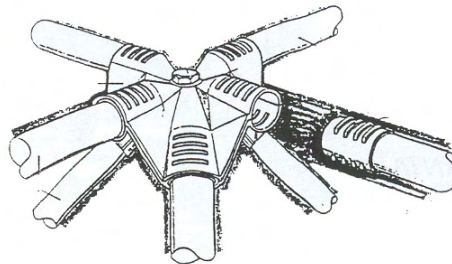


Figure 3.178: A system with bars of glassfibrepolyester by L. Hollaway

3.4.9 Stability

The stability must of course be guaranteed in the usability state as well as in the construction state.

3.4.9.1 Usability state

The different aspects which need to be dealt with will be mentioned here with just a short comment, because there is mostly not a general solution. These points should be considered as attention points, for which should be taken care in construction.

- Statically determinance or statically under- or overdeterminance
- Buckling of the bars, this is often leading in flat spaceframes. Also care should be taken that no bar has more than two hinges in longitudinal direction. This is often forgotten when dealing with in between connections in the joints themselves.
- Snap-through (Dutch: ‘doorslag’) or too little bending stiffness of single-layered systems with a too small curvature. To describe this phenomenon a non-linear calculation is needed. This is an iterative process in which the under loading constantly changing geometry is re-entered into the program until the end situation has been found.
- Buckling (Dutch: ‘uitspatten’) of the nodes because of little stiffness perpendicular to the plane. This is often repairable. A good example is the Alco-dome of the Eindhoven University of Technology. The so-called reducers that are welded to the ends of the bars are only reduced in width-direction, so the bars fit into the joint, but keep their internal height in the perpendicular direction to the width.
- The rotating out of joints because of too little rotational stiffness in horizontal sense. In the tie plate systems, like Octatube, it is needed to always use two bolts in the horizontal direction to prevent this effect.

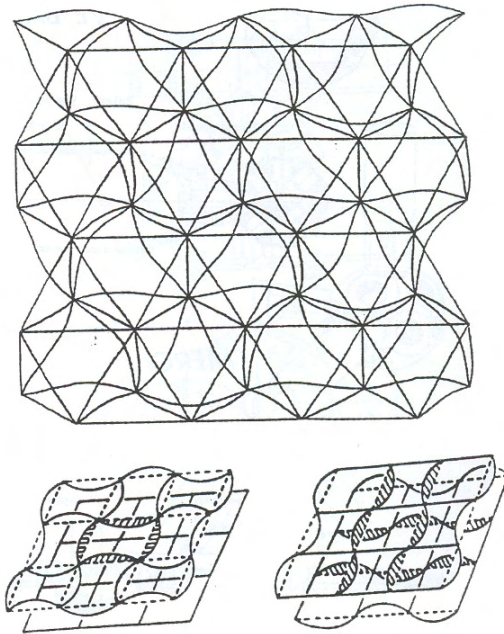


Figure 3.179: Possible problems with stability

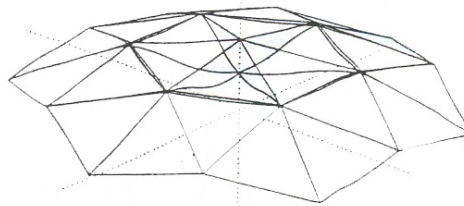


Figure 3.180: Snap through in a single layered domeframe

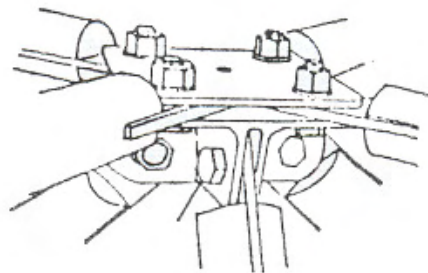


Figure 3.181: The Varitec system: too many hinges in a bar

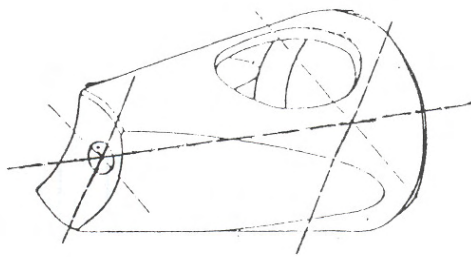


Figure 3.182: Reductor in a barend; Alcodome sistem of the TU Eindhoven

3.4.9.2 Construction state

The situation during construction can be very different from the usability state.

Possible problems during hoisting:

- Choice of hoisting points, because of cantilevers, which can lead to buckling of lower bars.
- Horizontal reaction force from hoisting cables, when no provisions are used, which can lead to:
 - buckling of lower bars
 - pinching together of the bottom side of the structure, when the hoisting points connect diagonally
- tilting of the hoisted structure, when the centre of gravity is not directly below the hoist point

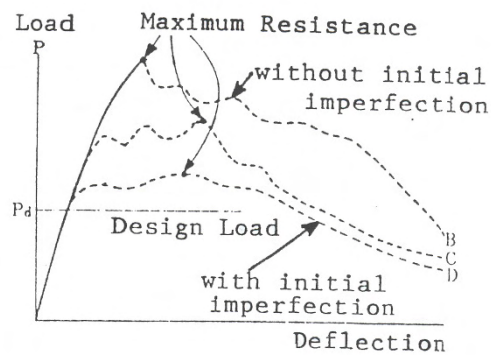


Figure 3.183: Failure behaviour of a spaceframe due to buckling of the bars

3.4.10 Calculation

3.4.10.1 Approximating calculation by hand

Spaceframes are too complicated to calculate by hand. When there were no computers yet, development in this field was therefore held back. Still it is possible to get a global insight into the strength and stiffness of the structure, as long as it is simple in essence. Reference is made here to an address by Beranek and Hobbelman (Wachsmann 1962), about a calculation method for the sketch design. Simple rules for design calculations are given in Merkblatt 10, by the Beratungsstelle für Stahlverwendung, under chair of H. Witte (1981).

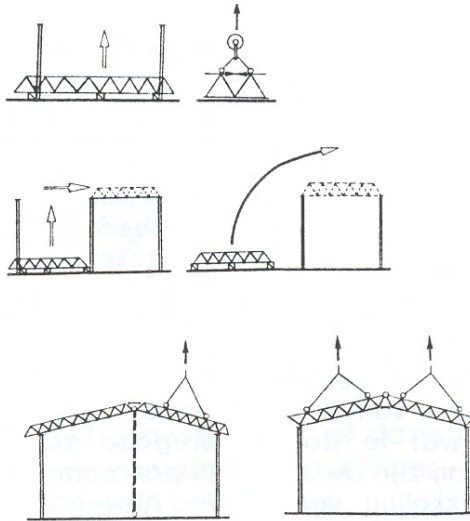


Figure 3.184: The construction of spaceframes

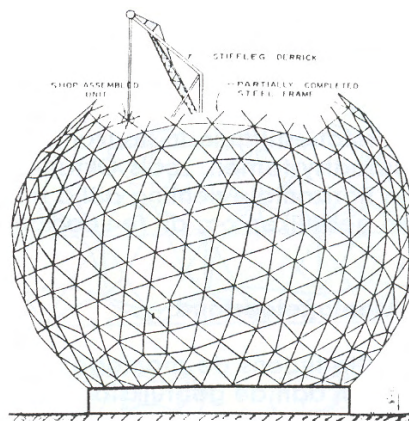


Figure 3.185: Construction of a dome

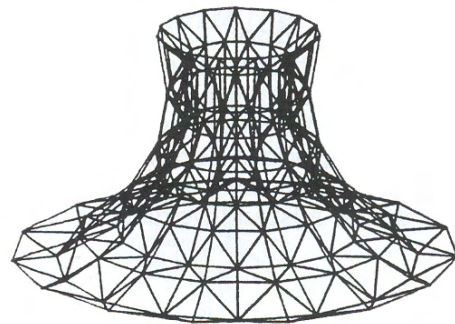


Figure 3.186: An example of a frame generated by FORMEX

3.5 Kinetic and adaptable structures

3.5.1 Adaptive structures

Adaptive structures are structures that adapt to their environment according to a certain set of rules and strategies. Mulder (Mulder 2003) researched some of the conceptual thoughts on these adaptive structures at the Delft University of Technology in 2003. They can be seen as physical form finding, since the structure finds its own form by adapting to the environment, not in a scaled-down model, but in a full scale reality. The rules and strategies of the system (physical, computational, man-made, artificial, etc.) are the driving force of the form finding process and the structure reaching its own structural optimality.

3.5.1.1 Large-Scale Linear Actuators

As already mentioned, a linear actuator can be described by two elements, namely a piston and a mechanism that applies a force to the piston and also controls the motion of the piston. This actuator type is the most commonly available and most often used, especially for applications demanding a large force and short response time. This usually implies a high energy demand. Three types of large-scale linear actuators will now be discussed: hydraulic, electromechanical, and electromagnetic systems.

Hydraulic systems create the force by using a hydraulic pressure on the face of a piston head contained with a cylinder; this is shown in Figure 3.187. Fluid is forced in or out of the cylinder through the mechanism to compensate for the piston displacement and to keep up a certain pressure. These systems have the highest force capacity of the linear actuator group, in the order of meganewtons (depending on the area of the piston).

The force can be described by:

$$F_c = \lambda \Delta P A_c \quad (3.38)$$

where λ is the friction, ΔP is the pressure and A_c is the area of the piston. From Equation 3.38 follows that the efficiency of the system is governed by friction. Precise control movement and force can be achieved with an appropriate control system. Protection against overload is provided by a pressure relief valve. When there is a small internal leakage the static load is kept. The disadvantages of this type of system are the requirements for fluid storage systems, complex valves and pumps to regulate the flow and pressure, seals and continuous maintenance. Durability of the seals and the potential for fluid spills are critical issues (Connor 2003).

Electromechanical linear actuators generate the force by moving the piston with a gear mechanism that is driven by an electric motor, i.e. electrical energy is transformed to mechanical energy. The motion, and therefore the force, is controlled by altering the power input to the motor. These devices are compact in size, environmentally safe, and economical. Figure 3.189 illustrates different sizes of rod-type linear electric actuator systems developed by the company Racal. The thrust (linear force) capacity of these devices goes from 0,5 kN up to 1,2 MN (homepage 2005)

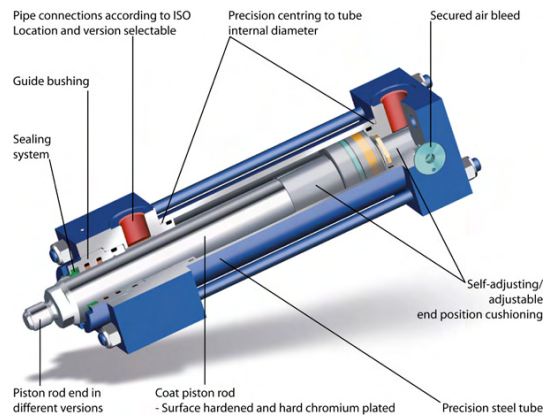


Figure 3.187: Tie-rod hydraulic system. Image from <http://www.birdair.com/birdair/flash.html>

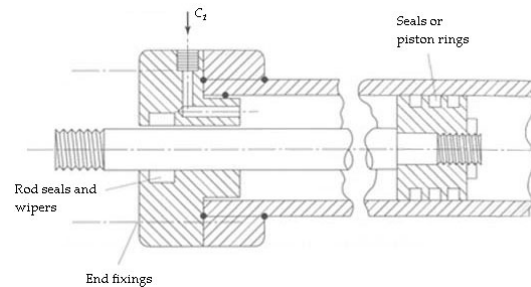


Figure 3.188: Schematic cross-section view of a hydraulic cylinder. Image by (Dorey & Moore 1996).

Hydraulic and electromechanical actuators are composed of many parts that are in contact with each other, and hence have a relatively high risk of failure. Since electromagnetic actuators are initiated by magnetic forces, which do not require mechanical contact, they are theoretically more reliable. Electromagnetic actuator devices operate on the principle that a magnetic field is produced in a high permeability core material that is wrapped with a current carrying coil. Small-scale electromagnetic actuators with a force capacity ranging from tens of newtons to several kilonewtons are already commercially available. Besides their compact nature and low voltage and amperage requirements, their response time is low, on the order of milliseconds. These characteristics are ideal for active force generation, and electromagnetic actuators are a popular choice for small-scale structures. Large-scale electromagnetic actuator technology is still in the research and development phase, and there is at the moment no commercial product available with a force capacity in the meganewton range (Connor 2003).

3.5.1.2 Large-scale Adaptive Composition-based Actuators

This category comprises mechanical devices such as dampers, artificial muscles, stiffness elements, and friction elements that have the capacity to produce a force by changing their physical composition. Their most distinctive features are their low ratio of energy demand to force output and, depending on the type of device, generally large-scale force capacity. These



Figure 3.189: Different sizes of rod-type electric linear actuators. Image from <http://www.racointernational.com>

features are very desirable for applications of large-scale civil structures. Adaptive devices that have a low energy demand and also operate as energy dissipation mechanisms are referred to as semi-active actuators since they behave like passive devices in the sense that they increase the stability of a structure and require no external energy. A semi-active actuator will never destabilize a system even though it has a low energy demand.

Figures 3.190 and 3.191 show the concept of a variable orifice damper. A variable orifice may be considered as a viscous damper with a variable damping coefficient. Its operation principle consists in controlling the damping coefficient by adjusting the opening of a valve according to the force demand specified by the feedback control algorithm. Given that the valve motion is perpendicular to the flow, the force required to alter the valve position is small, and therefore the energy demand is low; 50 watts of power to operate is a typical amount for such devices (Jr. & Sain 1997).

Artificial muscles At the Vrije Universiteit Brussel (VUB), department of Mechanical Engineering, Multi body Mechanics Research Group, Frank Daerden has recently developed the Pleated Pneumatic Artificial Muscle (PPAM), illustrated in Figure 3.192, the successor of the Pneumatic Artificial Muscle (PAM) e.g. the McKibben Muscle. A pneumatic artificial muscle is in essence, a membrane that will expand radially and contract axially when generating high pull forces along the longitudinal axis. In other words, pneumatic artificial muscles are contractile devices operated by pressurized air. The muscle is basically

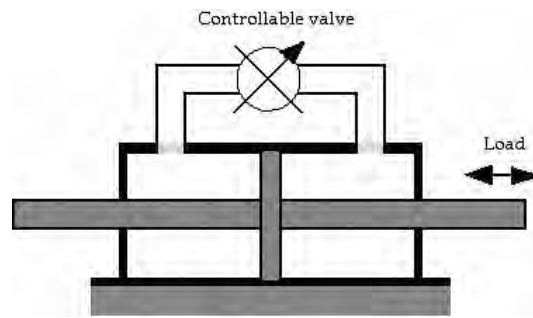


Figure 3.190: Schematic of a variable orifice damper. Image from (Jr. & Sain 1997)

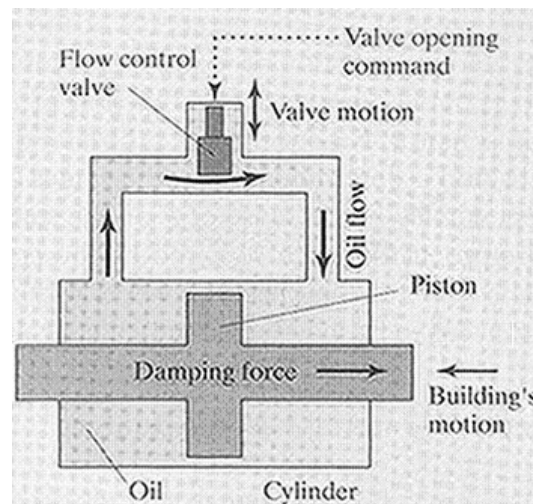


Figure 3.191: Variable damping mechanism. Image from <http://www.racointernational.com>

nothing more than a membrane, which makes it an extremely lightweight actuator. This muscle has a rubber tube which will expand when inflated, while adjacent netting transmits tension. Hysteresis (pressure/length course between contracting and relaxing), due to dry friction between the netting and the rubber tube, makes control of such a device rather complicated. Typical of this type of muscles is the need of (reaching) a lower boundary level of pressure before any action can take place.

The main goal of the new design was to avoid both friction and hysteresis, thus making control easier while avoiding the lower boundary. This was realized by arranging the membrane into radially laid out folds that can unfurl free of radial stress when inflated. The membrane's stiff longitudinal fibres transfer tension. As the pressure rises, the membrane can defold without the occurrence of friction and the muscle's elongation will not be hindered by material stresses, therefore optimising the contraction. When the artificial muscles are inflated, they swell, shorten and thus generate a contraction force. This means that for the geometry, the developed force (as a function of the length) and the maximum shortening, the bellows gets a 'pumpkin-like' shape when contracting. The (tensile) force depends on the applied pressure and on the muscle's length, ranging from an extremely high value at maximum length, i.e. zero contraction, to zero

at minimum length or maximum contraction. The maximum contraction depends on the initial slenderness (for the mathematical upper boundary case of an infinitely slender bellows, this slenderness can rise up to 54,3%) (Daerden & Lefeber 2001).

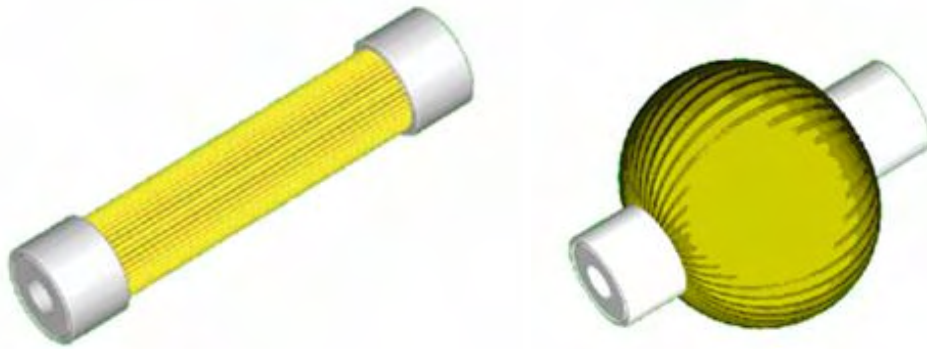


Figure 3.192: Deflated state of the PPAM and inflated state of the PPAM. Image from www.vub.ac.be

Each of the characteristics of this type of muscle can be expressed as the product of a scale factor with a dimensionless function depending only on the contraction and the slenderness. For the force for example, it holds:

$$F_t = pl \cdot f\left(\frac{\epsilon, l}{D}\right) \quad (3.39)$$

with D and l being the initial diameter and length, and the dimensionless contraction (referred to l). The scale factor is expressed by pl^2 . The following well known relation is also valid:

$$F_t = -p\left(\frac{dV}{dl}\right) \quad (3.40)$$

It unambiguously symbolizes the actuator's equilibrium length by the determined pressure and the external loading, meaning that the change of the volume over the length is directly decisive for the developed force (Daerden & Lefeber 2001).

The challenge is to efficiently integrate the muscles in a structure, both visually and structurally by knowing the possibilities and limitations of these elements.

The generated force is highly non-linear and proportional to the applied gauge pressure in the muscle. At a pressure of 300 kPa the force can be as high as 4000 N for a device with an initial length of 10 cm, weighing only 100 g. It has to be kept in mind that at increasing contraction, the force drastically (non-linearly) drops, as shown in Figure 3.193. So the muscles applied in a structure either supply a large force or make a large displacement possible, but not both.

To have a bi-directional working joint one has to couple two muscles antagonistically. At each joint the muscles are attached in a leverage mechanism by pulling rods. The points of attachment are essential in the design since they determine torque characteristics. Because of the one-way

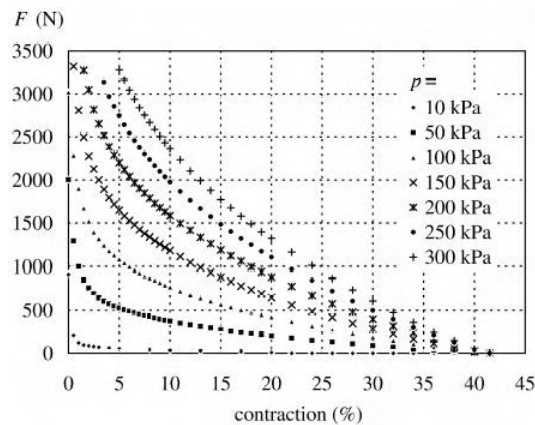


Figure 3.193: Force/contraction curve for PPAM for variable p . Image from (Daerden & Lefeber 2001)

force a paired or antagonistic set-up is needed in order to generate a restoring force or movement.

Another type of artificial muscles has been developed by the company Festo. In nature (for example the human being), biological muscles contract powerfully and relax in a controlled manner. Festo has tried to implement this principle in an industrial product, resulting in the meanwhile 'standard component' Fluidic Muscle MAS.

The Fluidic Muscle operates in the same way as the previously discussed PPAM, i.e. by membrane-contraction. The resulting 3-D grid pattern deforms when actuated by compressed air. As internal pressure is increased, an axial pulling force develops to cause the tubular unit to contract, turning it into a linear actuator.

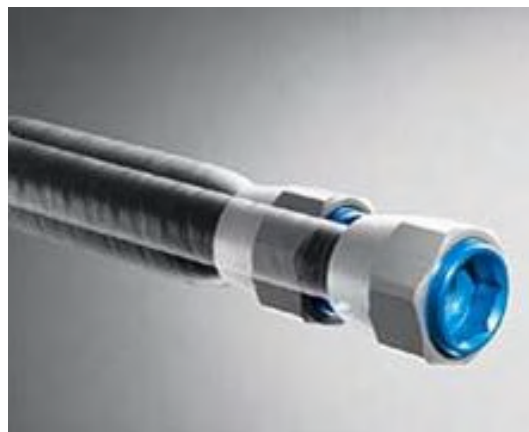


Figure 3.194: Festo Fluidic Muscle. Image from <http://www.festo.com/INetDomino>

The force capacity of the Fluidic Muscle MAS is comparable to the PPAM (a few kilonewtons), developed at the VU Brussels by Frank Daerden.

The advantages of the Fluidic Muscle as an (linear) actuator are its low self-weight, easy implementability in a structure, a reasonable response time and a contraction capacity up to 25% of its original length.

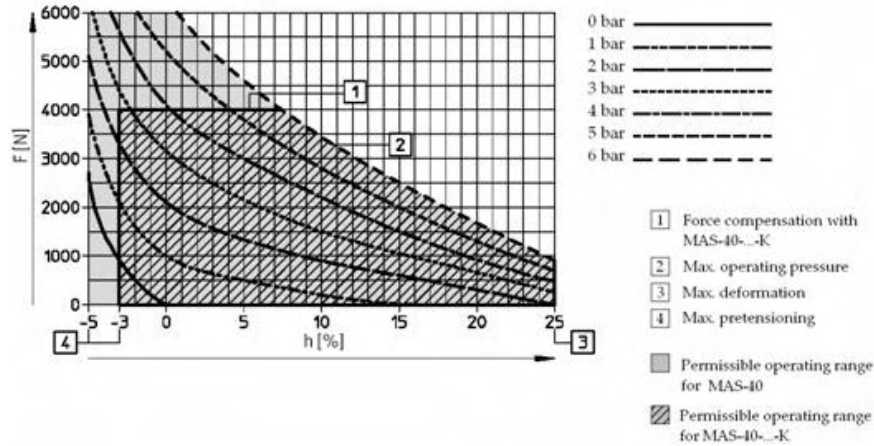


Figure 3.195: Permissible force F (N) as a function of contraction h [(%) of nominal length. Image from <http://www.festo.com/INetDomino>

Compared to the PPAM, the Fluid Muscle MAS has the disadvantage that it requires a high pressure and causes much hysteresis, making the control of the device more complicated.

3.5.1.3 Small-scale Adaptive Material-based Actuators

Low force capacity electromechanical and electromagnetic linear actuators are standard products presented by several suppliers. Here the attention will be focused on a new generation of small-scale force actuators that utilize the unique properties of adaptive materials to produce the force. Research and development in this area was started by the aerospace industry as a potential solution for shape control of satellite arms and airplane control surfaces. As the technology evolved, other applications associated to motion control of small-scale structures such as robot arms and biomedical devices have arisen. Although the reliability is still a major concern, technology continues to progress, and these devices are being seriously considered as candidates for force control where the required force level is on the order of a kilonewton. Several adaptive material based actuators will now be briefly discussed.

Piezoelectric actuators Piezoelectric materials belong to the category of electrostrictive materials. This implies that they deform elastically under the influence of an electric field, in a way similar to the Poisson effect for applied stress (Janocha 1999). Figure 3.21 illustrates this behavioural manner; a voltage V_z in the Z -direction produces extensional strains ϵ_x and ϵ_y in

the X and Y-directions (Connor 2003). The opposite behavioural characteristic occurs when the material is stressed in the X-Y plane, a voltage V'_z in the Z-direction is generated by σ_x and σ_y . Traditionally, piezoelectric actuators have been used as strain sensors. Their use as actuators is more recent and stimulated mainly by the aerospace industry.

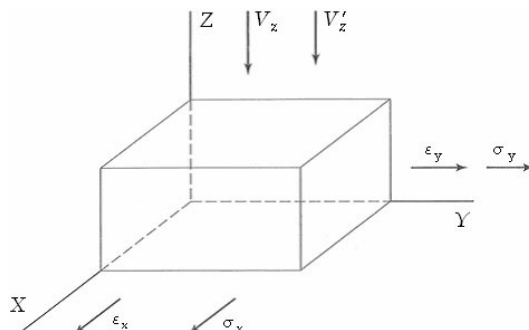


Figure 3.196: Piezoelectric electrical-mechanical interaction. Image from (Connor 2003)

Piezoelectric actuators are fabricated with piezoceramic block-type elements or piezopolymer films. Lead zirconate titanate (PZT) is the main piezoceramic composite used for transducer applications, i.e. sensors and actuators, in the frequency range up to 10^6 Hz. Artificially manufactured polymers on the basis of Polyvinylfluoride (PVDF) is most commonly used in piezoelectric films (Janocha 1999). As it has a quite low strength, PVDF is used mainly as a sensor, particularly for the high frequency range up to 10^9 Hz. The fundamental principle is the same for both mentioned materials. The piezoelectric object is attached to a surface which restrains its motion. When the object is subjected to a voltage, it inclines to expand immediately, and consequently contact forces are produced between the object and the restraining medium (Connor 2003).

So far, two actuator configurations have been realised. The first model is a conventional linear actuator such as shown in Figure 3.197. Piezoceramic wafers (small thin circular slices of a semi-conducting material) are piled up vertically, fastened, enclosed in a protective housing, and fitted with electrical connectors. These devices can deliver large forces, up to almost 30 kN, with a response time of several milliseconds (Homepage n.d.).

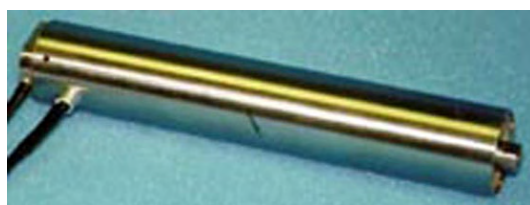


Figure 3.197: Cylindrical piezoceramic linear actuator. Image from <http://www.kineticceramics.com>

The second configuration has the form of a thin plate, as illustrated in Figure 3.198. Piezoceramic wafers are distributed over the area in a regular pattern. They may also be piled up through the thickness. This type of device is connected to a surface and applies a pair of self-equilibrating tangential forces to the surface. The peak force depends on the applied voltage

and degree of restraint. A force level of 500 N at 200 volts, and millisecond response, are typical upper limits for current plate-type piezoceramic actuators. Recent developments are concerned with lowering the voltage requirement (Connor 2003).

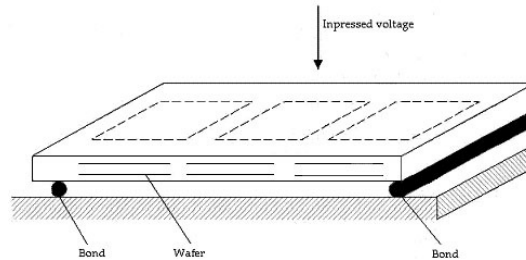


Figure 3.198: Plate-type piezoelectric actuator. Image from (Connor 2003).

Shape memory alloys. The shape memory effect (SME) refers to the ability of certain materials to deform at low temperature and then return to their original shape after heating to a higher temperature. They display the capacity to deform at a low temperature and then return to their original shape after heating to a higher temperature. Thus behaviour is illustrated in Figure 3.199. The initial straight form is deformed inelastically at room temperature to the triangular form. When the temperature is raised, the triangular form shifts back to the straight form and remains in that form when the temperature is lowered to room temperature. In the lack of any externally applied force, the transformation from austenite to martensite is during any subsequent thermal cycling invariant to shape change. This memory effect is caused by a phase transformation from martensite at room temperature to austenite at elevated temperature (F. Ansari & Leung 1997).

Inelastic deformation introduced during the martensite phase is eliminated when the state passes over to the austenite phase. The phase transitions without applied stress are illustrated in Figure 3.200. A_s and A_f define the temperatures for the start and finish of the transition from martensite to austenite for the case when the material is being heated; the corresponding temperatures for the cooling case are M_s and M_f . When T is greater than A_f , the phase is austenite but it is possible to change it back to martensite by applying stress. The magnitude M_d is the temperature beyond which austenite cannot be transformed to martensite by stress (i.e., the phase remains austenite for arbitrary applied stress).

Above the transition temperature, shape memory alloys show an exceptional elasticity. Like classically elastic materials, a load will cause a shape deformation that disappears during unloading. The difference is that shape memory alloys may be reversibly elongated or compressed five to ten times the amount of conventional materials, as illustrated in Figure 3.201. The restoring force is nearly independent of the strain. The upper straight line of the superelastic curve corresponds to the formation of stress induced martensite (SIM) while the lower straight line represents the reversion of SIM when the stress is reduced (F. Ansari & Leung 1997).

The stress-strain behaviour is strongly reliant on temperature. Figure 3.202 shows the limiting stress-strain curve for Nitinol, a nickel-titanium alloy.

The last category of the shape memory effect is the two-way effect, illustrated in Figure 3.28. The piece of wire deformed below M_f straightens itself when heated to above A_f . But, on being cooled down to below M_f , the wire changes back to its deformed shape. The wire straightens up on reheating and resumes its deformed shape on cooling. This behaviour repeats itself endlessly.

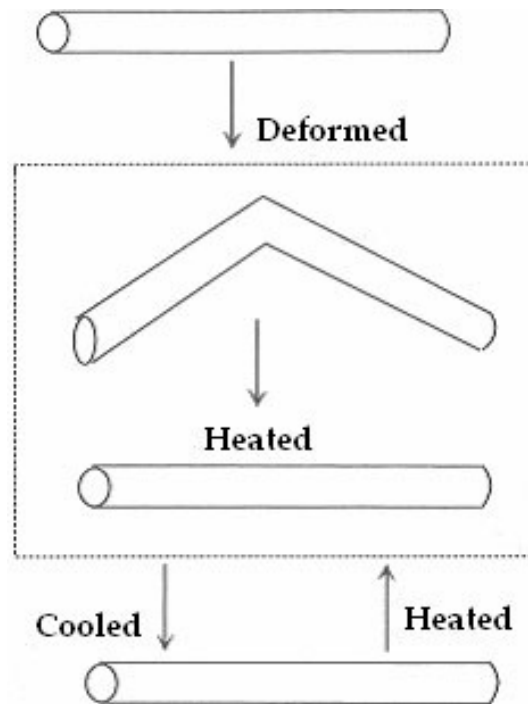


Figure 3.199: One-way shape memory behaviour. Image from (F. Ansari & Leung 1997)

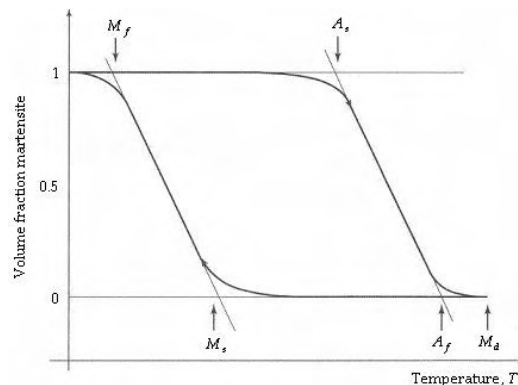


Figure 3.200: Martensitic transformation on cooling and heating. Image from (Connor 2003)

The realization of two-way behaviour implies thermo-mechanical treatment. This usually implicates several transformation cycles. This is achieved by cycling the material under the combination of stress and temperature.

The two-way shape memory behaviour gives the starting point for force actuation. If a trained shape memory alloy is restrained at low temperature in a way it cannot deform, a force is generated when the alloy is heated since it wants to return to its initial undeformed shape. The actuator does not need any additional (for instance electrical) power supplies, what increases the fail-safety.

Nitinol alloys in the form of small diameter wires (~ 0.4 mm) are used to assemble a force

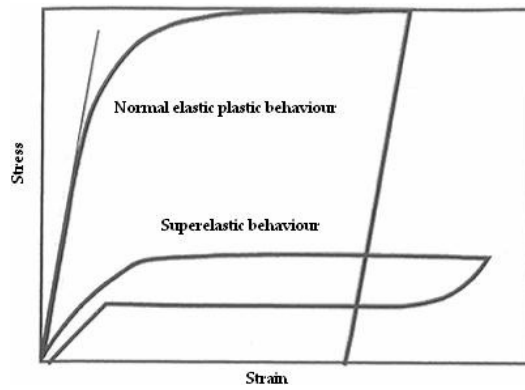


Figure 3.201: Schematic stress-strain diagram of superelastic behaviour of shape memory alloys. Image from (F. Ansari & Leung 1997)

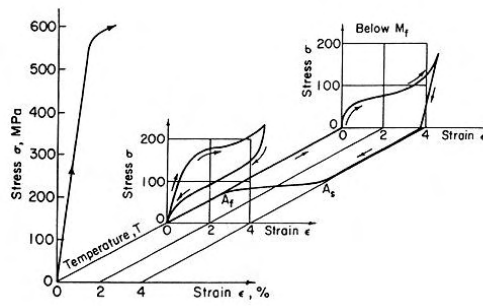


Figure 3.202: Effect of temperature on stress behaviour of Nitinol. Image from (F. Ansari & Leung 1997)

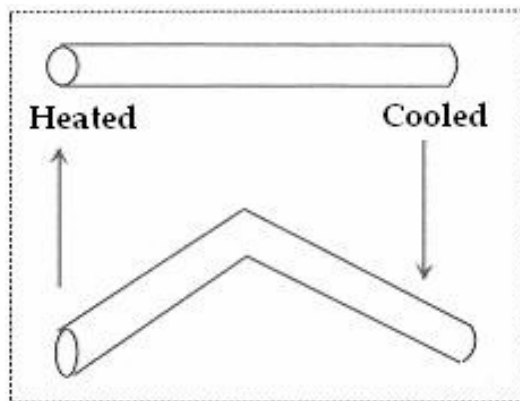


Figure 3.203: Two-way shape memory behaviour. Image from (F. Ansari & Leung 1997)

actuator. Heating is applied by passing an electric current through the wire. This process limits

the response time to seconds versus milliseconds for piezoelectric materials. Another restriction is the material cost; a usual price is in the order of €230/kg (Connor 2003). Most of the applications of shape memory actuators are for small-sized products thus requiring low capacity, and where cost and response time are not critical issues. Actuated civil structures like bridges and high-rise buildings with shape memory alloy prestressing tendons can be conceived but the required technology is still far too expensive (F. Ansari & Leung 1997). Another major topic is the issue of fatigue life. In order for these materials to gain acceptance in main stream civil engineering applications their fatigue performance has to improve considerable.

Controllable fluids Controllable fluids are categorized by their ability to change from a fluid to a semisolid in milliseconds when subjected to an electric or magnetic field. This effect was identified by Winslow in 1949. Two materials belonging to this category are electrorheological (ER) and magnetorheological (MR) fluids. In their initial state, they act as viscous fluids. Use of the (electric or magnetic) field introduces an additional plastic solid type behaviour mode, and the response is now a combination of plastic and viscous actions (Janocha 1999).

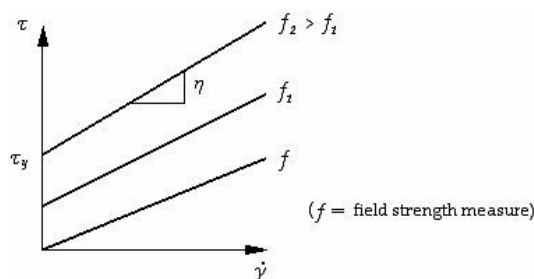


Figure 3.204: Effect of electric and magnetic fields on stress-strain relationship. Image from (Connor 2003)

Figure 3.204 illustrates this transformation for the situation when the material is idealized as a Bingham solid, which is defined as an ideal plastic solid in parallel with a linear viscous fluid.

The stress-strain relation for a Bingham solid subjected to shear deformation has the form

$$\tau = \tau_y \sin(\dot{\gamma}) + \eta \dot{\gamma} \quad (3.41)$$

where τ_y symbolizes the yield stress and η is the viscosity.

Experimental results show that the yield stress increases considerably when the field strength, f , augments to a limiting value τ_{max} . However, the viscosity is essentially constant. Therefore, it is reasonable to take η equal to a constant, η_0 , and consider the material behaviour as a combination of variable Coulomb hysteric damping and constant linear viscous damping. The equivalent linear material viscosity, η_{eq} , is reliant on the amplitude and frequency of the shear deformation. For the case of periodic excitation, η_{eq} , is given by

$$\eta_{eq} = \eta_0 + \frac{4\tau_y}{\pi\Omega\hat{\gamma}} \quad (3.42)$$

where $\hat{\gamma}$ is the strain shear amplitude and Ω is the excitation frequency. Devices containing controllable fluids can be used either as variable dampers or as semiactive force actuators. Figure 3.205 shows a schematic view of a prototype developed by the Lord Corporation. The main cylinder accommodates the piston, the MR fluid, and the magnetic circuit. A small electro-magnet is embedded in the piston head and supplied with current that generates the magnetic

circuit. A small electromagnet is entrenched in the piston head and supplied with current that generates the magnetic field across the annular orifice. Typical small-scale versions have a force capacity of about 3 kN, a millisecond response, and draw about 10 watts of power (Connor 2003).

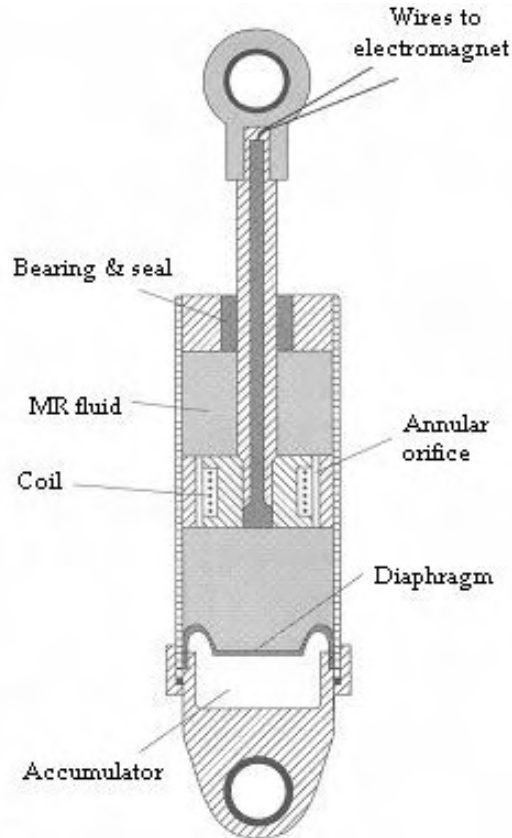


Figure 3.205: Damper. Image by (Janocha 1999)

Experimental results for quasi-static loading applied to the small scale version are plotted in Figure 3.206. These results show that the Bingham solid idealization is an acceptable approximation for the actual behaviour, and also that the plastic yield force is restricted by saturation of the fluid. For this device, saturation arises around 1.5 amps. When utilized as a force actuator, the amperage is attuned such that, for the observed value of velocity, the desired force magnitude is created.

A controllable fluid-type device is more operational than a variable orifice damper since the yield force is the primary component, and this force is independent of velocity. The low external power requirements, rapid response, and the potential for large capacity are attractive features. With further development, MR-based actuators should be applicable solutions for large-scale civil structures.

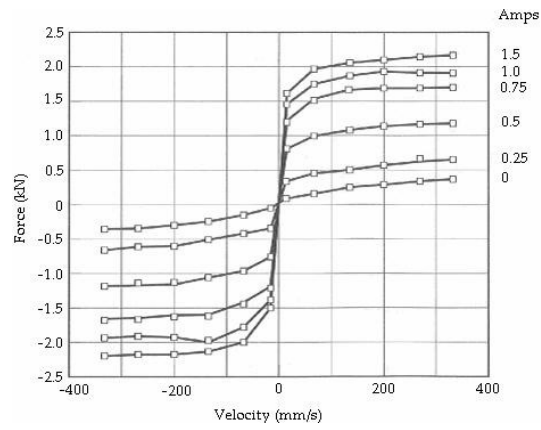


Figure 3.206: Quasi-steady force response for Rheonetics SD-1000-2MR damper. Image from (Connor 2003)

Advanced computation for Structural Design

4

Contents

4.1 Theory	292
4.1.1 Special structures	292
4.1.2 Opportunities and challenges	292
4.1.3 The structural design process	292
4.1.4 Fundamental problems between computation and the structural design process	293
4.2 Form description and generation	294
4.3 Descriptive techniques	294
4.3.1 Descriptive computational techniques	294
4.4 Generative Techniques	296
4.4.1 Generation techniques	296
4.4.2 Mesh techniques	296
4.5 Form finding	324
4.5.1 Minimal surfaces	324
4.5.2 Force density method	325
4.5.3 Dynamic relaxation	327
4.5.4 Shape form finding	330
4.5.5 Other form finding methods	330
4.6 Structural optimisation	331
4.6.1 Theory of optimisation	331
4.6.2 Classification of optimisation problems	334
4.6.3 Size optimisation	339
4.6.4 Classical optimisation methods	342
4.6.5 Genetic algorithms	346
4.6.6 Simulated annealing	351
4.6.7 Swarm behaviour and ant colony optimisation	352
4.6.8 Michell structures	358
4.6.9 Theory of Michell structures	362

RECOMMENDED STUDY MATERIAL

Title	Author	Year
Handbook for Grid Generation	Joe F. Thompson	1999
Numerical Recipes in C++	William H. Press, et al.	2001
An introduction to genetic algorithms	M. Mitchell	1996

4.1 Theory

Computational techniques are essential in the modern design of special structures, mainly because the advanced geometry of these structures make the design labourious to perform by hand. Computational tools can be used to define, describe, generate, calculate, produce, etc. these structures. It can even be said that currently it is almost impossible to perform any serious design step in an efficient manner without computation. However, still many difficulties with computation in the structural design of special structures (and in structural design in general) exist.

This chapter will cover the techniques, problems, challenges, opportunities, etc. for the computation of special structures, aimed on the structural design. Students will get insight in what is available in the world, what the problems and challenges are to solve in the near future and what the future might bring for the structural engineer.

4.1.1 Special structures

The structural design of special structures is specialistic work, often involving complex mathematics for geometry and complex structural behaviour. The techniques related to this are often not known to every engineer. Therefore, also the computation for special structures is complex, but also on a niche level, often consisting of custom-build tools. Special structures often involve advanced geometry, such as double-curvature and advanced definition methods. The mathematics of some of these techniques have been discussed in Chapter 2. Often these shapes will have to be segmented to create some kind of rationality to engineer, produce and assemble these structures.

4.1.2 Opportunities and challenges

One of the biggest challenges for the future of structural design is to create integral buildings, or as Ove Arup (the founder of the engineering firm Arup who did many special structures) called it, Total Architecture, which takes into account many aspects, such as architecture, structure, construction, production, installations, assembly, etc. etc. The related computational challenge is to create software tools which are also integral. Not only because they consider many aspects, but also because they are integrated because they can communicate with each other.

Another big challenge is to include more automation in the design process, for instance in the form of automated optimisation. This chapter will cover some techniques which currently can be used in some special cases.

4.1.3 The structural design process

It is important to understand the structural design process to understand some of the fundamental problems of computation in the structural design process. The structural design process is a complex process, which involves a lot of playing, varying and exploration by the engineer. This requires a high level of insight and craftsmanship. The design process is unique to any building, any design team and any engineer. This individuality of the design process is hard to capture in computation. The design process is also fast, with an evolutionary, cyclic, iterative nature, requiring good indications early in the design process when the important decisions are being made. Many disciplines are involved in the design, so it is a multi-disciplinary process and a team effort. Many aspects are being considered during the design process which the engineer needs to weight to an appropriate solution. A lot of the information involves implicit information, inside the head of the engineer, assumptions, codes, etc. while computation often requires very explicit information. Another important characteristic of the design process is that it involves a transition from a crude level to a finer, detailed level of information.

4.1.4 Fundamental problems between computation and the structural design process

Several fundamental problems can be found between computation and the structural design process, which leads to less use of computation than would be possible, purely on a technological level. This list does not attempt to be complete, but to give an idea what needs to be solved in the future to get to a situation where computation can be used in a more efficient manner in the structural design process.

- *Confidence*
The engineer currently often lacks confidence in the techniques which are used in computation. Confidence is important for the engineer, because he is primarily responsible for his design. Failure or collapse of a structure is a situation which he would like to avoid. Therefore, if he can eliminate some of the risk by using the methods he has insight in and can control, he will do this. This is one of the biggest problems in computation for structural design.
- *Insight*
The problem of the lack of insight in the used methods is often referred to as the 'black box' problem, because the engineer does not know what happens in the black box between input and output.
- *Control*
Next to the lack of insight, is also the lack of control a big issue for the use of computation in the structural design process. Engineers often do not know how to control advanced methods in a proper way, because every method, technique or application comes with their own knowledge, interface, etc.
- *Reusability*
A problem of computation is that while it often aims on reusability, still many applications, especially specialistic ones like the ones for special structures, are not very reusable.
- *The analysis versus design paradox*
An important issue is the analysis versus design paradox. Much software exists for analysis. However, this software can hardly be used for design work, since design in essence is another process than analysis and code checking. Hardly any software exists for design purposes, following the principles of the structural design process as discussed above.
- *The Swiss-army-knife versus the scalpel paradox* Chris Williams, lecturer of the University of Bath and engineer at Buro Happold, spoke about this paradox for software. Much software is able to do many things, like a Swiss-army-knife, but you would not want to operate a patient with it. While a scalpel makes very precise cuts, but is only fit for one specific purpose. The same currently still applies to software tools for structural design.
- *Software engineering*
Software engineering is often underestimated by structural engineers. These days building serious software applications requires control over high-level programming languages, knowledge of abstract frameworks, development environments (IDE's), testing tools, deployment tools, versioning tools, continuous building tools, etc. etc. Software engineering has become a discipline on its own and to build robust software a team of people is required to create this software. However, this does not mean that engineers are unable to build their own tools, since the level of adaptability has shifted from a programming level towards the user level by technologies, such as parametric associative design, scripting languages, etc.

- *Adaptation and customisation*

Because tools requires flexibility and individuality of the process, object and engineer, these tools need to be adaptable and customisable. However, currently very little software for structural design and engineering purposes is up to this task.

- *Interactivity and software integration*

Interactivity is a very important aspect for software for structural design, not only interactivity with the engineer and the design team, but also between software applications. The latter is often called 'software integration' or 'interoperability'.

4.2 Form description and generation

An important part in the design of building with special design is the description and generation of the buildings as computer models, often because of their complex geometrical nature and behaviour. Often these buildings consist of complex relationships in the geometrical design of the building. An essential step to design, produce, assemble or construct these building is to provide a unique geometrical description for the geometry and topology. As stated, since computation is essential for an efficient design process it is also essential to produce these computer models which relative ease. Since often the computer applications are complex, inaccessible and do not provide much inside in their behaviour, this is not an easy task.

One of the key differences between a regular design process of a rectangular building and a special structure is the step of the form description and generation which comes as an additional step within the design. As will become clear by reading this section often even most of the problems and liberations come from this techniques.

This section provides an insight and overview in the methods used to describe and generate form for special structures. It needs to be noted that these techniques can be used for regular buildings and structures as well. More complex techniques for generation of building, Form Finding and Structural Optimisation will be covered in Section 4.5. A close relation exists with Section 4.6 on geometry and mathematics.

4.3 Descriptive techniques

4.3.1 Descriptive computational techniques

Description of structures is an important aspect of the design of special structures. Many of the mathematical techniques have already been covered in Chapter 2. Purpose of the description of structures is providing an unique 'standard' for drafting, communication, setting out on site, etc. It is important for the coordination between all the disciplines in the design process, structural, architectural, building services, etc. Also for the analysis of the structure it is important to have a rigid and accurate definition of the geometry of the structure in the required format by the analysis tools. Some other purposes include the production, construction and visualisation of the design. Visualisation is often important for the presentation of the design to non-professional parties in the process. Computation for construction is often referred to as Virtual Construction, 4D, 5D, xD or nD modelling. These techniques aim on integrating a geometrical definition with databases of scheduling, cost, etc. However, for now mainly will be aimed on the geometrical techniques of description.

4.3.1.1 Description

Various things can be described by the various techniques. On a high level a subdivision can be made in the geometry (position, measurements) and topology (relationships) of the objects.

Another subdivision can be made in the description of the object or the description of the process, such as a generation, finding or optimisation process. Also here the distinction between continuous and discrete description exists.

Methods There are different methods of description. There are too many to mention, a few important ones include:

- **Mathematical description:** Mathematical description has already been covered in Chapter 2. Note that this form of description can be combined with other descriptive techniques, or even that often it is necessary to combine these techniques.
- **Physical:** Physical modelling techniques can be used for the description of objects (and processes). However, these can not directly be used in the computer.
- **Parametric design:** A parametric description derives the geometry (and sometimes topology) from parameters which can be manipulated by the user. Often this technique is only available for the generation of geometry.
- **Parametric associative or relational design:** In parametric associative design not only the parameters can be manipulated by the user, but also the relationships. Often this technique is only available for the generation of geometry.
- **Constraint solving:** In constraint solving only the constraints are defined and the computer 'solves' the geometry. Note that also this method is often only applicable to geometry.
- **Object-oriented design:** In this method objects are described with a state and a behaviour, rather than only geometry data, such as the variables for points (xyz) and lines (begin and end point numbers).
- **Scripting and programming:** Scripting and programming can be used to describe and (often) generate the geometry and topology of objects (and structures).

Objects Different objects can be used in the description:

- Points (or point clouds)
- Vectors, lines or curves, such as NURBS
- Planes or surfaces
- Grids and meshes
- Volumes, both regular and irregular
- Volumetric grids and meshes
- Higher dimensional objects

Objects: A computational data structure with a state and a behaviour. Also called Components or Features. These are used in Object-oriented programming (OOP).

Relationships: both mathematical and non-mathematical

Process: description, generation, finding or optimisation process

4.4 Generative Techniques

4.4.1 Generation techniques

Generation techniques are used to generate a structure from a set of parametric objects or a parametric dataset. Generation is a very powerful technique, because by controlling a small amount of parameters a large amount of data elements can be generated, even an entire building design with all related computational models. While this in theory only requires 'programmers sweat', generation for structural design is very hard to control by the engineer and several problems arise in the application of generation, such as the inability to 'solve back' variables, modify the generation process in an efficient way, etc.

Different generation techniques exist, of which parametric design, parametric associative design and mesh techniques are the most well known. Often, for free-form structures the engineer needs to describe a surface, with techniques, such as NURBS (Section 2.1.3), mesh this to a grid for various purposes, such as structural analysis, etc. and populate this mesh with an amount of (structural) elements. Also a different approach can be chosen where the engineer describes a generation of the structural elements and modifies the parameters of this generation in such a way that the final shape approaches the intended design.

While generation is often only used by specialists, able to write generative software or able to handle parametric associative modelling software, the basics of generation can already be applied with simple tools such as Excel.

4.4.2 Mesh techniques

Many software programs of grid generation techniques have been developed and still are under development. Grid generation is used in the field of computer fluid dynamics, EMAG, thermal and the environmental discipline in any dimension (surface, volume, etc.).

These software programs for structured, unstructured and variational grids have all in common the objective to generate an accurate grid over a complex surface, resulting in flat triangles or quadrangulans. The grid that we need to segment a shell surface must generate double curved elements and not flat elements. Thus, can be postulated that, especially, the node locations in relation to a certain accuracy of the grid, are of importance for the grid generation on the concrete shells. Double curved elements with least curvature follow from these node locations on the surface.

Figure 4.1 sketches the different node locations generated by a grid, with differing accuracy and element size.

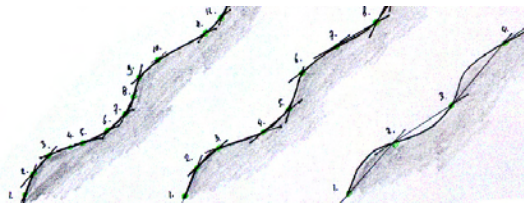


Figure 4.1: Grid with varying accuracy (and element size) on a certain surface.

The section about the type of grids and their grid generation techniques is divided in three parts. First the Structured Grids, following by the Unstructured Grids and subsequently the Variational Grids.

For the grid generation techniques, the shell is assumed to have no thickness.

4.4.2.1 Structured grids

Structured grids are grids where in the most general sense the local organization of the grid points and the form of the grid cells do not depend on their position but are defined by a general rule.

Structured grids are in structural engineering the most utilized grid, e.g. in Nervis shells. The main reasons are the simplicity to generate the grid because these follow often from the design of the shape and the predictable and regular shape of the elements.

The second reason is the easiness to adapt the mesh size, element size and element organization. Two techniques are often used in the practice, the Block-Structured Grids and Structured Grid by Analytical Approach. Boundary-Conforming Structured Grids is a third method, often used in other engineering disciplines. This method is suitable to generate grids over simple surfaces.

The method of these three grid generation techniques, the field of use and the results are considered in the following sections.

Boundary-Conforming Structured Grids

Method An efficient structured grid is one whose generation relies on a mapping concept. The idea is to choose a computational domain Ξ^n with a simpler geometry than that of the physical shell shape X^n and then to find a transformation $x(\xi)$ between these domains which eliminates the need for a non-uniform mesh when approximating the physical quantities (Haas 1962)

The corners of the element polygons are formed by the intersection of the coordinate lines, while the boundary of N^x is composed of a finite number of line-curves $\xi^i = \xi_0^i$. Consequently, in this case the computation region Ξ^n is a rectangular domain, the boundaries in R^n and the uniform grid in Ξ^n is the Cartesian grid. Thus the physical region is represented as a deformation of a rectangular domain and the generated grid as a deformed lattice. See Figure 4.2.

In practice there will be a trade-off between the difficulty of finding the transformation and the number of uniformly spaced points required to find the solution to a given accuracy and element size.

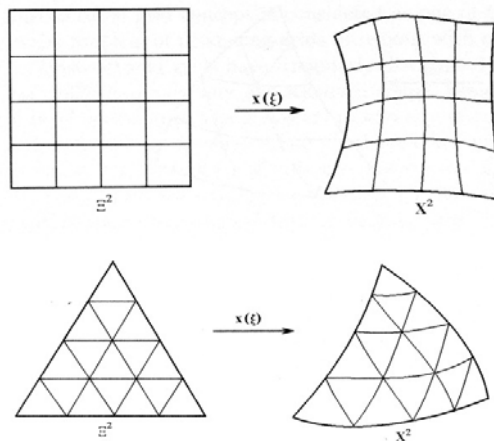


Figure 4.2: Boundary-conforming quadrangular & triangular grid.

Result A boundary-fitted coordinate grid in the region X^n is commonly generated first on the boundary of X^n and then successively extended from the boundary to the interior of X^n . This process is analogous to the interpolation of a function from a boundary or to the solution of a differential boundary value problem. On this base there have been developed three basic groups of methods of grid generation with the mapping approach;

- Algebraic methods, which use various forms of interpolation or special functions
- Differential methods, based mainly on the solution of elliptic, parabolic and hyperbolic equations in a selected transformed region
- Variational methods, based on optimisation of grid quality properties

For more information about these three methods, refer to the book *Grid Generation Methods*, by Vladimir Liseikin (Liseikin 1999).

In practice, the structured grid generated by mapping approach is today not in this form in use. This is because of the difficulty to find one transformation factor $x(\xi)$, to generate a grid over a complex 3D shape of the designed structure. For geometrical defined surfaces, the transformation factor can be found-

Block-Structured Grids Joe F. Thomson, Bharat K. Soni and Nigel P. Weatherill explain in the *Handbook of Grid Generation* (Thomson & et al. 1999) the block-structured grid as a sponge analogy. The best way to visualize the correspondence of a curvilinear grid in the physical field with a logically rectangular grid in the computational field is through the sponge analogy.

Method Consider a rectangular sponge within which an equally spaced Cartesian grid has been drawn. Now wrap the sponge around a circular cylinder and connect the two ends of the sponge together. Clearly the original Cartesian grid in the sponge now has become a curvilinear grid fitted to the cylinder. But the rectangular logical form of the grid lattice is still preserved and a programmer could still operate in the logically un-deformed sponge in constructing the loop and the difference expressions, simply having been given different equations to program. (Maeder & et al. 2004)

It is not hard to see, however, that for some boundary shapes the sponge may have to be so greatly deformed that the curvilinear grid will be so highly skewed and twisted that it is not usable in a numerical solution. The solution to this problem is to use not one, but rather a group of sponges to fill the physical field. Each sponge has its own logically rectangular grid that deforms to a curvilinear grid when the sponge is put in place in the field. The coordinate lines, defining the grid nodes of two adjacent blocks can join smoothly or non-smoothly (Figure 4.3). If the coordinates do not join smoothly, which is more efficient for load transferring and element connection, then during calculation, the solution values at the nodes of one block must be transferred to those of the adjacent block in the neighbouring of their intersection. This is achieved by interpolation.

Results Such a sponge could just as well be around a cylinder of noncircular cross section, regardless of the cross-sectional shape. To carry the analogy further, the sponge could, in principle, be wrapped around any shape, or could be expanded and compressed to fill any region (geometrical defined, free-form or form-finding shape), again producing a curvilinear grid filling the region and having the same correspondence to a logically rectangular grid.

This kind of grid generation is not only suitable for developable surfaces, but also for non-developable surfaces as the sponge can be stretched and squeezed. As a result at certain parts, a nice smooth grid will be generated; however strangely stretched and deformed elements on the

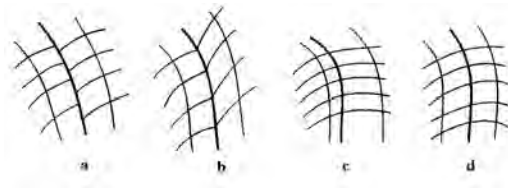


Figure 4.3: Types of interface between contiguous blocks; (a) discontinuous, (b & c) nonsmooth, (d) smooth. Image source:

surfaces will also unavoidably be generated.

The method could be utilized to generate a grid over all types of morphologies, including geometrical defined, free-form and form-finding shapes. The organization of the grid is, like all structured grids, logical.

The roof of the Neckarsulm grid dome is constructed with this block-structured method. Hans Schober says (Farin 1999):

‘ The base grid of the structure is manufactured from a quadrangular mesh of slats, square if laid flat on the ground. This plane mesh can be formed in almost any shape by modifying the original 90 degrees mesh angle. The square becomes rhombi.’

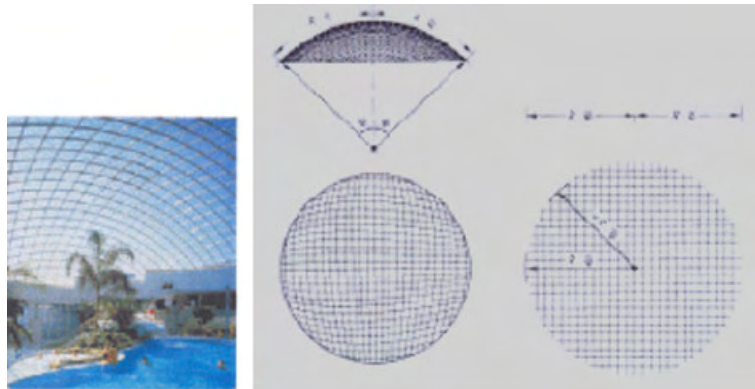


Figure 4.4: Neckarsulm grid dome (left), geometrical principle of the grid shell (middle) & a square mesh when laid out into a plane (right).

Translational Grid Configurations for flat or curved surfaces A number of basic grid patterns are illustrated in Figure 4.5. The two-way pattern, shown in (a), is the simplest pattern for a flat grid. It consists of two sets of line segments that run parallel to the boundary lines. The diagonal pattern, shown in (b), consists of two parallel sets of line segments that are disposed obliquely with respect to the boundary lines, forming quadrangulans. Figure 4.5 (c) to (f) show some basic three-way and four-way grid patterns. These grids form triangular elements (Hanisch 1996/1997). However, there are also many other grid patterns that are commonly used. These patterns are normally derived by removal of some elements from the basic patterns of the figure here above.

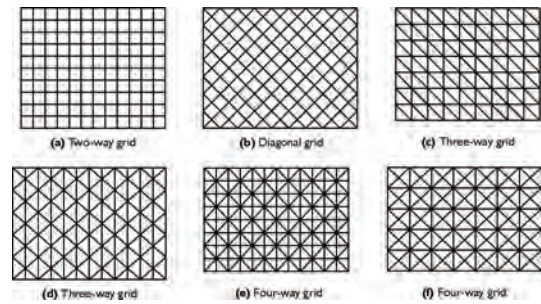


Figure 4.5: Six types of basic grid patterns. Image source:

The basic grid patterns of Figure 4.5 are frequently used in practice for complex (double) curved surfaces as geometrical defined, free-form and form-finding surfaces. The grids in the figure are composed by sliding one, two or three curves, the generatrix, over another curve, the directrix.

There can be two approaches perceived with this type of grid configuration. One method is the translational grids or directrix-generatrix grids. Second method is in fact an extension on the block-structured grid (Section 4.4.2.1).

Translational Grids The translational surfaces allow a vast amount of shapes for grid shells consisting of quadrangular planar mesh. Translating any spatial curve -one are more- (generatrix) against another random spatial curve (directrix) will create a spatial surface consisting solely of planar quadrangular mesh, as indicated in Figure 4.6 and Figure 4.7. Parallel vectors are the longitudinal and lateral edges of the surface. Subdividing the directrix and the generatrix equally results in a grid with constant length and planar mesh.

For the prefab elements generated by this methods this means that the elements have the same size (not the same shape) and the same weight. Varying by size is done by varying the generatrix distances, sliding over the directrix. This method is in particular suitable to generate a grid configuration for geometrical defined surfaces, generated by translation or ruling ‘Geometrical Defined Surfaces’ for the morphology.

A drawback of this method and the other structured grid methods- is that the translational generation of grids has no influence on and no optimisation tools to generate elements with low double-curvature (what is always easier to manufacture in a mould in concrete).

Specifically on this drawback, the unstructured grid techniques come in (Section 4.4.2.2).

The Hippo House at the Berlin Zoo (Figure 4.7), the Music Centre Gateshead and many more structures are designed by this method.

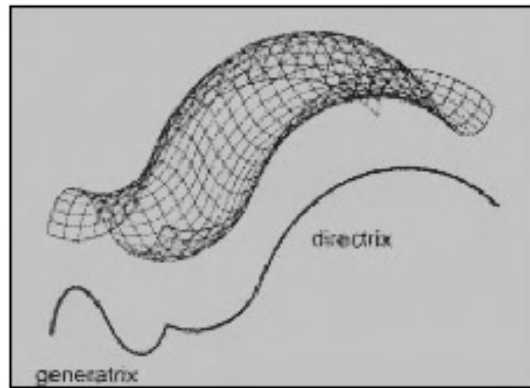


Figure 4.6: Translational surface, generated by two curves, directrix and generatrix.

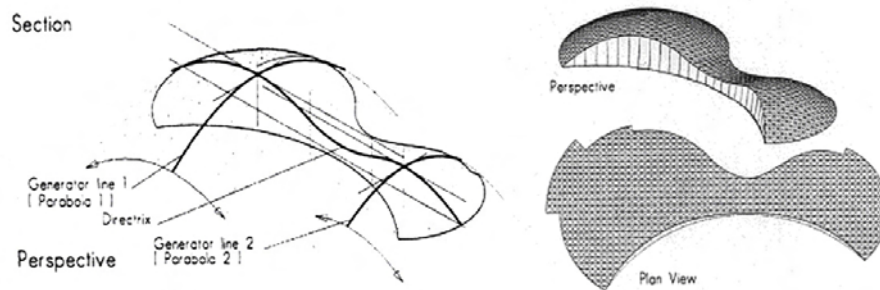
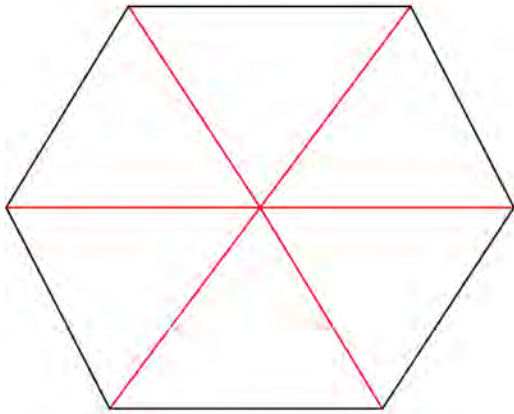


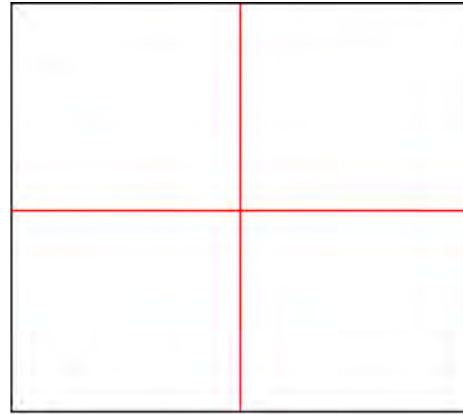
Figure 4.7: Translational surface generated by 1 directrix and 2 generatrixs, the Berlin Zoo Hippo House.

Quadrangular grid generation by Schlaich and Schober When describing free-form shapes with grids, usually triangular methods are chosen, since they can approximate any shape, always give planar surfaces (when the boundaries are straight lines) and can transfer the shell forces in an efficient manner. However, triangular shapes also have disadvantages. Schlaich Bergermann Partner (Schober 2003a, Schober 2002) has developed methods to create quadrangular grids which guarantee planar surfaces. Advantage of quadrangular grid is that they are more economic than triangular grids, because the glazing is only about half the cost and the joints are much easier to fabricate, since only four members come together, instead of six (see Figure 4.8). However, the quadrangular grids have to be braced by cables to transfer shell forces and extra in-plane stability (see Figure 4.9).

Both methods are based on the principle that two parallel vectors span a planar surface.



Six members come together for a triangular grid



Four members come together for a quadrangular grid

Figure 4.8: Joints for triangular and quadrangular grids.

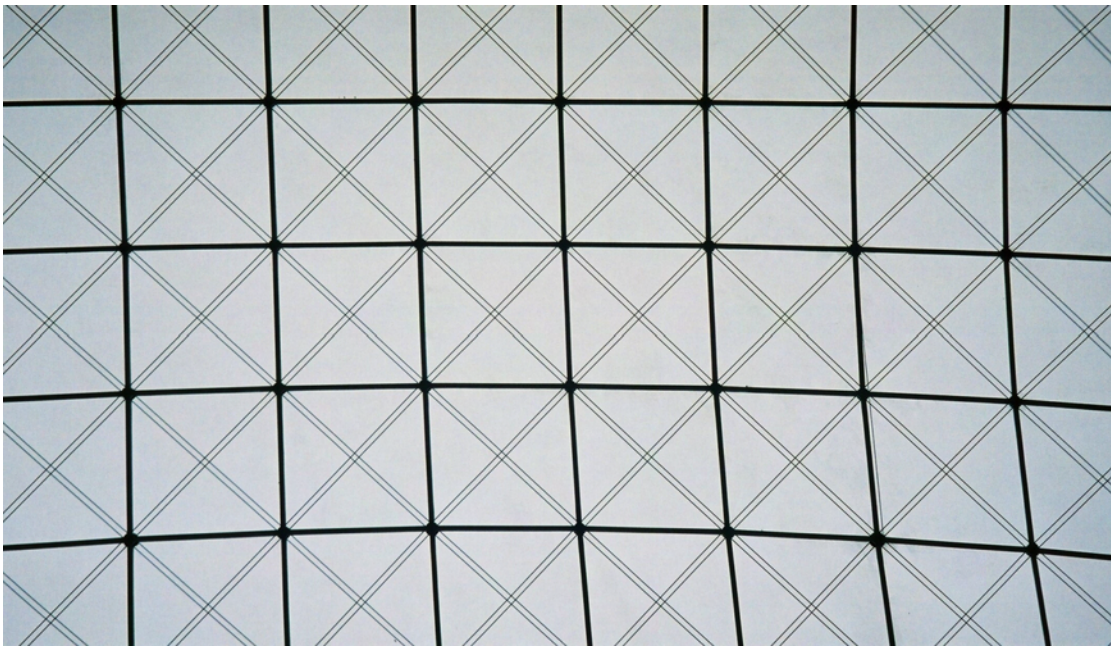


Figure 4.9: Close-up picture of the Bosch Area grid in Stuttgart by SBP.



Figure 4.10: Bosch Area grid in Stuttgart by SBP.

Translational surfaces Translational surfaces are based on the principle of translating sections (or a generatrix) along a describing curve, called the directrix (see Figure 4.11). Many shapes can be close approximated by this method.

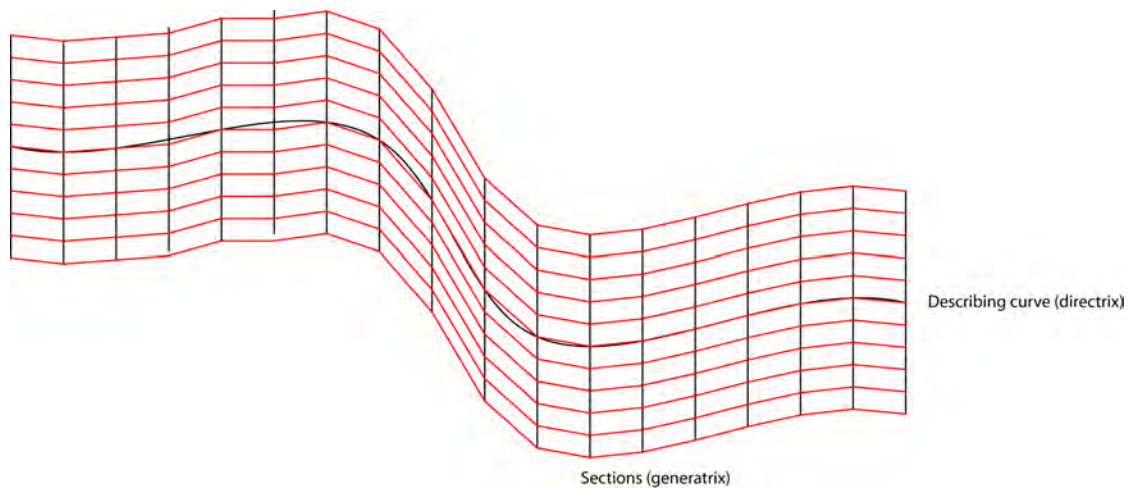


Figure 4.11: Translational Surfaces.

Scale-Trans surfaces Scale-Trans surfaces are based on the principle of scaling the generatrices and then translating the sections along the describing curve. This gives even more freedom of approximation than translational surfaces.

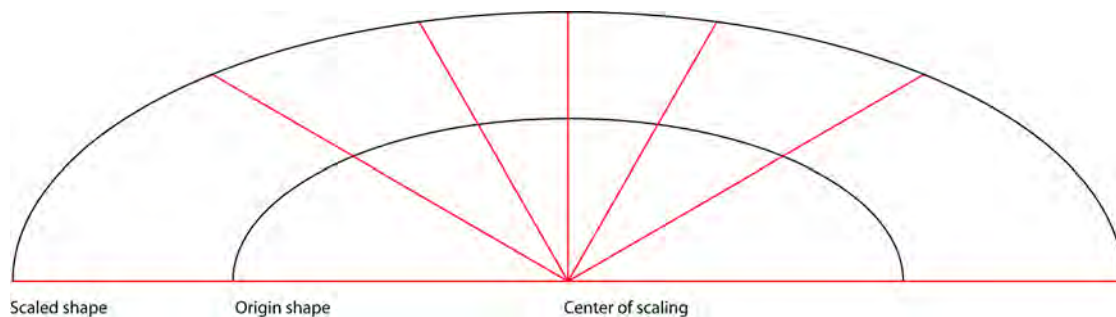


Figure 4.12: Scale-Trans Surfaces

Note that these methods can closely describe many surfaces, but that there are limits to the methods, such as highly curved parts in the directrix cannot be followed. Rotation will have to be added in that case, which does not always guarantee planar surfaces.

Extension to Block-Structured Grids The second approach is the one when the base grid of a structure is manufactured from a quadrangular mesh, square if laid flat on the ground. This approach is the same as the block-structured grid (Section 4.4.2.1). In fact, this method forms an extension to the block-structured grid, because with this technique the grid does not have to be the 90-degree rectangular grid when laying flat on the ground. The grid could be

diagonally, in two ways, three ways or four ways, as sketched in Figure 4.5. The diagonal pattern is utilized to segment the roof of the Orvieto airplane hangar.

Grid Configuration for Dome Shapes Figure 4.13, shows the grid configurations for a dome shape. Five types of grid generation could be distinguished: a Schwedler dome, a lamella dome, a diamatic dome, a grid dome and a geodesic dome (Vollers 2001). These grid configurations are suitable for all geometrical defined surfaces or parts of surfaces, generated by rotation.

A modified form of a ribbed dome (a) is obtained by bracing the quadrilateral panels of the dome. The result is a dome configuration that is referred to as a Schwedler dome. (Named after the nineteenth century German engineer J. W. Schwedler who built many domes of this kind) A simple example of a Schwedler dome is shown in (c) and (d). This dome configuration also involves trimming to avoid overcrowding of the elements at the upper part of the dome. A ribbed dome is generated by the rotation of a curve around an axis and by translation of a ring over the same axis.

An example of a lamella dome is shown in (e). A lamella dome has a diagonal pattern and may involve one or more rings. An example of a trimmed lamella dome with rings is shown in (f). The grid is composed by two curves rotating around an axis. The semi-cupola of the Turin exposition Hall and the Palazzetto dello Sport by Nervi are examples of a lamella dome.

The dome configurations shown in (g) and (h) are two examples of a family of domes that are referred to as diamatic domes. The dome shown in (g) is an example of a basic diamatic form consisting of triangulated sectors. The pattern of the diamatic dome of (h) is obtained from a denser version of the dome of (g) by removing every other line of elements.

The domes shown in (i) and (j) represent two examples of the family of grid domes. A grid dome is obtained by projecting a plane grid pattern, such as the grids in Figure 4.5, onto a curved surface.

A geodesic dome configuration is shown in (k). A dome of this kind is obtained by mapping patterns on the faces of a polyhedron and projecting the resulting configuration onto a curved surface. The dome of (k) is obtained by mapping a triangulated pattern on five neighbouring faces of icosahedrons (20-faced regular polyhedron) and projecting the result onto a sphere which is concentric with the icosahedrons. The geodesic dome of (l) is obtained in a similar manner with the initial pattern chosen such that the resulting dome has a honeycomb appearance.

For all these grid configurations of a dome it is not possible to point one out, that is better than the other. First, because the amount of repetitive elements is in relation to the amount of elements and shape of the structure. For all configurations apply that the elements in one ring (horizontally) contains the same shaped elements. Second, the total amount of elements segmenting the surface, can be varied by adjusting the mesh width, and so the curves distances, generating the mesh/surface. Third, because that the elements do not have to possess a certain shape; The radial grid configuration of the dome could also be used partially; the axis could lie outside the building, e.g. the Saint Maria Church in Storkow ¹ (Figure 4.14). The grid configuration is not only applicable to circular ground plans, but also to polygonal ground plans, e.g. the beams of the Noord Holland Pavilion are placed radial. See Figure 4.15. Of course, the elements do not possess the same shape and size all around the surface.

¹<http://www.sv.vt.edu/classes/> Access-date: 12-2005.

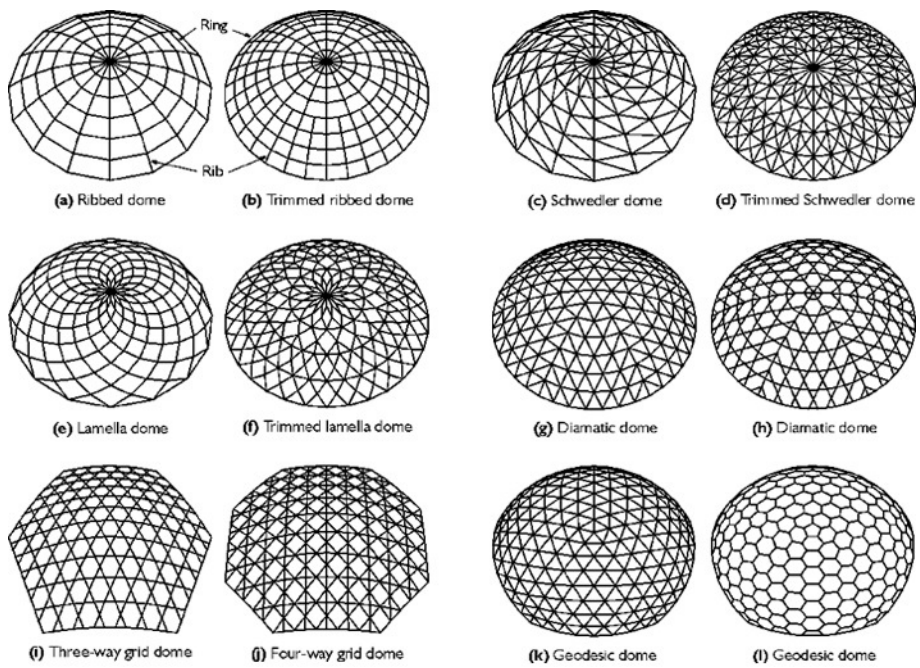


Figure 4.13: Grid configurations for dome shapes.

Isotope technique A grid generation technique that is derived from the techniques above is the isotope technique. With this method a shape is sliced in plural directions (one at least, two or three) by parallel curves, with a certain mutual distance (Rypl 2002). The quadrangular elements formed by these intersecting curves, are the final elements that should be fabricated in prefab concrete. The BMW pavilion Bubble, build for the IAA 99 in Frankfurt, is an example of a structure segmented in this way, in three directions. (Figure 4.16)

This method has not really any particular advantages; the method does not try to minimize the amount of different element shapes nor do the elements always have a good, optimal shape and size. This method however, is a suitable method to segment all types of morphologies with a structured and regularly organised grid.

Computer programs as Mathcad segment shapes by the isotope technique in two directions. The distance of the segmenting curves can be filled in as a parameter by hand in the program ². The node locations of the intersecting curves in space are given as x,y,z coordinates in space.

Other software programs able to generate structured grids are given in annexure, e.g. BUDMESH2D, ICEM CFD, Truegrid, VGM, i.e.

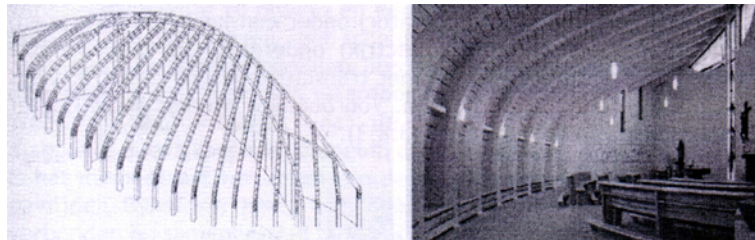


Figure 4.14: Radial grid, Storkow church.

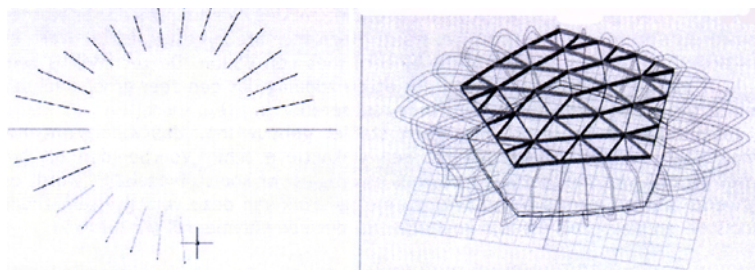


Figure 4.15: Radial grid of the 'Web Noord Holland.

²www.mathcad.com Access-date: 3-2006.

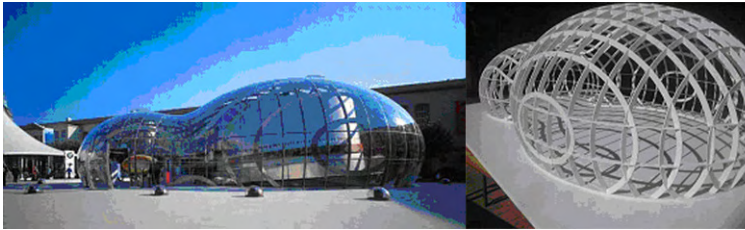


Figure 4.16: Isotope technique, BMW pavilion.

4.4.2.2 Unstructured Grids

Many free-form or form-finding designs involve complex regions that are not easily amenable to pure structured grids. Structured grids may lack the required flexibility and robustness for handling complex surfaces, or the grid cells may become too skewed or twisted. Therefore, the unstructured grid concept is considered as one of the appropriate solutions to the problem of producing grids in regions with complex shapes.

An unstructured grid has irregularly distributed nodes and their cells are not obliged to have a standard shape. Besides this, the connectivity of neighbouring grid cells is not subject to any restrictions. Thus, unstructured grids provide the most flexible tool for the description of a shapes geometry by a mesh. However, in practice, unstructured grids for architectural structures are not commonly used. It is even so that architects and engineers prefer to adapt the shape of the design in order to find a translational structured grid(Schober 2003b). If the structure will be executed in a steel lattice, this choice is understandable when considering the amount and costs of all differing joints to be fabricated. The grid generation techniques for unstructured grids fill in here as these techniques try to find, with certain accuracy, flat elements. But the elements we try to find could be double curved, but should be of least curvature. Thus, the grid generation techniques of unstructured grids help to find the elements with least double curvature, concerning a certain accuracy and element size.

There are today many techniques available, with all the research activity devoted to automatic grid generation, for the construction of unstructured grids. However, three approaches are widely used. They can be described as point insertion methods based on Delaunay triangulation, and Advancing Front Methods and tree-based methods, such as Octree approach. This section describes the methods.

Only the global idea, methods and results concerning the grid generation of complex shell surfaces, is described as this subject is too wide and complex to be fully described in this reader.

Delaunay Triangulation In general, the Delaunay approach connects neighbouring points, of some previously specified set of nodes in the region of the shell surface, to form tetrahedral cells in such a way that the circumsphere trough the four vertices of a tetrahedral cell does not contain any other point. (Figure 4.17) The following subsections discuss the three major techniques for generating triangles based on the Delaunay criterion; Voronoi Diagram, Edge Flipping Algorithm and Incremental Bowyer-Watson Algorithm.

Voronoi Diagram The Delaunay triangulation has a dual set of polygons referred to as the Voronoi Diagram or the Dirichlet Tessellation. The Voronoi Diagram can be constructed for a random set of points on the surface of a structure. Given a set of points in the plane, the idea is to assign to each point a region of influence in such a way that the regions decompose the surface of the structure. To describe a specific way to do that, let S element of R^2 be a set of n points and define the Voronoi region of p element of S as the set of points x element of R^2 that are at least as close to p as to any other point in S ; that is(Edelsbrunner 2001),

$$V_p = \{x \in R^2 \mid \|x - p\| \leq \|x - q\|, \forall q \in S\} \quad (4.1)$$

This definition is illustrated in Figure 4.18

The Delaunay triangulation is obtained by drawing each Delaunay edge from one endpoint straight to the midpoint of the shared Voronoi edge and then straight to the other endpoint. For each triangle formed in this way there is an associated vertex of the Voronoi diagram which is at the circum-centre of the three points which form the triangle. Thus each Delaunay

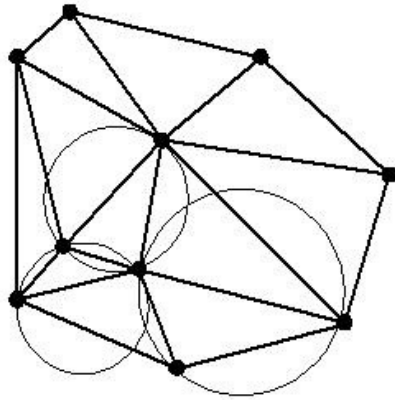


Figure 4.17: The circumcircle through 4 vertices does not contain any other point. Image source:

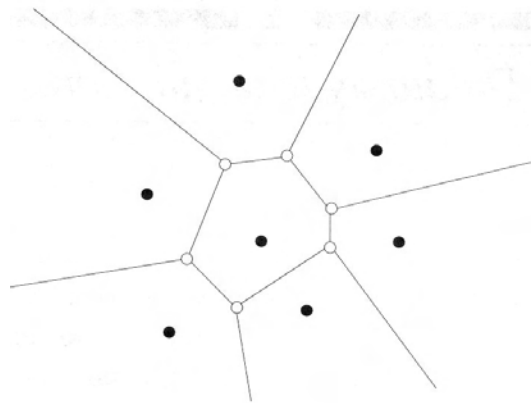


Figure 4.18: Seven points define the same number of Voronoi regions. One of the regions is bounded because the defining point is completely surrounded by the others.

triangle contains a unique vertex of the Voronoi diagram and no other vertex within the Voronoi structure lies within the circle centred at this vertex. Figure 4.19 depicts the Voronoi polygons and the associated Delaunay triangulation.

It is apparent from the definition of a Voronoi polygon that the degeneracy problems can arise in the triangulation procedure when

- Three points of a potential triangle lie on a straight line
- Four or more points are cyclic

These cases are readily eliminated by rejecting or slightly moving the point which causes the degeneracy from the original position.

More information about the ‘Circles and Power’ and ‘Acyclicity’ can be found in ‘Geometry and Topology for Mesh Generation’ written by Herbert Edelsbrunner(Edelsbrunner 2001).

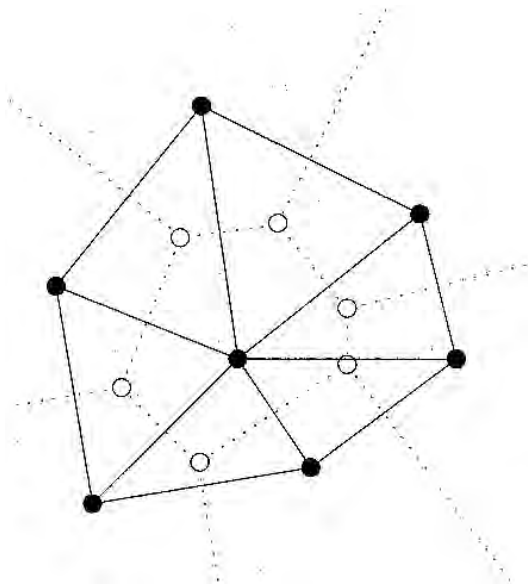


Figure 4.19: Voronoi edges are dotted and the dual Delaunay edges are solid. Image from (Edelsbrunner 2001)

Edge Flipping Algorithm The Edge Flipping Algorithm makes use of the equiangular property of the Delaunay-type triangulation, which states that the minimum angle of each triangle in the mesh, generated on the shell surface, is maximized (Liseikin 1999).

Assuming there is some triangulation of a given set of points, the swapping algorithm transforms it into a Delaunay triangulation by repeatedly swapping the positions of the edges in the mesh in accordance with the equiangular property. For this purpose, each pair of triangles which constitutes a convex quadrilateral is considered. This quadrilateral produces two of the required triangles when one takes the diagonal which maximizes the minimum of the six interior angles of the quadrilaterals, as shown in Figure 4.20. Each time an edge swap is performed, the triangulation becomes more equiangular. The end of the process results in the most equiangular triangulation.

This technique based on the Delaunay criterion re-triangulates a given triangulation in a unique way, such that the minimum angle of each triangle in the mesh is maximized. This has the advantage that the resulting meshes are optimal for the given point distribution, in that they do not usually contain many extremely skewed cells (Baker 1999).

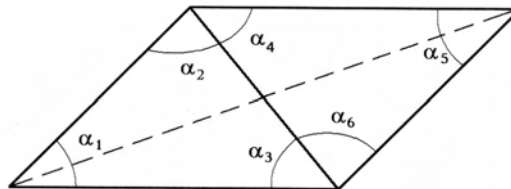


Figure 4.20: The triangulation which maximizes the minimum angle. The dashed line indicates a possible original triangulation.

Incremental Bowyer-Watson Algorithm The incremental technique, introduced by Bowyer and Watson in 1981 triangulates a set of points in accordance with the requirement that the circum-circle through the three vertices of a triangle does not contain any other point, such as mentioned in the previous subsection. The accomplishment of this technique starts from a Delaunay triangulation which is considered as an initial triangulation. The initial triangulation commonly consists of a square divided into two triangles which contains the given points. With this starting Delaunay triangulation, a new grid node is chosen from a given set of points or is found in accordance with some user-specified rule to supply new vertices. Check step (b) in Figure 4.21. In order to define the grid cells which contain this points as a vertex, all the cells whose circum-circles enclose the inserted points are identified and removed. The union of the removed cells forms the region which is referred to as the Delaunay or inserting cavity. A new triangulation is then formed by joining the new point to all boundary vertices of the inserting cavity created by the removal of the identified triangles step (c) in Figure 4.21(Liseikin 1999).

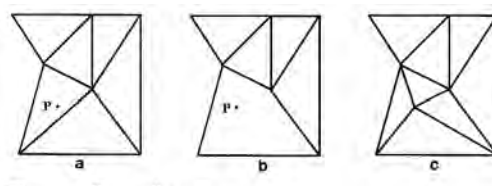


Figure 4.21: Stages of the planar incremental algorithm, three steps. Image from (Liseikin 1999)

Insertion of New Points The nature of the Boyer-Watson algorithm gives rise to a problem of choosing the position where to insert the new point in the existing mesh, because a poor point distribution can eventually lead to an unsatisfactory triangulation.

The new point should be chosen according to some suitable geometrical and physical solution. The geometrical criteria commonly consist in the requirement for the grid to be smooth and for the cell elements to be of a standard uniform shape and of the necessary size. The physical criterion commonly requires the grid cells to be concentrated in the zones of large solution variations. With respect to the geometrical criterion of generating uniform cells, the vertices and segments of the Dirichlet tessellation are promising locations for placing a new point since they represent a geometrical locus which falls, by construction, midway between the triangulation points.

Thus, in order to control the size and shape of the grid cells, there are commonly considered two different ways in which the new point is inserted. In the first, the new point is chosen at the vertex of the Voronoi polyhedron corresponding to the worst simplex. In the second way, the new point is inserted into a segment of the Voronoi polyhedron, in a position that guarantees the required size of the newly generated simplexes.

More information about point insertion strategies can be found in Chapter 11.3.6 in Grid Generation Methods written by Vladimir D. Liseikin(Liseikin 1999) and Chapter 16 in Handbook of Grid Generation written by Timothy J. Baker(Baker 1999)

Software Many computer programs are developed for Delaunay triangulation³. A full overview of meshing software can be found in annexure II of Grid Generation Software for Unstructured Grids, or on the internet; ⁴

³ <http://www.geom.uiuc.edu/software/cglist/ch.html> Access-date: 3-2006.

⁴<http://www.andrew.cmu.edu/user/sowen/softsurv.html> Access-date: 3-2006.

Some examples:

- ANSYS
- BAMG
- BL2D
- CADfix
- Geomagic Wrap
- Geopack90
- GMSH
- MEGA
- Mentat
- QHull

Of these programs, Ansys is the most common in use. On the internet site of Ansys the following can be found, considering the grid generation procedure:

'From automatic meshing to highly crafted mesh, ANSYS, Inc. provides the ultimate meshing solution. ANSYS provides powerful pre- and post-processing tools for mesh generation from any geometry source, to produce almost any element type, for nearly any physics, for virtually any application⁵.'

Other than Delaunay triangulation, Ansys is able to generate a triangular grid by the Advancing Front Technique and a quadrangular grid by Advancing Front Technique or Edge Sweeping Algorithm, Section 4.4.2.2. Except the structural calculation, other features of Ansys which improves the program utility for a good grid generation are the capability to adaptivity, refinement and mesh improvement.

Results The advantage of choosing an unstructured grid instead of a structured grid for the meshing of a complex surface is the geometric flexibility and suitability for adaptation inherent to the use of irregularly connected triangular elements. Herewith, the Delaunay triangulation is very popular in practical applications owing to the following optimality properties:

- Delaunay triangles are nearly equilateral
- The maximum angle is minimised
- The minimum angle is maximised(Liseikin 1999)

Figure 4.22 (left) shows how the Delaunay triangulation is derived from a convex 3D model by Qhull. Figure 4.22(right) represents a Delaunay triangulation executed with Ansys.

⁵<http://www.andrew.cmu.edu/user/sowen/softsurv.html> Access-date: 3-2006.

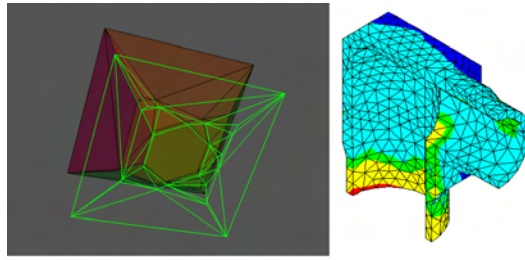


Figure 4.22: Delaunay triangulation with Qhull (left) with Ansys (right).

Advancing Front Technique A widely used algorithm for the design of FE meshes is based on the Advancing Front Method. The AFM was first published by Peraire et al (Peraire, Peiro & Morgan 1999). for the generation of meshes with triangular elements.

Method The generation problem consists of subdividing an arbitrarily complex domain into a consistent assembly of elements. The consistency of the generated mesh is guaranteed if the generated elements cover the entire domain and the intersection between elements occurs only on common points, sides or triangular faces. The final mesh is constructed in what may be defined as a bottom-up manner. This means that the process starts by discretizing each boundary curve in turn. Nodes are placed on the boundary curve components and then adjacent nodes are joined with straight line segments. In the later stages of the generation process, these segments will become sides of triangular faces. The length of these segments must therefore, be consistent with the desired local distribution of mesh size. This operation is repeated for each boundary curve in turn.

The next stage consists of generating planar faces. For each two-dimensional region or surface to be discretized, all the sides produced when discretizing its boundary curves are assembled into the so-called initial front. The relative orientation of the curve components with respect to the surface must be taken into account in order to give the correct orientation to the sides in the initial front. This front is used to generate a triangular mesh on the surface. The size and shape of the generated triangles must be consistent with the local desired size and shape (Farestam & Simpson 1994).

Daniel Ryppl (Ryppl 2002) describes the process of Advancing Front in eleven steps in a more mathematical manner, in an online document.

Figure 4.24 presents a flow chart for mesh generation using the Advancing Front Technique. Figure 4.23 demonstrates different stages during the triangulation process by the Advancing Front Technique.

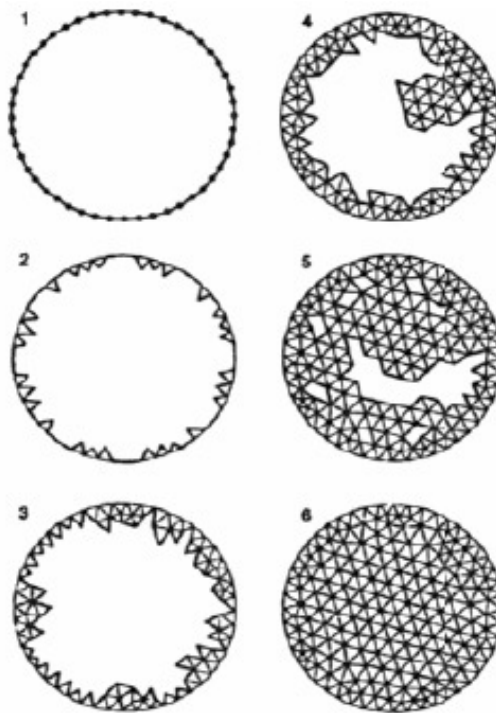


Figure 4.23: The Advancing Front Technique showing different stages during the triangulation process.

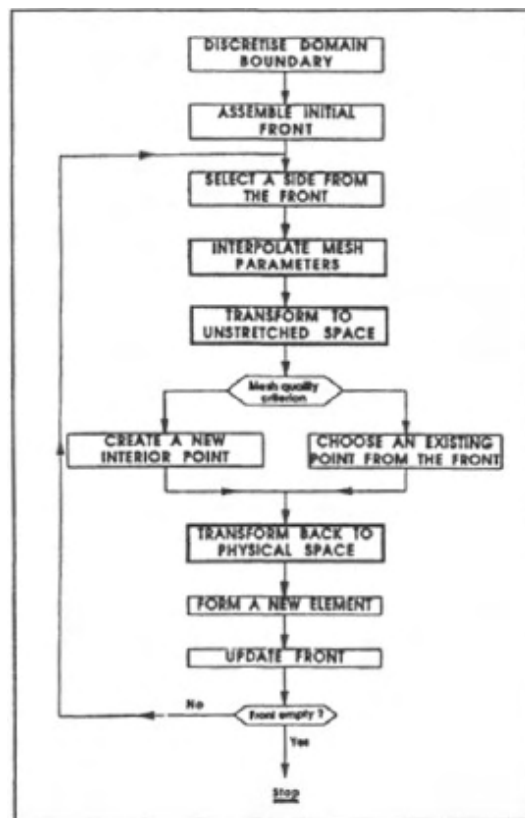


Figure 4.24: Flow chart of the Advancing Front Generation Technique.

Software Also for the advancing front technique, around 10 computer programs have been developed. Some programs are only used by a dozen of people; others are more common in use, such as ANSYS, for which is referred to Section 4.4.2.2.

Other programs used for structural discipline with the Advancing Front are ⁶:

- MeGA
- Mentat
- TMG

Figure 4.25 and Figure 4.26 are examples of the Advancing Front Grid Generation Technique with Ansys on a chair and a mechanical joint.



Figure 4.25: Model and mesh of a chair.

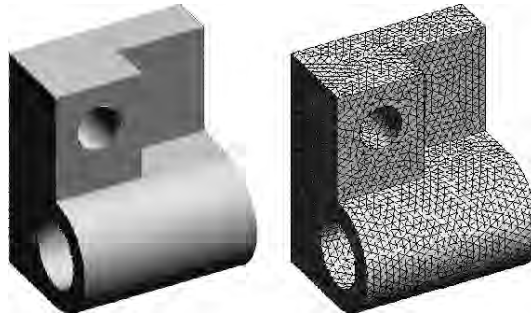


Figure 4.26: Model and mesh of a mechanical joint.

Results The basic disadvantage of this unstructured grid methodology lies in its incapability to handle multiple regions and multiple material domains. Also the deviation of the mesh from the original geometry together with a relatively large computational time is considered to be a drawback(Rypl 2002).

⁶<http://www.andrew.cmu.edu/user/sowen/softsurv.html> Access-date: 3-2006.

Same as Delaunay, easy parts of the surface are also generated by the Advancing Front Technique with result, that the grid of the surface becomes unnecessarily difficult and of different elements size and shape. This technique is suitable to be used for the complex surfaces in e.g. free-form or form-finding surfaces. Also, the elements with the lowest double curvature are found, just as with the Delaunay approach.

Octree approach

Method In the Octree approach the region of the shell is first covered by a regular Cartesian grid of cubic cells in 3D, or squares in 2D. Then the cubes containing segments of the domain surface are recursively subdivided in eight cubes until the desired resolution is reached. The cells intersecting the body surfaces are formed into irregular polygonal boundary cells, (Figure 4.27)

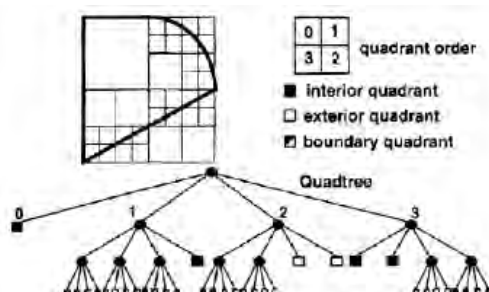


Figure 4.27: Example of the Octree approach.

The grid generated by this Octree approach is not considered as the final one, but serves to simplify the geometry of the final grid, which is commonly composed of tetrahedral cells built from the polygonal cells and the remaining cubes. (Liseikin 1999)

The process of meshing the boundary cell is a function of the level of geometric complexity supported by the mesh generator. In cases where there is only a limited amount of geometric complexity allowed per cell, simple templates are possible. When there is no specific limitation on the level of geometric complexity, the process of meshing the boundary octant requires all the functionality of an automatic mesh generator applied to the local region (Shephard 1999).

There are different approaches for the creation of elements in the boundary cells. The first two, create tetrahedral elements. The first of these approaches applies an element removal procedure starting from a basic cell level boundary representation. The second approach develops a Delaunay triangulation based on the mesh vertices of the cell level boundary representation, which is then followed by an algorithm that insures the resulting surface triangulation is topologically compatible and geometrically similar. Since the first two procedures operate strictly accounting for the intersections of the model and cell boundary entities, they are vulnerable to the small, poorly shaped elements caused by boundary cells touching the model boundary.

The third procedure creates tetrahedral elements from a given surface triangulation using an element removal procedure. The last boundary cell meshing procedure considers the creation of hexahedral elements to fill the region between the interior cell and the model boundary. These two procedures create the elements in the regions between the model boundary and interior cells without strict adherence to the boundary of the cell. Therefore, they are not susceptible to the

creation of poorly shaped elements caused by the boundary cells touching the model boundary.

Software Not too many software programs for Octree grid generation in the structural discipline have been developed. The most common in use is ICEM CFD:

ICEM CFD Engineering, a subsidiary of ANSYS, Inc., develops and markets software for pre- and post-processing of engineering applications such as computational fluid dynamics and structural analysis. Our major products include ICEM CFD, the leading software for 3-D grid generation for CFD and other engineering applications.

Our Direct CAD Interfaces link the parametric geometry creation tools available in CADD5, CATIA, ICEM Surf, Pro/ENGINEER, SDRC I-DEAS, SolidWorks, and Unigraphics to the grid generation, post-processing, and grid optimisation tools of ICEM CFD. We work closely with these CAD/CAM vendors to ensure that our Direct CAD Interfaces remain current.

The grid generation tools of ICEM CFD offer the capability to create grids from geometry in multi-block structured, unstructured hexahedral, tetrahedral, hybrid grids consisting of hexahedral, tetrahedral, pyramidal and prismatic cells, as well as Cartesian grid formats combined with boundary conditions.

The state of the art CFD post-processing and visualization tool, ICEM CFD Visual3, supports solutions in structured, unstructured, steady state, or transient data and contains powerful features while providing an open scripting system for easy customization.⁷

Results The computer program is relatively easy to use; the user brings the CAD surfaces or STL data that describe the space to be meshed into ICEM CFD Hexa. Then, Hexa automatically generates a global block around the CAD design. By subdividing this block into smaller blocks and assigning different materials the user can cut out the desired shape. To reflect the characteristic features of the geometry to be meshed, the block structure can be interactively adjusted to the underlying CAD geometry (Shaw 1999).

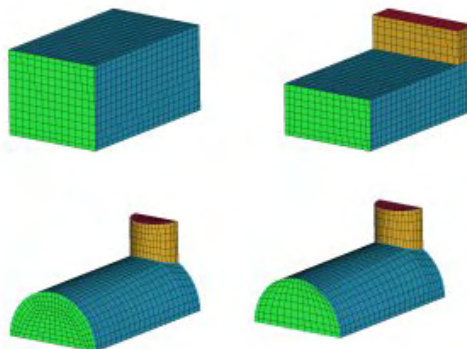


Figure 4.28: Octree discretization.

⁷<http://www-berkeley.ansys.com> Access-date: 12-2005.

The unstructured grid generation Octree is a good method to develop a mesh over a formfinding or free-form complex surface. Although, the main drawback of the Octree approach is the inability to match a prescribed boundary surface grid, so the grid on the surface is not constructed beforehand as desired but is derived from the irregular volume cells that intersect the surface. Another drawback of this grid is its rapid variation in cell size near the boundary. In addition, since each surface cell is generated by the intersection of a hexahedron with the boundary, problems arise in controlling the variation of the surface cell size and shape.

4.4.2.3 Variational Structured Grids

The mode of variable structured mesh design is required for preserving compatibility between the structured and unstructured parts of the surface. One method is the Hybrid Grid.

Hybrid Grids

Method Promoters of structured schemes highlight the efficiency and accuracy that is accomplished through the employment of regularly arranged volumes, while promoters of unstructured schemes emphasize the geometric flexibility and suitability for adaptation inherent to the use of irregularly connected tetrahedral volumes. All advantages of these techniques can be combined by replacing the use of only one grid generation type by the use of combined meshes composed of both structured and unstructured grids. This composed grid generation type is named a hybrid grid (Shaw 1999).

Commonly, a structured grid is generated about each chosen boundary segment. These structured grids are required not to overlap. The remainder of the domain is filled with the cells of an unstructured grid.

These kinds of meshes are widely used for the numerical analysis of boundary value problems in regions with a complex geometry and with a solution of complicated structure, e.g. free-form or form-finding structures.

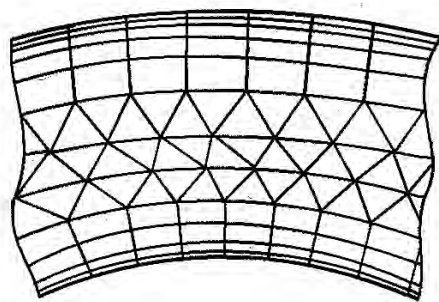


Figure 4.29: Fragment of a hybrid grid.

Software To generate hybrid grids, a software program which can not only generate unstructured grids, but also structured grids, can be utilised. The software program ICEM CFD is the one commonly in use for the structural discipline (Thompson 1995). This is also used for

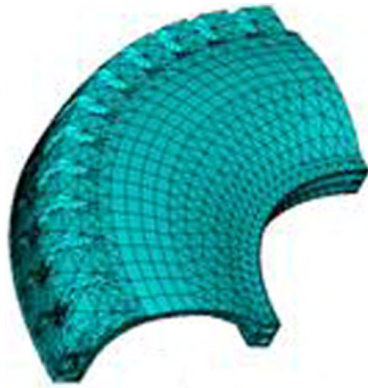


Figure 4.30: Fragment of a hybrid grid.

the Octree approach of unstructured grids.

Another program for the generation of Hybrid Grids is GRIDGEN. The structural part is generated by a block-structured grid, while the unstructured part is always generated by Delaunay triangulation.

In the GRIDGEN system of Pointwise (STEINBRENNER/CHAWNER/FOUTS 1990, STEINBRENNER/CHAWNER/ANDERSON 1992, STEINBRENNER/CHAWNER 1992, STEINBRENNER/CHAWNER 1993, CHAWNER/STEINBRENNER 1995) the user constructs curves which are in turn used to build the topological surface and volume components. The user then selects curves as the boundaries of surface grids, and finally surfaces as the boundaries of volume grids (blocks). With this system, grid generation is a user in-the-loop task. The data structure maintains the relationship among the curves, surfaces, and volumes so that changes can be propagated up or down the hierarchy automatically. The volume grid generation itself is finally done in the batch mode. (Thompson 1995)

Result This combination of grid types not only allows the benefits of structured and unstructured grids to be attained simultaneously, but also allows high grid quality to be achieved throughout the domain due to the appropriate use of each element type.

4.4.2.4 Configuration processing

Formex mathematics Formex (Nooshin, Space Structures Research Centre, Department of Civil Engineering, University of Surrey, Guildford, UK 1984, Nooshin & Disney 2002) algebra is a configuration processing mathematic language, which is implemented in a programming language, Formian (Delft University of Technology 2003) and (School of Engineering 2004). The configuration is an arrangement of parts of the structure. It is mostly used for generating (processing) regular shapes consisting of one or more-layered grids. The language works with so-called formices (plural of formex) which form a fundamental operation for the algebra. Very complex shapes can be generated with simple statements, as can be seen in the Formian examples below. This algebra could be seen as an early form of parametric geometry modeling. Simple parameters control complex structures.

Perspective view of Figure 4.31

```
(*) Perspective view (*)
TOP=rinid(7,8,2,2)|[0,0,1;2,0,1]#rinid(8,7,2,2)|[0,0,1;0,2,1];
BOT=rinid(6,7,2,2)|[1,1,0;3,1,0]#rinid(7,6,2,2)|[1,1,0;1,3,0];
WEB=rinid(7,7,2,2)|rosad(1,1)|[0,0,1;1,1,0];
GRID=TOP#BOT# WEB;
use vm(2),vt(2),vh(7,-14,7,7,7,0,7,7,1);
clear; draw GRID;
```

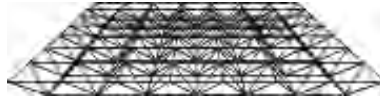


Figure 4.31: Image made in Formian of the Perspective View. Image from <http://www.bk.tudelft.nl/bt/dc/Formian/Formian.html>

Lamella dome of Figure 4.32

```
(*) Lamella dome (*)
ny=12; nz=8; rd=100; a=2; t=50;
e=[1,0,a;1,1,1+a];
f1=rinit(ny,nz,2,2)|rosat(1,1+a)|e;
f2=rinit(ny,2,2,2*nz)|[1,0,a;1,2,a];
f=bs(rd,180/ny,t/(2*nz+a))|(f1#f2);
use &,vt(1),vm(2),vh(10,10,20,0,0,0,0,0,1);
clear; draw f;
```

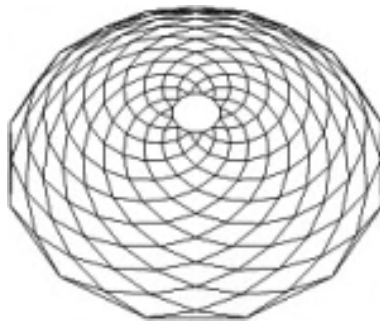


Figure 4.32: Image made in Formian of the Lamella dome. Image from <http://www.bk.tudelft.nl/bt/dc/Formian/Formian.html>

Onion with quadrangular elements of Figure 4.33

```

(*) Onion with quadrangular elements (*)
R=6;      (*) 1st radius (*)
Q=10;     (*) 2nd radius; conditon: R<Q (*)
M=24;     (*) no of elements along U2 (*)
N=20;     (*) no of elements along U4 (*)
T=acos|(R/Q);
P=asin|(R/Q);  (*) position angle (*)
A=[1,0,1,0;1,0,1,-1;1,1,1,-1;1,1,1,0];
B=rinic(2,4,M,N,1,-1)|A;
C=tran(4,-1*N*P/T)|B;
D=pex|dep(4)|ba(R,360/M,Q,T/N)|C;
use &,vm(2),c(3,8),vh(20*Q,-20*Q,20*Q,0,0,0,0,0,1);
clear; draw D;

```

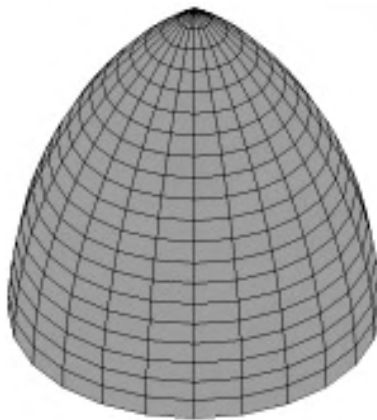


Figure 4.33: Image made in Formian of the Onion of quadrangular elements. Image from <http://www.bk.tudelft.nl/bt/dc/Formian/Formian.html>

Formian can be downloaded on: <http://www.surrey.ac.uk/eng/research/masss/ssrc/FMXJLY200.ZIP>.
 Another implementation, pyFormex, can be downloaded on: <http://pyformex.berlios.de>

4.5 Form finding

The techniques intended here are the 'classical Form Finding' techniques, aimed on the finding of shapes of structures such as membranes, cable-nets and when inverted, shells. These techniques can also be applied to other structures to find forms, but then need to be modified. An example of this is the British Museum Queen Elisabeth Great Court Roof, where Chris Williams modified the dynamic relaxation method to relax the generated grid for more efficient structural load bearing behaviour. Classical Form Finding follows the principle of 'Form follows Force'. The shape of the structure depends on the forces in the structure, but of course the forces also depend on the shape of the structure, leading to complex, non-linear behaviour which cannot be directly determined with analytical techniques. These problems have to be solved by an algorithmic approach. The history of Form Finding is rich, Gaudi, Isler, Candela and Torroja used the physical alternative in their structures, because computation was not yet available. People like Schek, Klaus Linkwitz, Frei Otto, Jorg Schlaich and Erik Moncrieff are inventors and users of the Force Density method, while people like Mike Barnes, Chris Williams, Ove Arup and Ted Happold prefer the Dynamic Relaxation methods.

4.5.1 Minimal surfaces

⁸ Minimal surfaces are defined as the smallest possible surface area between a given (closed) edge. Minimal surfaces are closely related to many form finding problems. This is caused by the soap film analogy (Bletzinger n.d.). The problem is considered as if it was a soap film and since soap films approximate minimal surfaces, often minimal surfaces are searched for. Minimal surfaces have some characteristics:

- Area variation is 0:
 $\delta a = 0$
- The mean surface curvature vanishes.

There are 2 approaches to calculating the minimal surface according to the principle of the area variation is 0. These work from the principle of the starting with a reference surface which is known, which has to be transformed to an actual surface, which has to be form found.

1. **Direct geometrical approach** which can be described by (Bletzinger n.d.):

$$\delta a = \int_A \delta(\det F) dA = \int_A \det F F^{-T} : \delta F dA = 0 \quad (4.2)$$

where

F deformation gradient

$$F = \frac{\partial x}{\partial X}$$

$x(\theta_1, \theta_2)$ is the coordinate on the actual surface

$X(\theta_1, \theta_2)$ is the coordinate on the reference surface

2. **Mechanical approach** which can be described by (Bletzinger n.d.):

$$\delta w = t \int_a \sigma : du_{,x} da = t \int_A (F \cdot S) : \delta F dA = 0 \quad (4.3)$$

⁸Bletzinger gives several good mathematical references for minimal surfaces (Bletzinger n.d.)

where

- σ the Cauchy stress tensor
- $\delta u_{,x}$ the derivative of the virtual displacement with respect to the geometry of the actual surface
- t thickness of the membrane
- S second order Piola-Kirchoff stress tensor

This methods works with the principle of virtual work of a stress field, which vanishes when in equilibrium.

When discretized and linearized form finding methods for cable-nets and membranes can be derived from these formulations, such as the force density method.

4.5.2 Force density method

The Force Density Method is a method to solve the non-linear system of equations of a cable-net structure by making the system linear. The method can also be used for membrane structures by discretization of the membrane to cable-net elements. A well-known force density application of the form finding, analysis and pattern-cutting of membranes is Easy (Stary 2003) and for an older application: Grundig, 1986 (Grundig & Bahndorf 1986) (formerly: FASNET). For detailed information, refer to Moncrieff (Moncrieff & Grundig 2000).

The force density method is a simplification for cable-net structures of the updated reference strategy (URS), which is defined by Equation 4.4 according to Bletzinger (Bletzinger n.d.).

$$K = A_c \int_L (F_c * S) : F_u ds = A_c \int_L \frac{1}{L} \left(\frac{L}{l} \frac{n}{A_c} \right) \frac{1}{L} ds = \frac{n}{l} = q \quad (4.4)$$

where

- K stiffness matrix
- A_c Reference surface area
- D_u Deformation gradient (u is the discretization parameter)
- $F = \frac{l}{L}$
- $F_u = \frac{1}{L}$
- S second Piola Kirchoff stress (in the reference surface), for minimal surfaces yields:
 $S = \frac{L}{l} \frac{n}{A_c} I$
- n Prescribed tension force in an element
- q Force density

This might be a quite complex formulation. A less complex problem illustrates the working of force density. Consider the problem in Figure 4.34. The three members are number 1,2 and 3. The four nodes are numbered a,b,c and d. Node a and d are supported by a hinged support. Node b and c are loaded by a load in the x direction and the y direction. The system of equations to describe this system is equation 4.7 which can be derived from among others equation 4.5 and 4.6.

$$\frac{L_1}{X_b - X_a} = \frac{S_1}{S_{x;1}} \quad (4.5)$$

$$\vec{S}_1 + \vec{S}_2 = \vec{F}_1 \quad (4.6)$$

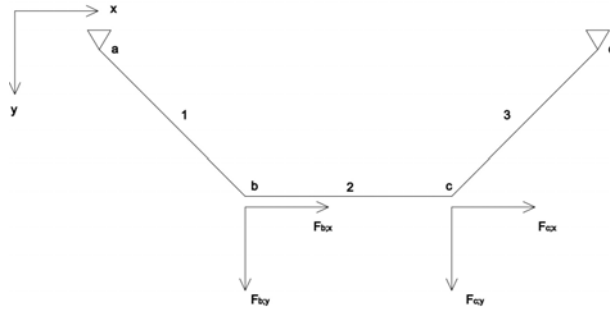


Figure 4.34: Example of a force density problem

$$\begin{aligned}
 (X_b - X_a) \frac{S_1}{L_1} + (X_b - X_c) \frac{S_2}{L_2} - F_{x;b} &= 0 \\
 (X_c - X_b) \frac{S_2}{L_2} + (X_c - X_d) \frac{S_3}{L_3} - F_{x;c} &= 0 \\
 (Y_b - Y_a) \frac{S_1}{L_1} + (Y_b - Y_c) \frac{S_2}{L_2} - F_{y;b} &= 0 \\
 (Y_c - Y_b) \frac{S_2}{L_2} + (Y_c - Y_d) \frac{S_3}{L_3} - F_{y;c} &= 0
 \end{aligned} \tag{4.7}$$

where

- X_p x coordinate of point p
- Y_p y coordinate of point p
- S_j force in member j
- L_j length of member j
- $F_{w;p}$ load in the direction of w in point p

$$L_j = \sqrt{(X_{end;j} - X_{begin;j})^2 + (Y_{end;j} - Y_{begin;j})^2} \tag{4.8}$$

where

- L_j length of member j
- $X_{end;j}$ x coordinate of the node at the end of member j
- $X_{begin;j}$ x coordinate of the node at the begin of member j
- $Y_{end;j}$ y coordinate of the node at the end of member j
- $Y_{begin;j}$ y coordinate of the node at the begin of member j

However, this system cannot be solved since there are 7 unknown variables: four coordinates (X and Y of b and c) and three forces (S_1 , S_2 and S_3). Note that the lengths are be found with equation 4.8, if the coordinates would be known.

This problem is solved by the introduction of the preset force density Q_j which is defined by equation 4.9. This simplification makes the system of equations linear and solvable, since only the four coordinates are unknown now.

$$Q_j = \frac{S_j}{L_j} \tag{4.9}$$

where

- Q_j force density in member j
- S_j force in member j
- L_j length of member j

In more complex problems this is used to converge to the equilibrium state of the cable-net or membrane. Important is to understand that the force density is a proportion between the

force in a member and the length of a member. When the lengths are held constant and the forces in the edges of the membrane or cable-net and the membrane or cable-net itself are equal, the shape is the same for each force density. However, when made unequal, the curvature in either the net or the cable-net or membrane itself will increase or decrease, and therefore the surface area of the cable-net or the membrane, depending on the force density (and the applied lengths and forces).

Force density method This method which is specifically developed (originally described by Sheck (Sheck 1974)) for tension structures, uses an analytic technique to linearize the form-finding equation for a tension net. This linearization makes the method independent of the material properties of the membrane. Force density ratios (cable force T divided by cable length l) need to be specified for each element, and different ratios give different equilibrium shapes. This means, the higher the force density, the shorter the element for a given force. When the force densities for a node are equal and evenly distributed around the node, a minimal surface (i.e. equilibrium shape) is generated.

The method is numerically robust, independent of the initial locations of the nodes, and the equilibrium shape is found easily. The force density solution applied to loads is non-linear, and requires iteration.

4.5.3 Dynamic relaxation

Dynamic relaxation can be used for finding the shape of net and membrane structures. Relaxation methods are not really 'form finding methods' but methods for structural calculation used for form finding purposes. Another well-known method is the solution of a stiffness matrix, either directly or iterative, to determine the equilibrium. However, in some situations, like local instability, these methods perform less good.

Dynamic relaxation is a method which lets the structure relax to a equilibrium situation. On one hand, the velocity of displacement converges to zero and the stiffness of the structure increases. The advantage of this method over matrix methods are that this method does not have to solve matrices, which takes a lot of calculation power, and although it takes more cycles to complete, each cycle takes much less time. Another advantage is the ability to deal with local instability, like wrinkling of the membrane, etc.

A couple of examples of software which use this principle are the dynamic relaxation programs by C.J.K. Williams (Williams 2004) and M.R. Barnes (Barnes 1986), the in-house Tensyl software (Wakefield 1986) by Buro Happold⁹ and the in-house software of Tensys¹⁰.

Dynamic relaxation in detail In this paragraph the procedure of dynamic relaxation will be explained and illustrated. Dynamic relaxation has an iterative, converging process where in the end an equilibrium should be reached. The success however depends on various parameters and of course the consistency the structure itself.

Each cycle of the process starts with the calculation of the lengths of each member j with Equations 4.10 and 4.11. The first equation calculates the differences in various directions. A schematic representation of a member can be seen in Figure 4.35.

$$\begin{aligned} dx_j &= x_{j;end} - x_{j;begin} \\ dy_j &= y_{j;end} - y_{j;begin} \\ dz_j &= z_{j;end} - z_{j;begin} \end{aligned} \tag{4.10}$$

⁹Buro Happold, <http://www.burohappold.com>

¹⁰Tensys, <http://www.tensys.com>

where

$x_{j;begin}$ x position of the node on the begin of the j-th member
 $x_{j;end}$ x position of the node on the end of the j-th member

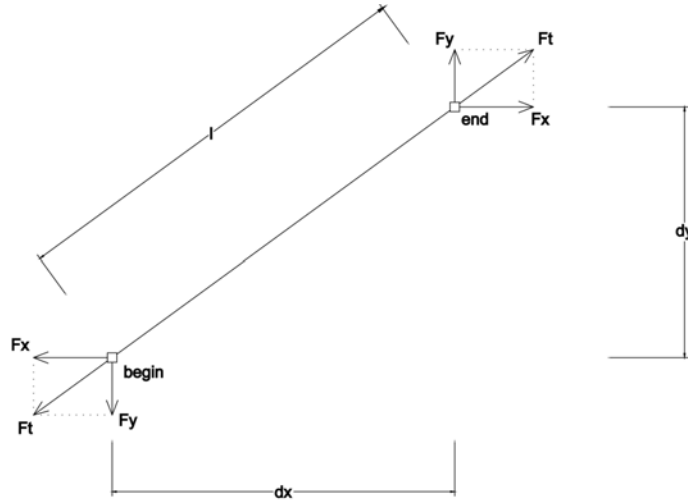


Figure 4.35: The schematic representation of a member in dynamic relaxation

$$l_j = \sqrt{dx_j^2 + dy_j^2 + dz_j^2} \quad (4.11)$$

where

l_j length of member j

With the Law of Hooke (4.12) the stress σ based on a strain ϵ can be determined. When multiplied with the section A the tension force F_t can be calculated from the strain (4.13). E is the modulus of elasticity.

$$\sigma = E\epsilon \quad (4.12)$$

$$F_t = \sigma A = EA\epsilon \quad (4.13)$$

The strain ϵ is the difference between the original length and the deformed length divided by the original length. In Equation 4.14 the tension force is calculated from the lengths.

$$F_{t;j} = EA_j \frac{l_j - L_j}{L_j} \quad (4.14)$$

The force F_t can be decomposed into the various directions to determine the force on each node, based on the original load and this extra force (Equation 4.15).

$$\begin{aligned}
F_{x;j;begin} &= F_{x;j;begin} + \frac{dx_j}{l_j} F_{t;j} \\
F_{x;j;end} &= F_{x;j;end} - \frac{dx_j}{l_j} F_{t;j} \\
F_{y;j;begin} &= F_{y;j;begin} + \frac{dy_j}{l_j} F_{t;j} \\
F_{y;j;end} &= F_{y;j;end} - \frac{dy_j}{l_j} F_{t;j} \\
F_{z;j;begin} &= F_{z;j;begin} + \frac{dz_j}{l_j} F_{t;j} \\
F_{z;j;end} &= F_{z;j;end} - \frac{dz_j}{l_j} F_{t;j}
\end{aligned} \tag{4.15}$$

The stiffness also changes when the lengths of the members change. This can be seen from Equation 4.16 where the change of stiffness in each direction is calculated.

$$\begin{aligned}
\Delta S_{x;j} &= \left(\frac{dx_j}{l_j}\right)^2 \frac{EA_j}{L_j} \\
\Delta S_{y;j} &= \left(\frac{dy_j}{l_j}\right)^2 \frac{EA_j}{L_j} \\
\Delta S_{z;j} &= \left(\frac{dz_j}{l_j}\right)^2 \frac{EA_j}{L_j}
\end{aligned} \tag{4.16}$$

From Equations 4.17, 4.18 and 4.19 the new stiffnesses of the system are being determined in each direction.

$$\begin{aligned}
S_{x;j;begin} &= S_{x;j;begin} + \Delta S_{x;j} \\
S_{x;j;end} &= S_{x;j;end} + \Delta S_{x;j}
\end{aligned} \tag{4.17}$$

$$\begin{aligned}
S_{y;j;begin} &= S_{y;j;begin} + \Delta S_{y;j} \\
S_{y;j;end} &= S_{y;j;end} + \Delta S_{y;j}
\end{aligned} \tag{4.18}$$

$$\begin{aligned}
S_{z;j;begin} &= S_{z;j;begin} + \Delta S_{z;j} \\
S_{z;j;end} &= S_{z;j;end} + \Delta S_{z;j}
\end{aligned} \tag{4.19}$$

Now the stiffness of each node can be determined for each node i in Equation 4.20.

$$S_i = S_{x;i} + S_{y;i} + S_{z;i} \tag{4.20}$$

In Equation 4.21 the velocities of each node are determined. However, as can be seen from Equation 4.22, where the node coordinates are adjusted, this velocity is not really a velocity, but a variable stepsize to change the node coordinates with. However, analogy with velocity is good to keep in mind for understanding the principles.

f is a factor which determines the amount of adjustment for the net. c is a convergence factor which is 0 or 1, to secure convergence and decreasing speeds. When all speeds summed are larger than the last cycle, this convergence safety trap goes to 0 and decreases the amount of speed.

$$\begin{aligned}
V_{x;i} &= c \cdot V_{x;i} + f \cdot \frac{F_{x;i}}{S_i} \\
V_{y;i} &= c \cdot V_{y;i} + f \cdot \frac{F_{y;i}}{S_i} \\
V_{z;i} &= c \cdot V_{z;i} + f \cdot \frac{F_{z;i}}{S_i}
\end{aligned} \tag{4.21}$$

$$\begin{aligned}
x_i &= x_i + V_{x_i} \\
y_i &= y_i + V_{y_i} \\
z_i &= z_i + V_{z_i}
\end{aligned} \tag{4.22}$$

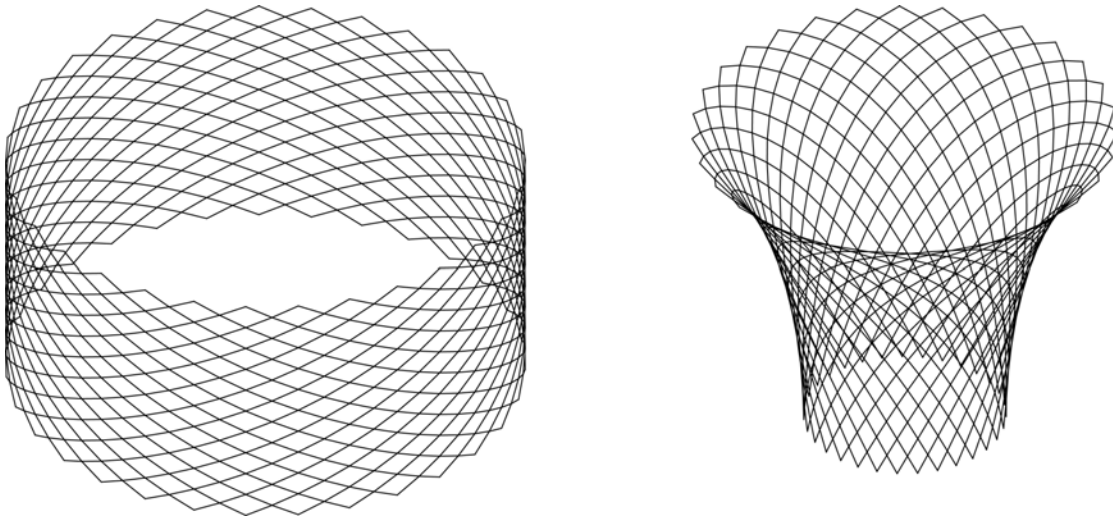


Figure 4.36: Dynamic relaxation, left the original net structure and right the relaxed structure. Image and software by C.J.K. Williams.

4.5.4 Shape form finding

Using a shape optimisation technique is another method of finding an equilibrium. This optimisation techniques finds the optimum between force and shape leading to a position where the structure is in equilibrium. Also principles of stress averaging can be used to find catenary shapes.

4.5.5 Other form finding methods

Other methods of Form Finding spring from the computer games industry and non-linear finite element analysis. A technique which has been used by Axel Kilian of MIT to create a virtual Gaudi hanging model application, is called particle-spring systems. These systems deals with masses on a spring. Another way of analysing membranes is to use non-linear finite element solvers to model and solve the behaviour of the membrane. The membrane is then modelled as membrane elements, with only in-plane forces.

4.6 Structural optimisation

Structural Optimisation deals with the optimisation of structures. Optimisation can be defined as the process to find the minimum (or maximum) of an object-function within a given set of boundaries or constraints. The object-function describes both the generation process as well as the evaluation process of the subject of the optimisation. The boundaries or constraints describe the freedom which is given to the algorithm to search the optimum.

4.6.1 Theory of optimisation

Mathematics In this section the basic mathematics of structural optimisation are covered in general form. In other words, not structural engineering problems, but mathematical problems and methods are described which can be used to solve structural engineering problems.

Note again that the purpose of this section is not to be a complete mathematical reference guide, but a general overview over problems and methods. Also should be noted that this section does not provide detailed explanation of each method.

For more detailed information, its recommended to read "Numerical Recipes in C++" (Press, Vetterling, Teukolsky & Flannery 2002), "Structural Optimisation" (Bletzinger 2001), "Advanced Techniques in the Optimum Design of Structures" (Hernandez 1993) and "Recent Advances in Optimal Structural Design" (Burns 2002).

To find a definition of optimisation the following references can be found:

(Kirsch 1993), (Liang 2005) and (Xie & Steven 1997a)

op·ti·mal *adj* the best or most suitable; extreme; highest; most favourable or most desirable possible under a restriction expressed or implied

op·ti·mise *v* the way that something is done or used as effective as possible; trying to make optimal; trying to reach the extreme; make optimal; get the most out of; use best

op·ti·mum *adj* the best or most suitable for a particular purpose; the best possible situation; conditions; amount of time etc for something to happen; the best; the highest achievable; the point at which the condition, degree, or amount of something is the most favourable

struc·tur·al *adj* relating to or having or characterized by structure; affecting or involved in structure or construction

In the context of a structure subject to multiple loads and support conditions the optimal shape is that which best satisfied the constraints, with the degree of satisfaction not necessarily the same for all the constraints.

General form of an optimisation problem. Equation 4.23. A function is linear if all functions f , g and h are linear. If one of these function is non-linear, the optimisation problem is also non-linear.

$$\begin{array}{ll}
\text{minimize} & F(\bar{x}); & \bar{x} \in R^n \\
\text{such that} & g_i \leq 0; & i = 1, \dots, p \\
& h_j = 0; & j = 1, \dots, q \\
\text{where} & F(X) = \begin{bmatrix} f_1(\bar{x}) \\ \dots \\ f_n(\bar{x}) \end{bmatrix} &
\end{array} \tag{4.23}$$

where

- F(x) object function
- g_i inequality restriction functions
- h_j equality restriction functions
- $f_i(x)$ i-th object function
- \bar{x} parameters

A special form of this problem are "variable bound problems" where also the variables \bar{x} are bounded by a restriction, for instance $\underline{x}_i \leq x_i \leq \bar{x}_i$.

The space spanned by the possible design variables is called the "search space". The space spanned by the possible design variables, satisfying all constraints, is called the "feasible domain".

Below several terms in optimisation will be explained which are important to understand before looking at the actual methods of optimisation.

Function approximation versus optimisation A possible classification of solution methods for these optimisation problems is the subdivision in function approximation methods and optimisation methods.

In function approximation methods the algorithm tries to approximate or 'learn' the object function and of this function the optimum is determined, for instance by determining the derivatives or searching this function. This often involves the optimisation of parameters of the function which models the object function. Neural networks are an example of an algorithm which 'learns' the object function.

In optimisation methods the algorithm tries to optimise the object function by searching the search space in some manner. The search space is the space spanned by the possible variables, boundaries and constraints.

Discrete versus continuous optimisation Often solution methods for the problem in Equation 4.23 assume continuous functions for f, g and h and the variables \bar{x} . These methods are often analytical and are called continuous optimisation.

Numerical methods often use a discrete definition of the variables. This is called discrete optimisation.

Local versus global optimisation One of the main problems of optimisation methods is the problem of local optima in the object function. The function possesses one or more local optima which have a derivative of zero, in other words are a top of the hill, or the bottom of a valley, but are not the highest top, or the lowest bottom in the object function, which is called the global optimum. Many classical methods have the problem that they get stuck in the local optima and cannot 'jump' out of these optima. Various techniques, such as genetic algorithms or simulated annealing, have this feature.

global and local maxima and minima The *feasible region* is the set of all solutions to the problem satisfying all the constraints. The *optimal solution* for a minimization problem is the solution with the smallest cost value in the feasible region. Similarly, for maximization problems, it is the solution with the largest objective function value. The cost function $f(x)$ has a local minimum (also called a relative minimum) at a point x^* in the feasible set S if the function value is the smallest at the point x^* compared to all other points x in a feasible neighbourhood N of x^* , that is

$$\begin{aligned} f(x^*) &\leq f(x) \\ \forall x &(\text{=for all } x \text{ in the feasible region.} \end{aligned} \tag{4.24}$$

If strict inequality holds, then x^* is called the strict or unique global minimum.

Function $f(x)$ has a local minimum at x^* if this equation holds for all x in a small neighbourhood of N of x^* in the feasible region. Neighbourhood N of the point x^* is mathematically defined as

$$N = \{x | x \in S \text{ with } \|x - x^*\| < \delta\} \tag{4.25}$$

for some small δ . Geometrically, it is a small feasible region containing the point x^* .

The global and local minima and maxima are shown in Figure 4.37.

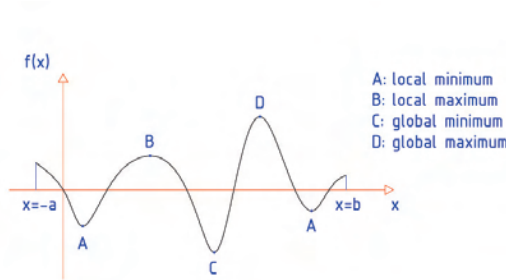


Figure 4.37: Global and local maximum and minimum points of a multimodal function.

Discrete versus continuous optimisation Often solution methods for the problem in Equation 4.23 assume continuous functions for f , g and h and the variables \bar{x} . These methods are often analytical and are called continuous optimisation.

Numerical methods often use a discrete definition of the variables. This is called discrete optimisation.

Fully stressed design In this strategy no redundancy of stress is allowed. Every element of the structure has to be stresses to the maximum. When considering a single load-case this is possible, however one can imagine that this is quite complex when considering more (paradoxical) load-cases.

For trusses Equation 4.26 applies (Bletzinger 2001) for convergencing to a fully stressed design. However, it needs to be noted that for statically indetermined structures the correct solution will not always be found:

$$A_i^{(k+1)} = \max_{(all\ loadcases)} \left[A_i^{(k)} \frac{\sigma_i^{(k)}}{\sigma_i^{admissible}} \right] \quad (4.26)$$

for all members $i = 1, \dots, n$

where

$A_i^{(k)}$ surface area of the profile section for member i
 $\sigma_i^{(k)}$ current stress for member i
k stepnumber

Multi-objective or multi-criteria optimisation Multi-objective or multi-criteria optimisation are characterized by more than one object-function. An example of this is Equation 4.27. The problem is how to define such a problem that these objectives can be optimised. An example of this is weighted summation of the objective functions (an example can be seen in Equation 4.28). Bletzinger (Bletzinger 2001) gives some examples of this optimisation.

$$\text{minimize } f(x) = \begin{bmatrix} f_1(x) \\ f_2(x) \\ \dots \\ f_n(x) \end{bmatrix} \quad (4.27)$$

$$\text{minimize } F(x) = \sum_{i=1}^n w_i f_i \quad (4.28)$$

where

f_i i-th object function
 $f(x)$ object function vector
 w_i weight of the i-th object function
 $F(x)$ weighted summation of object functions

4.6.2 Classification of optimisation problems

If an optimisation problem has linear objective and constraint functions, it is called a *linear programming problem*. An *integer programming problem* is a linear programming problem in which some or all variables must be non-negative integers. Otherwise, it is called a *non-integer programming problem*. The search for an optimal arrangement, grouping, ordering or selection of discrete objects is called *combinatorial optimisation*. A problem having a quadratic objective function and linear constraints is called a *quadratic programming problem*.

It is important to note the following points for the foregoing nonlinear problem model relative to structural and mechanical system design problems.

1. The model is applicable to all problems with continuous design variables. *Multi-objective* and *discrete variable* problems can also be treated after certain extensions of the model;
2. the functions of the problem are assumed to be *twice differentiable*. Problems having non-differentiable functions can be treated with additional computational effort. Also,

gradients of active constraints are assumed to be linearly independent at the optimum;

3. The cost and/or constraint functions may be *implicit* as well as *explicit* functions of the design variables. That is, their final form in terms of only the design variables may not be known. The functions, however, can be evaluated using analysis computer programs once a design is specified;
4. *Derivatives* of the functions are needed in numerical methods of optimisation. Efficient methods to calculate them taking advantage of the structure of engineering design problems have been developed.

Non-linear programming problem A nonlinear programming problem can be represented in the following manner.

Let x represent an n -dimensional design variable vector. Then any design optimisation problem can be stated as follows: find x to

$$\begin{aligned}
 &\text{minimise a cost function } f(x) \\
 &\text{subject to} \\
 &\text{equality constraints:} && g_h(x) = 0, h = 1 \text{ to } p \\
 &\text{inequality constraints:} && g_h(x) \leq 0, h = (p + 1) \text{ to } q \\
 &&& x_i^L \leq x_i \leq x_i^R \quad i = 1 \text{ to } k
 \end{aligned} \tag{4.29}$$

where p is the number of equality constraints and $(q-p)$ is the number of inequality constraints. x_i^L and x_i^R are the lower and upper bounds on the design variable x^i , and k is the total number of design variables. This optimisation problem is called a general mixed discrete-continuous variable nonlinear optimisation problem. In some situations, there may be two or more cost functions. This is called a *multi-objective optimisation problem*.

4.6.2.1 Analytical optimisation

Analytical optimisation usually involves the application of the mathematical methods from section on structural engineering problems. Usually the calculation is structural and the optimisation part is a certain mathematical technique. Since every problem brings its own method, there are no real types or categories in this field of optimisation. Also, these technique currently are only used for estimates of the final result of more complex calculation methods, since these techniques only work when the problem is quite simple and can be solved by analytical techniques. Since structural engineering problems usually involve complex search spaces with discrete and continuous variables, discrete and continuous object-functions, etc. not many problems can be solved in an analytic manner.

4.6.2.2 Size, shape and topology optimisation 1

Before the distinction between size, shape and topology optimisation will be made, it must be said that there are several understandings of this distinction. Below two of them will be described.

Information taken from: (Bendse 1995), (Bendse 2003), (Coenders 2004), (research group 2005) and (*Universtat Stuttgart, Institute for Structural Mechanics, Adaptive Finite Element Methods for fast transient, highly nonlinear processes* n.d.)

general introduction into shape, size, and topology optimisation Applications of numerical methods to truss problems and other discrete models were first described in the early sixties, but only recently have these challenging large-scale problems attracted renewed interest, especially for producing specialised algorithms.

In the design of the size, shape, and topology of a structure the interest is in the determination of the optimal placement of a given isotropic material in space, which means, it should be determined which points of space should be material points and which points should remain void (no material). The geometric representation of a structure is thought of as similar to a black-white rendering of an image. In discrete form this then corresponds to a black-white raster representation of the geometry, with pixels given by the finite element discretisation. So, in its most general setting shape, size and topology optimisation of continuum structures should consist of a determination for every point in space if there is material in that point or not. Alternatively, for a FEM discretisation every element is a potential void or structural member. In other words, the ground approach is that for an initially chosen layout of nodal points in the truss structure or in the finite element mesh, the optimum structure connecting the imposed boundary conditions and external loads is found as a subset of all the elements of the initially chosen set of connections between the truss nodal points or the initially chosen set of finite elements. The positions of nodal points are not used as design variables, meaning that these points are fixed.

Terminology and representation The three principles size, shape, and topology optimisation can be mentioned as one under the common denominator of layout optimisation (Figure 4.38)

Size optimisation The main feature of the size problem is that the domain of the design model and variables is known a priori and is fixed throughout the optimisation process. Only the size of certain elements is optimised without changing the shape or topology of the structure. Size optimisation is to find the optimal cross-sectional properties of members in a truss or frame structure or the optimal thickness distribution of a plate structure. It has the goal of maximising the performance of a structure in terms of the weight and overall stiffness or strength while the equilibrium condition and the design constraints are satisfied. The design variable is the cross-sectional area of truss members or the thickness of a plate.

Shape optimisation The goal in shape optimisation, or geometry optimisation, is to find the optimum geometry of the domain, that is, the shape problem is defined on a domain which is now the design variable. In shape optimisation, the objective is to find the optimal shape of the design domain, which maximises its performance. The shape of the design domain is not fixed but rather is a design variable. In shape optimisation, only the boundaries of the design domain are changed but not the topology of the domain.

Topology optimisation The purpose of layout optimisation is to find the optimal layout of a structure within a specified region. The only known quantities in the problem are the applied loads, the possible support conditions, the volume of the structure to be constructed and possibly some additional design restrictions such as the location and size of prescribed holes. In this problem the physical size and the shape and connectivity of the structure are unknown.

The topology, shape and size of the structure are not represented by standard parametric functions but by a set of distributed functions defined on a fixed design domain. These functions

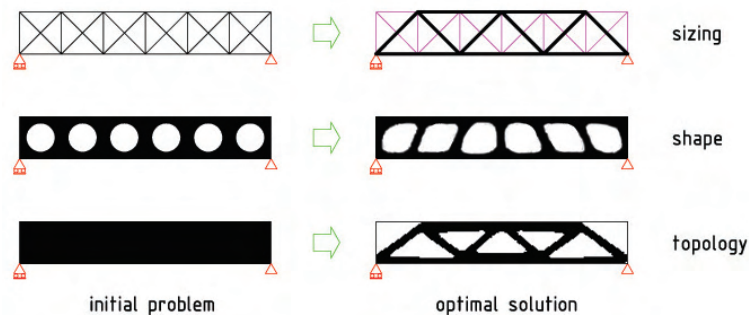


Figure 4.38: A representation of the size, shape and topology optimisation method

in turn represent a parameterisation of the rigidity tensor of the continuum and it is the suitable choice of this parameterisation which leads to the proper design formulations for layout optimisation.

The practical use of topology design to date often has been on the level of a creative sparring partner in the initial phase of a design process. Thus the output of the homogenisation method, as how use of topology optimisation is also called, has been used to identify potential good designs, the completion of the design being based entirely on traditional skills of the design office. One effect of the topology method that cannot be underestimated is the efficient testing of the appropriateness of the model of loads and supports. As the topology is very sensitive to a proper modelling of the load environment, one can immediately discover discrepancies or inaccuracies in this modelling. The results of using the homogenisation method for optimal topology design tend to favour the use of the sub-optimal microstructures, as these from a practical point of view results in more classically useful structures. In the future it will probably implement for example production requirements as constraints that will limit the final design. It is natural to integrate the material distribution method and the boundary variations approach into one design tool, employing the topology optimisation techniques as a pre-processor for boundary shape optimisation. The topology is of great importance for the performance of the structure, and it has turned out that the compliance optimised topologies generated using the homogenisation method are very good starting points for optimisation concerning several other criteria such as maximum stress, maximum deflection, etc.

In Figure 4.39 a flow of an integrated design system with topology design and boundary shape design modules is given.

4.6.2.3 Size, shape and topology optimisation 2

Form Finding versus Structural optimisation For structural optimisation the subdivision made by Ramm (Ramm & Bletzinger 1993) can also be used. Ramm describes structural optimisation as: "Parameters defining the layout of structures and material, the shape, the dimensions are taken as the unknown primary design variables; we define objectives, equality and inequality constraints, bounds for the design parameters and enter the world of mathematical optimisation. In more or less automated iterative process we loop through the three basic modules of structural optimisation: geometry, mechanics, mathematics."

He divides this field in four categories which will be covered in the next subsections:

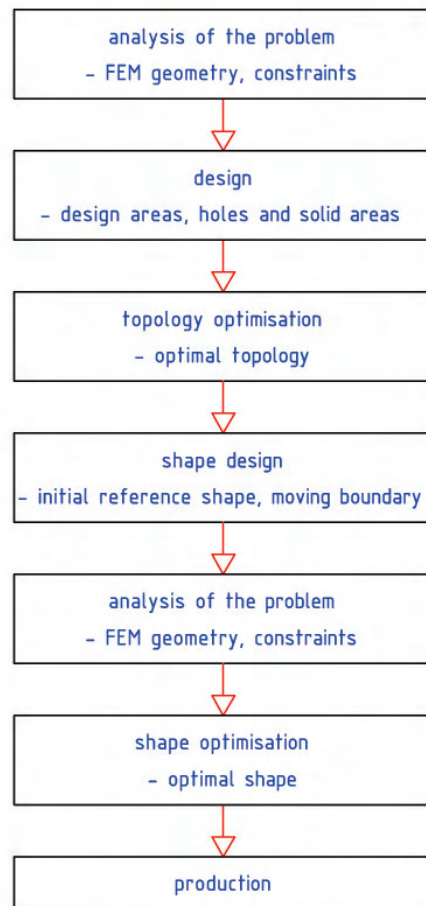


Figure 4.39: A flowchart of an integrated design system with topology design and boundary shape design modules

- Topology optimisation
- Shape optimisation
- Sizing
- Material optimisation

Important is to note that Ramm argues that providing additional information for the design process can speed up the optimisation process.

Shape optimisation With shape optimisation the shape of the structures (Ramm (Ramm & Bletzinger 1993): the overall contours of a given structure are adjusted) is the part which is optimised. The shape is closely related to the geometry of the structure, sometimes it is therefore called geometry optimisation. This type of optimisation is very close to form finding, but shape optimisation can involve more criteria than form finding, where often only the stress

is the ‘forming force’. Often shape optimisation involves the simulation of physical equilibrium models, like soap films or hanging chains and nets.

An example application of shape optimisation is for instance Sphere and Sphere2, developed at the Delft University of Technology by Nils Addink. The application can optimise the structure for very simple form finding criteria.

4.6.3 Size optimisation

Size optimisation is called sizing in the subdivision Ramm has made. Size optimisation is the optimisation of certain sizes of elements in the structure, without really adjusting the shape. One could also say that with sizing the initial geometry of the mechanical model is not changed.

Section optimisation A special case of size optimisation is the optimisation of sections or profiles. In this case the structure consists of certain predefined elements from which can be chosen. The optimisation process seeks the optimum.

Beam optimisation Beam optimisation is the same as section optimisation of beam elements and probably the simplest form of structural optimisation.

Truss optimisation Truss optimisation is a very old field in structural optimisation, which deals with the section optimisation of trusses. Quite old examples of optimisation of 2 and 3 member trusses are well known in structural optimisation, since they often can be solved analytically or with a simple iterative technique, and thus the computer was not necessary. From these examples much can be learned, even when studying more complex computer models, because often with these simple models great insight in the behaviour of systems can be acquired and the methods of the computer can be understood.

Czyz (Czyz & Lukaszewicz 1994) gives an example of truss optimisation for frequency constraints. Also Burns (Burns 2002) devotes a chapter to truss optimisation, but to the geometry (shape) and topology optimisation of trusses.

Material optimisation Material optimisation is mentioned by Ramm (Ramm & Bletzinger 1993) as a field in structural optimisation. Material optimisation is a daily practice for the structural engineer: defining the optimum material properties, such as dimensioning reinforcement bars.

4.6.3.1 Evolutionary structural optimisation (ESO)

A relative new method is the evolutionary structural optimisation (ESO) method. It is a simple concept of slowly removing (or shifting) inefficient material from a structure so that the resulting shape of the structure evolves towards an optimum. The ESO method is based on a simple concept that the step-by-step removal of the inefficient parts from the initial structure leads the structure toward an optimised configuration. There is, however, no consistent rule for determination of the control parameters needed in the evolutionary process of ESO such as, what is called, rejection ratios, evolution ratios and tolerance parameters for convergence. Additionally it has to be pointed out that the operations done in the process of the original ESO are only those for removing inefficient parts. It has been found that the evolutionary optimisation method can be effectively used for examination of the structural form, especially in the early stages of the design process. The organic form of the structure generated

through the usage of the computational morphogenesis scheme has not only a structural rationality but also a fresh appearance not easily acquired only through the usual designing process.

Structural optimisation methods can be enabled to obtain the structural form of which characteristic values are set to be extreme values while the subsidiary conditions imposed on the stress or displacement at specified portion of the structure are satisfied. The civil engineering industry has to satisfy all conditions required from the aspects of planning, architectural design, life facilities and other mathematically factors that are hard to prescribe, such as social impact on the human environment. It can be said that all these factors unsuitable for mathematical description have been keeping the civil and architectural engineering away from effective applications of optimising methods. However, regarding the conditions required from the planning or the life facility as the constraint conditions, there can be useful tools for civil and architectural engineering in the structural optimisation field.

4.6.3.2 Extended evolutionary structural optimisation (extended ESO)

Living things (flora and fauna) have been evolving their shapes to survive under various environments they have encountered. They are thought to evolve themselves toward better shapes by removing unnecessary parts, and, on the other hand, by extending necessary parts as well. Standing at this point of view, the extended evolutionary structural optimisation (extended ESO) method has been proposed, where two ideas are newly introduced

1. shape control scheme by the contour lines for two dimensional problems and the contour surfaces for three dimensional problems of sensitivity number;
2. bi-directional evolution.

An idea of contour line or contour surface is introduced for the determination of criteria of the boundary regions. Additionally, the bi-directional evolution which is the evolution scheme with not only deleting the concerned regions but also increasing them has been also newly introduced. Consequently, the proposed scheme makes the ordinary ESO method much more powerful.

In the ordinary ESO method, rejection of the inefficient part of the structure is carried out referring to the value of rejection ratio, which is given as a definite value in advance for computation. Consequently, the rejection procedure is performed throughout the whole evolutionary process of computation based upon that definite initial value and no attention is paid on the situation of the structure on evolution. In the extended ESO method, utilisation of the contour line is introduced as a new idea for evolutionary process to actively control the rejection ratio as well as the portion of evolution. This idea makes it possible to remove the inefficient parts of the structure largely at the early stage of the evolution and to gradually change the speed of the rejection process according to the actual situation of the evolution.

In the original ESO method, only the rejection procedure has been done and there must be the necessity of the additional procedure for the structure to keep up the proper evolutionary process. For this purpose, a new approach for the addition in the evolutionary process has been introduced. The procedure for addition is composed of two different steps, that is, the first step for calculation of the stress values at the cross points of the grid followed by the formation of the contour lines and the second step for settlement of the new design domain along the contour line corresponding to the prescribed value.

As had been mentioned above, deletions of the portions of the structure as well as addition are realised through usage of the contour lines for the 2-dimensional structures. In a similar manner, we can extend the way of thought to the evolutions of 3-dimensional structures, where the contour of the stress or the other prescribed characteristics values such as deflections, natural frequencies, linear buckling loads and so on should be replaced with the contour surface. Figure 4.40 shows the evolutionary process of the bridge type structures having the road on its upper part, for the case in which the relative stress of Von Mises is adopted for prescription of the contour surface, which can be written in the following form

$$\sigma^{VonMises} = \frac{1}{2} \sqrt{(\sigma_x - \sigma_y)^2 + (\sigma_y - \sigma_z)^2 + 6(\tau_{xy}^2 + \tau_{yz}^2 + \tau_{zx}^2)} \quad (4.30)$$

where $\sigma_x, \sigma_y, \sigma_z, \tau_{xy}, \tau_{yz}, \tau_{zx}$ represent the components of the normal stresses and the shear stresses in x-, y-, and z-direction. By using this characteristic value, we can get the mechanical information of the portion of the structure, by which the necessity of deletion or addition can be judged. It can be observed that in the evolutionary process of the bridge the form changes not only in the elevation but also in its thickness distribution.

As can be seen from Figure 4.40, the structure continuously changes its form in every point of itself and it is clear that only 3D approach can realise such characteristics.

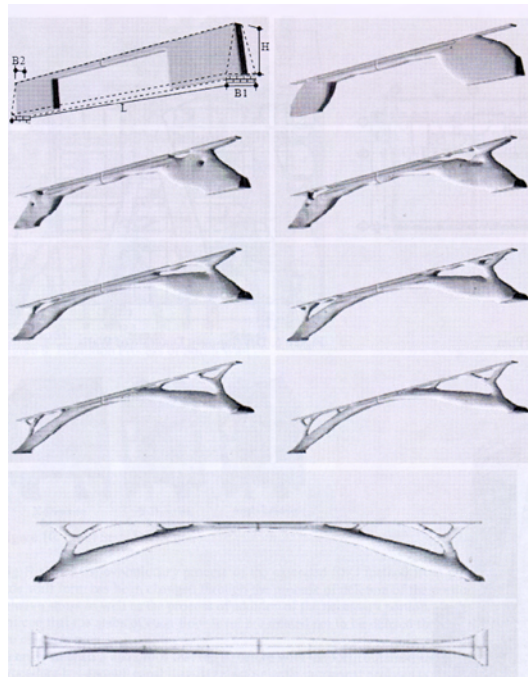


Figure 4.40: The elevation and the plan of a bridge structure obtained with the ESO process.

4.6.3.3 Performance based optimisation

The principles described above are also dealt with in the performance-based optimisation (PBO) method. Similarly, this method generates an optimal design by gradually removing inefficient material from a structure or adding efficient material to the structure until the performance of the structure is maximised. The main features of the PBO technique are its clarity in concepts, simplicity in mathematical formulation, ability to generate the global optimum and easy to understand. In PBO design, the weight of a structure is usually selected as the performance objective and structural response parameters such as stresses, displacements, overall stiffness and frequency are treated as performance-based constraints. It is realistic to minimise the weight or cost of a structure subject to geometrical constraints and performance-based constraints, which include stress, displacement, mean compliance, frequency and buckling load constraints. This is because performance-based constraints are usually prescribed in the design codes of practice.

4.6.4 Classical optimisation methods

Lagrangian function The Lagrangian function is defined in Equation 4.31 (Bletzinger 2001) which defines the Lagrangian multiplier or Lagrangian parameter λ .

$$L(x, \lambda) = f(x) + \lambda g(x) \quad (4.31)$$

for a problem

$$\begin{aligned} & \text{minimize} \quad f(x) \\ & \text{such that} \quad g(x) \leq 0 \end{aligned} \quad (4.32)$$

where

- L the Lagrangian function
- x parameter
- f(x) object function
- g(x) restriction function
- λ the Lagrangian multiplier

For this applies Equation 4.33 and 4.34, which have to be satisfied for the optimum:

$$\frac{dL(x, \lambda)}{dx} = 0 \quad (4.33)$$

$$\frac{dL(x, \lambda)}{d\lambda} = g(x) = 0 \quad (4.34)$$

Another often used definition is the dual function $D(\lambda)$ with respect to x, for a given λ :

$$D(\lambda) = \min_x L(x, \lambda) \quad (4.35)$$

where

- $D(\lambda)$ dual function of the Lagrangian function

Kuhn-Tucker conditions A solution of a general constrained optimisation problem needs to satisfy the 'Kuhn-Tucker' conditions. These are often used to check if a found solution is an optimum:

$$\begin{aligned} \frac{\partial L}{\partial x_i} &= \frac{\partial f}{\partial x_i} + \sum_{j=1}^p \lambda_j \frac{\partial g_j}{\partial x_i} + \sum_{j=1}^q \mu_j \frac{\partial h_j}{\partial x_i} = 0; & i &= 1, \dots, n \\ \frac{\partial L}{\partial \lambda_j} &= g_j(\mathbf{x}) = 0; & j &= 1, \dots, p \\ \frac{\partial L}{\partial \mu_j} &= h_j(\mathbf{x}) = 0; & j &= 1, \dots, q \\ \lambda_j g_j &= 0; & j &= 1, \dots, p \\ \lambda_j &\geq 0; & j &= 1, \dots, p \end{aligned} \quad (4.36)$$

where $L(x, \lambda, \mu) = f(x) + \sum_{j=1}^p \lambda_j g_j(x) + \sum_{j=1}^q \mu_j h_j(x)$ is the Lagrangian and λ and μ the vectors of Lagrangian multipliers of inequality and equality conditions.

Mathematical programming Below various types of mathematical programming, the solution methods for optimisation problems, are listed. Next to this subdivision other subdivisions could be made, such as constrained versus unconstrained, primal methods (genetic algorithms also are part of this category) versus penalty- or barrier methods versus dual methods versus Lagrange methods.

Penalty- or Barrier methods transform a constrained problem into an unconstrained problem. The methods can also be subdivided based on what kind of data they use: function values only (zero order methods or direct search methods), gradient (gradient or first order methods) or second order information (second order or Newton methods) (Bletzinger 2001).

- **Linear programming**
Linear programming is used for mathematical problems where for Equation 4.23 all function f , g and h are linear. These problems can be solved in finite iteration steps.
- **Non-linear programming**
Non-linear programming is used for mathematical problems where for Equation 4.23 one or more of the functions f , g and h are non-linear.
- **Quadratic programming**
Quadratic programming are mathematical problems where for Equation 4.23 the function f is quadratic and the functions g and h are linear. These problems can, like linear programming be solved in finite iteration steps.
- **Dual methods or algorithms**
Dual methods or algorithms are methods which use the dual function from Equation 4.35 to split the procedure of optimisation in a repeated sequence of minimization and maximization problems. Descent methods can be used for each subproblem.

Some other techniques, which will not be further explained are:

- **Integer programming (IP)**
Integer problems are problems where the variable require to take integer values. When the functions are linear, the problems is called Integer Linear Programming (ILP).
- **Feasible programming**
- **Penalty programming**
- **Dynamic programming**
- **Geometric programming**

Line search, 1-D minimization One of the simplest optimisation method class are the line search algorithms. These involve searching a line for a minimum.

First-order: Derivative is zero The simplest form of optimisation when the object function is known, and is differentiable, is to determine the first order derivative of the object function and calculate for what point the derivative is zero. Both the local and global optima can be determined by this

Bracketing or interval search A slightly more complex method is bracketing or interval search. The method focusses on closing in the optimum between an upper and lower boundary and reducing the size of this interval.

Golden section search The Golden section search method is a special kind of interval search where the reduction is the Golden Section: $\frac{1}{2}(\sqrt{5} - 1) \approx 0.618$.

Polynomial interpolation When first order information is available, polynomial interpolation is a good alternative to interval searching. With this method the algorithm interpolates along the function, based on the zero-order and first-order information to determine the next point.

Parabolic Interpolation An example of polynomial interpolation is parabolic interpolation, where parabolic functions are used for the interpolation

Linear programming methods Two linear programming methods which needs mentioning, because they are wide used, are the Simplex Method and the Branch and Bound Method.

Simplex Method The Simplex Method is a matrix method to solve linear programming equality problems. By write the equations in a matrix form and solving the matrix with this method, the optimum variable can be found. Many kinds of variants to this methods can be found, such as pivoting.

Branch and Bound Method (BBM) The Branch and Bound Method uses a kind of tree-representation to expand the branches of this tree until the constraints are met. Especially for inequality problems, this method has some advantages, such as the ability to find global optima.

For more information on this method, refer to Burns (Burns 2002).

Approximation techniques Various approximation techniques are known as optimisation techniques. A few types are:

- Sequence of linear problems (SLP: Sequential Linear Programming)
- Sequence of quadratic problems (SQP: Sequential Quadratic Programming)
- Convex approximation
- Sequence of linear problems based on intermediate variables

Examples of these methods are:

- Newton-Raphson method
- Quasi-Newton methods
- Neighborhood search method

Probing all combinations or direct search methods One of the simplest methods class of optimisation are direct search methods. They only use zero-order information, or direct information. When the gradients can be determined, often these methods are inefficient. However, they are often very general applicable and can be used for almost any search space.

Advantages

- When the optimum is possible, it will be found, eventually.

Disadvantages

- Requires a lot of time, maybe even an impossible amount of time.
- Works only in discrete problems.

Grid search Grid search determines for a number of points the values and compares them. The smallest (or highest) function is the first approximation for the optimum and a new grid can be determined.

Monte Carlo Method A well-known and often used method for this is the Monte Carlo Methods, which picks random points, calculates the values of the object-function and compares them.

Successive coordinate search This method is also a descent method and searches in each coordinate direction. The step size is determined by a line search close to the line minimum.

Hill-climbing methods and direction methods The idea behind descent methods is walking down the hill. This can involve gradient information, which make it a gradient method. The best known example is the steepest descent gradient method, which walks downhill along the steepest gradient. The big disadvantage of these methods is that they are very sensitive to local optima. Another problem is cycling, where the algorithms keep 'walking' around the optimum, instead of finding it.

A few examples of these methods are:

- Steepest Ascent Hill-climbing (SAHC)
- Next-Ascent Hill-climbing (NAHC)
- Random Mutation Hill-climbing (RMHC)
- Downhill Simplex Method
The Downhill Simplex Method uses a reflection of the highest point over the two lower points to determine a new (hopefully lowest) point. In this manner the algorithms walks downhill.
- Powell's Quadratic Convergent Method
- Conjugate gradient methods
- Generalized reduced gradient method (GRG)
- Modified feasible direction method

For more detailed information on these methods, refer to Press (Press et al. 2002) and Bletzing (Bletzing n.d.).

4.6.5 Genetic algorithms

Genetic algorithms are an optimisation method based on the Darwinian principle of "Survival of the Fittest" (Darwin 1859) and mimic the related evolution process. The problem and its parameters, forming the parametric model, are encoded in a chromosome (DNA-string) which can be decoded (grown) to a solution. This chromosome can be part of an individual, a cell or directly part of the population, based on the exact method. The success of the solution is evaluated by a fitness function.

By (sexual) reproduction the algorithms evolve the population to a better population. Usually reproduction implies crossover (crossing genetic material) and random mutation (mutating the children with a very small probability to increase the diversity).

Main advantages of this method are that Genetic Algorithms are general applicable, play well with large, complex search spaces and can find global optima. Main disadvantages are that they are slower than specific algorithms, because of their lack of knowledge about the problem.

For more information on Genetic Algorithms, read Mitchell (Mitchell 1996), who extensively cover all aspects of genetic algorithms important to structural optimisation. A sexy fact is that a principle called 'elitism' works very well, while this in reality would be the same as cloning.

History and basics

Genetic algorithms In the 60's genetic algorithms were invented and developed by John Holland, which lead to a book in 1975: "Adaption in Natural and Artificial Systems". Simultaneous, Rechenberg developed evolution strategies, a similar idea.

Currently the two ideas have been merged in one concept, with genetic algorithms benefitting from the performance improvements from evolution strategies.

In 1992 John Koza developed the idea of Genetic Programming (GP), which involves evolving programs with genetic algorithms.

Genetic algorithms are defined as a population-based model that uses selection and recombination operators to generate new sample points in a search space (Whitley 2003). Genetic algorithms are so-called nature-metaphores. They are based on ideas from nature, more specific the concept of evolution. Why evolution is being used will also be explained further.

Other systems which are nature-metaphores are for example neural networks and cellular automata.

Genetic algorithms are especially used in so-called NP problems, which stands for nondeterministic polynomial problems. This class of problems cannot be easily solved by analytical or simple numerical methods, since the calculation effort often increases exponentially with the order of the problem. However, it is possible to guess the solution and check it in polynomial time. A sub-class of NP-problems which is often mentioned is called NP-hard problems. Usually NP-problems are of the $O(2^n)$ order.

For example, imagine we have n cities. We want to define the shortest route for a salesman which is travelling between these cities. He wants to visit every city. It is very easy to just try all combinations, however with the increase of n , the possible combinations increase much more. This problem is known as the travelling salesman problem (TSP).

Typical GA process A typical genetic algorithm process looks like the process below. In pseudo-code:

- A. Creation of a population of chromosomes.
- B. Selection according to their fitness (Evaluation and selection).
- C. Breeding by crossover to produce new offspring (Crossover) and random mutation of new offspring. (Mutation)

D. Replacement of the old offspring by the new offspring (Replacement).

Like in nature, the process always starts with a certain population. This population is being evaluated, their fitness is being determined and usually based on this fitness the parents are selected. When the parents are selected the breeding starts by recombination, a process in which certain genes cross over between parents to the children. After this the children are being mutated with a very low probability. When this is done, the old population is replaced by the new one. In this process, hyperplanes in the solutions (the chromosomes) can be identified, which drive the search process.

The basic idea of the method is to start with a randomly generated set of design alternatives using the allowable values of each variable. Each design alternative is represented by a unique finite length binary string of 0s and 1s for binary coding. This set of designs is called the population in a given generation (iteration) Each design is also assigned a fitness value (usually the cost function or the penalty function). From the current population, a set of designs is selected randomly with a bias allocated to more fit members of the population. Random processes are used to generate a new set of designs for the next generation. The size of the population of each generation is kept fixed. Since more fit members of the population are used to create new designs, the successive generations have a higher probability of having designs with better fitness values. An advantage of this approach is that continuity and differentiability of functions are not required, as for the simulated annealing method.

The most common operators that are needed to implement a genetic algorithm are selection, crossover and mutation (Figure 4.41). Some of these operators were inspired by nature and, in the literature, many versions of these operators can be found. The choice or design of operators depends on the problem and representation scheme employed.

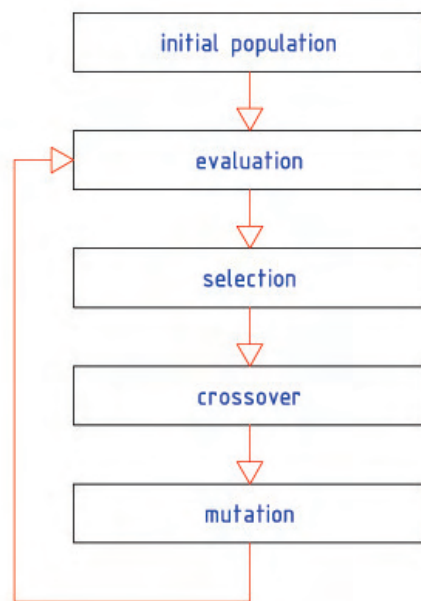


Figure 4.41: Flow chart of genetic algorithm.

Selection The aim of the selection procedure is to reproduce more copies of individuals whose fitness values are higher than those whose fitness values are low. The selection procedure has a significant influence on driving the search towards a promising area and finding good solutions in a short time. However, the diversity of the population must be maintained to avoid premature convergence and to reach the global optimal solution.

Crossover This operation is considered the one that makes the GA different from other algorithms. It is used to create two new individuals (children) from two existing individuals (parents) picked from the current population by the selection procedure. Some common crossover operations are one-point crossover, two-point crossover, cycle crossover and uniform crossover.

one-point crossover

```
parent 1    1 0 0 0 1 0 0 1 1 1 1
parent 2    0 1 1 0 1 1 0 0 0 1 1
```

```
new string 1 1 0 0 0 1 1 0 0 0 1 1
new string 2 0 1 1 0 1 0 0 1 1 1 1
```

two-point crossover

```
parent 1    1 0 1 0 0 0 1 1 0 1 0
parent 2    0 1 1 0 1 1 1 1 0 1 1
```

```
new string 1 1 0 1 0 1 1 1 1 0 1 0
new string 2 0 1 1 0 0 0 1 1 0 1 1
```

cycle crossover

```
parent 1    1 2 3 4 5 6 7 8
parent 2    a b c d e f g h
```

```
new string 1 1 b 3 d e 6 g 8
new string 2 a 2 c 4 5 f 7 h
```

uniform crossover

```
parent 1    1 0 0 1 0 1 1
parent 2    0 1 0 1 1 0 1
template    1 1 0 1 0 0 1
```

```
new string 1 1 0 0 1 1 0 1
new string 2 0 1 0 1 0 1 1
```

Mutation In this procedure, all individuals in the population are checked bit by bit and the bit values are randomly reversed according to a specified rate. Unlike crossover, this is a monadic operation. That is, a child string is produced from a single parent string. The mutation operator forces the algorithm to search new areas. Eventually, it helps the GA avoid premature convergence and find the global optimal solution.

mutation

```
old string 1 1 0 0 0 1 0 1 1 1 0
new string 1 1 0 0 1 1 0 1 1 1 0
```

The three steps are repeated for successive generations of the population until no further improvement in the fitness is attainable. The member in this generation with the highest level of fitness is taken as the optimum design.

The crossover rate determines the frequency of the crossover operation. It is useful at the start of optimisation to discover a promising region. A low crossover frequency decreases the speed of convergence to such an area. If the frequency is too high, it leads to saturation around one solution. The mutation operation is controlled by the mutation rate. A high mutation rate introduces high diversity in the population and might cause instability. On the other hand, it is usually very difficult for a GA to find a global optimal solution with too low a mutation rate.

The fitness evaluation unit acts as an interface between the GA and the optimisation problem. The GA assesses solutions for their quality according to the information produced by this unit and not by using direct information about their structure. In engineering design problems, functional requirements are specified to the designer who has to produce a structure which performs the desired functions within predetermined constraints. The quality of a proposed solution is usually calculated depending on how well the solution performs the desired functions and satisfies the given constraints. In the case of a GA, this calculation must be automatic and the problem is how to devise a procedure which computes the quality of solutions.

Fitness evaluation functions might be complex or simple depending on the optimisation problem at hand. Where a mathematical equation cannot be formulated for this task, a rule-based procedure can be constructed for use as a fitness function or in some cases both can be combined. Where some constraints are very important and cannot be violated, the structures or solutions which do so can be eliminated in advance by appropriately designing the representation scheme. Alternatively, they can be given low probabilities by using special penalty functions.

Conventional search techniques, such as hill-climbing, are often incapable of optimising non-linear multimodal functions. In such cases, a random search method might be required. However, undirected search techniques are extremely inefficient for large domains. A genetic algorithm is a directed random search technique, which can find the global optimal solution in complex multi-dimensional search spaces. A GA is modelled on natural evolution in that the operators it employs are inspired by the natural evolution process. These operators, known as genetic operators, manipulate individuals in a population over several generations to improve their fitness gradually. Individuals are likened to chromosomes and usually represented as strings of binary numbers.

GA's do not use much knowledge about the problem to be optimised and do not deal directly with the parameters of the problem. They work with codes which represent the parameters. Thus, the first issue in GA application is how to encode the problem under study, i.e. how to represent the problem parameters. GA's operate with a population of possible solutions, not only one possible solution, and the second issue is therefore how to create the initial population of possible solutions. The third issue in a GA application is how to select or devise a suitable set of genetic operators. Finally, as with other search algorithms, GA's have to know the quality of already found solutions to improve them further. Therefore, there is a need for an interface between the problem environment and the GA itself for the GA to have this knowledge. The design of this interface can be regarded as the fourth issue.

At the start of optimisation, a GA requires a group of initial solutions. There are two ways of forming this initial population. The first consists of using randomly produced solutions created by a random number generator. This method is preferred for problems about which no a priori knowledge exists or for assessing the performance of an algorithm. The second method employs a priori knowledge about the given optimisation problem. Using this knowledge, a set of requirements is obtained and solutions which satisfy those requirements are collected to form an initial

population. In this case, the GA starts the optimisation with a set of approximately known solutions and therefore converges to an optimal solution in less time than with the previous method.

Important control parameters of a simple GA include the population size (number of individuals in the population), crossover rate and mutation rate. A large population size means the simultaneous handling of many solutions and increases the computation time per iteration. However, since many samples from the search space are used, the probability of convergence to a global optimal solution is higher than when using a small population size.

4.6.6 Simulated annealing

Simulated annealing is an optimisation algorithm which provides a simulated analogy between an object function and the free energy of simple thermodynamics systems under the slow descendence of temperature. Annealing is a process where a solid is melted in a high temperature bath until all molecules can move independant of each other and after this it is cooled until all thermal mobility is lost. The molecules are able to rearrange themselves in a low energy state. The free energy of the solid is minized by this.

Simulated annealing is an approximation stochastic algorithm which towards the optimal solution. An important feature of this method is called 'accepting', where the better solutions are always accepted and the worse solutions sometimes get accepted. This way the algorithm can escape local optima. Like genetic algorithms, simulated annealing also provides a reasonable approximation of the optimum within a reasonable computation effort.

Orta-Rial (Orta-Rial 2000) provides an example of structural optimisation of trusses using simulated annealing.

Simulated annealing is inspired by an analogy between the physical annealing of solids (crystals) and combinatorial optimisation problems. In the physical annealing process a solid is first melted and then cooled very slowly, spending a long time at low temperatures, to obtain a perfect lattice structure corresponding to a minimum energy state. Simulated annealing transfers this process to local search algorithms for combinatorial optimisation problems. It does so by associating the set of solutions of the problem attached with the states of the physical system, the objective function with the physical energy of the solid, and the optimal solutions with the minimum energy states. Simulated annealing is a local search strategy which tries to avoid local minima by accepting worse solutions with some probability (Figure 4.42).

In the analogy between a combinatorial optimisation problem and the annealing process, the states of the solid represent feasible solutions of the optimisation problem, the energies of the states correspond to the values of the objective function computed at those solutions, the minimum energy state corresponds to the optimal solution to the problem and rapid quenching can be viewed as local optimisation.

The algorithm consists of a sequence of iterations. Each iteration consists of randomly changing the current solution to create a new solution in the neighbourhood of the current solution. The neighbourhood is defined by the choice of the generation mechanism. Once a new conclusion is created the corresponding change in the cost function is computed to decide whether the newly produced solution can be accepted as the current solution. If the change in the cost function is negative the newly produced solution is directly taken as the current solution. Otherwise, the current solution is unchanged.

In order to implement the algorithm for a problem, there are four principal choices that must be made.

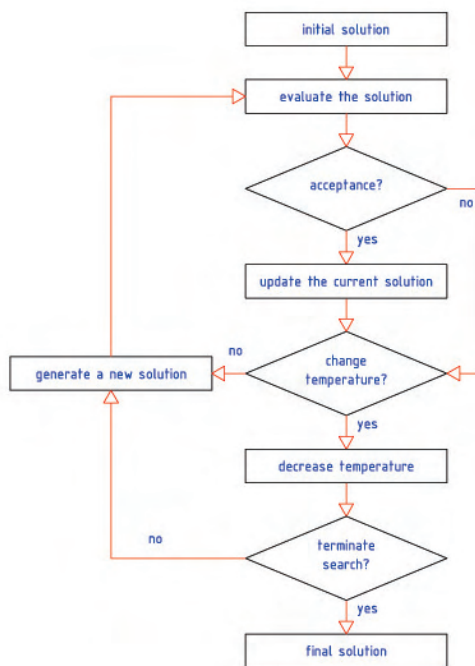


Figure 4.42: Flow chart of simulated annealing.

- representation of solutions
- definition of the cost function
- definition of the generation mechanism for the neighbours
- designing a cooling schedule

Solution representation and cost function definitions are as for GAs. Various generation mechanisms could be developed that again could be borrowed from GAs, for example, mutation and inversion. In designing the cooling schedule for a simulated annealing algorithm, four parameters must be specified. These are an initial temperature, a temperature update rule, the number of iterations to be performed at each temperature step and a stopping criterion for the search. One example of a cooling schedule is the geometric cooling rule. This rule updates the temperature by the following formula

$$T_{i+1} = cT_i, i = 0, 1, 2, \dots \quad (4.37)$$

where c is a temperature factor which is a constant smaller than, but close to 1.

4.6.7 Swarm behaviour and ant colony optimisation

Swarm behaviour or swarm algorithms are algorithms which use an analogy to the swarm behaviour of a swarm of birds. The birds always keep their distance from each other within certain limits. When they move too far from each other, they might lose their others, so

they move closer and when they move too close, they might collide, so they move further from each other. The movement of one bird influences every other bird directly or indirectly. This behaviour of one bird already resembles some behaviour of line searching or bracketing algorithms. When combining a lot of 'birds' in a three-dimensional or higher dimensional space one can imagine that the birds can search this space, especially when a 'bird' is preprogrammed with a certain "always moving" behaviour.

The emergent collective intelligence of groups of simple agents approach emphasises distributedness, direct or indirect interactions among relatively simple agents, flexibility, and robustness. Flexibility allows adaptation to changing environments, while robustness endows the colony with the ability to function even though some individuals may fail to perform their tasks. The number of its successful applications is exponentially growing in combinatorial optimisation, communication networks and robotics. However, it is fair to say that very few applications of swarm intelligence have been developed. One of the main reasons for this relative lack of success resides in the fact that swarm-intelligent systems are hard to program, because the paths to problem solving are not predefined but emergent in these systems and result from interactions among individuals and between individuals and their environment as much as from the behaviours of the individuals themselves. Therefore, using a swarm-intelligent system to solve a problem requires a thorough knowledge not only of what individual behaviours must be implemented but also of what interactions are needed to produce such or such global behaviour.

The daily problems solved by a colony include finding food, building or extending a nest, efficiently dividing labour among individuals, efficiently feeding the brood, responding to external challenges, spreading alarm, etc. Many of these problems have counterparts in engineering and computer science. One of the most surprising behavioural patterns exhibited by ants is the ability of certain ant species to find what computer scientists call shortest paths and it is this behavioural pattern that inspired computer scientists to develop algorithms for the solution of optimisation problems. The ant algorithm ant colony optimisation (ACO) is one outcome of these research efforts, and targets discrete optimisation problems. In fact, ACO algorithms are the most successful and widely recognised algorithmic technique based on ant behaviours.

Ant colonies, and more generally social insect societies, are distributed systems that, in spite of the simplicity of their individuals, present a highly structured social organisation. As a result of this organisation, ant colonies can accomplish complex tasks that in some cases far exceed the individual capabilities of a single ant. The field of ant algorithms studies models derived from the observation of real ants behaviour, and uses these models as a source of inspiration for the design of novel algorithms for the solution of optimisation and distributed control problems. The main idea is that the self-organising principles which allow the highly coordinated behaviour of real ants can be exploited to coordinate populations of artificial agents that collaborate to solve computational problems.

Ants coordinate their activities via *stigmergy*, a form of indirect communication mediated by modifications of the environment. Indirect interactions are very subtle: two individuals interact indirectly when one of them modifies the environment and the other responds to the new environment at a later time. For example, a foraging ant deposits a chemical on the ground which increases the probability that other ants will follow the same path. The idea behind ant algorithms is then to use a form of *artificial stigmergy* to coordinate societies of artificial agents. An important insight of early research on ants behaviour was that most of the communication among individuals, or between individuals and the environment, is based on the use of chemicals produced by the ants. These chemicals are called *pheromones*. By sensing pheromone trails foragers can follow the path to food discovered by other ants. This collective trail-laying and

trail-following behaviour whereby an ant is influenced by a chemical trail left by other ants is the inspiring source of ACO.

To test the *autocatalytic* or *positive feedback process* of the self-organising behaviour of the ants three double bridge experimental cases by Deneubourg are executed in 1990 (J.L. Deneubourg 1991).

In the first experiment the bridge between the ant nest and a food source consists of two branches of equal length (Figure 4.43). At the start, ants were free to move between the nest and the food source and the percentage of ants that chose one or the other of the two branches were observed over time. The outcome was that, although in the initial phase random choices occurred, eventually all the ants used the same branch. This result can be explained as follows. When a trial starts there is no pheromone on the two branches. Hence, the ants do not have a preference and they select with the same probability any of the branches. Yet, because of random fluctuations, a few more ants will select one branch over the other. Because ants deposit pheromone while walking, a larger number of ants on a branch results in a larger amount of pheromone on that branch; this larger amount of pheromone in turn stimulates more ants to choose that branch again, and so on until finally the ants converge to one single path.

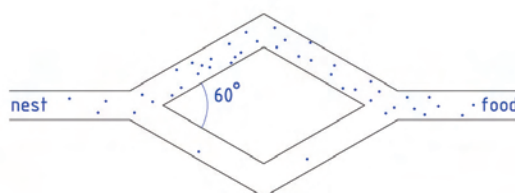


Figure 4.43: First experiment: two branches of equal length between the nest and the food source.

In the second experiment the bridge has two branches, with one branch twice as long as the other branch (Figure 4.44). In this case, in most of the trials, after some time all the ants chose to use only the short branch. As in the first experiment, ants leave the nest to explore the environment and arrive at a decision point where they have to choose one of the two branches. Because the two branches initially appear identical to the ants, they choose randomly. Therefore, it can be expected that, on average, half of the ants choose the short branch and the other half the long branch, although stochastic oscillations may occasionally favour one branch over the other. However, this experimental setup presents a remarkable difference with respect to the previous one: because one branch is shorter than the other, the ants choosing the short branch are the first to reach the food and to start their return to the nest. But then, when they must make a decision between the short and the long branch, the higher level of pheromone on the short branch will bias their decision in its favour. Therefore, pheromone starts to accumulate faster on the short branch, which will eventually be used by all the ants because of the autocatalytic process. Interestingly, it can be observed that, even when the long branch is twice as long as the short one, not all the ants use the short branch, but a small percentage may take the longer one. This may be interpreted as a type of path exploration.

In the third experiment, after convergence over the long branch, the ant colony is offered a new and shorter connection between the nest and the food source (Figure 4.45). This didn't affect the number of ants that was using the long branch; the short branch was only selected

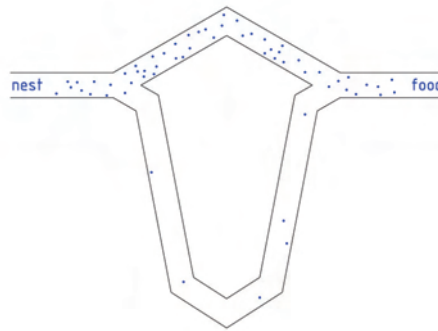


Figure 4.44: Second experiment: two branches of different length between the nest and the food source.

sporadically. This can be explained by the high pheromone concentration on the long branch and by the slow evaporation of it.

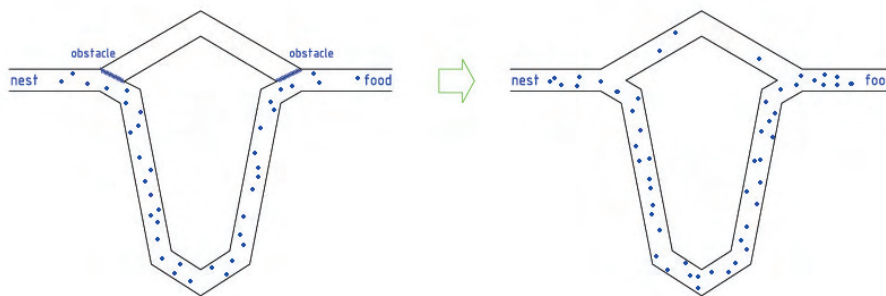


Figure 4.45: Third experiment: with the removal of the obstacles, the model again consists of two branches with different length between the nest and the food.

The double bridge experiments show that ant colonies have a built-in optimisation capability. By the use of probabilistic rules based on local information they can find the shortest path between two points in their environment.

The goal is to define algorithms that can be used to solve minimum cost problems on complicated graphs, where the minimum cost path (or the shortest path) between source and destination nodes needs to be determined. Unfortunately, the solving of a complicated graph can result in the following problem: the ants, while building a solution, may generate loops. As a consequence of the forward pheromone trail updating mechanism, loops tend to become more and more attractive and ants can get trapped in them. But even if an ant can escape such loops, the overall pheromone trail distribution becomes such that short paths are no longer favoured and the mechanism that in the simpler double bridge situation made the ant choose the shortest path with higher probability does not work anymore.

Because this problem is due to forward pheromone trail updating, it might seem that the

simplest solution to this problem would be the removal of the forward updating mechanism. In this way ants would rely only on backward updating. Still, this is not a solution. If the forward update is removed, the system does not work anymore, not even in the simple case of the double bridge experiment. Therefore, it is needed to extend the capabilities of the artificial ants in a way that, while retaining the most important characteristics of real ants, allows them to solve minimum cost path problems on generic graphs. In particular, artificial ants are given a limited form of memory in which they can store the partial paths they have followed so far, as well as the cost of the links they have traversed.

In experiments with foraging ants, it was shown that the pheromone evaporation rate is so slow compared to the time necessary for the ant colony to converge to the short path that, for modelling purposes, it can be neglected. When considering artificial ants things are different. Experimental results show that on very simple graphs, like the ones modelling the double bridge or the extended double bridge setups, pheromone evaporation is also not necessary. On the contrary, it improves the algorithms performance in finding good solutions to the minimum cost path problem on more complex graphs.

The experiments with the S-ACO method results in four conclusions

1. The differential path length effect, although important, is not enough to allow the effective solution of large optimisation problems;
2. Pheromone updates based on solution quality are important for fast convergence;
3. The larger the number of ants, the better the convergence behaviour of the algorithm, although this comes at the cost of longer simulation times;
4. Pheromone evaporation is important when trying to solve more complex problems

In the model of Deneubourg, the probability of choosing a branch at a certain time depends on the total number of ants that used the branch until that time. It is assumed that the amount of pheromone on a branch is proportional to the number of ants that used the branch to cross the bridge. With this assumption, pheromone evaporation is not taken into account: this is a plausible assumption, because the experiments typically last of the order of an hour, a time scale that may not be sufficient for the amount of pheromone to be reduced significantly. Let A_i and B_i be the number of ants that have used branches A and B after i ants have used the bridge. The probability $P_A(P_B)$ that the $(i + 1)th$ ant chooses branch $A(B)$ is

$$P_A = \frac{(k + A_i)^n}{(k + A_i)^n + (k + B_i)^n} = 1 - P_B \quad (4.38)$$

This equation quantifies the way in which a higher concentration on branch A gives a higher probability of choosing branch A , depending on the absolute and relative values of A_i and B_i . The parameter n determines the degree of nonlinearity of the choice function: when n is large, if one branch has only slightly more pheromone than the other, the next ant that passes will have a high probability of choosing it. The parameter k quantifies the degree of attraction of an unmarked branch: the greater k , the greater the amount of pheromone to make the choice non-random. The values of the parameters k and n that give the best fit to the experimental measures are $n \approx 2$ and $k \approx 20$.

The choice dynamics follows from the equation.

$$A_{i+1} = \begin{cases} A_i + 1 & \text{if } \delta \leq P_A \\ A_i & \text{if } \delta > P_A \end{cases} \quad (4.39)$$

and

$$B_{i+1} = \begin{cases} B_i + 1 & \text{if } \delta > P_A \\ B_i & \text{if } \delta \leq P_A \end{cases} \quad (4.40)$$

$$A_i + B_i = i \quad (4.41)$$

where δ is a random variable uniformly distributed over $[0,1]$.

Six design tasks as guidelines for attacking problems by ACO:

1. represent the problem in the form of sets of components and transitions or by means of a weighted graph, on which ants build solutions;
2. define appropriately the meaning of the pheromone trails, that is, the type of decision they bias. This is a crucial step in the implementation of an ACO algorithm and, often, a good definition of the pheromone trails is not a trivial task and typically requires insight into the problem to be solved;
3. define appropriately the heuristic preference for each decision that an ant has to take while construction a solution, that is, define the heuristic information associated with each component or transition. Notice that heuristic information is crucial for good performance if local search algorithms are not available or cannot be applied;
4. if possible, implement an efficient local search algorithm for the problem to be solved, because the results of many ACO applications to NP-hard combinatorial optimisation problems show that the best performance is achieved when coupling ACO with local optimisers;
5. choose a specific ACO algorithm and apply it to the problem being solved, taking the previous aspects into account;
6. tune the parameters of the ACO algorithm. A good starting point for parameter tuning is to use parameter settings that were found to be good when applying the ACO algorithm to similar problems or to a variety of other problems. An alternative to time-consuming personal involvement in the tuning task is to use automatic procedures for parameter tuning.

So, in conclusion, the ant colony optimisation approach has turned out to be more than just a fun metaphor. Recent developments, which combine the ant colony approach with local searches and/or other optimisation methods, are promising. What is the basic idea underlying all ant-based optimisation? It is to use a *positive feedback* mechanism, based on an analogy with the trail-laying trail-following behaviour of some species of ants and some other social insects, to reinforce those portions of good solutions that contribute to the quality of these solutions, or to directly reinforce good solutions. A virtual pheromone, used as reinforcement, allows good solutions to be kept in memory, from where they can be used to make up better solutions. Of course, one needs to avoid some good, but not very good, solutions becoming reinforced to the point where they constrain the search too much, leading to a premature convergence (stagnation) of the algorithm. To avoid that, a form of negative feedback is implemented through pheromone evaporation, which includes a time scale into the algorithm. This time scale must not be too large, otherwise suboptimal premature convergence behaviour can occur. But it must not be too short either, or otherwise no cooperative behaviour can emerge. Cooperative behaviour is the other important concept here: ant colony algorithms make use of the simultaneous exploration of different solutions by a collection of identical ants. Ants that perform well at a given iteration

influence the exploration of ants in future iterations. Because ants explore different solutions, the resulting pheromone trail is the consequence of different perspectives on the space of solutions. Even when only the best performing ant is allowed to reinforce its solution, there is a cooperative effect across time because ants in the next iteration use the pheromone trail to guide their exploration. The following makes ACO unique when considering other metaheuristics: it is a constructive, population-based metaheuristic which exploits an indirect form of memory of previous performance. This combination of characteristics is not found in any of the other metaheuristics.

4.6.8 Michell structures

Michell structures are structures of the least weight developed by A.G.M. Michell (an example of a Michell structure can be seen in Figure 4.46). A Michell structures assume the the tension and compression members of the structure lie in the direction of equal principal stress of form a structure of the least volume (and for a homogenous structure the least weight). A Michell structure is a redundant structure, which means that not all the forces can be found by statics.

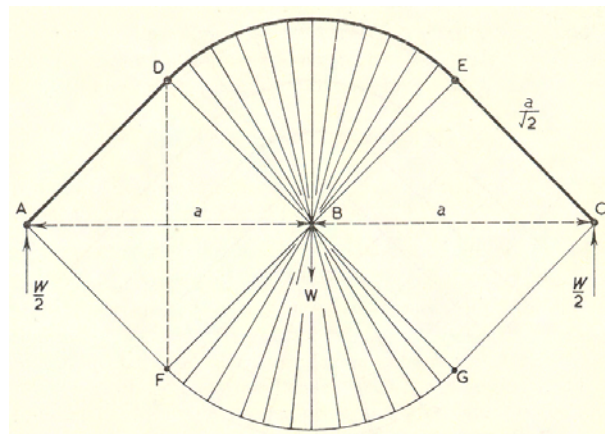


Figure 4.46: The most optimal Michell structure for carrying a point load. Image from (Owen 1965a)

Michell structures are well-known structures in the field of structural optimisation, sometimes outside the field of optimisation, such as the reference D'Arcy Thompson (Thompson 1942) makes to them when studying bone structures. However, not many structural engineers are familiar with these structures, probably because they are quite impractical and quite complex to understand. But they give a good insight in structures of the least weight and by creating structures close to these only little loss is achieved in structural efficiency.

Xie (Xie & Steven 1997b) shows that Michell structures are optimal with topology optimisation.

Michell structures in detail As stated, Michell structures are quite complex to understand since they require a lot of indepth mathematical knowledge. For the interested reader it is recommended to read Cox (Cox 1965), Owen (Owen 1965a) and Hemp (Hemp 1973) who give a good explanation on structures of the least weight in general, but also the different aspects of Michell structures. Also, Samyn (Samyn & Lateur 2000, Samyn 2000) gives some insight. However, he does not cover the real mathematics behind the structures.

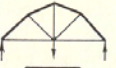
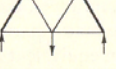
Column	(i)	(ii)	(iii)
Line	Structure	$\frac{\text{Vol.}}{WL(\frac{1}{f_c} + \frac{1}{f_t})^{1/2}}$	Efficiency %
1		$\frac{1}{2} \left(1 + \frac{\pi}{2} \right) = 1.28$	100
2		$\frac{\pi}{2} = 1.57$	81
3		$\frac{3}{2} = 1.5$	85
4		2	64
5		$\sqrt{3} = 1.73$	74

Figure 4.47: Table of Michell structures. Image from (Owen 1965a)

As stated, Michell structures assume a system of members (line elements) in the direction of the principal stresses σ_ϵ/σ_T (tension) and $-\sigma_\epsilon/\sigma_C$ (compression). The base of the layout of the field of orthogonal. The coordinates of such a system are α and β .

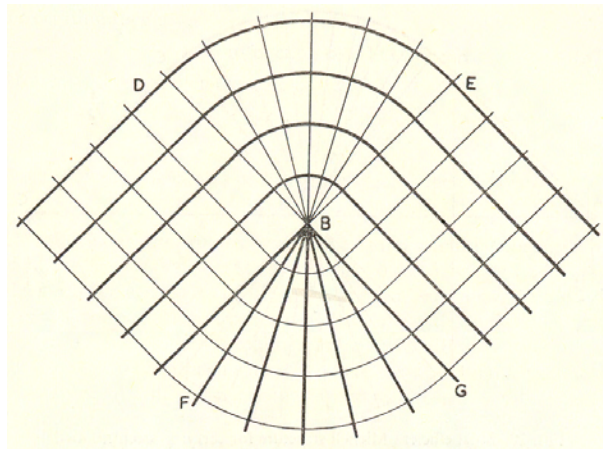


Figure 4.48: Michell strain field. Image from (Owen 1965a)

A line element ds is defined as

$$ds^2 = A^2 d\alpha^2 + B^2 d\beta^2 \quad (4.42)$$

where A and B are positive functions of α and β which describe the field. For these definitions applies:

$$\begin{aligned}
\frac{\partial x}{A\partial\alpha} &= \cos\phi \\
\frac{\partial y}{A\partial\alpha} &= \sin\phi \\
\frac{\partial x}{B\partial\beta} &= -\sin\phi \\
\frac{\partial y}{B\partial\beta} &= \cos\phi
\end{aligned}
\tag{4.43}$$

where x and y are the two-dimensional cartesian coordinates. Finally can be derived for the assumptions that all functions A and B must satisfy with (for more detailed explanation, refer to Hemp (Hemp 1973):

$$\left(\frac{\partial}{\partial\alpha}\right)\left(\frac{\partial B}{A\partial\alpha}\right) + \left(\frac{\partial}{\partial\beta}\right)\left(\frac{\partial A}{B\partial\beta}\right) = 0
\tag{4.44}$$

It can also be proved that equation 4.45 must be satisfied for Michell structures.

$$\frac{\partial^2\phi}{\partial\alpha\partial\beta} = 0
\tag{4.45}$$

When t_i is the thickness of each member along the lines, with for the α -lines t_1 and the β -lines t_2 , T_1 and T_2 can be defined as:

$$\begin{aligned}
T_1 &= \sigma_T B t_1 \\
T_2 &= -\sigma_C A t_2
\end{aligned}
\tag{4.46}$$

For the equilibrium then must be satisfied:

$$\frac{\partial T_1}{\partial\alpha} - T_2 \frac{\partial\phi}{\partial\beta} = 0
\tag{4.47}$$

and

$$\frac{\partial T_2}{\partial\beta} + T_1 \frac{\partial\phi}{\partial\alpha} = 0
\tag{4.48}$$

These equations are requirements for a solution, and cannot be directly written to one solution. That explains why there are more Michell structures, which satisfy these requirements. From now on an example shall be explained which meets these requirements.

The spoked wheel A well-known example of a Michell structure is a spoked wheel (which can be seen in Figure 4.49), which consists of a two-dimensional spokes field in tension and a rim in compression.

For this applies:

$$\begin{aligned}
\alpha &= r \\
\beta &= \theta \\
\phi &= \theta \\
A &= 1 \\
B &= r
\end{aligned}
\tag{4.49}$$

An equilibrium of the forces on a small length $Rd\theta$ on the rim requires:

$$P_\theta \cos\frac{d\theta}{2} = P_{\theta+d\theta} \cos\frac{d\theta}{2}
\tag{4.50}$$

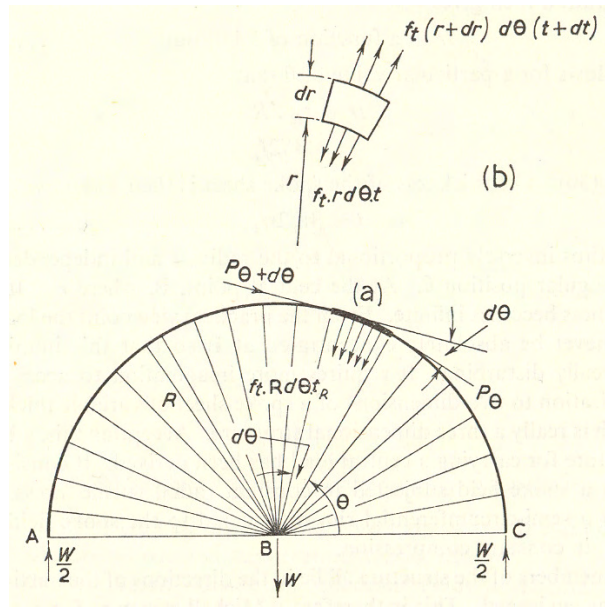


Figure 4.49: The spoked wheel. Image from (Owen 1965a)

from which can be derived:

$$P_{\theta} = P_{\theta+d\theta} \quad (4.51)$$

which means that the compressive forces in the rim must be constant. A vertical equilibrium of a small part of the rim requires:

$$P_{\theta} = \frac{W}{2} \quad (4.52)$$

A radial equilibrium of the rim requires:

$$2P_{\theta} \cdot \sin \frac{d\theta}{2} = f_t \cdot R \cdot d\theta \cdot t_R \quad (4.53)$$

which can be written to:

$$t_R R = \frac{P_{\theta}}{f_t} = \frac{W}{2f_t} \quad (4.54)$$

For the equilibrium of the spoke field can be written:

$$f_t \cdot r \cdot d\theta t = f_t (r + dr) d\theta (t + dt) \quad (4.55)$$

from which can be derived:

$$\frac{dt}{t} + \frac{dr}{r} = 0 \quad (4.56)$$

From this can be proven that for the spokefield applies:

$$V_s = \int_0^R \int_0^{\pi} t \cdot r d\theta dr = \frac{W}{2f_t} \cdot \pi \cdot R \quad (4.57)$$

where V_s is the volume of the spokefield.
 And for the rim applies:

$$V_r = \pi R \frac{W}{2} \frac{1}{f_c} \quad (4.58)$$

where V_r is the volume of the rim.
 For the total volume applies:

$$V = V_s + V_r = WR \frac{\pi}{2} \left(\frac{1}{f_t} + \frac{1}{f_c} \right) = \pi \left(\frac{WR}{f} \right) \quad (4.59)$$

The last only applies when $f = f_c = f_t$.

4.6.9 Theory of Michell structures

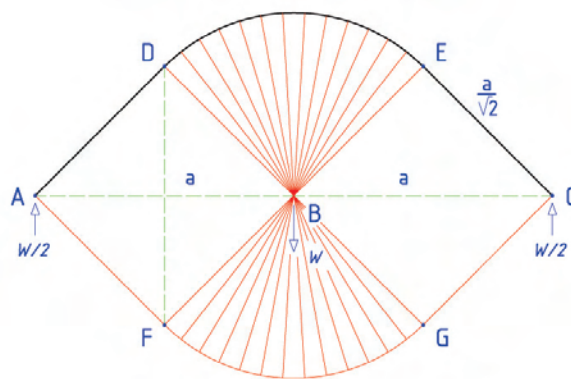


Figure 4.50: The most efficient Michell structure for carrying a central load w . All members are in tension or compression.

In another example, in *The analysis of light structures* Owen (Owen 1965b) studies structures of minimum volume of material as done by Michell.

Owen writes; suppose a typical compression member is designed to work to a mean compressive stress f_c and a typical tension member to a mean tensile stress f_t . If P_c is the compressive force in a typical strut, the area A_c of the member will be given by

$$A_c f_c = P_c \quad (4.60)$$

Similarly if P_t is the tensile force in a typical tie, the cross-sectional area A_t of the tie is given by

$$A_t f_t = P_t \quad (4.61)$$

However, Owen prefers to represent the force in a typical member jj of a structure by P_{jj} and to take this force as positive when it is tensile. P_{jj} will then be replaced when appropriate by either P_t or P_c , and both P_t and P_c , will be positive values. The x component of the force in jj exerted on the joint j will be

$$\frac{P_{if}(x_f - x_j)}{l_{jf}} \quad (4.62)$$

and the x component that it exerts on the joint f

$$-\frac{P_{if}(x_f - x_j)}{l_{jf}} \quad (4.63)$$

By denoting the external loadings acting on the joints j and f in the direction of the axes for equilibrium, Owen finally comes to a constant which can be written as

$$k_m = \Sigma(xX + yY + zZ) \quad (4.64)$$

so k_m is the sum of the products of coordinates and corresponding force components.

When f_t for all ties and f_c for all struts are constant and when V_t and V_c are respectively the volume of the tension and compression members, then

$$V_t f_t - V_c f_c = k_m \quad (4.65)$$

Or in words, the volumes of the tension and compression members (V_t and V_c) multiplied with respectively the tension and compression stresses should be in equilibrium with the external loads acting on the structure. The total volume of the whole structure can be written as

$$V = V_t + V_c V = V_t \left(1 + \frac{f_t}{f_c}\right) - \frac{k_m}{f_c} V = V_c \left(1 + \frac{f_c}{f_t}\right) + \frac{k_m}{f_t} \quad (4.66)$$

The volume of the joints is ignored.

Owen then states that since the volume of a structure cannot be negative these results indicate that when k_m is positive the structure of least volume, if this exists, will be one which has no compression members, i.e. $V_c = 0$, and the least volume will then be $\frac{k_m}{f_t}$. On the other hand, if k_m is negative, then a structure which has the least volume will be one which has no tension members and that this least volume will then be $-\frac{k_m}{f_c}$. When k_m vanishes a dilemma arises because the theoretical least weight may now be zero, corresponding to V_t or V_c zero. This indicates that structures composed entirely of compression or tension members are no longer possible means of connecting the specified loads. Such structures must then contain a combination of tension and compression members. Owen then uses the concepts of virtual work to give a formula from which it can be observed that a Michell structure will have the least volume.

The simplest Michell strain field which can be imagined is that in which all the strains are equal in all directions. A member in any direction in this field will be strained the same amount as any other member. The structure will then be all in compression or all in tension. There is often an infinity of possible minimum structures which will each have the volume $\frac{m_m}{(f_c \text{ or } f_t)}$, and this is the minimum possible volume of structural material to carry the given loads. Any geometry of such bars which maintains a specified set of loads in equilibrium is then as light as any other set of bars or any combination of such bars provided always equilibrium is maintained. Such arrangements of bars can range from mechanisms to highly redundant structures. So, structures as in Figure 4.51, where all the members work to a tensile stress f ,

are now recognisable as minimum structures.

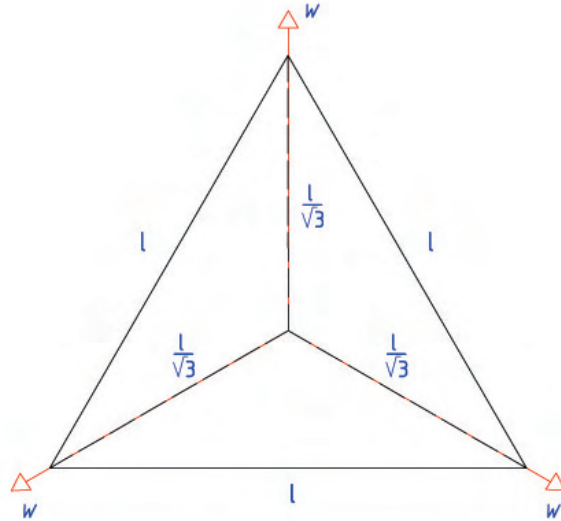


Figure 4.51: A minimum weight structure for concentric loads.

a Michell structure of a centrally loaded simply supported beam

In a plane, if one principal strain at a point is extensional and the other compressive, it is known that these strains must be at right angles. A simple set of plane curves which can depict a strain field is that of lines radiating from a point and concentric sectors of circles centred on this point. In this field, if the radial displacement u at a radial distance r is er and if the tangential displacement v here is $-2er\theta$, where θ is the angle between the radius and some given direction, then the radial strain is $\frac{\partial u}{\partial r} = \epsilon$, the tangential strain $\frac{u}{r} + \frac{\partial v}{r\partial\theta} = -\epsilon$, and the shear strains on radial and tangential planes vanish. These radial and tangential extensional strains are then principal strains and this field is of the kind that Michell postulates.

Analogy with pneumatic structures To give better insight, an analogy with pneumatic structures can be made.

The same results can be derived from the analogy with pneumatic structures. The rim under compression is replaced by a pneumatic structure (a membrane, which can only take tensile stresses) and the tensile stress in the spoke field can be replaced with the universal pressure of a gas. The spoked wheel can thus be inverted to a pneumatic structure as in Figure 4.53, where the radius of the half-circle shaped pneumatic structure is R and the overpressure is p over a length b . The opening angle α is 90° , therefore, the tensile forces per length at the supports (A and B) have only a vertical component, $n_v = n = pR$ (n is the support reaction per length) or $N_v = N = pbR$. This formula (also known as the kettle formula) is analogous with Equation 4.67.

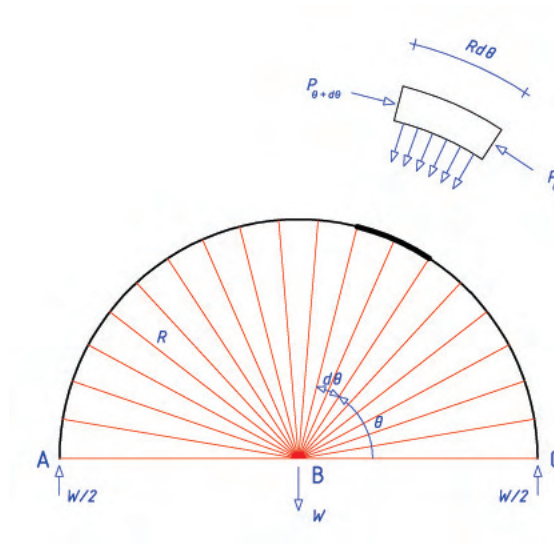


Figure 4.52: A Michell structure for carrying a central load w on two supports.

$$\begin{aligned}
 t \cdot r &= \frac{W}{2f_t} \approx N = nbR \\
 \text{with} \\
 t &\approx b \\
 r &\approx R \\
 W/2 &\approx N \\
 ft &\approx p
 \end{aligned}
 \tag{4.67}$$

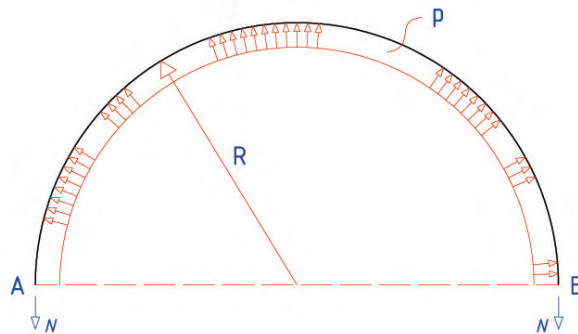


Figure 4.53: A pneumatic structure analogous to a Michell structure.

Returning to the Michell structure, the thickness of the spoke sheet is thus inversely proportional to the radius r and independent of the angular position θ . At the central point B , where $r = 0$, the thickness become infinite. From the practical viewpoint the load W can never be absolutely concentrated at B so that this infinity is not really disturbing. It requires more imagination to accept the idealisation to two dimensions of a spoke sheet of variable thickness which is really a three dimensional structure. Accepting this, a beam structure for carrying

a central load has been derived. It consists of (i) a spoke field subjected to constant radial tensile stress, and (ii) a semi-circumferential rim orthogonal to the spoke field and in constant compression.

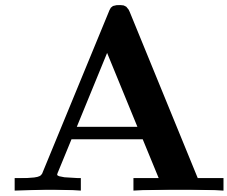
The members of the structures all lie in the directions of the maximum strains envisaged. This is therefore a Michell structure for carrying a central load. The volume of the spoke field is

$$\int_0^R \int_0^\pi t \cdot r d\theta \cdot dr = \int_0^R \int_0^\pi \frac{W}{2f_t} \cdot d\theta \cdot dr = \frac{W}{2f_t} \cdot \pi \cdot R \quad (4.68)$$

and the volume of the rim is

$$\frac{W}{2f_c} \cdot \pi \cdot R \quad (4.69)$$

Appendices



A.1 Example projects

The project descriptions below are not thorough descriptions of the structural design and engineering of these structures, but try to provide a tiny view in how the architects and structural engineers found the form of these structures, illustrated with images of the structures themselves.

A.1.1 Sagrada Familia - Barcelona, Spain (Gaudi)

RECOMMENDED STUDY MATERIAL

Title	Author	Year
The Essential Gaudi	J. Bonet	2001

As already explained, Antoni Gaudi is the absolute founding father of form finding with his hanging models. For his most famous building, the Sagrada Familia in Barcelona, Spain, he used a physical hanging chains model, built from wires and tiny sand bags. By adjusting the lengths of the wires he could find the shape he desired.

Next to this, Gaudi used mathematical principles, like ruled surfaces and surfaces of revolution, to create the geometry for parts of his buildings. Many methods and principles have been discovered (i Armengol 2001) in his shapes of the Sagrada Familia



Figure A.1: Sagrada Família in Barcelona, Spain. Image from (Zerbst 2002)

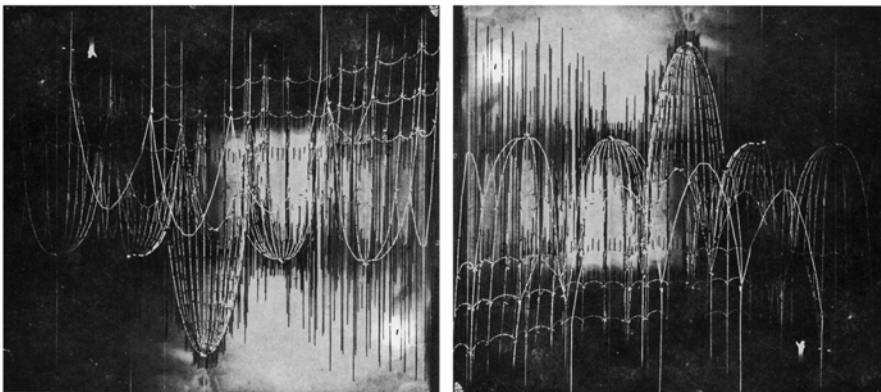


Figure A.2: Sagrada Família in Barcelona, Spain. Image from (Zerbst 2002)



Figure A.3: Sagrada Familia in Barcelona, Spain. Image from (Zerbst 2002)

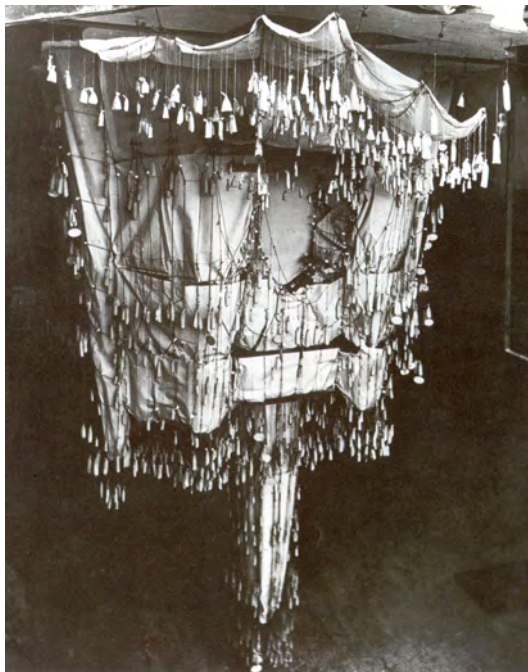


Figure A.4: Sagrada Familia in Barcelona, Spain. Image from (Zerbst 2002)

A.1.2 Multihalle Mannheim - Mannheim, Germany (Frei Otto)

RECOMMENDED STUDY MATERIAL

Title	Author	Year
IL13	Frei Otto, et al.	1978

A very famous building in the world of form finding is the Multihalle in Mannheim, Germany, which was researched by Frei Otto and the ILEK (für Leichtbau Entwerfen und Konstruieren 1978).

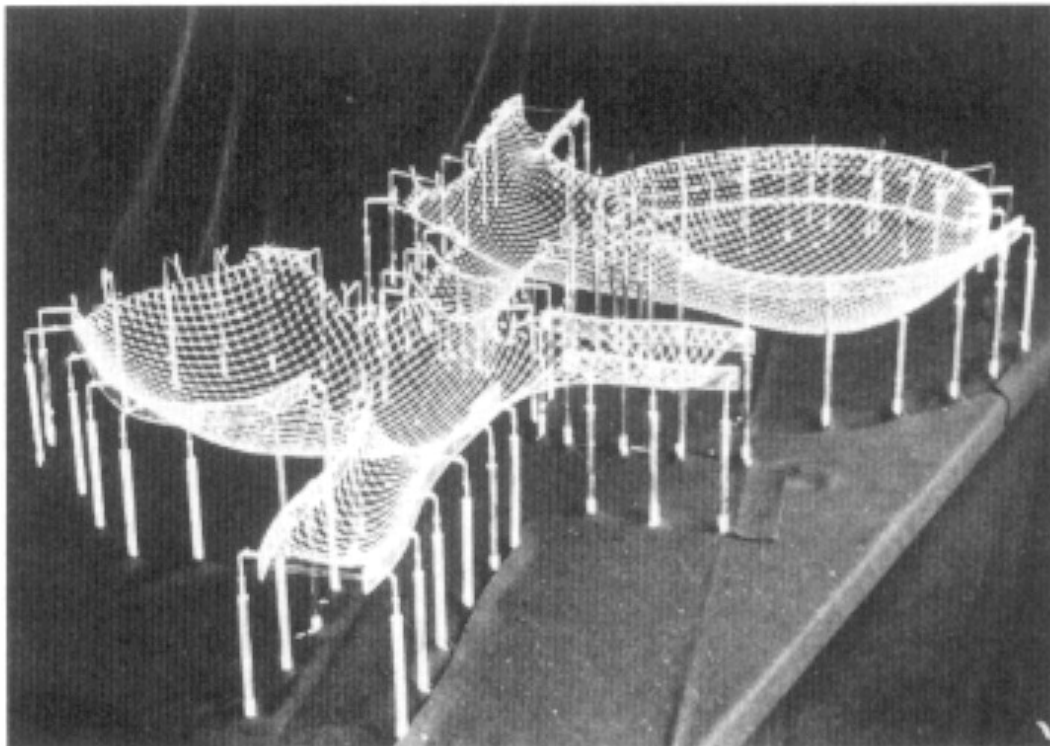


Figure A.5: Picture of the physical model of the Multihalle Mannheim. Image from Chris Williams

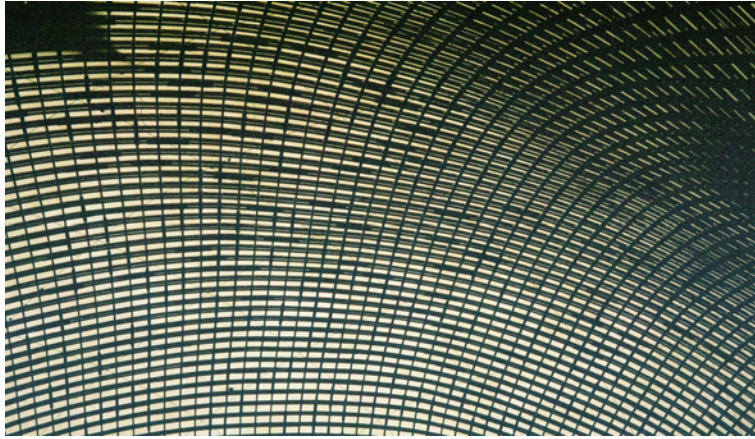


Figure A.6: Picture of the Multihalle Mannheim grid.



Figure A.7: Picture of the Multihalle Mannheim grid.



Figure A.8: Picture of the Multihalle Mannheim grid.

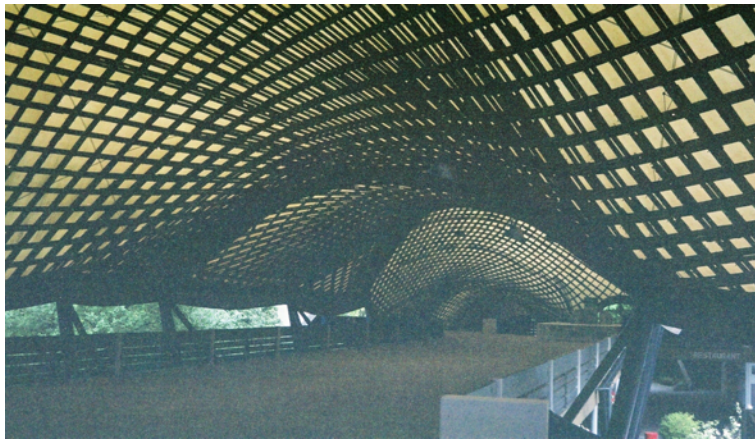


Figure A.9: Picture of the Multihalle Mannheim grid.

A.1.2.1 Background

Every two years a garden exhibition is held in one of the major cities in the Federal Republic of Germany. In 1970 it was decided that this Bundesgartenschau of 1975 was to be held in Mannheim (Happold & Liddell 1975). A master plan was developed for the area of Herzogenried park, where the festivities would take place. The plan included a large covered space, where a variety of activities could take place. The winning design for this space was the grid shell of Frei Otto and Ove Arup & Partners as structural engineers. Otto, famous for his structures of tension nets, used hanging models for his designs. Also the Multihalle of Mannheim was designed with hanging models.

The complex consists of a multi-purpose hall, where a range of activities can take place, such as exhibitions, flower shows, entertainment, concerts, theatre, sports activities, etc. In a second smaller hall a restaurant is situated. The halls are connected by a covered link. Figure A.10 shows an aerial view of the complex.



Figure A.10: Areal view of the Multihalle. Image from Burkhardt et al. 1978



Figure A.11: Inside view of the Multihalle. Image from Burkhardt et al. 1978

A.1.2.2 The roof

The Multihalle lies as an artificial hill in its surroundings. The grid shell is designed in such way that the shape continues the hilly landscape of the garden. The enclosed building area of 3600 m² is air conditioned and it is covered with PVC coated fabric. The grid has a maximum longitudinal span of 85m. It is built up out of a double layered mat of laths of Hemlock Pine. This performed best in test with respect to shrinkage and creep. It was also selected for its straight grain and availability in long lengths. The laths have a cross section of 50x50mm and are spaced on 500mm. Approximately 72000m of lath was used to construct the shell. The grid is supported by four different edge supports: concrete foundations, cables, laminated timber beams and arches. Diagonal stability is improved by applying cross ties. Pairs of 6mm cables are spaced at 4,5m in both directions.

After completion the roof was tested by loading it to 1,7 times the design load. This was applied by hanging dust bins filled with 90 l. of water on every ninth node. Deflections stayed well under the calculated deflection, proving the grid shell a safe structure.

A.1.2.3 Structural modelling and analysis

Physical modelling The initial form finding of the grid shell was entirely performed with physical modelling. At first, a wire model was made of the preliminary design. A second hanging model was made using the system line of the structure, to determine the initial data on node coordinates. This model had to be very accurate as an error will be enlarged when transferring the data on a full scale construction. Other methods of form finding, i.e. drawing and computing the coordinates were considered, but these appeared not to be better. To correctly compute the coordinates, input data was needed on form behaviour of the grid, but this was not available. Also the number of iterative steps to calculate the coordinates would be numerous and time consuming.

The model was made of rings and links (Figure A.13). Although these were machine manufactured, the sizes of the elements were not exact, due to tolerances in the manufacturing process and wearing of the tools, so it was impossible to rule out all imperfections. One of every 3 laths was modelled. In the model a mesh was used of 15mm, which represented 1,5m in the full scale structure. The intermediate nodes would be interpolated afterwards. The model was set up on a marble plate, so inaccuracies due to shrinkage or distortion of the base of the model was ruled out.

A fun detail is that some of the loads were provided by nuts hung on strings at the edges of the model, as can be seen on some of the photographs. A picture of one of the physical models can be seen in Figure A.5. Also other standing models were built from laths.

Computer form finding The coordinates of the nodes were determined by taking stereo photographs of the model. With these coordinated, the structure could be analysed by computer calculations. Because of inaccuracies of the model, not all members of the hanging model were in tension. To correct this, the correct geometry was calculated using the force density method. The intermediate results of the iterative steps were analysed. Deviations of a medium force smaller than 15% were considered non critical. When larger deviations occurred, adjustments were made in geometry. From this calculated suspended net, the data needed for production and erection was derived (fur Leichtbau Entwerfen und Konstruieren 1978).

Structural analysis When Ove Arup & Partners started with their designs, very little reference material was available. Only three much smaller grid shells were built before. Initial studies were performed to determine the design load and hand calculations on shell buckling were made. Structural design was started before the final geometry was finished. To gain

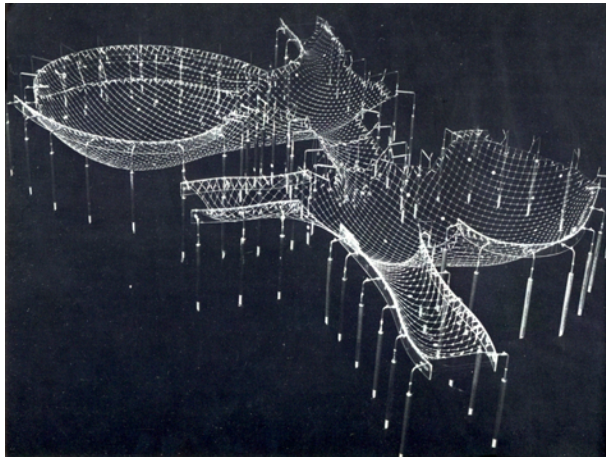


Figure A.12: Hanging model (Burkhardt et al 1978).

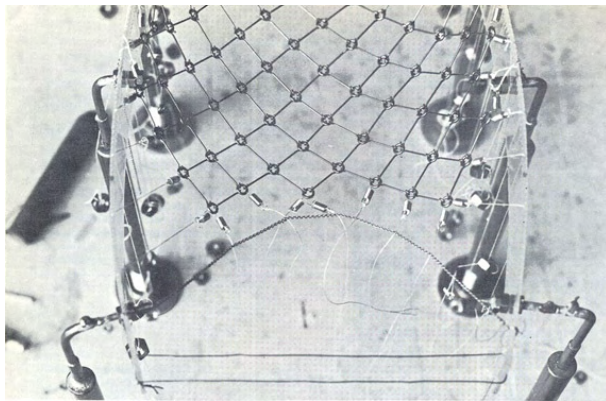


Figure A.13: Detail of the model (Burkhardt et al 1978).

knowledge on behaviour of grid shells, tests on a working model of the Essen grid shell were executed. The results showed that lath size had to be increased to enhance buckling resistance, to 100x100mm. This would give problems however with forming the shell, as more force is needed to bend the laths with a bigger cross section. Also the contract was already let and a lath size of 50x50mm was agreed. Decided was to apply a double layered mat, so bending flexibility was maintained during construction. After applying shear blocks between the layers, sufficient out of plane bending strength will be provided.

Design loading was determined by using wind and snowfall records in the area and by wind tunnel testing on a 1:200 scale model. This way, the design could be fully optimized, instead of just using normative average loading values. Also tests were carried out on the nodes and to investigate stress relaxation of the timber.

To determine a collapse load, tests were executed on a model of the grid shell. To correctly model the full size structure, dimensional analysis was used, which means scaling the factors that govern the behaviour of the physical system. Perspex members were used to model the grid. One model member represented six double layer members on full scale (Figure A.14).

The model was tested by hanging 100mm nails on the nodes and dial gauges were used to measure the deflections (Figure A.15).

The test results were compared with the results of computer calculations. The collapse load determined by the tests was $2,8 \text{ kN/m}^2$. The calculations gave a value slightly over 1 kN/m^2 . This difference occurs because the model does not scale the shear deformation of the full scale structure. This shear resistance is largely controlled by the individual slip per unit of force of the joints. The Perspex model corresponds to a full size structure with a very high value of joint stiffness, thus resulting in a high collapse load.

Grundig describes some of the computation, which seems to be an early force density method.

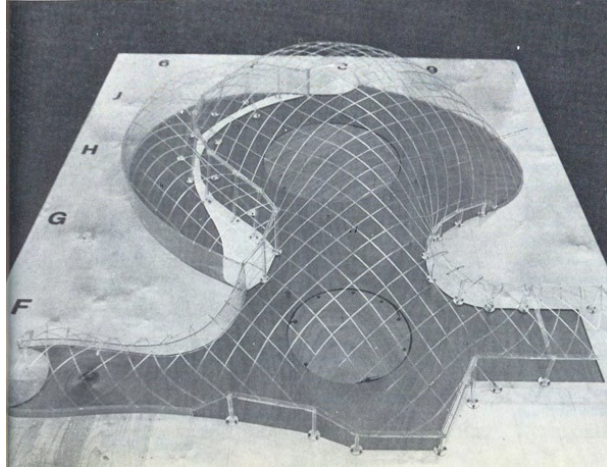


Figure A.14: Test model. Image from Burkhardt et al. 1978

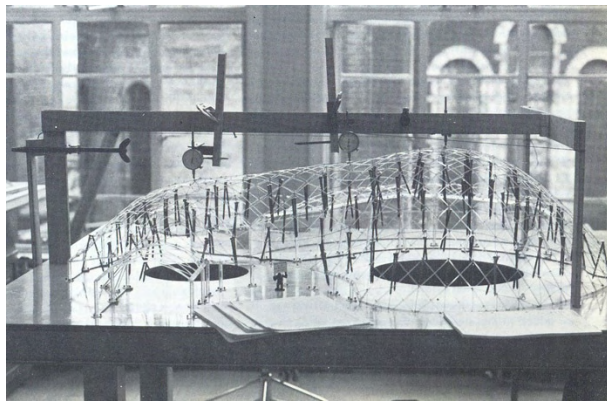


Figure A.15: Tests on the model. Image from Burkhardt et al. 1978

A.1.2.4 Connection details

Typical node joint The laths are bolted together in the nodes. To provide slipping of the outer layers during erection, these layers have slotted holes. After erection, shear resistance is needed, so the bolts are tightened to provide sufficient friction. Testing indicated that tension in the bolts would decrease in time, due to shrinkage of the timber. To prevent this, spring washers are applied (Figure A.16 and Figure A.18).

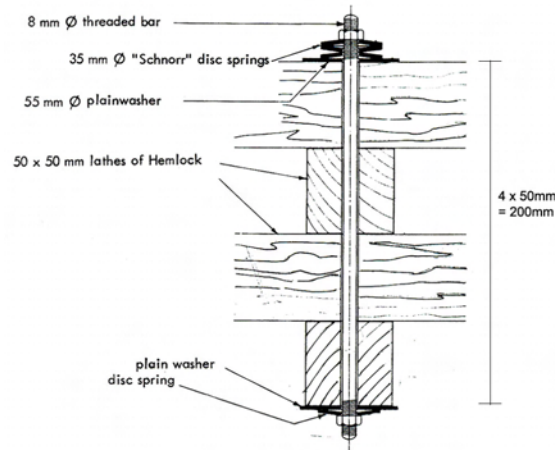


Figure A.16: Typical node joint. Image from Burkhardt et al. 1978



Figure A.17: Photo of a typical node joint. Image from www.kunst.uni-stuttgart.de

Joints in the laths The laths are prefabricated into laths up to 40m by finger jointing. The joints used was 20mm with a 6mm root, to suit the machines of the factory. Quite a lot of joints broke during site handling and erection due to this short connection length. The laths were

repaired by nailing 50x25mm lapping pieces to each side. This was also used to lengthen the laths into the required length.

Boundary connections Four types of edge connections are used in the Multihalle (Figure A.18). Originally, Frei Otto designed all boundaries on columns as cable edges. Cable edge supports are possible where boundary forces are more or less constant and where the change in angle of the boundary system line at the column is not that large that excessive support reactions are caused. These conditions were only met at parts of the restaurant. To connect the grid shell to the cable, it is first connected to a plywood board. This board also helps to cope with the differences in distributed lath forces and the cable reaction force. At the columns the cables are brought together (Figure A.19).

Where cable supports could not be applied, edge beams are used. 60x500mm laminated timber beams are connected on either side of the grid. The laths are bolted to these beams. Also where the grid is connected to the concrete support, it is first connected to timber beams. The timber beams are connected to the steel columns with steel plates. These plates are bolted to the beams and welded to the columns (Figure A.21). The connection itself was simple, but the geometry was not as for every connection the angles were different. The cutting profile for the plates had to be determined accurately to provide production drawings. A special computer program was written for this task. Also the production drawings for the arches were produced by a specially written computer program.

At the valley between the Banana and the Multihalle a laminated timber beam is applied with a circular section. Steel connectors connect the grid to the valley beam (Figure A.20).

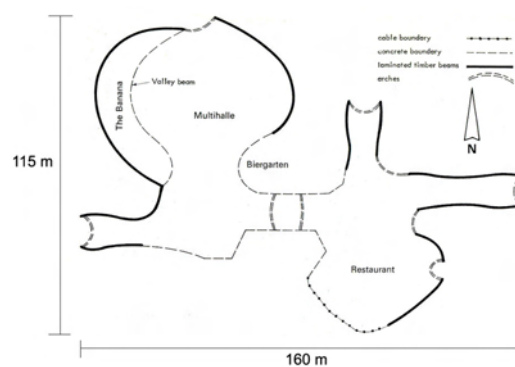


Figure A.18: Edge layout. Image from Burkhardt et al. 1978

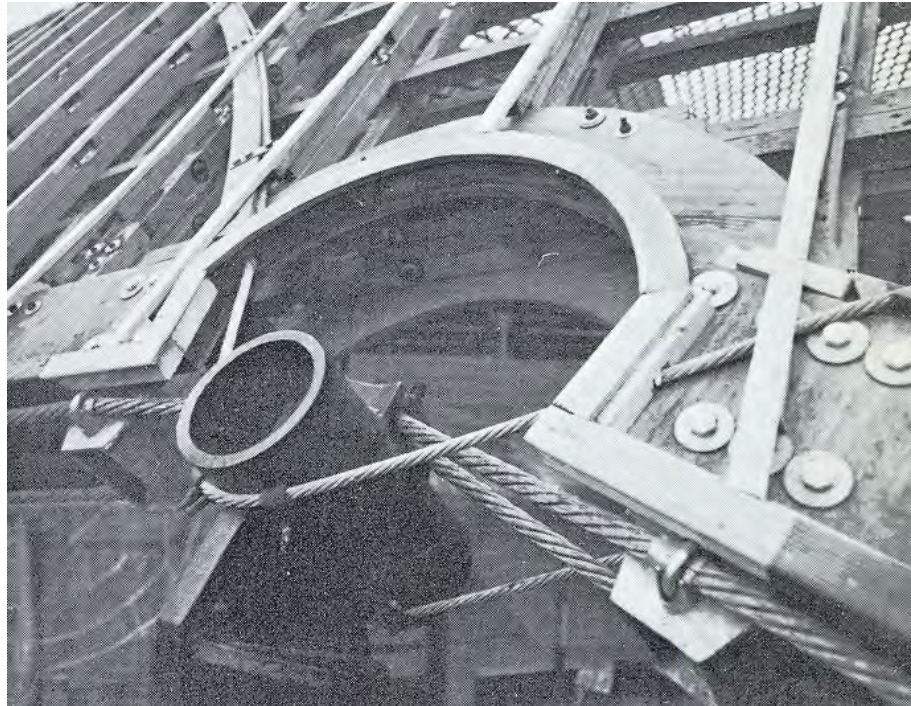


Figure A.19: Cable edge connection. Image from Burkhardt et al. 1978

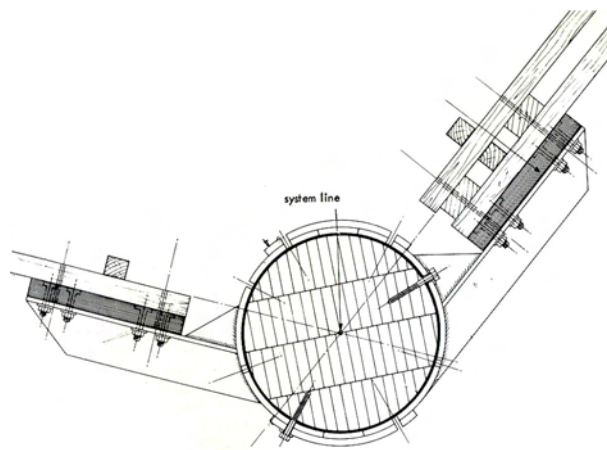


Figure A.20: Valley beam connection. Image from Burkhardt et al. 1978

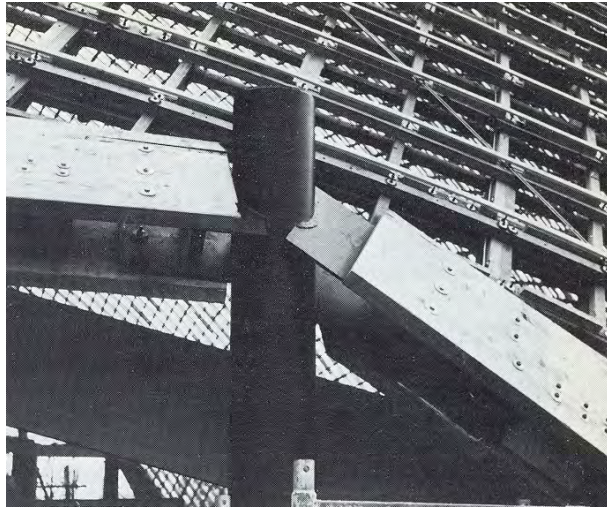


Figure A.21: Edge column connection. Image from Burkhardt et al. 1978

A.1.2.5 Assembly

As with the Essen grid shell, the Mannheim grid was supposed to be lifted into shape by cranes. Calculations however, showed that four 200 tonnes cranes were needed over a period of three weeks. The high costs of this forced the contractors to think of other options. Finally, the grid shell was erected by pushing up the lattice from underneath. Fork lifts were used to lift the scaffolding towers (Figure A.23). By using these, the horizontal movement of the scaffolds as the shape of the lattice changed could be followed easily. To spread the forces on the grid, H-shaped timber spreaders were used. A ball joint between the scaffold and spreader provided rotation to fit the curve of the shell. To reduce costs, as few scaffolds as possible were used. This resulted in quiet long spans between the scaffolds. To eliminate low areas between the scaffolds, flying struts were used (Figure A.24).

The PVC coated fabric is applied and fitted to the structure on site (Figure A.25). It is made of sheets of the fabric, hot welded together, and attached to the grid with over 400.000 staples.

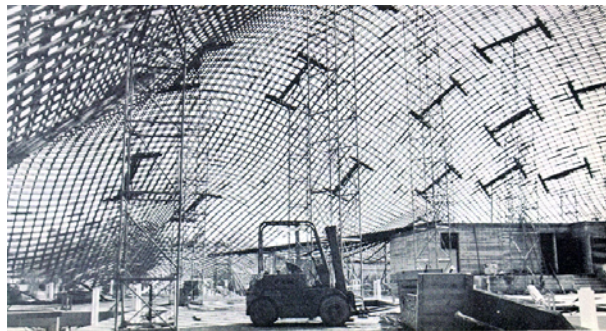


Figure A.22: Under construction. Image from Burkhardt et al. 1978

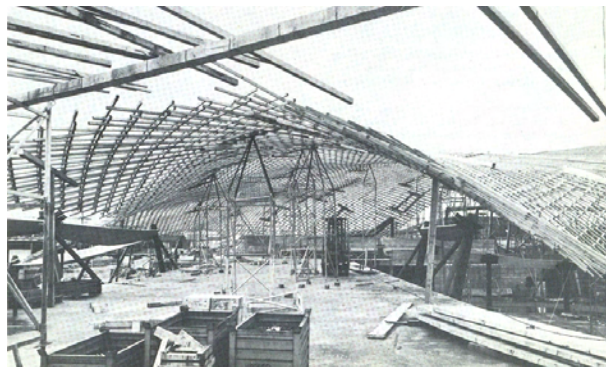


Figure A.23: Scaffolding towers. Image from Burkhardt et al. 1978

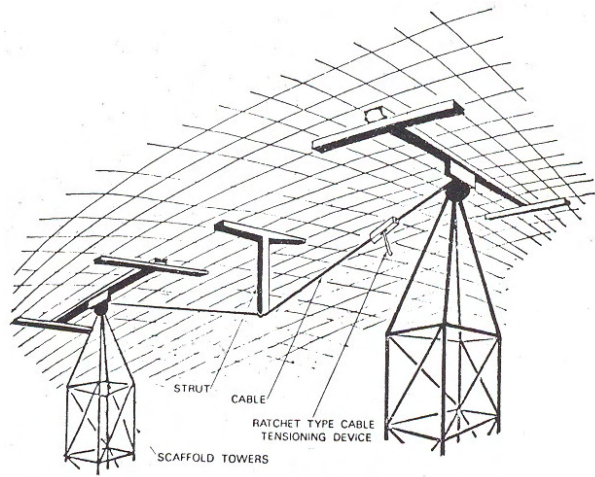


Figure A.24: Intermediate strut. Image from Burkhardt et al. 1978



Figure A.25: Applying the roof skin. Image from Burkhardt et al. 1978

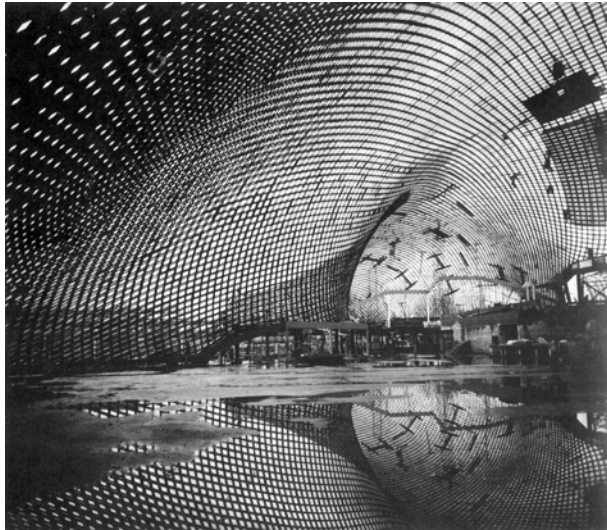


Figure A.26: Interior.

A.1.3 British Museum - London, United Kingdom (sir Norman Foster)

RECOMMENDED STUDY MATERIAL

Title	Author	Year
The definition of curved geometry for widespan enclosures. (enclosed in this reader)	C. Williams	2000
The Analytic and numerical definition of the geometry of the British museum great court roof	C. Williams	2000
The design and manufacture of the British museum great court roof	S. Brown and M. Cook	2002

For the Great Court Yard roof of the British Museum in London, UK, by sir Norman Foster a combination of various analytic and numerical methods have been used by Buro Happold and C.J.K. Williams to find the form of the roof.

First the shape of the roof was described by a function (Williams 2000) (Equation A.1 to A.4).

$$z = z1 + z2 + z3 \quad (\text{A.1})$$

where

$$z1 = (h_{centre} - h_{edge})\eta + h_{edge} \quad (\text{A.2})$$

$$\begin{aligned} \frac{z2}{\alpha} = (1 - \lambda) & \left(\begin{array}{l} (35.0 + 10.0\psi)\frac{1}{2}(1 - \cos 2\theta) + \\ \frac{24.0}{2} \left(\frac{1}{2}(1 - \cos 2\theta) \right) + \sin\theta + \\ (7.5 + 12.0\psi) \left(\frac{1}{2}(1 - \cos 2\theta) - \sin\theta \right) \end{array} - 1.6 \right) \\ & - \frac{10.0}{2}(1 + \cos 2\theta) + 10.0 \left[\frac{1}{2} \left(\frac{1}{2}(1 - \cos 2\theta) + \sin\theta \right) \right]^2 (1.0 - 3.0\alpha) \\ & + 2.5 \left[\frac{1}{2} \left(\frac{1}{2}(1 - \cos 2\theta) - \sin\theta \right) \right]^2 \left(\frac{r}{a} - 1 \right)^2 \end{aligned} \quad (\text{A.3})$$

$$\begin{aligned} \frac{z3}{\beta} = & \lambda \left(\frac{3.5}{2}(1 + \cos 2\theta) + \frac{3.0}{2}(1 - \cos 2\theta) + 0.3\sin\theta \right) \\ & + 1.05 \left[e^{-\mu(1-\frac{r}{b})} + e^{-\mu(1+\frac{r}{b})} \right] \left[e^{-\mu(1-\frac{r}{c})} + e^{-\mu(1+\frac{r}{c})} \right] \end{aligned} \quad (\text{A.4})$$

On this function the grid was projected.

Then, a dynamic relaxation procedure was used to relax the grid. Then was executed by removing the normal direction to the shape from the relaxation procedure. The nodes could only move along the grid with that procedure.

Eventually the limitation of the size of the glass was the restriction and controlling factor for the shape of the structural grid. This 'form finding' procedure was executed by running a lot of procedures as described above by hand with different parameters for the grid.

Brown (Brown & Cook 2002) also describes that spirals were used to define the grid. He further describes the procedure of the form finding and more details of the structural design.

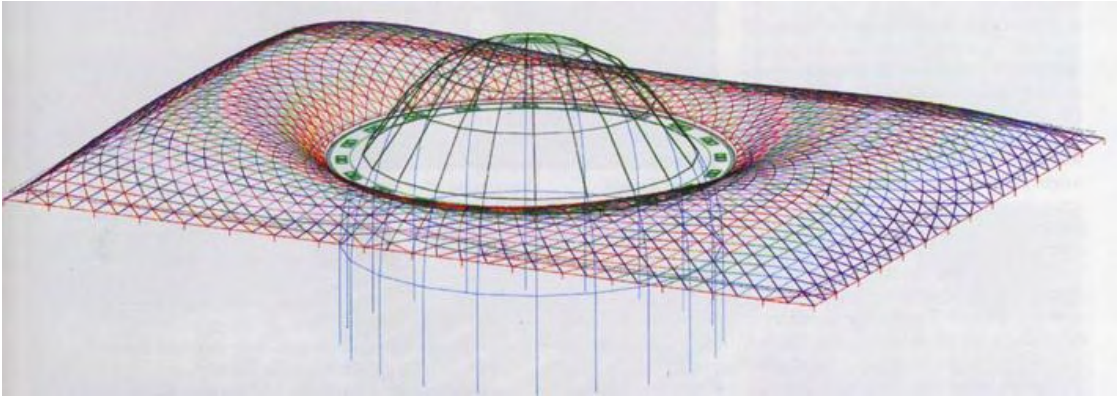


Figure A.27: British museum computer model. Image by Chris Williams.

A.1.4 Esplanade theatres - Singapore, China (M. Wilford)

RECOMMENDED STUDY MATERIAL

Title	Author	Year
The geometrical processing of the free-formed envelopes for the Esplanade Theatres in Singapore	J. Sanchez Alvarez	2002
The envelopes of the arts centre in Singapore	H. Klimke et al.	2002

In Sanchez (Sanchez-Alvarez 2002) and Klimke (Klimke, Sanchez, Vasilu, Stuhler & Kaspar 2002) the structural design and the geometrical description of the Esplanade theaters in Singapore is described. The 'form finding' in this form was not really done by a form finding method. This project is mentioned because this is sometimes referred to as form finding, but is more a geometrical description with NURBS curves and a mesh (grid) projected on the surfaces. This could also be seen as form finding, when looking from an abstract point of view, because it involves the definition of form.

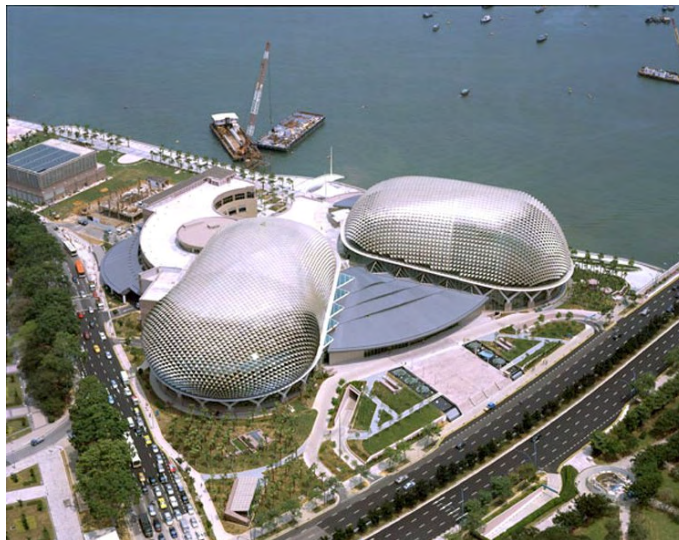


Figure A.28: The Esplanade theatres in Singapore.

A.1.5 Downland Grid Shell - Singleton, United Kingdom (E. Cullinan, Buro Happold)

RECOMMENDED STUDY MATERIAL

Title	Author	Year
Downland Grid Shell	F. Jensen	2000
The structural engineering of the Downland Gridshell	R. Harris and O. Kelly	2002

The Downland Grid Shell, at the Weald and Downland Museum in Sussex, UK, is the roof of the new Archive Store and the Workshop building.



Figure A.29: Physical model of the Downland Grid shell. Image by Frank Jensen.

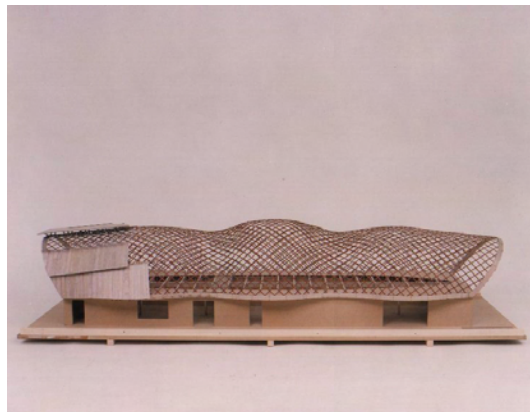


Figure A.30: Physical model of the Downland Grid shell. Image by Frank Jensen.



Figure A.31: Computer model of the Downland Grid shell,. Image by Frank Jensen.

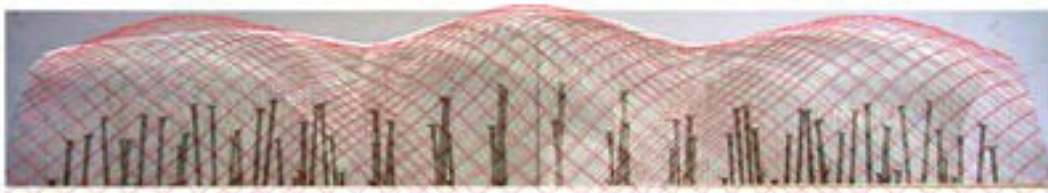


Figure A.32: Physical model of the Downland Grid shell with the computer model projected on the surface. Image by Frank Jensen.

A.1.5.1 Background

The Weald and Downland grid shell, shown in Figure A.33 and Figure A.34 is built at the Weald and Downland Open Air Museum in Sussex in the UK, and was finished in 2002. This museum has over 45 historical buildings from South East England, which have been rescued and rebuilt there. The museum needed a new building for study and practice of building conversation, especially the timber framing tradition in England. Also a new conservation store for collection items was needed. To extend the collection of timber structures into the 21st century, the new building should be an example for modern rural buildings. The result of the combination of skills of the architect Edward Cullinan Architects, the engineer Buro Happold and the carpenter, Green Oak Carpentry Company, truly is a display of modern craftsmanship (Harris & Kelly 2002). The basement of the building is sunken into the hillside and houses the conservation store. The workshop is situated on the ground floor and is roofed by the grid shell. The roof has the shape of a triple-bulb hourglass, to mirror the rolling shapes of the West Sussex Downs.



Figure A.33: The Weald & Downland grid shell. Image from www.wealddown.co.uk



Figure A.34: Inside view of the grid shell. Image from www.wealddown.co.uk

A.1.5.2 The roof

The triple-bulb hourglass roof is 48m long and between 11-16m wide. It has an internal height of 7-10m. The roof is clad with Red Cedar boards and polycarbonate glazing. The grid is built up out of 50x35mm oak laths in four layers, like the grid shell in Mannheim, to provide good out of plane resistance. The laths have a spacing of 500mm in areas with high load, and 1000mm in other areas. Original designs were made with 500mm spacing for the whole structure. Careful examination of the forces and stresses by computer analysis lead to increasing of the spacing, which saved construction time and reduced costs significantly. Shear blocks are screwed between the different layers to provide composite action between the layers. To increase stability, diagonal bracing is applied. In the lower parts the bracing laths run in longitudinal direction, at the top in transverse direction. These also provide support for the cladding boards.

The cladding consists of polycarbonate glazing, which covers the upper part of the roof, and Western Red Cedar boards. This closed part is insulated with a multi-layered composite insulation material (Weald & open air museum 2005).

A.1.5.3 Structural modelling and analysis

Physical modelling Physical modelling involved an important part of the modelling process. It provided a lot of information on form, structure and construction of the shell. Scheme models of wire mesh were made to research the form. After this a larger 1:30 model using wood strips was built. This proved to be very instructive. The geometry of the model was used to determine the boundary conditions for the computer model. It also served as presentation model (Harris & Kelly 2002).

After this an accurate wire mesh model was made, to explore the formation of the shape and to determine self weight bending. Dimensional analysis was used to correctly model the full scale structure (Jensen 2000). A boundary template was used to determine if the correct shape was reached. Also internal scaffolding was modelled to approximate the formation procedure as good as possible. The wire mesh was loaded by hanging large steel nail on the nodes.

Main conclusion of the experiment was that the saddles would not form themselves under dead weight. External forces are needed to reach the final shape. As the lattice becomes more curved, larger forces are needed to stretch the lattice, so the initial lay out of the lattice should be already stretched instead of with square angles. It was also concluded that formation of the waists costs a lot of force when first a barrel shape is adopted. Formation of the valleys and tops should be formed simultaneously to prevent breakage of the laths.

Computer form finding Using a modified dynamic relaxation method, the shape of the structure was determined. Dynamic relaxation is an iterative process that modifies an initial approximation to the desired shape by monitoring the kinetic energy of the model as it is made to oscillate. The method is generally used to examine oscillations of a pure catenary shape to generate a final shape. The W&D grid shell however is not a purely catenary shape. It is not possible to create the saddles with a hanging chain model. The method had to be modified by including the bending stiffness of the laths, to correctly model the shape.

Structural analysis The structure is analysed and designed in accordance with the eurocode 5, using timber grade D30 with a characteristic bending strength of 30N/mm². Structural analysis was performed using the elastic analysis software STAAD Pro. Two methods were used. Dynamic relaxation was used for second order analysis of buckling instability. Using the STAAD model a deflection analysis to compare the deflected shape with the non-linear analysis under the same load. This proved that under working load the behaviour is elastic, with adequate factor of safety against buckling. Detailed stress checks were made using the information provided by the

STAAD model.

It was also concluded that the shape of the grid enhanced the load bearing capacity. The waisting along the building improved the strength and stiffness against asymmetric loads (Harris & Kelly 2002).

A.1.5.4 Timber

Selection A number of species of timber were considered for construction of the grid shell. Based on their properties and the results of a series of tests, oak was selected for the grid. This species performed best in the structural tests carried out at Bath University, with respect to bending behaviour. It proved to be stiffer than other species and has a considerably higher bending strength. Although it needs more force than other species to be bended it can achieve a smaller bending radius prior to failing. Also it showed a somewhat plastic failure mode, compared to more brittle timber. Additionally, oak has high natural durability, so no treatment would be necessary. Possible leakages will not lead to decay of the timber (R. Harris, pers. email comm. 14 March 2006).

Another reason is that, oak is one of the most common used materials in the museum's collection of buildings and the species was readily available from sustainable sources in UK. Strangely enough, eventually the timber was sourced in Normandy, because better timber with a lower rejection rate was available there.

The main disadvantage of oak is that the direction of grain varies significantly, due to the growth characteristics. This was overcome by cutting out the defects and joining the pieces together to create laths of the required length. Selection was made on the following requirements (Harris & Kelly 2002):

- A maximum slope of grain of 1:10
- No dead knots or live knots. Only small pin knots were allowed, provided that they formed no more than 20% of the width of any face.
- No shakes or splits
- No sapwood (sapwood is not naturally durable and not resistant to infestations)

Lath production Although tests indicated that the shell could be formed using dry oak, green oak was used. Green timber is easier to bend, thus making the forming process of the shell easier. One disadvantage of oak is its acidity, making it difficult to joint with adhesives. Using green oak only make this worse, also because of the moisture content of the green timber. After an adhesive was found which is not affected by this acidity and the moisture content, the use of it was no problem anymore.

In total, approximately 6000 linear meters of lath were needed. The average length of individual pieces was 0.6m so 10.000 finger joints were used in the structure. Laths of 6m length were made off site, using a special machine, to maximize the quality with a minimum wastage. The finger joints are hardly visible, so despite the amount the joints have minimal visual impact (Figure A.35).

On site the laths were jointed into laths up to 37m long. Here, a scarf joints with a slope of 1:7 was used (Figure A.36). The joints were made in a tunnel tent to avoid weather influences. There is an interesting contrast between the two jointing techniques used. Finger jointing was the latest technology, while scarf jointing has been used for centuries.

The joints performed well during construction. There were approximately 145 breakages during forming. Almost all broken joints were finger joints. Main causes were (Harris & Kelly 2002):

- Pinching of the lattice on scaffold supports

- Tight curvature
- Tension build-up because restriction of the relative slipping between the layers
- Dry joints



Figure A.35: The Weald & Downland grid shell. Image from www.wealddown.co.uk



Figure A.36: Scarf joint. Image from www.wealddown.co.uk

A.1.5.5 Connection details

Typical node joint For the connection between the laths a special connector was designed. It consists of three plates, connected with four bolts (Figure A.37). The middle plate has a pin in the centre, keeping the connection into place. The outer layers can slide freely in their direction during shaping of the structure. Two of the four bolts can be used to connect the diagonal bracing. The connector proved to be very successful and has been patented.

Edge connection At the edges the grid shell is connected to the floor of the structure. The laths are bolted between two layers of plywood and connected to the floor beams. The floor and floor beams are cut into shape and the first layer of plywood boarding is connected to the glulam floor beams with angle brackets prior to the erection of the roof. Holes are drilled in the boarding aligned with the holes in the brackets. Figure A.39 shows one of the positions of the brackets. After the grid is lowered, blocks are installed on this location to fix the sandwich



Figure A.37: Assembly of a typical node joint. Image from www.wealddown.co.uk

structure firmly to the brackets on the inside (Figure A.40). Also the gaps between the layers are filled up with timber where the grid overlaps the boarding to create a solid section four times the depth of a lath. The second layer of plywood is attached and the laths and plywood layers are bolted together (Figure A.41). The whole sandwich is bolted to the brackets on the inside to create a rigid edge connection.



Figure A.38: Floor and beams are cut into shape. Image from www.wealddown.co.uk



Figure A.39: Location of the brackets. Image from www.wealddown.co.uk



Figure A.40: Connection to the edge. Image from www.wealddown.co.uk



Figure A.41: Edge detail. Image from www.wealddown.co.uk



Figure A.42: Finished connection. Image from www.wealddown.co.uk

A.1.5.6 Assembly

Instead of pushing or lifting up the grid against gravity, the Weald and Downland grid shell was lowered into position. The flat grid of laths was laid out on a special scaffolding system at the level of the valleys of the shape. This scaffolding system used adjustable jacks to accurately alter the heights to form the shape of the grid shell.

The mat was laid out at a height of 7m. As concluded from the experiences of physical modelling, the mat was not laid out with 90 angles between the laths. 96 and 84 angles were used and the resulting mat was 47x25m (Kelly, HARRIS & ROWE 2001). The process of lowering the grid was carefully monitored visually and with the information provided by scaffolding jacks system. The longitudinal centre line was used as a reference line, as this line was not to move transversely. The nodes on this line were painted white, to be able to visually check if the nodes remained on a straight line.

The scissoring and sliding of the laths was influenced with straps in plane of the grid. By tensioning the straps in the desired direction, the scissoring was stimulated. The strapping arrangement was continuously monitored. Failing of the lattice to scissor or of the laths to slide relatively to each other would lead to breakages so the process was observed carefully.

After formation was finished, the valleys resembled the designs very well. The domes however appeared to be too low. Also the perimeter nodes around the domes were 300mm too low. Adjustments were made by pushing up the perimeter nodes using small jacks.

The formation process was very successful. Observation was seen as the key control of the formation process. Potential problems could be isolated and dealt with continuously by observing the behaviour of the lattice.



Figure A.43: Flat mat of laths. Image from www.wealddown.co.uk



Figure A.44: Start of lowering. Image from www.wealddown.co.uk



Figure A.45: Adjustable jack. Image from www.wealddown.co.uk



Figure A.46: Angled jacks. Image from www.wealddown.co.uk



Figure A.47: Halfway down. Image from www.wealddown.co.uk



Figure A.48: Completed form. Image from www.wealddown.co.uk

A.1.6 Eden Project - Bodelva, United Kingdom (Grimshaw)

RECOMMENDED STUDY MATERIAL

Title	Author	Year
The Eden Project glass houses world environments	A. Whalley	2000

The Eden project (see figure A.49) by Nicolas Grimshaw & Partners (Whalley 2000) has been formed by structural morphology, by geometrical techniques to form a grid from hexagonal elements in the desired shape. Much has been learned from nature's efficiency, not only as a structural but also an architectural motive, since the structure itself is also close related to nature (it houses many plants).



Figure A.49: Image of the Eden project

A.1.7 Groningen Twister - Groningen, The Netherlands (KCAP)

RECOMMENDED STUDY MATERIAL

Title	Author	Year
The Groningen Twister - an experiment in applied generative design.	F. Scheurer	2003

The Groningen Twister is a collaborative project between the design team of Kees Christiaanse Architects & Planners (KCAP) in Rotterdam, an engineering team of Ove Arup & Partners in Amsterdam and the chair for Computer Aided Architectural Design (CAAD) at the ETH Zurich. The project was initiated in February 2003. The aim of the project was to develop a CAD-tool which would help the architects of KCAP to solve a complex design task: Underneath a pedestrian area that links the main station to the city centre of Groningen, there was a need for parking space for approximately 3000 bicycles (Figure A.50). To support the concrete slab of the pedestrian level, the desired design called for more than one hundred columns of different sizes to be placed in a random pattern, but to be then sized and controlled according to structural, functional and aesthetic needs.

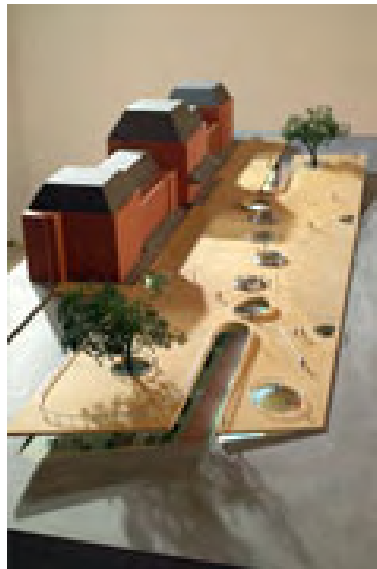


Figure A.50: Model view of the Groningen Stadsbalkon. (Scheurer 2003)

To solve this problem, software was developed at the chair for CAAD that simulates a growth process for the columns. The distribution of the columns is defined by structural rules, provided by ARUP's engineers, as well as functional and design rules provided by KCAP's designers. The results are presented to the user as a three dimensional, dynamically evolving model. At any time during this process the user is able to control the model on the screen interactively. The user can control the process in two distinct ways, on the one hand by directly controlling the placement of single columns, on the other hand by adjusting various parameters that define the properties of the columns and the environment. The system provides real time feedback, as the column distribution tries to adapt to the changed configuration. This allows the user to test various alternative solutions in very short time (Figure A.51).

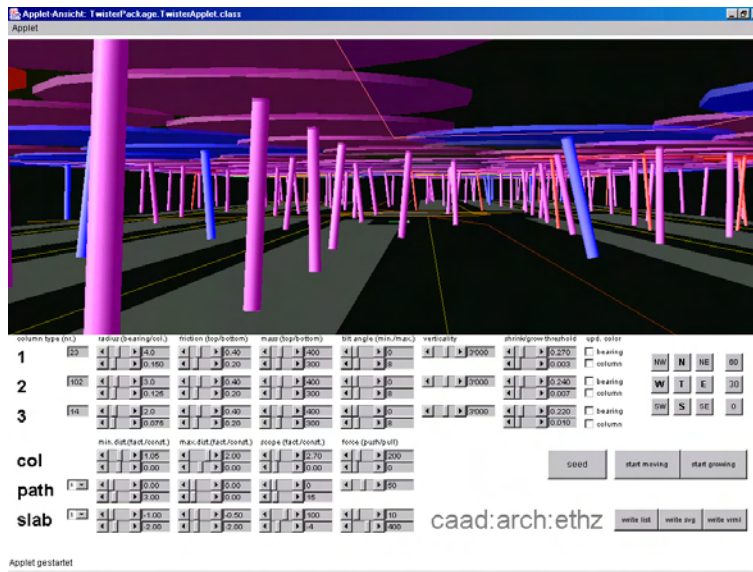


Figure A.51: Screenshot of the Groningen Twister model. (Scheurer 2003)

After a stable and satisfactory condition is achieved, the resulting column locations can be exported for construction documents in various digital file formats (Figure A.52).

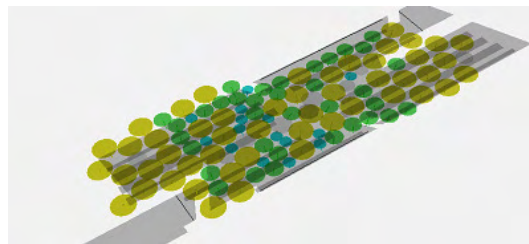


Figure A.52: Color coding by kinetic energy. (Scheurer 2003)

The columns represent particles in a swarm system. Each column in the system is an autonomous individual, exploring the habitat and reacting to its neighbouring columns. According to the two layers of the habitat, the column model consists of two independent parts. The bottom end can move freely within the ground plane of the model, whereas the top end can move in the plane described by the slab. The actual column position, length and tilt is defined by the connecting line. It has to be assured, that the tilt angle stays below the assigned maximum (Figure A.53).

This behaviour is easily described by a spring-mass-system (called particle spring system): punctual masses are connected by a virtual spring that pulls depending on the distances between the masses. In the model each organism is composed of two masses which describe the top and bottom end of the column and a spring in between. The force of this spring is proportional to the horizontal distance and, since the move of the masses is confined within the two planes of the habitat, they are drawn to positions above each other.

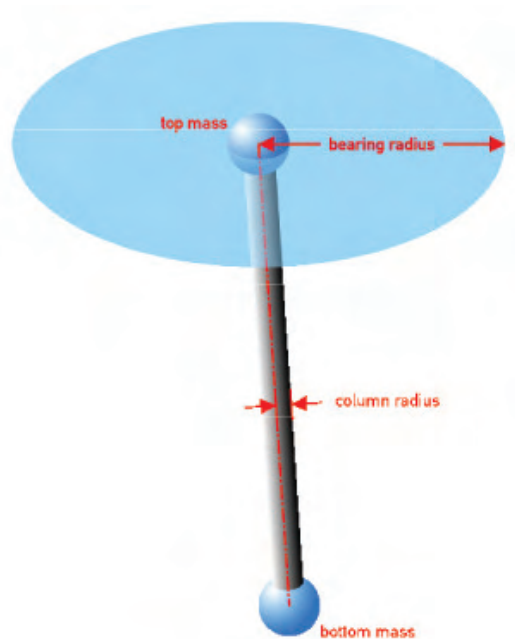


Figure A.53: The column model with a maximum bearing capacity and tilt. (Scheurer 2003)

The columns are interacting with their adjacent columns as well as with the surrounding habitat following the same simple principles of attraction and repulsion by virtual springs. If they come too close, the top masses of each column are repelled by the slab outline, the holes, and the areas without cellar. The bottom masses are attracted by the closest bike stand.

To get the desired effect of distributing the columns, they seek to stay at a certain “social distance” to each other. This distance is defined by the maximum spanning distance of the slab and the bearing capacities of the respective columns. The bearing capacity of a column defines a circle around the top end marking the area where column is able to support the slab. Neighbouring columns therefore have to be aligned so that their radii touch or overlap slightly. This is also accomplished by virtual springs that push or pull between their respective top masses.

The specifications of the columns were given by Arup. There are three types of columns with different diameters and bearing capacities. The maximum radius of the column results from the bearing capacity and defines the distance between the columns. The tilt angle of the columns was limited to 10 degrees so that this factor could be ignored in structural calculations. Also the height differences between the ground plane and the slab were not cared for and an average height of 3,0 meters was used throughout the habitat. The approximate number of columns needed was estimated by Arup based on the maximum radii and the building budget which would only allow for a certain number of columns.

By making the columns pressure sensitive and able to change their type, an actual growth process was possible. Instead of assigning a column diameter and bearing radius from the beginning, the columns are able to adapt to their surroundings by changing their size autonomously.

A column that is too far away from its neighbours detects a low surrounding pressure and

starts to grow in discrete steps, matching the column types. If it reaches the largest possible state and still has no close neighbours, it splits into two small columns which both start growing again. If a column gets too close with its neighbours or the edges of the habitat the resulting pushing increases the pressure and it starts shrinking in just the same way. And if it reaches the smallest state while the pressure remains high, it finally dies. Thus, by “seeding” a single column the whole area of the slab is filling up with columns over time (Figure A.54).

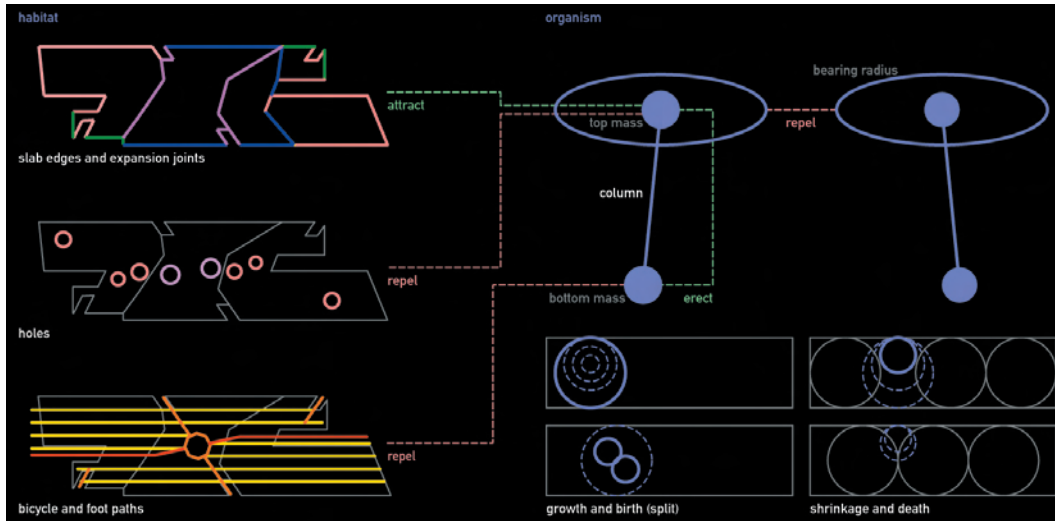


Figure A.54: The relation between the habitats and the 'agents' in the growth, birth, shrinkage and death of the columns. (Scheurer 2003)

A.1.8 Web of North Holland - Haarlemmermeer/Delft, The Netherlands (ONL)

RECOMMENDED STUDY MATERIAL

Title	Author	Year
Architectural design and mass customization.	S. Boer and K. Oosterhuis	2004

Design conception

For the Dutch province of North Holland ONL designed a pavilion for the world horticultural exhibition 'Floriade' 2002. Architecturally there is no distinguishable difference between wall, floor or ceiling (Figure A.55).

The design was based on a topological surface that governs the logical aesthetic continuity of the shape. The specific shape of the surface came about in a design process which combined milled physical models of the computer model with again computer modelling of adaptations to the milled models to attain a good space for its program as well as introducing the rigorous styling requirements of ONL. During this process a clear vision arose of the concave / convex dynamics and the shaping lines, the folding lines that fade in and fade out of the shape. ONL described the styling requirements in a number of shaping rules of the design. It was important

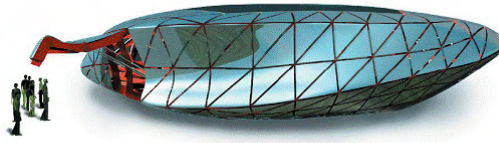


Figure A.55: A rendering of the Web of North Holland. Image from (Boer & Oosterhuis 2004).

to describe the design not in mass, but in a number of design rules and guidelines since its internal program was still to change. To control the shape and the look of the design a NURBS surface was created (Figure A.56).

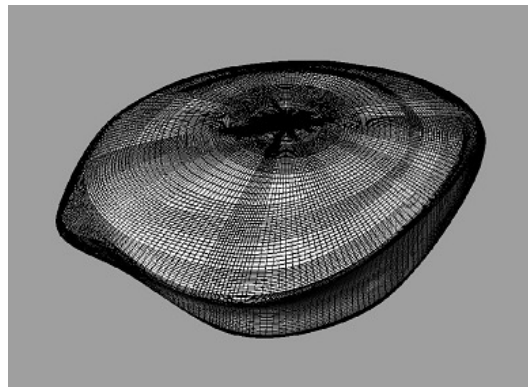


Figure A.56: The NURBS surface of the design. Image from (Boer & Oosterhuis 2004).

Expanding on the conventional paradigm of a construction grid ONL mapped a triangular grid with the internal integrity of an icosahedron (a 20-faced polyhedron on the NURBS surface). The icosahedron system was chosen for a number of reasons, the main reason being that it is a closed system, like the design (Figure A.57).

With the pavilion for the Web of North Holland ONL reaffirmed their strong beliefs acquired by previous projects [Elhorst-Vloedbelt, saltwater pavilion] that one can gain a maximum design freedom and keep the budget in check by gaining control over a system of similar, but different elements. A number of techniques can be determined that make this possible:

1. File to Factory: A construction process is greatly simplified by connecting the file created by the architect to the machine, eliminating intermediate steps that are inefficient - and even more so - susceptible to errors.
2. Mass customization: An irregular shape can only exist by the grace of irregular elements, therefore control over mass customization greatly increases design freedom.
3. Parameterisation: One Building, One Detail. Ideally, in a mass customized solution more

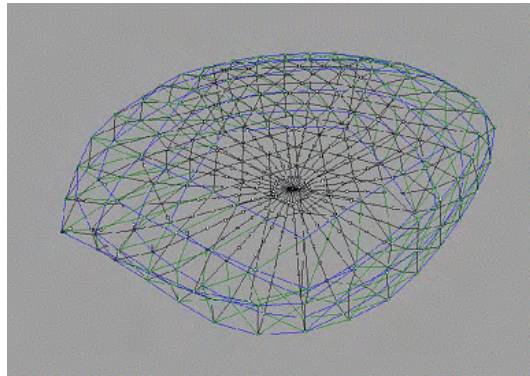


Figure A.57: Mapping of a constructive grid based on a icosahedron. Image from (Boer & Oosterhuis 2004).

parameters can be found than those that account for shape alone. These can be utilized to optimise the design.

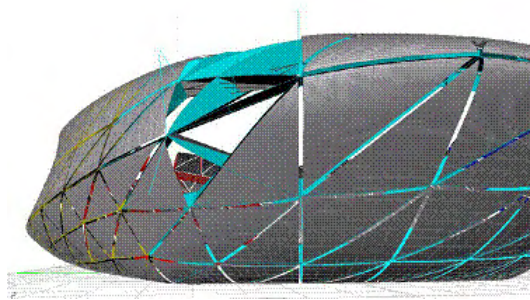


Figure A.58: 3D model of the panels with the construction showing. Image from (Boer & Oosterhuis 2004).

4. Design control hierarchy: In this specific pavilion the shape is described in a single NURBS surface, essentially all that follows will refer to this surface. A NURBS surface is created using NURBS lines, keeping this creation link intact yields control on a higher level, by changing the line, the surface changes and the entire system changes. Primarily for designers this notion is paramount.
5. Body Styling: These techniques give the architect / designer full freedom to shape the volume of the building, to propose styled creases and smooth transitions of creases disappearing into the surface of the overall body. ONL has two other projects in the production phase that have been designed with the above in mind: the Cockpit building and the Acoustic Barrier. The Cockpit building is part of a fluid design of the Acoustic Barrier, to accommodate the transition from the one to the other the design control hierarchy proved to be essential, both projects share the same outlines, but differ in construction principle. Construction is based on a streamlined File-to-Factory process described earlier.

This pavillion was designed to be open-air, meaning that in essence the construction is open and that rain would essentially fall through it. In respect to cladding this building, things were pretty simple in terms of insulation and waterproofing. However, ONL invested in creating a construction that already describes the shape exactly, therefore the cladding must be able to follow this shape with a minimum of processing. As was stated earlier, ONL wanted to build this building only once, with creating a mold, the building is built more than once and half of it is thrown away. Prior to the design of this pavilion ONL conducted a small study of the material 'Hylite', an aluminum laminate produced by the Corus group that consists of aluminum on both sides and polyethylene in the middle (Figure A.59). It has the look of aluminum, but the flexibility and pliability of a polymer. ONL found this to be a flexible material that will let itself be fitted on a triangle of three spatial curves in a form of pseudo double curvedness.

In 2006, the Web was placed in front of the faculty of Architecture, Delft University of Technology.



Figure A.59: Specific view to illustrate the effectiveness of the application of the Hylite. Image from (Boer & Oosterhuis 2004).

A.1.9 Akutagwa River Side Project - Takatsuki City, Japan

RECOMMENDED STUDY MATERIAL

Title	Author	Year
Computational morphogenesis and its application to structural design.	H. Ohmori et al.	2005

Akutagwa River Side project is the project which brought a practical project to appeal the potential and possibility of the computational morphogenesis method for the future. It has been planned at the site along the shopping arcade which runs from the north front of Takatsuki JR station in Japan, where a large scale redevelopment of the urban district has been planned to activate the shopping area by renewing the decrepit shopping area through both introduction of the new buildings as well as renovation of conventional stock of urban district. The present project has been designed not only as to be effective as a leading project to the campaign but also to have an attractive appearance even if it does not have a big mass.

The west and south side wall development diagram of the building after completion (April of 2004) is shown in Figure A.60. Figure A.61 shows a rendering of the complete building. As can be seen from the diagram and the rendering, the west side and south side wall structures have non-geometrical form which is even that of organisation, which has been generated through the proposed process of computational morphogenesis through usage of the extended ESO method.

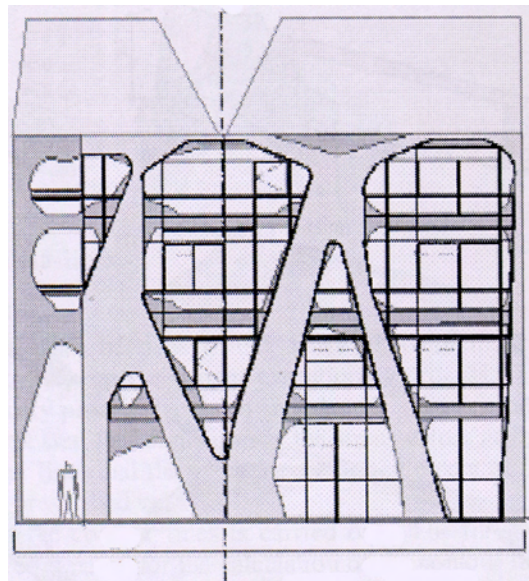


Figure A.60: The west and south side wall development diagram of the building. Image from (Ohmori & et al. 2005).

Figure A.62 shows the evolutionary process of the extended ESO method from which we can observe how the south side wall form has been changed through the process of deletion of the portion with low density of Von Mises' relative stress as well as the process of addition of the necessary portion. In the evolutionary process, it has to be noticed that the slabs of each floor

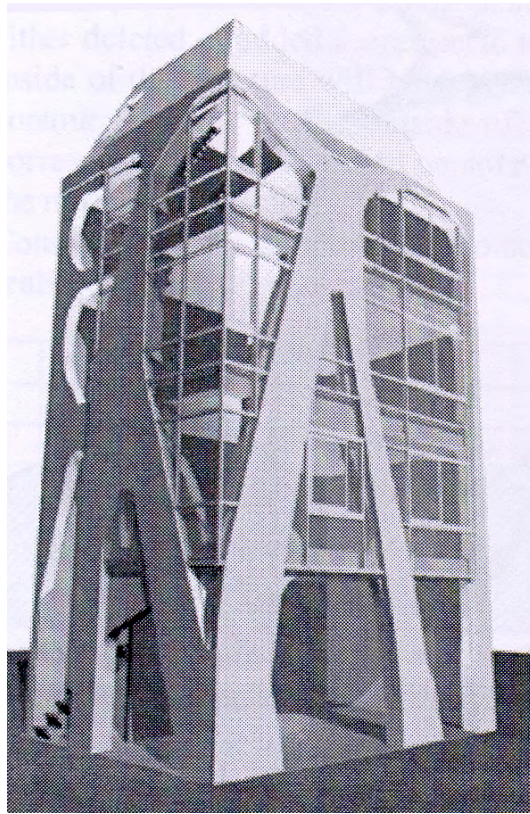


Figure A.61: A perspective view of the building in a rendering. Image from (Ohmori & et al. 2005).

level are treated not to be deleted through the evolutionary process and so is the east side wall.

In order to ensure and proof that the structure with the form obtained through the computational morphogenesis procedure has enough capability, 3D elasto-plastic numerical analysis is carried out. Figure A.63 shows the deflection state of the whole structure subjected to the horizontal loads in x-, y-direction and also in the direction at an angle 45 degrees to the x-axis, respectively.

Some photos of the construction site and the inside and the outside view of the building just after the completion are shown in Figures A.64 up to A.69.

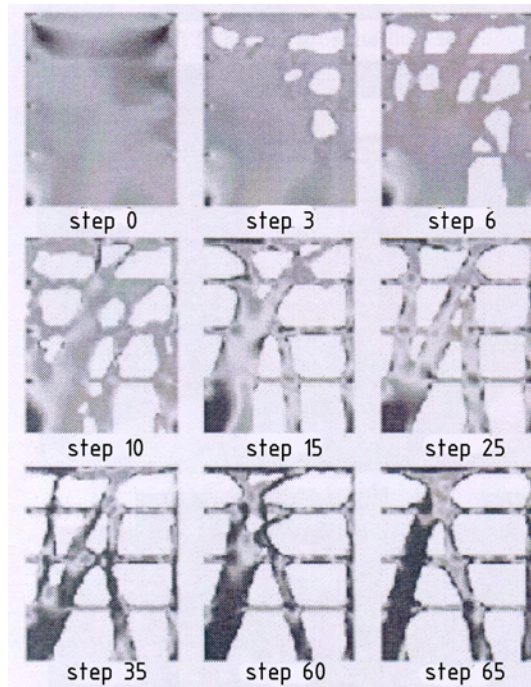


Figure A.62: The evolution process of the south wall. Image from (Ohmori & et al. 2005).

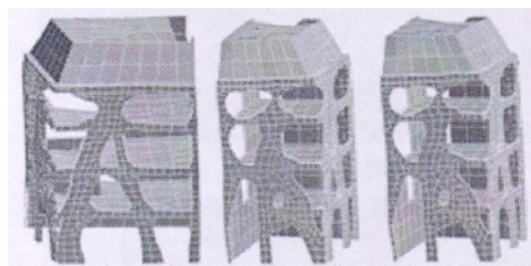


Figure A.63: The limit state deflection of the whole structure subjected to horizontal loads in x-, y-direction and under an angle. Image from (Ohmori & et al. 2005).

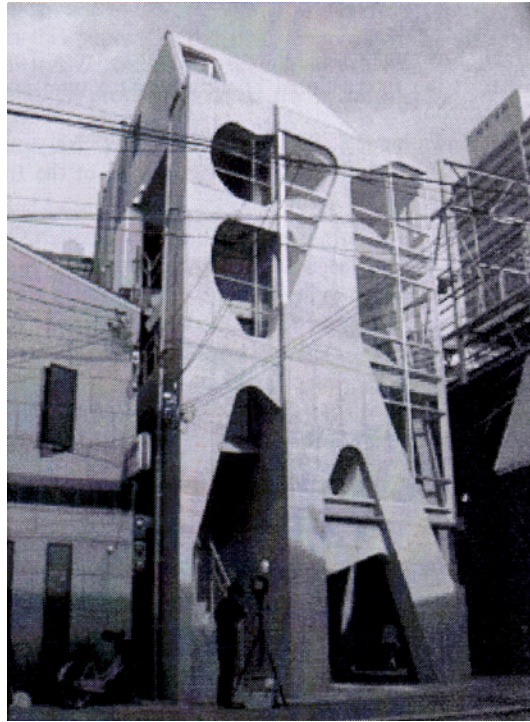


Figure A.64: outside view. Image from (Ohmori & et al. 2005).

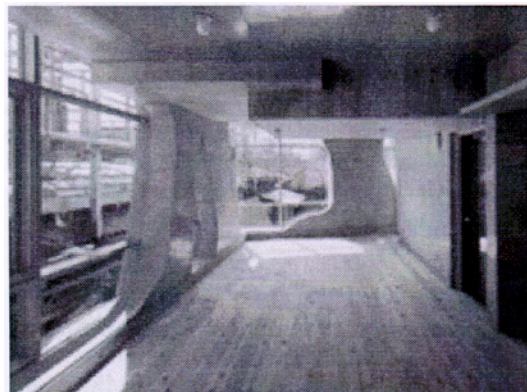


Figure A.65: inside view. Image from (Ohmori & et al. 2005).



Figure A.66: inside view. Image from (Ohmori & et al. 2005).

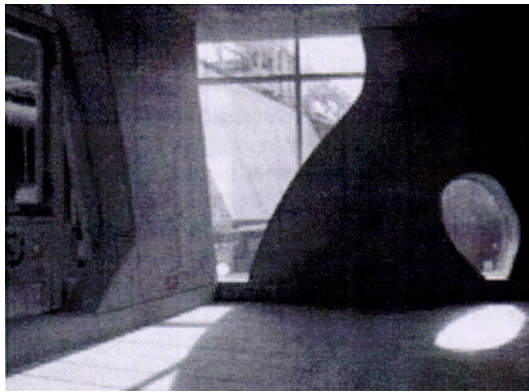


Figure A.67: inside view. Image from (Ohmori & et al. 2005).



Figure A.68: outside view. Image from (Ohmori & et al. 2005).



Figure A.69: outside view. Image from (Ohmori & et al. 2005).

A.1.10 Palazzetto dello Sport - Rome, Italy (P.L. Nervi)

For the Olympics 1960 in Rome, Nervi executed three stadiums; a small Palazzetto dello Sport (Figure A.71, designed with architect A. Vitellozzi, a larger covered Palazzo dello Sport, with architect Piancentini and the Stadio Flaminio, a 50.000-seat stadium designed with his son Antonio.

The flute-edged roof shell of the Palazzetto dello Sport is composed of 1620 prefabricated, diamond-shaped sections, joined by poured-in-place concrete that makes their connecting ribs, creating a webbed ceiling network, like a lamella dome. (Figure A.70

Nervi employed diamond shaped ferro-cement waffle units (2,5 cm thick) as permanent formwork for this shell. The ferro-cement waffle units were produced from fine-aggregate concrete and wire reinforcement. They were laid on scaffolding. Then, the reinforcement to the ribs was placed in the intermediate spaces. By casting the ribs and pouring a layer of concrete over the diamond shaped elements the actual load-bearing structure was formed. A compression ring in the centre forms a cupola, providing a central source of natural light. The forces that flow through these ribs are gathered in prefabricated, triangular sections, which transfer the load to exterior Y-shaped buttresses and vertical supports. The building seats 5000 spectators. The prefabricated elements are put in place in just 30 days as can be seen in Figures A.72 & A.73.

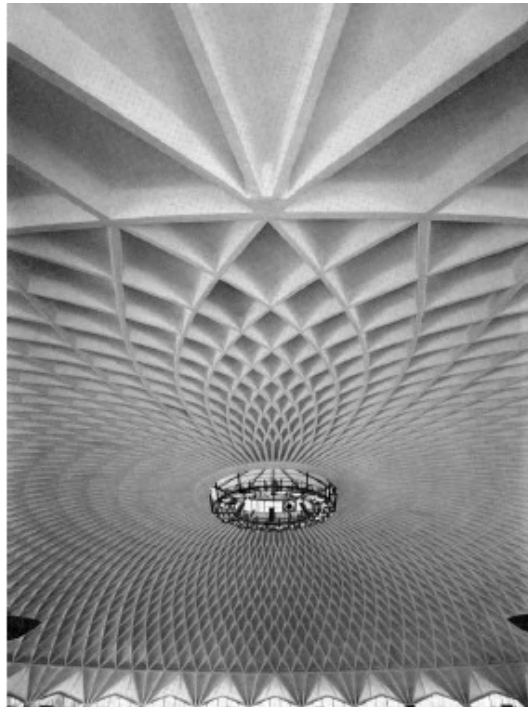


Figure A.70: Internal view of the Palazzetto dello Sport; h=21m, d=60m

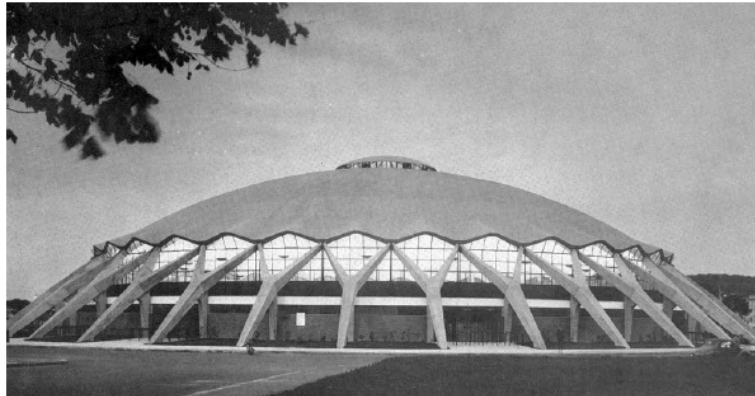


Figure A.71: Palazzetto dello Sport

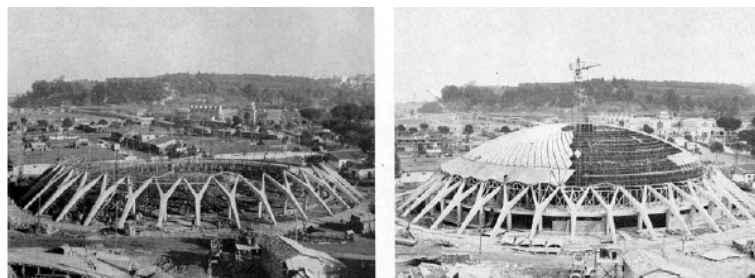


Figure A.72: Placement of the prefabricated elements

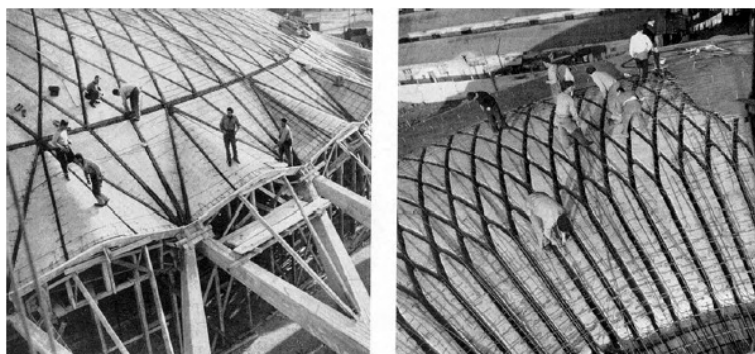


Figure A.73: Finishing of the structures, before pouring concrete

A.1.11 Sydney Opera House - Sydney, Australia (J. Utzon)

RECOMMENDED STUDY MATERIAL

Title	Author	Year
IABSE proceedings	IABSE	2006

The beautiful sail-like vaults of the Opera House, designed by Jørn Utzon, were a great success for architect and engineer, but also had some disappointments. The shape of the vaults as drawn in the sketches could not be built, nor be calculated by the engineers. It took years and years and a lot of money to find a possible solution to build the vaults in an easy, economic and the preferred, prefabricated way. Finally the solution was to change the shape of the vaults in such a way that the curvature of the elements would all be the same. Finally, the vaults and the tile lids are made as concrete, prefabricated elements, which have, due to the chosen shape, the same curvature. The repetition of the elements was maximized. The process of transition from free-form to spherical geometry, the segmentation process and the realization of the superstructure and the tile lids are described in the following paragraphs.



Figure A.74: Sydney Opera House

A.1.11.1 Morphology; from Free-form to Geometrical Defined

Between 1956 and 1961 analytical work and model tests were directed towards finding a comprehensive statical solution to the problems posed by Utzon's scheme. The first approaches were aimed at finding a structural solution, one that would both provide stability and retain the roof profiles as they had been initially conceived: single-skin concrete shells strengthened by their curves. The ideal shell needed to unify the various surfaces, form a structure that would prove stable under all climatic conditions and respond to the requirements for erection and cladding.[12] The geometry of the shells, as presented in the first design book, in 1961, was based on a parabola. The simple concrete skin was, nevertheless, reinforced by the use of internal ribs. The following year, this construction principle was modified. The parabolic shells evolved into two thin concrete membranes, approximately 1,2 m apart, with a web placed between the layers capable of transmitting shear forces. Tests revealed that the shear forces and the bending moments in the system were far higher than had been anticipated and that it was impossible to calculate the load distribution to the foundations. The engineers continued to explore the geometry and construction techniques of the double skin system. The shell profile became circular, then elliptical. The three-dimensional metal structure was transformed so that it could be constructed in a naval dockyard. Uncertainties remained respecting the behaviour of such shell in the instance of violent

winds and in the repercussions of vibration on the glazed facades. Again, Utson indicated his reservations as to their internal appearance and the acoustical problems were far from resolved. The engineers re-examined the two geometries in the light of other construction techniques. In June 1961, the structural principles were altered radically. From now on, concrete members of triangular section, fanning out from the base of each shell and joined to a ridge beam describing either elliptical or circular sections, formed the shells. Complex scaffolding was envisaged for their construction, but the question of the cost of this technique was still insolvable and Utson was not really satisfied with any of these proposals (Figure A.75). In the autumn of 1961, the design team came up with a simple idea that, in a single stroke, resolved all the problems that had been encountered over some years. He altered the given of the problem by proposing that the surfaces of all the shells should be calculated from one potential sphere. (Figure A.77) The solution had great geometric rigor; an assembly of cast elements would replace the long-contemplated in-situ formation of the shells scaffolding would be redundant this would mean that every segment of the shell was identical.

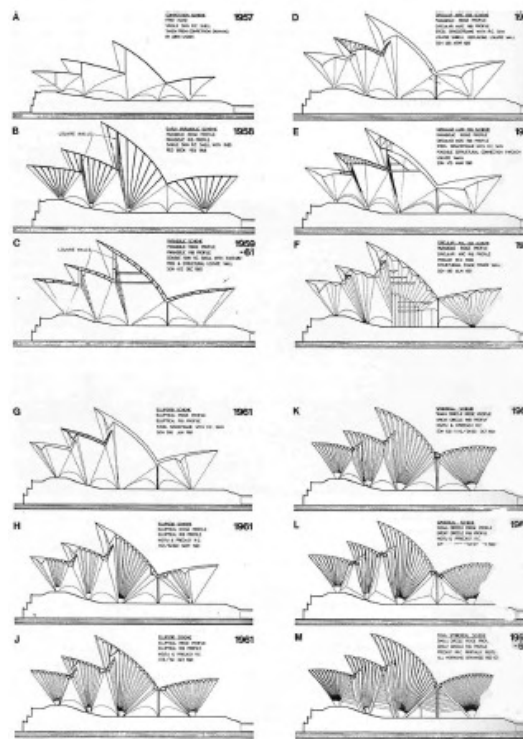


Figure A.75: Summary of the roof solutions

A.1.11.2 Segmentation and shape of the superstructure

All the half-shells of the roofs were developed from the quarters of the same theoretical sphere with a radius of 75m. The ribs forming the half-shells gathered together into a fanshaped. The ribs were formed of hollow concrete segments prefabricated on site using the land between Botanical Gardens and Sydney Cove, which was to be transformed into an immense casting yard. The section of each rib widened continuously from the base to the summit. At pedestal level the rib was a simple T-section becoming, at the ridge beam, an open Y with the two arms thus



Figure A.76: Presentation of the spherical solution

formed being braced by a series of crosspieces, also in concrete. See Figures A.77 and A.78.

A.1.11.3 Fabrication of the Rib Segments

The ribs curve in two directions and were cast in plywood lined, double curved steel formwork. The plywood was treated with several layers of fibreglass-bonded resin to give a smooth and precise finish. Each form could produce five rib segments of 4,6m length, which would be located in an equivalent position on the different ribs.

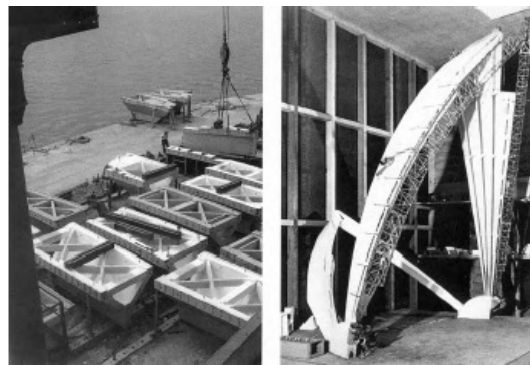


Figure A.77: Y-shaped prefab elements (a) Fan shaped element of the vault (b)

A.1.11.4 Fabrication of the Cladding Elements

Like the vault segments, the tile-lids were prefabricated on site. Spherical geometry again made series production possible here there were 18 types of lid. Ultimately, a total of 4253 lids were made. For the lower parts of the vault certain lids were replicated up to 280 times. The prefabrication process was a relatively simple operation that did not require specially qualified personnel. A bronze plate of double curved form, overlaid by a diagonal grid of square aluminium strips, locating and spacing the tiles, formed the base of each mould. The base and side of the mould were first cleaned by compressed air; then lubricated. The tiles were sorted by type, rather like printing types, and these were then fitted into the framework with their surfaces facing the base. The joints were filled with a layer of heated animal glue, which set on cooling, to prevent grout penetration onto the surface of the panels. Three layers of pre-cut galvanized steel mesh were placed on top of the tiles, separated by small pieces of asbestos cement to allow a sufficient layer of concrete between the mesh and the tile back. Reinforcement in the ribs had been cut, bent and galvanized prior to being fixed into position. (Figure A.79) Three hours after the concrete had been poured and compacted by vibrators the panel was covered by a PVC tent and treated with steam to accelerate curing. This eight-hour process took place at night in order to optimize

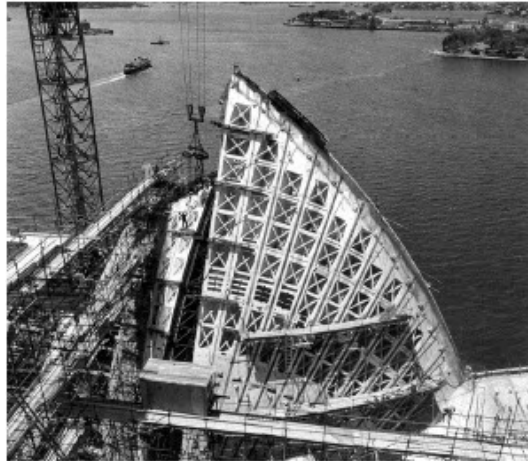


Figure A.78: The prefab vault during construction

the use of the moulds. In the morning the sides of the moulds were taken off and the lateral panels were raised with the assistance of a winch, a delicate process, as it was difficult to avoid damaging the sharp edges of the tiles that bordered each lid. The animal glue, which had melted during the steam curing process, left a concave meniscus in the tile joints and this was filled with an epoxy compound. The finished lids were classified according to their final position and then stored.

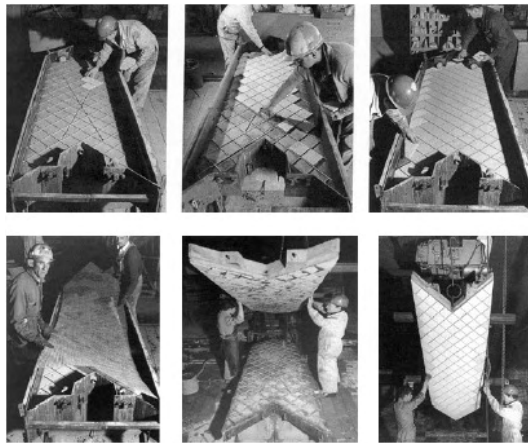


Figure A.79: Fabrication of a tile lid

A.1.11.5 Installation of the Prefab Elements

A crane track was installed along the rising axes of each set of vaults to be constructed. The pedestals for the rib sections were cast in-situ, symmetrically, on either side of the vault axis onto the steel rods that anchored them to the foundations. Pre-stressing cables fixed on the pedestals formed a supple pre-structure. Cranes capable of lifting the twelve ton segments up to a height of fifty meters were specially supplied and the elements were installed using an ingenious mechanism

developed for the scheme; a telescopic arch able to pivot on a base fixed to the pedestals. As its extrados was able to simulate the interior surface of any arch to be raised, it was possible to rotate and adjust the length of the cast arms to deal with all possible scenarios. The exact position of the segments was adjusted by the surveyors from measurements taken by theodolite and calculated by computer. The segments were then bolted together by hydraulic jacks before the anchorage cables were stressed to ensure that they maintained their exact position. See Figure A.78. The tile lids had to be applied to the structure as it was erected. Since they follow the same geometry as the arch segments, their width and lateral joints corresponded with their underlying ribs. The larger panels weighted up to four ton. Finally, the joints were waterproofed with lead flashing. See Figure A.80 for the installation of the tile lids on the vaults.

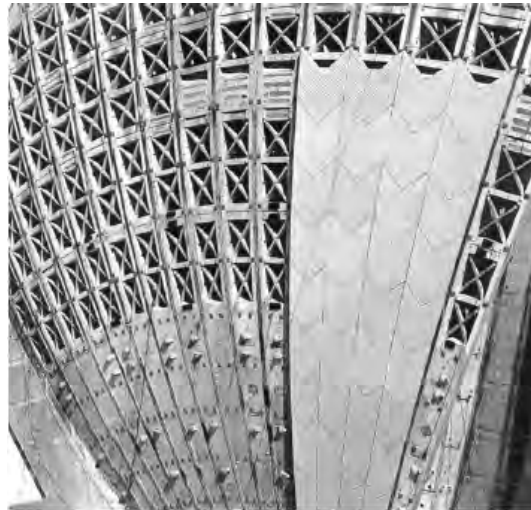


Figure A.80: Tiles lids attached to the ribs segments

A.1.12 Luifel Zonnestraal, Hilversum, The Netherlands (H.-J. Henket)

A pavilion on the terrain of the previous sanatorium De Zonnestraal presents the latest developments on the domain of concrete technology and construction techniques; prefab, demountable and high strength concrete elements.

A.1.12.1 Shape of the shed

The basic surface of the shed is 9 by 9m and 3.5m high. The plate is segmented in 4 elements of identical properties and size, to make the fabrication, transport and montage easier. The plate is just, thanks to the use of high strength concrete, 2.5cm thick and stiffened by transversal and radial ribs with a thickness of 4cm. The 4 quadrants are connected to each other with bolts, trough stainless steel elements inserted in the concrete during moulding.

A.1.12.2 Composition of the Concrete

The shed roof is constructed with UHPC, Ultra High Performance Concrete, which is, due to the higher amount of cement and specific additives, 5 times stronger than ordinary concrete. And, also 5 to 10 times more expensive than standard concrete. The four arms of the shed roof are composed of fibre-reinforced UHPC. The fibres have a diameter of 1mm.



Figure A.81: The roof of the shed is 25mm thick and the stiffening ribs are 40mm thick

A.1.12.3 Formwork

The double curved components of the roof are composed with the file-to-factory method; on the basis of 2D drawings, 3D drawings are composed. The formwork is made out of 2 thick multiplex laminated plates; where with the aid of the 3D-CAD-file, a grinder turning around 3 axes, drill out the shape of the arms. The components are not treated with a finishing material; this is not necessary due to the low porosity of the UHPC and the exact fitting of the components.

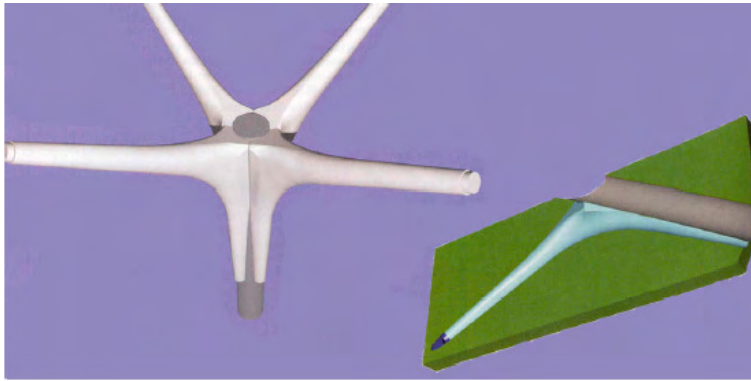


Figure A.82: The roof of the shed rests on a steel column onto which the fibre reinforced UHPC arms are attached.

A.1.13 Hessing Cockpit

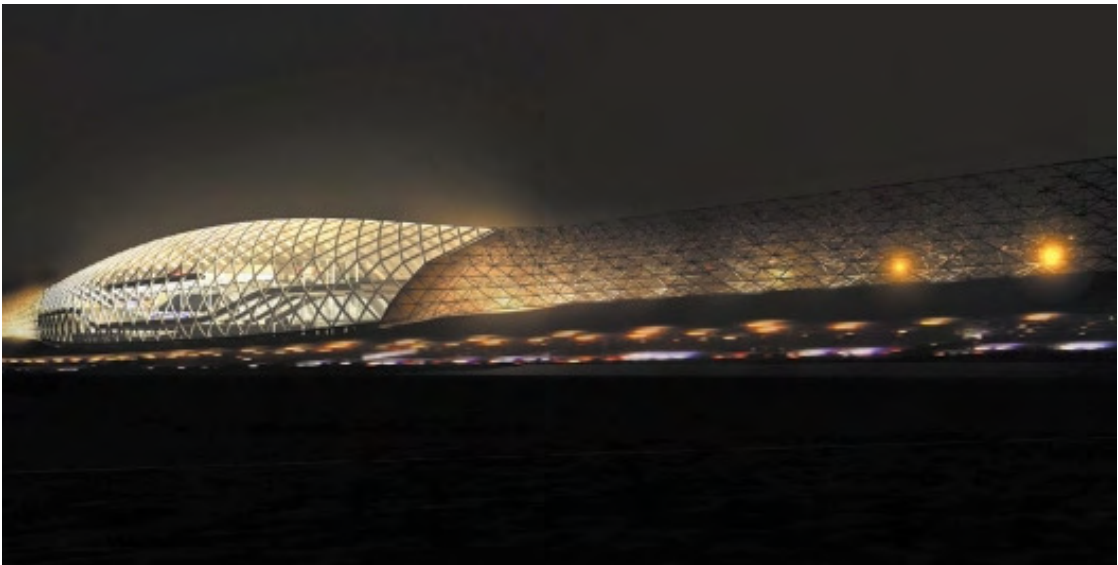


Figure A.83: Design impression of the Hessing Cockpit by ONL

Architect: ONL

Contractors and engineers: Meijers Staalbouw, Pilkington Glass, Polyned

Year: 2005

Geometry The cockpit building is designed as a prestigious car showroom and garage for the Hessing Company, displaying Rolls Royces, Bentleys, Lamborghinis, Maseratis and Lotuses. Special about this showroom is that it is integrated in a sound barrier alongside the A2 motorway nearby Utrecht. The total project, the ‘Acoustic Barrier’ together with the ‘Cockpit Building’, has a length of 1500 meters. In the whole combination of barrier and building, lines are continued and curves fluently transform between convex and concave, see Figure A.83. The Cockpit spans in its length 120m, and in its maximum width more than 25m. One of the main design rules applied by ONL states that the length of the cockpit has to measure at least 10 times its height to guarantee that the cockpit keeps its smooth appearance when passed by at a speed of 120 km/h. The maximum height of the building is therefore 12 meters. The total floor space is 6400 m².

Structure The free formed shape of the cockpit building is only present on the motorway side of the building. The backside of the cockpit is build of with standard rolled profiles, covered with profiled steel plates. The other ‘leg’ of the three hinged truss is formed by the curved façade on the A2 motorway side, see Figure A.84.

Inside the building, 3 different levels for the car-showroom are located. These floors are connecting façades, but they have their own load bearing structure. No significant vertical loads from the floors are transmitted to the curved façade. The connection of the façades through the floors is beneficial for the stability of the façades, outward buckling of the curved façade is hindered by this coupling. The curved façade structure is build up of (over dimensioned) tubular steel profiles (total steel usage: 1000 tons), see Figure A.85. These

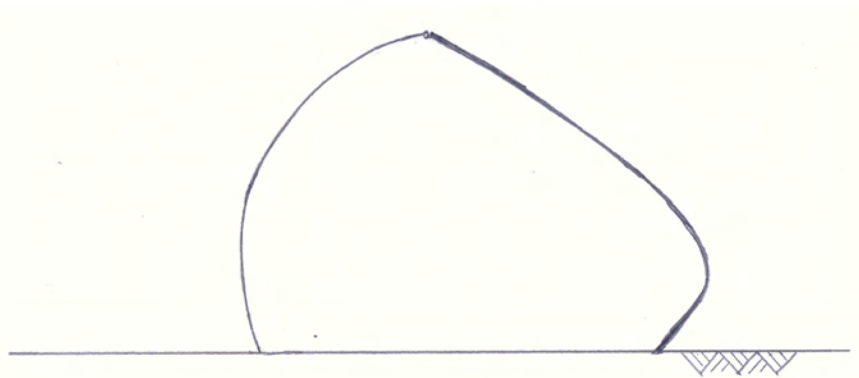


Figure A.84: Cross section of Hessing Cockpit

profiles are connected by a standard parametric node detail, in which 4 tubes come together. This way a quadrangular grid is formed. In order to make the grid form retaining, horizontal coupling profiles are added to divide the quadrangular grid into a triangular grid. On the outside of the structural steel, profiles are placed for supporting the triangular glazing (2000 m²).

Design and Construction process In the whole structural design process, no structural engineering firm has been involved. The structural design and the development of the construction process have been performed by a combination of the architect and the steel contractor. As with the Web of North Holland, a file to factory production process was used to feed the production machinery of the steel supplier with the design specific data. The production principle behind the steel structure is ‘Mass Customisation’. Production according to the principle of mass customisation follows a completely different path from the normal ‘Mass Production’ processes. There are no catalogues, the products are produced starting from raw material (which in most cases still is mass produced) for a specific purpose, to become a unique part on a unique location in a specific building. The ‘mass produced’ part will not fit anywhere else, it is a unique element.

The point cloud that forms the basis for the 3D model for the Acoustic Barrier and Cockpit Building is generated in a parametric way. Only a few parameters describe the total geometry of both the barrier and the building. These parameters are based on rules that are initiated by the architect. Client, contractor and façade supplier were able to alternate the parameters to optimise the design. The parametric lines that define the contours and cross sections are the base for the file to factory process. This geometrical envelope is divided into a structural grid, again by making use of parameters. The values of these parameters are defined in consultation with the steel- and façade supplier. This way the length and weight of the profiles can be economically optimised by increasing or decreasing the density of the grid. The intersection points of the geometrical envelope and the structural grid result in a point cloud that forms the base for the geometry of the main load bearing structure and the façade structure.

To get from a point cloud to a realisable design, several scripts are developed. These scripts are developed in such a way that each point of the point cloud (each structural node) can be elaborated iterative. If the geometry of the design changes, calculations, drawings, dimensioning and nodes are again generated by the scripts. In total three scripts were used.



Figure A.85: Structure of the Hessing Cockpit

The first two define the geometrical data of an element. The third script, written by the steel supplier, generates the main load bearing structure. This is an iterative process that creates a detail around each point of the point cloud based on parameters that are supplied by the architect and steel supplier. An optimisation routine is built in to realise a grid that is most economical for the combination of steel and glass supplier.

A.1.14 The Esplanade Theatres Singapore



Figure A.86: Esplanade Theatres in Singapore

Architect: DP Architects
Structural Engineer: Atelier One
Year: 2002

Geometry The Esplanade, a centre for performing arts, is located in the cultural heart of Singapore by the Marina Bay waterfront, see Figure A.86. The project consists of two domelike free formed buildings and incorporates an 1800 seat concert hall and a 2000 seat theatre, a 200 seat black box theatre and a 200 seat Recital Studio. The two main domes are referred to as The Concert Hall and the Lyric Theatre (according to the main functions that are accommodated). Both the Concert Hall and Lyric Theatre were designed and equipped to meet the needs of the most demanding performance events.

Because Singapore is almost on the Equator, the sun's position and movement is almost constant during the year. Therefore, the architect designed a fixed cladding system consisting of a glazed steel space frame with triangular sun shields. These shields are set to be more open or closed, depending on the angle the sun hits them. This way, the glass facades are protected from direct sunlight without limiting the views, see Figure A.86.

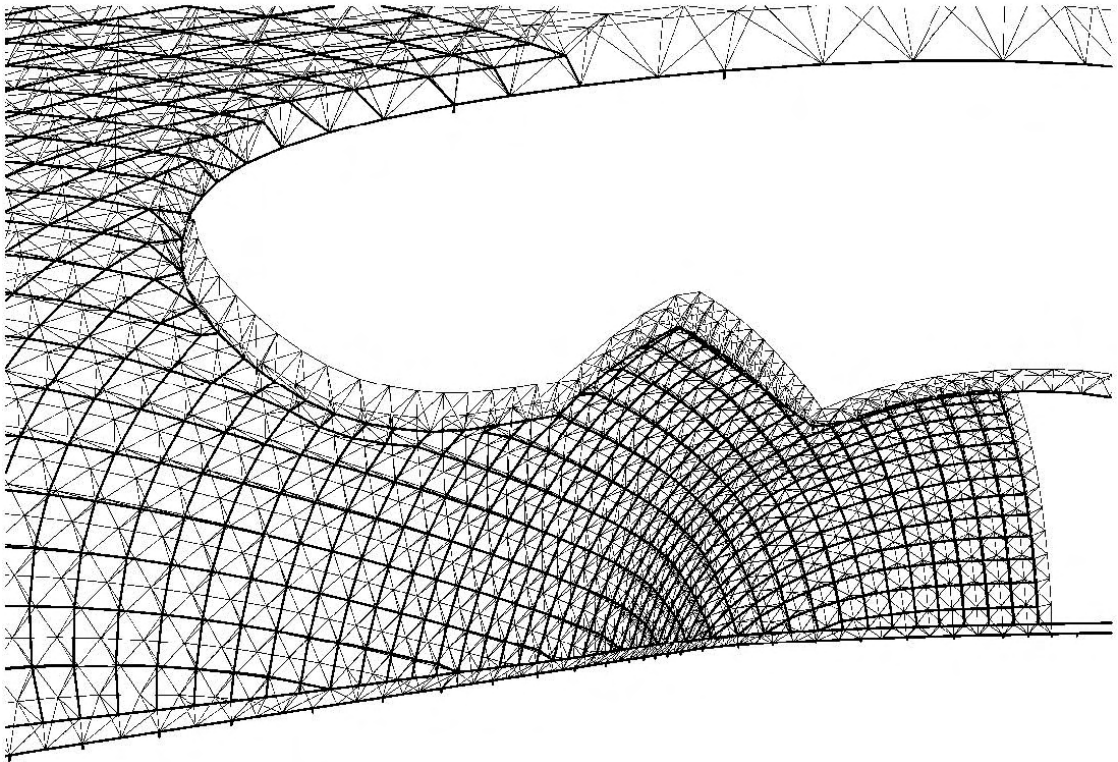


Figure A.87: Double layered Spaceframe for the Free Formed structure

Both the concert hall and theatre are housed in separate spaces. One of the main reasons to do this is to be able to comply with the high acoustic requirements for the both spaces. Therefore, both theatres are also supported by rubber footings to isolate them from the vibrations of nearby subway lines. Around the primary spaces (the actual performance spaces), lobbies and foyers are created by the free formed façade structure. These multi level secondary spaces are not linked to the free formed façade structure, and therefore are not causing any point concentrated loads on the dome like façade structure.

The curvature of the free formed envelope is irregular, but convex on all points of the surface. In comparison to other free formed buildings, the curvature of the envelope of the Esplanade is less irregular. Because there are no transitions from convex to concave curvature, bending moments in the façade structure are limited. What makes the domes even less irregular is the fact that they are symmetric around their long axis. The dimensions of the Concert Hall are: length 93 meters, width 59 meters, height from the inclined base edge, 26 meters and for the Lyric theatre: length 102 meters, width 61 meters, height from the inclined base edge, 24 meters.

Structure The shape of the domes is designed to fit tightly around the boxes of the Concert Hall and Lyric Theatre. The designed NURBS surfaces were meshed into rhombic grids by the architect to get the desired look of the building. The grid that was generated on the surface

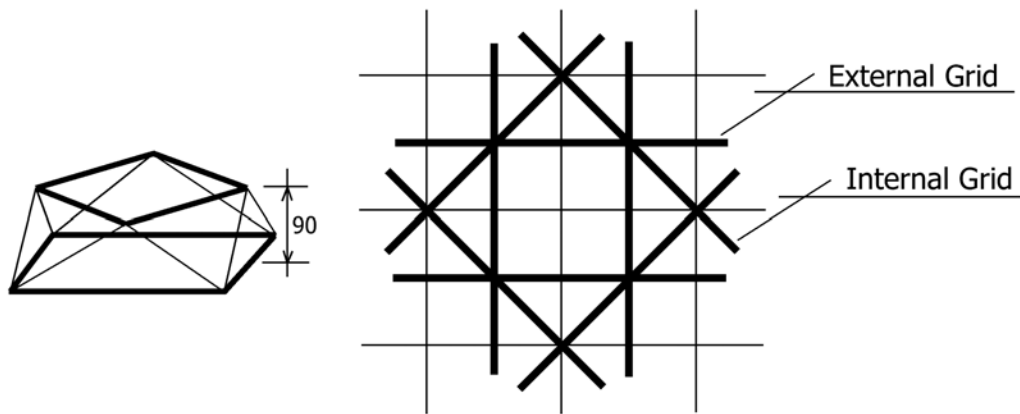


Figure A.88: Square-On-Diagonal Double Layered grid topology

has a constant mesh length of 1,5 meter. The difference between the two rhombic grids of the shells is the orientation of the meshes. For the Concert Hall, the main polygons run either along or across the base edge of the shell, whereas in the Lyric Theatre these polygons run diagonally to the base line. As structural solution for the envelopes of the Esplanade Theatres, a double layered spaceframe was chosen, see Figure A.87. The geometrical topology of the double layered grid is known as the square-on-diagonal double layered grid. This type of geometrical arrangement is used when a square on square layout is too dense. Because a high transparency is desired by the architect, the square-on-diagonal typology is chosen, see Figure A.88. The external grid matches the lines of the basic rhombic grid that was designed by the architect, the nodal points of the internal diagonal grid lie at a constant distance of 90 cm inside the external grid. The nodal points of internal grid are acquired by offsetting lines through the midpoints of the external net by 90 cm; the intersections between these offset lines form the nodes of the internal grid. The underlying grid is acquired by connecting the nodal points diagonally in a chessboard layout. The result is a $\sqrt{2}$ times as wide grid. To obtain the square-on-diagonal double layered grid, the nodes of the external grid are connected to the nodes of the internal grid. The rhombic external grid is split to obtain a triangulated grid. This triangular grid was required for the structural stability as well as for the support of the triangular glass planes.

The by MERO designed steel space trusses are supported at the bottom at each second or third top chord on concrete edge girders. The upper edges of the space trusses are supported by the concrete box of the Concert Hall / Lyric Theatre. To stabilise the envelope structure it was necessary to support the lower and upper edges of the space frames. At the lower edges, the bearing points are fully restraint, at the upper edges, it was necessary to allow for thermal expansion. At the top, the space frames are rigidly fixed to the non resilient stair towers; other bearing points are only supported horizontally where this is statically required. The solution for the upper bearings had to deliver an unrestrained support and take care of the vibration insulation to prevent the transfer of sound from the cladding into the concert and theatre auditorium. A special rubber composite was applied for the upper supports. For the structural analysis, besides the dead loads and live loads, wind- and thermal loads were considered.

The designed double layered spaceframe provides high accuracy through machined fabrication and can therefore be easily shaped into the designed free form geometry. The top chord members are square hollow sections to allow direct support for the triangular glass panels, see Figure A.89. The nodes of the top chord members are special bowl type nodes.

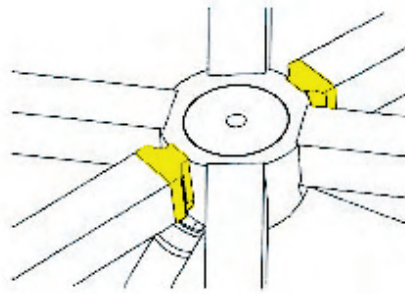


Figure A.89: Node detail, designed by MERO

To keep the nodes small, special head plates are applied for the square diagonal members, which divide the rhombic configurations into triangles. The space diagonal members and the bottom chord members are standard MERO round tubes, the nodes are forged spheres. All components were produced at the MERO workshops in Germany. In total, over 32.000 line elements and almost 8.500 nodes were necessary to construct the space frames for both domes.

The façade of the Esplanade Theatres is closed by triangular glass panels that are directly supported by the top chord of the space frame. In theory, only every second of the 10.500 glass panels is identical. When a tolerance of 2,5 millimeters is allowed, which can be adjusted in the joints, the number of different panels can be reduced to about 1.500. The panels are fixed to withstand wind suction by means of aluminium discs at the top chord nodes and by two additional clamps at each top chord member.

The façades of the Lyric Theatre and the Concert Hall are covered by 4.900 shading panels. The design steps for these panels were first to determine the rise of each panel and second to optimise the cutting patterns, similar to the glass panels. Result was thirty basic cutting patterns and thirty more special patterns for the edge panels. Panels are made of 4 mm thick aluminium sheets, which are supported at 300 mm above the top chord of the space trusses.

For the construction process a special erection sequence was planned. The domes were divided into sections that can best be described as vertical orientated strips. The erection was to follow these sections from top to bottom and proceed to the horizontally adjacent sections. Scaffolding was applied to allow adjustment to the hardly predictable requirements of the three dimensional spaceframe geometry. Spaceframe units of 4,5 meter by 4,5 meter to a maximum of 9 meter were pre assembled on the ground and lifted onto the concrete structure. After connection to the bearings, the erection succeeded with the single members and nodes. Two independent groups started erecting on one end of the symmetry line, both constructing towards the other end of the symmetry line, keeping each other in balance. The small tolerances in the fabrication of the nodes and members, together with permanent measurements of the node positions, enabled the erected structure to meet the described geometry.

A.2 Papers by Chris Williams

In this paragraph two papers by Dr. Chris Williams, an Engineer, formerly at Arup and later at Buro Happold, and tutor at the University of Bath. Amongst others he was responsible for the

structural design of the glass roof of the British Museum. He often uses form finding techniques to help him with his designs.

THE ANALYTIC AND NUMERICAL DEFINITION OF THE GEOMETRY OF THE BRITISH MUSEUM GREAT COURT ROOF

Chris J K Williams
University of Bath, UK

Abstract: The steel and glass British Museum Great Court Roof covers a rectangular area of 70 by 100 metres containing the 44 metre diameter Reading Room. The paper describes in detail how the spiralling geometry of the steel members was generated working closely with the architects, Foster and Partners, and the engineers, Buro Happold. A combination of analytic and numerical methods were developed to satisfy architectural, structural and glazing constraints. Over 3000 lines of computer code were specially written for the project, mainly for the geometry definition, but also for structural analysis.

Introduction

Figure 1 is a computer generated image of the original scheme for the roof and this paper will describe the process of generating the final geometry from this starting point.

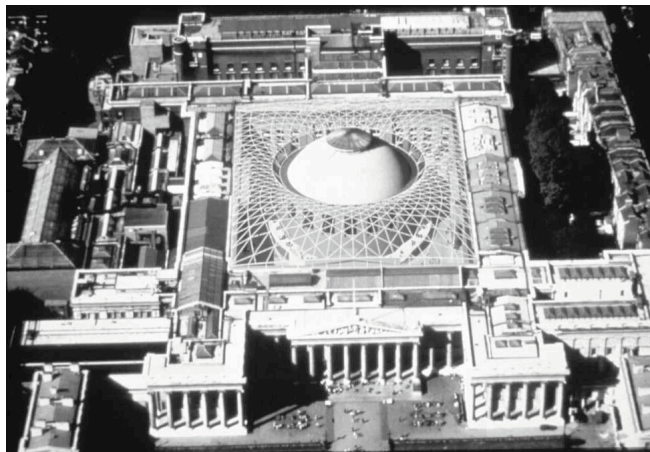


Figure 1. Computer generated image of the original scheme

The British Museum Great Court is 73m east-west and 97m north-south. The centre of the 44m diameter Reading Room is offset 3m to the north of the centre of the Court. The space in the Court outside the Reading Room was used for temporary book store buildings, but with the completion of the new British Library at St Pancras the book storage was no longer required.

The new roof over the Court was designed by Foster and Partners, architects, and Buro Happold, engineers, and was fabricated and erected by Waagner Biro. The roof is constructed of a triangular grid of steel members welded to node pieces. The members are boxes welded from plate and are tapered to change depth. The grid is triangulated for structural stiffness and so that it can be glazed with one flat panel of double glazing for each triangle of the structural grid.

The roof is supported around the Reading Room and on the rectangular boundary where it sits on sliding bearings to avoid imposing lateral thrusts on the existing building. This means that the roof can only push outwards at the corners where it can be resisted by a tension in the edge beam. Internal tension ties were considered, but rejected on architectural grounds.

The surface geometry

The shape of the roof is defined by a surface on which the nodes of the steel grid lie. The height of the surface, z , is a function of x in the easterly direction and y in the northerly direction. The origin lies on a vertical line through the centre of the Reading Room. The function is: $z = z_1 + z_2 + z_3$ where $z_1 = (h_{\text{centre}} - h_{\text{edge}})\varphi + h_{\text{edge}}$,

$$\frac{z_2}{\varphi} = (1 - \varphi) \left[\frac{35.0 + 10.0\varphi}{2} (1 + \cos 2\varphi) + \frac{24.0}{2} (1 - \cos 2\varphi) + \sin \varphi \right] + (7.5 + 12.0\varphi) \frac{1}{2} (1 - \cos 2\varphi) - \sin \varphi + 1.6$$

$$+ \frac{10.0}{2} (1 + \cos 2\varphi) + 10.0 \frac{1}{2} \frac{1}{2} (1 - \cos 2\varphi) + \sin \varphi (1.0 - 3.0\varphi)$$

$$+ 2.5 \frac{1}{2} \frac{1}{2} (1 - \cos 2\varphi) - \sin \varphi \frac{r}{a} + 1$$

and

$$\frac{z_3}{\varphi} = \frac{3.5}{2} (1 + \cos 2\varphi) + \frac{3.0}{2} (1 - \cos 2\varphi) + 0.3 \sin \varphi$$

$$+ 1.05 \left[e \frac{x}{b} + e \frac{x}{b} + e \frac{y}{c} + e \frac{y}{d} \right]$$

In these expressions the polar co-ordinates, $r = \sqrt{x^2 + y^2}$ and $\varphi = \cos^{-1} \frac{x}{r} = \sin^{-1} \frac{y}{r}$, and

$$\varphi = \frac{1}{r} \left[\frac{x}{b} + \frac{x}{b} + \frac{y}{c} + \frac{y}{d} \right], \quad \varphi = \frac{1}{r} \left[\frac{x}{b} + \frac{x}{b} + \frac{y}{c} + \frac{y}{d} \right], \quad \varphi = \frac{r}{a} + 1$$

$$\frac{1}{r} \frac{a}{r} = \frac{ax}{rb} + \frac{ax}{rb} + \frac{ay}{rc} + \frac{ay}{rd}$$

$$\frac{1}{r} \frac{a}{r} = \frac{\sqrt{(b-x)^2 + (c-y)^2}}{(b-x)(c-y)} + \frac{\sqrt{(b-x)^2 + (d+y)^2}}{(b-x)(d+y)} + \frac{\sqrt{(b+x)^2 + (c-y)^2}}{(b+x)(c-y)} + \frac{\sqrt{(b+x)^2 + (d+y)^2}}{(b+x)(d+y)}$$

The constants are $a = 22.245$, $b = 36.625$, $c = 46.025$, $d = 51.125$, $\varphi = 0.5$, $\varphi = 14.0$, $h_{\text{centre}} = 20.955$ and $h_{\text{edge}} = 19.71$.

The functions z_1 , z_2 and z_3 are each built up from its own fundamental function. The first, shown in figure 2, supplies the correct change in level between the rectangular boundary and the circular Reading Room. The vertical scale in the figure is chosen arbitrarily. The original scheme had the roof level arching up along each of the rectangle edges, and this would have had certain structural advantages, but the final scheme has a constant height along the edges. The remaining two fundamental functions give $z = 0$ around the rectangular and circular boundaries.

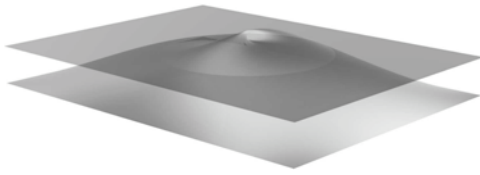


Figure 2. Level change function,

$$\frac{\frac{x}{b} + \frac{x}{b} + \frac{y}{c} + \frac{y}{d}}{\frac{ax}{rb} + \frac{ax}{rb} + \frac{ay}{rc} + \frac{ay}{rd}}$$

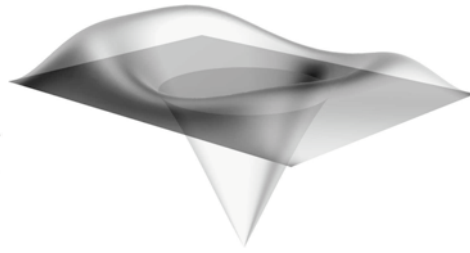


Figure 3. Function with finite curvature at corners

$$\frac{r}{a} \left(\frac{x}{b} + \frac{x}{b} + \frac{y}{c} + \frac{y}{d} \right)$$

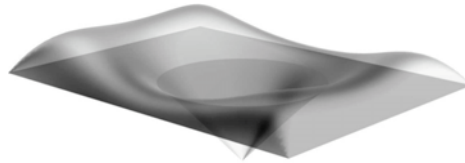


Figure 4. Function with conical corners

$$\frac{1 - \frac{a}{r}}{\frac{\sqrt{(b-x)^2 + (c-y)^2}}{(b-x)(c-y)} + \frac{\sqrt{(b-x)^2 + (d+y)^2}}{(b-x)(d+y)} + \frac{\sqrt{(b+x)^2 + (c-y)^2}}{(b+x)(c-y)} + \frac{\sqrt{(b+x)^2 + (d+y)^2}}{(b+x)(d+y)}}$$

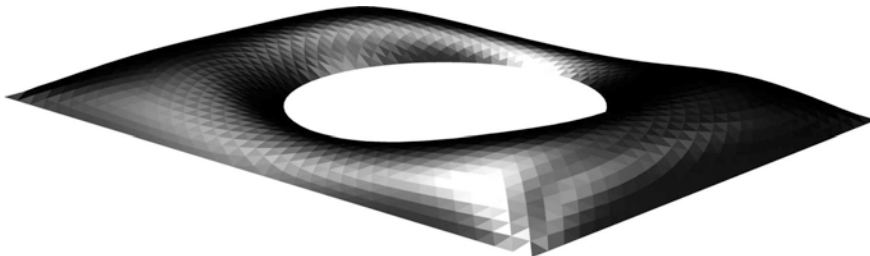


Figure 5. Final surface

The second fundamental function is shown in figure 3. Both this function and the first produce a horizontal surface at the corners. This is inevitable unless the curvature tends to infinity at the corners, like approaching the tip of a cone and this is what happens with the third fundamental function shown in figure 4.

The issue of the curvature of the corners was important for architectural and structural reasons and the relative amount of the second and third fundamental functions was chosen to balance these constraints. The corners were important structurally because of the thrusts coming down to the corners to be balanced by tensions in the edge beam. The corners are reinforced locally by external trusses which cannot be seen from inside the Court.

The final shape was obtained by adding a constant times the first fundamental function to the second and third fundamental functions multiplied by two different functions of x and y . These extra functions were chosen to satisfy planning, architectural and structural constraints.

Figure 5 shows the final surface on which the faceting is that of the glazing grid. The concentration of curvature at the corners can be seen.

The structural grid

The structural grid passed through many stages before arriving at the final form as shown in the right hand drawing in figure 6. In the early scheme on the left of figure 6 the grid meets the rectangular boundary in an unsatisfactory way in that some triangles are cut through, leading to a combination of triangles and quadrilaterals. The central drawing overcomes this problem, but is still coarse compared to the final form.

The starting point in producing the final grid is shown in figure 7. This is a simple geometric drawing in which points equally spaced around the Reading Room are joined to equally spaced points around the rectangular boundary. The radial lines so formed are then divided into varying numbers of equal segments. The structural grid is produced from this 'mathematical grid' by 'joining the dots' as seen in the right hand half of figure 7.

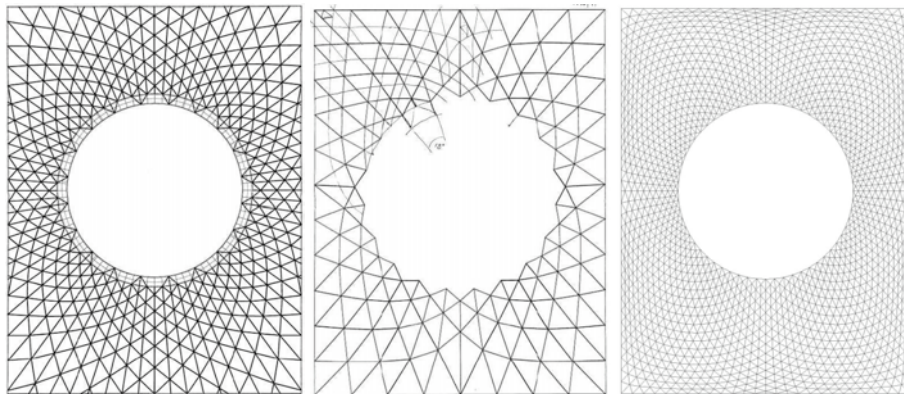


Figure 6. Evolution of the structural grid

However this produces discontinuities, particularly on the diagonal directions. These were removed by 'relaxing' the grid to produce figure 8. The relaxation process was as follows.

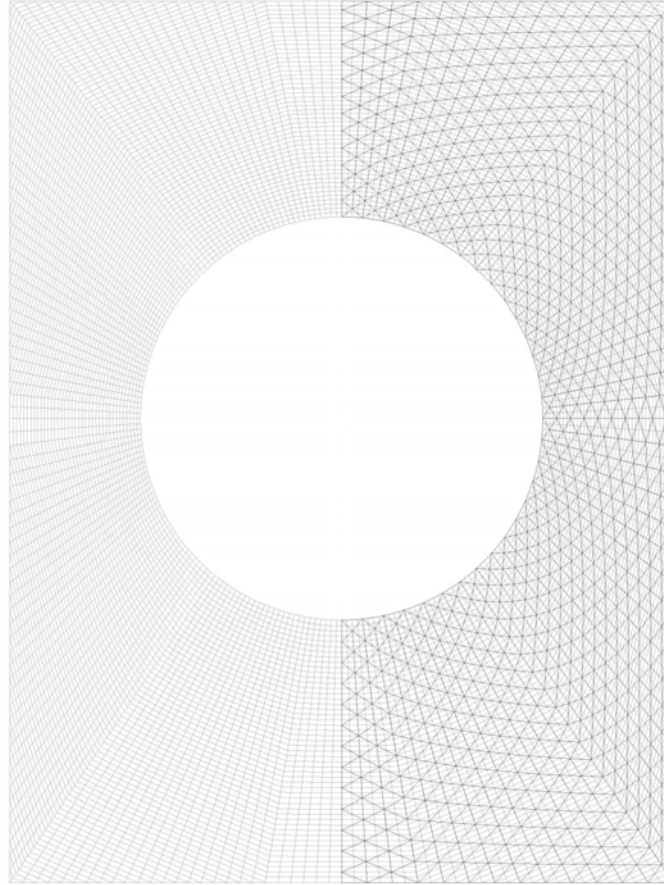


Figure 7. Starting grid

Figure 9 shows a typical node, i, j of the mathematical grid surrounded by its four neighbours. If $\mathbf{p}_{i,j}$ is the position vector of the typical node at some point during the relaxation process, then

$$\mathbf{f}_{i,j} = (\mathbf{p}_{i-1,j} - \mathbf{p}_{i,j}) + (\mathbf{p}_{i+1,j} - \mathbf{p}_{i,j}) + (2 - \Delta)(\mathbf{p}_{i,j-1} - \mathbf{p}_{i,j}) + \Delta(\mathbf{p}_{i,j+1} - \mathbf{p}_{i,j})$$

would be the fictitious force applied to the node by 'strings' attached to the neighbouring nodes if the tension coefficients of the strings are 1, 1, $(2 - \Delta)$ and Δ . The tension coefficient is the tension in a member divided by its length. The purpose of the variable Δ will be described later.

Now imagine that the nodes of the mathematical grid are free to slide with no friction over the surface defining the shape. The force $\mathbf{q}_{i,j} = \mathbf{f}_{i,j} - (\mathbf{f}_{i,j} \cdot \mathbf{n}_{i,j})\mathbf{n}_{i,j}$ (where $\mathbf{n}_{i,j}$ is the unit normal to the surface) is the component of $\mathbf{f}_{i,j}$ tangential to the surface and therefore the nodes will slide until all the $\mathbf{q}_{i,j} = 0$.

The quantity $\Delta = 1 - 0.004(1.5m - j)(1 - \cos 2\theta)$ where $m = 70$ is the value of j on the Reading Room boundary and θ is the polar co-ordinate. This function was chosen so as to

control the maximum size of the glass triangles which occur near the centre of the southern boundary. It was the limitation on glass size which was the controlling factor in choosing the structural grid.

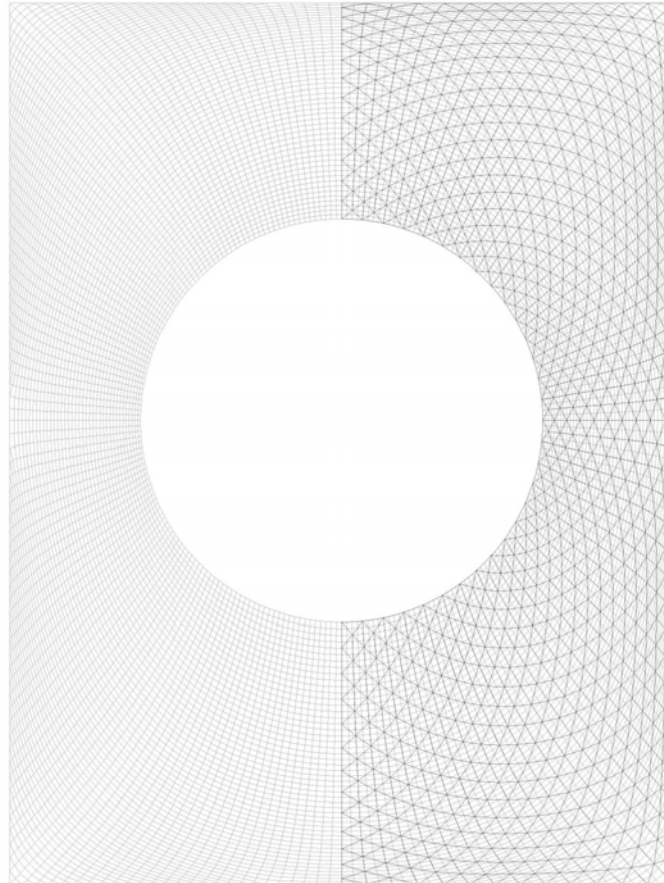


Figure 8. Relaxed grid

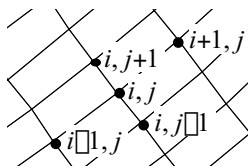


Figure 9. Typical grid nodes

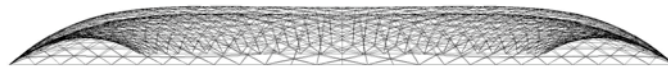


Figure 10. Elevation of structural grid looking north

The non-linear equations $\mathbf{q}_{i,j} = 0$ were solved by repeated application of the algorithm $(\Delta \mathbf{p}_{i,j})_{\text{this cycle}} = c_1 \mathbf{q}_{i,j} + c_2 (\Delta \mathbf{p}_{i,j})_{\text{the previous cycle}}$ where $\Delta \mathbf{p}_{i,j}$ is the movement of the typical node and the constants c_1 and $c_2 \leq 1.0$ are chosen to optimise the speed of convergence. The larger the constants, the faster the convergence, but if they are too high,

numerical instability occurs. This process is known as *dynamic relaxation* and was invented by Alister Day. The whole mathematical grid was run through 5000 cycles before the process was judged to have converged. Convergence was speeded by using setting $c_2 = 0$ when the sum of the squares of the $\Delta p_{i,j}$ passed through a maximum.

Figures 10, 11 and 12 show the final structural grid.



Figure 11. Elevation of structural grid looking west

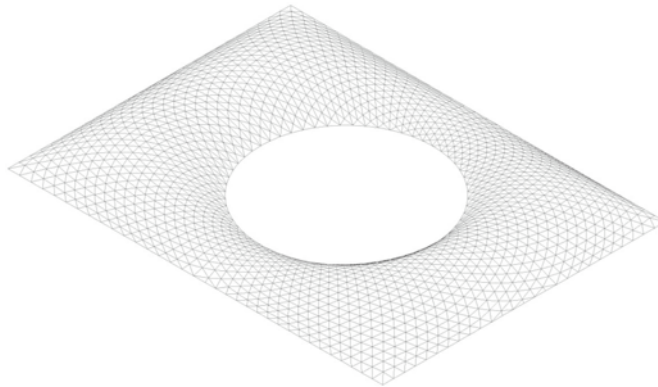


Figure 12. Isometric of structural grid

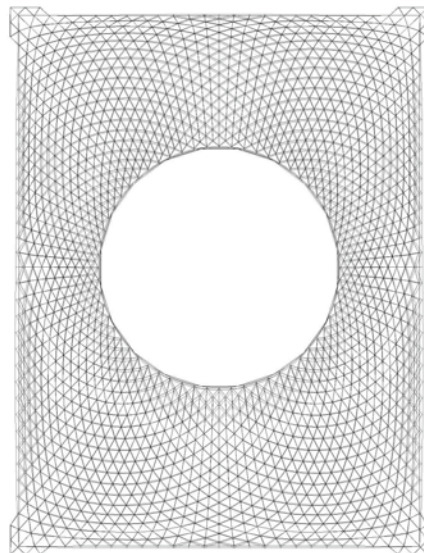


Figure 13. Outwards deflections due to loading

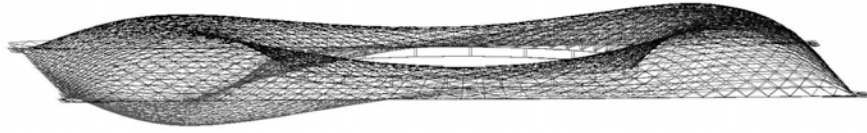


Figure 14. View showing south side collapsed while north remains standing

Structural analysis

A detailed description of the structural analysis of the roof is beyond the scope of this paper. A specially written computer program was used, together with commercial software. Figures 13 and 14 show the deflections due to a large vertical load, much larger than possible on the roof. The spreading of the boundaries can be seen on the plan and on figure 14 it can be seen that the south side has collapsed, hanging in tension, while the north side still stands.



Figure 15. Day and night views

Conclusion

This paper discusses one aspect of one project and figure 15 contains photographs of the completed Great Court. Papers by the architects, engineers and builders of this and other recent projects are contained in Barnes and Dickson (2000).

References

Michael R. Barnes and Michael G.T. Dickson, Thomas Telford, *Widespan roof structures*, London 2000

The definition of curved geometry for widespan enclosures

Chris J K Williams
Department of Architecture and Civil Engineering
University of Bath
UK

1 Introduction

If an enclosure is to be constructed of curved lines and surfaces rather than straight lines and flat planes, the questions arise as to how the geometry is first to be chosen and then how it can be defined with sufficient accuracy for the structure to be built and clad.

There are clearly many ways that the geometry can be chosen and defined, but they fall into three broad categories and the methods used on any one project may fall into more than one of these categories. The categories are:

Sculptural in which a model is sculpted by hand or a computer model is constructed that can be deformed interactively.

Geometric in which the form is defined in terms of geometrical objects which might be simple spheres, cylinders or cones, or much more complicated objects which can only be visualised using computers.

Physical in which the shape is controlled by some physical process such as a soap film or a hanging chain. The physical process may be modelled by an actual physical model or a mathematical model which may be analytic or numerical in a computer.

An example of a mixed sculptural and physical approach would be bending a piece of wire by hand (the sculptural part) and then dipping it into soap solution and withdrawing it to form a soap film (the physical part).

An example of a mixed geometric and physical approach would be forming a soap film between two parallel circular rings so that the rings are simple geometric entities. In this case the soap film forms a catenary of revolution so that one might say that it is a relatively simple geometric object formed by a physical process.

The methods used for any one project will depend upon many factors. Perhaps the most important of these is the relative importance of structural, architectural and other constraints. Another is the experience of the design team in using various techniques, especially since the technology may have evolved in other disciplines such as sculpture, medicine or automobile, aerospace or ship design.

In the following I shall discuss some recent experience using a number of methods to try and illustrate the possibilities of the three approaches.

2 Sculptural

Traditionally large sculptures or even car bodies were first made as small clay models or maquettes which were measured and enlarged. Now much of this work is done using computers employing software written for the automobile and aerospace

industries. Frank O. Gehry & Associates use aerospace software, but the starting point is still physical models.

Such software is expensive and time is needed to learn how it can be used. Curved lines are divided up into a series of spline curves which fit together with an appropriate continuity of orientation and curvature. Curved surfaces are constructed from curved patches. These patches, developed for Computer Aided Design are very similar to the finite elements developed for the analysis of shell structures.

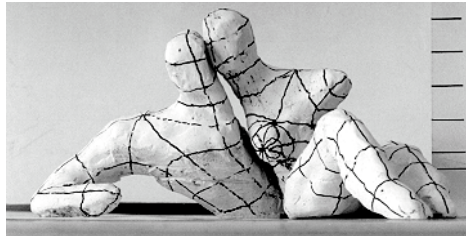


Figure 1 Body Zone sculpture

Architect: Branson Coates Architecture

Engineer: Buro Happold

Figures 1 to 5 show the Body Zone in the Millennium Dome. The shape was defined by the small physical model in the photographs in figure 1. A structural grid was drawn on the model and this was measured using a standard CAD package from scanned images of the photographs. This data was used to construct the computer model shown in figure 2.



Figure 2 First computer model

Architect: Branson Coates Architecture

Engineer: Buro Happold

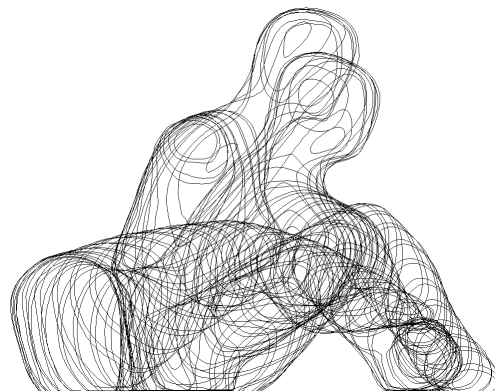


Figure 3 Sections through sculpture

Architect: Branson Coates Architecture

Engineer: Buro Happold

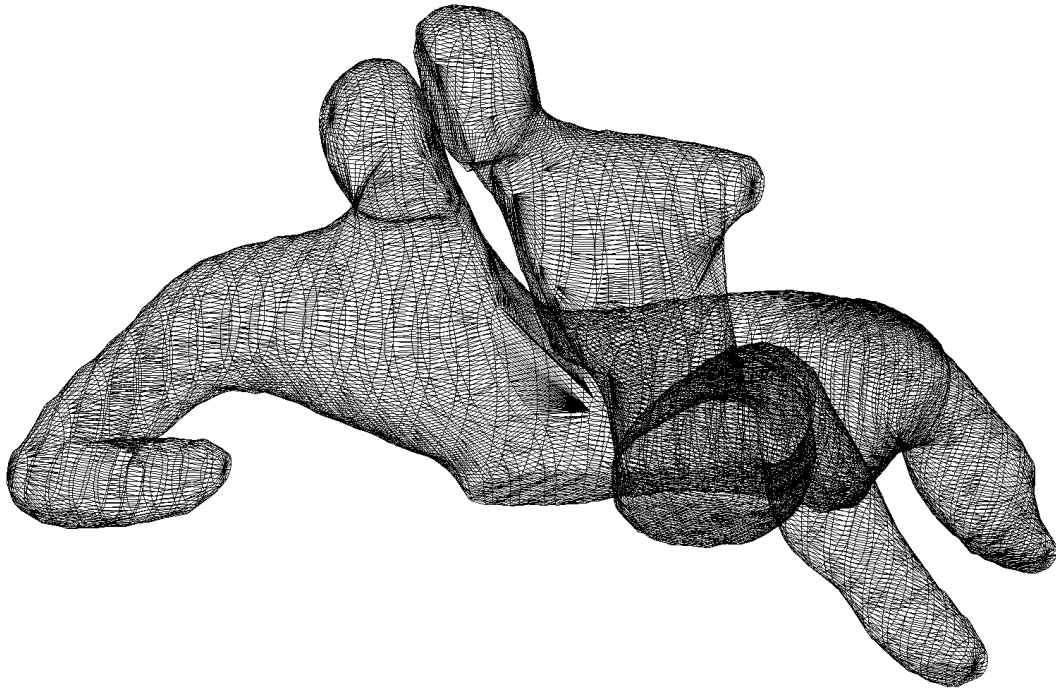


Figure 4 Computer model from sections

Architect: Branson Coates Architecture

Engineer: Buro Happold

Following this work it was decided to concentrate on defining the figures in terms of parallel cross-sections. A copy of the physical model was sliced using a saw and the resulting cross-sections were scanned and 'traced' to produce figure 3. These cross-sections were joined to produce the three dimensional image shown in figures 4 and 5.

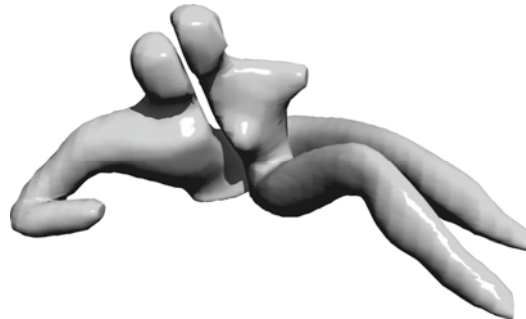


Figure 5 Rendered image

Architect: Branson Coates Architecture

Engineer: Buro Happold

The software used to produce figures 2, 3 and 4 was specially written for the project.

3 Geometric

The limit of what can be done using geometry is the mathematical knowledge and imagination of the individual. As an example let us consider Le Corbusier's Modulor¹ shown in figure 6b. Modulor is based upon the Fibonacci series, examples of which are

1, 1, 2, 3, 5, 8, 13, 21, 34,

and

1, 3, 4, 7, 11, 18, 29, 47,


```

#include <iostream.h>
#include <math.h>
int i,j,k,m,nhalfcycles,finish;
float PI,x,y,z,U,V,W,alpha,beta,
      A,C,phi;
ofstream Julia("Modulor.dxf");
int main(void)
{
PI=4.0*atan(1.0);
Julia<<"0\nSECTION\n2\nENTITIES\n";
nhalfcycles=18;m=20*nhalfcycles;
phi=(1.0+sqrt(5.0))/2.0;C=216.0;
for(j=1;j<=4;j+=1)
{
if(j==4)finish=90.0;
else finish=60;
for(k=0;k<=finish;k+=3)
{
A=1.2*cos((PI*k)/180.0);
for(i=0;i<=m;i+=1)
{
beta=-(1.0*i*nhalfcycles)/(2.0*m);
alpha=beta;if(j<=2)alpha-=0.5;
y=C*pow(phi,alpha);
if(j==1||j==3)
x=A*y*fabs(sin(beta*PI));
if(j==2||j==4)
x=A*0.5*y*fabs(sin(2.0*beta*PI));
if(j<=2)x=-x;
x=x/8.0;
z=0.0;
if(i!=0)
{
Julia<<"0\nLINE\n8\n0\n";
Julia<<"10\n"<<U<<"\n20\n"<<
V<<"\n30\n"<<W<<"\n";
Julia<<"11\n"<<x<<"\n21\n"<<
y<<"\n31\n"<<z<<"\n";
}
U=x;V=y;W=z;
}
}
}
Julia<<"0\nENDSEC\n0\nEOF\n";
Julia.close();
cout<<"DXF file written\n";
return 0;
}

```

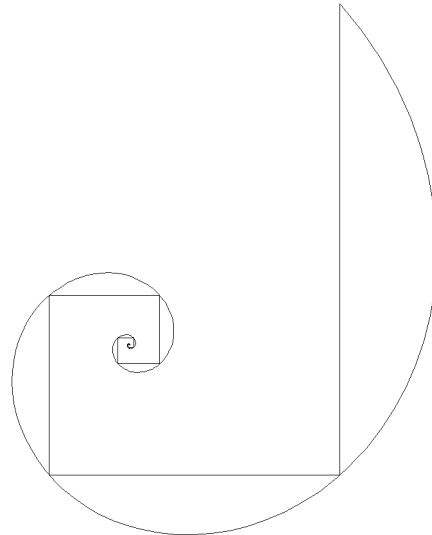


Figure 7 Golden section log spiral

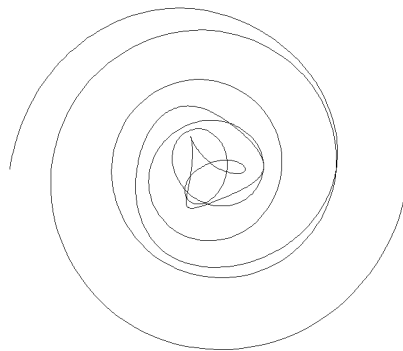


Figure 8 Two spirals

The program will run on any computer (Macintosh, PC etc.) with a C++ compiler and very little work would be required to convert the program to Basic or Fortran.

An unlimited variety of curves and surfaces can be produced by such programs. For example, figures 7, 8 and 9 were produced using the formulae

$$x = r^2 \cos 2\theta$$

$$y = r^2 \sin 2\theta$$

$$x = r^2 \cos 2\theta + r^3 \cos \theta$$

$$y = r^2 \sin 2\theta + r^3 \sin \theta$$

and

$$x = (1 + r) r^2 + (1 - r) r^3 \cos \theta$$

$$y = (1 - r) r^3 \sin \theta$$

respectively.

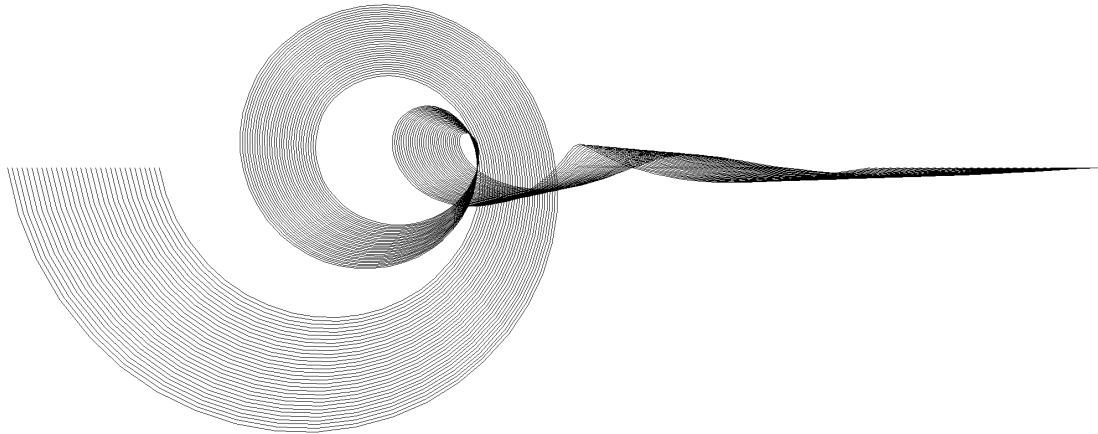


Figure 9 Spirals to lines

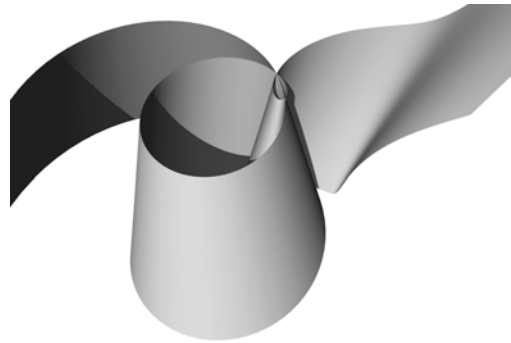


Figure 10 Rendered image

In each case \square is varied to draw a curve and in the case of figure 9, a different value of \square is used for each curve.

The surface in figure 10 was obtained from the curves in figure 9 by giving each curve a different value of z .



Figure 11 Bridge study

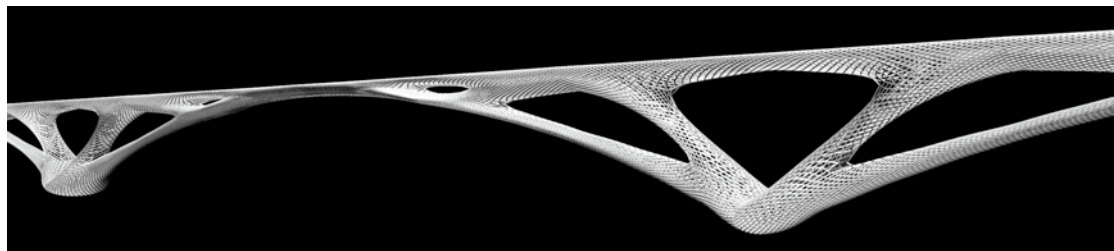


Figure 12 Bridge study

The bridge studies in figures 11, 12 and 13 were also produced by purely mathematical methods as was the shell study in figure 14. In each case the whole object is defined by the just one set of mathematical formula so that there is complete continuity of all derivatives, orientation, curvature, rate of change of curvature etc.



Figure 13 Bridge study

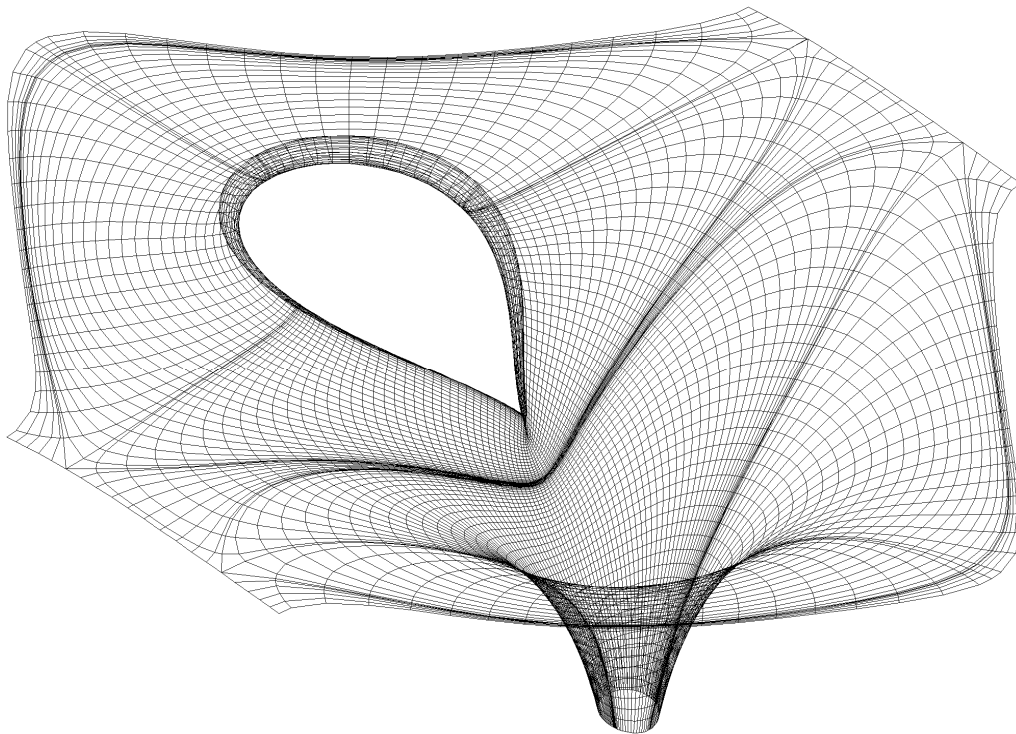


Figure 14 Shell study for Stuttgart railway station

Architect: Ingenhoven Overdiek Kahlen und Partner

Consultant Architect: Professor Frei Otto

Engineer: Buro Happold

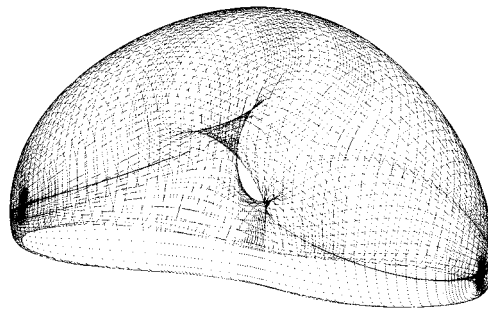


Figure 15 Millennium Dome Rest Zone - system geometry

Architect: Richard Rogers Partnership

Engineer: Buro Happold

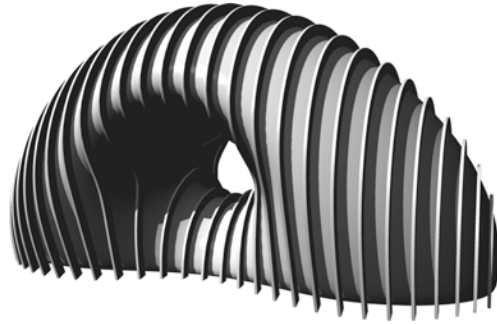


Figure 16 Rest Zone

Architect: Richard Rogers Partnership

Engineer: Buro Happold

Figures 15 and 16 show the Rest Zone in the Millennium Dome which was produced by deforming a torus. Again there is complete continuity of all derivatives.

4 Physical

In the membrane theory of shell structures the geometry of the structure and the loads are assumed to be known and the three membrane stresses - two tensile or compressive and one shear are unknown.

There are three equations of equilibrium, one in the direction normal to the surface,

$$\sigma^{\alpha\alpha} b_{\alpha\alpha} + p = 0,$$

and two in the plane of the surface,

$$\sigma^{\alpha\beta}{}_{;\beta} + p^{\alpha} = 0.$$

The notation here is similar to that in Green and Zerna². In these equations the geometry of the shell is determined by the components of the metric tensor, $g_{\alpha\beta}$, and of the curvature tensor, $b_{\alpha\beta}$. The components of load are p^{α} and p , and the unknown membrane stress components are σ^{11} , σ^{22} and $\sigma^{21} = \sigma^{12}$.

The fact that there are three equilibrium equations and three unknown membrane stress components means that shells are essentially statically determinate if the overall shape and boundary supports permit. An inappropriate shape or lack of support may mean that a shell is a mechanism.

It is not at all obvious which shapes and support conditions lead to mechanisms and which do not. Spivak³ discusses this issue in purely geometric terms, for example the Cohn-Vossen theorem states that any complete convex surface with positive Gaussian curvature is not a mechanism if membrane strains are prevented.

A cooling tower on the ground is not a mechanism, but a spherical shell with a hole in the top is.

A shell may also be a mechanism if it is made of masonry, so that the principal membrane stresses must be compressive, or if it is made of fabric in which case they must be tensile.

A mechanism can carry certain loads if it has the correct shape. In the case of a masonry structure, the dominant load is the dead load and in the case of a fabric structure it is prestress upon which wind and snow are added.

Form finding is the process of establishing a structural geometry for a mechanism to carry a particular load.

Gaudi used hanging models which, when inverted, defined the shape of masonry arches and vaults for the Colonia Guell and the Sagrada Familia. Professor Frei Otto pioneered the use of physical models for fabric structures, cable nets and grid shells.

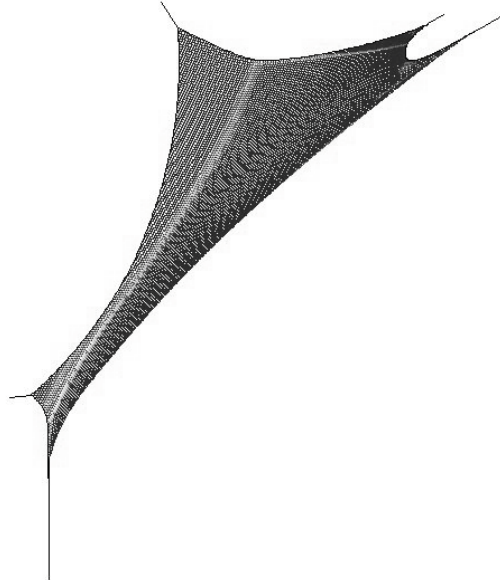


Figure 17 Tree of the Future

Architect: Mark Fisher Associates

Engineer: Atelier One

Form finding: Lynne Mabon, University of Bath

Now much of this work is done with numerical models, although physical models are indispensable for initial studies. Form finding a fabric structure with a soap film or minimal surface is done by setting the membrane stress components

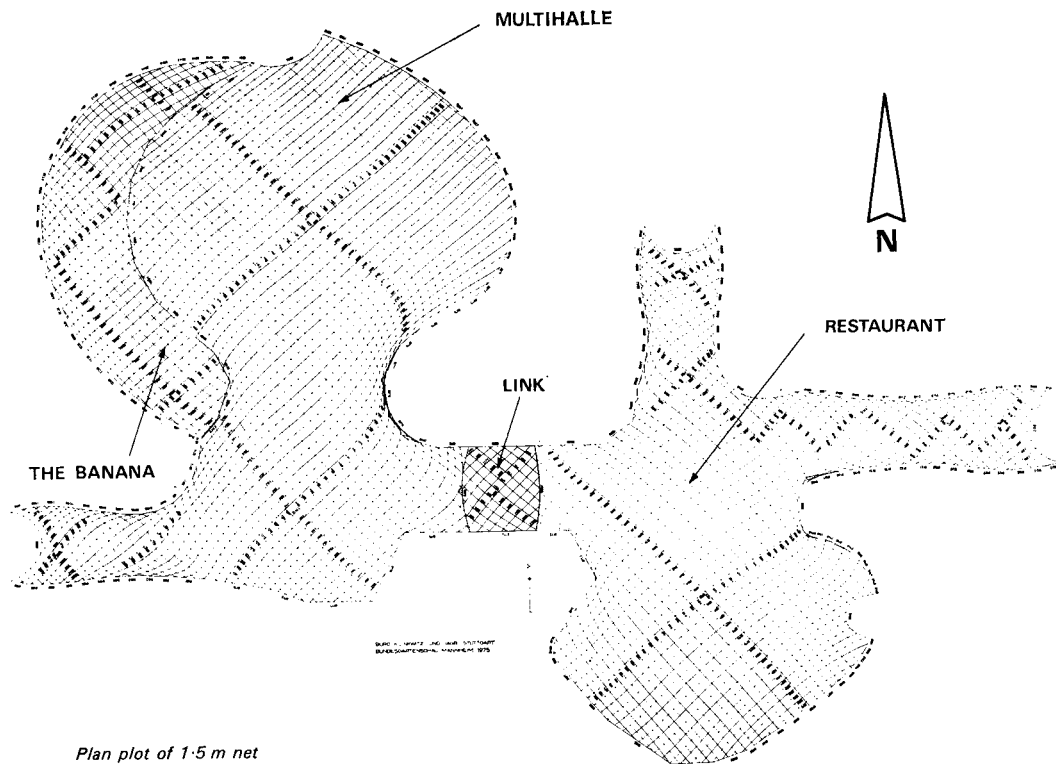
$$\sigma_{\alpha\alpha} = Tg_{\alpha\alpha}$$

where T is the surface tension. In addition a geodesic co-ordinate system for generating the cutting the pattern is obtained by imposing the conditions $g_{12} = 0$ and $g_{22} = \text{constant}$.

An equal mesh net is produced by writing

$$g_{12} = 0 \text{ and } g_{11} = g_{22} = \text{constant},$$

if there is no elastic extension, otherwise g_{11} and g_{22} increase with tension. Equal mesh nets are more difficult to form find than fabric structures due to the adjustment of cable lengths at the boundary.



Plan plot of 1.5 m net

Figure 18 Mannheim Bundestgartenschau 1.5m grid

Architect: Mutschler & Partners

Consultant Architect: Atelier Warmbronn (Professor Frei Otto)

Form finding: Büro Linkwitz

Engineer: Ove Arup & Partners (Ted Happold and Ian Liddell)

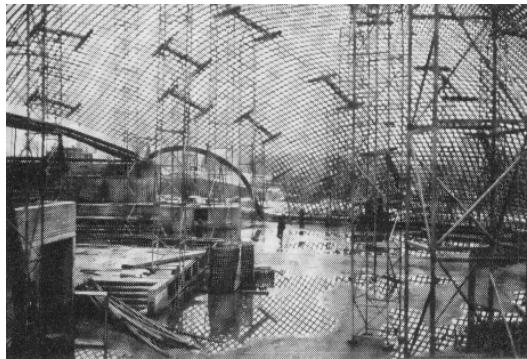


Figure 19 Mannheim erection

Figure 17 shows one of the equal mesh nets of the Tree of the Future intended for the Central Show in the Millennium Dome. In this case a computer program was specially written by Lynne Mabon of Bath University which automatically generated the boundary data.

Figure 18 shows the hanging chain model for the Mannheim Bundestgartenschau. This is a computer generated model by Büro Linkwitz, based upon Frei Otto's accurate physical model. Figures 19 and 20 show the erection and load testing of the shells.

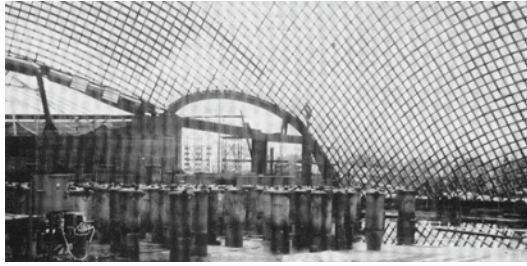


Figure 20 Mannheim load test

Figures 21 and 22 show computer generated models of the Weald and Downland Museum. In this case the mathematical model had to contain bending stiffness during form finding, otherwise compressive stresses produced wrinkling.

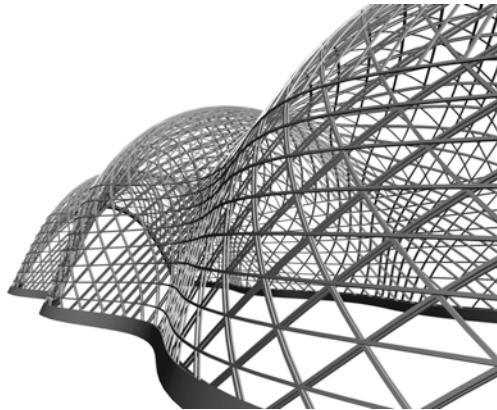


Figure 21 Weald and Downland Museum

Architect: Edward Cullinan Architects

Engineer: Buro Happold

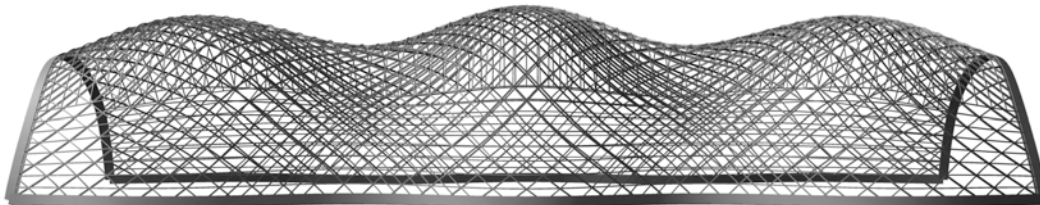
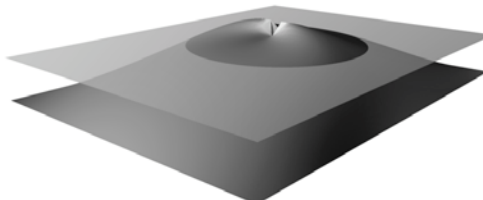


Figure 22 Weald and Downland Museum

Architect: Edward Cullinan Architects Engineer: Buro Happold

5 The British Museum Great Court Roof

Figure 30 is an image of the computer model of the British Museum Great Court Roof. It was generated by a mixed approach.



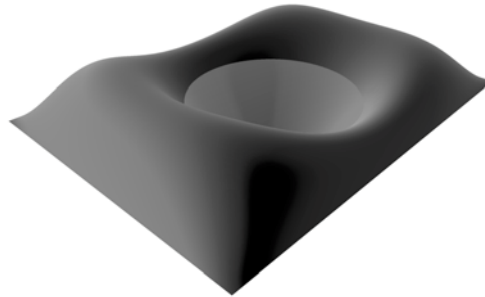
$$\frac{z}{h} = \frac{\left(1 - \frac{x}{b}\right) \left(1 + \frac{x}{b}\right) \left(1 - \frac{y}{c}\right) \left(1 + \frac{y}{d}\right)}{\left(1 - \frac{ax}{rb}\right) \left(1 + \frac{ax}{rb}\right) \left(1 - \frac{ay}{rc}\right) \left(1 + \frac{ay}{rd}\right)} \text{ where } r = \sqrt{x^2 + y^2}$$

Figure 23 British Museum Great Court Roof - first function

Architect: Foster and Partners

Engineer: Buro Happold

The shape of the surface was defined analytically by weighting and summing functions based on those shown in figures 23, 24 and 25. The weightings also varied with position to satisfy architectural, planning, structural and clearance requirements.



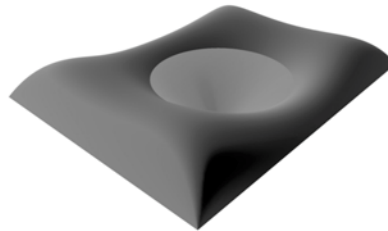
$$\frac{z}{H} = \left(1 - \frac{x}{b}\right) \left(1 + \frac{x}{b}\right) \left(1 - \frac{y}{c}\right) \left(1 + \frac{y}{c}\right) \left(\frac{\sqrt{x^2 + y^2}}{a} - 1\right)$$

Figure 24 British Museum Great Court Roof - second function

Architect: Foster and Partners

Engineer: Buro Happold

The positions of nodes on the surface were obtained from the starting grid shown in figure 26. A displacement was calculated for each interior node of this grid to make its x , y and z co-ordinates the weighted average of the current co-ordinates of the four surrounding nodes. However, before moving a node, the component of displacement normal to the surface (see figure 27) was removed so that the node remained on the surface. This relaxation procedure was repeated thousands of times for the whole structure until the geometry settled down to that in figure 28.



$$\frac{z}{\lambda} = \frac{\sqrt{x^2 + y^2} - 1}{\frac{a}{\sqrt{(b-x)^2 + (c-y)^2} + \sqrt{(b+x)^2 + (c-y)^2} + \sqrt{(b-x)^2 + (d+y)^2} + \sqrt{(b+x)^2 + (d+y)^2}}}$$

Figure 25 British Museum Great Court Roof - third function

Architect: Foster and Partners

Engineer: Buro Happold

The weighting of the surrounding nodes was varied at different points on the surface to control the distribution of the nodes, in particular in relation to the sizes of the glass panels.

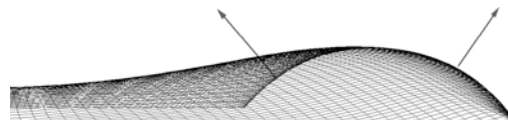


Figure 27 British Museum Great Court Roof - surface normals

Architect: Foster and Partners

Engineer: Buro Happold

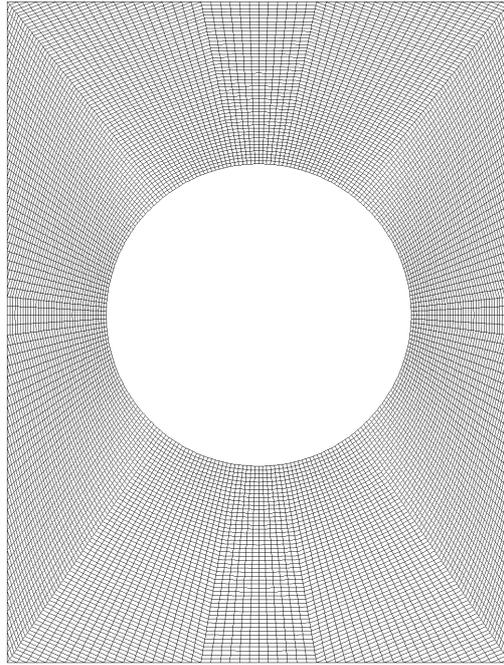


Figure 26 British Museum Great Court Roof - original grid

Architect: Foster and Partners

Engineer: Buro Happold

The spiraling members were obtained by joining points in the form finding grid as shown in figure 29 to produce figures 30 and 31.

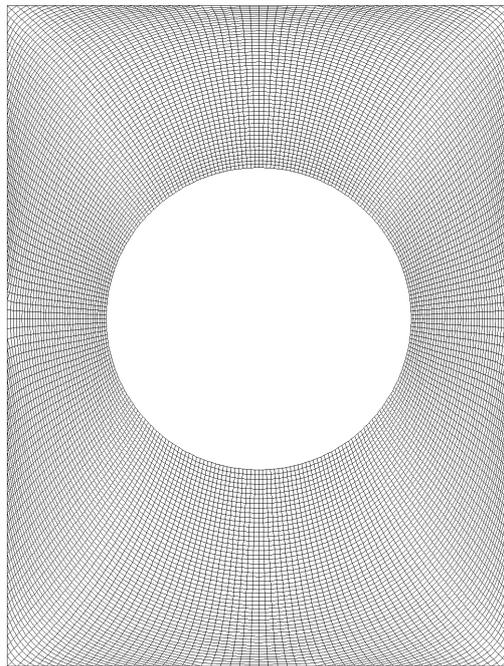


Figure 28 British Museum Great Court Roof - relaxed grid

Architect: Foster and Partners

Engineer: Buro Happold

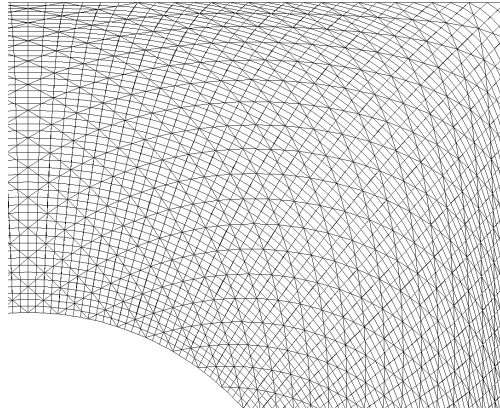


Figure 29 British Museum Great Court Roof - steel members on grid

Architect: Foster and Partners

Engineer: Buro Happold

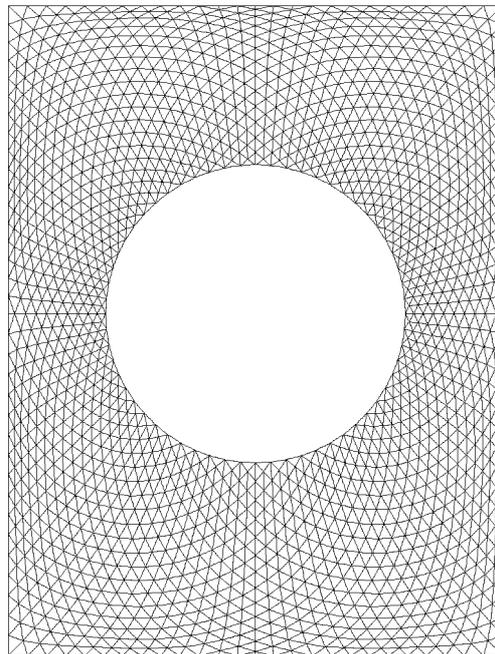


Figure 30 British Museum Great Court Roof - steel members

Architect: Foster and Partners

Engineer: Buro Happold

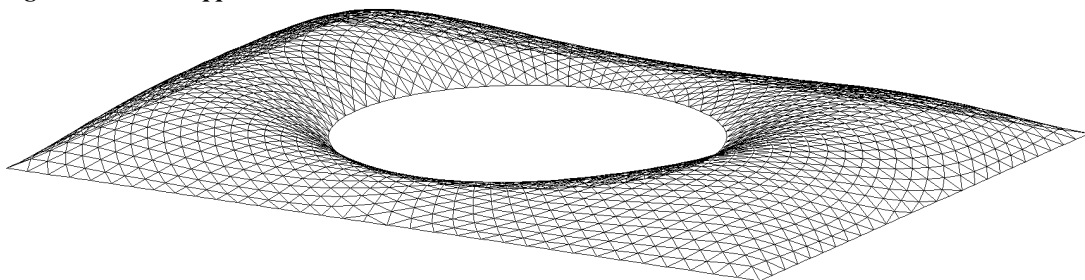


Figure 31 British Museum Great Court Roof - steel members

Architect: Foster and Partners

Engineer: Buro Happold

6 Conclusion

This paper discusses some of the ways in which curved forms can be generated. It is not possible to say that any one method is the optimum, because there are so many

possibilities and the architectural, structural and environmental constraints will never be the same on two projects.

References

- 1 Le Corbusier, *The Modulor*, translated by Peter de Francia and Anna Bostock, Faber and Faber, London 1961.
- 2 Green, A.E. and Zerna, W., *Theoretical elasticity*, 2nd edition, Oxford University Press, 1968.
- 3 Spivak, Michael, *A comprehensive introduction to differential geometry*, volume 5, 2nd edition, Publish or Perish Inc., Delaware, 1975, 1979.

Bibliography

- (2005a). World Wide Web: <http://www.ticam.utexas.edu/CCV/projects/shastra/projects/visualization/me-joint-sim.htm>.
- (2005b). World Wide Web: <http://www.beakman.com/beakman/spider/spider.html>.
- (2005c). World Wide Web: www.brantacan.co.uk.
- (2006). World Wide Web: www.phycomp.technion.ac.il.
- (n.d.). World Wide Web: <http://www.midcoast.com/bo/CloseFromTop.jpg>.
- Alexander, R. M. (1992). *Op Verkenning in de Biomechanica, Dieren in Beweging (Original title: Exploring biomechanics, Animals in motion)*, dutch edition (1995) edn, The Scientific American Library (De Wetenschappelijke Bibliotheek).
- Argebau (1971). Argebau, richtlijnen voor de bouw en de exploitatie van dragende constructies.
- Baant, Z. & Cedolin, L. (1991). *Stability of Structures, Elastic Inelastic, Fracture and Damage theories*, New York; Oxford University Press.
- Bach, K., Burkhardt, B. & Otto, F. (eds) (1987). *IL18 Seifenblasen, Forming bubbles*, number 18 in *IL*, Institut für leichte flächentragwerke.
- Bach, K. (ed.) (1971). *IL3 Biology and Building, part 1, Information of the Lightweight Structures Institute (IL)*, number IL3 in *IL*, Institut für Leichtbau Entwerfen und Konstruieren.
- Bach, K. (ed.) (1973). *IL6 Biology and Building, part 3, Information of the Institute for Lightweight Structures (IL)*, number IL6 in *IL*, Institut für Leichtbau Entwerfen und Konstruieren.
- Bach, K. (ed.) (1974). *IL10 Grid Shells, Gitterschalen*, number IL10 in *IL*, Institut für Leichtbau Entwerfen und Konstruieren.
- Bach, K. (ed.) (1975). *IL 8 Netze in natur und technik, Nets in nature and technics*, number IL8 in *IL*, Institut für Leichtbau Entwerfen und Konstruieren.
- Bach, K. (ed.) (1990). *IL33 Radiolarien, Radiolaria*, number 33 in *IL*, Institut für leichte flächentragwerke.
- Baecke, W. (2005). *Het ontwerpen van vouwschalen bestaand uit prefab elementen*, Master's thesis, Delft University of Technology.
- Baer, S. (1970). *Zome Primer*, Albuquerque, Zomeworks Corporation.
- Baker, T. J. (1999). *Delaunay-Voronoi Methods. Handbook of Grid Generation, online version*, CRC Press.
- Barnes, M. (1986). Computer-aided design of cable and membrane structures, with applications to expo 88 and dqdc, riyadh, in V. Sedlak (ed.), *LSA86, Lightweight Structures in Architecture, The First International Conference on Lightweight Structures in Architecture, Sydney, Australia, 24-29 August 1986, Proceedings, Volume I*, Lightweight Structures in Architecture, Unisearch Limited, The University of New South Wales, PO Box I Kensington, NSW Australia 2033, pp. 254–270.

- Bauer, U. (1968). Traglufthallen und ihren klimatischen bedingungen, *Sport und Baderbauten* **January**: 9–27.
- Bendse, M. (1995). *Optimization of structural topology, shape, and material*, Berlin Heidelberg, Springer-Verlag.
- Bendse, M. (2003). *Topology optimization - Theory, methods and applications*, Berlin Heidelberg, Springer-Verlag.
- Beranek, P. W. (1976). *Berekening van platen*, TU Delft.
- Beranek, P. W. (1988a). *Understanding of structures, Proceedings of the International Updating Course on Structural Consolidation Stable-Unstable? Structural Consolidation Of Ancient Buildings, Center For The Conservation Of Historic Towns And Buildings*, Leuven University.
- Beranek, P. W. (1988b). *Understanding of structures, stable-unstable*, *Leuven University Press*.
- Beukers, A. & Hinte, E. (2001). *Lightness, the inevitable renaissance of minimum energy structures*, 3rd edn, 010 publishers, Rotterdam.
- Bletzinger, K. (n.d.). *Structural optimization lecture papers*, Printed.
- Bletzinger, P. (2001). *Structural optimization, Reader for the Lehrstuhl für Statik*, Technische Universität München.
- Boer, S. & Oosterhuis, K. (2004). *Architectural parametric design and mass customization, Proceedings of the 5th European Conference on Product and Process Modelling in the AEC Industry*.
- Borrego, J. (1967). *Space Grid Structures*, Cambridge, MIT Press.
- Brown, S. & Cook, M. (2002). *The design and manufacture of the british museum great court roof, IABSE Symposium Melbourne*, IABSE.
- Brylka, R. (1970). *Traglufthalle Heute, technische mitteilungen Krupp Werksberichte, Band 28*, Krupp.
- Buerger, M. (1968). *Elementary Crystallography*, M.I.T.
- Burkhardt, B. e. a. (n.d.). *Multihalle Mannheim, Institut für leichte Flächentragwerke*.
- Burns, S. (2002). *Recent advances in optimal structural design*, Reston: American Society of Civil Engineers.
- Calladine, C. (1998). *Deployable structures: What can we learn from biological structures*, in S. Pellegrino & S. Guest (eds), *Proc. IUTUM-IASS Symp. on Deployable Structures: Theory and Applications*, Kluwer Academic Publisher, Dordrecht, pp. 63–75.
- Cattan, A. & Reissig, P. (2000). *Hard models of manual and visual operation for the generation and reading of spatial forms*, in J. Gerrits (ed.), *Bridge between civil engineering and architecture*, International Association for Shell and Spatial Structures (IASS), Working Group no. 15 'Structural Morphology' (SMG), Delft University of Technology, Delft University of Technology, The Netherlands, pp. 42–47. 1st edition.
- Chalmers, B., Holland, J., Jackson, K. & Williams, R. (1965). *Crystallography, A Programmed Course in three Dimensions*, New York: Appleton-Century-Crofts.

- Chilton, J. (2000). *Space Grid Structures*, Architectural Press, Oxford.
- Clark, R. (1970). *KINETIC ARCHITECTURE*, New York; van Nostrand Reinhold Company.
- Coenders, J. (2004). Structural form finding, new life through a new definition, World Wide Web, Delft University of Technology. Part of Master's thesis.
- Connor, J. (2003). *Introduction to Structural Motion Control*, Upper Saddle River, NJ; Prentice Hall Pearson Education, Inc.
- Cox, H. (1965). *The Design of Structures of Least Weight*, Pergamon Press Ltd.
- Coxeter, H. & R.W.W.Ball (1947). *Mathematical Recreations and Essays*, New York, Macmillan.
- Critchlow, K. (1980). *Time Stands Still*, G. Fraser.
- Cundy, H. & A.P.Rollett (1961). *Mathematical Models*, London: Clarendon.
- Czyz, J. & Lukasiewicz, S. (1994). Optimization of space lattice structures with multimodal frequency constraints, in J. Abel, J. Leonard & C. Penalba (eds), *Spatial, Lattice and Tension Structures*, IASS-ASCE, American Society of Civil Engineering, 345 East 47th Street, New York 10017-2398, pp. 419–428.
- Daerden, F. & Lefeber, D. (2001). The concept and design of pleated pneumatic artificial muscles, *International Journal of Fluid Power* **2,3**: 41–50.
- Darwin, C. (1859). *The Origin of Species*, Oxford University Press.
- Delft University of Technology, F. o. A. (2003). Formian - formex, World Wide Web, <http://www.bk.tudelft.nl/bt/dc/Formian/Formian.html>.
- Dorey, A. & Moore, J. (1996). *Advances in actuators*, Bristol, UK: Institute of Physics Publishing.
- Edelsbrunner, H. (2001). *Geometry and Topology for Mesh Generation*, Cambridge University Press.
- Eekhout, M. (1989). *Architecture in Space Structure*, 010 Publishers.
- Engel, H. (1999). *Tragsysteme, Structure Systems*, 2nd edn, Verlag Gert Hatje, Senefelderstrasse 12, 73760 Ostfildern-Ruit.
- Eppstein, D. (1996). Zonohedra and zonotopes, *Mathematica in Educ. Res.* **5**: 15–21.
- F. Ansari, A. M. & Leung, C. (eds) (1997). *Intelligent Civil Engineering Materials and Structures*, New York, American Society of Civil Engineers.
- Farestam, S. & Simpson, R. (1994). A framework for advanced front techniques of finite element mesh generation.
- Farin, G. (1999). *NURBS, from Projective Geometry to Practical Use.*, 2nd edn, Natick, Massachusetts; AK Peters.
- Farshad, M. (1992). *Design and Analysis of Shell Structures*, Dordrecht; Kluwer Academic Publishers.
- Festo (2005). Festo homepage, World Wide Web, <http://www.festo.com/INetDomino/>.
- Flügge, W. (1960). *Stresses in Shells*, Springer Verlag, Berlin.

- Frank, F. & Kasper, J. (1959). Complex alloy structures regarded as sphere packings. ii. analyses and classification of representative structures., *Acta Crystallographica* **12**: 483–499.
- fur Leichtbau Entwerfen und Konstruieren, I. (1978). *IL13 Multihalle Mannheim*, number IL13 in *IL*, Institut fur Leichtbau Entwerfen und Konstruieren.
- Gibson, L. & Ashby, M. (1997). *Cellular solids, structure and properties*, 2nd edn, Cambridge University Press.
- Grundig, L. & Bahndorf, J. (1986). Form finding of a roof structure for a health spa, in V. Sedlak (ed.), *LSA86, Lightweight Structures in Architecture, The First International Conference on Lightweight Structures in Architecture, Sydney, Australia, 24-29 August 1986, Proceedings, Volume I*, Lightweight Structures in Architecture, Unisearch Limited, The University of New South Wales, PO Box I Kensington, NSW Australia 2033, pp. 246–253.
- Haas, A. (1962). *Design of thin concrete shells*, Vol. 1, positive Curvature Index, New York, John Wiley and Sons.
- Hanegraaf, A. & et al. (1975). Primary zonohedra, *Preprint 2nd Conference on Space Structures*.
- Hanisch, F. (1996/1997). B-spline curves, Applet on Internet. <http://www.cs.technion.ac.il/cs234325/homepage/applets/doc/html/etc/appletIndex.html> (sept. 2005).
- Hanselaar, H. (2003). *Snowplace*, Master's thesis, Delft University of Technology.
- Happold, E. & Liddell, W. (1975). lattice roof for the mannheim bundesgartenschau, *The Structural Engineer* **53**, no3.
- Harris, R. & Kelly, O. (2002). The structural engineering of the downland gridshell, in G. Parke & P. Disney (eds), *Space Structures 5*, University of Surrey, Guildford, UK, Thomas Telford Publishing, pp. 161–172.
- Hemp, W. (1973). *Optimum structures*, Oxford University Press.
- Hernandez, S. (1993). *Advanced Techniques in the Optimum Design of Structures*, Vol. 12 of *Topics in Engineering*, Computational Mechanics Publications, Southampton, UK and Boston, USA.
- Hoefakker, J. & Blaauwendraad, J. (2003). *Theory of Shells, Lecture book*, Delft University of Technology.
- Holgate, A. (1986). *The art in structural design*, Oxford University Press.
- Homepage, K. C. I. (n.d.). World Wide Web, <http://www.kineticceramics.com>.
- homepage, R. I. (2005). World Wide Web, <http://www.racointernational.com>.
- Honeycombs (n.d.). World Wide Web, <http://www.mse.mtu.edu/dr-john/my4150/honey/h1.html>.
- Houtman, R. (1996). *The influence of distorsion introduced by cloth flattening on stress behaviour of tensile structures*, Delft University of Technology, department of Civil Engineering.
- H.S.M.Coxeter, H. (1963). *Regular Polytopes*, New York: Macmillan.
- H.S.M.Coxeter, Longuet-Higgins, M. & Miller, J. (1954). *Uniform Polyhedra. Philosophical Transactions*, Londen: Royal Society.

- Huybers, D. (2000a). 38 years of morphology, an anthology, Printed for the Delft University of Technology.
- Huybers, D. & Ende, G. (1994). Prisms and antiprisms, in J. Abel, J. Leonard & C. Penalba (eds), *Spatial, Lattice and Tension Structures*, IASS-ASCE, American Society of Civil Engineering, 345 East 47th Street, New York 10017-2398, pp. 142–151.
- Huybers, P. (1983). *Een koepelconstructie van rondhout*, Delft University of Technology, department of Civil Engineering.
- Huybers, P. (1994). *Draagconstructies Gebouwen Deel 2: Vorm en Functie*, Fac. Civiele Techniek TU Delft.
- Huybers, P. (2000b). Polyhedriods, in J. Gerrits (ed.), *Bridge between civil engineering and architecture*, International Association for Shell and Spatial Structures (IASS), Working Group no. 15 'Structural Morphology' (SMG), Delft University of Technology, Delft University of Technology, The Netherlands, pp. 100–107. 1st edition.
- i Armengol, J. B. (2001). *The Essential Gaudi, The geometric modulation of the Church of the Sagrada Familia*, 2nd edn, ECSA. Translation by Mark Burry.
- IASS, W. . (1985). *Recommendations for air-supported structures.*, IASS.
- Isler, H. (2000). Creating shell shapes, in J. Gerrits (ed.), *Bridge between civil engineering and architecture*, International Association for Shell and Spatial Structures (IASS), Working Group no. 15 'Structural Morphology' (SMG), Delft University of Technology, Delft University of Technology, The Netherlands, pp. 108–115. 1st edition.
- Janocha, H. (ed.) (1999). *Adaptronics and Smart Structures*, Berlin, Springer.
- Jensen, F. (2000). *Downland grid shell*, Master's thesis, University of Bath, UK. Final year dissertation.
- J.L. Deneubourg, e. a. (1991). Swarm-made architecture, *Proc. European conference on Artificial Life*.
- Jr., B. S. & Sain, M. (1997). Controlling buildings: A new frontier in feedback., *IEEE Control Systems Magazine on Engineering Technology; Special Issue* **17 nr. 6**: 19–35.
- K. Bach, B. B. F. O. (ed.) (1988). *IL25*, number 25 in *IL*, Institut fur Leichtbau Entwerfen und Konstruieren.
- Kelly, O., HARRIS, R.J.L., D. M. & ROWE, J. (2001). Construction of the downland gridshell, *The Structural Engineer* **79**(17).
- Kirsch, U. (1993). *Structural optimization - Fundamentals and applications*, Berlin Heidelberg, Springer-Verlag.
- Kitrick, C. (1990). A unified approach to class i, ii and iii geodesic domes, *International Journal of Space Structures* **5, nr. 3&4**: 223–246.
- Klimke, H., Sanchez, J., Vasilu, M., Stuhler, W. & Kaspar, C. (2002). The envelopes of the arts centre in singapore, *Space Structures* **5**, Thomas Telford, London, pp. 795–806.
- Knebel, K. & et al. (2002). The structural making of the eden domes, *Space Structures* **5 1**: 245–254.
- Koiter, W. (1945). *Over de Stabiliteit van het Elastisch Evenwicht*, Amsterdam; H.J. Paris.

- Koiter, W. (1967). Nasa technical translation, *NASA Technical F10,833*.
- Lalvani, H. (1991). *Morphological Aspects of Space Structures*, -. p1-68.
- Lauletta, E. (ed.) (1961). *Statics Of Hyperbolic Paraboloidal Shells Studied By Means Of Models*, Vol. Proceedings of the symposium on shell research.
- Lewis, F. (1923). The typical shape of polyhedral cells in vegetable parenchyma and the restoration of that shape following cell division, *Proceedings of the American Academy of Arts and Sciences* **58**: 527–552.
- Liang, Q. (2005). *Performance-based optimization of structures - Theory and applications*, Oxon, Spon Press.
- Liseikin, V. (1999). *Grid generation methods*, New York, Scientific Computation.
- Loeb (1966). *The architecture of Crystal*, Proportion, Symmetry and Rhythm, Georgy Kepes, New York: Braziller.
- Macior, W. & Matzke (1951). An experimental analysis of cell-wall curvatures, and approximations to minimal tetrakaidekahedra in the leaf parenchyma of rhoeo discolor, *American Journal of Botany* **38**: 783–793.
- Maeder, U. & et al. (2004). *Ceracem, a new high performance concrete: characterisations and applications*, Kassel University press.
- Marvin, J. (1938). The shape of compressed lead shot and its relation to cell shape, *American Journal of Botany* **25**: 280–287.
- Mathworld (2008). World Wide Web: www.mathworld.com.
- Matzke, E. (1939). Volume-shape relationships in lead shot and their bearing on cell shapes, *American Journal of Botany* **26**: 288–295.
- Membrane, B. T. & Welcome!, L. S. B. H. (2005). Birdair homepage: Welcome!, World Wide Web, <http://www.birdair.com/birdair/flash.html>.
- Mengerlinghausen, M. (1975). *Komposition im Raum, Band 1, Raumbachwerke aus Staben und Knoten*, Wiebaden/Berlijn, Bauverlag GMBH.
- Mitchell, M. (1996). *An Introduction to Genetic Algorithms*, 2nd edn, MITPress.
- Montcrieff, E. & Grundig, L. (2000). Computational modelling of lightweight structures: Form-finding, load analysis and cutting pattern generation, *Proceedings Symposium VU Brussel*, VU Brussel.
- Mulder, H. (2003). *Adaptive structures*, Master's thesis, Delft University of Technology, Delft University of Technology, NL.
- Mutoh, I. (2002). How does a metal cobweb behave?, in G. Parke & P. Disney (eds), *Space Structures 5*, University of Surrey, Guildford, UK, Thomas Telford Publishing, pp. 47–55.
- Nachtigall, W. (1985). *Warum die Vgel fliegen*, Raschen und Rhring.
- Nachtigall, W. (2001). *Das groe Buch der Bionik; Neue Technologien nach dem Vorbild der Natur*, Stuttgart, Deutsche Verslags-Ansalt.
- Nooshin, H. & Disney, P. (2002). Formex configuration processing, Reader for the Faculty of Architecture, Structural Design Group, Delft University of Technology.

- Nooshin, Space Structures Research Centre, Department of Civil Engineering, University of Surrey, Guildford, UK, H. (1984). *Formex Configuration Processing in Structural Engineering*, Elsevier Applied Science Publishers.
- Ohmori, H. & et al. (2005). Computational morphogenesis and its application to structural design, *Proceedings of the international symposium in shell and spatial structures*.
- Orta-Rial, B. (2000). Optimisation of shape and topology of statically determined trusses under worse loading conditions using simulated annealing, in J. Gerrits (ed.), *Bridge between civil engineering and architecture*, International Association for Shell and Spatial Structures (IASS), Working Group no. 15 'Structural Morphology' (SMG), Delft University of Technology, Delft University of Technology, The Netherlands, pp. 321–328. 1st edition.
- Otto, F. (1973). *Tensile Structures (Original title: Zugbeanspruchte Konstruktionen)*, Vol. 1 and 2, paperback, english translation edn, MIT Press.
- Otto, F., Trostel, R. & Schleyer, F. (1962). *Zugbeanspruchte Konstruktionen, dl 1*, Ulstein Fachverlag, Frankfurt.
- Owen, J. (1965a). *The Analysis and Design of Light Structures*, Edward Arnold (Publishers) Ltd.
- Owen, J. (1965b). *The analysis and design of light structures.*, American Elsevier Publ. co.
- Pearce, P. (1978). *Structure in Nature is a Strategy for Design*, Cambridge/Massachusetts; MIT Press.
- Peraire, J., Peiro, J. & Morgan, K. (1999). *Advancing Front Grid Generation. Online version*, CRC Press.
- Popko, E. (1968). *Geodesics*, Detroit, University of Detroit Press.
- Press, W., Vetterling, W., Teukolsky, S. & Flannery, B. (2002). *Numerical Recipes in C++, The Art of Scientific Computing*, 2nd edn, Cambridge University Press.
- Prusinkiewicz, P. & Lindenmayer, A. (1990). *The Algorithmic Beauty of Plants*, New York, Springer-Verlag.
- Ramm, E. & Bletzinger, K. (1993). Structural optimization, *International Association for Shell and Spatial structures (IASS) newsletter 112* p. 6.
- research group, T. (2005). Topology optimization, World Wide Web, <http://www.topopt.dtu.dk/>.
- Rypl, D. (2002). Grid generation, World Wide Web:<http://power2.fsv.cvut.cz/dr/papers/Thesis>. viewed: july 2005.
- Samyn, P. (2000). The volume indicators for michell-type structures and telescopic beams, in J. Gerrits (ed.), *Bridge between civil engineering and architecture, Proceedings of the 4th International Colloquium on Structural Morphology, August 17-19, 2000, Delft, NL*, IASS, Delft University of Technology, pp. 305–308.
- Samyn, P. & Lateur, P. (2000). Volume and displacement indicators of isostatic structures the case of the horizontal isostatic span, vertically loaded, in J. Gerrits (ed.), *Bridge between civil engineering and architecture, Proceedings of the 4th International Colloquium on Structural Morphology, August 17-19, 2000, Delft, NL*, IASS, Delft University of Technology, pp. 294–307.

- Sanchez-Alvarez, J. (2002). The geometrical processing of the free-formed envelopes for the esplanade theatres in singapore, *Space Structures 5*, Thomas Telford, London, pp. 1025–1035.
- Scheurer, F. (2003). The groningen twister - an experiment in applied generative design, *Milan, In Generative Art 2003. Proceedings of the 4th International Conference*, ed. C. Soddu .
- Schippers, J. (1975). *Pneumatische constructies*, Master's thesis, Delft University of Technology, faculty of Civil Engineering and GeoSciences.
- Schlaich, J. (2000). Lightweight structures, in M. Barnes & U. Michael Dickson, University of Bath (eds), *Widespan Roof Structures*, University of Bath, UK, Thomas Telford Publishing, London, UK, Thomas Telford Ltd, 1 Heron Quay, London E14 4JD, UK, pp. 178–188.
- Schober, D. (2002). Geometrie-prinzipien fur wirtschaftliche und effiziente schalentragwerke, *Bautechnik 79*: 16–24.
- Schober, D. (2003a). Freeform glass structures, Distributed as a paper copy, Schlaich Bergerman Partner.
- Schober, H. (2003b). *Freeform Glass Structures*, Stuttgart, Schlaig, Bergermann und Partner.
- Schodek, D. (1998). *Structures*, Prentice Hall.
- School of Engineering, U. o. S. (2004). Formian 2.0, World Wide Web, <http://www.surrey.ac.uk/eng/research/ems/ssrc/formian.htm>.
- Schulz, H. (1962). Die traglufthalle, *Technische mitteilungen Krupp March*: 133–138.
- Shaw, J. (1999). *Hybrid Grids. Handbook of grid generation, online version*, CRC Press.
- Sheck, H. (1974). The force density method for form-finding and computation of general networks., *Computation Methods in Applied Mechanics and Engineering* .
- Shephard, M. e. a. (1999). *Automatic Grid Generation Using Spatially based Trees. Handbook of Grid Generation, online version.*, CRC Press.
- Shubnikov, A. & Kopstik, V. (1974). *Symmetry in Science and Art*, Plenum.
- Smith, C. (1952). *Grain Shapes and Other Metallurgical Applications of Topology,* in *Metal Interfaces*, Cleveland: American Society of Metals. pages 65-113.
- Stary, B. (2003). Technet gmbh, World Wide Web, <http://www.technet-gmbh.com>.
- Struik, D. (1950). *Differential Geometry*, Addison-Wesley Mathematics Series, Addison-Wesley Press, inc., USA.
- Struik, D. (1953). *Analytic and projective geometry*, Addison-Wesley Publishing Company, inc., USA.
- Tarnai, T. (1987). *Spherical Grid Structures*, Budapest; Hungarian Inst. for Building Science.
- Thompson, D. (1942). *On Growth and Form*, Cambridge University Press.
- Thompson, D. (1963). *Growth and Form*, Cambridge University Press.
- Thompson, J. (1995). *A Reflection on Grid Generation in the 90's, Trends Needs and Influences.*, NSF Engineering Research Center for Computational Field Simulation.

- Thomson, J. & et al. (1999). *An elementary Introduction*, CRC Press.
- Universtat Stuttgart, Institute for Structural Mechanics, Adaptive Finite Element Methods for fast transient, highly nonlinear processes (n.d.). World Wide Web, <http://www.uni-stuttgart.de/ibs/research/adaptive/index.html>.
- Vollers, K. (2001). *Twist and Build creating non-orthogonal architecture*, Rotterdam, 010 Publishers.
- Wachsmann, K. (1962). *Wendepunkt im Bauen*, Munchen, Rowohlt Verlag.
- Wakefield, D. (1986). Tensyl, the development of an integrated cad system for stressed membrane structures, in V. Sedlak (ed.), *LSA86, Lightweight Structures in Architecture, The First International Conference on Lightweight Structures in Architecture, Sydney, Australia, 24-29 August 1986, Proceedings, Volume I*, Lightweight Structures in Architecture, Unisearch Limited, The University of New South Wales, PO Box I Kensington, NSW Australia 2033, pp. 271–278.
- Weald & open air museum, D. (2005). World Wide Web: <http://www.wealddown.co.uk/downland-gridshell.htm>.
- Weingarten, V., Morgan, E. & Seide, P. (1965). Elastic stability of thin-walled cylindrical and conical shells under combined internal pressure and axial compression, *AIAA Journal* **3**: 500–505.
- Wellesley-Miller, S. (1972). *Pneumatische constructies*, Documentatie bouwwezen.
- Werkman, H. (2003). *Een podiumoverkapping voor het openluchttheater in soest*, Master's thesis, Delft University of Technology.
- Wester, T. (1994). The nature of structural morphology and some interdisciplinary examples, in J. Abel, J. Leonard & C. Penalba (eds), *Spatial, Lattice and Tension Structures*, IASS-ASCE, American Society of Civil Engineering, 345 East 47th Street, New York 10017-2398, pp. 1000–1009.
- Whalley, A. (2000). The eden project glass houses world environments, in M. Barnes & U. Michael Dickson, University of Bath (eds), *Widespan Roof Structures*, University of Bath, UK, Thomas Telford Publishing, London, UK, Thomas Telford Ltd, 1 Heron Quay, London E14 4JD, UK, pp. 75–84.
- Whitley, D. (2003). A genetic algorithm tutorial, World Wide Web, <http://www.cse.msu.edu/~cse848/papers/whitleyTutorial.ps>. Online article.
- Williams, C. (2000). The definition of curved geometry for widespan enclosures, in M. Barnes & M. Dickson (eds), *Widespan Roof Structures*, University of Bath, UK, Thomas Telford Publishing, London, UK, Department of Architecture and Civil Engineering, University of Bath, UK.
- Williams, C. (2004). Dynamic relaxation c++ programs, World Wide Web, <http://www.bath.ac.uk/~abscjkw>.
- Xie, Y. & Steven, G. (1997a). *Evolutionary structural optimization*, Londen, Springer-Verlag.
- Xie, Y. & Steven, G. (1997b). *Evolutionary Structural Optimization*, Springer-Verlag Berlin Heidelberg New York.

Yoshimura, Y. (1955). On the mechanism of buckling of a circular shell under axial compression,
NACA Tech. Note **1390**, Sec 7.7.

Zerbst, R. (2002). *Antoni Gaudi, The Complete Buildings*, Taschen GmbH.

List of Figures

2.1	Tree column and the sections. Image from (i Armengol 2001).	19
2.2	One of the geometry definitions which was found in Gaudí's buildings. Image from (Zerbst 2002).	19
2.3	Proposal by Gaudí for a hotel. Image from (Zerbst 2002).	20
2.4	Parabolic shape in one of Gaudí's buildings. Image from (Zerbst 2002).	21
2.5	Basic pressure-response diagram showing relationship between the set of pressures and the form. A change in any of the pressures within the set or in the technology which stands at the interface between pressure and form will alter the diagram and ultimately the form. Image from (Clark 1970).	23
2.6	Comparison of square and triangular packings of equal circles in a given area, with triangular packing approximately 7 percent more circles may be placed. Image from (Pearce 1978).	23
2.7	Triangulation of two-dimensional closest packed arrays. Changing closest packed circles into closest packed hexagons. Image from (Pearce 1978).	24
2.8	Figures formed by closest packed equal spheres. Image from (Pearce 1978).	24
2.9	Soap Bubbles. Image from (Pearce 1978).	25
2.10	Triangulation of planar array of random bubbles viewed from above. Image from (Pearce 1978).	26
2.11	Surface of heated aluminum sheet. Image from (Smith 1952).	26
2.12	n-dimension table.	28
2.13	4-sided polygon. Image from (Lalvani 1991).	29
2.14	4-star. Image from (Lalvani 1991).	30
2.15	Table with zonogons derived out of regular polygonal stars. Image from (Lalvani 1991).	31
2.16	Axes of symmetry.	33
2.17	Tessellation of flat plane with squares. Image from (Chilton 2000).	33
2.18	Tessellation of flat plane with rotated squares. Image from (Chilton 2000).	34
2.19	Tessellation of flat plane with triangles. Image from (Chilton 2000).	34
2.20	Tessellation of flat plane with hexagons. Image from (Chilton 2000).	34
2.21	Regular and semi-regular plane tessellations (left) and their duals (right). Image from (Pearce 1978).	35
2.22	Compound Tessellations and Islamic patterns. Image from (Lalvani 1991).	37
2.23	Parallelogram and rectangular tessellations and vertex placements. Image from (Lalvani 1991).	38
2.24	Triangular tessellations and vertex placements. Image from (Lalvani 1991).	38
2.25	Zonogonal tessellation. Image from (Lalvani 1991).	39
2.26	Central tessellations. Image from (Lalvani 1991).	40
2.27	Concentric repeating patterns with regular pentagons with regular decagons. Image from (Pearce 1978).	41
2.28	Non-periodic rhombic tessellations and non periodic hexagonal tessellations. Image from (Lalvani 1991).	41
2.29	Non-periodic Pattern-generation. Image from (Lalvani 1991).	42
2.30	Tessellation with Non-convex polygons. Image from (Lalvani 1991).	43
2.31	Platonic polyhedra as bar and node or pure plate structures. Image from (Chilton 2000).	44
2.32	Dual regular polyhedra. Image from (Pearce 1978).	45
2.33	The 13 Archimedean polyhedra. Image from (Pearce 1978).	46

2.34	The duals of the 13 Archimedean polyhedra. Image from (Pearce 1978).	47
2.35	Semi-regular prisms (top) and semi-regular anti-prisms. Image from (Pearce 1978).	48
2.36	Dipyramids (top), the duals of prisms (top) Trapezohedra (down), the duals of antiprisms. Image from (Pearce 1978).	48
2.37	The convex deltahedra. b: Triangular dipyramid. d: Pentagonal dipyramid. e: 12-hedron. f: 14-hedron. g: 16-hedron. Image from (Pearce 1978).	49
2.38	Three families of polyhedra: tetrahedral, octahedral and icosahedral, the last two families are here turned into n-stars. Image from (Lalvani 1991).	49
2.39	The dodecahedron has 5 rhombohedra from two types of rhombii, $70^{\circ}32'$ and $41^{\circ}49'$, and the icosidodecahedron has fourteen types of rhombohedral cells from four types of rhombii 90° , 72° , 60° , 36° . Image from (Lalvani 1991).	51
2.40	Vertex placements. Image from (Lalvani 1991).	51
2.41	Edge combinations. Image from (Lalvani 1991).	52
2.42	The fundamental regions of a single rhombohedron, a cube in higher space, are shared. Image from (Lalvani 1991).	52
2.43	Seven polyhedra of octahedral symmetry corresponding to one cube. Image from (Lalvani 1991).	53
2.44	Triangles of frequencies 1 to 4 (top) and minimal triangles. Image from (Lalvani 1991).	54
2.45	Division of spherical surfaces Class I Method I. Image from (Lalvani 1991).	55
2.46	The tetrahedron, octahedron and icosahedron can be converted into a sphere by using the minimal triangle. Image from (Knebel & et al. 2002) (Huybers & Ende 1994).	55
2.47	Two methods for the subdivision of polyhedron-edges and surfaces. Image from (Huybers & Ende 1994).	55
2.48	Generation of the Fullerdome. Image from (Knebel & et al. 2002).	56
2.49	Volvox. Image from (Pearce 1978).	57
2.50	Class II and III and their subdivisions. Image from (Huybers & Ende 1994).	58
2.51	Other basis divisions of spheres. Image from (Huybers & Ende 1994).	58
2.52	Dihedral Angle. Image from (Pearce 1978).	59
2.53	The seven symmetry classes. Image from (Pearce 1978).	60
2.54	Bravais lattices. Image from (Pearce 1978).	62
2.55	Space fillings: Triangular prisms, hexagonal prisms, cube, rhombic dodecahedron and the truncated octahedron. Image from (Pearce 1978).	63
2.56	Tetrahedron-Octahedron space filling. Image from (Pearce 1978).	64
2.57	Central space filling with a single rhombohedron, hexacontrahedral star (n=6) with icosahedral symmetry. Image from (Lalvani 1991).	65
2.58	Non periodic space fillings. Image from (Lalvani 1991).	66
2.59	Models built by Pieter Huybers.	68
2.60	A study of stacking regular shapes. Models by Pieter Huybers.	68
2.61	Some shapes from the field of Structural Morphology.	69
2.62	A model in Tekkit.	70
2.63	Mero model material.	70
2.64	The earliest presentation of a tensile-stressed suspended model describing the load-bearing behaviour of a compressive stressed vaulting structure by Giovanni Poleni (1748), used to check the stability of the dome of St. Peter's in Rome. Image from (K. Bach 1988).	71
2.65	Funiculars of a semi-circular, a parabola and a catenary arch.	72
2.66	Model geometry used to model hanging lines.	73
2.67	Two hanging models by Gaudí. Image from Williams.	73
2.68	Hanging model by Gaudí. Image from (i Armengol 2001).	74

2.69	Hanging models by Gaudí.	74
2.70	Hanging chain model.	75
2.71	Hanging chain model upside down to find the pressure shape.	75
2.72	A hanging paperclip model.	75
2.73	Soap bubbles. Image from (Otto 1973).	77
2.74	Soap film model.	78
2.75	Soap film model.	78
2.76	Soap film model. Image from (Bach et al. 1987).	79
2.77	Soap film model. Image from (Bach et al. 1987).	80
2.78	Soap film pneumatic model. Image from (Bach et al. 1987).	80
2.79	Soap film pneumatic model.	81
2.80	Soap film pneumatic model.	81
2.81	Two prestressed pantymodels.	82
2.82	Picture of the physical pneu model. Image courtesy of P.C. van Hennik.	82
2.83	Inverted hanging cloth model, strengthened with plaster. Models by P.C. van Hennik.	83
2.84	Relation between Lamy's Theorem and the Cosines Rule.	86
2.85	Three situations (a) $P = R \gg S$; (b) $P = R$ and S is a little smaller; (c) $P = R = S$	86
2.86	Different types of cellular structures. Image from (Gibson & Ashby 1997).	87
2.87	Different types of two-dimensional shapes. Image from (Gibson & Ashby 1997).	87
2.88	Different types of three-dimensional shapes. Image from (Gibson & Ashby 1997).	88
2.89	Different types of grid topologies. Image from (Gibson & Ashby 1997).	88
2.90	(a) Picture of a part of a dragonfly wing; (b) vector drawing of the venation. Based on this vector drawing the distribution of the 235 angles of Figure 2.91 is made.	90
2.91	(a) Distribution of 235 angles between cell partition walls; (b) Graphical illustration of the distribution of 235 measured angles between the partition walls of a dragonfly wing. Image from Dumans 2005.	90
2.92	Introduction of the parameters used for the calculations.	91
2.93	Detail of the wing of a dragonfly. The characteristic angles 90° and 120° are clearly visible.	92
2.94	Two wings of a dragonfly, a fore and a hind wing. Both wings look quite similar, although they differ at some points, nevertheless, nature seems to have reasons to form the venation in this way and it may be assumed that is not a random configuration.	92
2.95	Fresh and dried leaf of <i>Dieffenbachia</i> . Nature does not always follow the 'simple' laws and rules made by human beings. In this leave the regular pattern with 180° and 120° which may be expected based on Equation 2.24 is missing. Nature has its own, more complex reasons to form the partition walls the way they are formed.	93
2.96	Pattern of soap-partition walls. The characteristic angle of 120° is easy to recognize. Image from (K. Bach 1988).	93
2.97	Dragonfly wing. Image from (Bach et al. 1987).	94
2.98	Dragonfly wing. Image from (Bach et al. 1987).	94
2.99	The most famous hexagonal structure; the bee's cell.	95
2.100	Mathematical model of the bee's cell. Image from (Thompson 1942).	95
2.101(a)	Schematically representation of the folding of eight hexagons. (b) Foldable bee's cell structure. Image from (n.d.).	96
2.102	Model for elastic analysis of hexagonal structure.	96
2.103	Section over two layers of bee's cells. The small slope results in the collection of the honey in the lowest part of the cell.	98

2.104	Bone analogy with Michell structures (see Section 4.6.8). Image from (Thompson 1942).	99
2.105	Bone structure. Image from (Bach 1973)	99
2.106	Bone structure. Image from (Bach 1973)	100
2.107	Very simple model of the human <i>tibia</i> (a) The bone can be simplified as a cylinder with a flat top plate. (b) Without stiffening-elements, the flat plate shows significant deflections. (c) With stiffening-elements, the deflection is much less. The stiffening-elements in bone structures have strong similarities with Michell structures.	100
2.108	X-ray photo of the head of the human <i>femur</i> . Image from (Thompson 1942). . .	101
2.109	Head of the <i>femur</i> (upper leg). Image from (Thompson 1942).	102
2.110	Optimisation of a structure. In every step the required bars are thinner. The most complicated one is called 'Michell structure'. Image from (Beukers & Hinte 2001).	102
2.111	Michell structures for two different configurations; a cantilever structure and a structure one two supports loaded by a force in the center. Image by (Holgate 1986).	103
2.112	3D model of joint <i>tibia</i> and <i>femur</i> , the flat plate on top of the <i>tibia</i> is clearly visible. Image from (2005a).	103
2.113	Leaf structure of the <i>Victoria Amazonica</i>	104
2.114	Hangar structure by Nervi.	104
2.115	(a) The ribs of a Boeing airplane show strong similarities with (b) the rib structure of the wings of butterflies at micro-level. Image from (Nachtigall 2001).	105
2.116	Underside of the <i>Victoria amazonica</i> , a typical example of a natural rib structure.	105
2.117	Compilation of pictures of the Palazzetto dello Sport in Roma. Especially the picture at the right-bottom side shows in a nice way the ribs. They have strong similarities with the Michell structures which can be found in bones.	106
2.118	Oriente railway station, Lisbon, Portugal and departure hall Stuttgarter airport.	107
2.119	Generated branching structures for $L_0 = 1$, $n = 10$, $R = 0.6868$ and a changing angle α (95° , 85° , 75° , 65° , 45° , 35° , 25° and 15°).	108
2.120	Explanation of parameters used in model.	109
2.121	Three-dimensional representation of branching structure of the Stuttgarter airport.	109
2.122	Output from GSA8.0 (a) Displacements by point loads in the direction of the structure; (b) Axial-stresses belonging to the loads of (a); (c) Axial-stresses after the sections are changed according to formula 2.37; (d) Displacements by point loads in vertical direction; (e) Axial-stresses after the sections are changed according to Equation 2.37.	110
2.123	(a) Feasibility study Tree Structures for an exhibition hall, Yale University, USA 1960 (Students of Frei Otto during a seminar) (b) Support pillars of a six-angle gridshell in the Kings Office, Council of Ministers, Majlis al Shura, Riyadh, Saudi Arabia, 1979 (Rolf Gutbrod, Frei Otto, Buro Happold, Ove Arup and Partners.)	110
2.124	(a) Tree-like branching structure; (b) tensile-stressed branching structure; (c) under compression; (d) slenderness increase from top to bottom. Image from (K. Bach 1988).	111
2.125	Different examples of branching structures found in nature. Image from (K. Bach 1988).	112
2.126	A spiderweb.	113
2.127	Spider web analogy of a membrane structure. Image from (Bach 1975).	113
2.128	Dewdrops on the threads of a spider web.	114
2.129	Microscopic photo of a thread of a spider web. The small blobs are made of a sticky viscous liquid.	114
2.130	Grid shells based on hanging models. Image from (K. Bach 1988).	115
2.131	Reconstruction of hanging model from Gaudí. Image from (K. Bach 1988).	115

2.132	Basic geometry of catenary curves. Image from (K. Bach 1988).	116
2.133	Spider web and structures based on webs. Image from (K. Bach 1988).	116
2.134	Radiolaria. Image from (Beukers & Hinte 2001).	117
2.135	Spiral shell. Image from (Thompson 1942).	118
2.136	Spiral analogy of the spiral shell. Image from (Thompson 1942).	118
2.137	X-ray image of a sea shell.	119
3.1	Line of thrust of the load (Funicular line) in relation to the Shell surface and the corrective hoopforces. Image from (Schodek 1998).	123
3.2	Graphical determination of the forces in masonry dome due to it's own weight. Image from (Beranek 1988a).	124
3.3	Shell combined of several straight edge hypars.	125
3.4	Principal stresses in a shell model combined of several straight edge hypars. Image from (Lauletta 1961)	125
3.5	Contourplot and gradientplot of the flow of forces of a shell combined of several straight edge hypars.	126
3.6	Shell-like structure with contourplot of the vertical displacements determined with an elastic calculation (FEM).	126
3.7	Sketch of gradientplot in top view.	127
3.8	Line of thrust of the load (funicular line) in relation the axis of a circular arch.	127
3.9	Line of thrust of the load (funicular line) in relation to the dome (shell) surface.	128
3.10	Polygon of forces in dome section.	128
3.11	Hoop forces (N_{HH}) and meridional forces (N_{RR}) in a dome pinned in one point and on rollers round the hemisphere at its spring (picture above) and a dome pinned round the hemisphere at its spring (picture below).	129
3.12	Deformation of a dome pinned in one point and on rollers round the hemisphere at its spring (picture above) and deformation of a dome pinned round the hemisphere at its spring (picture below).	129
3.13	Equilibrium of forces in a section of a dome with an oculus.	130
3.14	Hoop (ring) forces in a dome with an oculus.	130
3.15	Hoop forces (N_{HH}) and meridional Forces (N_{RR}) in a section.	131
3.16	Polygon of forces in a section.	131
3.17	Hoop forces (N_{HH}), above, and meridional forces (N_{RR}), below, numerically calculated.	132
3.18	Support reactions.	132
3.19	picture above: dome with an oculus, picture below: axisymmetric "donut like" shell.	133
3.20	Equilibrium of forces in a section of an axisymmetric "donut like" shell.	134
3.21	Hoop forces (N_{HH}) and meridional Forces (N_{RR}) in a section.	134
3.22	Polygon of forces in a section.	135
3.23	Hoop forces (N_{HH}) numerically calculated.	135
3.24	Meridional forces (N_{RR}) numerically calculated.	135
3.25	Deformations with sharp dip at the hole.	136
3.26	Hoop forces (N_{HH}) and meridional forces (N_{RR}) plotted on the deformed surface.	136
3.27	The hoop forces will cause extensions in the tangential direction, compression hoop forces will shorten the rings, and tensile hoop forces will elongate the rings, thus resulting in a sharp dip of the deformations.	136
3.28	Three collapsed cooling towers at Ferrybridge.	137
3.29	Buckling modes of an axially compressed cylinder (Baant & Cedolin 1991) (only half the cylinder is shown).	138
3.30	Experiment on an aluminium cylinder (Note the Yoshimura pattern).	138
3.31	A simple beer can.	139

3.32	Experimental maximum loads of 172 axially loaded cylinders. (Weingarten et al. 1965)	140
3.33	Buckling of cylinders for different unevenness size β . (Weingarten et al. 1965) . .	140
3.34	Basic types of post buckling behaviour.	141
3.35	Maximum load as a function of the imperfection amplitude.	141
3.36	Shell finite element analysis of a shallow dome (Farshad 1992).	142
3.37	Preliminary design for a mobile stage covering.	145
3.38	New model for the mobile stage covering.	146
3.39	The left figure has cutting patterns which meet at right angles. The other figure has cutting patterns which flow into each other.	148
3.40	By means of a dotted line the stress compensation is indicated. It is on a scaled base. The boundaries should stay at the same length and just rotate a little bit. After stressing they will rotate into their meant position. Because the opening angle at the bottom point will become larger, this needs to be regarded when designing the detailing.	152
3.41	A welding machine.	152
3.42	In the overlap of this pocket is folded back, the border will be much too short. By means of perpendicular cuts it will be possible to solve this problem. It is not a very nice solution. It is better to use a strip of fabric which has threads which make an angle of 45 degrees with the boundaries and add it to the cloth. Because of the disability to resist shear forces, it is easy to deform the strip to make it follow the boundary of the cloth.	154
3.43	A round wood dome structure generated with EASY.	155
3.44	Modelling the membrane.	155
3.45	Radial pattern orientation.	156
3.46	Planview of a radial pattern orientation.	157
3.47	Geodesic lines.	157
3.48	Eight cutting patterns.	158
3.49	Entrance canopy in Helsinki.	159
3.50	To examine the influence of the seam in the middle, the created cutting patterns are sewn together and re-analyzed under snow load. It can be seen that the middle line takes much force under load. The use of the seam line in the middle prevents the occurrence of sags.	160
3.51	The seam line in the middle of the fabric.	161
3.52	Two parts of the large cloths are sewn together.	161
3.53	The building without the membrane.	162
3.54	The anchoring points.	162
3.55	The membrane.	163
3.56	Installing the side points.	163
3.57	Erecting the mast.	163
3.58	The membrane after pretensioning.	164
3.59	The principles of the air-supported structure.	165
3.60	The first designs for an air-supported structure by Lancaster.	166
3.61	Patent request by F.W. Lancaster.	167
3.62	A design for an aircraft hangar by H.H. Stevens.	168
3.63	The first pneumatic dome structure ever built; design by W. Bird (1949).	168
3.64	The Telstar radome in Maine.	169
3.65	An exhibition hall by Krupp in Hannover, shape like a toroid (=part of a cylindrical ring).	169
3.66	Air-supported halls on a longitudinal base; often applied shapes.	169
3.67	The common stress distribution in a double curved surface under internal pressure.	170

3.68	The stress distribution in spherical and cylindrical shaped roof surfaces.	171
3.69	The effect of the shape on the membrane stresses; $M = p * \frac{r}{2}$	171
3.70	Shapes of air-supported surfaces over random plans.	172
3.71	Stress-strain curves for different types of fibres.	174
3.72	Often applied types of membrane (costs are not realistic anymore).	175
3.73	An example of a high strength membrane build up.	175
3.74	The basic shape of an ellipse.	176
3.75	Superellipses with different values for the exponent; in this case a proportion of 1,5 between the axis is chosen.	177
3.76	Section through the stainless steel roofstructure in Halifax.	177
3.77	Overview Halifax.	178
3.78	Structural lay-out of the air-supported stainless steel roof (82mx64m) with contraction joint.	178
3.79	Cylinder and sphere.	180
3.80	The two hall types, compared in Tables 3.7 & 3.8.	181
3.81	Often used patterns in two common shapes.	183
3.82	Different possibilities for seams: A. Sowing; B. Gluing or welding; C. Combinations.	183
3.83	Some characteristic principles of anchorage.	186
3.84	The temperature profile for single and double layered skins.	187
3.85	Necessary provisions for entering while maintaining the over-pressure.	189
3.86	Tensioning around a door.	189
3.87	Different solutions for an airlock.	190
3.88	Loading on circular shaped air-supported halls.	192
3.89	Time taken to collapse at different door widths.	193
3.90	The principle of stabilisation by tying down.	194
3.91	The principle of tying down with line shaped ties.	194
3.92	The American pavilion at the Osaka World Fair.	195
3.93	The B.C. Place Amphitheatre in Vancouver (top) and the Aquatic centre in Calgary, Canada (bottom).	195
3.94	Soap bubble configurations.	196
3.95	Principles of double layered pneumatic structures.	197
3.96	The Boston Arts Centre Theatre by Koch, Ross and Weidlinger.	198
3.97	Structural lay out of the covering of a shoppingcentre in Marl.	199
3.98	Structural detail of the covering in Marl.	200
3.99	Double layered exhibition hall by V. Lundy.	200
3.100	Fuji Group pavilion in Osaka.	201
3.101	Showboat of the Electric Energy pavilion by Y. Murata.	202
3.102	The video-pavilion in Sonsbeek by the ERG-group.	202
3.103	Inflated bridge structure by P.S. Bulson.	203
3.104	An inflated dam structure, with water as medium.	204
3.105	Principle of the air sandwich.	204
3.106	Noteworthy pneumatic structures at the Osaka World Fair 1970.	205
3.107	The principle of rigidising air-supported structures.	206
3.108	A point load supported by one individual simple truss. Image from (Chilton 2000)	210
3.109	Deflection of a system of individual trusses. Image from (Chilton 2000)	210
3.110	A point load supported space grid of intersecting trusses. Image from (Chilton 2000)	211
3.111	The deflection of a two-way spanning double-layer grid of intersecting trusses demonstrating the load distribution advantage. Image from (Chilton 2000)	211
3.112	Relationship between span aspect ratio and proportion of the total load carried out by the longer span beam, L2 of the simple two-beam intersection grid ratio L_2/L_1 , equal to 1, 2, 3, 5. Image from (Chilton 2000)	213

3.113Regular geometry can gives nice views. Pallafolls sports hall.Image from (Chilton 2000)	214
3.114MERO System. Image from http://www.columbia.edu	215
3.115Space Deck System. Image from (Nooshin, Space Structures Research Centre, Department of Civil Engineering, University of Surrey, Guildford, UK 1984)	216
3.116Different principle shapes of spaceframes	218
3.117Different single layer shapes	220
3.118Combinations of single and double curved systems	221
3.119Stacking of octahedrons and tetrahedrons, in which the most often used offset grid appears as horizontal layer	222
3.120Two-layered systems	225
3.121Cubic rasters with octahedrons, tetrahedrons and cuboctahedrons	226
3.122Spacefilling stacking of a 14-plane	226
3.123Typical node element in a cubic system	227
3.124Spatial system of cubes with plane diagonals	227
3.125rhombic dodecahedron	228
3.126Spatial view of cubic systems	228
3.127Zone-eders	229
3.128Examples of cubic rasters in possible applications	231
3.129Principle of a two-way grid	232
3.130parallel raster	232
3.131Two-layered, two-directional diagonal raster	233
3.132A sphere shaped spaceframe based on a cubic raster	234
3.133A three-way grid with a reduced height	234
3.134A three-way grid built from identical bars	235
3.135Edge-endings of two-layered spaceframes	237
3.136Reductions	238
3.137Support types	239
3.138Design for a three-layered spaceframe with a span of 300m	240
3.139Design of a three-layered structure for a hangar in India, with the cuboctahedron as base element	240
3.140Large and small circle on a sphere	241
3.141Projection of a triangular division of the circumscribed sphere	242
3.142First degree subdivisions of polyhedrons	242
3.143Orientation on a sphere	243
3.144The different classes of subdivision	246
3.145Some other types of often used sphere subdivisions	247
3.146The two most important methods of subdividing triangular planes	247
3.147Different possible connectionpatterns, after the definition of the topological division of the points	248
3.148Project: Structural Bay System by H. Caminos	249
3.149System of prefabricated pyramids	250
3.150Cylindershell of plastic tetrahedrons	250
3.151Tetragrid System consisting of muliplex and planks	251
3.152Antiprismatisch vouwsysteem	252
3.153Spaceframe in rectangular tubes	253
3.154Detail with pinched profiles and eight cornered nodeplates, by W. Beckett	253
3.155Cut over a bar according to the Tuball-plus system	254
3.156Composed cut over a bar, by Schuco	254
3.157Spaceframe in roundwood poles	254
3.158Some examples of facetted nodes	255

3.159	A Japanese sphere-shaped node	256
3.160	A solution with tie plates, with which most common spaceframes can be built	256
3.161	The triodetic system with aluminium nodes and bars	257
3.162	The positioning of the holes in a node	259
3.163	The SDC-system	259
3.164	A disjoint in a single layer sphereshaped frame	260
3.165	The Japanese NS space truss system	260
3.166	Solutions by R.B. Fuller without separate joints	261
3.167	A system, developed by TU Delft, with a U-shaped bar-ending	262
3.168	The Radial System	262
3.169	A welded joint	263
3.170	The meeting of different bars in a common spaceframe	264
3.171	The Unistrut system	264
3.172	A composed joint according to a Russian patent	265
3.173	Some examples of solutions for single layered spaceframes	265
3.174	Some special solutions with clamping or slide connections	266
3.175	Joints with tie plates	267
3.176	Different massive sphere shaped joints	268
3.177	A number of hollow sphere shaped joints	269
3.178	A system with bars of glassfibrepolyester by L. Hollaway	270
3.179	Possible problems with stability	272
3.180	Snap through in a single layered domeframe	272
3.181	The Varitec system: too many hinges in a bar	272
3.182	Reductor in a bar-end; Alcodome system of the TU Eindhoven	273
3.183	Failure behaviour of a spaceframe due to buckling of the bars	274
3.184	The construction of spaceframes	275
3.185	Construction of a dome	275
3.186	An example of a frame generated by FORMEX	276
3.187	Tie-rod hydraulic system. Image from http://www.birdair.com/birdair/flash.html	278
3.188	Schematic cross-section view of a hydraulic cylinder. Image by (Dorey & Moore 1996).	278
3.189	Different sizes of rod-type electric linear actuators. Image from http://www.racointernational.com	279
3.190	Schematic of a variable orifice damper. Image from (Jr. & Sain 1997)	280
3.191	Variable damping mechanism. Image from http://www.racointernational.com	280
3.192	Deflated state of the PPAM and inflated state of the PPAM. Image from www.vub.ac.be	281
3.193	Force/contraction curve for PPAM for variable p. Image from (Daerden & Lefebvre 2001)	282
3.194	Festo Fluidic Muscle. Image from http://www.festo.com/INetDomino	282
3.195	Permissible force F (N) as a function of contraction h [(%) of nominal length. Image from http://www.festo.com/INetDomino	283
3.196	Piezoelectric electrical-mechanical interaction. Image from (Connor 2003)	284
3.197	Cylindrical piezoceramic linear actuator. Image from http://www.kineticceramics.com	284
3.198	Plate-type piezoelectric actuator. Image from (Connor 2003).	285
3.199	One-way shape memory behaviour. Image from (F. Ansari & Leung 1997)	286
3.200	Martensitic transformation on cooling and heating. Image from (Connor 2003)	286
3.201	Schematic stress-strain diagram of superelastic behaviour of shape memory alloys. Image from (F. Ansari & Leung 1997)	287

3.202	Effect of temperature on stress behaviour of Nitinol. Image from (F. Ansari & Leung 1997)	287
3.203	Two-way shape memory behaviour. Image from (F. Ansari & Leung 1997)	287
3.204	Effect of electric and magnetic fields on stress-strain relationship. Image from (Connor 2003)	288
3.205	Damper. Image by (Janocha 1999)	289
3.206	Quasi-steady force response for Rheonetics SD-1000-2MR damper. Image from (Connor 2003)	290
4.1	Grid with varying accuracy (and element size) on a certain surface.	296
4.2	Boundary-conforming quadrangular & triangular grid.	297
4.3	Types of interface between contiguous blocks; (a) discontinuous, (b & c) nonsmooth, (d) smooth. Image source:	299
4.4	Neckarsulm grid dome (left), geometrical principle of the grid shell (middle) & a square mesh when laid out into a plane (right).	299
4.5	Six types of basic grid patterns. Image source:	300
4.6	Translational surface, generated by two curves, directrix and generatrix.	301
4.7	Translational surface generated by 1 directrix and 2 generatrixs, the Berlin Zoo Hippo House.	301
4.8	Joints for triangular and quadrangular grids.	302
4.9	Close-up picture of the Bosch Area grid in Stuttgart by SBP.	302
4.10	Bosch Area grid in Stuttgart by SBP.	303
4.11	Translational Surfaces.	304
4.12	Scale-Trans Surfaces	304
4.13	Grid configurations for dome shapes.	306
4.14	Radial grid, Storkow church.	307
4.15	Radial grid of the 'Web Noord Holland.	307
4.16	Isotope technique, BMW pavilion.	308
4.17	The circumcircle through 4 vertices does not contain any other point. Image source:	310
4.18	Seven points define the same number of Voronoi regions. One of the regions is bounded because the defining point is completely surrounded by the others.	310
4.19	Voronoi edges are dotted and the dual Delaunay edges are solid. Image from (Edelsbrunner 2001)	311
4.20	The triangulation which maximizes the minimum angle. The dashed line indicates a possible original triangulation.	311
4.21	Stages of the planar incremental algorithm, three steps. Image from (Liseikin 1999)	312
4.22	Delaunay triangulation with Qhull (left) with Ansys (right).	314
4.23	The Advancing Front Technique showing different stages during the triangulation process.	315
4.24	Flow chart of the Advancing Front Generation Technique.	316
4.25	Model and mesh of a chair.	317
4.26	Model and mesh of a mechanical joint.	317
4.27	Example of the Octree approach.	318
4.28	Octree discretization.	319
4.29	Fragment of a hybrid grid.	320
4.30	Fragment of a hybrid grid.	321
4.31	Image made in Formian of the Perspective View. Image from http://www.bk.tudelft.nl/bt/dc/Formian/Formian.html	322
4.32	Image made in Formian of the Lamella dome. Image from http://www.bk.tudelft.nl/bt/dc/Formian/Formian.html	322

4.33	Image made in Formian of the Onion of quadrangular elements. Image from http://www.bk.tudelft.nl/bt/dc/Formian/Formian.html	323
4.34	Example of a force density problem	326
4.35	The schematic representation of a member in dynamic relaxation	328
4.36	Dynamic relaxation, left the original net structure and right the relaxed structure. Image and software by C.J.K. Williams.	330
4.37	Global and local maximum and minimum points of a multimodal function.	333
4.38	A representation of the size, shape and topology optimisation method	337
4.39	A flowchart of an integrated design system with topology design and boundary shape design modules	338
4.40	The elevation and the plan of a bridge structure obtained with the ESO process.	341
4.41	Flow chart of genetic algorithm.	348
4.42	Flow chart of simulated annealing.	352
4.43	First experiment: two branches of equal length between the nest and the food source.	354
4.44	Second experiment: two branches of different length between the nest and the food source.	355
4.45	Third experiment: with the removal of the obstacles, the model again consists of two branches with different length between the nest and the food.	355
4.46	The most optimal Michell structure for carrying a point load. Image from (Owen 1965a)	358
4.47	Table of Michell structures. Image from (Owen 1965a)	359
4.48	Michell strain field. Image from (Owen 1965a)	359
4.49	The spoked wheel. Image from (Owen 1965a)	361
4.50	The most efficient Michell structure for carrying a central load w. All members are in tension or compression.	362
4.51	A minimum weight structure for concentric loads.	364
4.52	A Michell structure for carrying a central load w on two supports.	365
4.53	A pneumatic structure analogous to a Michell structure.	365
A.1	Sagrada Familia in Barcelona, Spain. Image from (Zerbst 2002)	368
A.2	Sagrada Familia in Barcelona, Spain. Image from (Zerbst 2002)	368
A.3	Sagrada Familia in Barcelona, Spain. Image from (Zerbst 2002)	369
A.4	Sagrada Familia in Barcelona, Spain. Image from (Zerbst 2002)	369
A.5	Picture of the physical model of the Multihalle Mannheim. Image from Chris Williams	370
A.6	Picture of the Multihalle Mannheim grid.	371
A.7	Picture of the Multihalle Mannheim grid.	371
A.8	Picture of the Multihalle Mannheim grid.	371
A.9	Picture of the Multihalle Mannheim grid.	372
A.10	Areal view of the Multihalle. Image from Burkhardt et al. 1978	373
A.11	Inside view of the Multihalle. Image from Burkhardt et al. 1978	373
A.12	Hanging model (Burkhardt et al 1978).	375
A.13	Detail of the model (Burkhardt et al 1978).	375
A.14	Test model. Image from Burkhardt et al. 1978	376
A.15	Tests on the model. Image from Burkhardt et al. 1978	376
A.16	Typical node joint. Image from Burkhardt et al. 1978	377
A.17	Photo of a typical node joint. Image from www.kunst.uni-stuttgart.de	377
A.18	Edge layout. Image from Burkhardt et al. 1978	378
A.19	Cable edge connection. Image from Burkhardt et al. 1978	379
A.20	Valley beam connection. Image from Burkhardt et al. 1978	379

A.21 Edge column connection. Image from Burkhardt et al. 1978	380
A.22 Under construction. Image from Burkhardt et al. 1978	381
A.23 Scaffolding towers. Image from Burkhardt et al. 1978	381
A.24 Intermediate strut. Image from Burkhardt et al. 1978	382
A.25 Applying the roof skin. Image from Burkhardt et al. 1978	382
A.26 Interior.	383
A.27 British museum computer model. Image by Chris Williams.	385
A.28 The Esplanade theatres in Singapore.	386
A.29 Physical model of the Downland Grid shell. Image by Frank Jensen.	387
A.30 Physical model of the Downland Grid shell. Image by Frank Jensen.	387
A.31 Computer model of the Downland Grid shell,. Image by Frank Jensen.	388
A.32 Physical model of the Downland Grid shell with the computer model projected on the surface. Image by Frank Jensen.	388
A.33 The Weald & Downland grid shell. Image from www.wealddown.co.uk	389
A.34 Inside view of the grid shell. Image from www.wealddown.co.uk	389
A.35 The Weald & Downland grid shell. Image from www.wealddown.co.uk	392
A.36 Scarf joint. Image from www.wealddown.co.uk	392
A.37 Assembly of a typical node joint. Image from www.wealddown.co.uk	393
A.38 Floor and beams are cut into shape. Image from www.wealddown.co.uk	393
A.39 Location of the brackets. Image from www.wealddown.co.uk	394
A.40 Connection to the edge. Image from www.wealddown.co.uk	394
A.41 Edge detail. Image from www.wealddown.co.uk	395
A.42 Finished connection. Image from www.wealddown.co.uk	395
A.43 Flat mat of laths. Image from www.wealddown.co.uk	396
A.44 Start of lowering. Image from www.wealddown.co.uk	397
A.45 Adjustable jack. Image from www.wealddown.co.uk	397
A.46 Angled jacks. Image from www.wealddown.co.uk	398
A.47 Halfway down. Image from www.wealddown.co.uk	398
A.48 Completed form. Image from www.wealddown.co.uk	399
A.49 Image of the Eden project	400
A.50 Model view of the Groningen Stadsbalkon. (Scheurer 2003)	401
A.51 Screenshot of the Groningen Twister model. (Scheurer 2003)	402
A.52 Color coding by kinetic energy. (Scheurer 2003)	402
A.53 The column model with a maximum bearing capacity and tilt. (Scheurer 2003) .	403
A.54 The relation between the habitats and the 'agents' en the growth, birth, shrinkage and death of the columns. (Scheurer 2003)	404
A.55 A rendering of the Web of North Holland. Image from (Boer & Oosterhuis 2004).	405
A.56 The NURBS surface of the design. Image from (Boer & Oosterhuis 2004). . . .	405
A.57 Mapping of a constructive grid based on a icosahedron. Image from (Boer & Oosterhuis 2004).	406
A.58 3D model of the panels with the construction showing. Image from (Boer & Oosterhuis 2004).	406
A.59 Specific view to illustrate the effectiveness of the application of the Hylite. Image from (Boer & Oosterhuis 2004).	407
A.60 The west and south side wall development diagram of the building. Image from (Ohmori & et al. 2005).	408
A.61 A perspective view of the building in a rendering. Image from (Ohmori & et al. 2005).	409
A.62 The evolution process of the south wall. Image from (Ohmori & et al. 2005). . .	410
A.63 The limit state deflection of the whole structure subjected to horizontal loads in x-, y-direction and under an angle. Image from (Ohmori & et al. 2005).	410
A.64 outside view. Image from (Ohmori & et al. 2005).	411

A.65 inside view. Image from (Ohmori & et al. 2005).	411
A.66 inside view. Image from (Ohmori & et al. 2005).	412
A.67 inside view. Image from (Ohmori & et al. 2005).	412
A.68 outside view. Image from (Ohmori & et al. 2005).	412
A.69 outside view. Image from (Ohmori & et al. 2005).	413
A.70 Internal view of the Palazetto dello Sport; h=21m, d=60m	414
A.71 Palazetto dello Sport	415
A.72 Placement of the prefabricated elements	415
A.73 Finishing of the structures, before pouring concrete	415
A.74 Sydney Opera House	416
A.75 Summary of the roof solutions	417
A.76 Presentation of the spherical solution	418
A.77 Y-shaped prefab elements (a) Fan shaped element of the vault (b)	418
A.78 The prefab vault during construction	419
A.79 Fabrication of a tile lid	419
A.80 Tiles lids attached to the ribs segments	420
A.81 The roof of the shed is 25mm thick and the stiffening ribs are 40mm thick	421
A.82 The roof of the shed rests on a steel column onto which the fibre reinforced UHPC arms are attached.	422
A.83 Design impression of the Hessing Cockpit by ONL	423
A.84 Cross section of Hessing Cockpit	424
A.85 Structure of the Hessing Cockpit	425
A.86 Esplanade Theatres in Singapore	426
A.87 Double layered Spaceframe for the Free Formed structure	427
A.88 Square-On-Diagonal Double Layered grid topology	428
A.89 Node detail, designed by MERO	429

List of Tables

3.1	Critical loading and critical membrane forces for elementary shells.	139
3.2	Max. radii depending on the material strength and internal pressure.	173
3.3	Different types of fibre materials	173
3.4	Applied coating materials.	174
3.5	Fibre properties	174
3.6	Comparison of windspeeds and wind pressures;	179
3.7	Needed energy for keeping hall type one from Figure 3.80 pressurized.	182
3.8	Needed energy for keeping hall type two from Figure 3.80 pressurized.	182
3.9	Span Ratio. (Chilton 2000) Note: E and I constant, L_2 longer span and L_1 shorter span.	213